

DOT/FAA/TC-19/21

Federal Aviation Administration
William J. Hughes Technical Center
Aviation Research Division
Atlantic City International Airport
New Jersey 08405

Adhesively Bonded Repairs to Metallic Fuselage Structure: Test 4, Effect of Temperature and Humidity on Mechanical and Fatigue Behavior

September 2019

Final Report

This document is available to the U.S. public through the National Technical Information Services (NTIS), Springfield, Virginia 22161.

This document is also available from the Federal Aviation Administration William J. Hughes Technical Center at actlibrary.tc.faa.gov.



U.S. Department of Transportation
Federal Aviation Administration

NOTICE

This document is disseminated under the sponsorship of the U.S. Department of Transportation in the interest of information exchange. The U.S. Government assumes no liability for the contents or use thereof. The U.S. Government does not endorse products or manufacturers. Trade or manufacturers' names appear herein solely because they are considered essential to the objective of this report. The findings and conclusions in this report are those of the author(s) and do not necessarily represent the views of the funding agency. This document does not constitute FAA policy. Consult the FAA sponsoring organization listed on the Technical Documentation page as to its use.

This report is available at the Federal Aviation Administration William J. Hughes Technical Center's Full-Text Technical Reports page: actlibrary.tc.faa.gov in Adobe Acrobat portable document format (PDF).

Technical Report Documentation Page

1. Report No. DOT/FAA/TC-19/21		2. Government Accession No.		3. Recipient's Catalog No.	
4. Title and Subtitle Adhesively Bonded Repairs to Metallic Fuselage Structure: Test 4, Effect of Temperature and Humidity on Mechanical and Fatigue Behavior.				5. Report Date September 2019	
				6. Performing Organization Code ANG-E281	
7. Author(s) Ryan J. Neel ¹ , John G. Bakuckas, Jr. ² , Yongzhe Tian ² , Cong Duong ³ , Jeong-Beom Ihn ³ , Kelly M. Greene ³ ¹ FAA (Ph.D. Candidate, Drexel University) ² FAA ³ Boeing Research & Technology				8. Performing Organization Report No.	
9. Performing Organization Name and Address William J. Hughes Technical Center Aviation Research Division Structures and Materials Section Atlantic City International Airport, NJ 08405				10. Work Unit No. (TRAIS)	
				11. Contract or Grant No. N/A	
12. Sponsoring Agency Name and Address U.S. Department of Transportation Federal Aviation Administration Transport Standards Branch Airframe & Cabin Safety Section, AIR-675 2200 South 216 th Street Des Moines, Washington 98198				13. Type of Report and Period Covered Final Report	
				14. Sponsoring Agency Code AIR-675	
15. Supplementary Notes The FAA William J. Hughes Technical Center Aviation Research Division COR was John G. Bakuckas, Jr.					
16. Abstract In a collaborative effort, the FAA and The Boeing Company investigated the structural robustness and damage-resistance capabilities of adhesively bonded repair patches through the testing and analysis of metallic B727 fuselage panels using the FAA's Full-Scale Aircraft Structural Test Evaluation and Research laboratory. The program objectives were to characterize the durability and fatigue performance of adhesively bonded boron/epoxy and aluminum (Al) repair patches subjected to simulated service load conditions over the typical design service goal (DSG) of an airplane (60,000 cycles for a B727) and to investigate tools used to evaluate and monitor the integrity of the repair patches over the life of the part. This report summarizes the results of the fourth and final fuselage panel test conducted in this ongoing program. The objective was to determine the effect of environmental conditions (i.e., temperature and humidity) on the mechanical and fatigue behavior of adhesively bonded repair patches installed on a metallic fuselage structure. Hot-wet (165°F and 85% humidity), cold-dry (-25°F), and ambient environmental conditions were considered. B/Ep and Al doublers were used to patch active, through-thickness, center-bay cracks in the skin of a fuselage panel harvested from a retired B727 aircraft. Repair patches included those that were properly designed and those that were intentionally made deficient through under-design and the insertion of disbonds to encourage damage growth. This allowed for the generation of data for analysis verification and assessment of non-destructive inspection methods used to monitor repair integrity. Efforts were focused on assessing residual strains that developed during the curing cycle of patch installation and during the four-week period of hot-wet conditioning that occurred immediately after repair patch installation (i.e., prior to load application) for select repair patches. Following the completion of this period, the fuselage panel was subjected to fatigue testing under cold-dry environmental conditions up to the typical DSG of 60,000 cycles. For the B/Ep repair patches, high residual strains developed during curing as a result of mismatches in the thermal properties of the repair and fuselage skin. The magnitude of notch-tip strains increased as temperature decreased. Consequently, the fatigue crack growth increased as the temperature decreased for the B/Ep repairs. Results for the Al repairs indicated the limited effect of environment on the notch-tip mechanical strains and the fatigue crack-growth behavior under hot-wet or cold-dry conditions. Because both the repair and the fuselage skin are made of Al, residual strains due to thermal mismatch were limited. Multi-site damage formed in the panel lap-joint area outside the test section during fatigue cycling, resulting in crack linkup to a 20-inch-long crack after the completion of 92,834 cycles. Because of stress redistribution, data analysis was terminated at that point. Data from this program will be used to assess tools and methods for evaluating and monitoring the repair integrity.					
17. Key Words Bonded repairs, Boron/epoxy, aluminum, Fuselage structure, Disbond, Crack, Non-destructive inspection, Structural health monitoring, Test, Analysis			18. Distribution Statement This document is available to the U.S. public through the National Technical Information Service (NTIS), Springfield, Virginia 22161. This document is also available from the Federal Aviation Administration William J. Hughes Technical Center at actlibrary.tc.faa.gov .		
19. Security Classif. (of this report) Unclassified		20. Security Classif. (of this page) Unclassified		21. No. of Pages 568	22. Price

TABLE OF CONTENTS

	Page
EXECUTIVE SUMMARY	x
1. INTRODUCTION	1
2. EXPERIMENTAL PROCEDURE	4
2.1 Test Fixture Description	4
2.2 Test Specimen Description	6
2.3 Load History	8
2.4 Damage Scenarios	9
2.5 Repair Types	10
2.5.1 Type-1 Repair Patches	12
2.5.2 Type-2 Repair Patches	13
2.5.3 Type-3 Repair Patches	14
2.6 Applied Loads and Test Matrix	16
2.7 Inspection and Monitoring Methods	18
2.7.1 Bonded Foil Strain Gauges	19
2.7.2 Temperature and Humidity Sensors	21
2.7.3 High-Magnification Camera Systems	23
2.7.4 Three-Dimensional (3D) Digital Image Correlation (DIC)	25
2.7.5 Eddy Current	26
2.7.6 Flash Thermography	27
2.7.7 Resonance Ultrasonic	28
2.7.8 Piezoelectric-Based Structural Health Monitoring (SHM)	28
3. RESULTS AND DISCUSSION	30
3.1 Unexpected Occurrence of Multi-Site Damage (MSD)	30
3.2 Strain Monitoring	32
3.2.1 Thermal Residual Strain During Repair Patch Installation	32
3.2.2 Thermal Residual Strain During Hot-Wet Conditioning	33
3.2.3 Effect of Fatigue Loading on Mechanical Strain	36
3.2.4 Effect of Environment on Mechanical Strain	43
3.3 Fatigue Crack-Growth Monitoring	44
3.3.1 Effect of Repair Quality on Fatigue Performance	45
3.3.2 Effect of Hot-Wet Conditioning on Fatigue Crack Growth	45
3.3.3 Effect of Environment on Fatigue Crack Growth	46
3.3.4 Correlation Between Crack Growth Inspections	47

3.4	Disbond Detection	48
	3.4.1 Disbond Detection With Flash Thermography	48
	3.4.2 Disbond Detection With Resonance Ultrasonic	49
3.5	Structural Health Monitoring	50
3.6	Preliminary Thermal Residual Stress Analysis by Viscoelastic Modeling	52
4.	SUMMARY	52
5.	REFERENCES	54

APPENDICES

A	FUSELAGE PANEL ENGINEERING DRAWINGS
B	REPAIR PATCH INSTALLATION PROCEDURE
C	STRAIN GAUGE LAYOUTS
D	STRAIN GAUGE RESPONSE DURING REPAIR PATCH INSTALLATION
E	STRAIN GAUGE RESPONSE DURING HOT-WET CONDITIONING
F	STRAIN GAUGE RESPONSE DURING STRAIN SURVEYS
G	3D DIGITAL IMAGE CORRELATION RESULTS
H	FATIGUE CRACK GROWTH RESULTS
I	FLASH THERMOGRAPHY RESULTS
J	RESONANCE ULTRASONIC RESULTS
K	PRELIMINARY THERMAL RESIDUAL STRESS ANALYSIS BY VISCOELASTIC MODELING

LIST OF FIGURES

Figure		Page
1	Full-scale aircraft structural test evaluation and research (FASTER) fixture: FASTER fixture and supporting components and exploded view of the FASTER fixture	4
2	External view of the fuselage panel and section A-A view of the fuselage panel	5
3	Environmental chamber: internal view and strapped to fuselage panel	6
4	Airplane at a salvage yard and location of the panel with respect to the airplane	6
5	Fuselage panel after initial modifications: external view and internal view	7
6	Fuselage panel after installation of elastomeric pressure box seal and axial loader shims	7
7	Dimensions of the fuselage panel following preparatory modifications	8
8	Environmental and mechanical fatigue load history of fuselage panel 4	8
9	Location of cracks with respect to the fuselage panel and a typical notch	9
10	Typical development of a naturally sharp crack during fatigue pre-cracking	9
11	Location and designation of bonded repair patches	11
12	Overview of the reference B/Ep repair patch	12
13	Overview of the reference Al repair patch	13
14	Overview of the under-designed B/Ep repair patch	14
15	Overview of the under-designed Al repair patch	14
16	Overview of the partially disbanded B/Ep repair patch	15
17	Overview of the partially disbanded Al repair patch	16
18	Strain gauges installed before cutting notches in the panel: external fuselage panel surface, internal fuselage panel surface, stringer detail, and frame detail	20
19	Layout of strain gauges during the first 40,000 cycles of testing: 3-inch-wide repairs, RAC, UAC, UBC, UDBC, UDAC; and 5-inch-wide repair, RBC	21
20	Layout of strain gauges during the final 52,834 SL cycles of testing: 3-inch-wide repairs, RAC, UAC, UB, UBC, UDC, UDBC, UDAC; and 5-inch-wide repair, RBC	21
21	Location of temperature/humidity probes with respect to the panel during testing	22
22	Location of thermocouples with respect to the panel during installation of repair patches: UBC and RBC, UAC and UDAC, UB and UDB, and UDBC and RAC	23
23	RCCM system mounted above the FASTER fixture, motion control assembly, cameras, and a typical image captured by the RCCM system during fatigue pre-cracking	24
24	The pressure box camera system underneath a fuselage panel, and a typical image captured by the pressure box camera system during fatigue cracking	25

25	ARAMIS 3D DIC system mounted on the motion control assembly of the RCCM system, and typical stochastic pattern painted on, and in the vicinity of, each repair patch	26
26	Portable Eddy Current Flaw Detector, PowerLink™ Absolute Shielded Metal Detachable Pencil Probe, and PowerLink™ Standard Bridge Detachable Surface Probe	27
27	TWI ThermoScope® II high-performance PC system complete with MOSAIQ® analysis software, and TWI ThermoScope® II integrated illumination head	27
28	Olympus BondMaster 1000e+, and S-PR-5 - 250 kHz Resonance Probe	28
29	Position of piezoelectric transducers installed in the vicinity of repair patches UB and UDB: external fuselage panel surface and internal fuselage panel surface	29
30	MSD that occurred along lap joint S-4R between stringers STA580 and STA600	31
31	Hoop strain response recorded between 90,000 cycles and 92,800 cycles of testing: hoop strain time history SGS1 and hoop strain time history SGS2	31
32	Thermal residual strains measured during the patch installation cure process	33
33	Thermal residual strains measured during the 4-week hot-wet conditioning period	34
34	Comparison between hoop strains measured before and after 4 weeks of hot-wet conditioning by crack-tip strain gauges: damage scenario, repair patch UBC, and; repair patch UAC	35
35	Comparison between hoop strains measured before and after 4 weeks of hot-wet conditioning by 3D DIC for repair patches: RBC, UBC, and UDBC	36
36	Comparison between hoop strains measured before and after 4 weeks of hot-wet conditioning by 3D DIC for repair patches: RAC, UAC, and UDAC	36
37	Hoop strain results obtained by strain gauges in the vicinity of repair patch UAC: hoop strain as a result of pressure, and strain history throughout the test	37
38	Hoop strain results obtained by strain gauges in the vicinity of repair patch UBC: hoop strain as a result of pressure, and strain history throughout the test	38
39	Comparison of the average strain measured along the boundary of repair patches and the locations of strain gauges with respect to the repair patches	38
40	Comparison of the average strain measured at the centers of repair patches and the location of strain gauges with respect to the repair patches	39
41	Comparison of the average strain measured along the boundary of repair patches and the locations of strain gauges with respect to the repair patches	40
42	Comparison of the average strain measured at the centers of repair patches and the location of strain gauges with respect to the repair patches	40
43	DIC WFOV hoop strain results measured for repair patch UDBC after: hot-wet conditioning, 20,000 cycles, 40,000 cycles, and 60,000 cycles	41

44	DIC NFOV hoop strain results measured for repair patch UDBC after: hot-wet conditioning, 20,000 cycles, 40,000 cycles, and 60,000 cycles	43
45	Comparison between strains measured in cold-dry, ambient, and hot-wet environmental condition by crack-tip strain gauges underneath repairs: typical damage scenario underneath each adhesively bonded repair patch, UBC, and UAC	44
46	Comparison of the fatigue crack growth exhibited by Type-1, Type-2, and Type-3 repair patches: typical damage scenario underneath each adhesively bonded repair patch, B/Ep repair patches, and Al repair patches	45
47	Comparison between the fatigue crack growth exhibited by repairs that were and were not pre-conditioned in a hot-wet environment: typical damage scenario underneath each adhesively bonded repair patch, UB and UBC, and UDB and UDBC	46
48	Average fatigue crack growth observed for fuselage Panel 2 (ambient), fuselage Panel 3 (hot-wet), and fuselage Panel 4 (cold-dry) for repair patches: typical damage scenario underneath each adhesively bonded repair patch, UB and UA and UAC	47
49	Comparison of fatigue crack-growth measurements conducted with visual, HFEC, and LFEC inspections: typical damage scenario underneath each adhesively bonded repair patch, Type-2 B/Ep repair patch, UBC; and Type-2 Al repair patch, UAC	48
50	Flash thermography results for the Type-3 B/Ep repair patch, UDBC: 0 cycles, 20,000 cycles, 40,000 cycles, 60,000 cycles, and 92,834 cycles.	49
51	Resonance ultrasonic results for the Type-3 B/Ep repair patch, UDBC: 0 cycles, 20,000 cycles, 40,000 cycles, 60,000 cycles, and 92,834 cycles.	50
52	Comparison between predictions by the local SHM model and crack-growth measurements obtained via HFEC inspections for Panel 4 repair patches UB and UDB: type 2 B/Ep repair patch, UB; type 3 B/Ep repair patch UDB; model correlation, UB; blind measurements, UB; model correlation, UDB, and blind measurements, UDB	51
53	Comparison between predictions by the global SHM model and crack-growth measurements obtained via HFEC inspections for Panel 3 repair patches UB and UDB	52

LIST OF TABLES

Table		Page
1	Summary of visual crack length measurements obtained after pre-cracking	10
2	Overview of repair types	11
3	Overview of the mechanical loads to which the fuselage panel was subjected	17
4	Overview of the environmental conditions to which the fuselage panel was subjected	17
5	Summary of the fatigue load history of each repair patch	18
6	Overview of the frequency with which intermittent inspections were conducted	19
7	Overview of SHM test conditions, algorithms, and validation approaches	30

LIST OF ACRONYMS

3D	Three-dimensional
Al	Aluminum
B/Ep	Boron/epoxy
DIC	Digital image correlation
DSG	Design service goal
FASTER	Full-Scale Aircraft Structural Test Evaluation and Research
FEP	Fluorinated ethylene propylene
FTO	Flash trigger offset
HFEC	High-frequency eddy current
LFEC	Low-frequency eddy current
MSD	Multi-site damage
NDI	Non-destructive inspection
NFOV	Narrow field-of-view
RCCM	Remote controlled crack monitoring
SHM	Structural health monitoring
SSL	Simulated service load
TSR	Thermographic signal reconstruction
TWI	Thermal wave imaging
VPG	Vishay Precision Group
WFOV	Wide field-of-view

EXECUTIVE SUMMARY

In a collaborative effort, the FAA and The Boeing Company investigated the structural robustness and damage-resistance capabilities of adhesively bonded repair patches through the testing and analysis of metallic B727 fuselage panels using the FAA's Full-Scale Aircraft Structural Test Evaluation and Research laboratory. The program objectives were to characterize the durability and fatigue performance of adhesively bonded boron/epoxy and aluminum (Al) repair patches subjected to simulated service load conditions over the typical design service goal (DSG) of an airplane (60,000 cycles for a B727) and to investigate tools used to evaluate and monitor the integrity of the repair patches over the life of the part.

This report summarizes the results of the fourth and final fuselage panel test conducted in this ongoing program. The objective was to determine the effect of environmental conditions (i.e., temperature and humidity) on the mechanical and fatigue behavior of adhesively bonded repair patches installed on a metallic fuselage structure. Hot-wet (165°F and 85% humidity), cold-dry (-25°F), and ambient environmental conditions were considered. B/Ep and Al doublers were used to patch active, through-thickness, center-bay cracks in the skin of a fuselage panel harvested from a retired B727 aircraft. Repair patches included those that were properly designed and those that were intentionally made deficient through under-design and the insertion of disbonds to encourage damage growth. This allowed for the generation of data for analysis verification and assessment of non-destructive inspection methods used to monitor repair integrity. Efforts were focused on assessing residual strains that developed during the curing cycle of patch installation and during the 4-week period of hot-wet conditioning that occurred immediately after repair patch installation (i.e., prior to load application) for select repair patches. Following the completion of this period, the fuselage panel was subjected to fatigue testing under cold-dry environmental conditions up to the typical DSG of 60,000 cycles.

For the B/Ep repair patches, high residual strains developed during curing as a result of mismatches in the thermal properties of the repair and fuselage skin. The magnitude of notch-tip strains increased as temperature decreased. Consequently, the fatigue crack growth increased as the temperature decreased for the B/Ep repairs. Results for the Al repairs indicated limited effect of environment on the notch-tip mechanical strains and the fatigue crack-growth behavior under hot-wet or cold-dry conditions. Because both the repair and the fuselage skin are made of Al, residual strains due to thermal mismatch were limited. Multi-site damage (MSD) formed in the panel lap-joint area outside the test section during fatigue cycling, resulting in crack linkup to a 20-inch-long crack after the completion of 92,834 cycles. Because of stress redistribution, data analysis was terminated at that point. Data from this program will be used to assess tools and methods for evaluating and monitoring the repair integrity.

1. INTRODUCTION

Installing mechanically fastened repair patches to a damaged structure is a common maintenance practice for ensuring continued airworthiness of a commercial aircraft. During the installation process, the damaged area is removed, an array of through-thickness holes is drilled around the void, and metallic sheets are rivet-attached to the aircraft structure. This method is sufficient for restoring the structural strength of aircraft components but can lead to potential problems intrinsic to the fastening method. The drilling of through-thickness holes and subsequent installation of rivets generates areas of high-stress concentration that could, under low-stress conditions, develop cracks. Significant efforts have been made to evaluate alternative repair methods using adhesively bonded repair patches [1]. Pioneered by the Defense Science and Technology Organization of Australia more than 3 decades ago, adhesively bonded repair patches have been demonstrated to be viable alternatives to traditional mechanically fastened repairs. Comparisons of the two shows that adhesively bonded repair patches are more aerodynamically efficient, mitigate removal of baseline material from the damaged structure, and facilitate continuous load transfer from the aircraft component to the repair patch.

Although the effectiveness of adhesively bonded repair patches has been demonstrated to maintain aging military fleets worldwide, challenges remain with respect to commercial aircraft applications. A particular challenge pertains to the integrity of the bond between the repair patch and the damaged structure, which depends on a myriad of installation parameters. Errors during installation, including exposure of the repair patch to a humid environment, improper surface preparation, contamination of the bond line, insufficient control of the curing temperature (e.g., over-heating or under-curing), and loss of vacuum pressure can lead to a reduction in bond-line strength. Furthermore, bond integrity cannot be detected by existing non-destructive inspection (NDI) techniques. Consequently, the FAA issued a policy statement (PS-AIR-100-14-130-001) regarding the installation of adhesively bonded repair patches on primary structure [2]. According to this policy statement: “All critical structures must have a repair size limit no larger than a size that maintains limit load residual strength capability with the repair completely failed or failed within arresting design structures.”

To expand the size limits of a given bonded repair patch, repair designs must have structural substantiation based on tests or analyses supported by tests. Additional datasets are required to qualify bonded material and process compatibilities to demonstrate the proof of structure and establish reliable inspection procedures.

To gain better insight into the performance of adhesively bonded repairs and help address issues cited in the FAA policy statement, the FAA and The Boeing Company have been investigating adhesively bonded repair patches through structural testing of B727 fuselage panels using FAA’s Full-Scale Aircraft Structural Test Evaluation and Research (FASTER) facility. The program objectives are to characterize the durability and fatigue performance of adhesively bonded boron/epoxy (B/Ep) composite and aluminum (Al) repair patches subjected to simulated service load (SSL) conditions over the typical design service goal (DSG) of an airplane (60,000 cycles for a B727) and to investigate methods and tools used to conduct analyses and performance predictions of the repair patches and those used to monitor and evaluate repair quality over the life of the part.

The damage scenarios considered in this program were primarily active, through-thickness, center-bay cracks. Center-bay cracks are not common; however, this approach simplifies the analysis, repair installation, and inspection. Normally, a crack is completely removed from the structure prior to repair application; however, for the purpose of this research, the cracks were not removed. Active damage was left underneath each repair patch to facilitate the collection of data that can be used to support efforts to verify fracture mechanics-based analysis and design tools and to facilitate the ability to evaluate monitoring systems, such as structural health monitoring (SHM) and other conventional NDI techniques. This program does not advocate leaving active damage under a repair in nonresearch-related applications.

Multiple fuselage panel tests were conducted in a phased approach in this program. A variety of damage scenarios, repair configurations, mechanical load configurations, and environmental conditions were considered. In each case, conventional and prototype NDI techniques were used to evaluate the integrity of the repair patches throughout testing. As part of this program, three fuselage panel tests were conducted as reported in references 3–5. During the Panel 1 test, properly designed repair patches were tested under ambient environmental conditions. Baseline results indicated that properly designed and installed adhesively bonded repair patches are durable under fatigue to at least one DSG under SSL conditions and capable of effectively containing large damage under severe loading conditions [3].

For the Panel 2 test, properly designed repair patches and those which were intentionally made deficient for the purpose of promoting damage growth were tested under ambient environmental conditions [4]. Emphasis was placed on assessing several conventional NDI techniques used to monitor the integrity of the repair patches throughout testing, including eddy current, flash thermography, and resonance ultrasonic in addition to a prototype piezo-electric-based SHM system. In terms of fatigue performance, results indicated that adhesively bonded repair patches that are made deficient by improper design or installation procedures are less effective at resisting damage growth when compared with their properly designed and installed counterparts. The capability of conventional NDI to detect growing flaws underneath adhesively bonded repair patches and to monitor the effectiveness of the adhesively bonded repair patches was demonstrated. In general, predictions using a fracture mechanics-based model were in good agreement with crack-growth results for the majority of the repair patch configurations, though test and analysis correlations revealed that further research was needed to better account for the thermal residual stresses.

The first two panel tests were conducted in ambient (laboratory) environmental conditions. Follow-on phases of the program studied the effect of other environmental conditions on the durability and fatigue performance of the adhesively bonded repair patches. Major modifications were made to fully integrate an environmental system with the FASTER fixture to apply synchronous mechanical, temperature, and humidity load profiles. With this enhanced capability, fuselage panels can be subjected to environmental conditions ranging from hot and wet (165°F and 85% to 95% humidity) to cold and dry (-25°F). During the Panel 3 test, properly designed repair patches and those which were intentionally made deficient for the purpose of promoting damage growth were tested under hot-wet (165°F and 85% humidity) environmental conditions [5]. In terms of fatigue performance, slower crack growth was observed under hot-wet conditions for the B/Ep repair patches when compared to counterparts tested under ambient conditions. Mismatches between the thermal coefficients of expansion of the repair patches and the panel skin

resulted in the development of residual stresses ahead of the notch tip during the patch-installation curing process. At elevated temperatures, residual stresses relaxed, which could have contributed to slower crack growth.

In this report, results from the fourth and final panel test of this program are summarized. The objective was to investigate the effect of hot-wet and cold-dry environmental conditions on the performance of adhesively bonded repair patches. Emphasis was placed on assessing residual strains that developed during the curing cycle of patch installation and during the 4-week period of hot-wet conditioning that occurred immediately after repair patch installation (i.e., prior to load application) for select repair patches. Following the completion of this period, the fuselage panel was subjected to fatigue testing under cold-dry environmental conditions up to and exceeding the typical DSG of 60,000 cycles. Results and other major findings include:

- Thermal residual strains that developed in and around the repair patch regions during the repair patch installation process were measured for model development purposes. For the B/Ep repair patches, high thermal residual strains developed within the repair patch footprint and surrounding areas as a result of the mismatches between the thermal properties of the B/Ep repair patch and the Al fuselage panel skin. For the Al repair patches, thermal residual strains were much lower and often insignificant.
- Following the completion of the repair patch installation process, select repair patches were subjected to 4 weeks of hot-wet conditioning. During this time, strain gauges installed in the vicinity of each repair patch were continuously monitored. For the B/Ep repair patches, thermal-viscoelastic-plastic behavior was observed in which thermal strains relaxed. Conditioning of the B/Ep repair patches resulted in lower notch-tip strains when compared with similar repair patches that were not subjected to hot-wet conditioning. For the Al repair patches, the effects of hot-wet conditioning were insignificant.
- Throughout the duration of the test, mechanical strains were measured along the notch centerline during the application of a quasistatic load under ambient, hot-wet, and cold-dry environmental conditions. For the B/Ep repair patches, the mechanical strains increased as temperature decreased. For the Al repair patches, the environment effects were limited.
- Fatigue loading was conducted under cold-dry conditions up to and exceeding one DSG. During this time, fatigue crack growth and strains were monitored continuously. Post-test, comparisons were made between the results obtained from this test to those obtained during the Panel 2 test (conducted under ambient conditions) and the Panel 3 test (conducted under hot-wet conditions). The fatigue crack growth observed under the cold-dry conditions for the as-installed B/Ep repair patches (Panel 4) was the highest, followed by ambient (Panel 2), and then hot-wet (Panel 3). These followed similar trends in which the notch-tip strains were highest under cold-dry conditions, followed by ambient, and then hot-wet. The pre-conditioned B/Ep repair patches installed on Panel 4 exhibited slower crack growth compared to the as-installed B/Ep repair patches, which correlated with lower notch-tip strains.

2. EXPERIMENTAL PROCEDURE

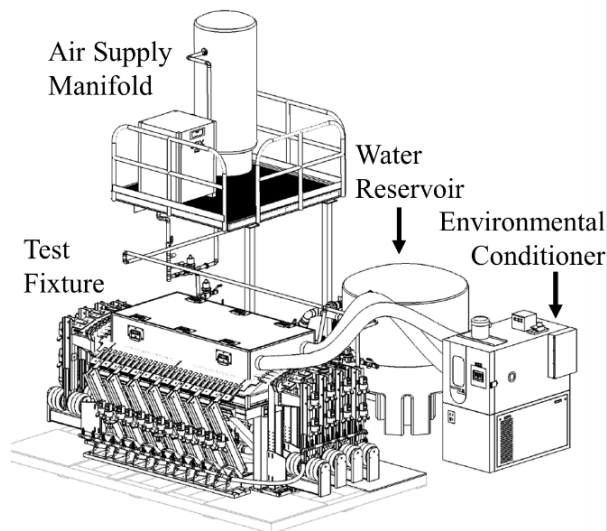
This section provides information on the experimental procedure used for the full-scale test. First, the test fixture and fixture modifications are discussed. Next, a description of the test panel, including aircraft history, panel dimensions, materials, and panel preparation for the test, are provided. Then, the test phases and the applied loads are provided. Finally, an overview of the inspection and monitoring methods employed are described.

2.1 Test Fixture Description

Located at the FAA William J. Hughes Technical Center in Atlantic City, NJ, the FASTER fixture was developed to conduct static and fatigue testing of full-scale fuselage panels (see figure 1). Using a novel combination of mechanical and electrical components, the FASTER fixture is capable of simulating aircraft service load conditions through synchronous application of various mechanical and environmental loading conditions. A detailed description of the FASTER fixture features and capabilities is provided in reference 6.

In general, the FASTER fixture consists of a base structure, hoop load assemblies, axial load assemblies, frame load assemblies, a fuselage pressure box, and an environmental system with a remote conditioner and an environmental chamber (see figure 1). The test fixture is capable of dynamically cycling the internal pressure and performing a static pressurization. The frame and hoop load assemblies are designed to react to the applied pressure, whereas the axial load assembly is designed to apply both tension and compression to simulate fuselage vertical bending conditions.

(a) FASTER Fixture and Supporting Components



(b) Exploded View of the FASTER Fixture

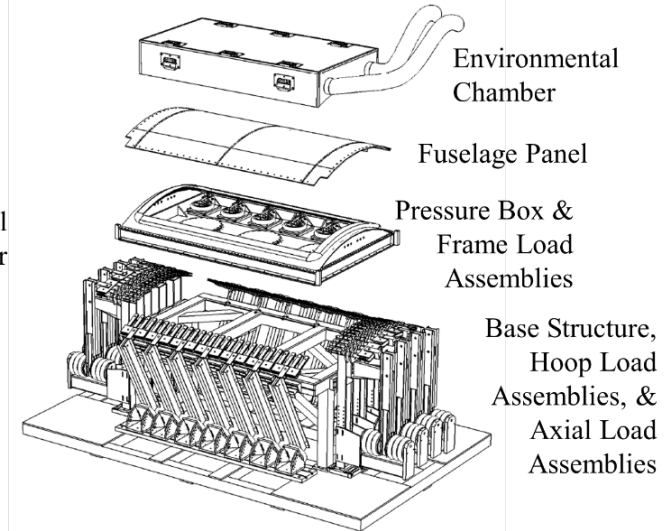


Figure 1. Full-scale aircraft structural test evaluation and research (FASTER) fixture: (a) FASTER fixture and supporting components and (b) exploded view of the FASTER fixture

External load application is accomplished using pressurized fluid (e.g., air or water). Internal pressurization is applied by pumping fluid into the pressure box to desired levels. Axial, hoop, and frame loads are generated by leveraging the pressurized fluid through mechanical lever assemblies. Applied hoop and axial loads are simulated by the controlled application of distributed loads

around the perimeter of the test panel (see figure 2). Forces are distributed by individual loading linkages using a two-tier coaxial whiffle tree assembly, which generates four equal forces from each load actuator. Seven hoop load assemblies are used on each side of the specimen, creating 28 load attachment points. Four bi-axial load mechanisms are used on each end for 16 load application points. Similar devices are available to apply hoop tension loads at the ends of up to six frames.

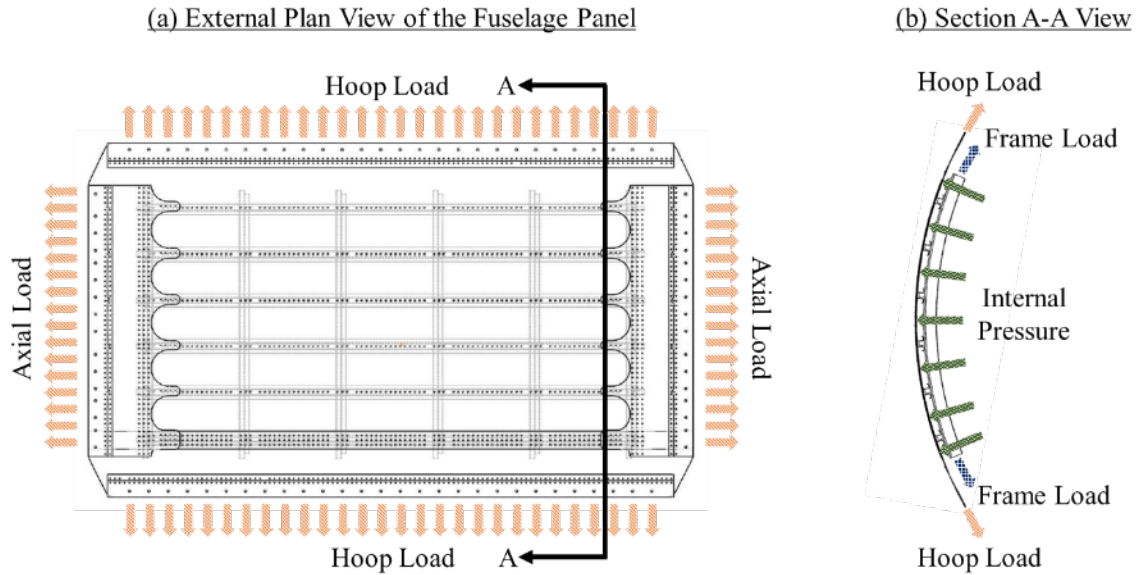


Figure 2. (a) External view of the fuselage panel and (b) section A-A view of the fuselage panel

The most recent modification to the fixture provides the capability to subject fuselage panels to humidity and temperature environmental conditions ranging from hot and wet (165°F and 85%–95% RH) to cold and dry (-25°F). This system consists of an environmental chamber and a remote conditioner (see figure 3). The environmental chamber, which is strapped to the external surface of the fuselage structure, as shown in figure 3b, consists of four external vertical walls and a lid that define its external volume, and an internal vertical wall that separates the internal volume into two regions, as shown in figure 3a: 1) the conditioned region and 2) the ambient region. Each wall is comprised of polystyrene foam core insulation sandwiched between 26-gauge galvanized steel sheets. An impermeable interface between the environmental chamber and the external surface of the fuselage structure was achieved using rubber bulb seals and weather-resistant neoprene foam.

The remote conditioner, a Cincinnati Sub-Zero Z-plus remote conditioner (P/N Model ZPRCHS-816-6-6-SC/AC), is connected to the environmental chamber through two insulated, 8-inch diameter ducts that facilitate passage of conditioned air into and out of the environmental chamber. The section of the chamber connected to the ducts is the conditioned region, whereas the section on the other side of the internal vertical wall is the ambient region. The two internal volumes allow for simultaneous testing of both conditioned and unconditioned repairs to a fuselage structure. Similar to the mechanical loading mechanisms described previously, instrumentation of the environmental chamber and remote conditioner facilitates the ability to control and monitor the performance of the system remotely via a laboratory computer.

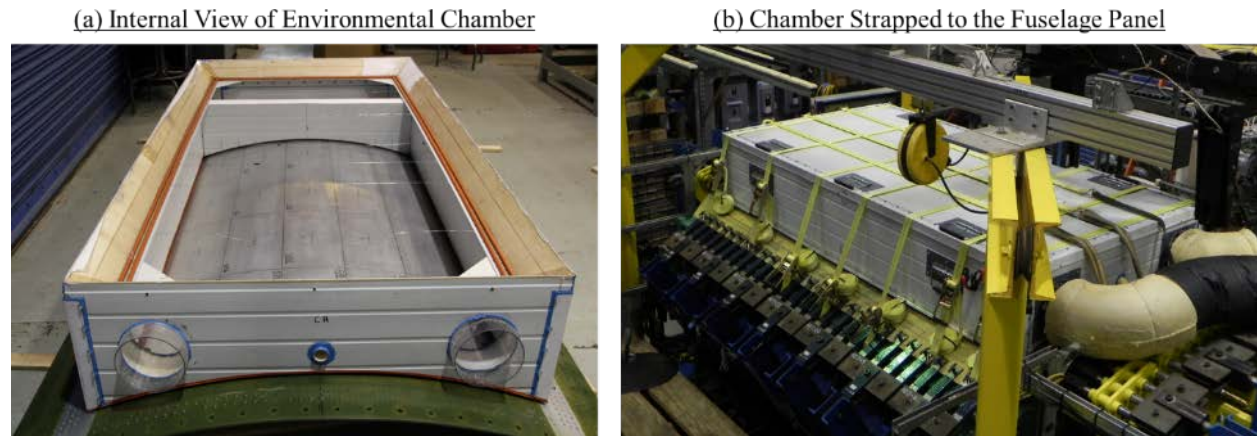


Figure 3. Environmental chamber: (a) internal view and (b) strapped to fuselage panel

2.2 Test Specimen Description

The fuselage panel was removed from a retired passenger B727-225 aircraft with tail number N676MG and serial number 22554, with 47,724 accumulated flight hours and 29,326 flight cycles while in service (see figure 4). Located on the crown of the aircraft, the fuselage panel included frame stations STA520 to STA620 and stringer stations S-9R to S-4R. Components of the fuselage section included the skin, frames, shear clips, stringers, and an axial skin splice joint.

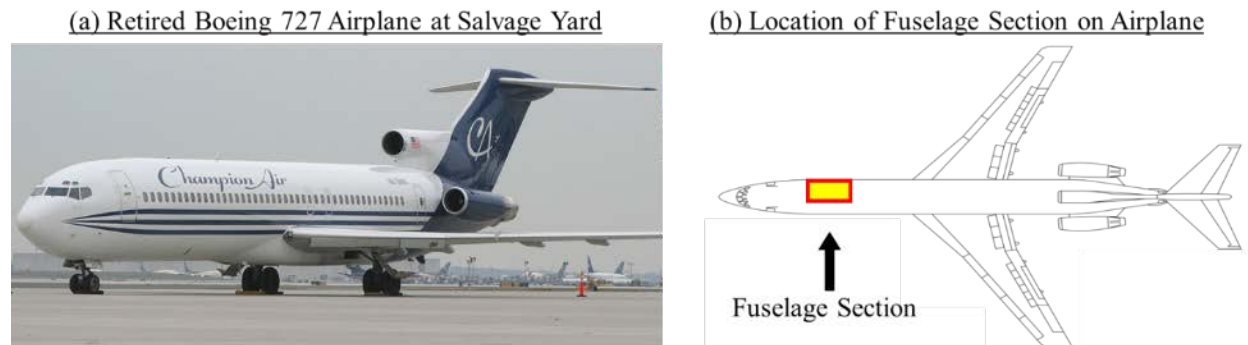


Figure 4. (a) Airplane at a salvage yard and (b) location of the panel with respect to the airplane

When the fuselage panel was removed from the aircraft, NDIs were conducted to determine the condition of the test section. Following these inspections, modifications were made to ensure that the form and condition of the fuselage section were sufficient for testing. Modifications included: 1) extraction of the test specimen (i.e., the area of the fuselage covered by frame stations STA520 to STA620 and stringer stations S-9R to S-4R) from the fuselage section; 2) reduction of frame and stringer lengths to ensure proper connectivity to the FASTER fixture; 3) installation of 2024-T3 Al doublers along the perimeter of the fuselage panel on both the internal and external fuselage panel surfaces; 4) installation of 2024-T3 Al doublers on the frame ends; 5) drilling of 0.5-inch diameter load attachment holes through the frame end doublers and fuselage panel perimeter doublers; 6) installation of 2024-T3 Al shims at the axial load attachment points on both the internal and external fuselage panel surfaces; and (7) the installation of an elastomeric pressure

box seal. Figure 5 shows the fuselage panel following modifications (1) through (5), whereas figure 6 shows the fuselage panel following modifications (6) and (7).

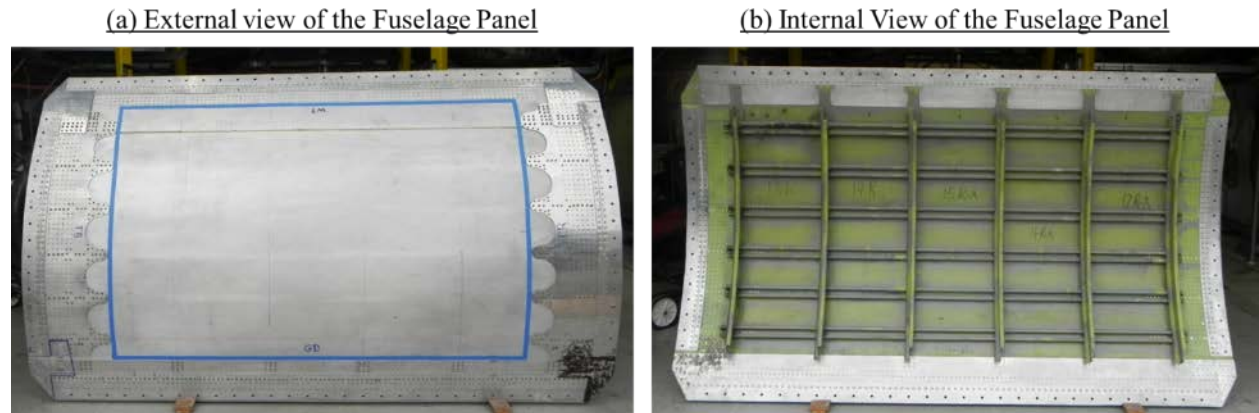


Figure 5. Fuselage panel after initial modifications: (a) external view and (b) internal view



Figure 6. Fuselage panel after installation of elastomeric pressure box seal and axial loader shims

The final version of the fuselage panel was 125 inches long and 73 inches wide with a radius of 74 inches and a skin thickness of 0.040 inch throughout the test section. The substructure included six stringers oriented in the axial direction with 9.5-inch spacing, six frames oriented in the hoop direction with 20-inch spacing, and a lap joint along stringer station S-4R. A schematic depicting the dimensions of the fuselage panel is shown in figure 7. Detailed engineering drawings of the fuselage panel are provided in appendix A.

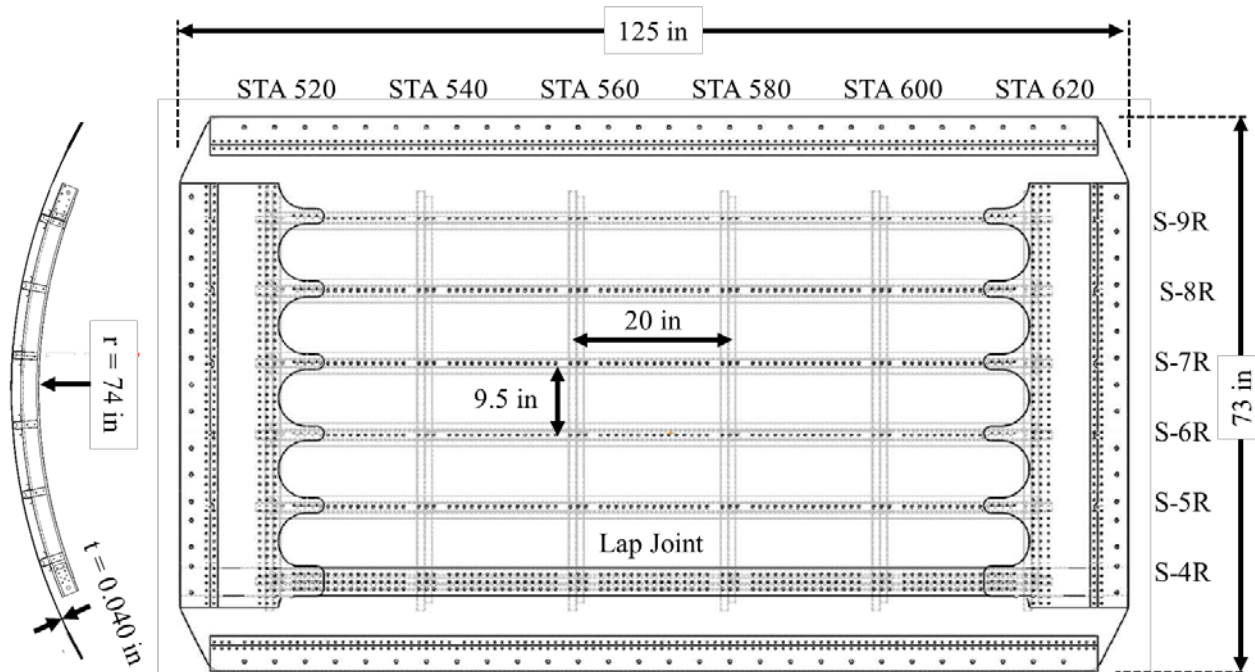


Figure 7. Dimensions of the fuselage panel following preparatory modifications

2.3 Load History

The complete load history of the fuselage panel is shown in figure 8. During service, the aircraft accumulated 29,326 flight cycles. In subsequent testing, the panel with a subset of repairs was subjected to four weeks of hot-wet (165°F and 85% RH) conditioning (without mechanical loading). This was followed by two phases of extended fatigue testing under simulated SL conditions in a cold-dry (-25°F) environment for an additional 92,834 cycles. During the extended fatigue testing, MSD formed, resulting in a 20-inch-long crack. Because of stress redistribution, data analysis and results are presented up to 90,000 cycles in this report. The details of the MSD are provided in the results section.

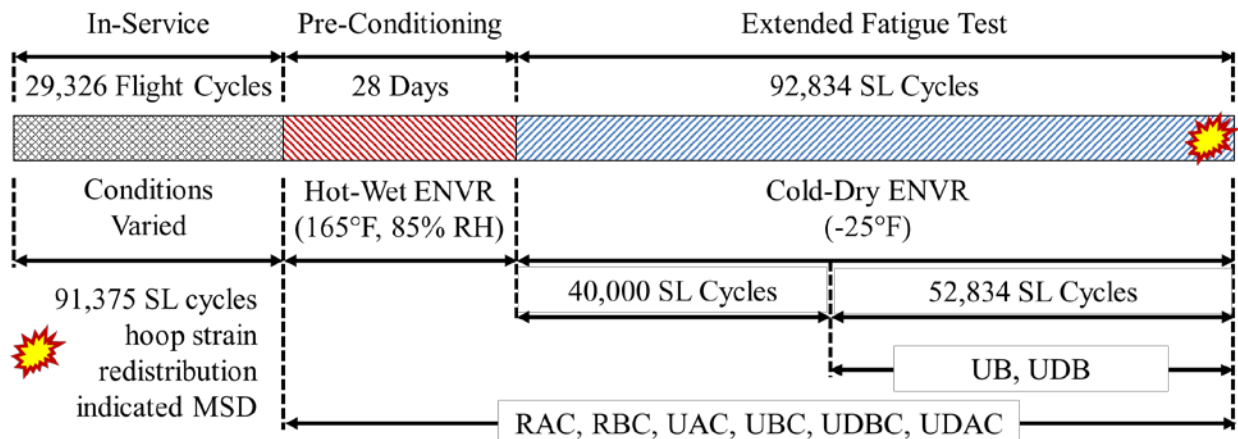


Figure 8. Environmental and mechanical fatigue load history of fuselage panel 4

2.4 DAMAGE SCENARIOS

The initial damage scenario for each repair patch was a 3-inch, center-bay, through-thickness crack, as shown in figure 9. Using a grind wheel and jeweler's saw, damage was inserted in the form of a crack starter notch with a length of 2.8 inches and notch-tip width of 0.006 inch. Subsequently, fatigue pre-cracking was conducted at an applied load equivalent to 75% of SL conditions to generate naturally sharp crack tips. Although natural occurrence of this damage scenario is not common, it does simplify repair installation, inspection, and analytical procedures; therefore, it was chosen for this research study. As emphasized earlier, this program does not advocate leaving active damage under a repair in non-research related applications. Figure 10 shows the development of naturally sharp crack tips from this notch during fatigue pre-cracking.

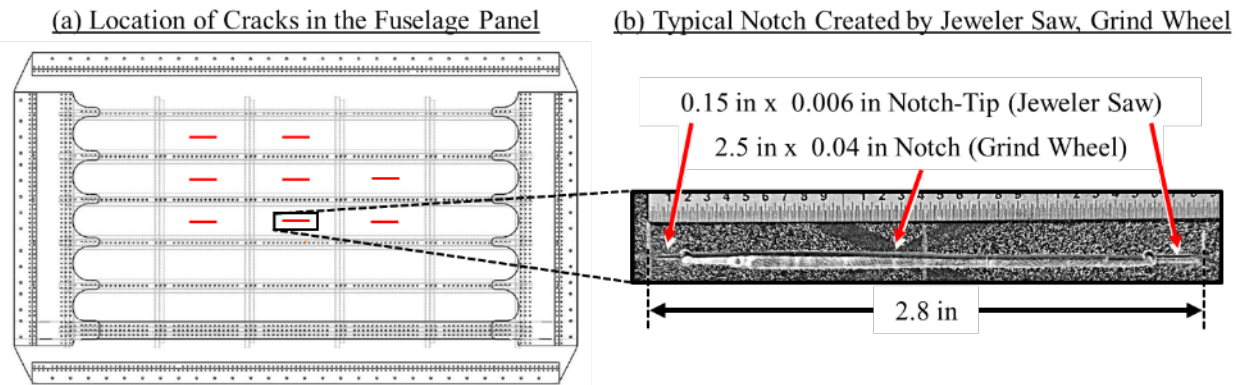


Figure 9. (a) Location of cracks with respect to the fuselage panel and (b) a typical notch

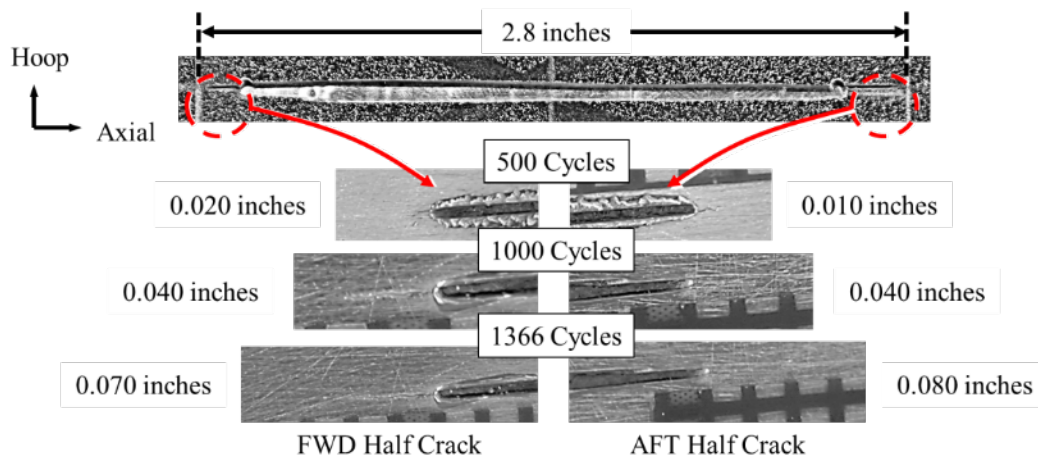


Figure 10. Typical development of a naturally sharp crack during fatigue pre-cracking

Crack lengths determined through visual inspection of the fuselage panel following the completion of the pre-cracking phase are provided in table 1. In general, FWD and AFT half crack lengths were approximately equal for each instance of damage. The average half crack length was approximately 1.49 inches, whereas the average total crack length was approximately 2.97 inches.

Table 1. Summary of visual crack length measurements obtained after pre-cracking

Repair Patch Designation	FWD Half Crack Length (in)	AFT Half Crack Length (in)	Total Crack Length (in)
RAC	1.50	1.49	2.99
RBC	1.47	1.48	2.95
UAC	1.48	1.49	2.97
UB	1.50	1.51	3.01
UBC	1.49	1.46	2.95
UDAC	1.47	1.48	2.95
UDB	1.50	1.50	3.00
UDBC	1.50	1.48	2.98

2.5 Repair Types

Several types of adhesively bonded B/Ep and Al repair patches were considered in this study. Irrespective of the repair patch material, each repair patch discussed in this report can be classified as one of three different types: 1) Type 1 (reference); 2) Type 2 (under-designed), or 3) Type 3 (partially disbonded), as summarized in table 2. In general, these three repair patch types were identical to those considered in the Panel 2 test conducted under ambient conditions [3], and the Panel 3 test conducted under hot-wet conditions (165°F and 85% humidity) [4]. Each configuration was retained to compare the results with those of prior panel tests. The location of the repair patches in the conditioned region of Panel 4 is shown in figure 11.

Table 2. Overview of repair types

Repair Types	Designation	Description
Type 1: Reference	RAC	Reference A1 repair patch installed at the onset of the test.
	RBC	Reference B/Ep repair patch installed at the onset of the test.
Type 2: Under-Designed	UAC	Under-designed A1 repair patch installed at the onset of the test.
	UB	Under-designed B/Ep repair patch installed after 40,000 cycles.
	UBC	Under-designed B/Ep repair patch installed at the onset of the test.
Type 3: Partially Disbonded	UDAC	Partially disbonded A1 repair patch installed at the onset of the test.
	UDB	Partially disbonded B/Ep repair patch installed after 40,000 cycles.
	UDBC	Partially disbonded B/Ep repair patch installed at the onset of the test.

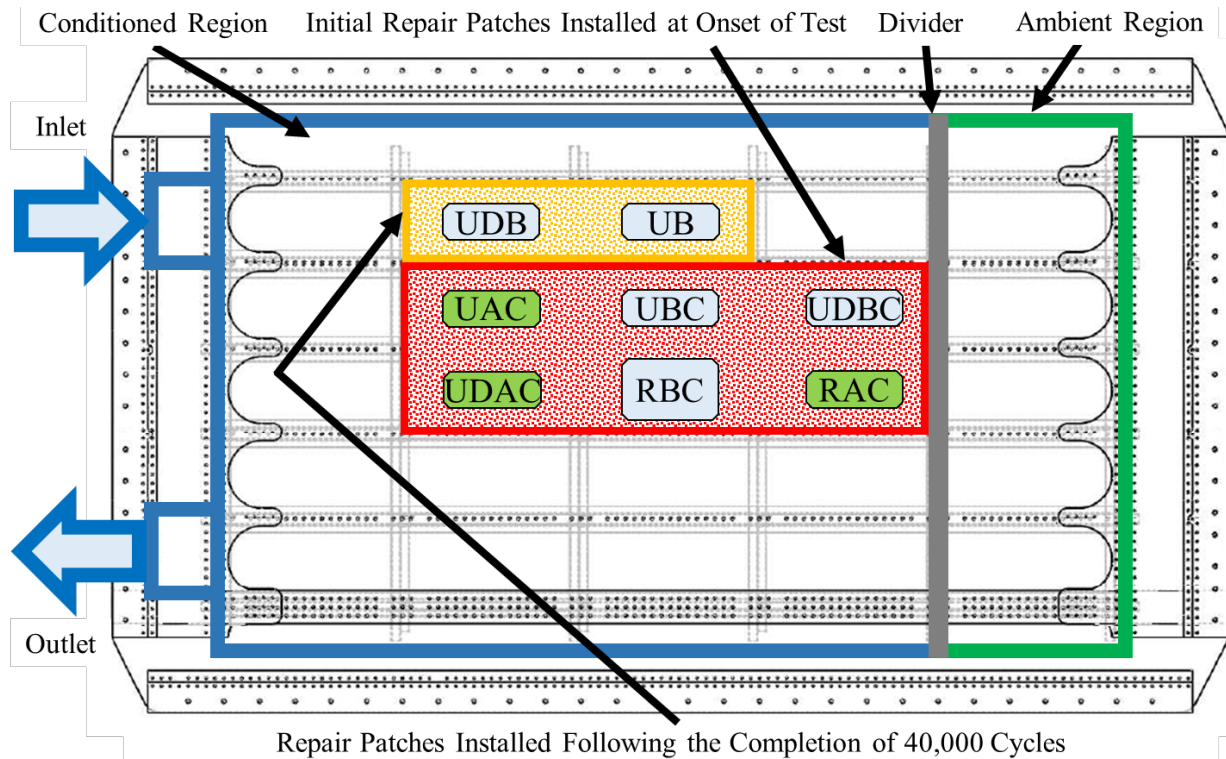


Figure 11. Location and designation of bonded repair patches

Before each repair patch installation, the external fuselage panel surface area to which the repair patch was to be installed was stripped of all paint and adhesive residues, solvent cleaned, deoxidized with a grit blaster, and coated with 3M™ Surface Pre-Treatment AC-130. A detailed overview of the repair patch installation procedure is provided in appendix B. Descriptions of each adhesively bonded repair patch layout are provided in the subsequent sections.

2.5.1 Type-1 Repair Patches

The reference repair patches, designed to contain damage and withstand SSL conditions up to one DSG of a B727, and including a 9-ply B/Ep repair patch and a three-layer Al repair patch. A description of each Type-1 repair patch is provided in the subsequent sections.

2.5.1.1 Reference B/Ep

The reference B/Ep repair patch studied during this test consisted of a thin layer of bonding primer, one layer of Henkel EA 9696 Epoxy Film Adhesive, and nine octagon-shaped layers of 5521 B/Ep prepreg tape (see figure 12). All nine layers of the 5521 B/Ep prepreg tape were precured together on a flat surface before being installed on the fuselage panel. Each layer featured a fiber direction of $+20^\circ$, 0° , or -20° , where 0° is perpendicular to the crack. Fiber directions were 20° , -20° , 20° , -20° , 0° , -20° , 20° , -20° , and 20° for the bottommost layer to the topmost layer, respectively. Following repair patch installation, all eight sides of the repair patch featured a taper ratio of 20:1, transitioning from the bottommost layer, which was 5 inches wide and 8 inches long, to the topmost layer, which was 3 inches wide and 6 inches long.

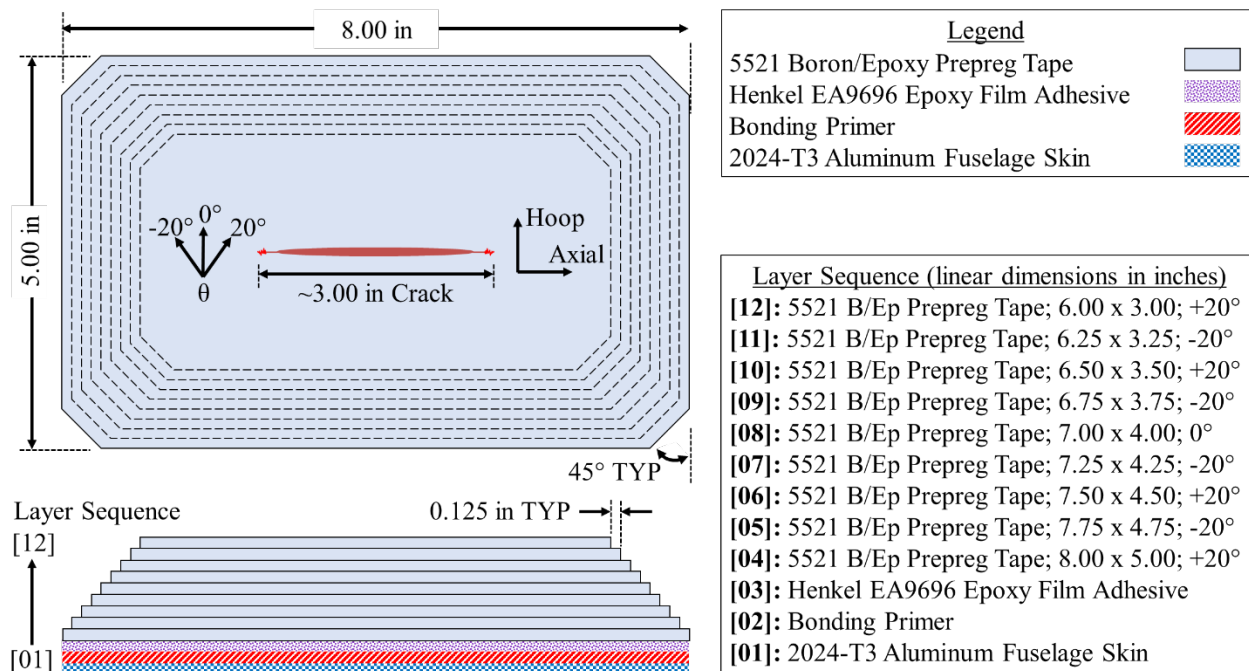


Figure 12. Overview of the reference B/Ep repair patch

2.5.1.2 Reference Al

The reference Al repair patch studied during this test consisted of a thin layer of bonding primer, three layers of Henkel EA9696 Epoxy Film Adhesive, and three octagon-shaped layers of 2024-T3 Al sheet (see figure 13). All three layers of the 2024-T3 Al sheet were cured while the layer sequence was being installed on the fuselage panel. Following repair patch installation, all eight sides of the repair patch featured a taper ratio of 20:1, transitioning from the bottommost layer, which was 3 inches wide and 8 inches long, to the topmost layer, which was 1.4 inches wide and 6.4 inches long.

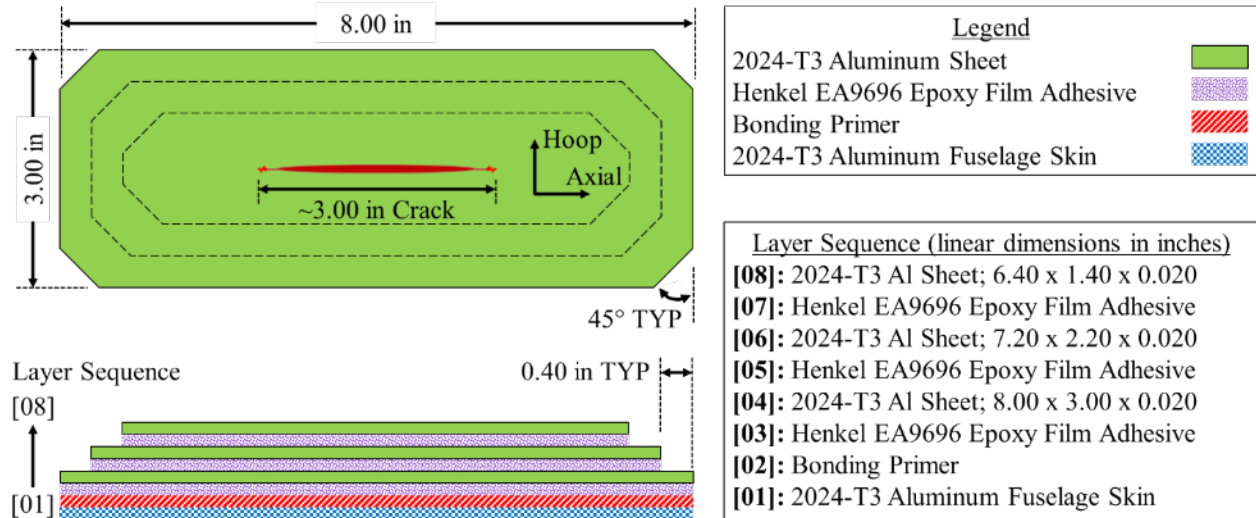


Figure 13. Overview of the reference Al repair patch

2.5.2 Type-2 Repair Patches

The under-designed repair patches, intentionally under-designed for the purpose of encouraging damage growth during fatigue loading, included two 5-ply B/Ep repair patches and a two-layer Al repair patch. The B/Ep repair patches were under-designed by reducing the number of reinforcing B/Ep plies and by reducing the footprint in the hoop direction, whereas the Al repair patches were under-designed by simply reducing the number of Al doublers. A description of each Type-2 repair patch is provided in the subsequent sections.

2.5.2.1 Under-Designed B/Ep

The under-designed B/Ep repair patch studied during this test consisted of a thin layer of bonding primer, one layer of Henkel EA9696 Epoxy Film Adhesive, and five octagon-shaped layers of 5521 B/Ep prepreg tape (see figure 14). All five layers of the 5521 B/Ep prepreg tape were precured together on a flat surface before being installed on the fuselage panel. Each layer featured a fiber direction of +20°, 0°, or -20°, where 0° is perpendicular to the crack. Fiber directions were 20°, -20°, 0°, -20°, and 20 for the bottommost layer to the topmost layer, respectively. Following repair patch installation, all eight sides of the repair patch featured a taper ratio of 20:1, transitioning from the bottommost layer, which was 3 inches wide and 8 inches long, to the topmost layer, which was 2 inches wide and 7 inches long.

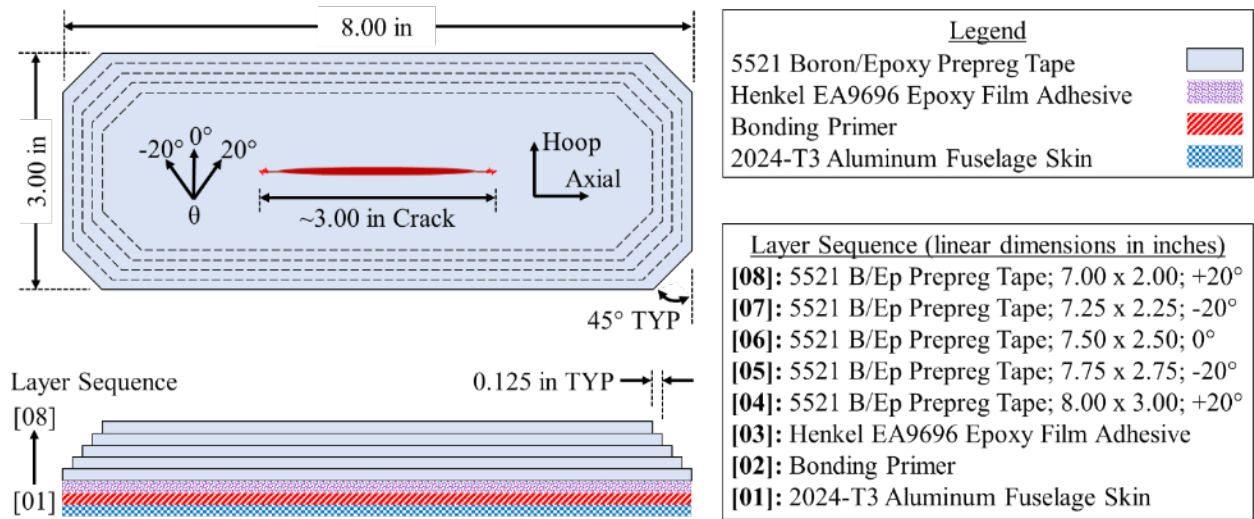


Figure 14. Overview of the under-designed B/Ep repair patch

2.5.2.2 Under-Designed Al

The Type-2 under-designed Al repair patch studied during this test consisted of a thin layer of bonding primer, two layers of Henkel EA9696 Epoxy Film Adhesive, and two octagon-shaped layers of 2024-T3 Al sheet (see figure 15). Both layers of the 2024-T3 Al sheet were cured while the layer sequence was being installed on the fuselage panel. Following repair patch installation, all eight sides of the repair patch featured a taper ratio of 20:1, transitioning from the bottommost layer, which was 3 inches wide and 8 inches long, to the topmost layer, which was 2.2 inches wide and 7.2 inches long.

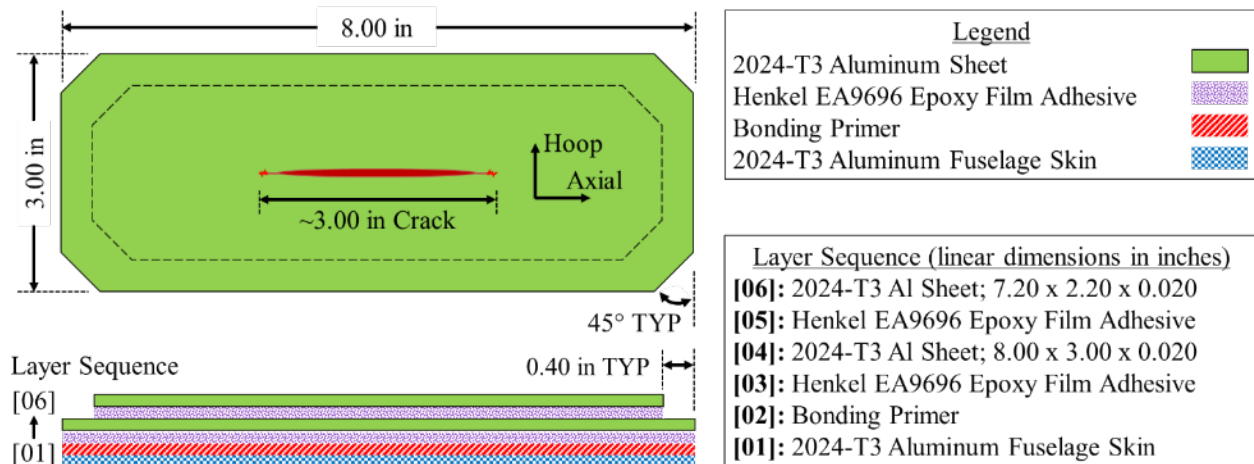


Figure 15. Overview of the under-designed Al repair patch

2.5.3 Type-3 Repair Patches

The partially disbanded repair patches, under-designed similar to the Type-2 repair patches and made further deficient through the inclusion of engineered disbonds, included two five-ply B/Ep repair patches and a two-layer Al repair patch. Each repair patch featured disbonds under the

central footprint of the repair patches and several disbonds along the footprint edges. Disbonds under the central footprint were created using fluorinated ethylene propylene (FEP) tabs, whereas disbonds along the footprint edges were created using Al shims coated with a mold release agent. In general, the diameters of the circular flaws were chosen such that they are representative of the minimum delamination flaw size detectable using NDI such as resonance ultrasonic. A description of each Type-3 repair patch is provided in the subsequent sections.

2.5.3.1 Partially Disbonded B/Ep

The partially disbonded B/Ep repair patch studied during this test consisted of a thin layer of bonding primer, one layer of Henkel EA9696 Epoxy Film Adhesive, two 0.5-inch diameter FEP inserts, and five octagon-shaped layers of 5521 B/Ep prepreg tape (see figure 16). All five layers of the 5521 B/Ep prepreg tape were precured together on a flat surface before being installed on the fuselage panel. Each layer featured a fiber direction of $+20^\circ$, 0° , or -20° , where 0° is perpendicular to the crack. Fiber directions were 20° , -20° , 0° , -20° , and 20° for the bottommost layer to the topmost layer, respectively.

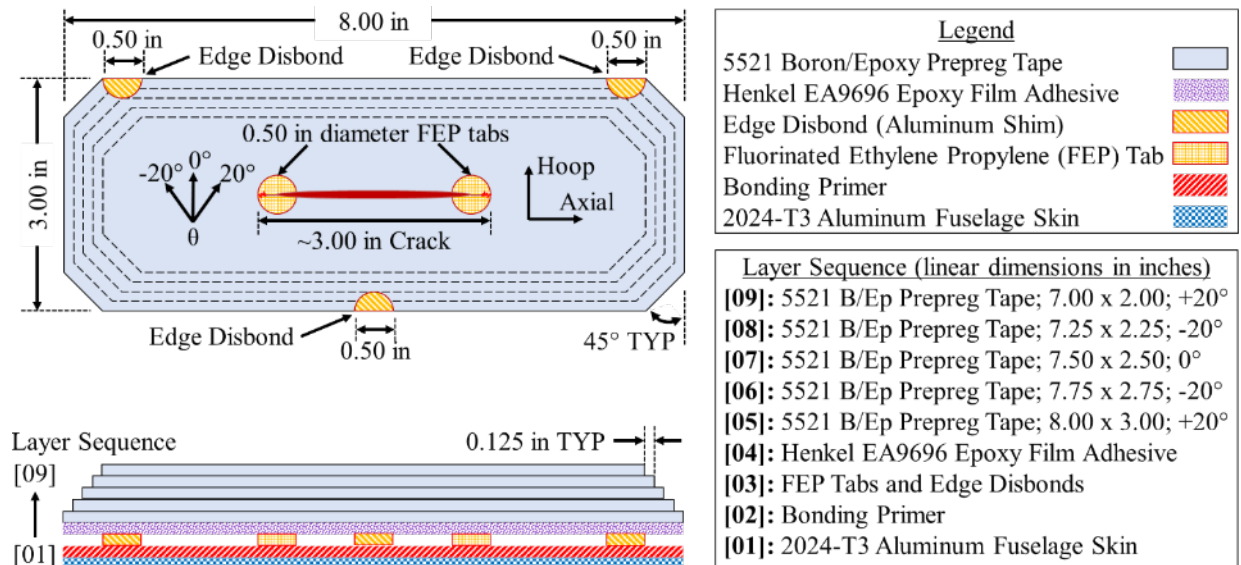


Figure 16. Overview of the partially disbonded B/Ep repair patch

During repair patch installation, the two 0.5-inch diameter FEP tabs were inserted between the adhesive and the fuselage panel surface and positioned such that the center of each tab was directly over each notch tip (see figure 16). Similarly, three Al shims coated in a mold release agent were inserted between the adhesive and the fuselage panel surface and positioned such that the shape of the shim beneath the repair patch was a 0.5-inch diameter semi-circle (see figure 16). When the repair patch installation process was complete, the Al shims were removed from underneath the repair patch, whereas the FEP tabs remained in place (the former were accessible, but the latter were not). All eight sides of the repair patch featured a taper ratio of 20:1, transitioning from the bottommost layer, which was 3 inches wide and 8 inches long, to the topmost layer, which was 2 inches wide and 7 inches long.

2.5.3.2 Partially Disbonded Al

The partially disbonded Al repair patch studied during this test consisted of a thin layer of bonding primer, two layers of Henkel EA9696 Epoxy Film Adhesive, one 3.5-inch-by-0.5-inch FEP insert, and two octagon-shaped layers of 2024-T3 Al sheet (see figure 17). Both layers of the 2024-T3 Al sheet were cured while the layer sequence was being installed on the fuselage panel. During repair patch installation, the 3.5-inch-by-0.5-inch FEP tab was inserted between the adhesive and the fuselage panel surface and positioned such that the tab was directly over the center of the crack (see figure 17). Similarly, three Al shims coated in a mold release agent were inserted between the adhesive and the fuselage panel surface and positioned such that the shape of the shim beneath each patch was a 0.5-inch diameter semi-circle (see figure 17). When the repair patch installation process was complete, the Al shims were removed from underneath the repair patch, whereas the FEP tabs remained in place (the former were accessible, but the latter were not). All eight sides of the repair patch featured a taper ratio of 20:1, transitioning from the bottommost layer, which was 3 inches wide and 8 inches long, to the topmost layer, which was 2.2 inches wide and 7.2 inches long.

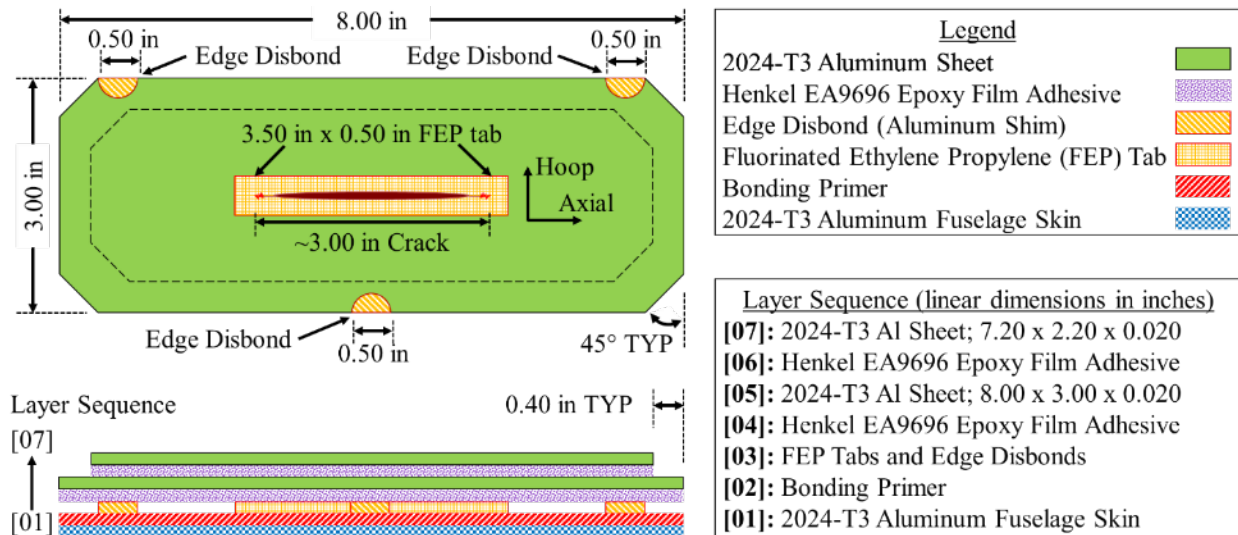


Figure 17. Overview of the partially disbonded Al repair patch

2.6 Applied Loads and Test Matrix

A summary of applied loads is provided in table 3. The loads used for the fatigue test simulated the SL conditions, including cabin pressurization (8.9 psi) and fuselage vertical bending, and were represented by an equivalent constant-amplitude spectrum. The magnitude of the applied loads used in the strain survey and fatigue pre-cracking to insert the initial damage was 75% of the SL conditions used for the fatigue test. For the baseline strain survey tests, quasistatic loadings were applied in 10 increments up to the maximum loads. For the pre-cracking and fatigue test, constant-amplitude loading was applied at a frequency of 0.033 Hz (resulting in two pressurization cycles per minute) with an *R* ratio (minimum to maximum load) of 0.1.

Table 3. Overview of the mechanical loads to which the fuselage panel was subjected

Test Phase	Load Type	Maximum Load			
		Pressure (psi)	Hoop (lbf)	Axial (lbf)	Frame (lbf)
Fatigue Cracking (100% SSL Conditions)	Cyclic (R = 0.1)	8.9	9520	8900	1510
Fatigue Pre-Cracking (75% SSL Conditions)	Cyclic (R = 0.1)	6.7	7140	6675	1133
Strain Survey (75% SSL Conditions)	Quasistatic	6.7	7140	6675	1133

SSL = Simulated service load

In addition to the mechanical loading, the fuselage panel was also subjected to environmental conditions throughout the duration of the test. Environmental conditions included ambient (80°F and 60% RH), cold-dry (-25°F), and hot-wet (165°F and 85% RH). Immediately following the installation of repair patches RAC, RBC, UAC, UBC, UDAC, and UDBC, the fuselage panel was subjected to 4 weeks of hot-wet conditioning (without mechanical load). Following the completion of this pre-conditioning period, extended fatigue testing was conducted in a cold-dry environment. Quasistatic strain surveys conducted during the first 40,000 cycles were conducted in cold-dry, ambient, and hot-wet environments, whereas quasistatic strain surveys conducted during the final 52,834 cycles were only conducted in cold-dry and ambient environments. A summary of the environmental conditions considered during this test is provided in table 4.

Table 4. Overview of the environmental conditions to which the fuselage panel was subjected

Environmental Conditions	Temperature (°F)	Relative Humidity (%)
Cold-Dry	-25	-
Ambient	80	60
Hot-Wet	165	85

Repair patches were installed at various phases of testing. A summary of the environmental conditions and extended fatigue load history of each repair patch is provided in table 5 and shown in figure 8. Repair patches RAC, RBC, UAC, UBC, UDAC, and UDBC were all installed at the onset of the test; therefore, they were all subjected to 4 weeks of hot-wet conditioning, followed by 92,834 cycles in a cold-dry environment (-25°F). Repair patches UB and UDB were installed after 40,000 cycles; therefore, they were subjected to 52,834 cycles in a cold-dry environment.

Table 5. Summary of the fatigue load history of each repair patch

Repair Types	Designation	Description
Type 1: Reference	RAC	Four weeks of hot-wet conditioning, followed by 92,834 fatigue cycles in cold-dry conditions.
	RBC	Four weeks of hot-wet conditioning, followed by 92,834 fatigue cycles in cold-dry conditions.
Type 2: Under-Designed	UAC	Four weeks of hot-wet conditioning, followed by 92,834 fatigue cycles in cold-dry conditions.
	UB	52,834 cycles of fatigue loading under cold-dry environmental conditions.
	UBC	Four weeks of hot-wet conditioning, followed by 92,834 fatigue cycles in cold-dry conditions.
Type 3: Partially Disbonded	UDAC	Four weeks of hot-wet conditioning, followed by 92,834 fatigue cycles in cold-dry conditions.
	UDB	52,834 cycles of fatigue loading under cold-dry environmental conditions.
	UDBC	Four weeks of hot-wet conditioning, followed by 92,834 fatigue cycles in cold-dry conditions.

2.7 Inspection and Monitoring Methods

Various inspection and monitoring methods were used to measure the distribution of strain using strain gauges and digital image correlation (DIC), record the environmental conditions using temperature/humidity probes, and detect damage formation and growth in the vicinity of each repair patch using a variety of NDI techniques, including high-magnification cameras, eddy current, flash thermography, and resonance ultrasonic. An overview of the various inspection and monitoring methods and the inspection intervals is provided in table 6. Further details of these methods are provided in the subsequent sections.

Table 6. Overview of the frequency with which intermittent inspections were conducted

Method	Inspection Purpose	Repair Patches	Interval (Cycles)	Applied Loads	
				MECH	ENVR
DIC	Determine the continuous distribution of hoop strain	All	5,000–20,000	Strain Survey	Ambient
Flash Thermography	Detect the delamination, disbonds, general damage	B/Ep	5,000–20,000	None	Ambient
High-Frequency Eddy Current	Measure crack growth by probing ext. panel surface	All	5,000–20,000	None	Ambient
Low-Frequency Eddy Current	Measure crack growth by probing top of patches	All	5,000–20,000	None	Ambient
Resonance Ultrasonic	Detect the delamination, disbonds, general damage	All	5,000–20,000	None	Ambient
Piezoelectric-Based SHM	Collect waveforms captured by transducers	UB & UDB	10,000	None	Ambient
Strain Gauges	Determine the discrete distribution of hoop strain	All	5,000–20,000	Strain Survey	Ambient, Cold-Dry, Hot-Wet

2.7.1 Bonded Foil Strain Gauges

The fuselage panel was instrumented with over 200 strain gauges to monitor strain distribution during repair patch installation, hot-wet conditioning, and extended fatigue. Strain gauges were installed on the fuselage panel skin, frames, stringers, and in the vicinity of each repair patch. Gauges used were Vishay Precision Group (VPG) uniaxial (gauge designation CEA-13-062UW-350) and VPG rectangular rosette (gauge designation CEA-13-062UR-350).

In general, strain gauges installed throughout the test can be organized into four distinct groups: 1) those installed and monitored prior to notch cutting; 2) those installed and monitored during the 4-week period of hot-wet conditioning; 3) those installed and monitored during the first 40,000 cycles of testing; and 4) those installed and monitored during the final 52,834 cycles of testing.

Locations of strain gauges installed on external fuselage panel surface, stringers, the internal fuselage panel surface, and frames prior to notch cutting are shown in figures 18a–18d, respectively. Schematics showing the layout of strain gauges in the vicinity of each repair patch are shown in figures 19–20 for the first 40,000 and the last 52,834 cycles of extended fatigue testing, respectively. Further details of strain gauge layouts are provided in appendix C, and results are provided in appendices D, E, and F.

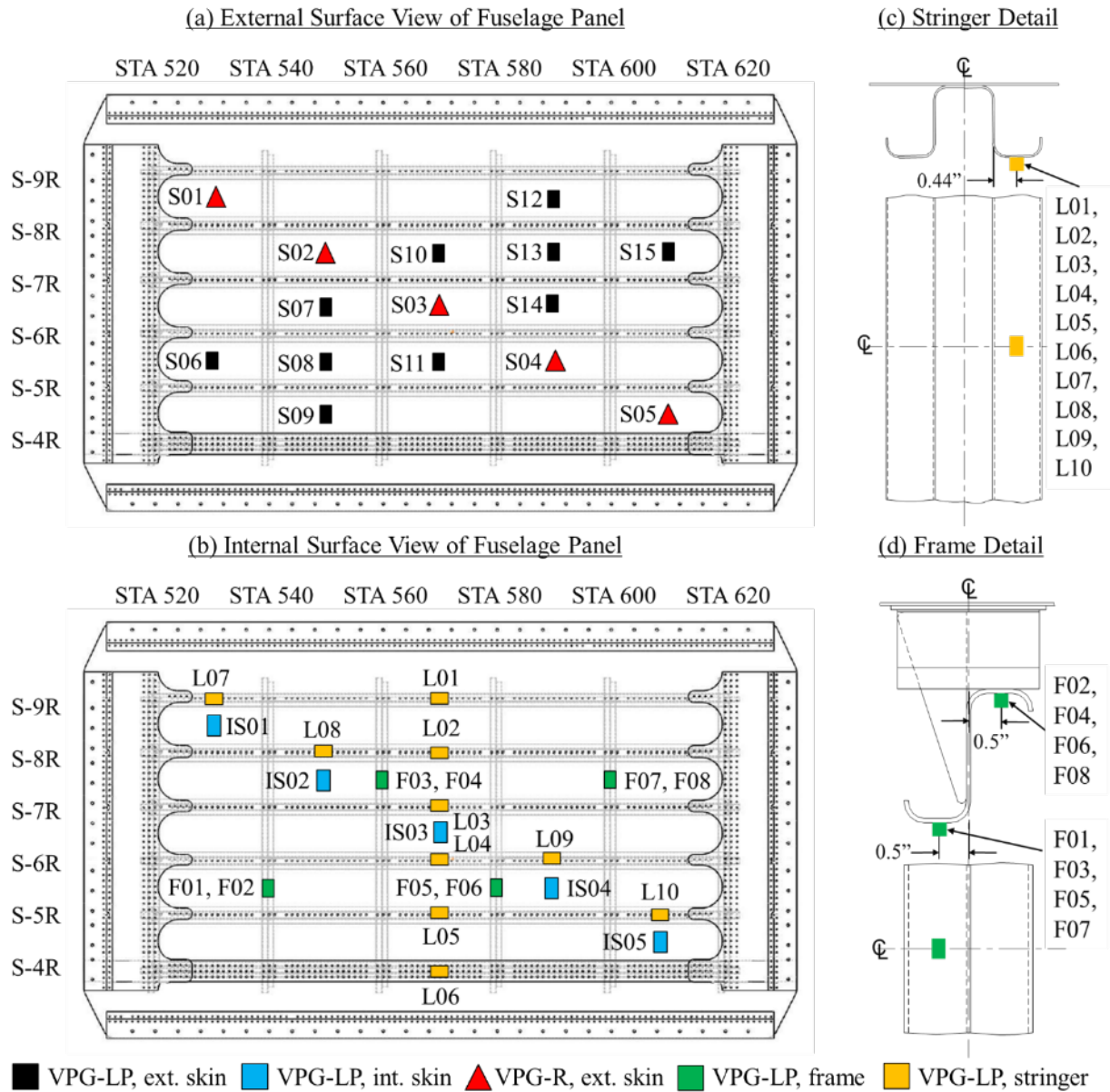


Figure 18. Strain gauges installed before cutting notches in the panel: (a) external fuselage panel surface, (b) internal fuselage panel surface, (c) stringer detail, and (d) frame detail

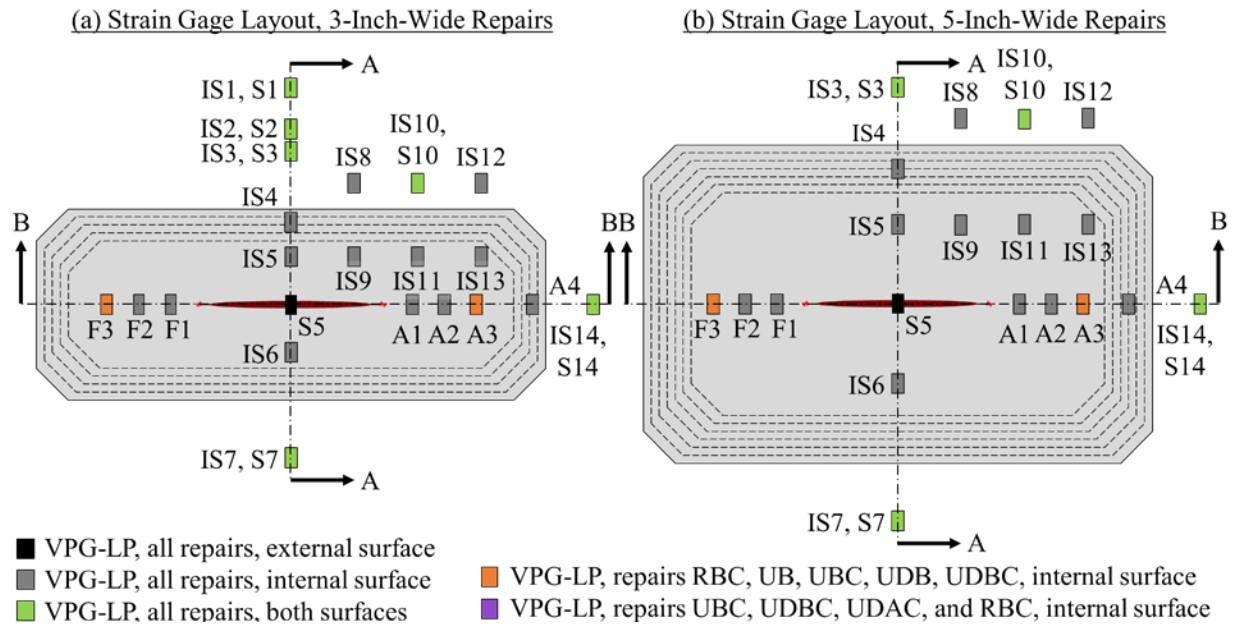


Figure 19. Layout of strain gauges during the first 40,000 cycles of testing: (a) 3-inch-wide repairs, RAC, UAC, UBC, UDBC, UDAC; and (b) 5-inch-wide repair, RBC

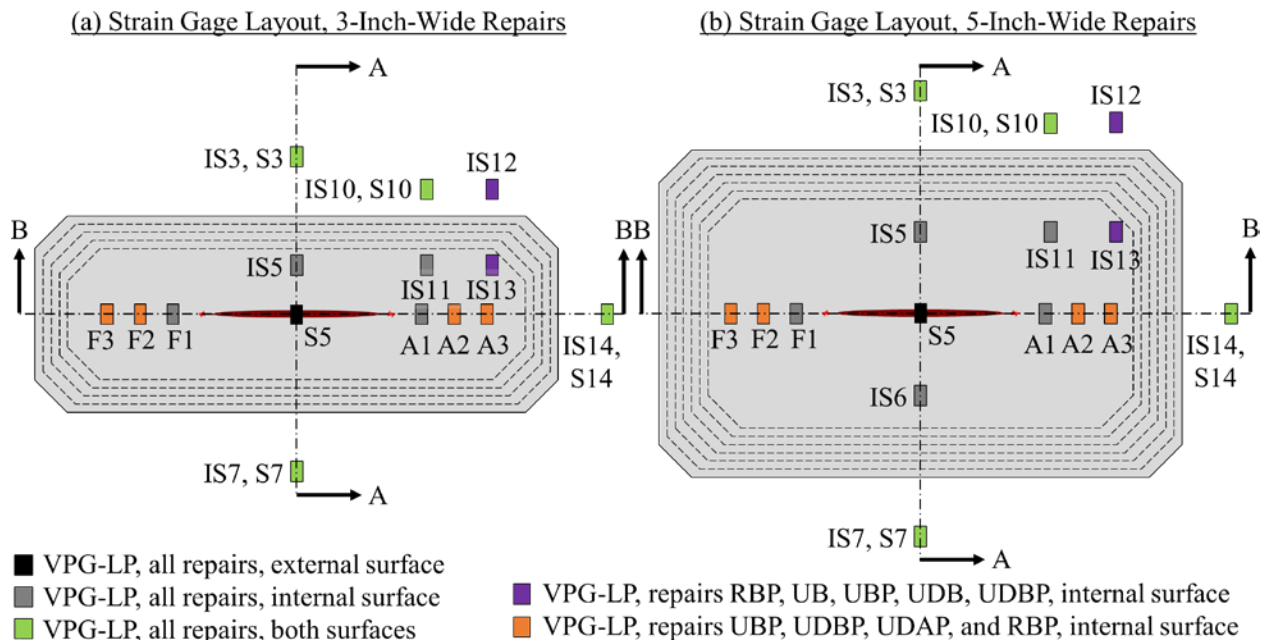


Figure 20. Layout of strain gauges during the final 52,834 SL cycles of testing: (a) 3-inch-wide repairs, RAC, UAC, UB, UBC, UDC, UDBC, UDAC; and (b) 5-inch-wide repair, RBC

2.7.2 Temperature and Humidity Sensors

The fuselage panel was instrumented with OMEGA k-type thermocouples (designation 5TC-TT-K-24-72) used to monitor temperature during repair patch installation process and ROTRONIC temperature/humidity probes (designation HC2-S) to monitor and record temperature and

humidity distributions. Figure 21 shows the location of temperature/humidity probes positioned within the environmental chamber. Probes B, C, D, and Z were positioned within the conditioned region of the environmental chamber, whereas temperature humidity probe A was positioned within the ambient region of the environmental chamber.

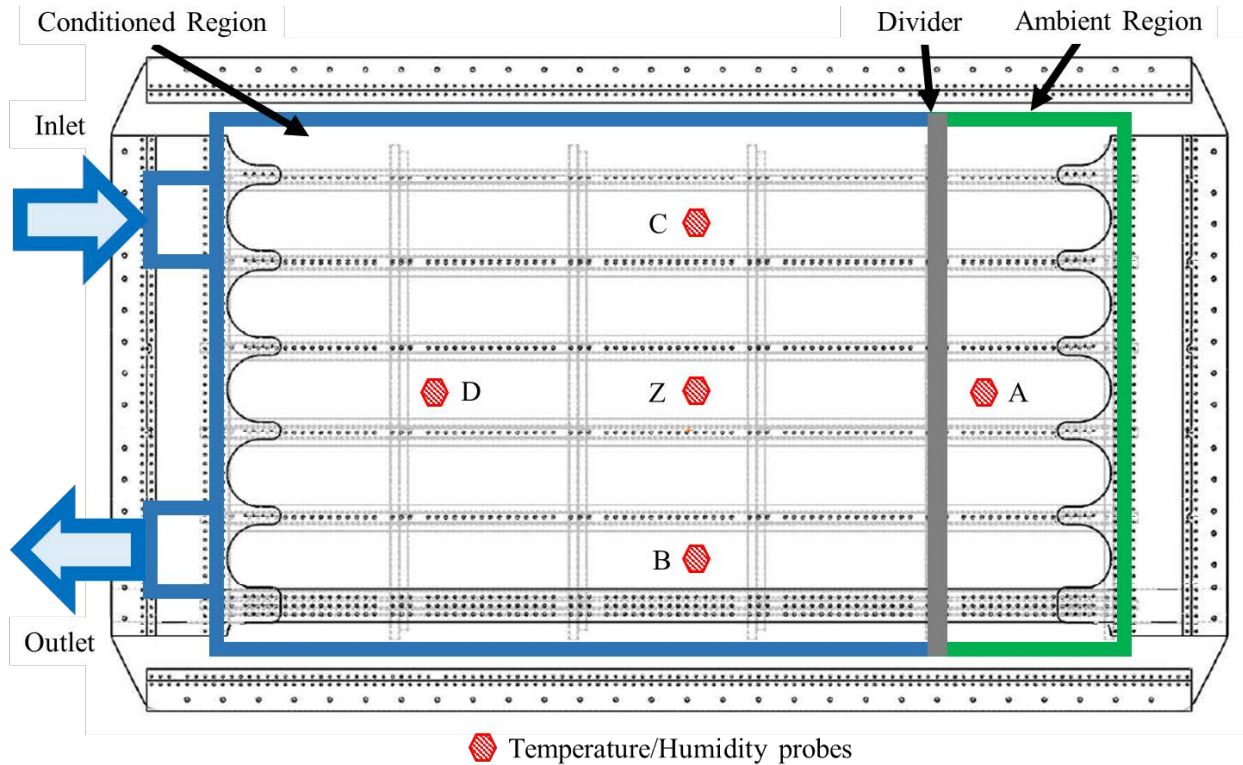
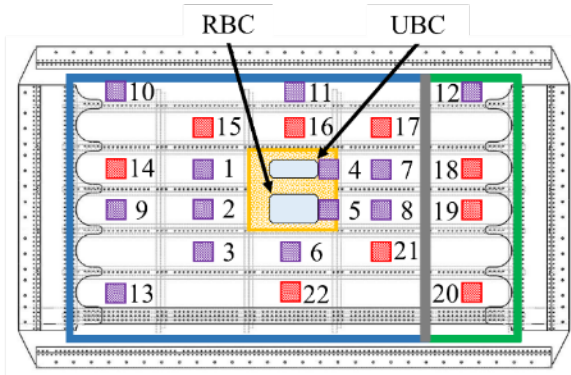


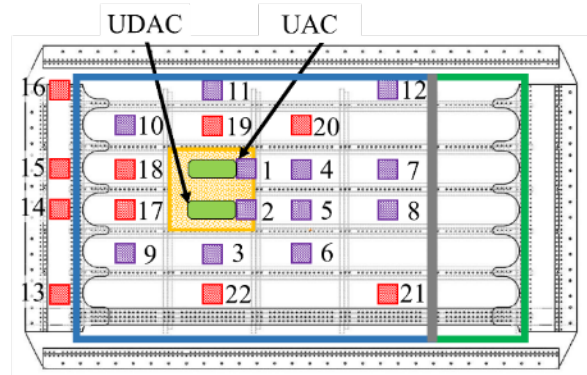
Figure 21. Location of temperature/humidity probes with respect to the panel during testing

Figure 22 shows the locations of thermocouples used to monitor temperature during patch installation. Thermocouples were positioned in an array around each repair patch during patch installation. Repair patches were installed in pairs; therefore, four schematics are provided. In general, the precise position of thermocouples varied from installation to installation.

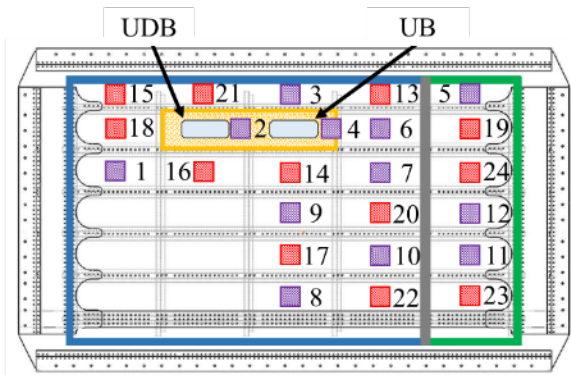
(a) Thermocouples During Installation of UBC, RBC



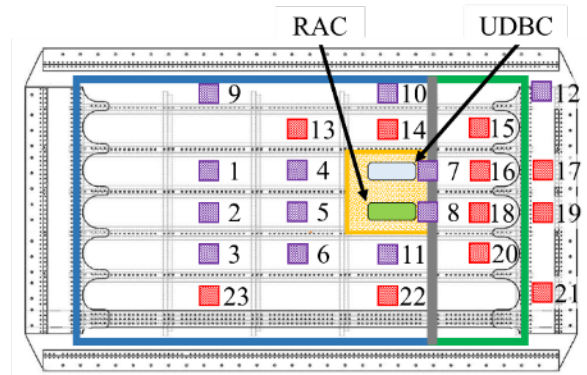
(b) Thermocouples During Installation of UAC, UDAC



(c) Thermocouples During Installation of UB, UDB



(d) Thermocouples During Installation of UDBC, RAC



Thermocouples, internal surface
 Thermocouples, external surface

Figure 22. Location of thermocouples with respect to the panel during installation of repair patches: (a) UBC and RBC, (b) UAC and UDAC, (c) UB and UDB, and (d) UDBC and RAC

2.7.3 High-Magnification Camera Systems

Two high-magnification, remote-controlled camera systems were used to monitor crack growth during this test on the outer and inner surfaces of the panel, as described in the subsequent sections.

2.7.3.1 Remote-Controlled Crack Monitoring (RCCM) System

The RCCM system consists of a mechanical frame assembly, motion-control assembly, and a video data-acquisition system. The mechanical frame assembly (see figure 23a) includes a rectangular frame mounted on top of the four columns at the corners of the test fixture and two nesting frames that provide the capability to adjust the axial and transverse positions of the attached assembly. The motion-control assembly (see figure 23b) consists of three bidirectional and two unidirectional translation stages that provide additional positioning ability and is the attachment point for four high-magnification cameras, two of which are shown in figure 23c. A video data-acquisition system provides real-time crack-length measurements, recording images and videos with frame rates of up to 30 frames per second. Because of the nature of the test, the external surface of the panel was not visible during fatigue cracking; therefore, the RCCM system was used

only during fatigue pre-cracking. A typical image captured by this system during pre-cracking is shown in figure 23d.

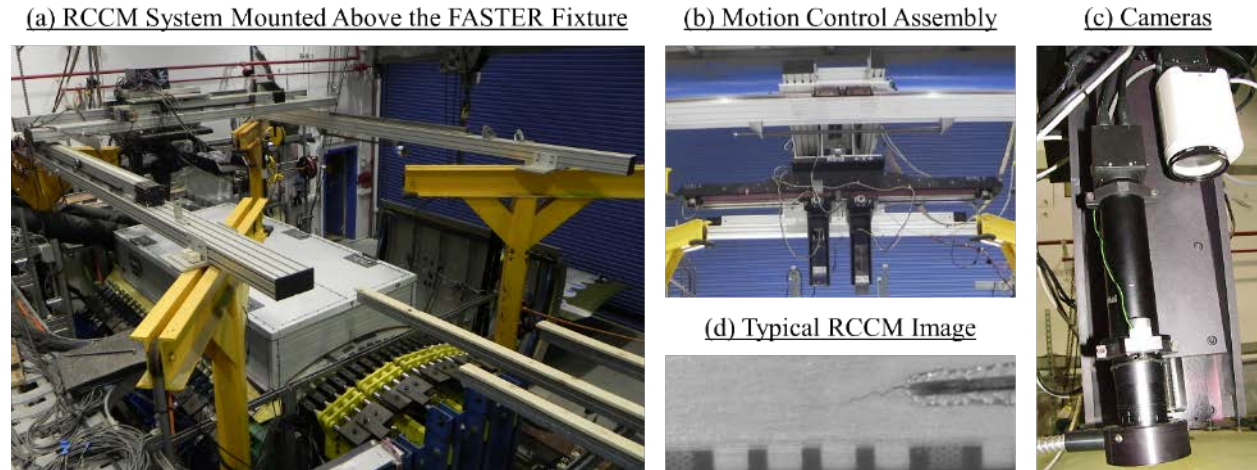


Figure 23. (a) RCCM system mounted above the FASTER fixture, (b) motion control assembly, (c) cameras, and (d) a typical image captured by the RCCM system during fatigue pre-cracking

2.7.3.2 Pressure Box Camera System

The pressure box camera system consists of a Spectrum 120™ High-Definition camera, a MicroTrac Flat Platform, a tether, and a Versatrax Rack Mount Controller. Mounted to the chassis of the MicroTrac Flat Platform, the Spectrum 120™ High-Definition camera features four high-intensity LEDs and is capable of zooming up to 432x, tilting up to 280°, and panning up to 360°. The complete system is tether-connected to a break-out box that connects to a computer monitor and the Versatrax Rack Mount Controller, both of which were located in the laboratory control room. The assembled system (see figure 24a) is rated to operate under a hydrostatic pressure of approximately 42 psi. Because of the nature of the test, only the internal surface of the panel was viewable during fatigue cracking; therefore, the pressure box camera system was the only system capable of monitoring the formation and growth of damage in the fuselage panel during fatigue cracking. A typical image captured by this system during fatigue is shown in figure 24b.

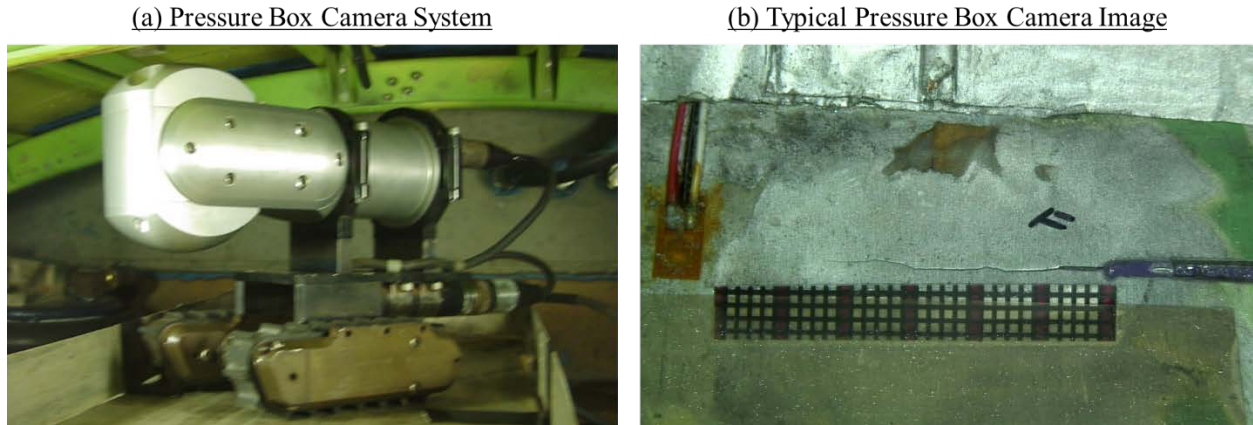
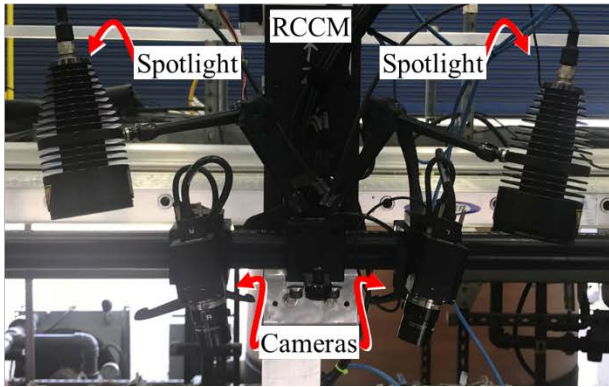


Figure 24. (a) The pressure box camera system underneath a fuselage panel, and (b) a typical image captured by the pressure box camera system during fatigue cracking

2.7.4 Three-Dimensional (3D) Digital Image Correlation (DIC)

Three-dimensional (3D) DIC is a non-contact, material-independent NDI method that uses sequential digital images of a specimen subjected to mechanical loading to measure in-plane deformation, displacement, and strain. Throughout the duration of the test, a 5M ARAMIS 3D DIC system was used to monitor strains exhibited in the vicinity of each repair patch during quasistatic strain surveys. The 5M ARAMIS 3D DIC system consisted of a sensor unit, a sensor controller, a high-performance PC system, and ARAMIS 3D DIC analysis software. The sensor unit, which featured two 5-megapixel cameras with 12-mm focal length lenses, a laser pointer, and two adjustable LED spotlights mounted on a circular support bar, was connected to the sensor controller and the high-performance PC system, both of which were located in the laboratory control room. Prior to each inspection, the ARAMIS sensor assembly was mounted on the motion control assembly of the RCCM system (see figure 25a). Similar to the high-magnification cameras mentioned in section 2.7.3.2, this connection to the motion control assembly facilitated the ability to precisely and efficiently relocate the ARAMIS sensor unit throughout the test section of the fuselage panel.

(a) ARAMIS System Mounted on the RCCM System



(b) Typical Pattern Painted on the Repair Patches

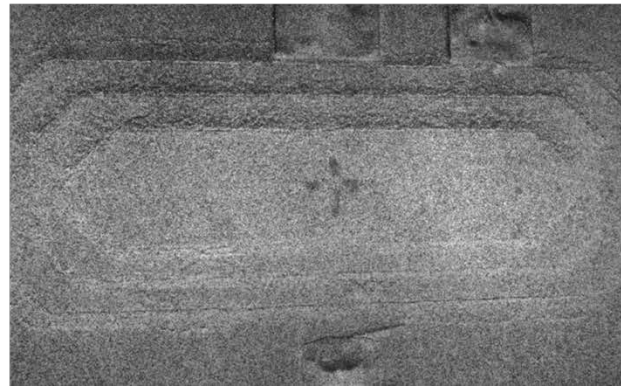


Figure 25. (a) ARAMIS 3D DIC system mounted on the motion control assembly of the RCCM system, and (b) typical stochastic pattern painted on, and in the vicinity of, each repair patch

Prior to each inspection, the top surface of each repair patch and the external fuselage panel surface in the immediate vicinity of each repair patch was coated with a dull, highly contrasted, monochromatic, stochastic pattern by sporadically spraying flat black paint over a consistent layer of flat white paint (see figure 25b). Subsequently, to ensure appropriate resolution of results, digital images of each repair patch were captured independently using two fields of view: 1) narrow field-of-view (NFOV), which was 7.87 inches by 6.69 inches; and 2) wide field-of-view (WFOV), which was 11.81 inches by 9.84 inches. For each field-of-view, a rotational inspection approach was applied in which the RCCM system was used to position the ARAMIS sensor unit directly above each repair patch. When the system was in position, the fuselage panel was subjected to the quasistatic strain survey load spectrum while the high-resolution cameras captured digital images of the repair patch at each load stage. More detailed descriptions of the system are provided in appendix G.

2.7.5 Eddy Current

Eddy current is an NDI method that utilizes measured changes in electrical impedance to detect surface and subsurface flaws (e.g., cracks) in electrically conductive specimens. Throughout the duration of the test, an Olympus Nortec[®] 500D Eddy Current Flaw Detector (P/N 7720140.00), shown in figure 26a, was used in conjunction with two detachable probes to monitor the growth of the through-thickness, center-bay cracks underneath each adhesively bonded repair patch. For high-frequency inspections of cracks on the panel surface, a PowerLink[™] Absolute Shielded Metal Detachable Pencil Probe (P/N 9403410) was used featuring a tip diameter of 0.13 inch and an operating frequency range of 50 to 500 kHz (see figure 26b). For low-frequency inspections of cracks from the top of the repairs, a PowerLink[™] Standard Bridge Detachable Surface Probe (P/N 9222161) was used featuring a tip diameter of 0.31 inch and an operating frequency range of 1–50 kHz (see figure 26c). Prior to each inspection, the system was calibrated using reference standards provided by Boeing. Further details are given in appendix H.

(a) Olympus Nortec® 500D Eddy Current Flaw Detector



(b) PowerLink™ Detachable Pencil Probe



(c) PowerLink™ Detachable Surface Probe



Figure 26. (a) Portable Eddy Current Flaw Detector, (b) PowerLink™ Absolute Shielded Metal Detachable Pencil Probe, and (c) PowerLink™ Standard Bridge Detachable Surface Probe

2.7.6 Flash Thermography

Flash thermography is an NDI method that uses measured changes in the surface temperature of a specimen subjected to a spatially uniform flash of light, captured via sequential infrared images, to detect subsurface irregularities such as delaminations and disbonds. Throughout the duration of the test, a Thermal Wave Imaging (TWI) ThermoScope® II system was used to monitor the formation and growth of areas of disbond, cracks, and general damage in the vicinity of each B/Ep repair patch from the exterior surface. The ThermoScope® II system consists of: 1) a portable high-performance PC system pre-equipped with MOSAIQ® analysis software, shown in figure 27a; and 2) an integrated illumination head with two xenon flash lamps, an infrared camera, and an LCD monitor, shown in figure 27b. Further details are provided in appendix I.

(a) TWI Portable High-Performance PC System



(b) TWI Integrated Illumination Head



Figure 27. (a) TWI ThermoScope® II high-performance PC system complete with MOSAIQ® analysis software, and (b) TWI ThermoScope® II integrated illumination head

2.7.7 Resonance Ultrasonic

Resonance Ultrasonic is an NDI method that uses measured changes in the phase and amplitude of ultrasonic waveforms induced in a specimen to detect delaminations and disbonds. An Olympus BondMaster 1000e+ instrument (P/N 7720140.00) system was used to conduct inspections on the top of each repair patch in conjunction with a S-PR-5 - 250 kHz Resonance Probe (P/N 9317795) featuring a tip diameter of 0.37 inch and Sonotech ULTRAGEL II® (P/N 25-901) couplant (see figure 28). A system description is provided in appendix J.

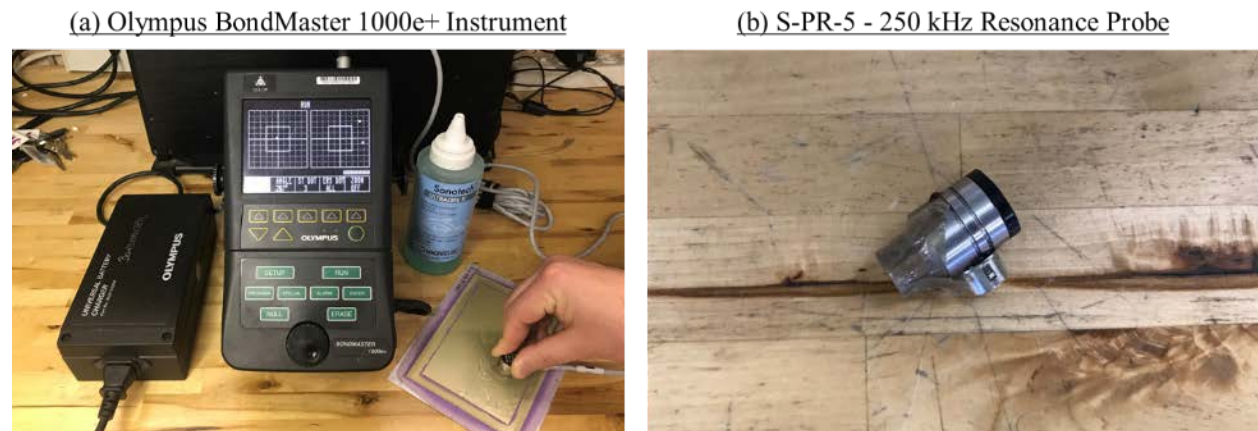


Figure 28. (a) Olympus BondMaster 1000e+, and (b) S-PR-5 - 250 kHz Resonance Probe

2.7.8 Piezoelectric-Based Structural Health Monitoring (SHM)

Piezoelectric-based SHM utilizes measured changes in the characteristics of ultrasonic waveforms induced in a specimen to detect adverse changes (e.g., the formation or growth of cracks). A Metis Design MD7 IntelliConnector™, a Boeing prototype data-acquisition device, and a network of Acellent SMART Layer Transducers (P/N SML-SP-1/4-0) were used in a pitch-and-catch approach to monitor the growth of the through-thickness, center-bay cracks underneath the Type-2 and Type-3 B/Ep repair patches, UB and UDB. The layout of sensors installed in the vicinity of each repair patch is shown in figure 29.

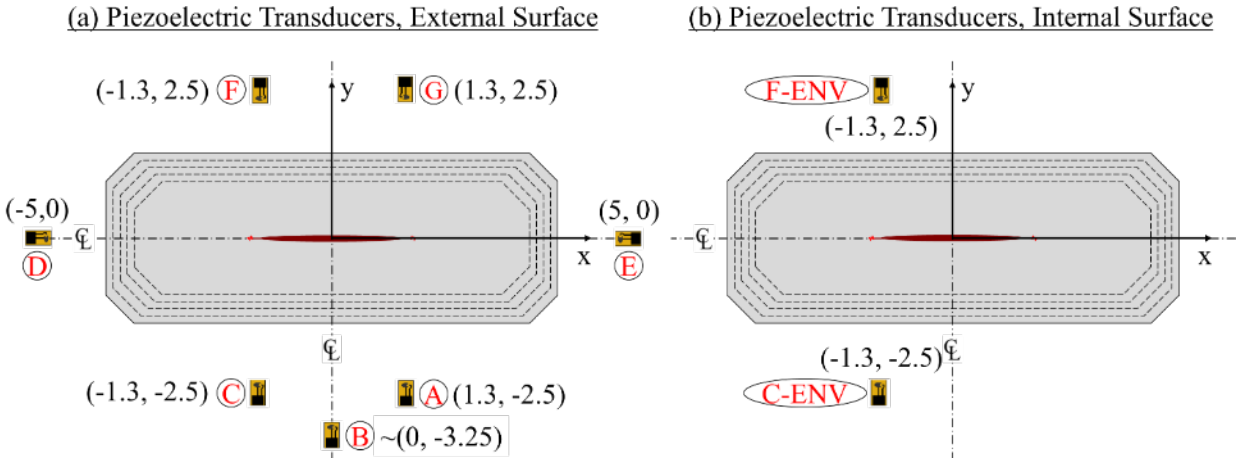


Figure 29. Position of piezoelectric transducers installed in the vicinity of repair patches UB and UDB: (a) external fuselage panel surface and (b) internal fuselage panel surface

During testing of panels 2, 3, and 4, a variety of signal characteristics were collected for each wave path and used in conjunction with other empirically obtained datasets (i.e., crack growth obtained via visual and high-frequency eddy current (HFEC) inspections) by Boeing to train a linear regression model to understand crack growth [3, 4]. Changes in the characteristics of the generated waveforms as they propagated from active to passive transducers, influenced by reflections off of irregularities (e.g., voids, inclusions, specimen boundaries) were of particular interest. An overview of SHM test conditions, algorithms, and validation approaches for the three panel tests is provided in table 7.

Table 7. Overview of SHM test conditions, algorithms, and validation approaches

	Panel 2 Test	Panel 3 Test	Panel 4 Test
Test Condition	Ambient	Hot-wet (96°F, 85-95% RH) Hot-dry (96°F, 3-8% RH) Cold-dry (-25°F)	Cold-dry (-25°F)
Algorithm/ Model Approach	Damage indices manually selected via trial and error	Optimal damage index combinations for improved damage measurement accuracy chosen via parametric analyses	Environmental compensation algorithm developed to minimize baseline variability; Advanced regression model developed to further reduce model variance and bias via cross validation
Model Validation	Models applied to repairs individually	Local model developed to blindly measure damage for repairs individually	Universal model developed to measure damage blindly for each repair and panel
Sensor Types	Only commercially available laboratory PZT sensors used	Commercial laboratory PZT sensors + Boeing prototype PZT sensors (operational in extreme environment) used	Only commercially available laboratory PZT sensors used

During this test, a blind test of the model was conducted (i.e., the local model used to detect crack growth on Panel 3 was applied to Panel 4 to calculate crack growth). To address and minimize the panel-to-panel variability on SHM system performance, a new and improved algorithm based on Lasso regression technique was also adopted to create a “global” crack correlation model that aims to further reduce variance and biased errors associated with crack-length predictions.

3. RESULTS AND DISCUSSION

Similar to previous fuselage panel tests, various inspection methods were used to monitor and assess the distribution of strain, and the formation and growth of areas of disbond, cracks, and general damage in the vicinity of each adhesively bonded repair patch. Representative results of strain surveys, fatigue crack growth, and NDI are described in the subsequent sections. Comparisons to previous fuselage panel tests are also provided where relevant.

3.1 Unexpected Occurrence of Multi-Site Damage (MSD)

MSD unexpectedly formed during fatigue cycling, resulting in the formation of a 20-inch-long crack along lap joint S-4R between stringer stations STA580 and STA600 (see figure 30). As shown in figure 30, MSD linkup is evident from the clearly visible saw tooth cracking pattern.

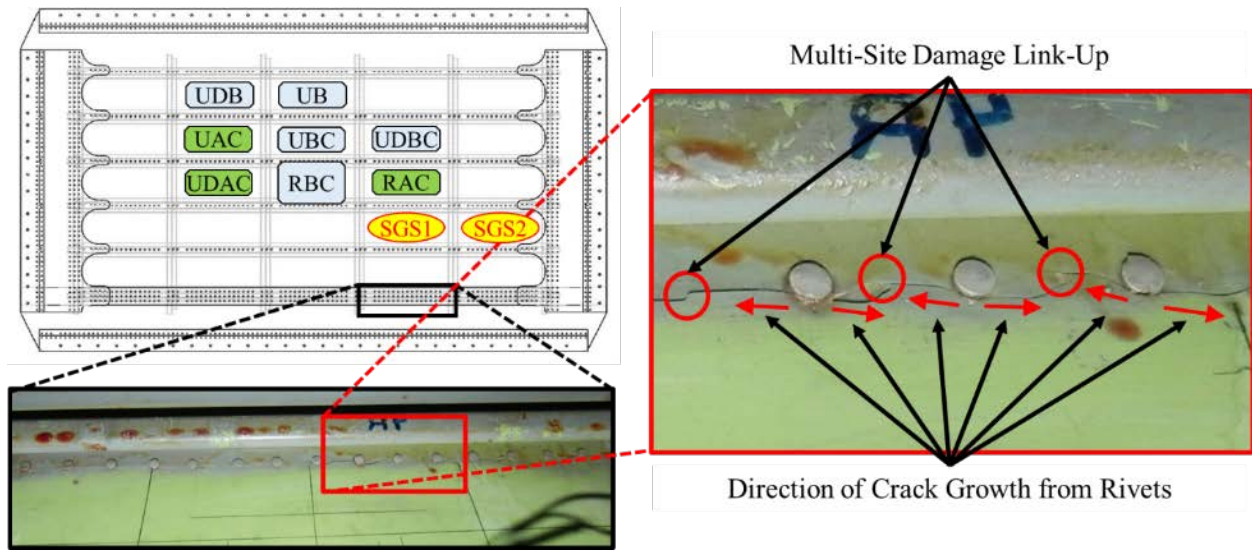


Figure 30. MSD that occurred along lap joint S-4R between stringers STA580 and STA600

The MSD linkup also impacted the strain distribution during fatigue at gauge sets SGS1 and SGS2, which were in the vicinity of the cracking. Figure 31 shows the differences between hoop strains measured by these gauges at the maximum fatigue load level and the minimum fatigue load level for every 100 cycles from 90,000 cycles to 92,800 cycles. As shown, significant load transfer was observed following the completion of approximately 91,375 cycles. The hoop strain measured by set SGS1 reduced, whereas those measured by set SGS2 increased, indicating that this was the point at which MSD linkup occurred. Because of this large strain redistribution, results can be compared only up to the last inspection, which occurred prior to MSD linkup (i.e., 90,000 cycles).

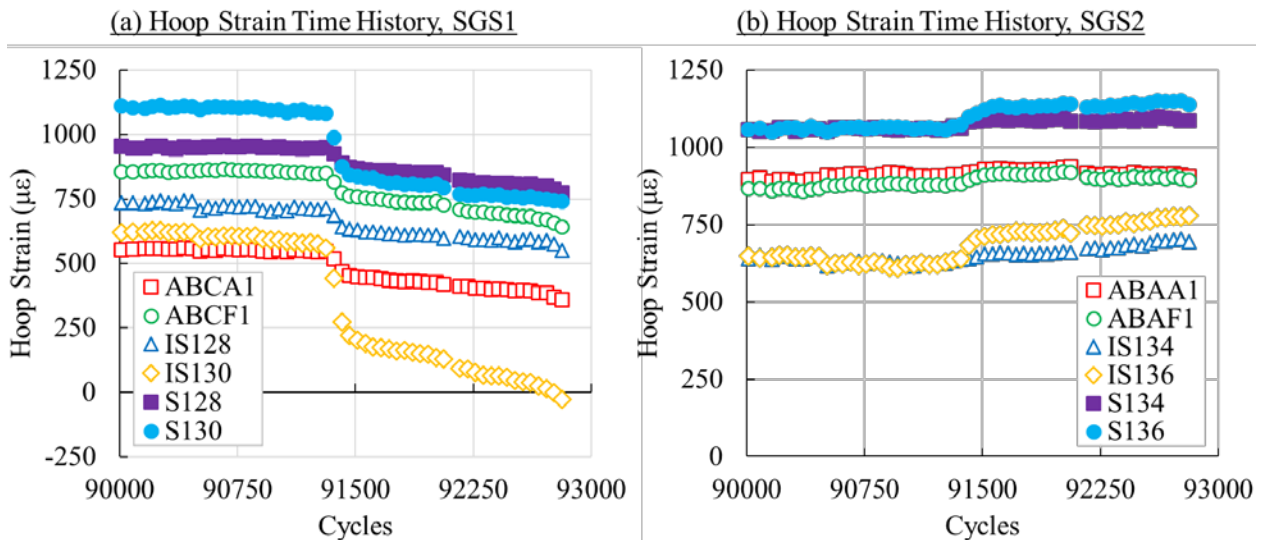


Figure 31. Hoop strain response recorded between 90,000 cycles and 92,800 cycles of testing: (a) hoop strain time history SGS1 and (b) hoop strain time history SGS2

3.2 Strain Monitoring

Throughout the duration of the test, a 3D DIC system and strain gauges installed on the fuselage panel skin, frames, stringers, and the top of each repair patch were used to monitor the distribution of strain. Subsequent sections review results obtained using these methods.

3.2.1 Thermal Residual Strain During Repair Patch Installation

For model-development purposes, heavy emphasis was placed on monitoring the development of thermal residual strains during the curing process of repair patch installation for select repair patches. Approximately 26 strain gauges and 22 thermocouples installed within the vicinity of each repair patch (see figure 19 and figure 22) were continuously monitored. During each curing process, a vacuum was applied under a temperature profile (see figure 32c). The temperature was ramped linearly from ambient environmental conditions to the cure temperature of 250°F, at which it was held constant for 90 minutes, and then decreased to ambient environmental conditions. Figure 32 shows representative results captured during this process for repair patches UDAC and UDBC. Time-dependent strain results are shown in figures 32c and 32e, whereas strains remaining after the cool-down phase (i.e., the thermal residual strains) are shown in figures 32d and 32f. Results obtained during the installation of all other repair patches are provided in appendix D.

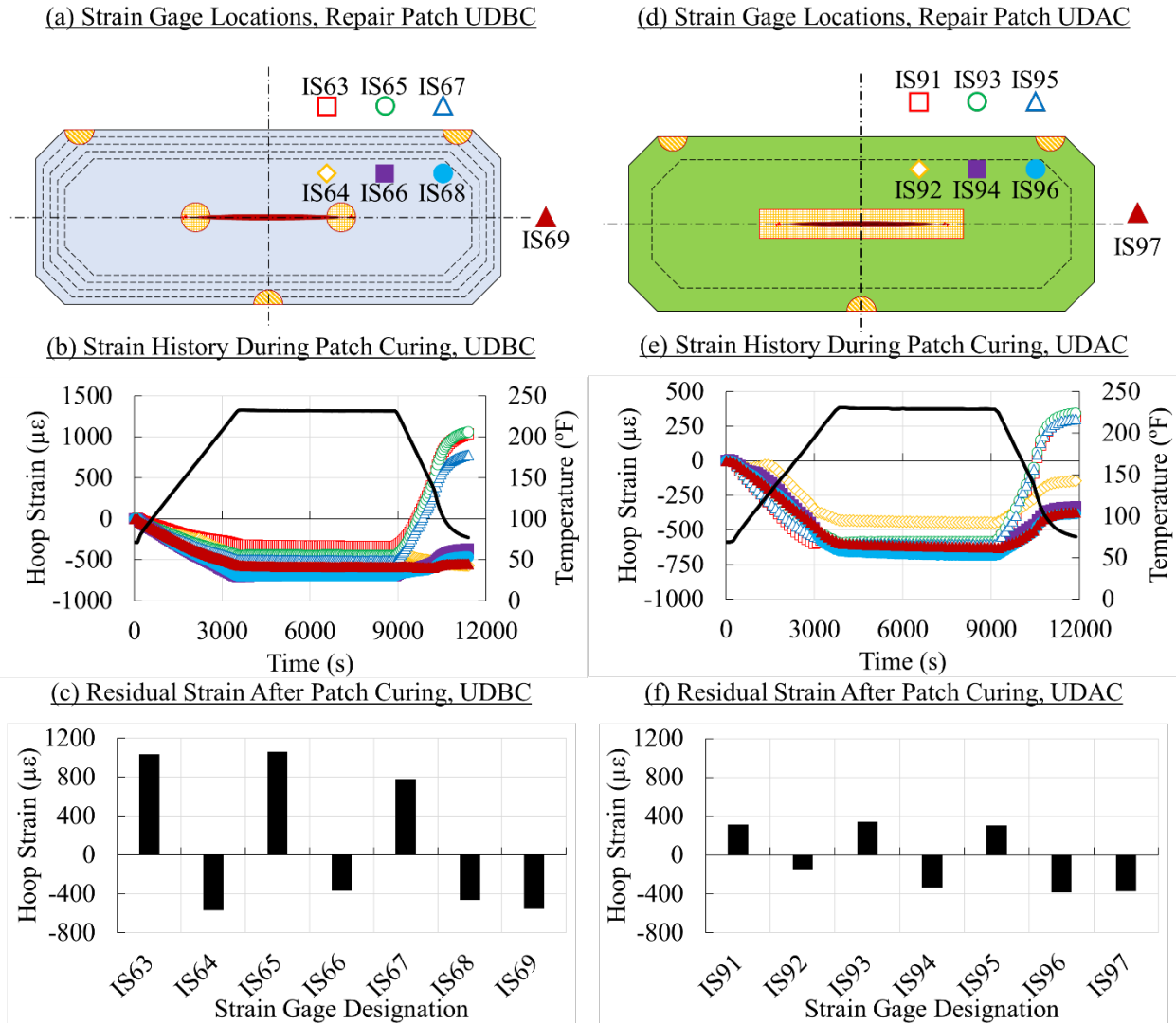


Figure 32. Thermal residual strains measured during the patch installation cure process

As shown in figure 32 for a representative B/Ep repair patch, high thermal residual strains developed within the patch footprint and surrounding areas because of mismatches between the thermal coefficient of expansion of the B/Ep repair patch and Al fuselage panel. For the Al repair patches, thermal residual strains after curing were much lower and often insignificant.

3.2.2 Thermal Residual Strain During Hot-Wet Conditioning

Heavy emphasis was also placed on monitoring the development of thermal residual strains during the 4-week period of hot-wet conditioning. Figure 33 shows representative results captured during this period for repair patches UDAC and UDBC. Time-dependent strain results are shown in figures 33c and 33e, whereas strains remaining after the cool-down phase (i.e., the thermal residual strains) are shown in figures 33d and 33f. Results obtained during the hot-wet conditioning of all other repair patches are provided in appendix E.

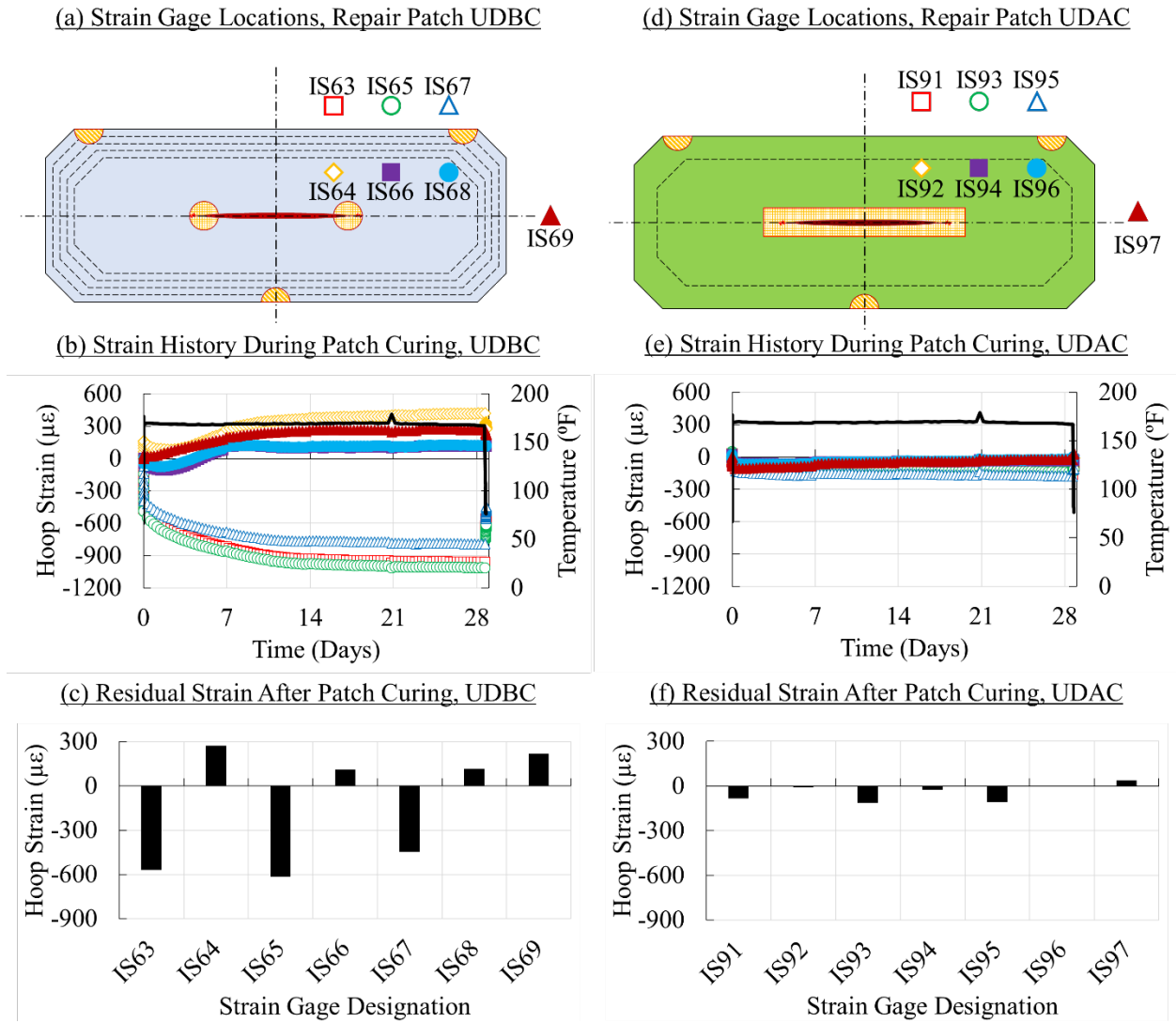


Figure 33. Thermal residual strains measured during the 4-week hot-wet conditioning period

As shown, the magnitude of residual strains after hot-wet conditioning were comparatively higher for the B/Ep repair patches than the AI repair patches. For the B/Ep repair patches, thermal-viscoelastic-plastic behavior was observed in which thermal strains relaxed because of hot-wet conditioning.

Hoop strain values measured ahead of the crack tip for repair patches UBC and UAC are shown in figure 34. As shown, the strains ahead of the UBC crack tip reduced following hot-wet conditioning, whereas strains ahead of the UAC crack tip remained relatively constant.

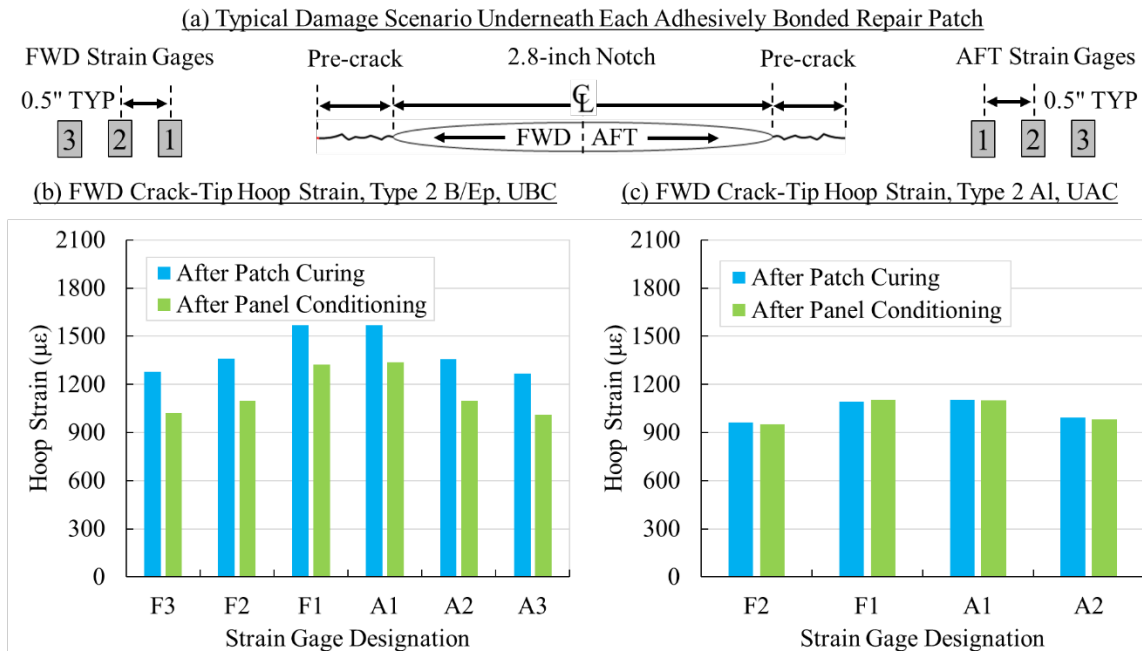


Figure 34. Comparison between hoop strains measured before and after 4 weeks of hot-wet conditioning by crack-tip strain gauges: (a) damage scenario, (b) repair patch UBC, and; (c) repair patch UAC

The mechanical strains measured under strain survey loads (75% of SL conditions) using the DIC for all three B/Ep repair types is shown in figure 35 before and after conditioning. As shown in the figure, the magnitude of strains on the outer surface of the repair patches reduced. The AI repairs were not affected by the conditioning (see figure 36). Mechanical strains measured using DIC under strain survey loads were similar before and after conditioning.

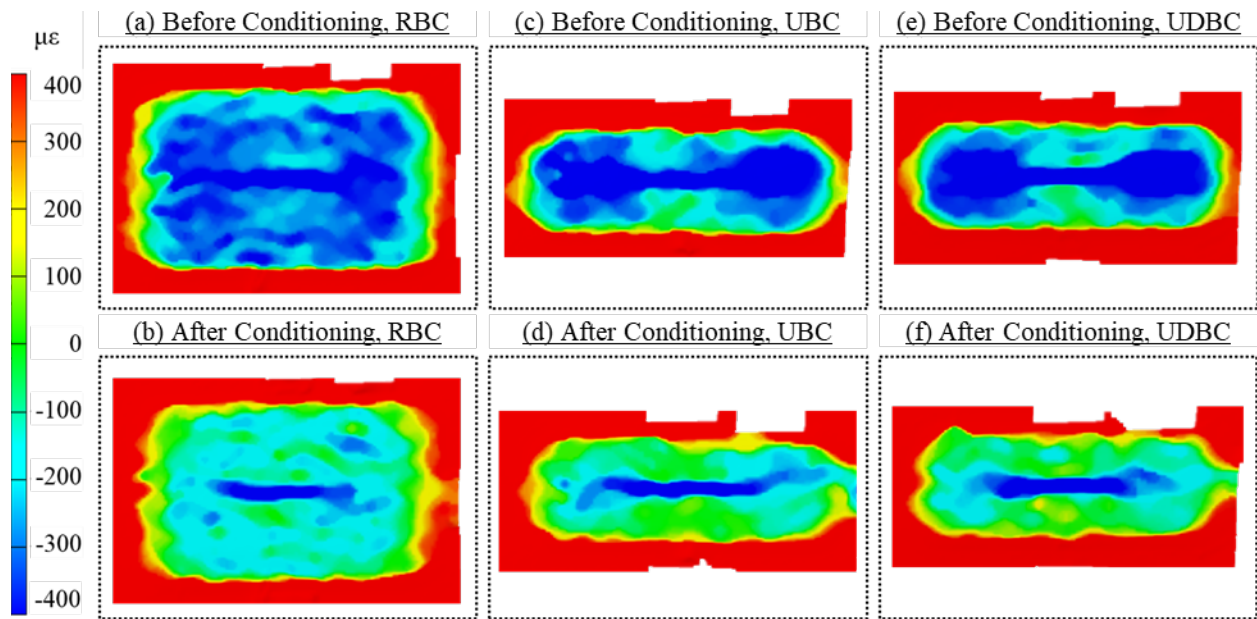


Figure 35. Comparison between hoop strains measured before and after 4 weeks of hot-wet conditioning by 3D DIC for repair patches: (a–b) RBC, (c–d) UBC, and (e–f) UDBC

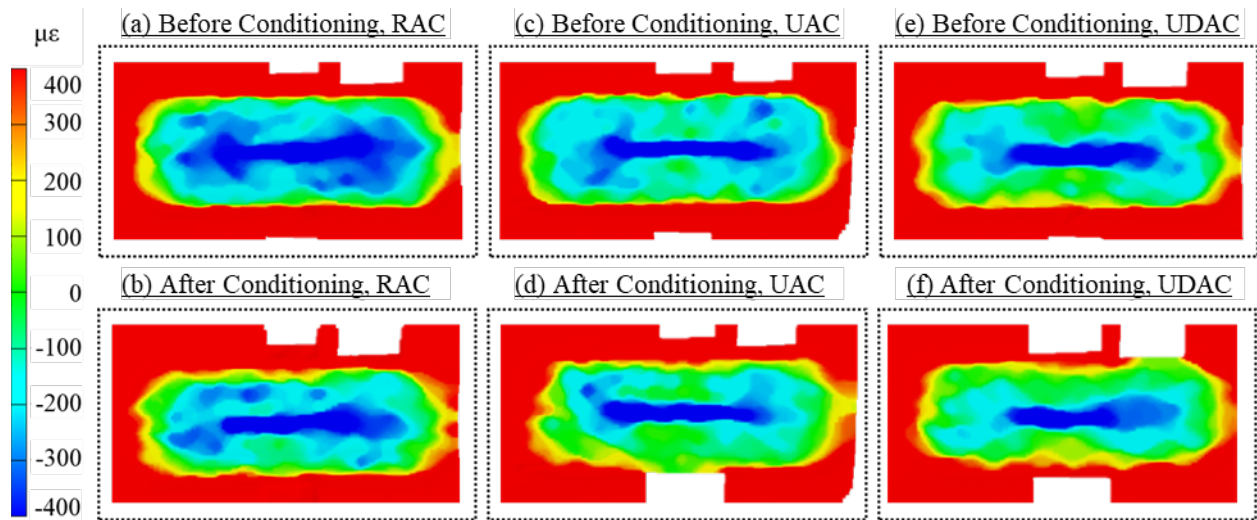


Figure 36. Comparison between hoop strains measured before and after 4 weeks of hot-wet conditioning by 3D DIC for repair patches: (a–b) RAC, (c–d) UAC, and (e–f) UDAC

3.2.3 Effect of Fatigue Loading on Mechanical Strain

Throughout the duration of the test, the fuselage panel was intermittently subjected to a quasistatic load spectrum for the purpose of monitoring the distribution of strain in the test section. During these strain surveys, which were conducted in a variety of environmental conditions, the applied loads (i.e., pressure, hoop, frame, and longitudinal loads) were incrementally increased from 0%–75% of SL conditions. Provided in the subsequent sections are representative results obtained during these surveys. More expansive representations of strain gauge and ARAMIS 3D DIC results are provided in appendices F and G, respectively.

3.2.3.1 Discrete Hoop Strain Distribution

Provided in the subsequent sections are hoop strain results captured by strain gauges installed at the top of, and in the immediate vicinity of, each adhesively bonded repair patch.

3.2.3.1.1 Under-Designed AI Repair

Representative discrete hoop strain results for repair patch UAC are shown in figure 37a. As shown, results indicate bending along the patch boundary as the outer skin surface is in a higher state of tension than that of the inner skin surface. Additionally, high compressive strains were measured on the top surface of the repair patch in the region directly above the notch centerline. A comparison of results obtained throughout the test is shown in figure 37b. Results include those obtained immediately after curing, after conditioning, after 20,000 cycles, after 40,000 cycles, after 60,000 cycles, and after 90,000 cycles. As shown, strains remained relatively constant throughout the duration of the fatigue test. For each gauge, fluctuations in hoop strain throughout the history can be attributed to the replacement of disbonded strain gauges.

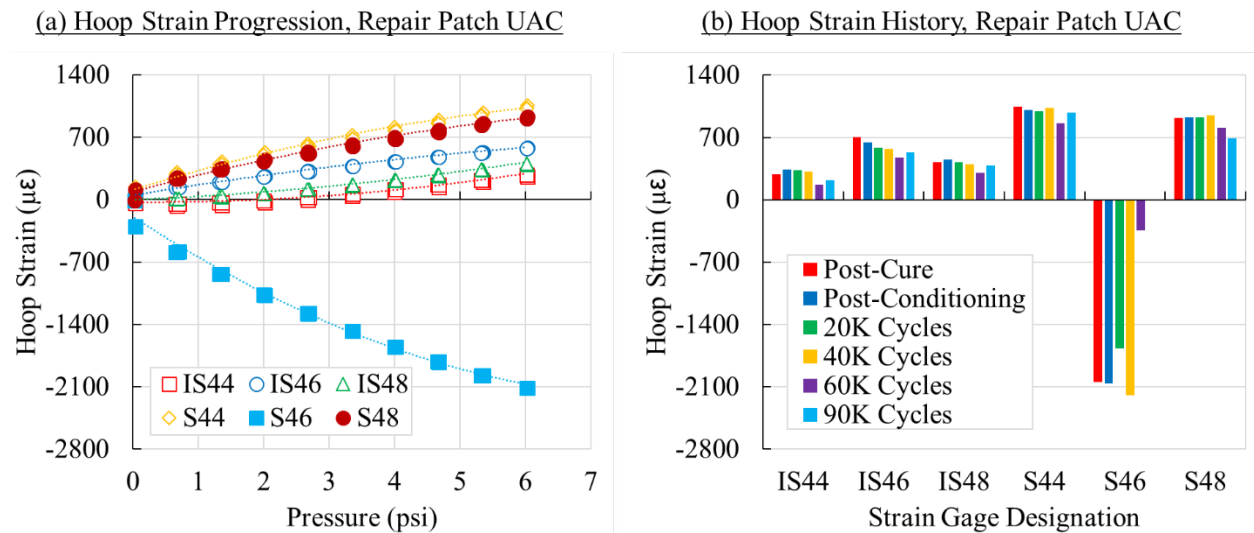


Figure 37. Hoop strain results obtained by strain gauges in the vicinity of repair patch UAC: (a) hoop strain as a result of pressure, and (b) strain history throughout the test

3.2.3.1.2 Under-Designed B/Ep Repair

Similar results for the Type-2 B/Ep patch, designated UBC, are shown in figure 38. As shown in figure 38a, there is a large amount of bending along the patch boundary as the outer skin surface is in a state of tension, whereas the inner skin surface is in a slight state of compression. Additionally, high compressive strains were measured on the top surface of the repair patch in the region directly above the notch centerline. A comparison of results obtained throughout the test is shown in figure 38b. Results include those obtained immediately after curing, after conditioning, after 20,000 cycles, after 40,000 cycles, after 60,000 cycles, and after 90,000 cycles. As shown, a reduction in strains was observed, particularly during the early stages of fatigue testing, indicating that the residual strains induced during the curing process of repair patch installation may have relaxed.

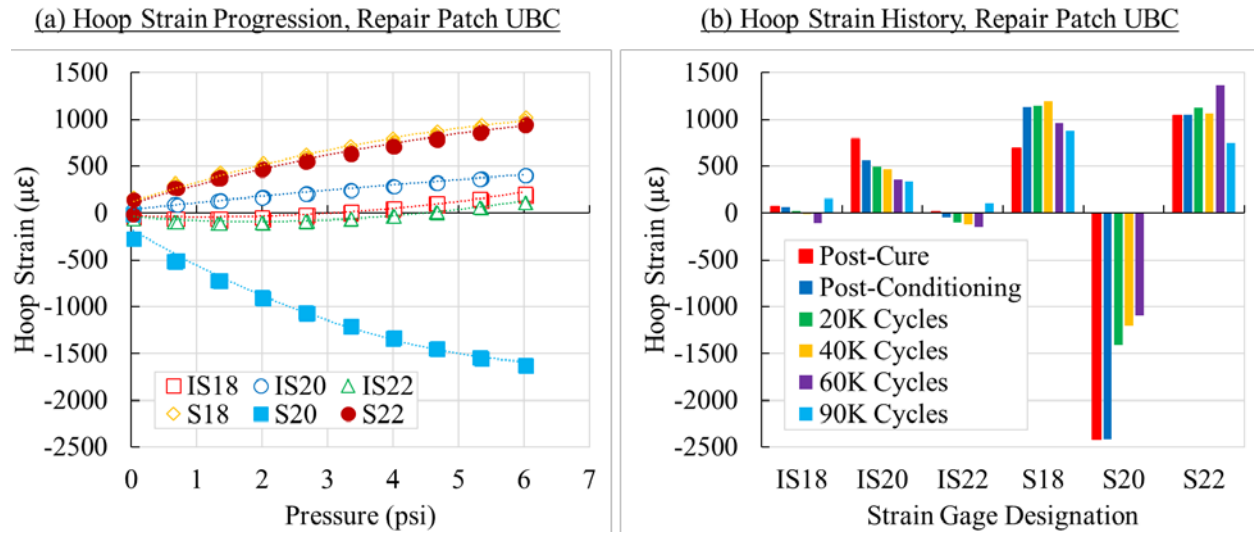


Figure 38. Hoop strain results obtained by strain gauges in the vicinity of repair patch UBC: (a) hoop strain as a result of pressure, and (b) strain history throughout the test

3.2.3.1.3 Comparison of Type-1, Type-2, and Type-3 Al Repairs

Representative results of the Type-1 (reference) Al repair patch, RAC; the Type-2 (under-designed) Al repair patch, UAC; and the Type-3 (partially disbanded) Al repair patch, UDAC, are provided in this section. Measurements by back-to-back strain gauges installed along the repair patch boundaries are shown in figure 39, whereas measurements by strain gauges installed within the central footprint are shown in figure 40. In general, bending hoop strains measured along the patch boundary were similar for all three types of Al repair patches. Differences between the strains measured by central gauges on the internal and external surfaces was greatest for repair patch UAC, followed by RAC and UDAC, which were second and third, respectively.

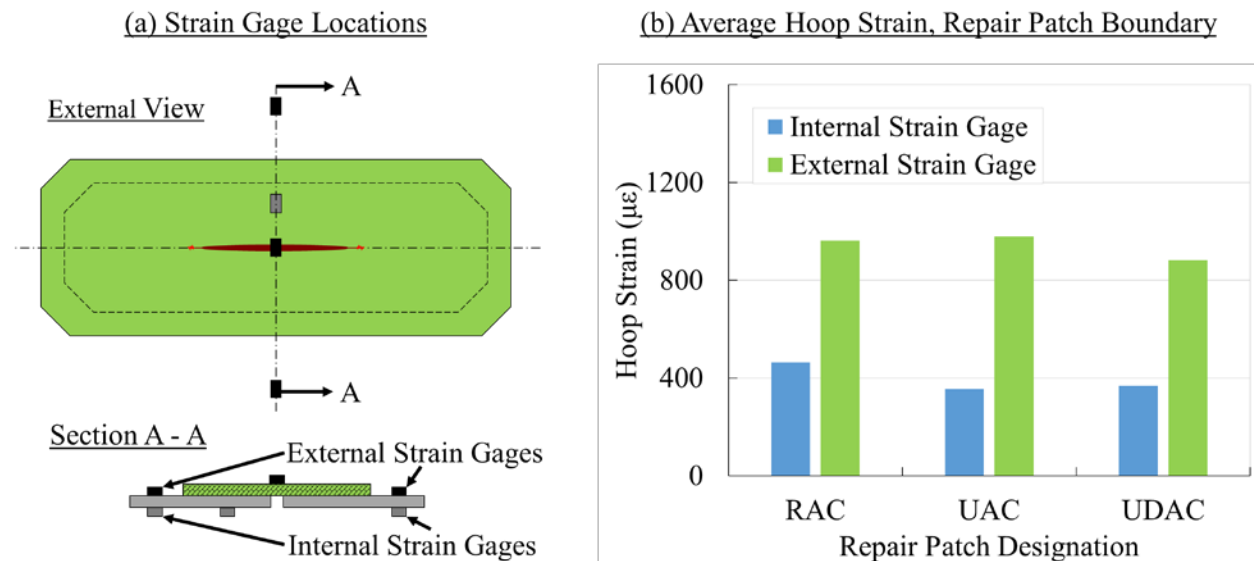


Figure 39. (a) Comparison of the average strain measured along the boundary of repair patches and (b) the locations of strain gauges with respect to the repair patches

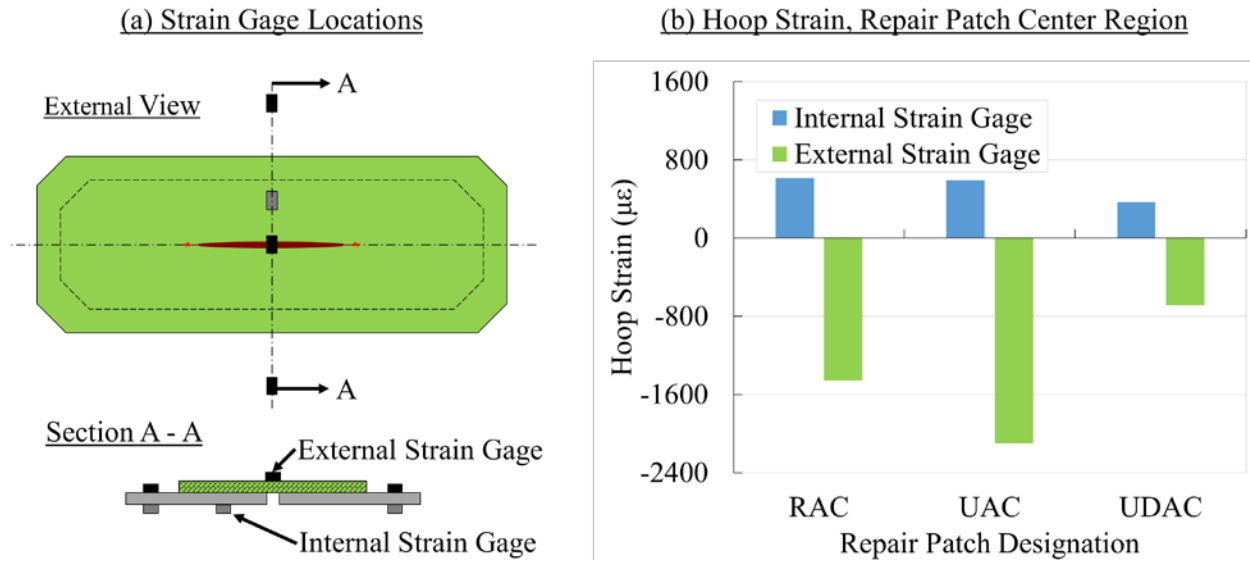


Figure 40. (a) Comparison of the average strain measured at the centers of repair patches and (b) the location of strain gauges with respect to the repair patches

3.2.3.1.4 Comparison of Type-1, Type-2, and Type-3 B/Ep Repairs

Representative results of the Type-1 (reference) B/Ep repair patch, RBC; the-Type 2 (under-designed) B/Ep repair patches, UB and UBC; and the Type 3 (partially disbonded) B/Ep repair patches, UDB and UDBC, are provided in this section. Measurements by back-to-back strain gauges installed along the repair patch boundaries are shown in figure 41, whereas measurements by strain gauges installed within the central footprint are shown in figure 42. In general, bending hoop strains measured along the patch boundary were similar for the conditioned repairs, which featured relatively smaller magnitudes when compared with the un-conditioned counterparts.

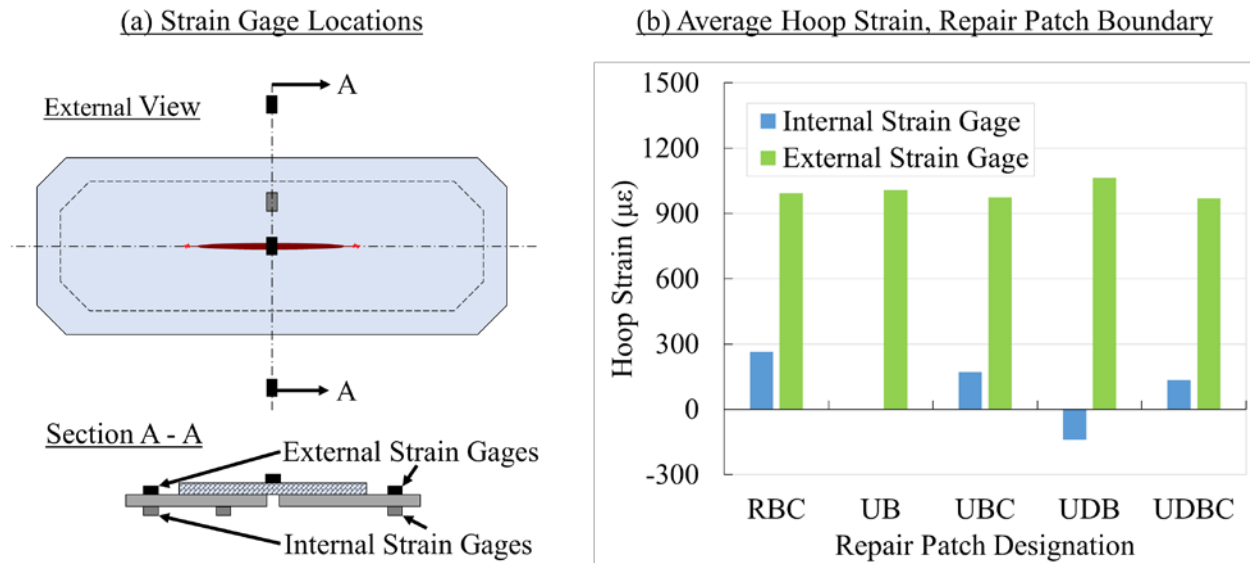


Figure 41. (a) Comparison of the average strain measured along the boundary of repair patches and (b) the locations of strain gauges with respect to the repair patches

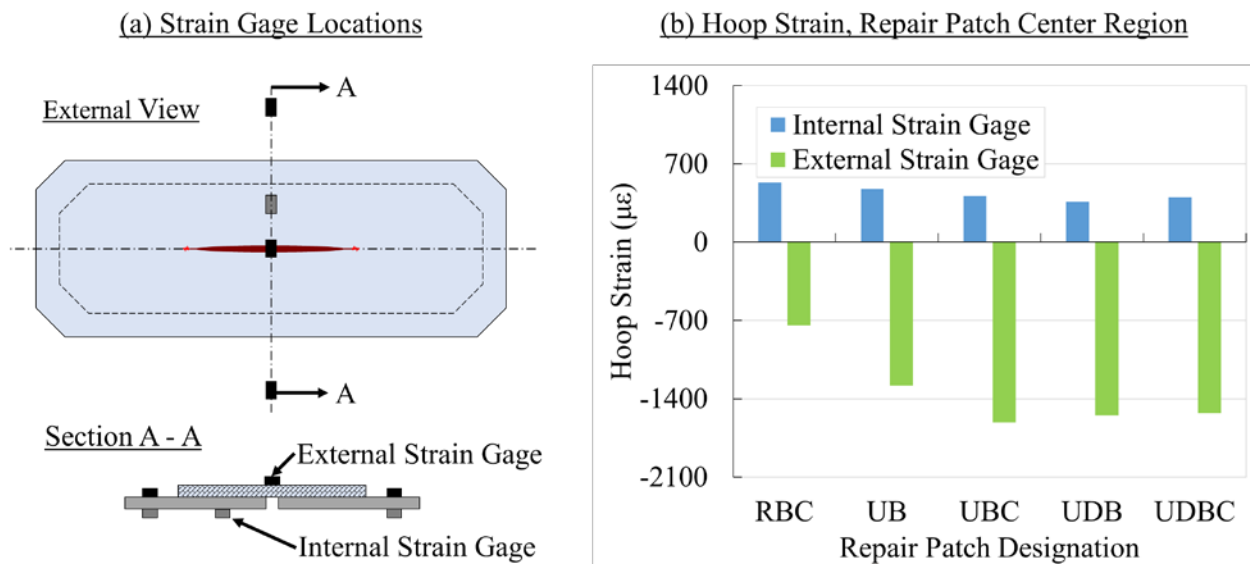


Figure 42. (a) Comparison of the average strain measured at the centers of repair patches and (b) the location of strain gauges with respect to the repair patches

As shown in figure 42, the bonded surface area apparently has a correlation with the strains measured at the central footprint region. Repair patches UB and UBC had identical geometries and dimensions and, therefore, identical bonded surface areas. Repair patches UDB and UDBC featured the same geometries and dimensions, but also included several intentional areas of disbond; therefore, the bonded surface areas of these patches were comparatively lower than that of repair patches UB and UBC. Furthermore, the overall size of repair patch RBC was much greater than the other B/Ep repair patches; therefore, the bonded surface area was comparatively greater than that of all other B/Ep repair patches. With the exception of repair patch UBC, an increase in bonded surface area correlated with a decrease in the difference between strains measured at the

internal and external surfaces. The smallest difference was observed for repair patch RBC, which featured the largest bonded surface area, whereas the largest differences were observed for repair patches UBC, UDB, and UDBC, which featured the smallest bonded surface areas.

3.2.3.2 Continuous Hoop Strain Distribution

Provided in the subsequent sections are hoop strain results captured by the ARAMIS 3D DIC system in the WFOV and NFOV settings, respectively.

3.2.3.2.1 WFOV Full-Field Hoop Strain Distribution

Representative full-field hoop strain results captured in the WFOV for repair patch UAC are shown in figure 43. Results include digital images captured immediately after the 4-week period of hot-wet conditioning, after 20,000 cycles, after 40,000 cycles, and after 60,000 cycles. As shown, a sharp transition from a slight state of compressive strain to a high state of tensile strain was measured along the repair patch boundary, whereas a state of high compressive strain was measured in the center region of the patch along the notch centerline. In general, the global strains on the external surface remained relatively constant throughout the fatigue test up to 60,000 cycles.

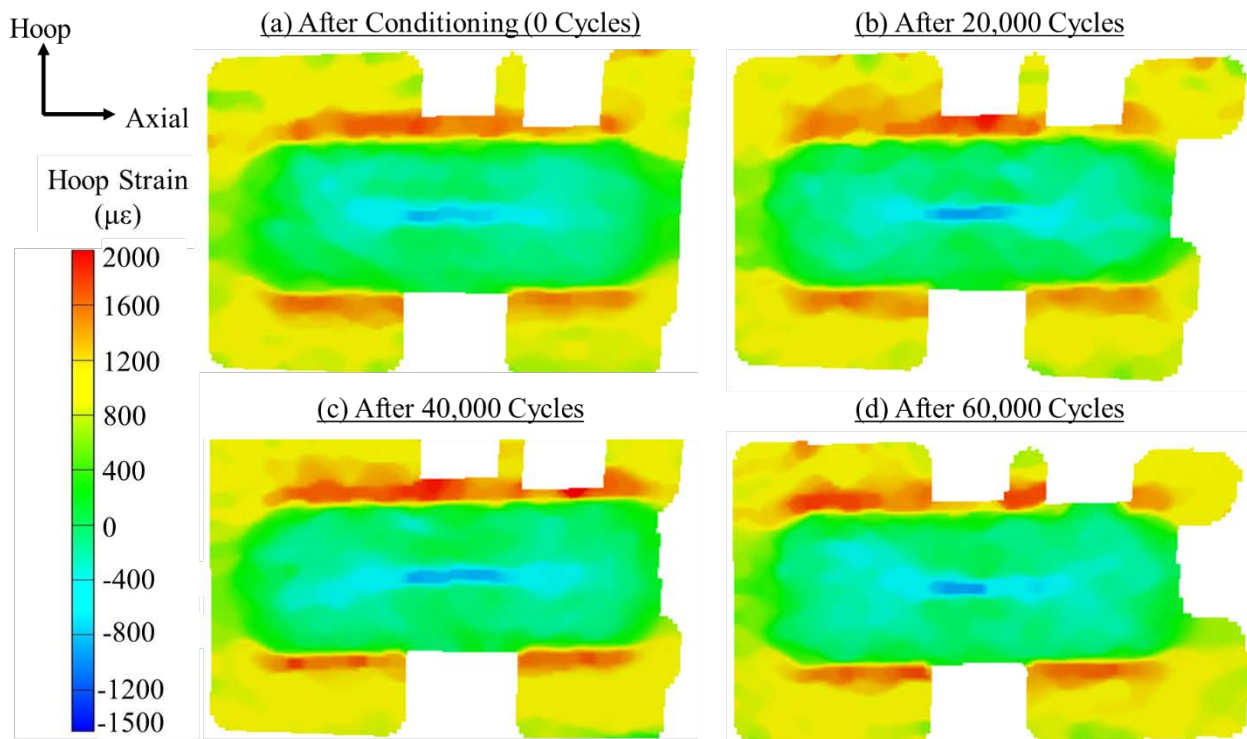


Figure 43. DIC WFOV hoop strain results measured for repair patch UDBC after: (a) hot-wet conditioning, (b) 20,000 cycles, (c) 40,000 cycles, and (d) 60,000 cycles

3.2.3.2.2 NFOV Full-Field Hoop Strain Distribution

Representative full-field hoop strain results captured in the NFOV for repair patch UAC, which highlight finer details of the notch region, are shown in figure 44. Results include digital images captured immediately after hot-wet conditioning, 20,000 cycles, 40,000 cycles, and 60,000 cycles.

In each case, hoop strain variations across the hoop footprint of the repair patch are provided via three sections spaced 1.5 inches apart. Section 1 is located along the centerline of the repair patch, section 2 is located at the original crack-tip region, and section 3 is located at the region ahead of the original crack tip. In general, hoop strains varied most along the patch boundaries and at the center of the patch where the notches were located. The central region of the repair patch, directly above the notch centerline, featured the highest state of compression, whereas the region outside the patch boundary featured the highest state of tension. Along section 1, the hoop strain values ranged from approximately 2000 $\mu\epsilon$ in the skin outside the patch to approximately -1680 $\mu\epsilon$ in the center of the patch for the baseline measurement (see figure 44a). High strain gradients were evident over short distances at the patch boundary and the notch region. Across the patch boundary, the strain was reduced from 2000 $\mu\epsilon$ to 0 $\mu\epsilon$ over a distance of approximately 0.2 inch. The strain gradient was also quite high in a narrow band of approximately ± 0.5 inch around the notch. Over this short distance, the strain ranged from approximately 0 $\mu\epsilon$ to -1680 $\mu\epsilon$.

As shown in figure 44, local strain redistribution at the center of the repair patch, a result of crack extension, is evident by the expansion of the compression zone along the top of the notch centerline. At the same time, the magnitude of these compressive strains reduced to approximately -1370 $\mu\epsilon$ as the number of cycles increased, as shown in figures 44b, 44c, and 44d for 20,000, 40,000 and 60,000 cycles, respectively. Similar trends were displayed along section 2, where high strain gradients occurred over short distances at the patch boundary and the notch region. Values ranged from approximately 3000 $\mu\epsilon$ in the skin outside the patch to approximately -1000 $\mu\epsilon$ in the center throughout the fatigue test. Along section 3, high strain gradients were initially only measured at the patch boundary. Hoop strain values ranged from approximately 2000 $\mu\epsilon$ in the skin outside the patch to approximately 0 $\mu\epsilon$ at the center, as shown in figures 44a and 44b for the baseline and 20,000 cycles, respectively. Figure 44d shows as the compressive region began to cross section 3, the compressive hoop strain increased from approximately 0 $\mu\epsilon$ to -350 $\mu\epsilon$.

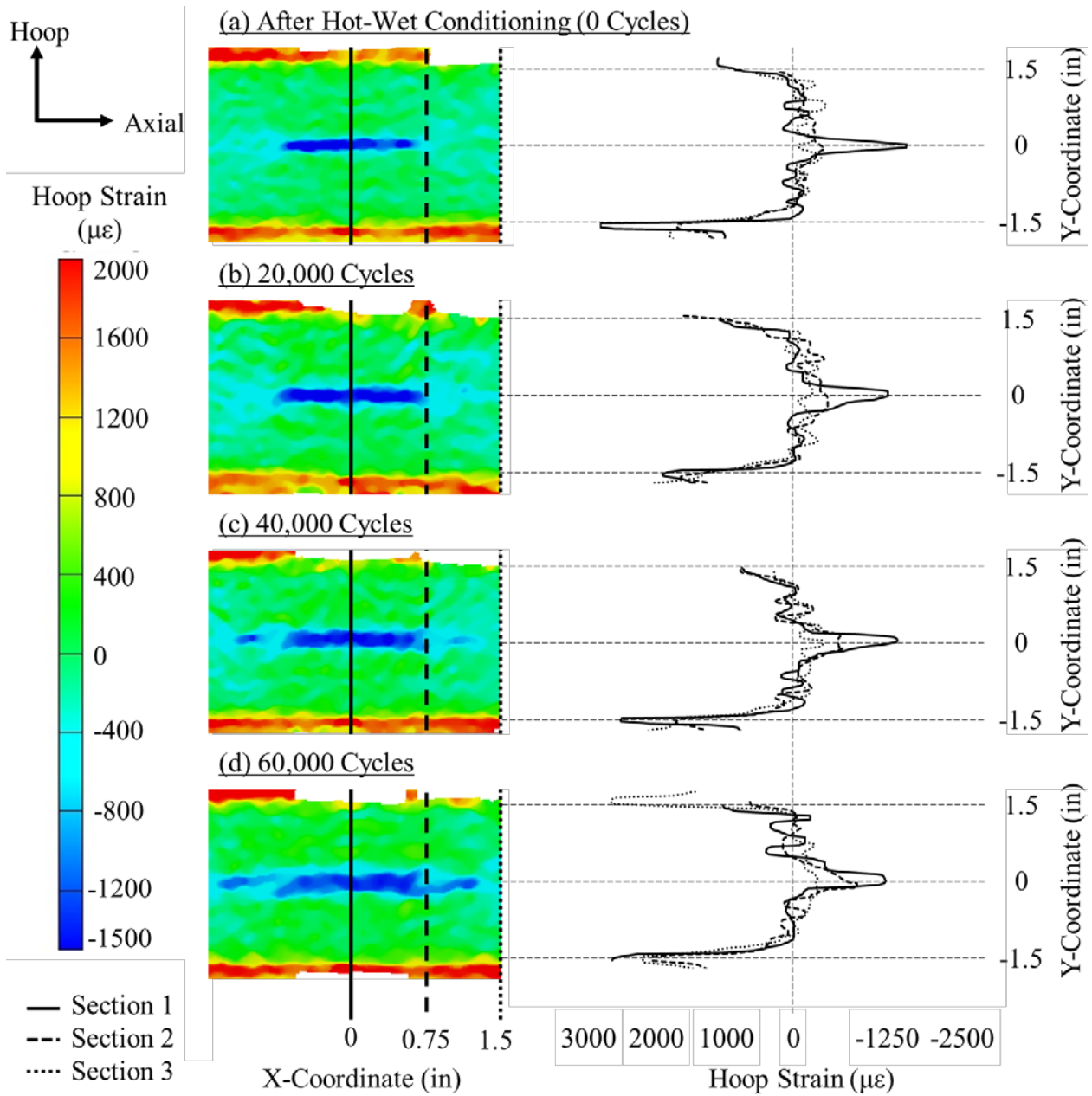


Figure 44. DIC NFOV hoop strain results measured for repair patch UDBC after: (a) hot-wet conditioning, (b) 20,000 cycles, (c) 40,000 cycles, and (d) 60,000 cycles

3.2.4 Effect of Environment on Mechanical Strain

During the first 20,000 cycles of testing, strain surveys were conducted in cold-dry, ambient, and hot-wet environmental conditions every 10,000 cycles. For each environmental condition, the fuselage panel was subjected to a quasistatic load spectrum during which the applied loads were incrementally increased from 0%–75% of conditions. While the load spectrum was being applied, strain gauges monitored and recorded the pointwise hoop strain response in the vicinity of each repair patch at each load step. Figures 45a and 45b show results captured by FWD and AFT crack-tip strain gauges during the maximum strain survey load step (75% conditions) following the

completion of the four-week, hot-wet conditioning period for repair patches UBC and UAC, respectively. Both figures include a comparison of strains measured at three notch-tip gauges between results obtained in cold-dry, ambient, and hot-wet environmental conditions.

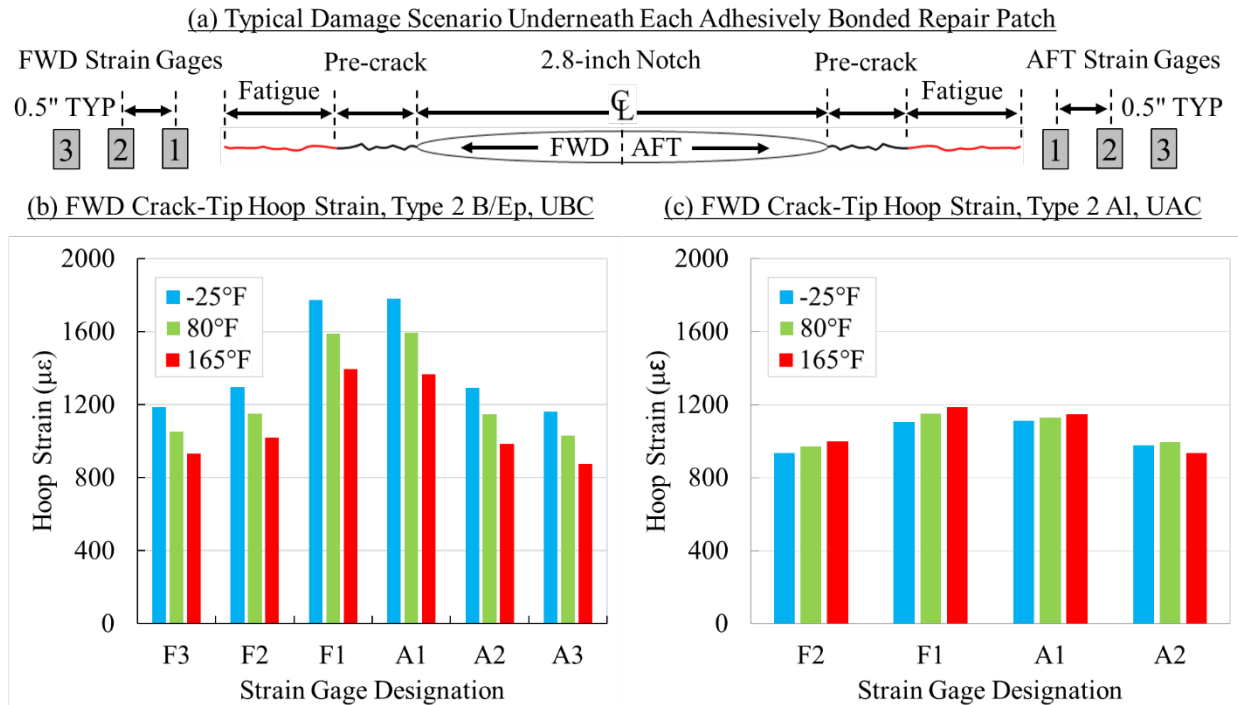


Figure 45. Comparison between strains measured in cold-dry, ambient, and hot-wet environmental condition by crack-tip strain gauges underneath repairs: (a) typical damage scenario underneath each adhesively bonded repair patch, (b) UBC, and (c) UAC

As shown, high-tensile hoop strains were measured ahead of the FWD and AFT crack tips for repair patches UBC and UAC. Irrespective of environmental conditions, a steady decrease in hoop strain was observed as the distance between the strain gauge and the crack tip increased. Comparing the hoop strains measured in cold-dry, ambient, and hot-wet environmental conditions, there is apparently a fundamental difference between the effect that environmental conditions have on the mechanical response of repair patches UBC and UAC. For repair patch UBC, hoop strains increased as temperature decreased. The FWD strain gauge closest to the crack tip measured 1395 µε, 1588 µε, and 1774 µε under hot-wet, ambient, and cold-dry environmental conditions, respectively. For repair patch UAC, hoop strains remained relatively constant irrespective of the environmental conditions. The FWD strain gauge closest to the crack tip measured 1188 µε, 1150 µε, and 1106 µε under hot-wet, ambient, and cold-dry environmental conditions, respectively.

3.3 Fatigue Crack-Growth Monitoring

Throughout the duration of the test, visual, HFEC, and low-frequency eddy current inspections (LFEC) were conducted to monitor the growth of the through-thickness, center-bay cracks in the fuselage panel underneath each repair patch. Representative results using these methods are summarized in the subsequent sections. Tabulated results for each repair patch are provided in appendix H.

3.3.1 Effect of Repair Quality on Fatigue Performance

The effect of repair quality and condition on fatigue performance is shown in figure 46. The average half-crack growth for B/Ep repair patches is shown in figure 46a, whereas the average half-crack growth for Al repair patches is shown in figure 46b. For the B/Ep patches, the fatigue crack growth increased as the repair quality reduced. The Type-1 (reference) B/Ep repair patch, RBC, which was properly designed, yielded the least amount of crack growth whereas the Type-3 (partially disbonded) B/Ep repair patch, UDBC, which featured the worst quality as it was intentionally under-designed with disbonds, yielded the most crack growth. The performance of the Type-2 (under-designed) B/Ep repair patch, UBC, was in between. For the Al patches, the fatigue crack growth was quite limited with no discernable differences in the response of the three types.

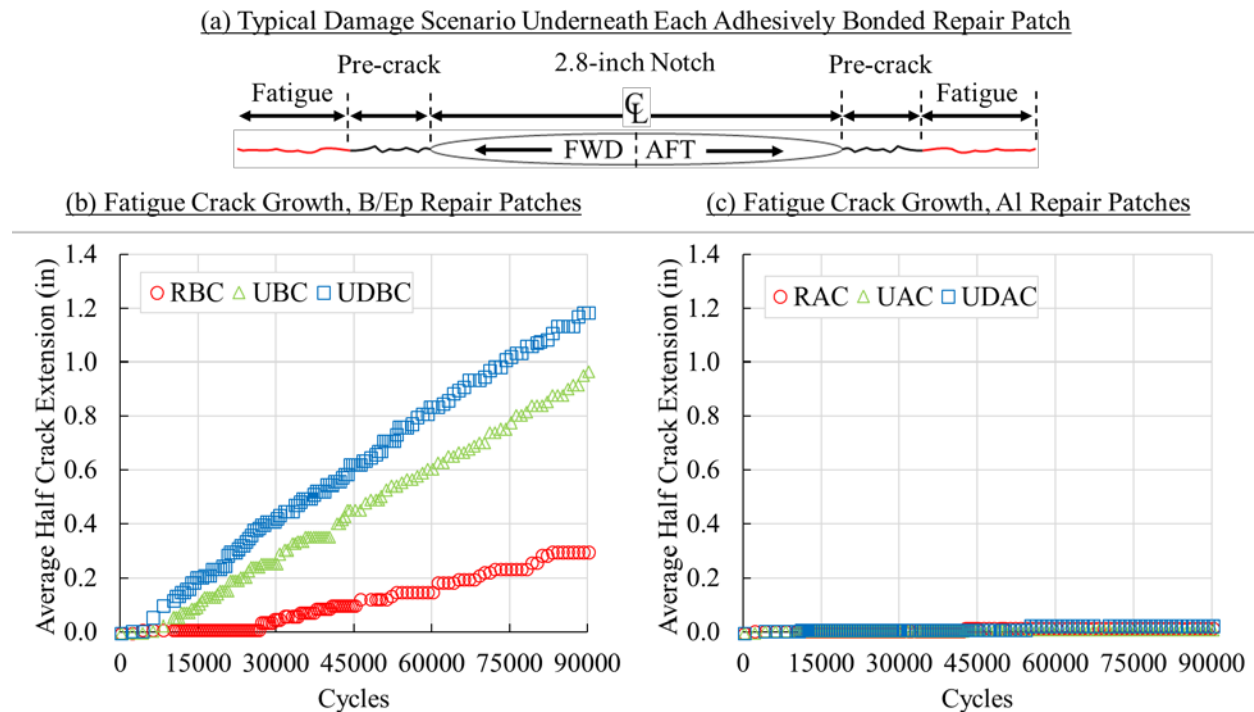
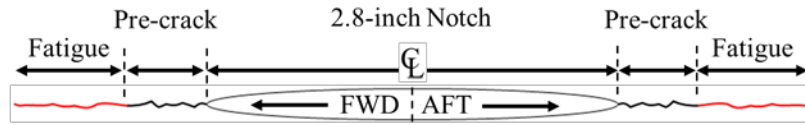


Figure 46. Comparison of the fatigue crack growth exhibited by Type-1, Type-2, and Type-3 repair patches: (a) typical damage scenario underneath each adhesively bonded repair patch, (b) B/Ep repair patches, and (c) Al repair patches

3.3.2 Effect of Hot-Wet Conditioning on Fatigue Crack Growth

The effect of conditioning the repairs for four weeks under hot-wet environment is shown in figure 47. Figure 47a shows a comparison between the average half-crack extension exhibited by the Type-2 B/Ep repairs, UB and UBC. Figure 47b shows a comparison between the average half-crack extension exhibited by Type-3 B/Ep repairs, UDB and UDBC.

(a) Typical Damage Scenario Underneath Each Adhesively Bonded Repair Patch



(b) Fatigue Crack Growth, Type 2 B/Ep, UB & UBC

(c) Fatigue Crack Growth, Type 3 B/Ep, UDB & UDBC

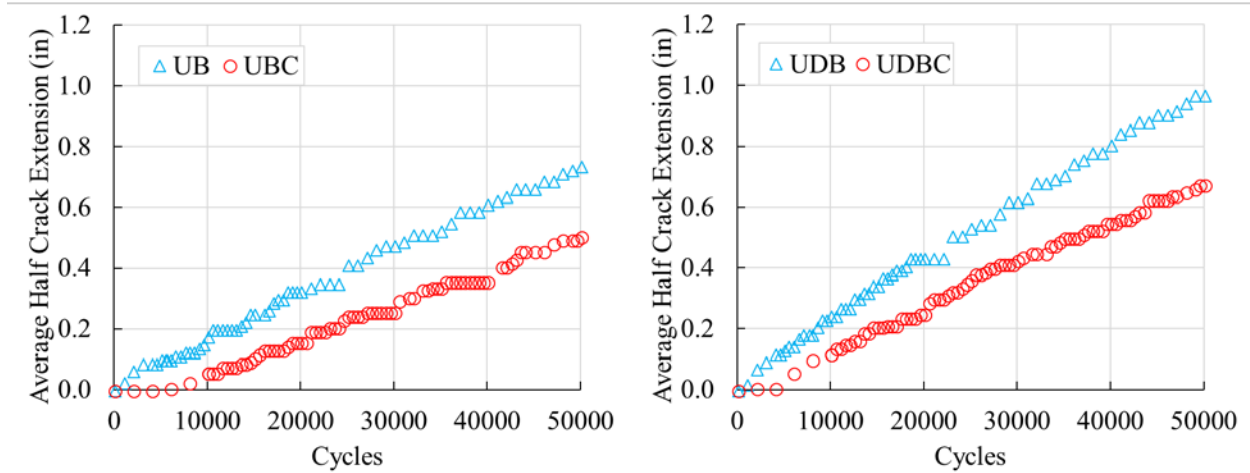


Figure 47. Comparison between the fatigue crack growth exhibited by repairs that were and were not pre-conditioned in a hot-wet environment: (a) typical damage scenario underneath each adhesively bonded repair patch, (b) UB and UBC, and (c) UDB and UDBC

As shown in figure 47, the pre-conditioned B/Ep repair patches exhibited slower crack growth compared to the counterparts that were not pre-conditioned. This correlates with lower notch-tip strains measured in the pre-conditioned repairs, as discussed previously and shown in figure 34.

3.3.3 Effect of Environment on Fatigue Crack Growth

Results from this test, conducted under cold-dry conditions, were compared with results obtained during the Panel 2 test, conducted under ambient conditions, and the results obtained during the Panel 3 test, conducted under hot-wet conditions. For the B/Ep repair patches, shown in figure 48a, the fatigue crack-growth rate under the cold-dry conditions (Panel 4) was the highest, followed by that which was observed under ambient conditions (Panel 2), and then by that which was observed under hot-wet conditions (Panel 3). The fatigue crack-growth rate was approximately 1.56×10^{-5} inches/cycle under cold-dry environmental conditions, approximately 1.48×10^{-5} inches/cycle under ambient environmental conditions, and approximately 1.29×10^{-5} inches/cycle under hot-wet environmental conditions. As shown in figure 45b, these rates are consistent with the trend observed for notch-tip strains in which those measured under cold-dry conditions were the highest, followed by those which were observed under ambient conditions, and then by those which were observed under hot-wet conditions.

For the AI repair patches, shown in figure 48c, the fatigue crack-growth rates were quite limited during all panel tests as no discernable effect from the applied environment was observed. The fatigue crack-growth rate was approximately 0.76×10^{-5} inches/cycle under cold-dry

environmental conditions, approximately 0.05×10^{-5} inches/cycle under ambient environmental conditions, and approximately 0.02×10^{-5} inches/cycle under hot-wet environmental conditions. Similar to the B/Ep repair patches, as shown in figure 45c, these rates are consistent with the trend observed for notch-tip strains in which those measured were relatively consistent, irrespective of the environmental conditions that were applied.

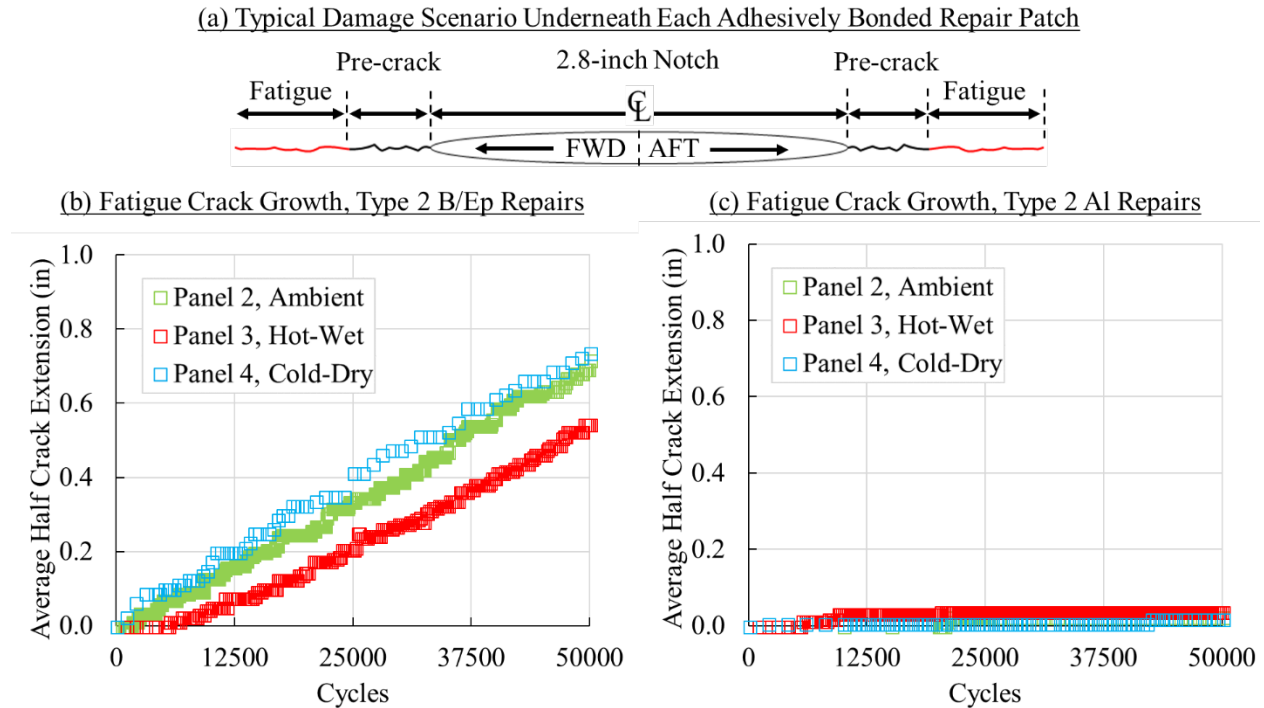
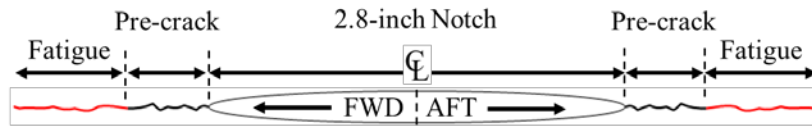


Figure 48. Average fatigue crack growth observed for fuselage Panel 2 (ambient), fuselage Panel 3 (hot-wet), and fuselage Panel 4 (cold-dry) for repair patches: (a) typical damage scenario underneath each adhesively bonded repair patch, (b) UB and (c) UA and UAC

3.3.4 Correlation Between Crack Growth Inspections

Shown in figures 49a and 49b are comparisons between the average half-crack length measurements obtained through visual, HFEC, and LFEC inspections for repair patches UBC and UAC, respectively. As shown, measurements conducted through visual, HFEC, and LFEC inspections were consistently in good agreement.

(a) Typical Damage Scenario Underneath Each Adhesively Bonded Repair Patch



(b) Crack Inspection Correlation, Type 2 B/Ep, UBC

(c) Crack Inspection Correlation, Type 2 AI, UAC

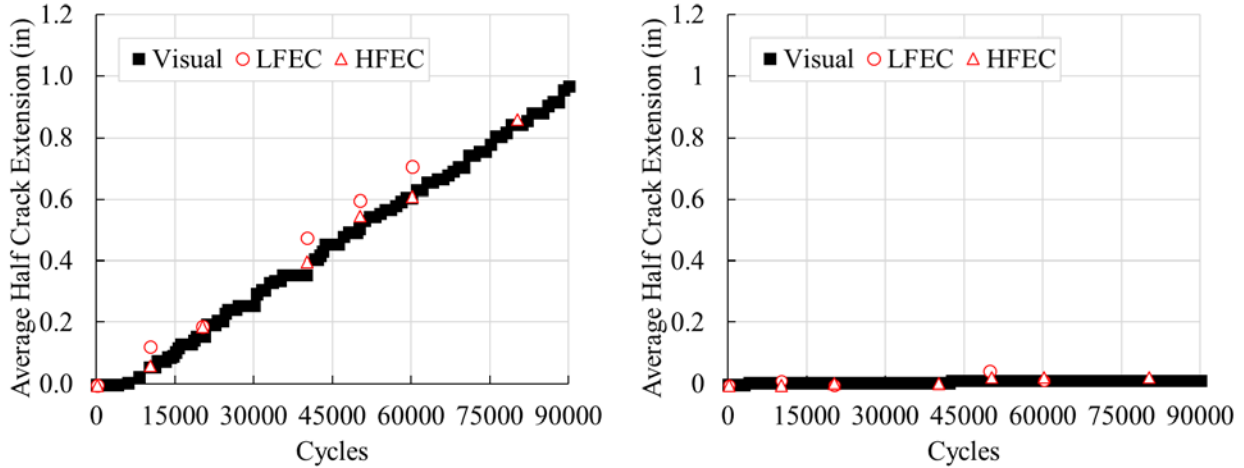


Figure 49. Comparison of fatigue crack-growth measurements conducted with visual, HFEC, and LFEC inspections: (a) typical damage scenario underneath each adhesively bonded repair patch, (b) Type-2 B/Ep repair patch, UBC; and (c) Type-2 AI repair patch, UAC

3.4 Disbond Detection

Throughout the duration of the test, flash thermography and resonance ultrasonic inspections were conducted to monitor the formation and growth of damage and areas of disbond in the vicinity of each repair. The following sections contain results obtained using these methods.

3.4.1 Disbond Detection With Flash Thermography

Flash thermography inspections were conducted every 5,000 to 20,000 cycles throughout the duration of the test to monitor the formation and growth of areas of disbond and damage in the vicinity of B/Ep repair patches. Figure 50 shows results obtained for repair patch UDBC following repair patch installation and the completion of 20,000, 40,000, 60,000, and 92,834 cycles. In each case, digital images represent the second logarithmic derivative of temperature captured 2.502 seconds into acquisition. Results obtained for the other patches are provided in appendix I.

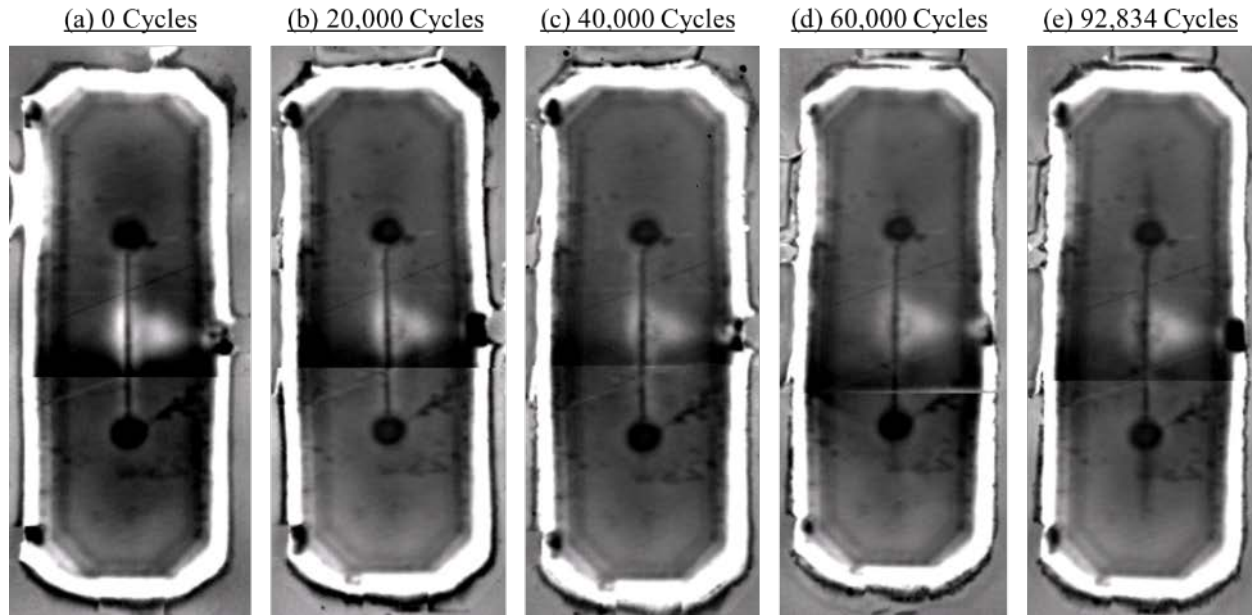


Figure 50. Flash thermography results for the Type-3 B/Ep repair patch, UDBC: (a) 0 cycles, (b) 20,000 cycles, (c) 40,000 cycles, (d) 60,000 cycles, and (e) 92,834 cycles.

As shown in figure 50, the intentional damage (i.e., the through-thickness, center-bay crack) and intentional areas of disbond (i.e., the three semi-circular edge disbonds and the two circular FEP tabs located directly over each crack tip) were clearly detectable at each stage. As the cumulative cycle count increased, the size of the intentional areas of disbond remained the same, whereas the length of the center-bay crack extended. Flash thermography inspections provided no substantial indications that damage or disbond growth occurred.

3.4.2 Disbond Detection With Resonance Ultrasonic

Resonance ultrasonic inspections were conducted every 5,000 to 20,000 cycles throughout the duration of the test to monitor the formation and growth of areas of disbond and damage in the vicinity of each repair patch. Figure 51 shows results obtained for repair patch UDBC following repair patch installation and the completion of 20,000, 40,000, 60,000, and 92,834 cycles. Results obtained for the other repair patches are provided in appendix J.

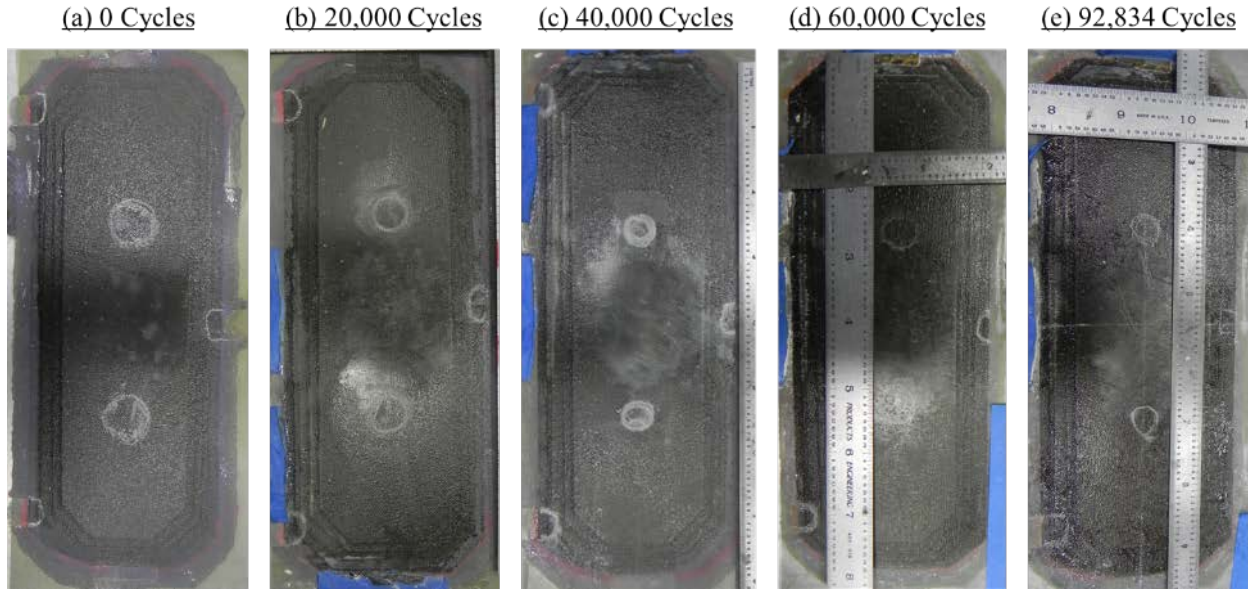


Figure 51. Resonance ultrasonic results for the Type-3 B/Ep repair patch, UDBC: (a) 0 cycles, (b) 20,000 cycles, (c) 40,000 cycles, (d) 60,000 cycles, and (e) 92,834 cycles.

As shown in figure 51, the intentional areas of disbond (i.e., the three semi-circular edge disbonds and the two circular FEP tabs located directly over each crack tip) were clearly detectable at each stage. As the cumulative cycle count increased, the size of the intentional areas of disbond remained the same. Resonance ultrasonic inspections provided no substantial indications that damage or disbond growth occurred.

3.5 Structural Health Monitoring

During the final 52,834 cycles of testing, SHM inspections of repair patches UB and UDB were conducted every 10,000 cycles, resulting in the collection of 44 data packages that were used to improve on a predictive linear regression model developed during the second and third fuselage panel tests [5, 6]. Characteristics of wave propagation signals were correlated to crack-length measurements obtained through visual and HFEC inspections. A “local” crack correlation model was developed for each side of the crack-growth zone (i.e., the FWD half-crack and the AFT half-crack) and blindly applied to the other side for prediction validations (i.e., crack correlation models were developed for the FWD half-crack of each repair patch and applied to predict the AFT half-crack of each repair patch). Figure 52 shows crack-growth measurements at each data interval performed by the SHM system for repair patches UB and UDB. As shown, crack growth has been accurately predicted by the SHM system within the tolerance of conventional crack-length measuring techniques (e.g., HFEC). Further, the correlation of SHM signals to physical damage in the host structure is shown to be accurate and reliable even when the host structure and repair patch system have undergone extreme hot-wet conditions.

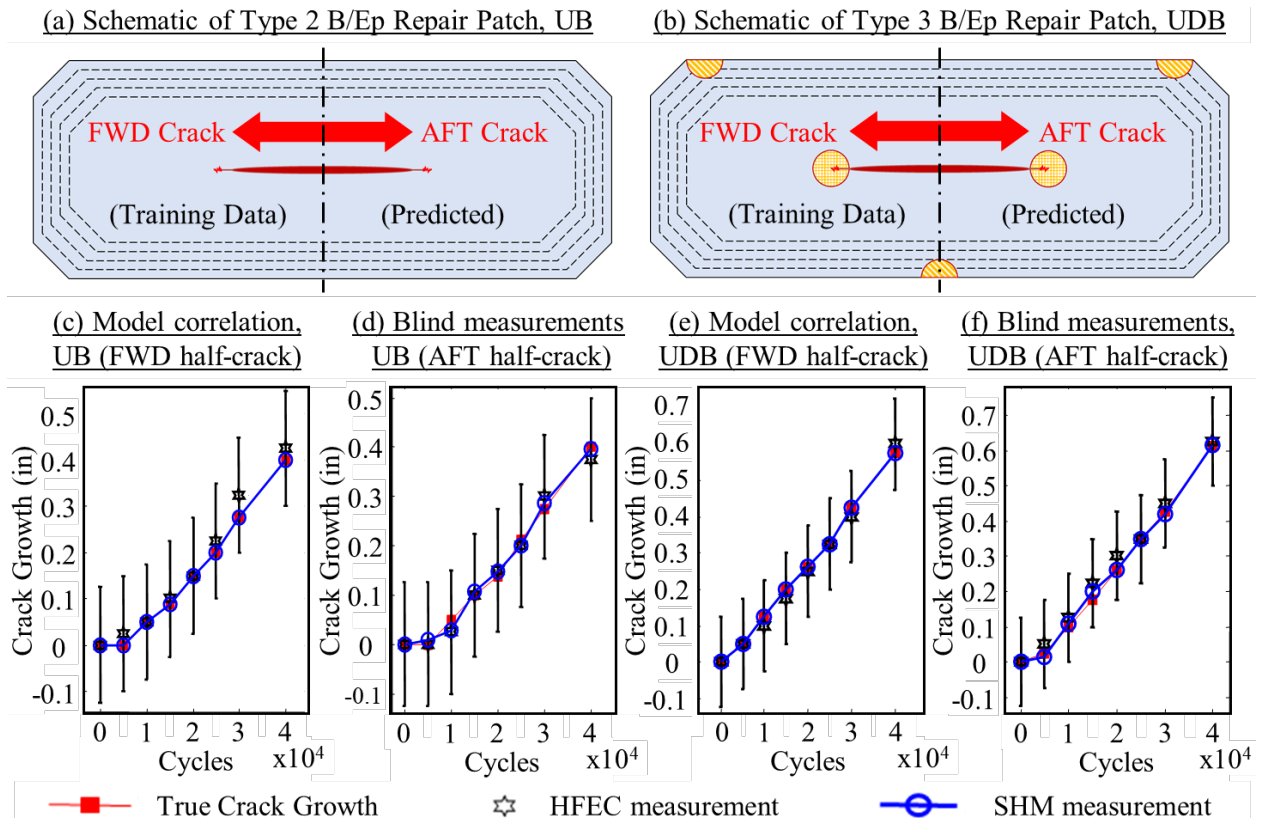


Figure 52. Comparison between predictions by the local SHM model and crack-growth measurements obtained via HFEC inspections for Panel 4 repair patches UB and UDB: (a) type 2 B/Ep repair patch, UB; (b) type 3 B/Ep repair patch UDB; (c) model correlation, UB; (d) blind measurements, UB; (e) model correlation, UDB, and (f) blind measurements, UDB

To address and minimize the panel-to-panel variability on SHM system performance, a new and improved algorithm based on the Lasso regression technique was adopted to create a “global” crack correlation model that aims to further reduce variance and biased errors associated with crack-length predictions. Figure 53 shows the results of the “global model” when cross validated against the NDI data from different crack sides (i.e., FWD and AFT) and repair zones (i.e., UB and UDB). As shown, the global model consistently shows good correlation with results across the entire Panel-3 dataset. The crack growth calculated from the SHM system based on the global model will be compared to the NDI crack-growth data collected from Panel 4 testing.

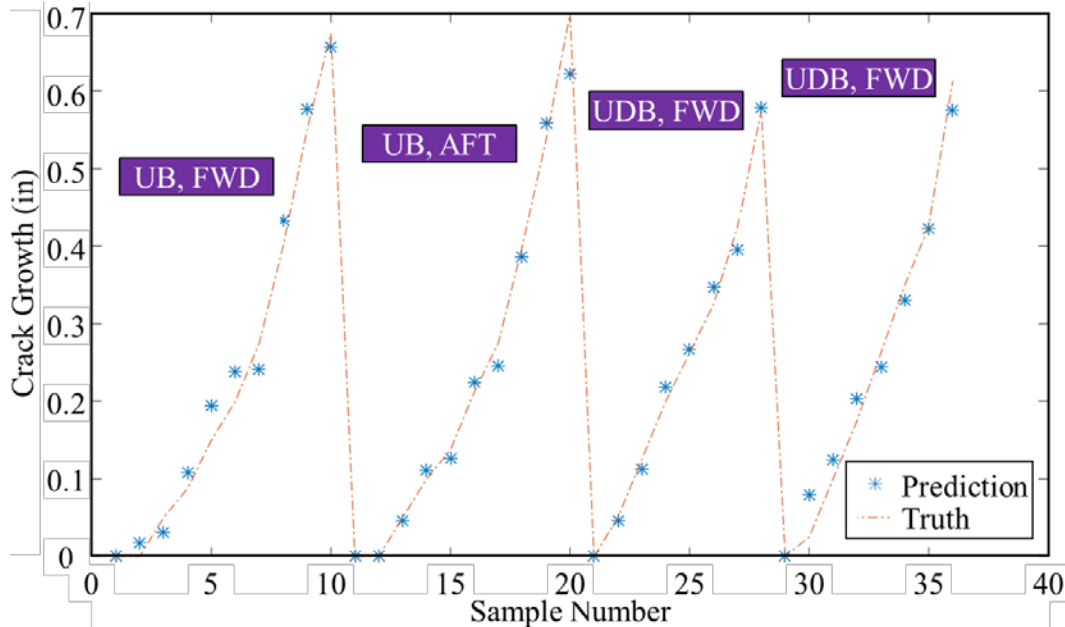


Figure 53. Comparison between predictions by the global SHM model and crack-growth measurements obtained via HFEC inspections for Panel 3 repair patches UB and UDB

3.6 Preliminary Thermal Residual Stress Analysis by Viscoelastic Modeling

To improve the predictive capability of thermal residual stresses in adhesively bonded repair patches, a preliminary study was conducted by Inhar University using a newly developed viscoelastic material model. Details of this study are provided in appendix K.

4. SUMMARY

In a collaborative effort, the FAA and The Boeing Company studied the performance of adhesively bonded repair patches installed on fuselage panels harvested from retired B727 aircraft. This report summarizes representative results of the fourth and final fuselage panel test in this program. The objective was to investigate the effects of hot-wet and cold-dry environmental conditions on the performance of adhesively bonded B/Ep and Al repair patches installed over active, center-bay cracks. Emphasis was placed on assessing residual strains that developed during the curing cycle of patch installation and during the four-week period of hot-wet conditioning that occurred immediately after repair patch installation (i.e., prior to load application) for select repair patches. Following the completion of this period, the fuselage panel was subjected to fatigue testing under cold-dry environmental conditions up to 90,000 cycles.

Throughout the duration of the test, various inspection methods were used to monitor and assess the distribution of strain, and the formation and growth of areas of disbond, cracks, and general damage in the fuselage panel. A 3D digital image correlation system and strain gauges installed on the fuselage panel skin, frames, stringers, and the top of each repair patch were used to monitor the distribution of strain. High-magnification camera systems, a prototype structural health monitoring (SHM) system, and conventional non-destructive inspection (NDI) methods, including

eddy current, flash thermography, and resonance ultrasonic, were used to monitor the formation and growth of damage.

Results and other major findings include:

- Thermal residual strains that developed in and around the repair patch regions during the repair patch installation process were measured for model development purposes. For the B/Ep repair patches, high thermal residual strains developed within the repair patch footprint and surrounding areas as a result of the mismatches between the thermal properties of the B/Ep repair patch and the Al fuselage panel skin. For the Al repair patches, thermal residual strains were much lower and often insignificant.
- Following the completion of the repair patch installation process, select repair patches were subjected to 4 weeks of hot-wet conditioning. During this time, strain gauges installed in the vicinity of each repair patch were continuously monitored. For the B/Ep repair patches, thermal-viscoelastic-plastic behavior was observed in which thermal strains relaxed. Conditioning of the B/Ep repair patches resulted in lower notch-tip strains when compared with similar repair patches that were not subjected to hot-wet conditioning. For the Al repair patches, the effects of hot-wet conditioning were insignificant.
- Throughout the duration of the test, mechanical strains were measured along the notch centerline during the application of a quasistatic load under ambient, hot-wet, and cold-dry environmental conditions. For the B/Ep repair patches, the mechanical strains increased as temperature decreased. For the Al repair patches, the environment effects were limited. Global strains remained relatively constant during tests, whereas local strain redistribution was observed as the skin crack extended.
- Fatigue loading was conducted under cold-dry conditions up to 90,000 cycles. During this time, fatigue crack growth and strains were monitored continuously. Post-test comparisons were made between the results obtained from this test and those obtained during the Panel-2 test (conducted under ambient conditions) and the Panel-3 test (conducted under hot-wet conditions). The fatigue crack growth observed under the cold-dry conditions for the as-installed B/Ep repair patches (Panel 4) was the highest, followed by ambient (Panel 2) and then hot-wet (Panel 3). These followed similar trends in which the notch-tip strains were highest under cold-dry conditions, followed by ambient, and then hot-wet. The pre-conditioned B/Ep repair patches installed on Panel 4 exhibited slower crack growth compared to the as-installed B/Ep repair patches, which correlated with lower notch-tip strains.
- Fatigue performance reduced for the defective repairs as compared to the reference. The reference B/Ep repair patch, which was properly designed, yielded the least amount of crack growth, whereas the partially disbanded B/Ep repair patch, intentionally under-designed with disbonds, yielded the most crack growth. No discernable effect was observed for the Al repair patches as limited fatigue crack growth was observed.
- The primary methods used to monitor disbonds included resonance ultrasonics and flashed thermography. Both NDI techniques were successful in detecting initial disbonds inserted in the B/Ep repairs. However, there were no indications that disbond growth occurred using

these methods. Skin crack growth was successfully monitored and measured using high-magnification cameras and eddy current. A prototype SHM system was demonstrated to track crack growth.

5. REFERENCES

1. Baker, A. A., Rose, L. R. F., and Jones, R., (eds.) (2002). *Advances in the Bonded Composite Repair of Metallic Aircraft Structure, Volumes 1 and 2*, Amsterdam, Netherlands: Elsevier.
2. Warren, A.S. (2004). Developments and challenges for aluminum – A Boeing Perspective. *Materials Forum*, 28.
3. FAA Policy Statement, U.S. Department of Transportation, Federal Aviation Administration, Bonded Repair Size Limits, 11/24/14, Policy No. PS-AIR-100-14-130-001, Initiated By: AIR-100
4. FAA Report. (2013). Adhesively Bonded Repairs to Metallic Fuselage Structure: Test 1, Fatigue and Residual Strength Performance. (DOT/FAA/AR-11/4).
5. FAA Report. (2015). Adhesively Bonded Repairs to Metallic Fuselage Structure: Test 2 Monitoring Damage Growth. (DOT/FAA/TC-15/3).
6. FAA Report. (n.d.). Adhesively Bonded Repairs to Metallic Fuselage Structure: Test 3 Effect of Environmental Conditions. (DOT/FAA/TC-18/24)

APPENDIX A—FUSELAGE PANEL ENGINEERING DRAWINGS

A.1 INTRODUCTION

The fuselage panel studied in this test was removed from a retired B727-225 aircraft with tail number N676MG and serial number 22554. Owned and operated by Champion Air, as shown in figure A-1a, the structure, which accumulated 47,724 flight hours and 29,326 flight cycles while in service, was well-maintained and had a well-documented and accessible service history. Originating from the crown of the aircraft, as shown in figure A-2b, the fuselage panel included the area of the fuselage covered by frame stations STA520 to STA620 and stringer stations S-9R to S-4R. Components included the skin, shear clips, stringers, and an axial skin splice joint. When the fuselage section was removed from the aircraft, non-destructive inspections were conducted to determine the condition of the test section. Following these inspections, modifications were made to ensure that the form and condition of the fuselage section were sufficient for testing.

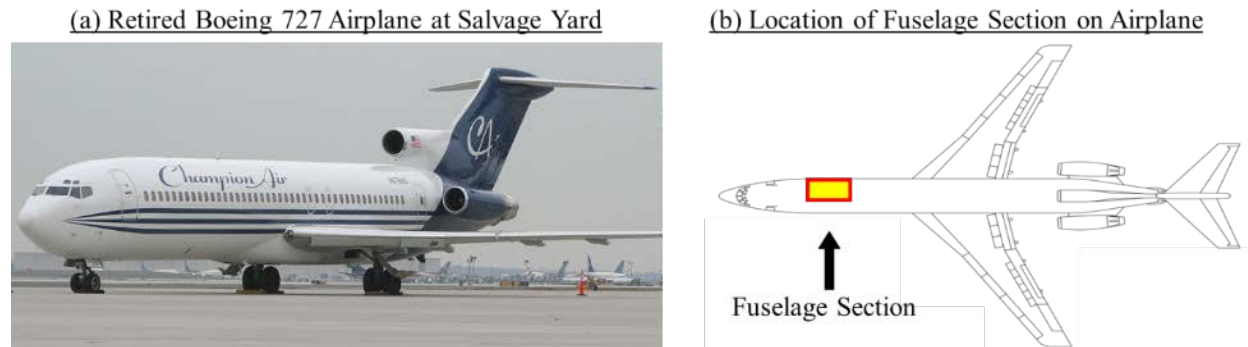
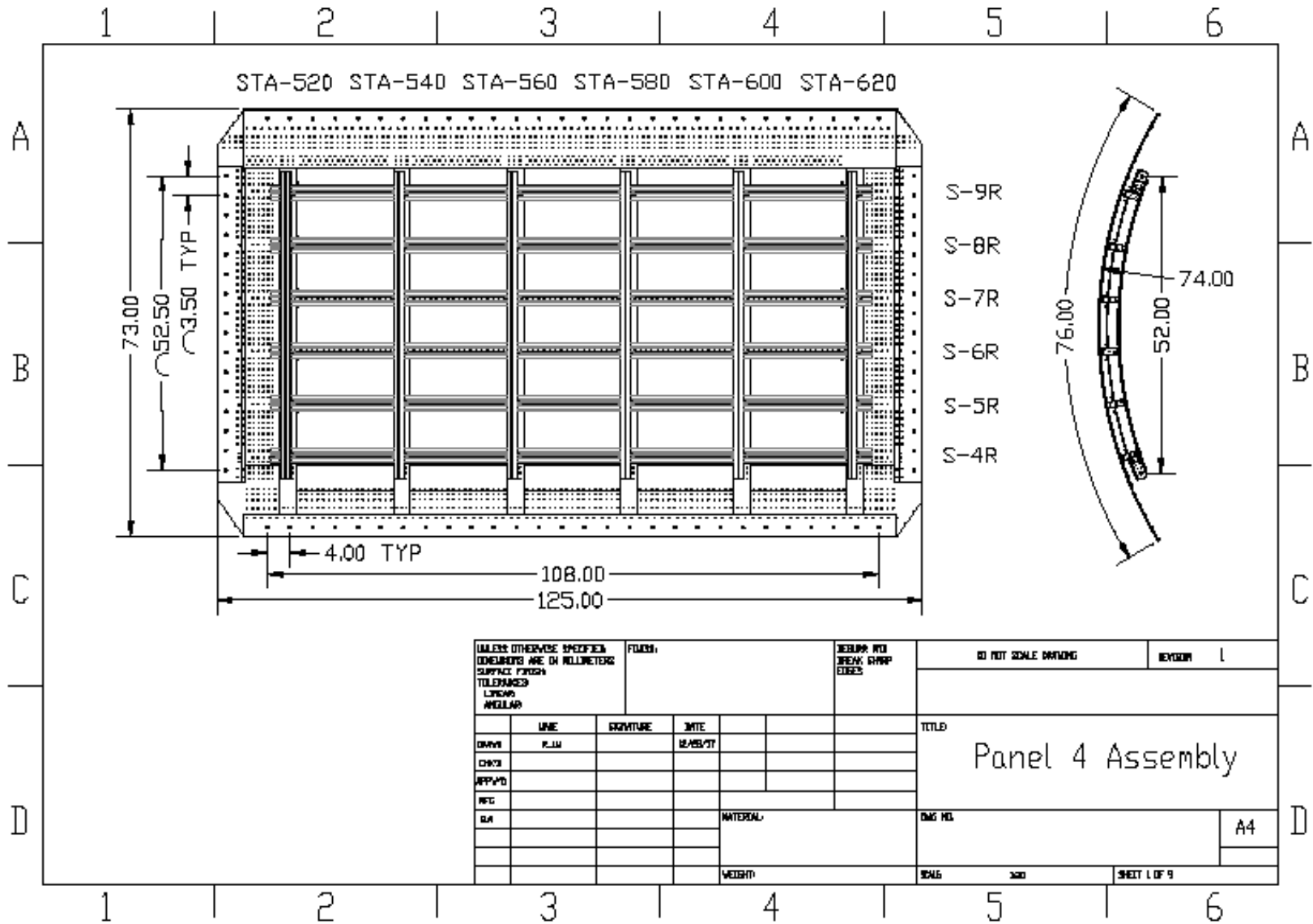


Figure A-1. External view of the fuselage panel depicting the location of the repair patches: (a) retired Boeing 727 airplane at salvage yard and (b) location of fuselage section on airplane

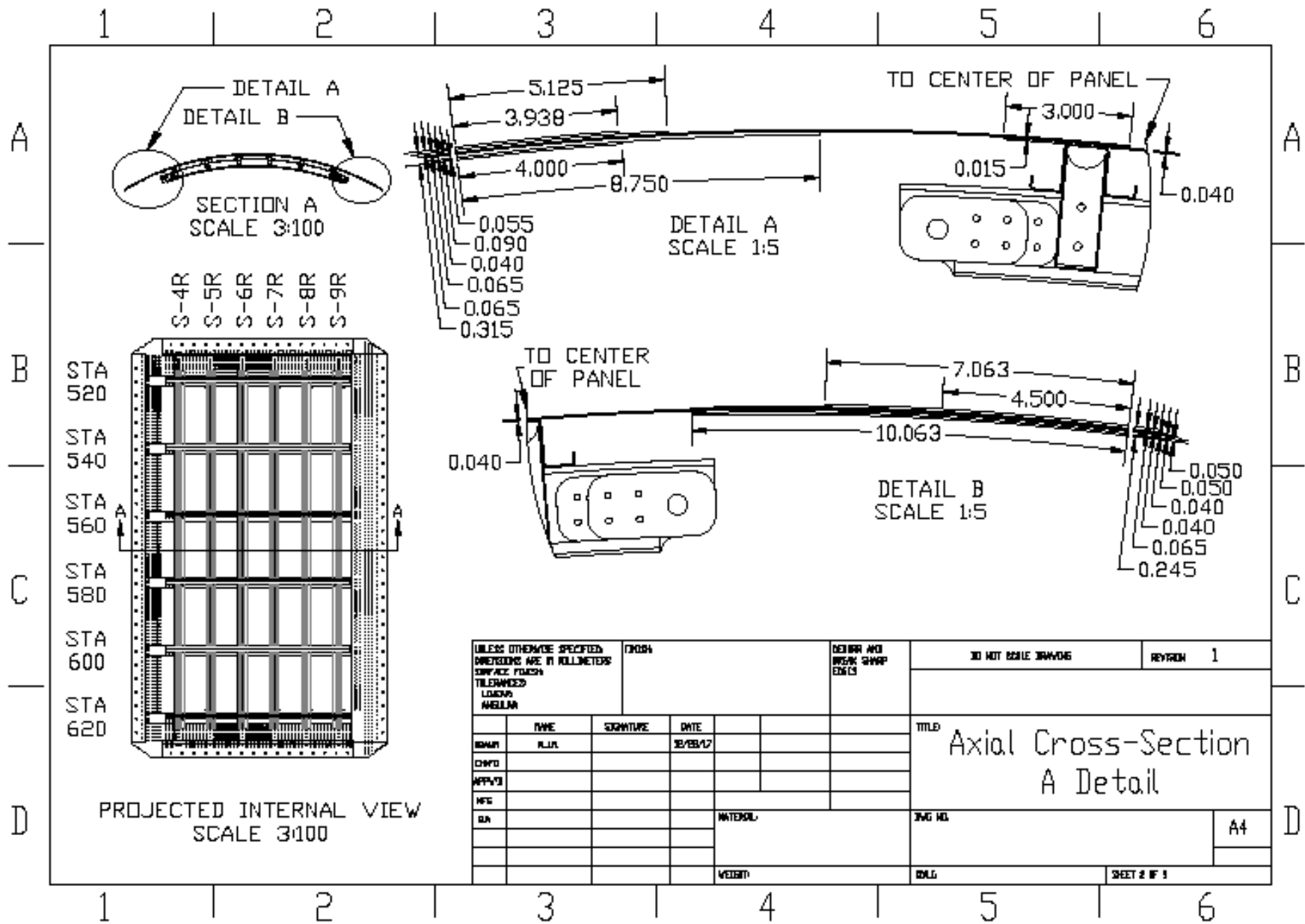
Modifications included: 1) extraction of the test specimen (i.e., the area of the fuselage covered by frame stations STA520 to STA620 and stringer stations S-9R to S-4R) from the fuselage section; 2) reduction of frame and stringer lengths to ensure proper connectivity to the FASTER fixture; 3) installation of 2024-T3 aluminum doublers along the perimeter of the fuselage panel on both the internal and external fuselage panel surfaces; 4) installation of 2024-T3 aluminum doublers on the frame ends; 5) drilling of 0.5-inch diameter load attachment holes through the frame end doublers and fuselage panel perimeter doublers; 6) installation of 2024-T3 aluminum shims at the axial load attachment points on both the internal and external fuselage panel surfaces; and 7) the installation of an elastomeric pressure box seal. Provided in the subsequent section are drawings showing the fuselage panel following the completion of modifications 1–5.

A.2 FUSELAGE PANEL ENGINEERING DRAWINGS

A-2

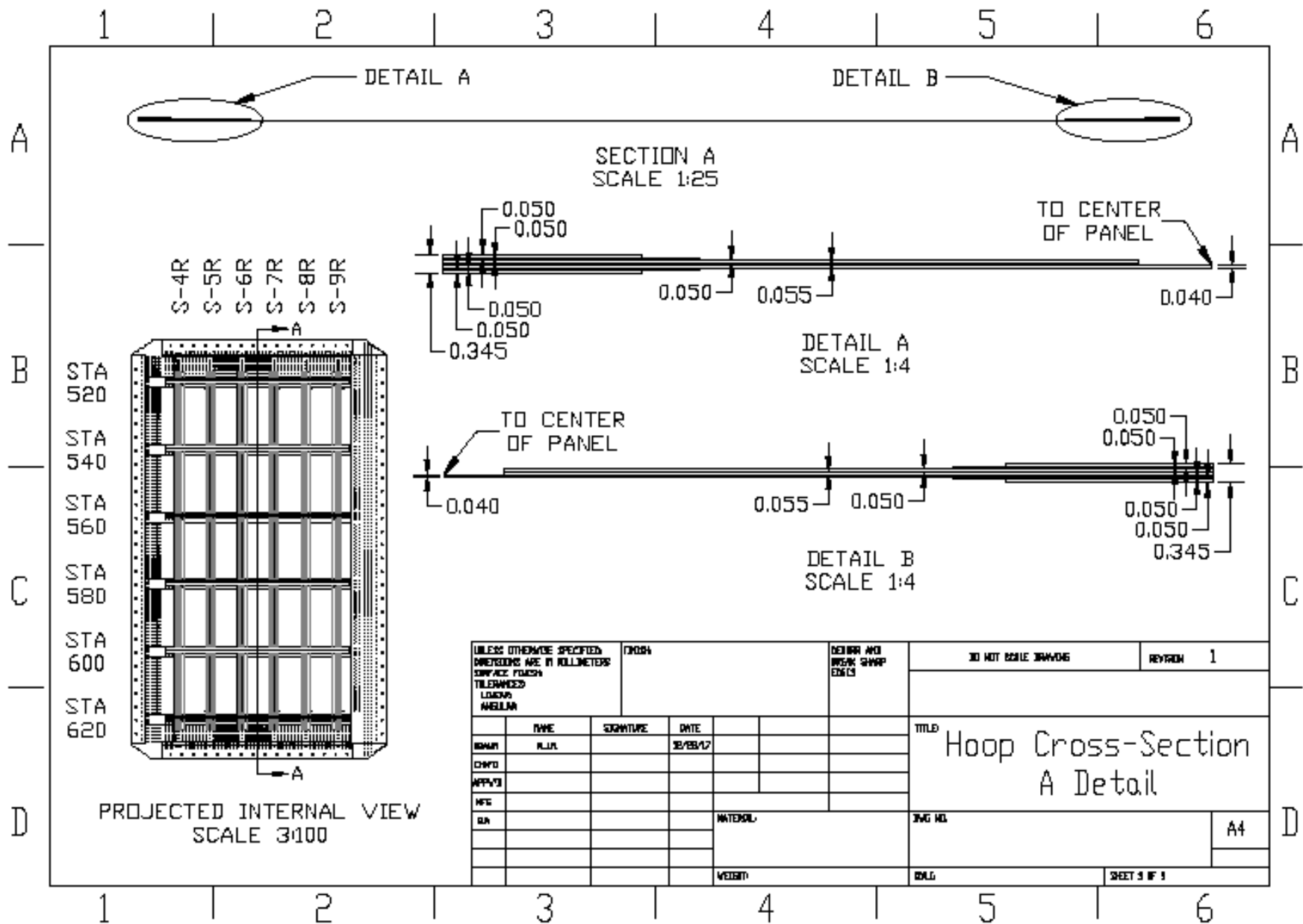


A-3



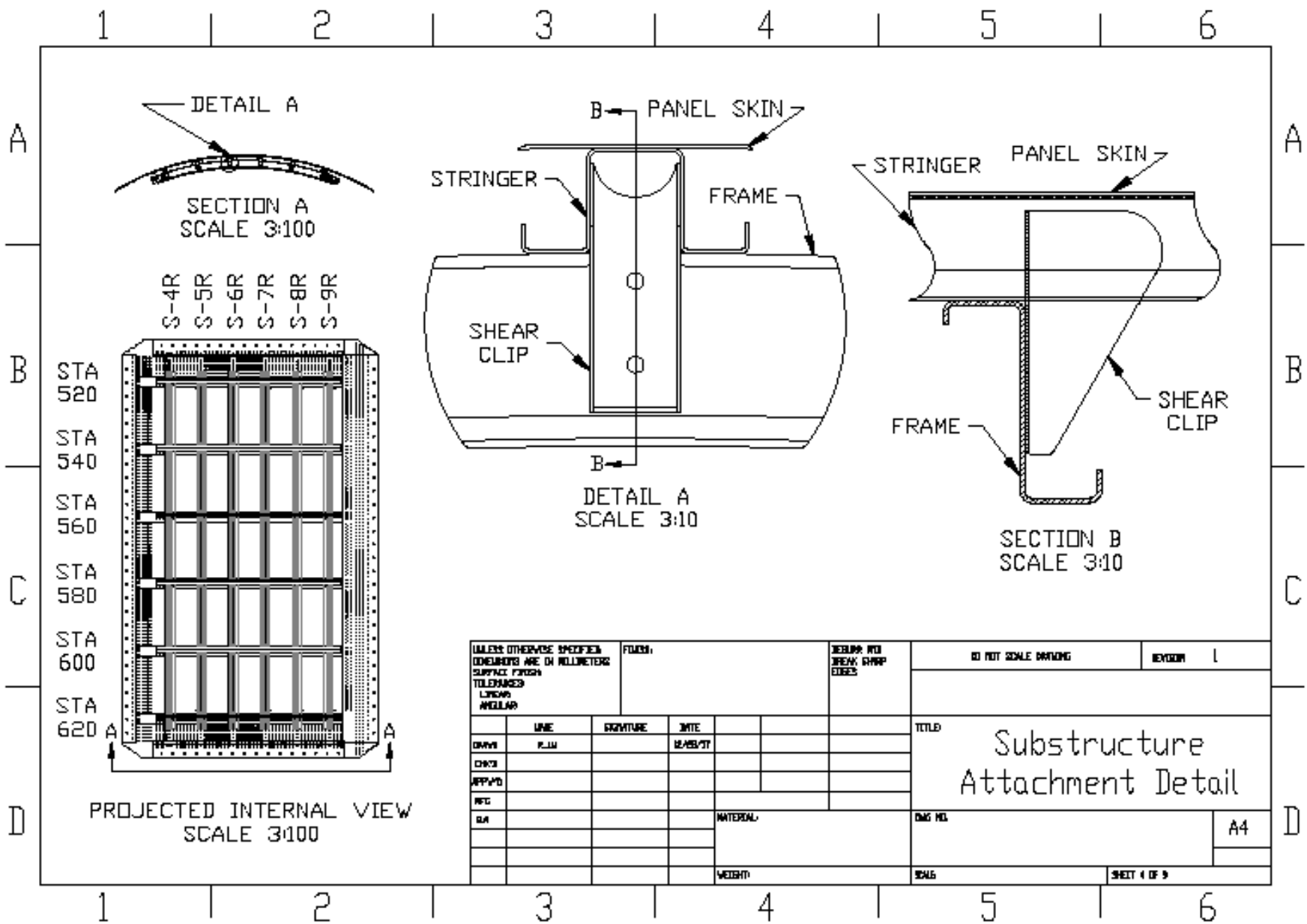
UNLESS OTHERWISE SPECIFIED: DIMENSIONS ARE IN MILLIMETERS SURFACE FINISH TOLERANCES UNLESS NOTED		FINISH	DESIGN AND WORK SHOP ENGS		DO NOT SCALE DIMENSIONS	REVISION 1
DATE	SIGNATURE	NAME	TITLE Axial Cross-Section A Detail			
3/28/17		ALJ	SHEET NO. A4			
			MATERIAL		DRG. NO.	
			WEIGHT		ENCL.	SHEET 2 OF 3

4-V



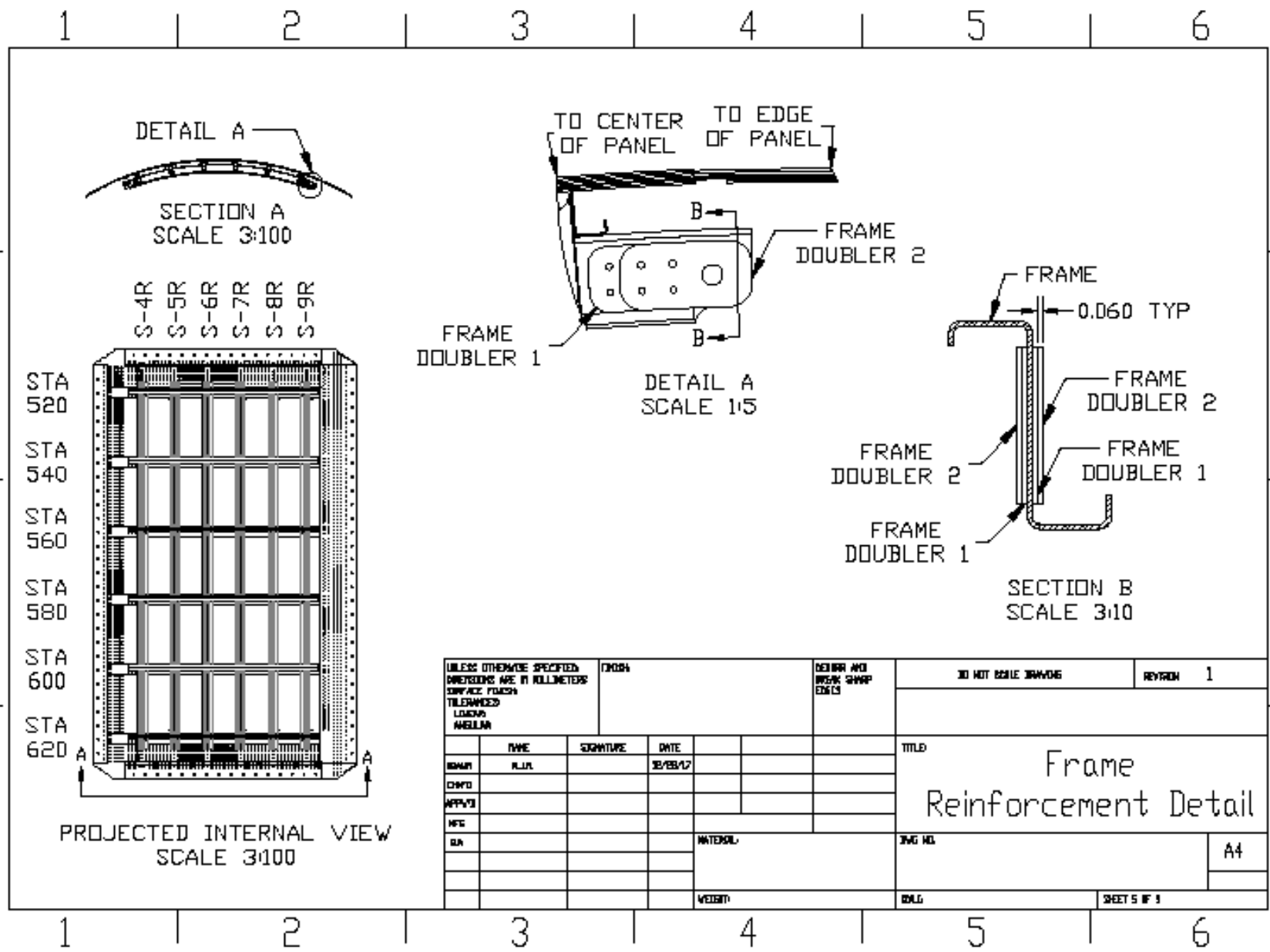
UNLESS OTHERWISE SPECIFIED DIMENSIONS ARE IN MILLIMETERS SURFACE FINISH TOLERANCES UNLESS NOTED		FINISH		DESIGN AND DRAWING GROUP ENCL		DO NOT SCALE DIMENSIONS		REVISION 1	
NO.	DATE	SIGNATURE	DATE			TITLE Hoop Cross-Section A Detail			
DESIGN	11/17		10/25/17						
CHKD						SHEET NO. A4			
APPRD									
MFG						SHEET 3 OF 3			
QA									

A-5



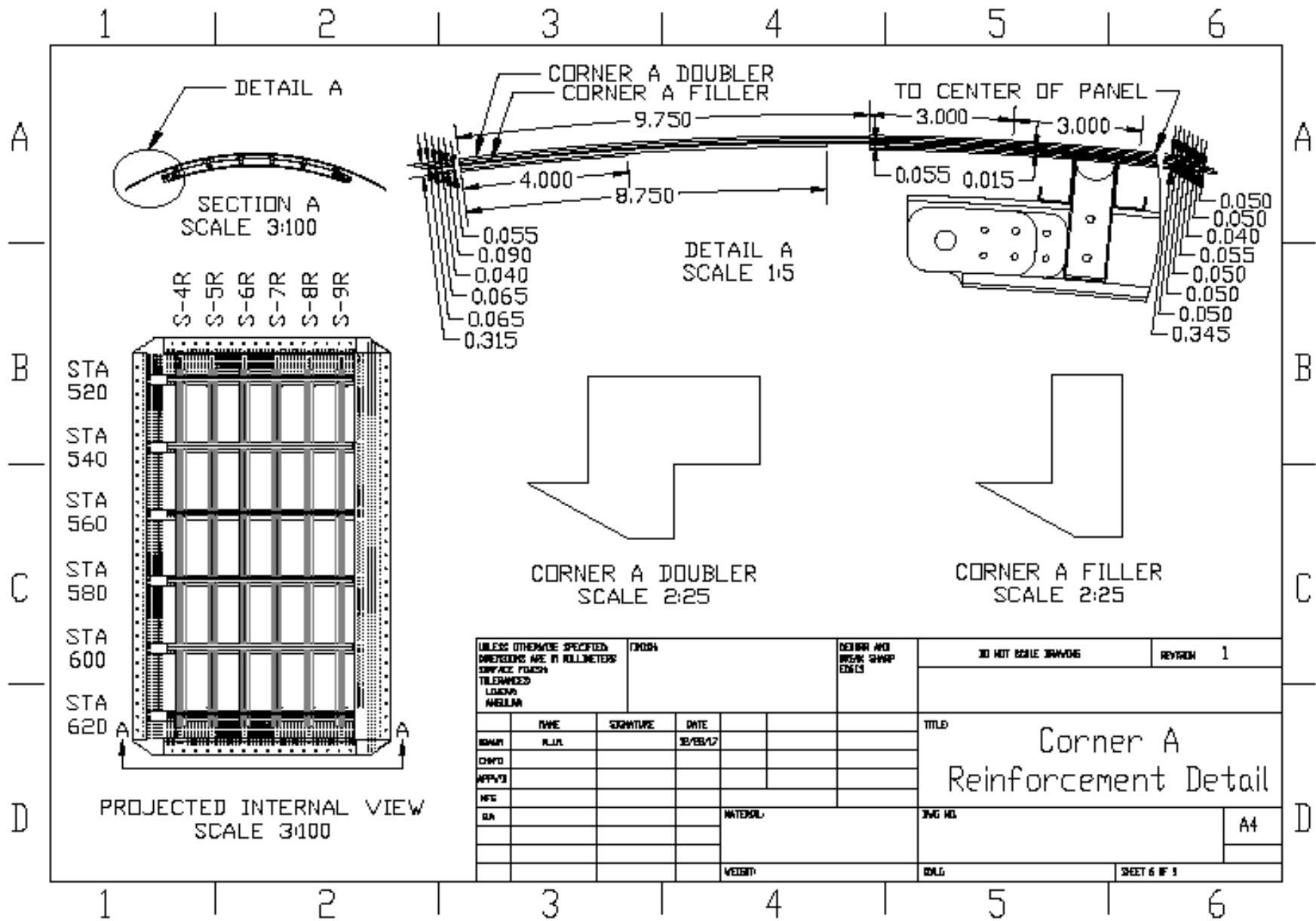
UNLESS OTHERWISE SPECIFIED DIMENSIONS ARE IN MILLIMETERS SURFACE FINISH TOLERANCES LINEAR ANGULAR		FINISH		WELDS: NOT BREAK SHARP EDGES		DO NOT SCALE DRAWING		REVISION 1	
DATE	NAME	SIGNATURE	DATE			TITLE Substructure Attachment Detail			
CHKD			REVISED						
APPRD						DWG NO.		A4	
WGT				MATERIAL		SCALE		SHEET 4 OF 9	
BA				WEIGHT					

9-V

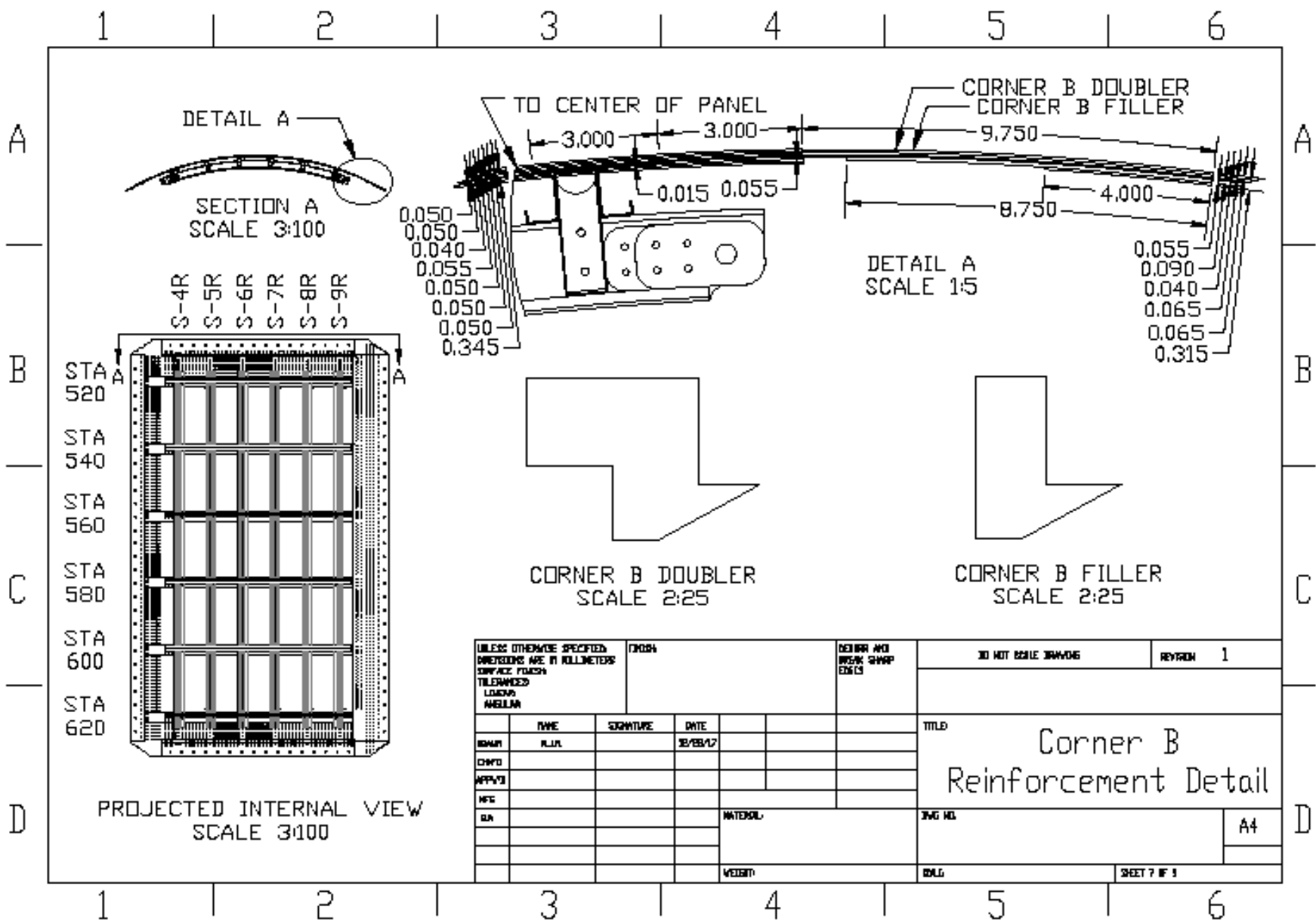


UNLESS OTHERWISE SPECIFIED, DIMENSIONS ARE IN MILLIMETERS		TYPICAL		DESIGN AND WORK SHOWN		DO NOT SCALE DRAWING		REVISION 1	
SURFACE FINISH									
TOLERANCES									
LOADING									
WELDED									
NO.	NAME	SIGNATURE	DATE			TITLE			
10001	ALJA		28/FEB/17			Frame Reinforcement Detail			
01002									
01003									
01004									
01005									
01006									
01007									
01008									
01009									
01010									
						SHEET NO.		A4	
						SHEET 5 OF 5			

A-7

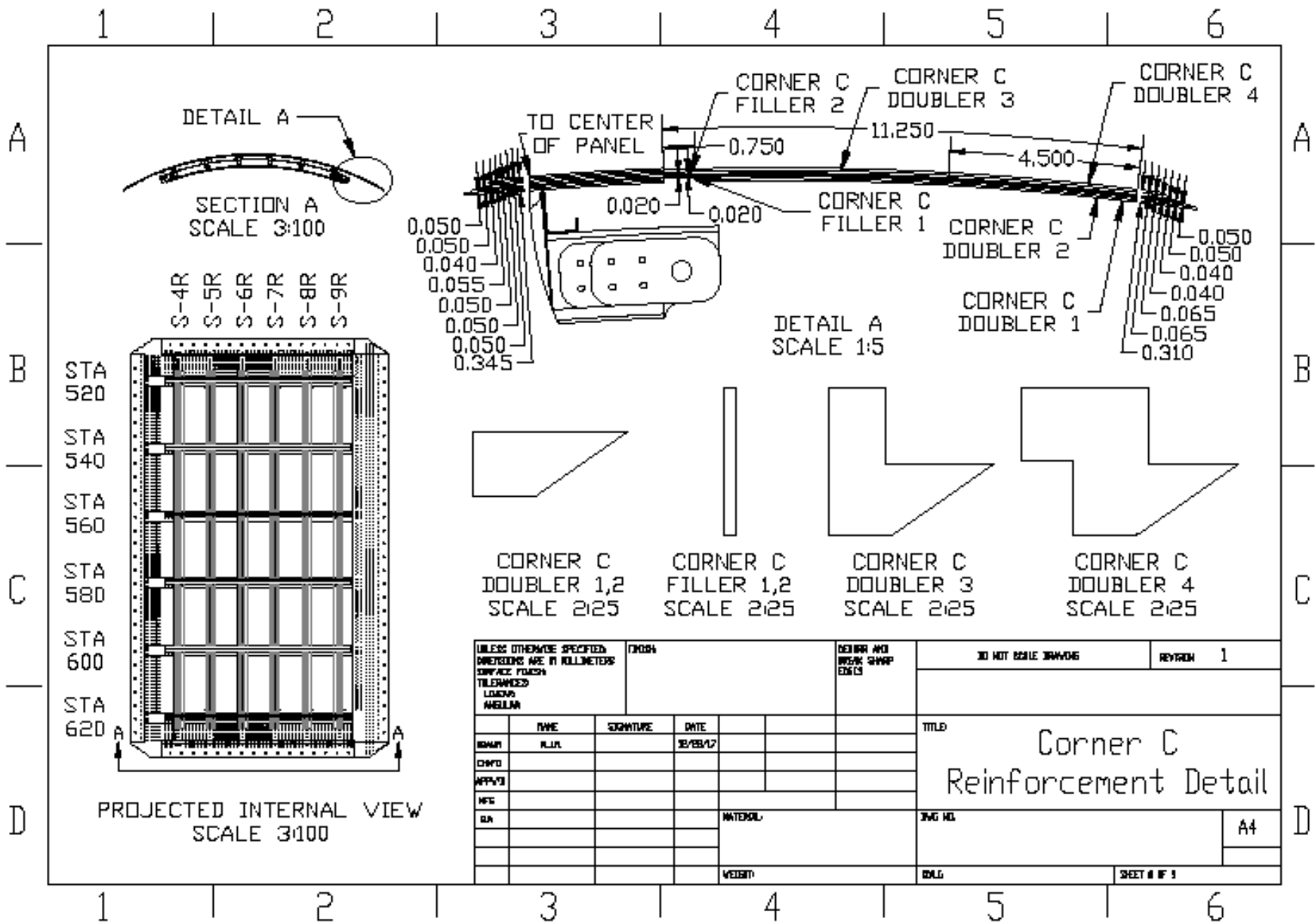


8-V



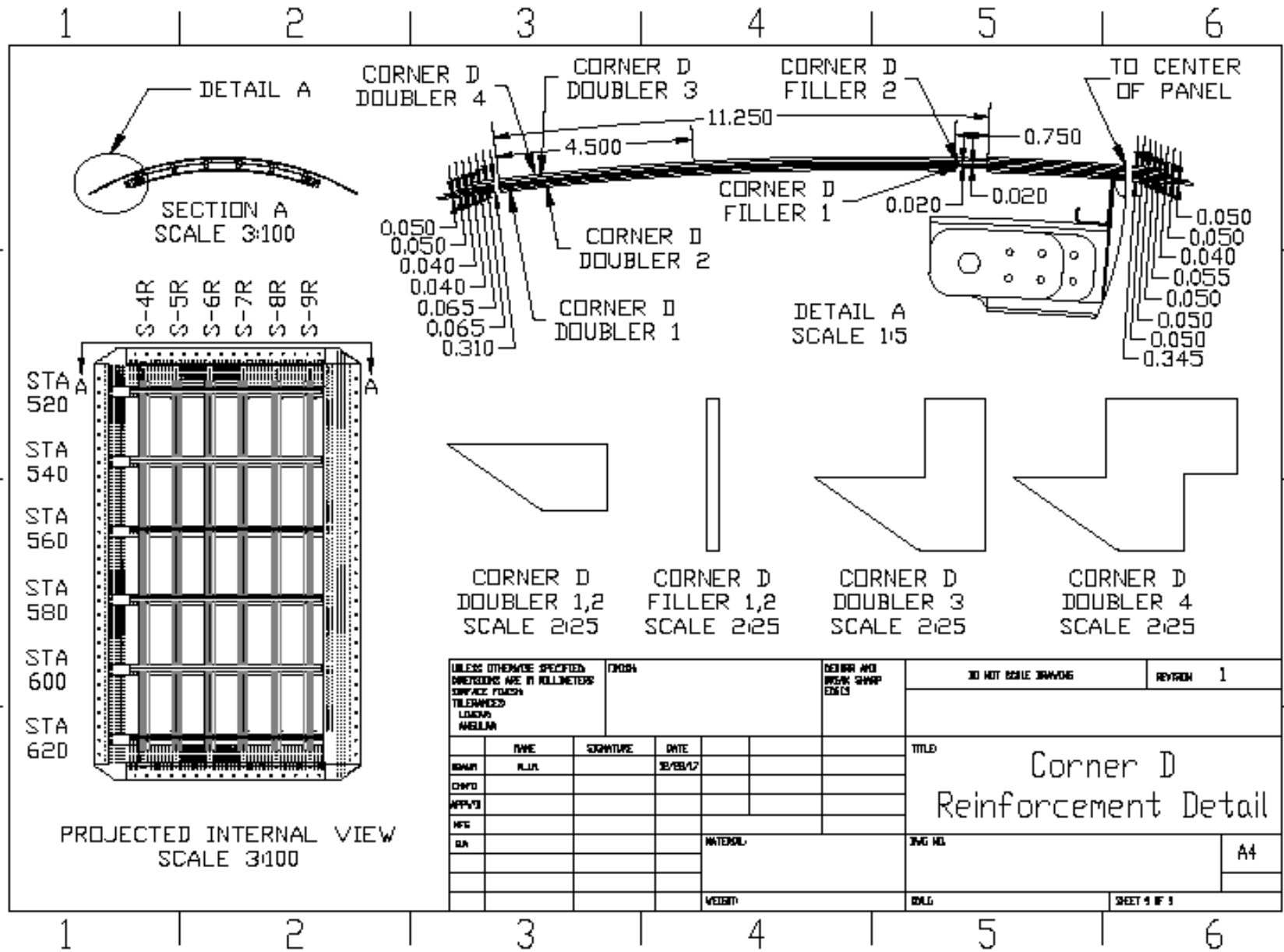
UNLESS OTHERWISE SPECIFIED, DIMENSIONS ARE IN MILLIMETERS				TYPICAL		CORNER AND WEDGE SHARP EDGES		DO NOT SCALE DIMENSIONS		REVISION 1	
SURFACE FINISH											
TOLERANCES											
LAPING											
WELDING											
NO.	DATE	SIGNATURE	DATE			TITLE					
ISSUED	KLJL		12/28/17			Corner B Reinforcement Detail					
CHG'D											
APPR'D											
CHK'D											
QA					MATERIAL	DWG NO.		A4			
					WEIGHT	DWG NO.		SHEET 7 OF 8			

6-V



UNLESS OTHERWISE SPECIFIED DIMENSIONS ARE IN MILLIMETERS SURFACE FINISH TOLERANCES LOADING WELLING				FINISH	DESIGN AND WORK SHOP DATE	30 NOT SCALE DRAWING	REVISION 1
DATE	TIME	SIGNATURE	DATE			TITLE Corner C Reinforcement Detail	
CHKD	ALJ		10/28/17			DWG NO. A4	
APPRD						SHEET # OF 3	
WFG							
BA				MATERIAL			
				WEIGHT			

A-10



UNLESS OTHERWISE SPECIFIED DIMENSIONS ARE IN MILLIMETERS SURFACE FINISH TOLERANCES LOADS WELLS				TYPICAL		REINBAR AND WREN SWAMP E2613		DO NOT SCALE DRAWING		REVISION 1	
DATE	TIME	SIGNATURE	DATE	TITLE				Corner D Reinforcement Detail			
BY	ALJ		10/28/17	DWG NO.				A4			
CHKD				MATERIAL							
APPRD				WEIGHT				DWG			
WFS								SHEET 4 OF 3			

APPENDIX B—REPAIR PATCH INSTALLATION PROCEDURE

B.1 INTRODUCTION

Six instances of damage were established prior to the onset of the test, and two instances of damage were established following the completion of 40,000 cycles. Directly following the completion of fatigue pre-cracking, adhesively bonded repair patches were installed directly over each sharp, through-thickness, center-bay crack, as shown in figure B-1. Provided in the subsequent sections are details of the repair patch installation procedure.

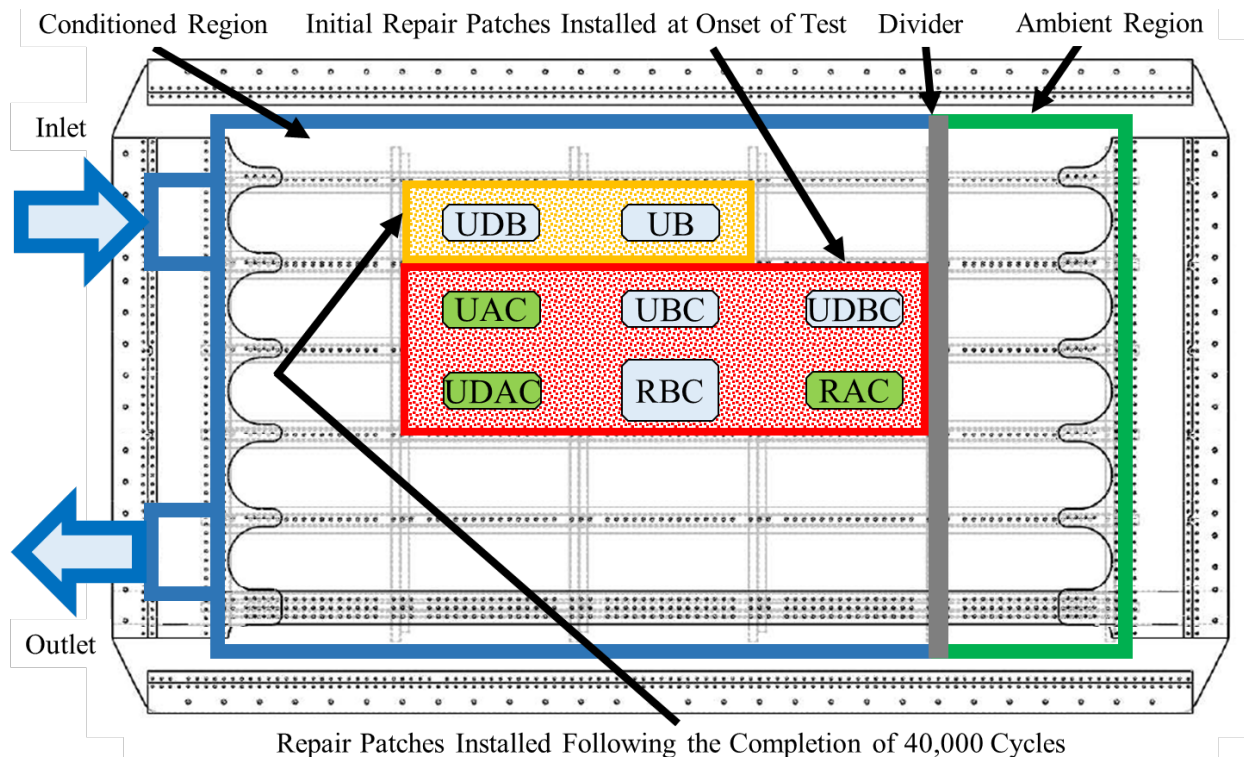


Figure B-1. Locations of the repair patches with respect to an external view of the fuselage panel

B.2 REPAIR PATCH INSTALLATION PROCEDURE

Each of the repair patches depicted in the previous section (i.e., RAC, RBC, UAC, UB, UBC, UDB, and UDBC) were installed using the same installation procedure. In general, the procedure consisted of five main steps: 1) external fuselage panel surface preparation; 2) deoxidization; 3) application of sol-gel coating; 4) application of bonding primer; and 5) co-curing. For each step, inherent details were developed and provided by The Boeing Company. A brief overview of these steps is provided in the subsequent sections.

B.2.1 External Fuselage Panel Surface Preparation

1. All the surface coatings and residual adhesive residues were removed down to the bare Al.

2. The bare Al surface was cleaned with solvent, and all contaminants were removed.

B.2.2 Deoxidization

1. A region slightly larger than the bond area was grit-blasted, as shown in figure B-2.
2. Loose grit residue was removed with clean, dry compressed air or nitrogen.



Figure B-2. Grit blasting

B.2.3 Application of Sol-Gel Coating

1. Sol-gel solution was applied by brushing with a natural bristle brush. The surface was kept wet during application, as shown in figure B-3.
2. Sol-gel parts were left to dry under ambient conditions for a minimum of 60 minutes.

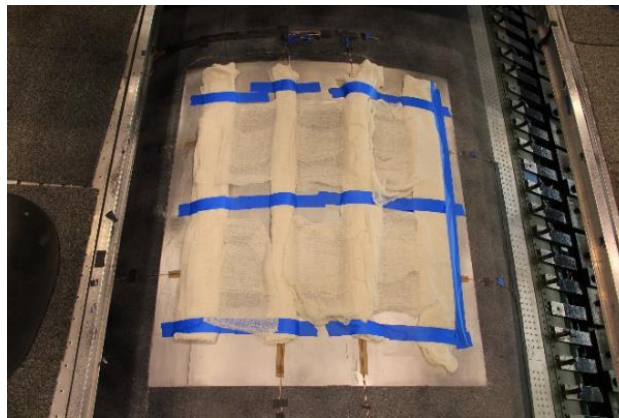


Figure B-3. Applying sol-gel solution

B.2.4 Application of Bonding Primer

1. Bonding primer was thoroughly mixed by agitation in the original container.

2. The primer was transferred to a reservoir with continued agitation during application.
3. The adhesive primer was applied to the bond surface to obtain a cured film thickness of 0.00015–0.00040 inch (0.15–0.40 mil).
4. Primed parts were allowed to dry at 135°F using a heat gun for 60 minutes before curing.

B.2.5 Co-Curing

1. The Henkel EA9696 OST (one tacky side) film adhesive and patch were applied to the sol-gel-treated and primed surface using standard bond procedures.
2. Both the adhesive and primer were co-cured for 90 minutes at $250^{\circ} \pm 10^{\circ}\text{F}$ using standard heat blanket and vacuum bag processes, as shown in figure B-4.

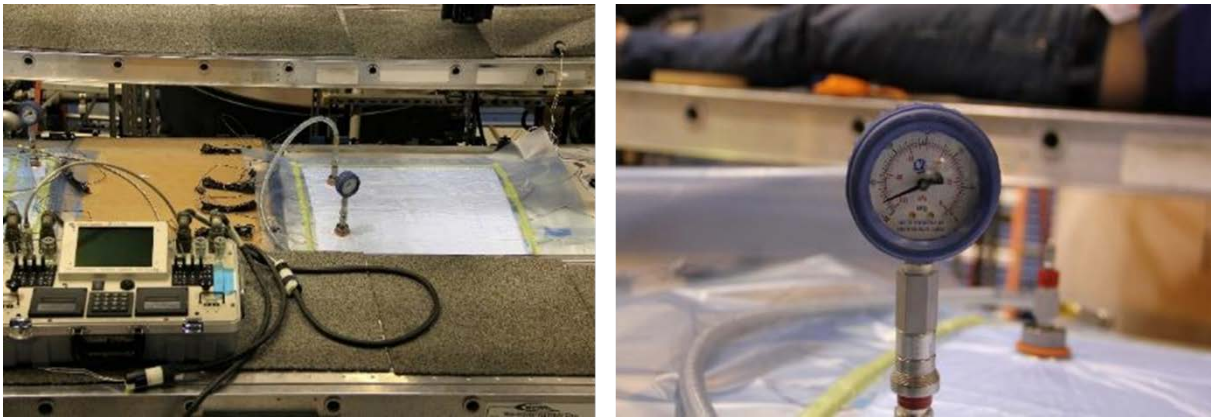


Figure B-4. Co-curing process

APPENDIX C—STRAIN GAUGE LAYOUTS

C.1 INTRODUCTION

The fuselage panel was instrumented with strain gauges for the purpose of continuously monitoring hoop strain distribution during fatigue pre-cracking, repair patch installation, hot-wet conditioning, fatigue cracking, and quasistatic strain surveys. Among the specific instruments used were Vishay Precision Group (VPG) linear pattern strain gauges (gauge designation CEA-13-062UW-350) and VPG rectangular rosette strain gauges (gauge designation CEA-13-062UR-350), as shown in figure C-1a and C-1b, respectively. In general, strain gauges installed throughout this test can be organized into four distinct groups: 1) those installed and monitored prior to damage initiation (i.e., prior to notch cutting); 2) those installed and monitored during the repair patch installation and the 4-week hot-wet conditioning period; 3) those installed and monitored during the first 40,000 cycles of testing; and 4) those installed and monitored during the final 52,834 cycles of testing. In each case, surface areas were prepared in accordance with VPG Bulletin B-129-8, and strain gauges were bonded in accordance with VPG Bulletins B-137 and B-127-14. Three-conductor Teflon®-coated twisted cables (designation 330-FTE) were used to connect the strain gauges to the data acquisition (DAQ). Strain gauges located on the external surface of the fuselage panel were covered with Teflon® tape and sealed with B-1/2 sealant.

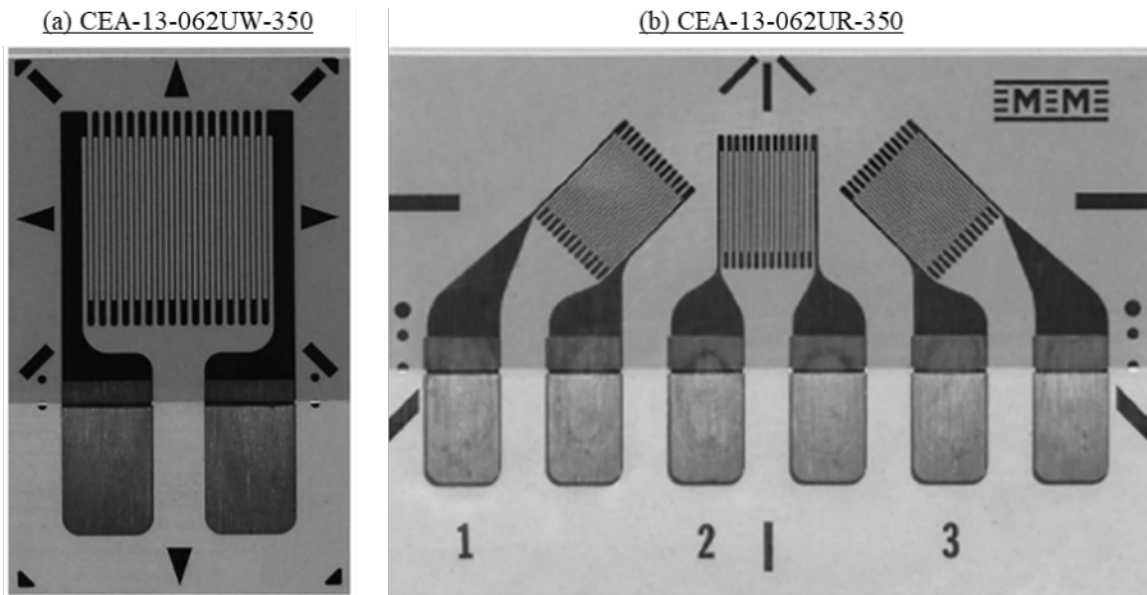


Figure C-1. Strain gauge used throughout the duration of the test: (a) uniaxial and (b) rosette

C.2 STRAIN GAUGE INSTRUMENTATION PRIOR TO NOTCH CUTTING

Prior to the initiation of damages in the fuselage panel, select areas of the internal fuselage panel skin, select areas of the external fuselage panel skin, select fuselage panel frames, and select fuselage panel stringers were instrumented with VPG linear pattern strain gauges and VPG rectangular rosette strain gauges. These strain gauges were specifically installed for the purpose of conducting quasistatic strain surveys prior to the initiation of damage in the fuselage panel. When

these strain surveys were complete, because the location of several of these strain gauges interfered with the location of a repair patch and because the number of data acquisition channels were limited, they were either removed or no longer monitored (i.e., disconnected from the DAQ). Schematics depicting the precise location of strain gauges installed on external fuselage panel surface, stringers, the internal fuselage panel surface, and frames are provided in figures C-2a–C-2d, respectively.

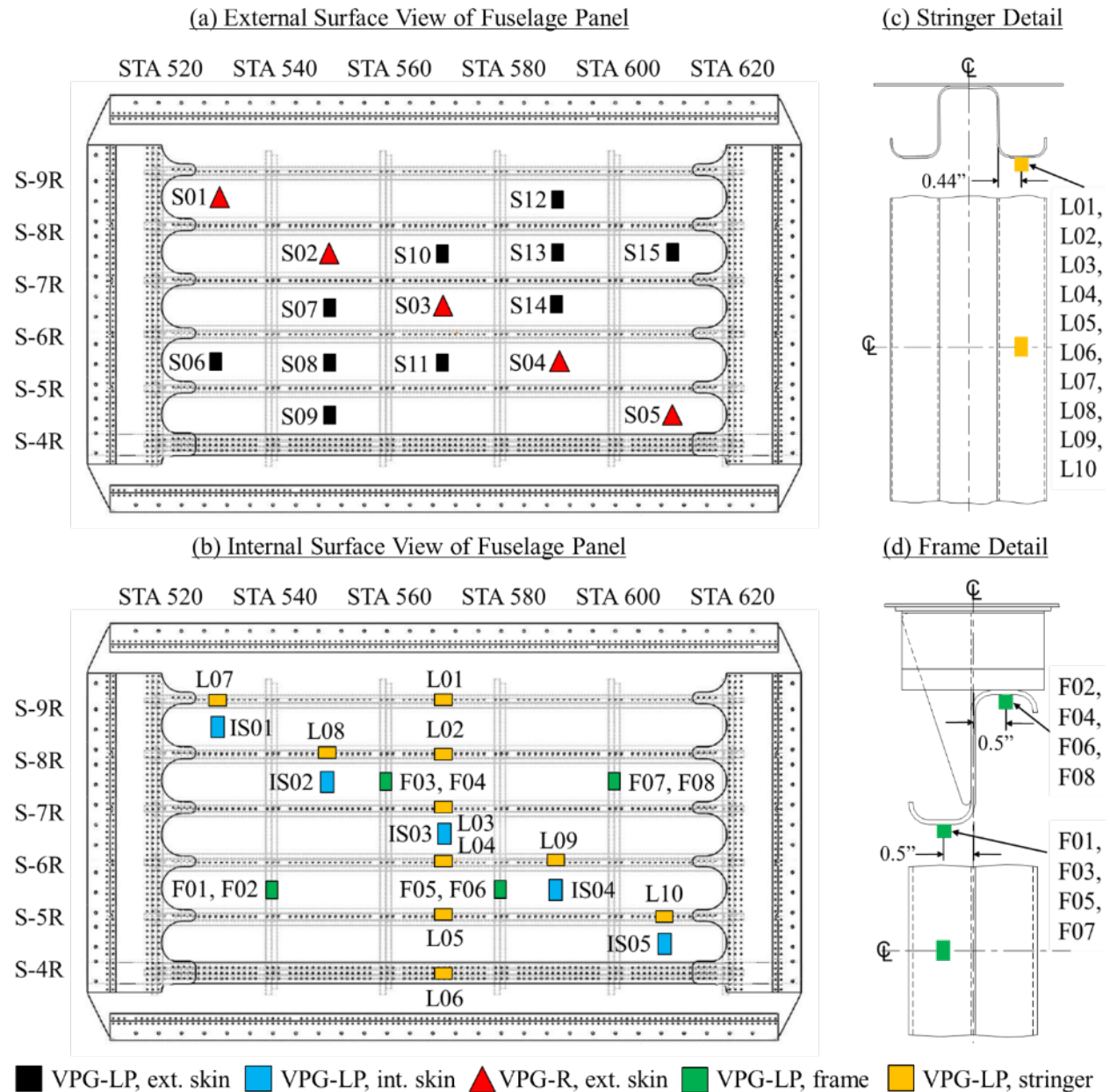


Figure C-2. Strain gauges installed before cutting notches in the panel: (a) external fuselage panel surface, (b) internal fuselage panel surface, (c) stringer detail, and (d) frame detail

C.3 STRAIN GAUGE INSTRUMENTATION DURING FIRST 40,000 CYCLES

Following the initiation of damages in the fuselage panel and prior to patch installation, VPG linear pattern strain gauges were installed on the internal fuselage panel skin and the external fuselage panel skin in the vicinity of each instance of damage. These strain gauges were specifically installed for the purpose of monitoring the distribution of strain during fatigue pre-cracking, patch installation, 4 weeks of hot-wet conditioning, and the application of quasistatic strain survey load spectrums. Following repair patch installation, VPG linear pattern strain gauges were also installed on the top surface of each repair patch. In general, the quantity and location of the strain gauges installed in the vicinity of each repair patch depended on the size and type of repair patch. A summary of strain gauges installed in the vicinity of each repair patch during the first 40,000 cycles of testing is provided in table C-1. Schematics depicting the location of strain gauges in the vicinity of each repair patch during this period are provided in the subsequent sections.

Table C-1. Strain gauges in the vicinity of each repair patch during the first 40,000 cycles

Repair Patch	Strain Gauge Type	Strain Gauge Count	Quantity of Strain Gauges Per Location		
			Internal Panel Surface	External Panel Surface	Top of Repair Patch
RAC	Rosette	0	0	0	0
	Uniaxial	26	19	6	1
RBC	Rosette	0	0	0	0
	Uniaxial	24	19	4	1
UAC	Rosette	0	0	0	0
	Uniaxial	26	19	6	1
UBC	Rosette	0	0	0	0
	Uniaxial	28	21	6	1
UDAC	Rosette	0	0	0	0
	Uniaxial	26	19	6	1
UDBC	Rosette	0	0	0	0
	Uniaxial	28	21	6	1

C.3.1 REPAIR PATCH RAC

Twenty-six uniaxial strain gauges were installed in the vicinity of repair patch RAC—on the internal and external panel surfaces and on top of the repair patch—as shown in figures C-3 and C-4.

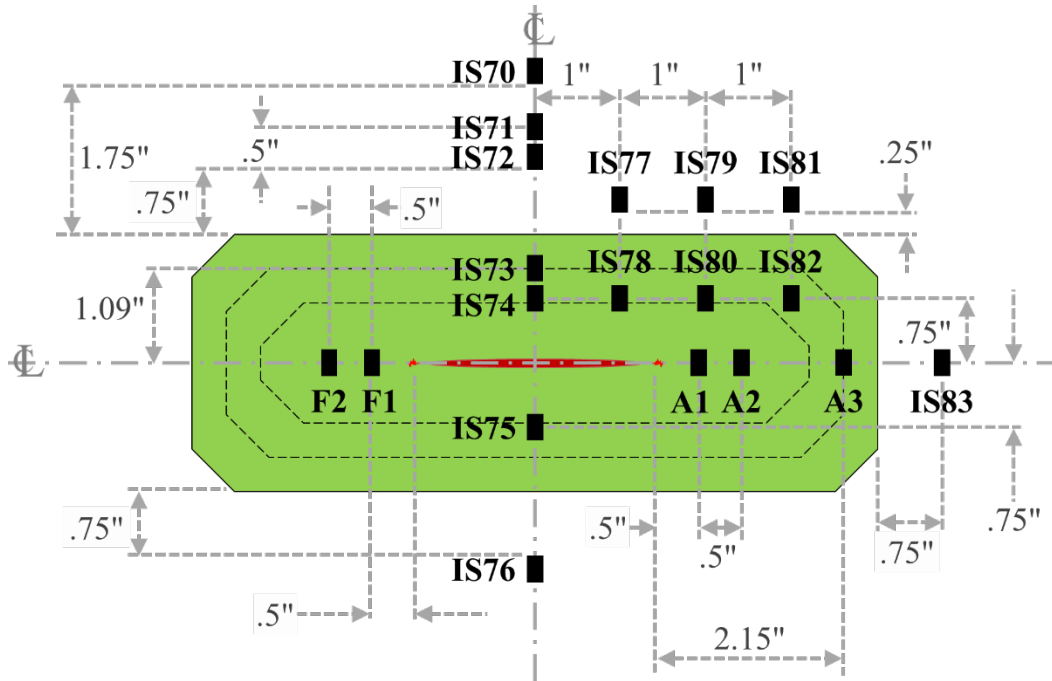


Figure C-3. Internal strain gauges during first 40,000 cycles of testing, repair patch RAC

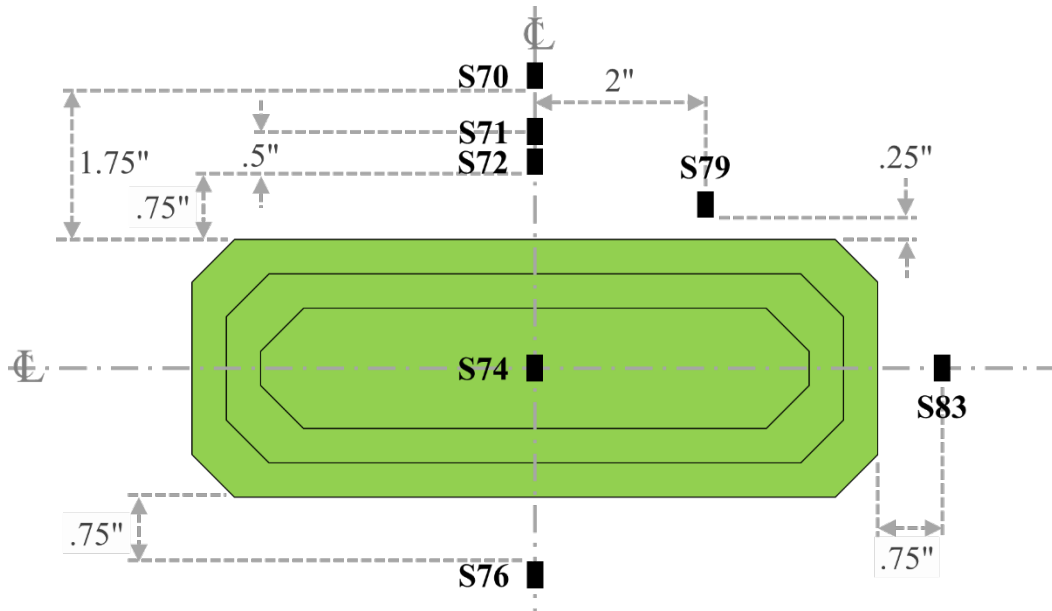


Figure C-4. External strain gauges during first 40,000 cycles of testing, repair patch RAC

C.3.2 REPAIR PATCH RBC

Twenty-four uniaxial strain gauges were installed in the vicinity of repair patch RBC—on the internal and external panel surfaces and on top of the repair patch—as shown in figures C-5 and C-6.

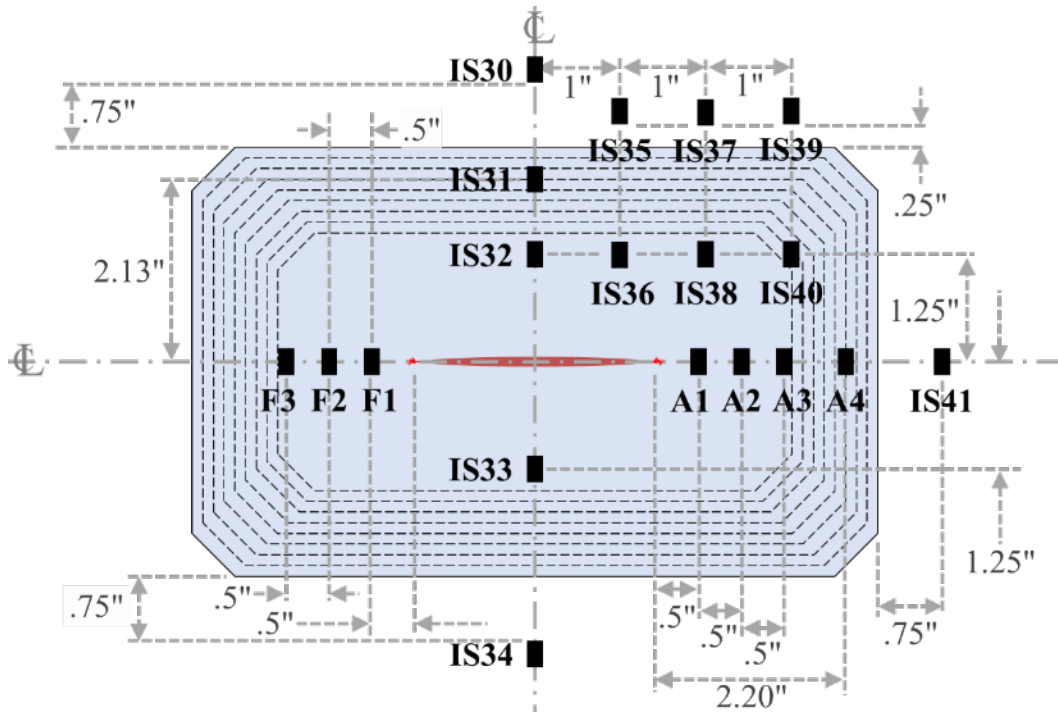


Figure C-5. Internal strain gauges during first 40,000 cycles of testing, repair patch RBC

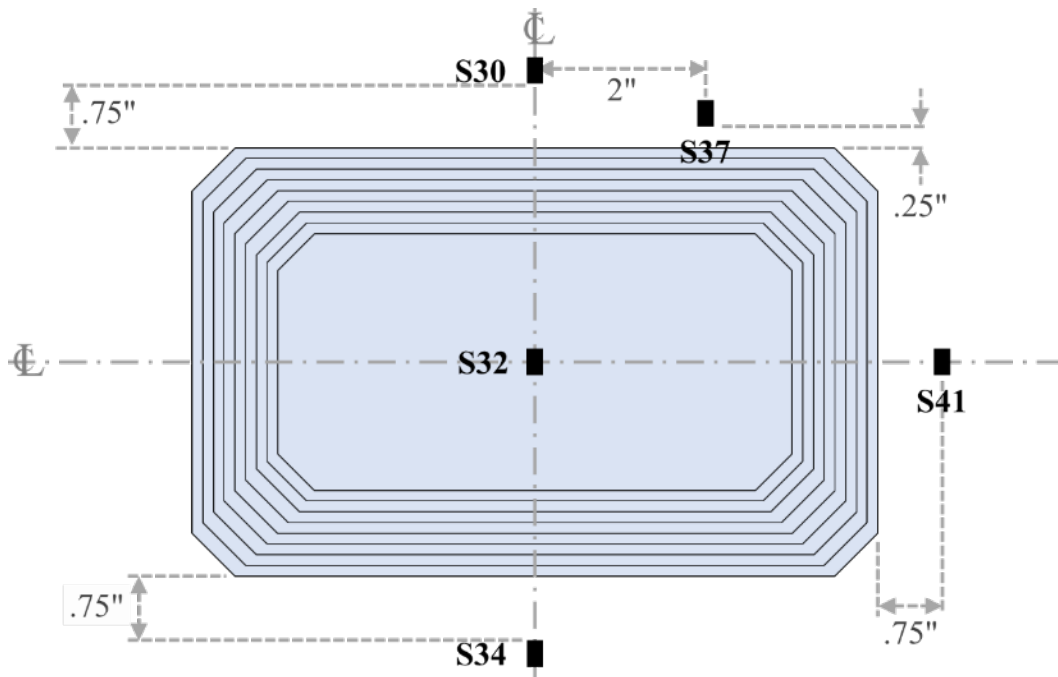


Figure C-6. External strain gauges during first 40,000 cycles of testing, repair patch RBC

C.3.3 REPAIR PATCH UAC

Twenty-six uniaxial strain gauges were installed in the vicinity of repair patch UAC—on the internal and external panel surfaces and on top of the repair patch—as shown in figures C-7 and C-8.

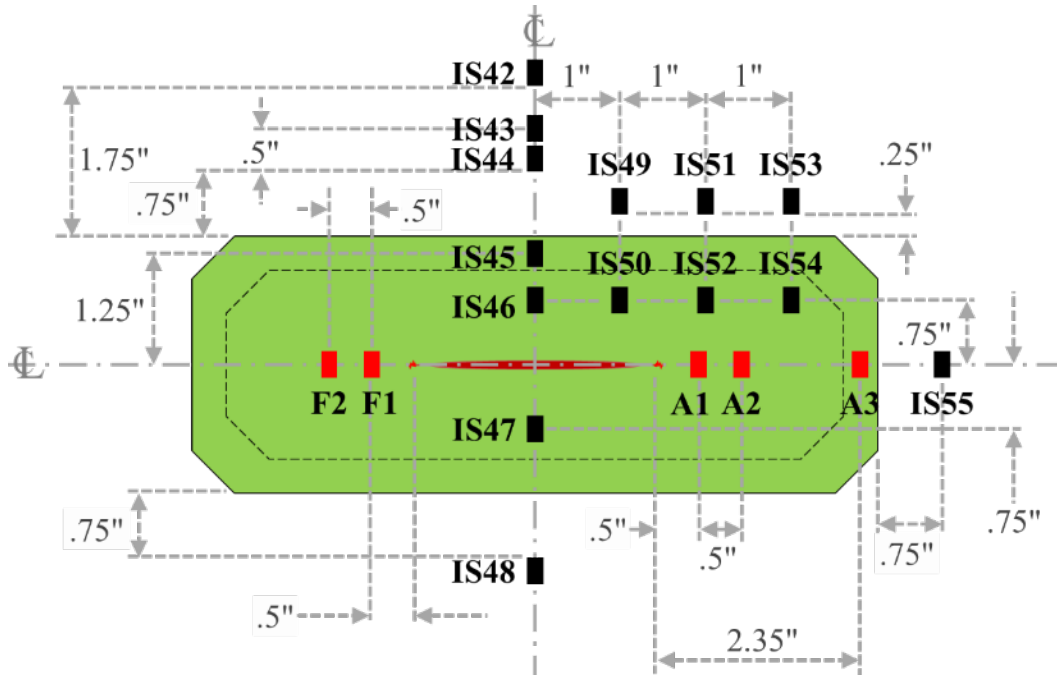


Figure C-7. Internal strain gauges during first 40,000 cycles of testing, repair patch UAC

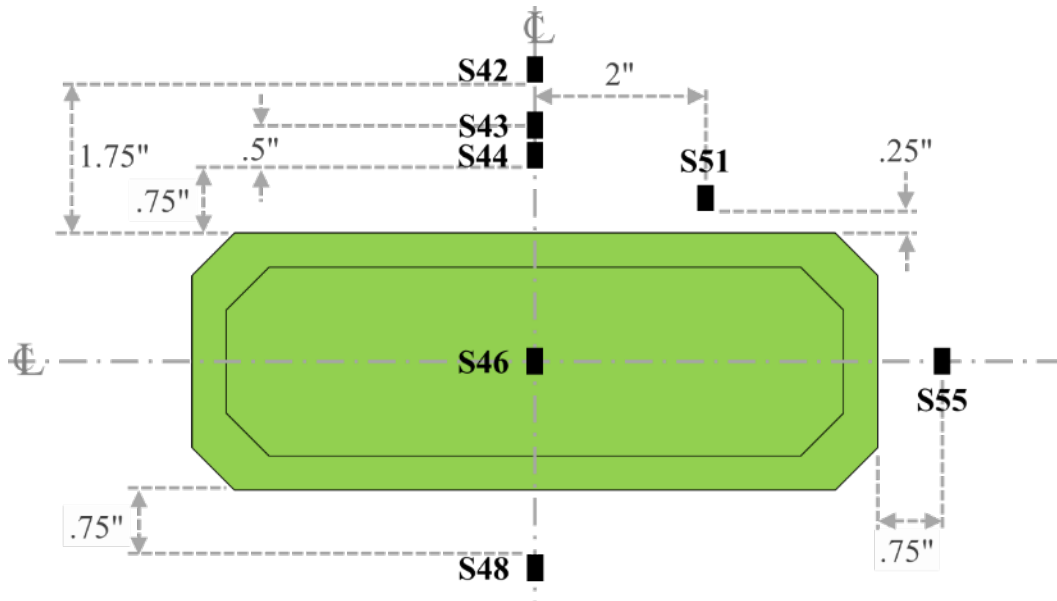


Figure C-8. External strain gauges during first 40,000 cycles of testing, repair patch UAC

C.3.4 REPAIR PATCH UBC

Twenty-eight uniaxial strain gauges were installed in the vicinity of repair patch UBC—on the internal and external panel surfaces and on top of the repair patch—as shown in figures C-9 and C-10.

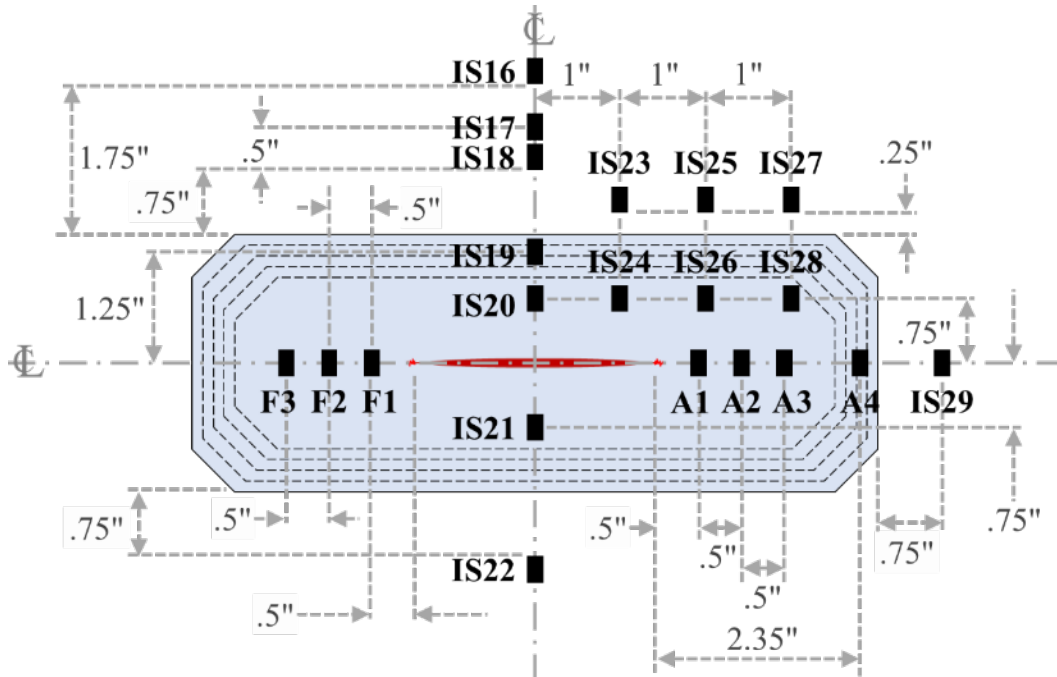


Figure C-9. Internal strain gauges during first 40,000 cycles of testing, repair patch UBC

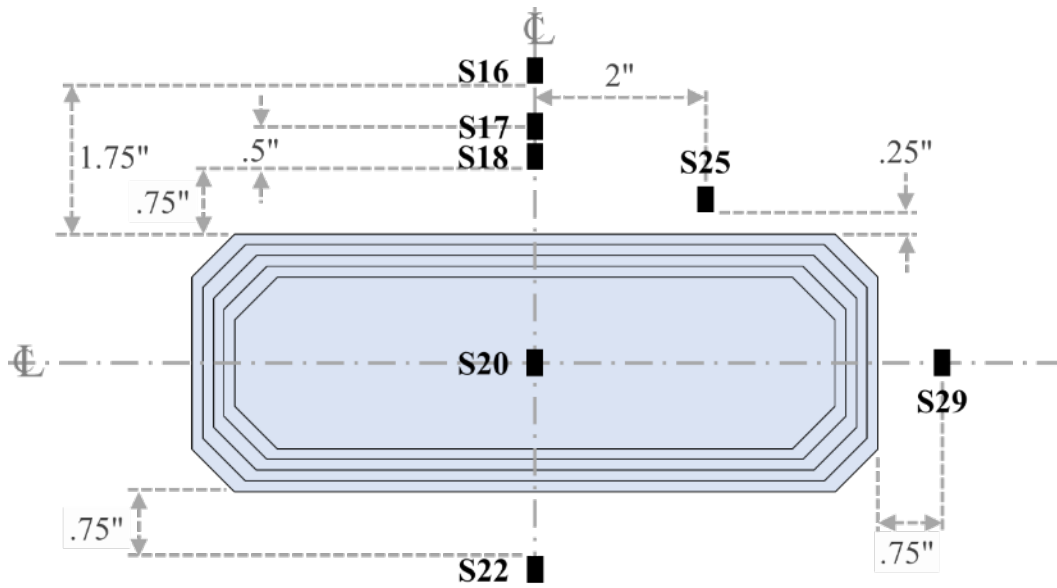


Figure C-10. External strain gauges during first 40,000 cycles of testing, repair patch UBC

C.3.5 REPAIR PATCH UDAC

Twenty-six uniaxial strain gauges were installed in the vicinity of repair patch UDAC—on the internal and external panel surfaces and on top of the repair patch—as shown in figure C-11 and figure C-12.

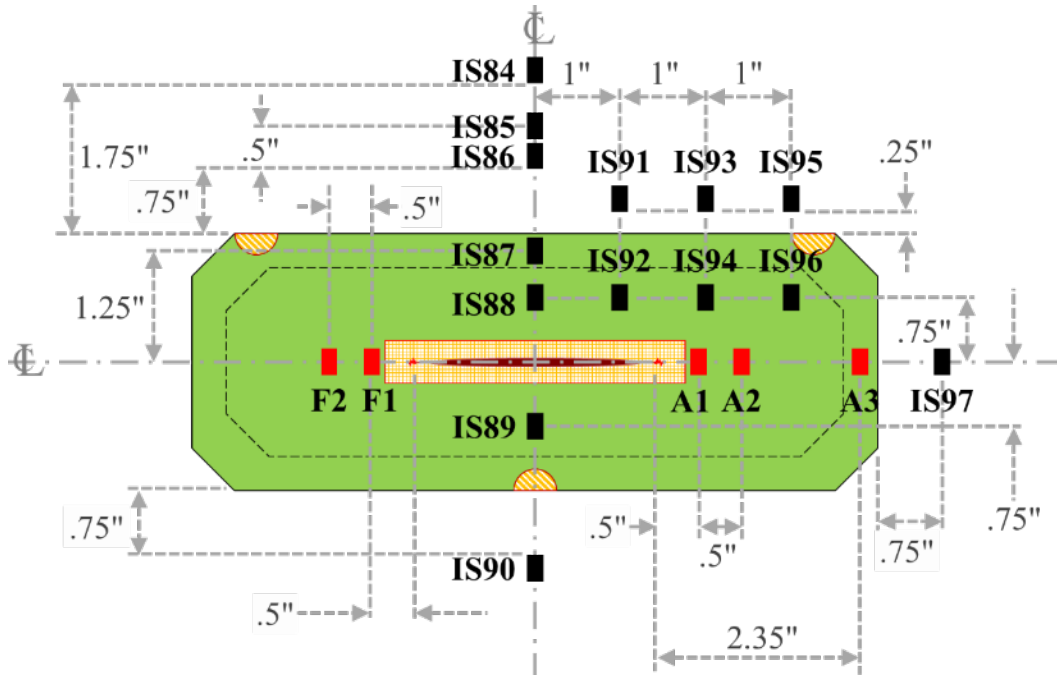


Figure C-11. Internal strain gauges during first 40,000 cycles of testing, repair patch UDAC

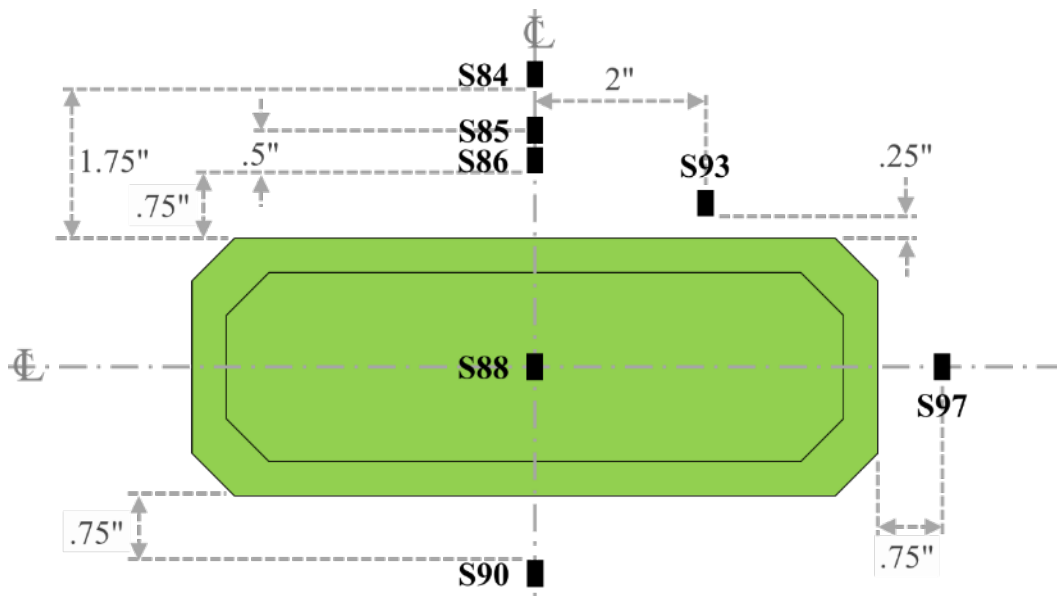


Figure C-12. External strain gauges during first 40,000 cycles of testing, repair patch UDAC

C.3.6 REPAIR PATCH UDBC

Twenty-eight uniaxial strain gauges were installed in the vicinity of repair patch UDBC—on the internal and external panel surfaces and on top of the repair patch—as shown in figures C-13 and C-14.

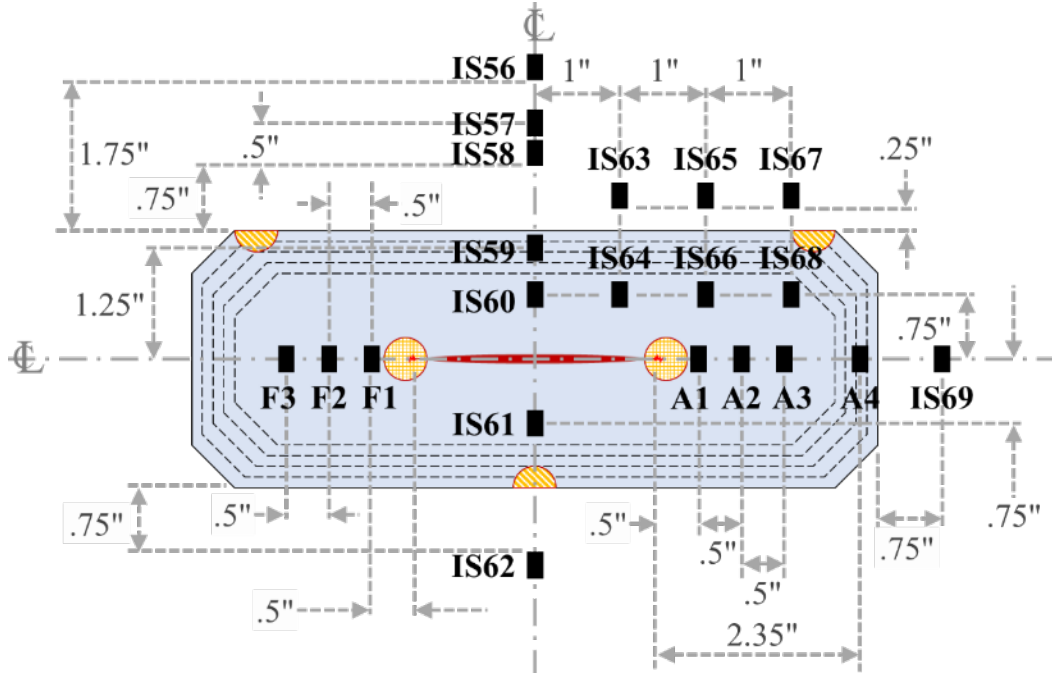


Figure C-13. Internal strain gauges during first 40,000 cycles of testing, repair patch UDBC

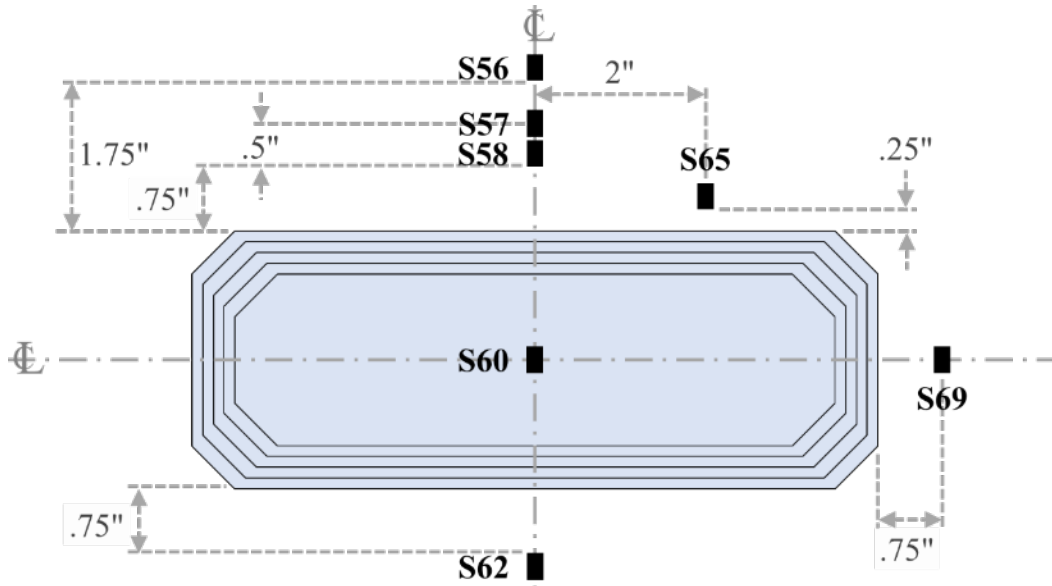


Figure C-14. External strain gauges during first 40,000 cycles of testing, repair patch UDBC

C.4 STRAIN GAUGE INSTRUMENTATION DURING FINAL 52,834 CYCLES

Following the completion of 40,000 cycles, the installation of two additional repair patches facilitated the need to install a new batch of strain gauges. Because the number of DAQ channels were limited, a significant number of previously installed strain gauges were removed. In general, a majority of the strain gauges that were removed were those that were installed outside of the vertical and horizontal axes of symmetry. When these strain gauges were removed, the DAQ channels were used to accommodate the strain gauges installed in the vicinity of the two new repair patches. The quantity and location of all other strain gauges remained the same. A summary of strain gauges installed in the vicinity of each repair patch during the final 52,834 cycles of testing is provided in table C-2. Schematics depicting the location of strain gauges in the vicinity of each repair patch during this period are provided in the subsequent sections.

Table C.2. Strain gauges in the vicinity of each repair patch during the final 52,834 cycles

Repair Patch	Strain Gauge Type	Strain Gauge Count	Quantity of Strain Gauges Per Location		
			Internal Panel Surface	External Panel Surface	Top of Repair Patch
RAC	Rosette	0	0	0	0
	Uniaxial	13	8	4	1
RBC	Rosette	0	0	0	0
	Uniaxial	19	14	4	1
UAC	Rosette	0	0	0	0
	Uniaxial	13	8	4	1
UB	Rosette	0	0	0	0
	Uniaxial	17	12	4	1
UBC	Rosette	0	0	0	0
	Uniaxial	19	14	4	1
UDAC	Rosette	0	0	0	0
	Uniaxial	17	12	4	1
UDB	Rosette	0	0	0	0
	Uniaxial	17	12	4	1
UDBC	Rosette	0	0	0	0
	Uniaxial	19	14	4	1

C.4.1 REPAIR PATCH RAC

Thirteen uniaxial strain gauges were installed in the vicinity of repair patch RAC—on the internal and external panel surfaces and on top of the repair patch—as shown in figures C-15 and C-16.

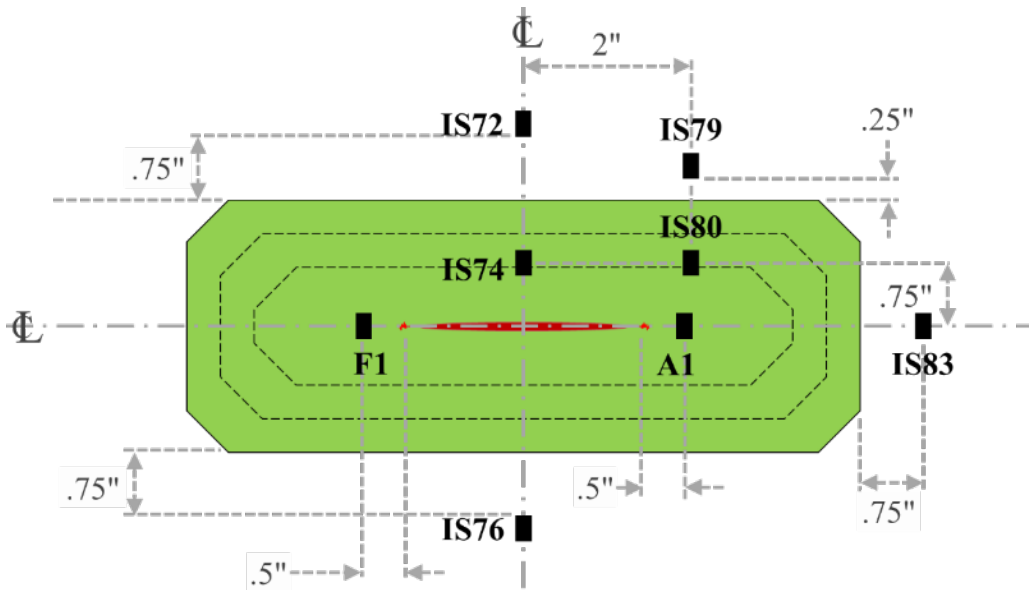


Figure C-15. Internal strain gauges during final 52,834 cycles of testing, repair patch RAC

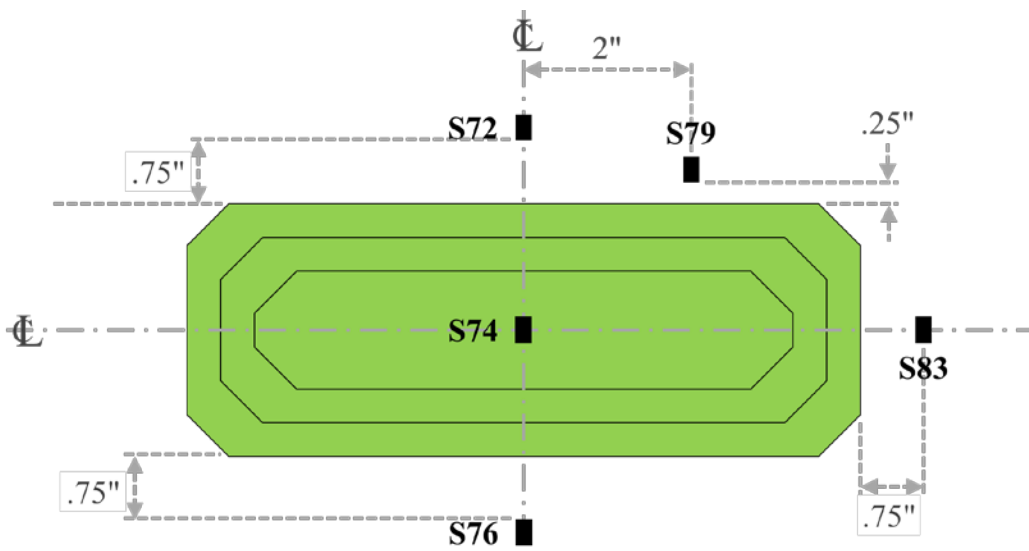


Figure C-16. External strain gauges during final 52,834 cycles of testing, repair patch RAC

C.4.2 REPAIR PATCH RBC

Nineteen uniaxial strain gauges were installed in the vicinity of repair patch RBC—on the internal and external panel surfaces and on top of the repair patch—as shown in figures C-17 and C-18.

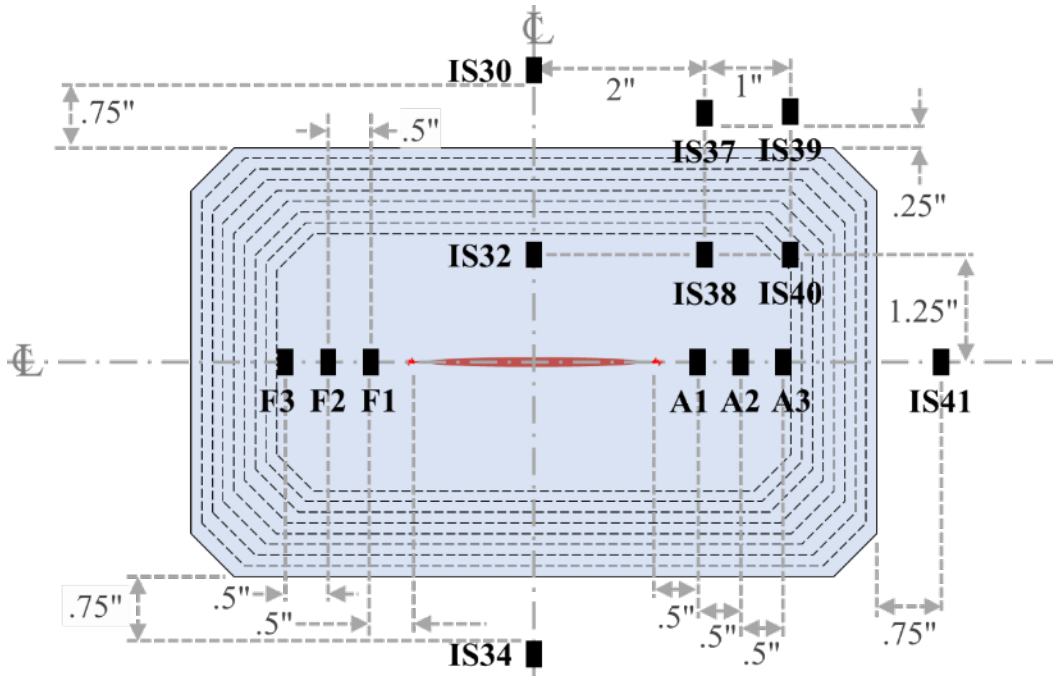


Figure C-17. Internal strain gauges during final 52,834 cycles of testing, repair patch RBC

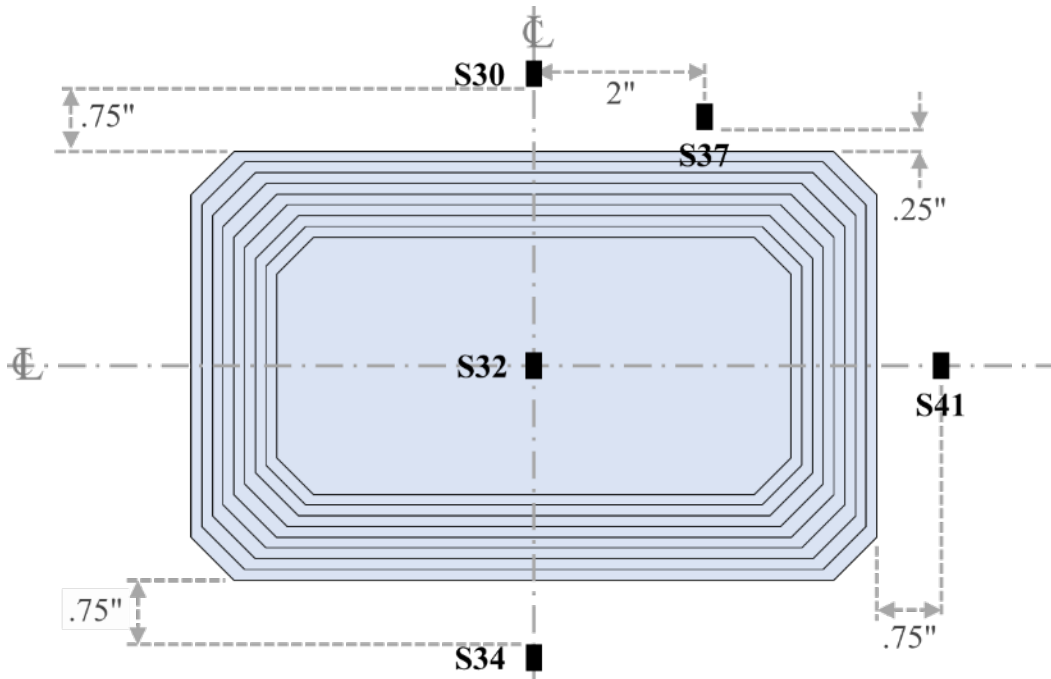


Figure C-18. External strain gauges during final 52,834 cycles of testing, repair patch RBC

C.4.3 REPAIR PATCH UAC

Thirteen uniaxial strain gauges were installed in the vicinity of repair patch UAC—on the internal and external panel surfaces and on top of the repair patch—as shown in figures C-19 and C-20.

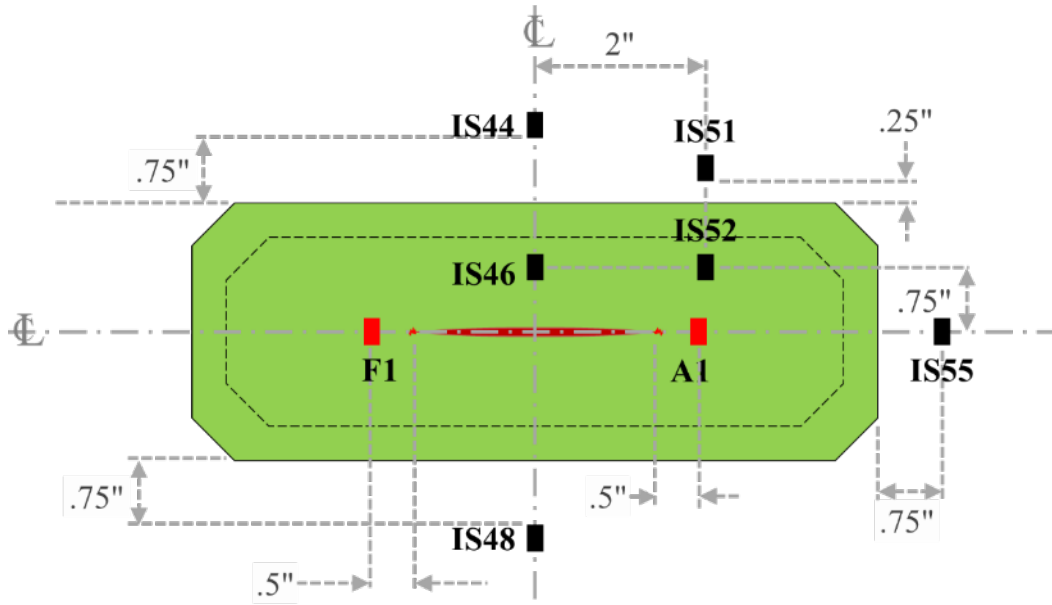


Figure C-19. Internal strain gauges during final 52,834 cycles of testing, repair patch UAC

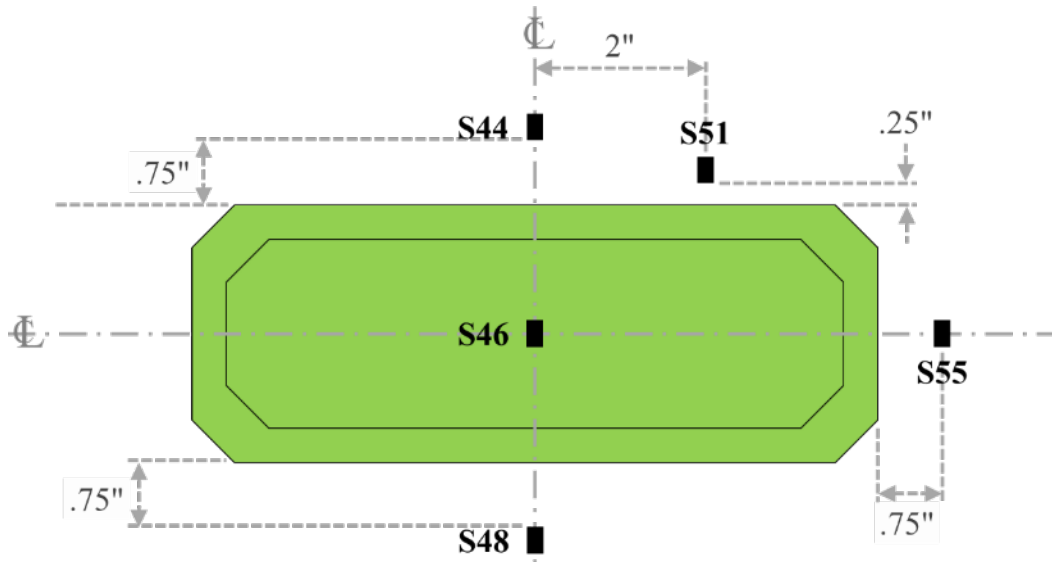


Figure C-20. External strain gauges during final 52,834 cycles of testing, repair patch UAC

C.4.4 REPAIR PATCH UB

Seventeen uniaxial strain gauges were installed in the vicinity of repair patch UB—on the internal and external panel surfaces and on top of the repair patch—as shown in figures C-21 and C-22.

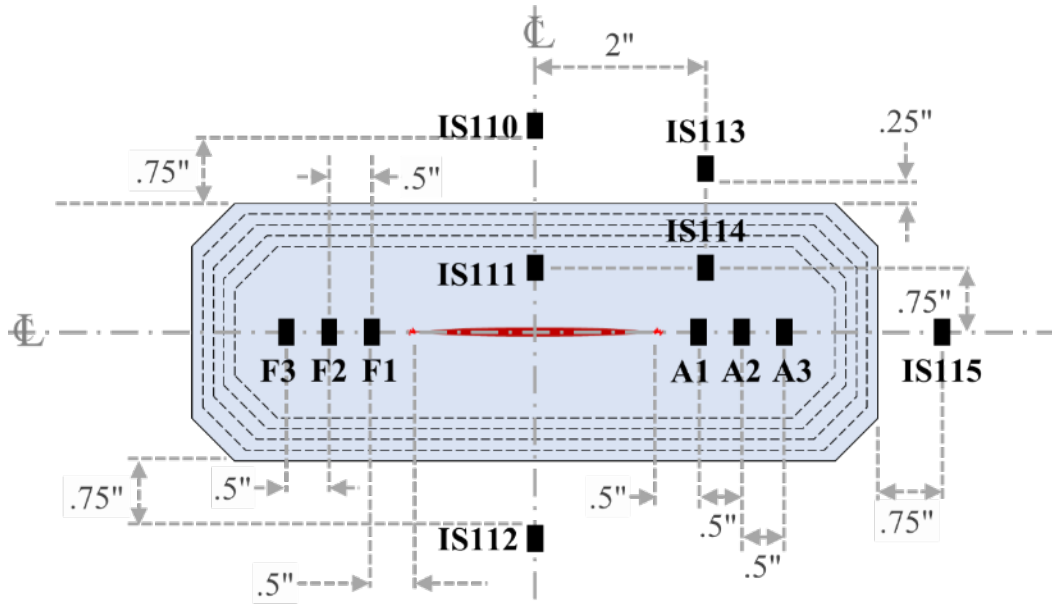


Figure C-21. Internal strain gauges during final 52,834 cycles of testing, repair patch UB

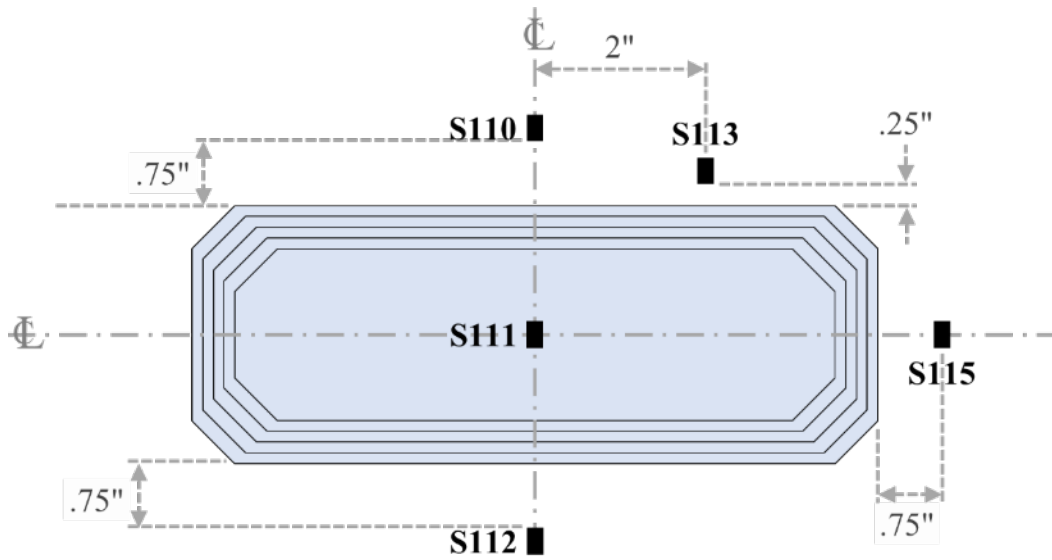


Figure C-22. External strain gauges during final 52,834 cycles of testing, repair patch UB

C.4.5 REPAIR PATCH UBC

Nineteen uniaxial strain gauges were installed in the vicinity of repair patch UBC—on the internal and external panel surfaces and on top of the repair patch—as shown in figures C-23 and C-24.

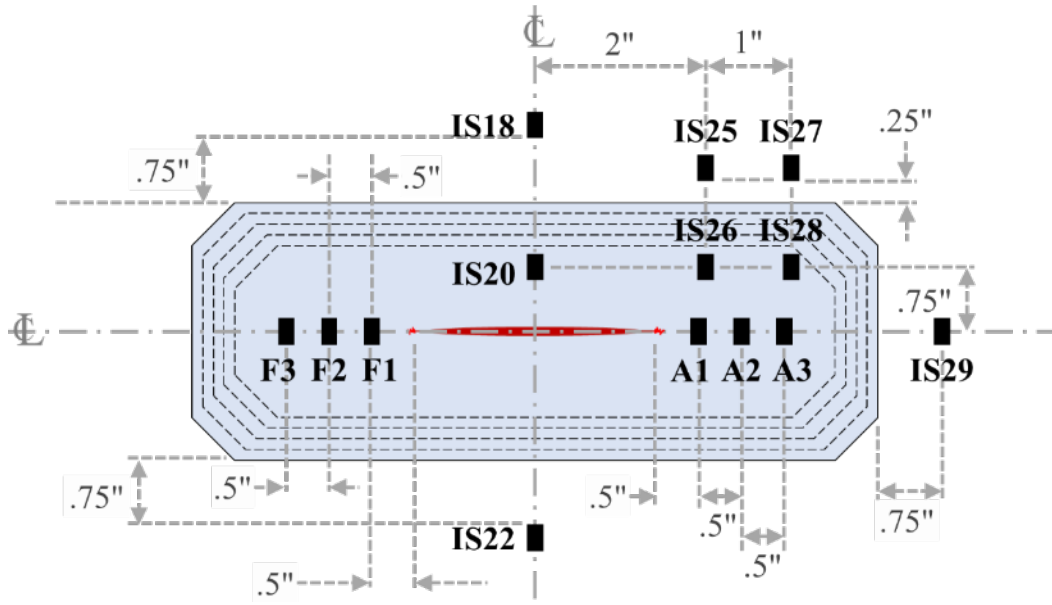


Figure C-23. Internal strain gauges during final 52,834 cycles of testing, repair patch UBC

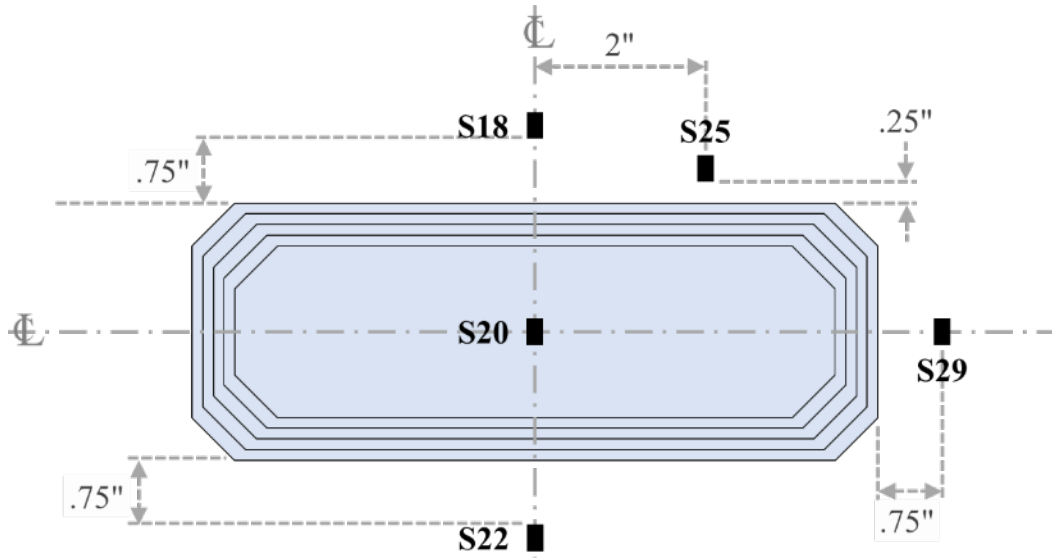


Figure C-24. External strain gauges during final 52,834 cycles of testing, repair patch UBC

C.4.6 REPAIR PATCH UDAC

Seventeen uniaxial strain gauges were installed in the vicinity of repair patch UDAC—on the internal and external panel surfaces and on top of the repair patch—as shown in figures C-25 and C-26.

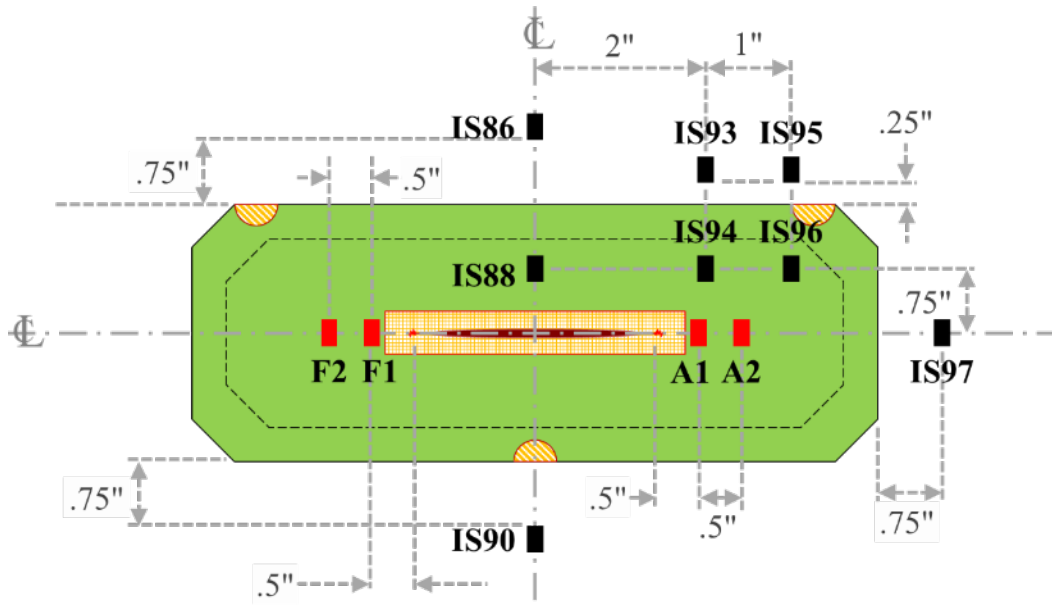


Figure C-25. Internal strain gauges during final 52,834 cycles of testing, repair patch UDAC

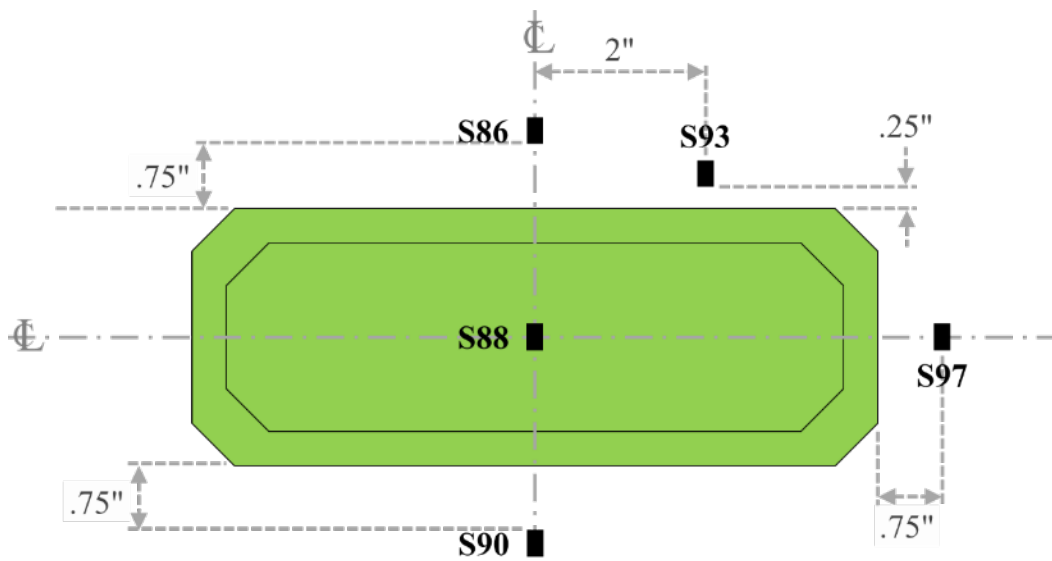


Figure C-26. External strain gauges during final 52,834 cycles of testing, repair patch UDAC

C.4.7 REPAIR PATCH UDB

Seventeen uniaxial strain gauges were installed in the vicinity of repair patch UDB—on the internal and external panel surfaces and on top of the repair patch—as shown in figures C-27 and C-28.

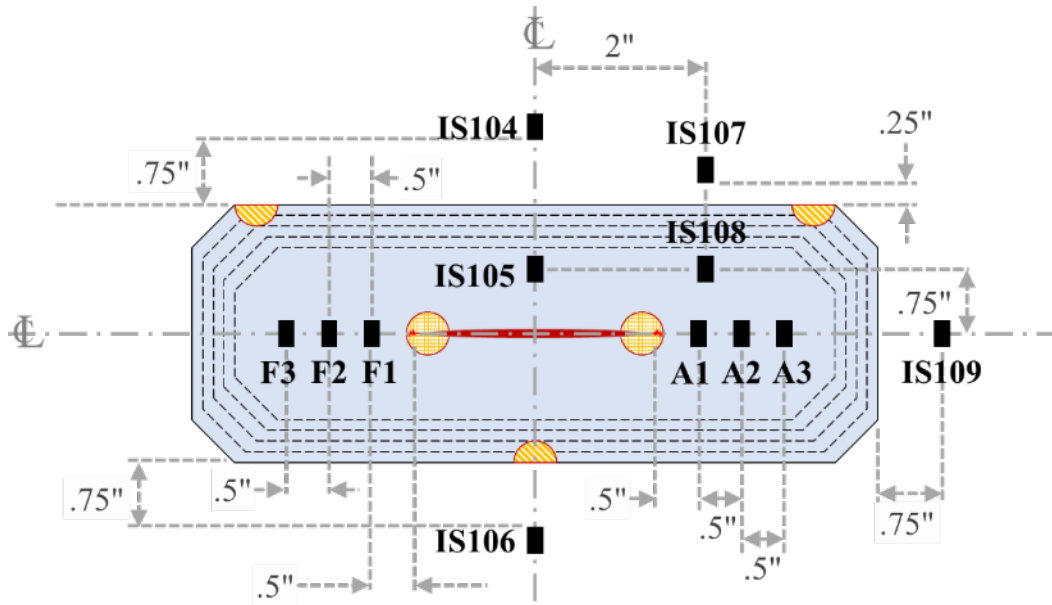


Figure C-27. Internal strain gauges during final 52,834 cycles of testing, repair patch UDB

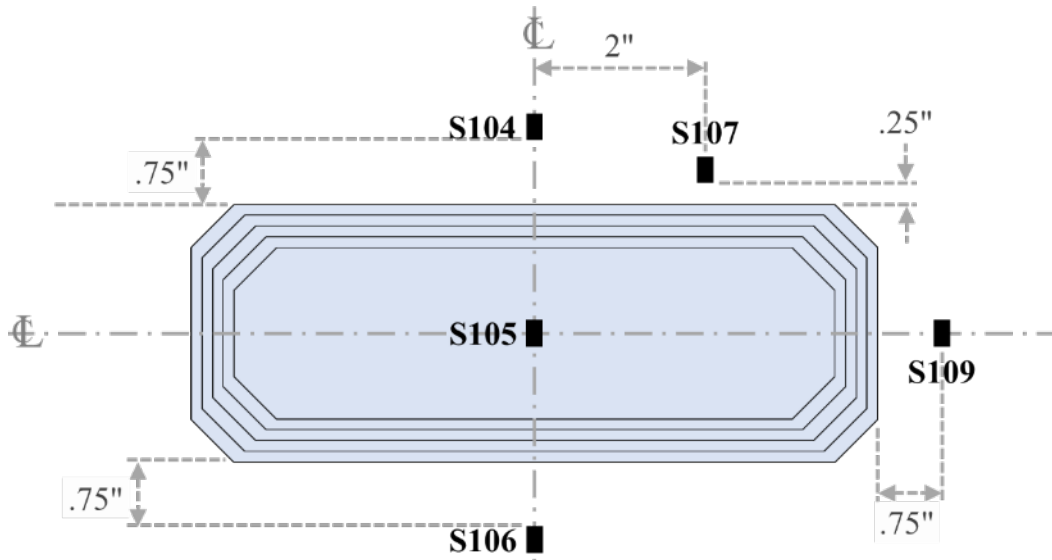


Figure C-28. External strain gauges during final 52,834 cycles of testing, repair patch UDB

C.4.8 REPAIR PATCH UDBC

Nineteen uniaxial strain gauges were installed in the vicinity of repair patch UDBC—on the internal and external panel surfaces and on top of the repair patch—as shown in figures C-29 and C-30.

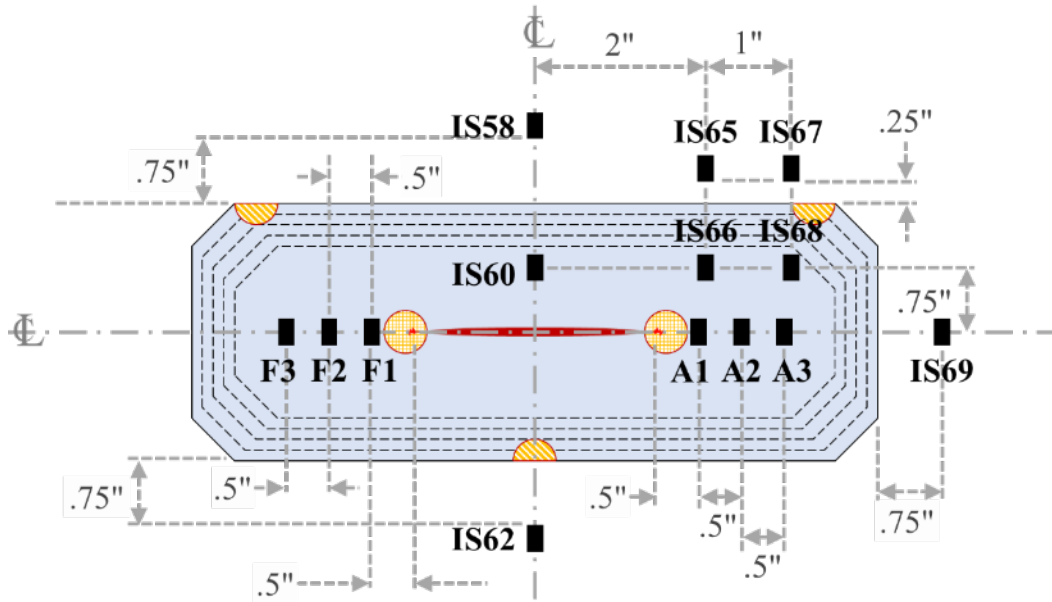


Figure C-29. Internal strain gauges during final 52,834 cycles of testing, repair patch UDBC

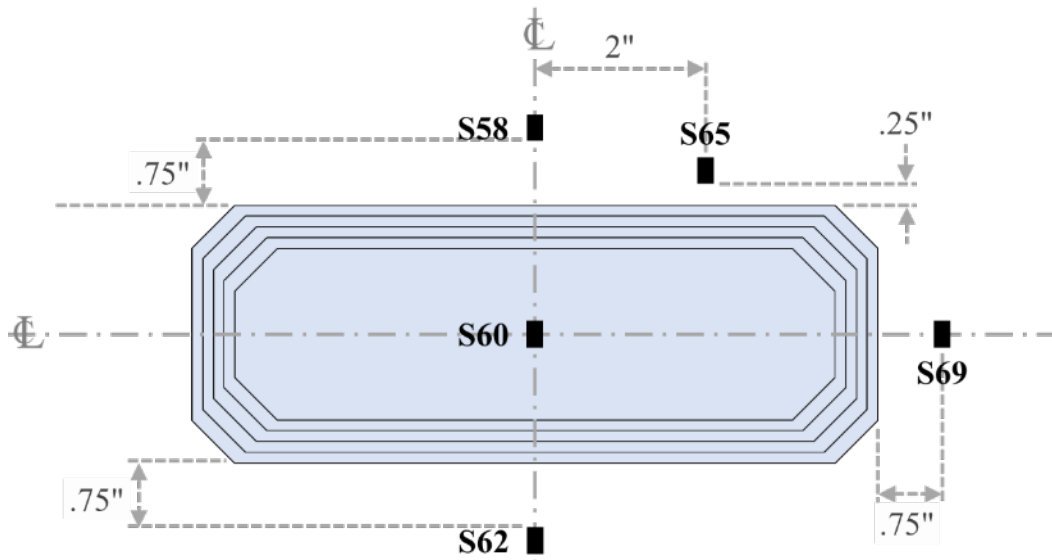


Figure C-30. External strain gauges during final 52,834 cycles of testing, repair patch UDBC

APPENDIX D—STRAIN GAUGE RESPONSE DURING REPAIR PATCH INSTALLATION

D.1 INTRODUCTION

During the curing cycle of each repair patch installation, strain gauges installed on the internal and external fuselage panel surfaces in the vicinity of each repair patch and the top of each repair patch were used to monitor the development of thermal residual strains while thermocouples installed on the internal and external fuselage panel surfaces in the vicinity of each repair patch and the top of each repair patch were used to monitor the distribution of temperature. Provided in section D-2 is an overview of the reduction procedure applied to the raw dataset. Provided in section D-3 are plots displaying the reduced time-dependent strain and temperature measurements obtained during the curing cycle for each adhesively bonded repair patch. For each point, measured strains are provided in units of $\mu\epsilon$, whereas measured temperatures are provided in $^{\circ}\text{F}$.

D.2 REDUCTION PROCEDURE

During acquisition, measurements by strain gauges and thermocouples were captured and stored every 2 seconds, resulting in prohibitively large data file sizes. To remedy this issue, the frequency of the dataset was reduced to 1 data point for every 2 minutes of acquisition. This reduced frequency was specifically chosen because it reduced the overall size of the dataset and simultaneously maintained the accuracy of the measured responses.

D.3 RAW STRAIN GAUGE RESPONSE DURING REPAIR PATCH CURING, GRAPHED

D.3.1 Repair Patch RAC

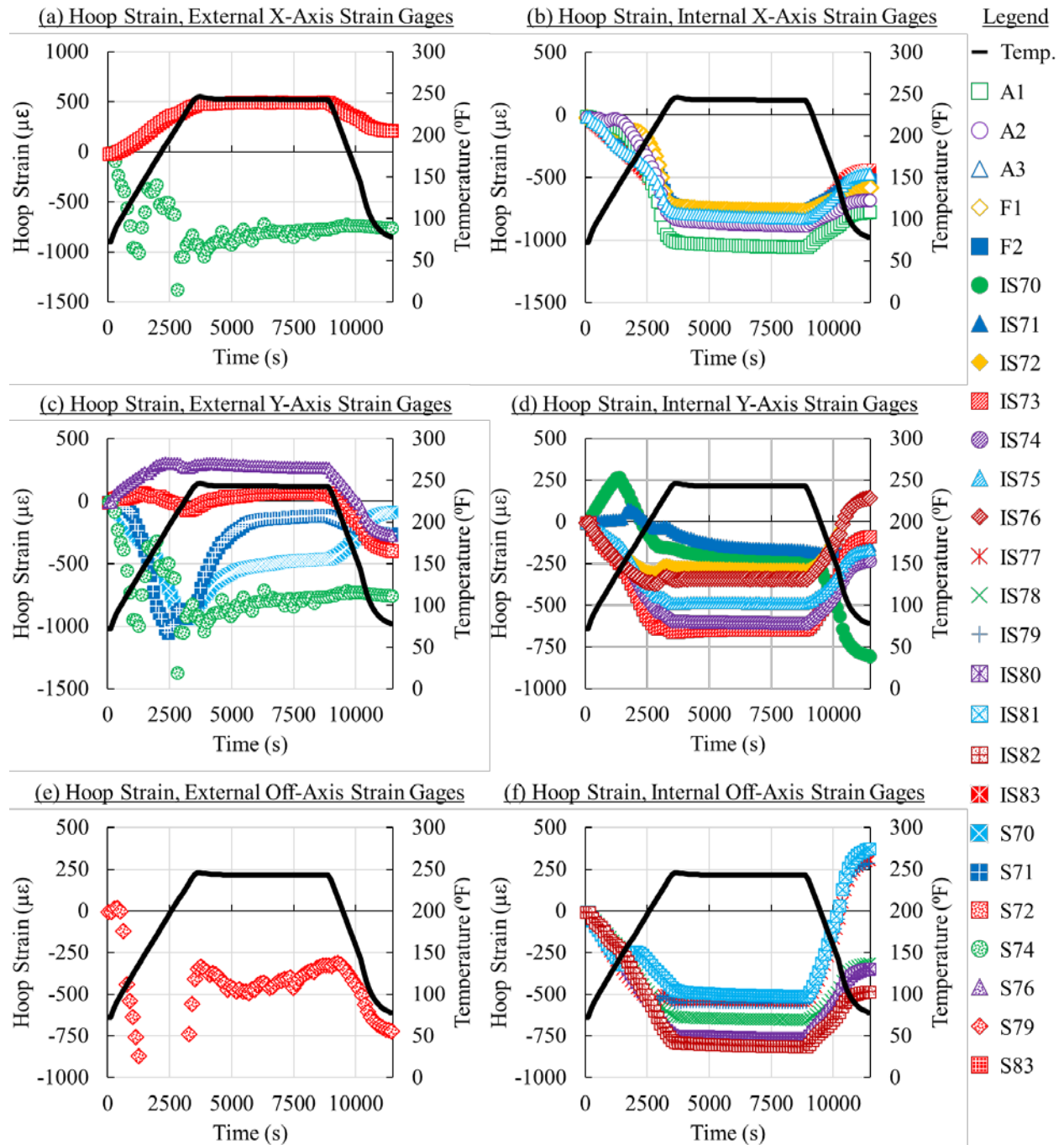


Figure D-1. Hoop strain response measured during curing process for repair patch RAC: (a) hoop strain, external X-axis strain gauges, (b) hoop strain, internal X-axis strain gauges, (c) hoop strain, external Y-axis strain gauges, (d) hoop strain, external Y-axis strain gauges, (e) hoop strain, external off-axis strain gauges, and (f) hoop strain, internal off-axis strain gauges

D.3.2 Repair Patch RBC

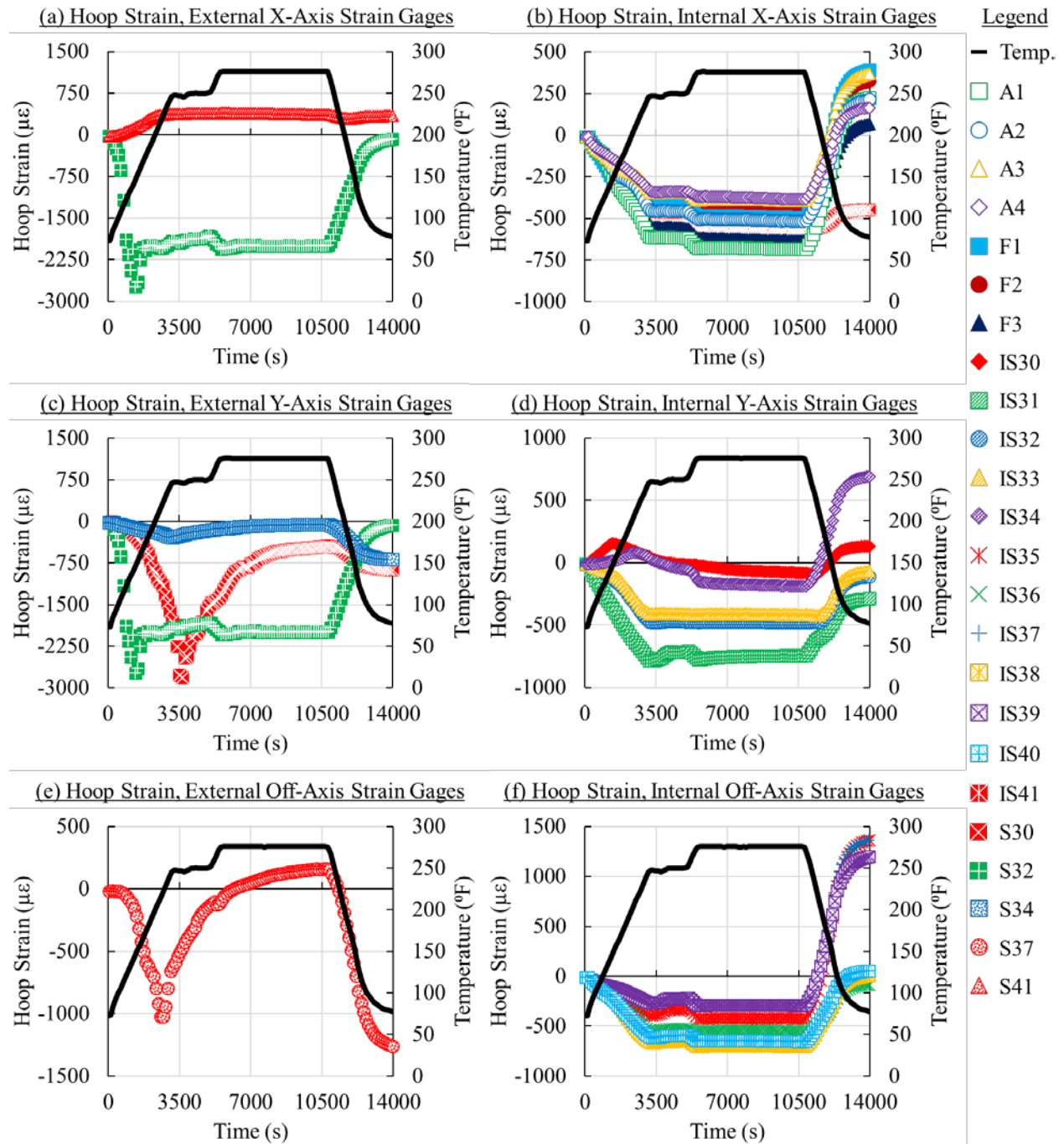


Figure D-2. Hoop strain response measured during curing process for repair patch RBC: (a) hoop strain, external X-axis strain gauges, (b) hoop strain, internal X-axis strain gauges, (c) hoop strain, external Y-axis strain gauges, (d) hoop strain, external Y-axis strain gauges, (e) hoop strain, external off-axis strain gauges, and (f) hoop strain, internal off-axis strain gauges

D.3.3 Repair Patch UAC

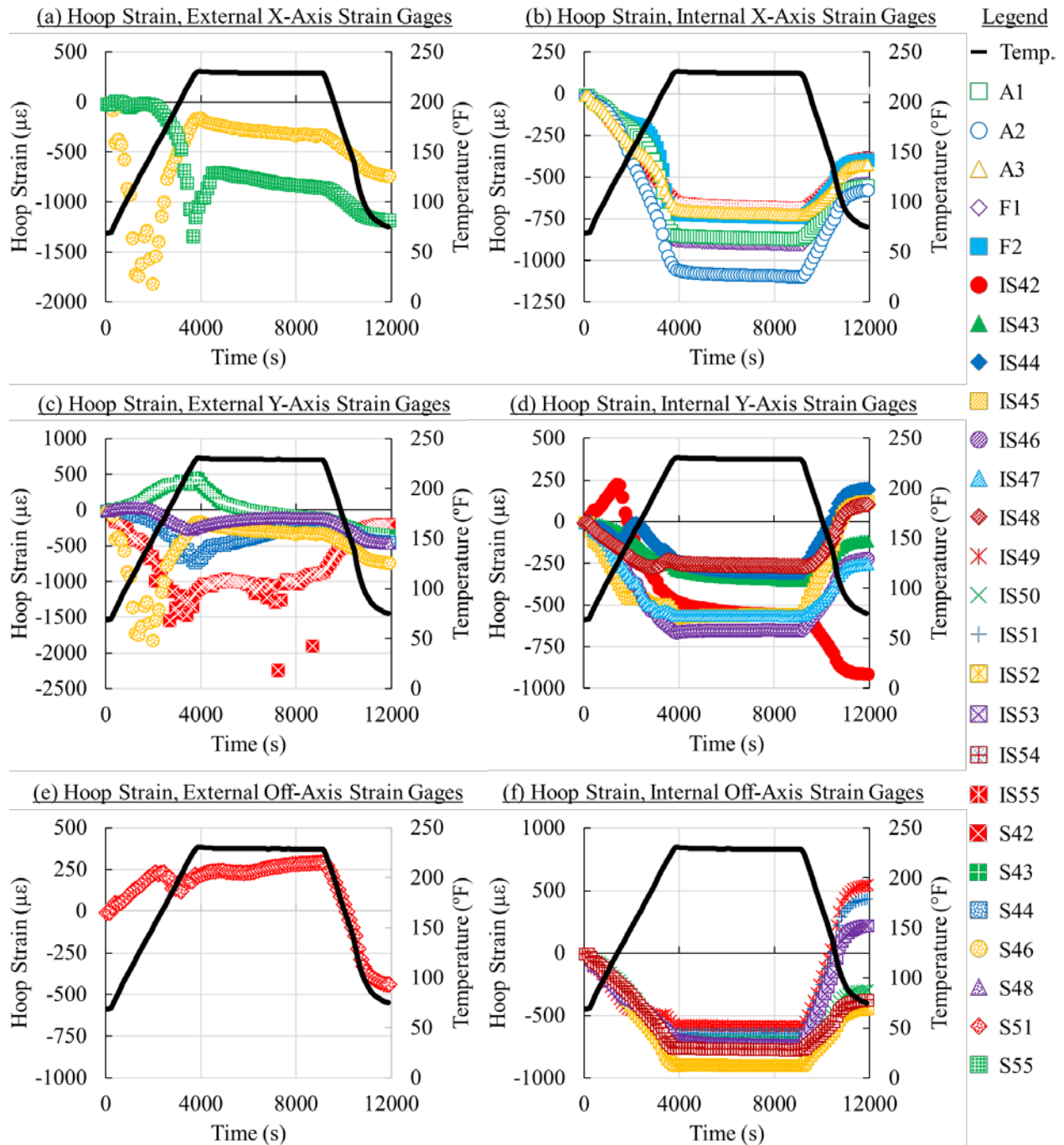


Figure D-3. Hoop strain response measured during curing process for repair patch UAC: (a) hoop strain, external X-axis strain gauges, (b) hoop strain, internal X-axis strain gauges, (c) hoop strain, external Y-axis strain gauges, (d) hoop strain, external Y-axis strain gauges, (e) hoop strain, external off-axis strain gauges, and (f) hoop strain, internal off-axis strain gauges

D.3.4 Repair Patch UB

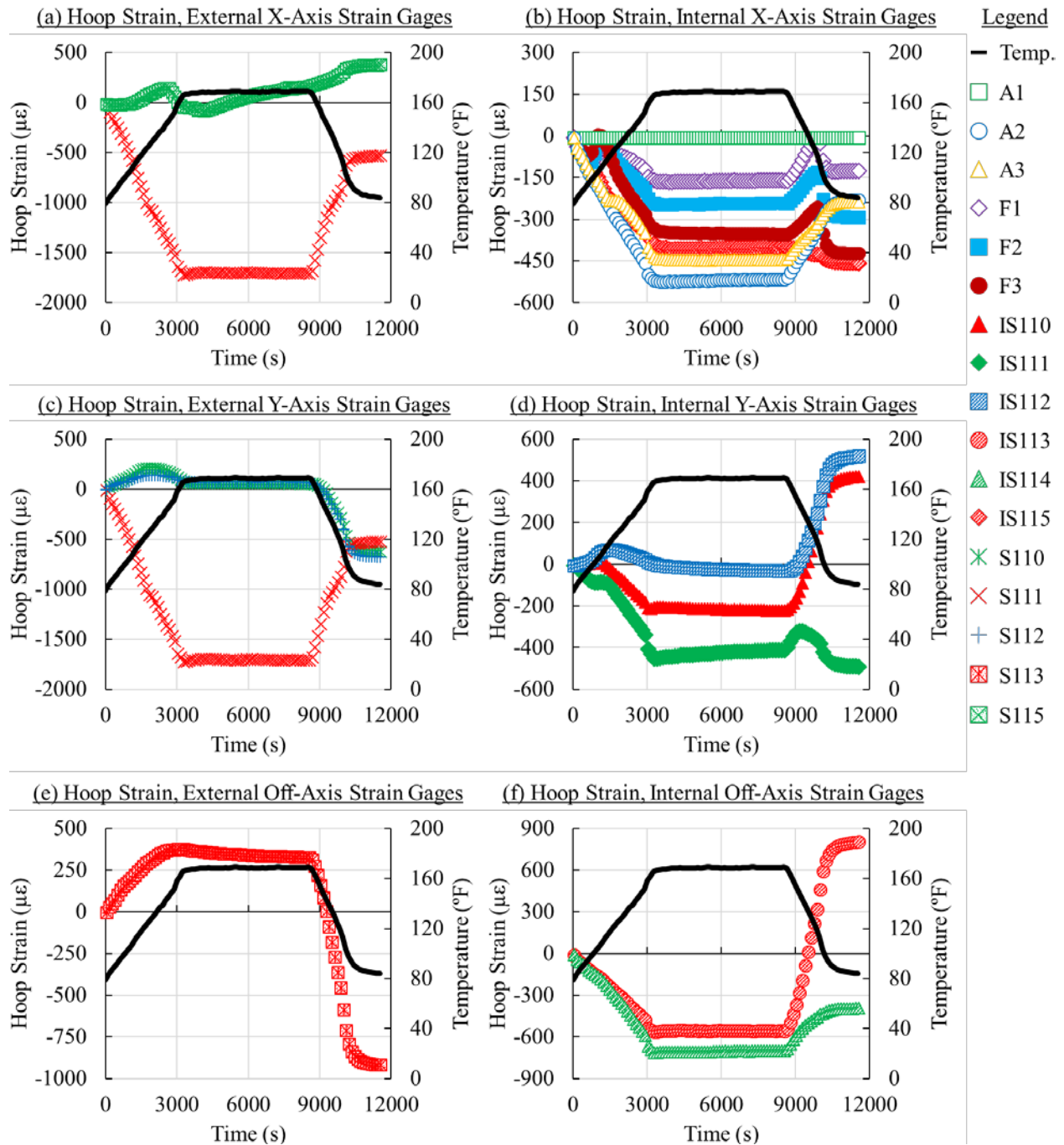


Figure D-4. Hoop strain response measured during curing process for repair patch UB: (a) hoop strain, external X-axis strain gauges, (b) hoop strain, internal X-axis strain gauges, (c) hoop strain, external Y-axis strain gauges, (d) hoop strain, internal Y-axis strain gauges, (e) hoop strain, external off-axis strain gauges, and (f) hoop strain, internal off-axis strain gauges

D.3.5 Repair Patch UBC

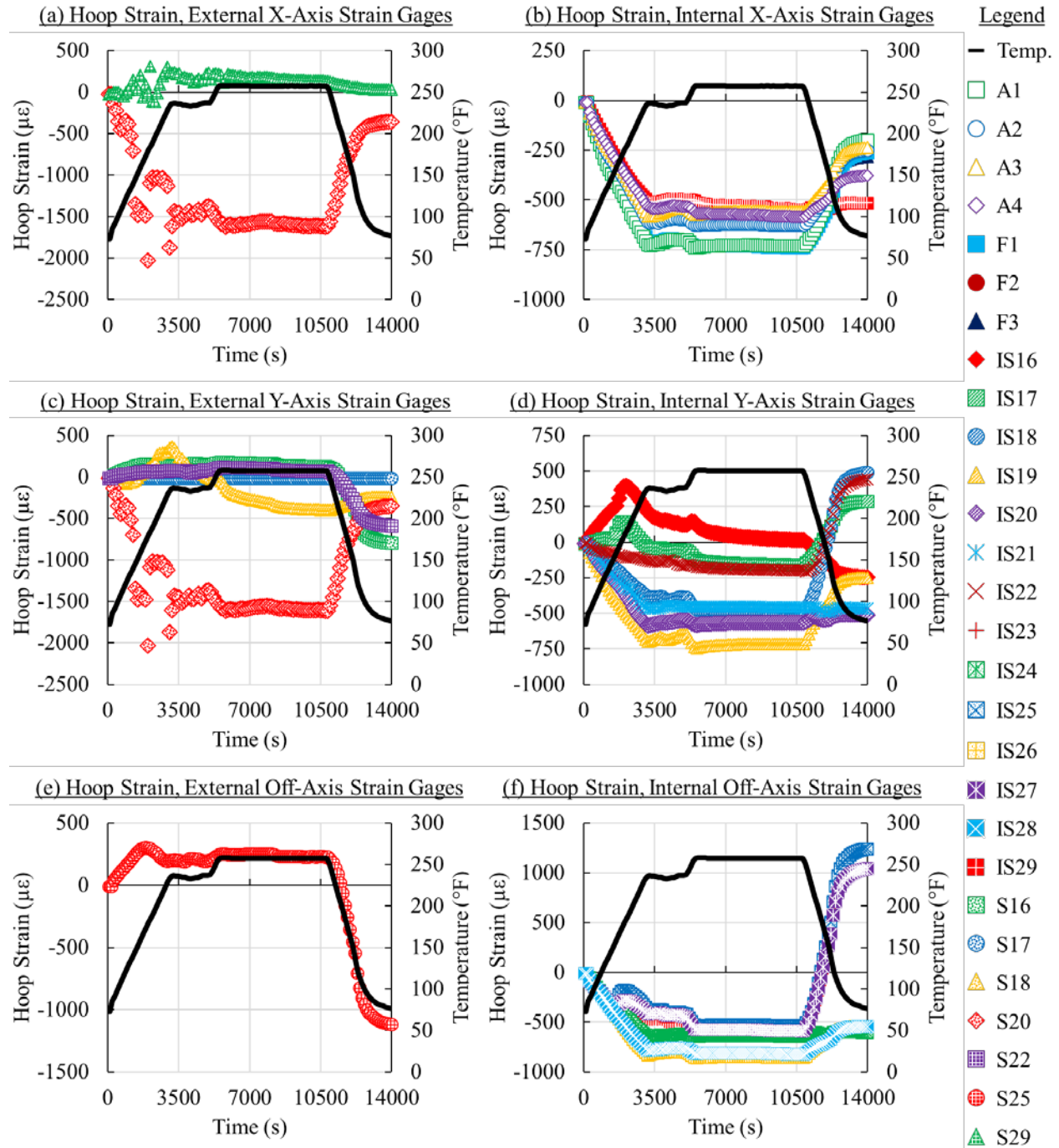


Figure D-5. Hoop strain response measured during curing process for repair patch UBC: (a) hoop strain, external X-axis strain gauges, (b) hoop strain, internal X-axis strain gauges, (c) hoop strain, external Y-axis strain gauges, (d) hoop strain, external Y-axis strain gauges, (e) hoop strain, external off-axis strain gauges, and (f) hoop strain, internal off-axis strain gauges

D.3.6 Repair Patch UDAC

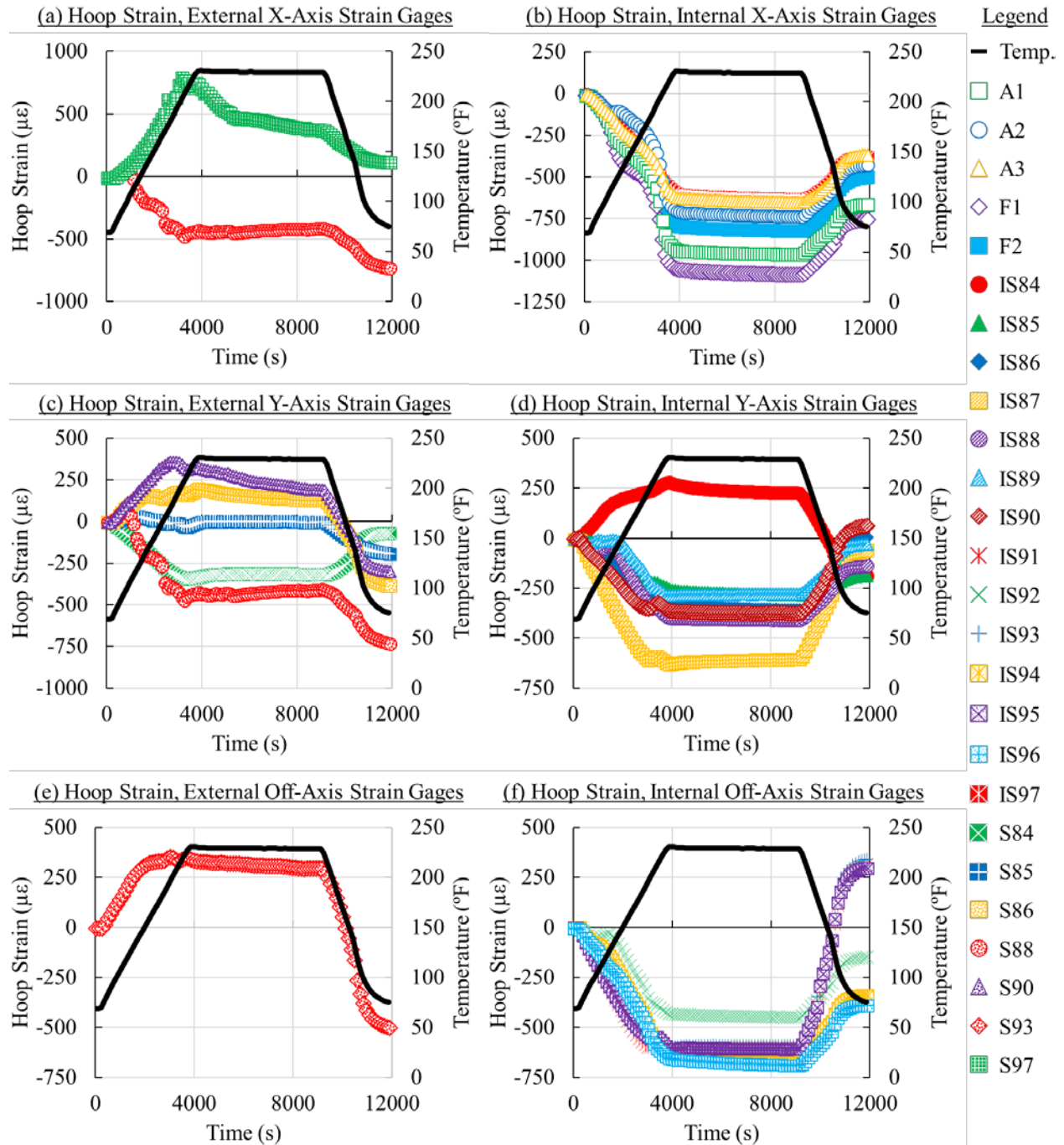


Figure D-6. Hoop strain response measured during curing process for repair patch UDAC: (a) hoop strain, external X-axis strain gauges, (b) hoop strain, internal X-axis strain gauges, (c) hoop strain, external Y-axis strain gauges, (d) hoop strain, external Y-axis strain gauges, (e) hoop strain, external off-axis strain gauges, and (f) hoop strain, internal off-axis strain gauges

D.3.7 Repair Patch UDB

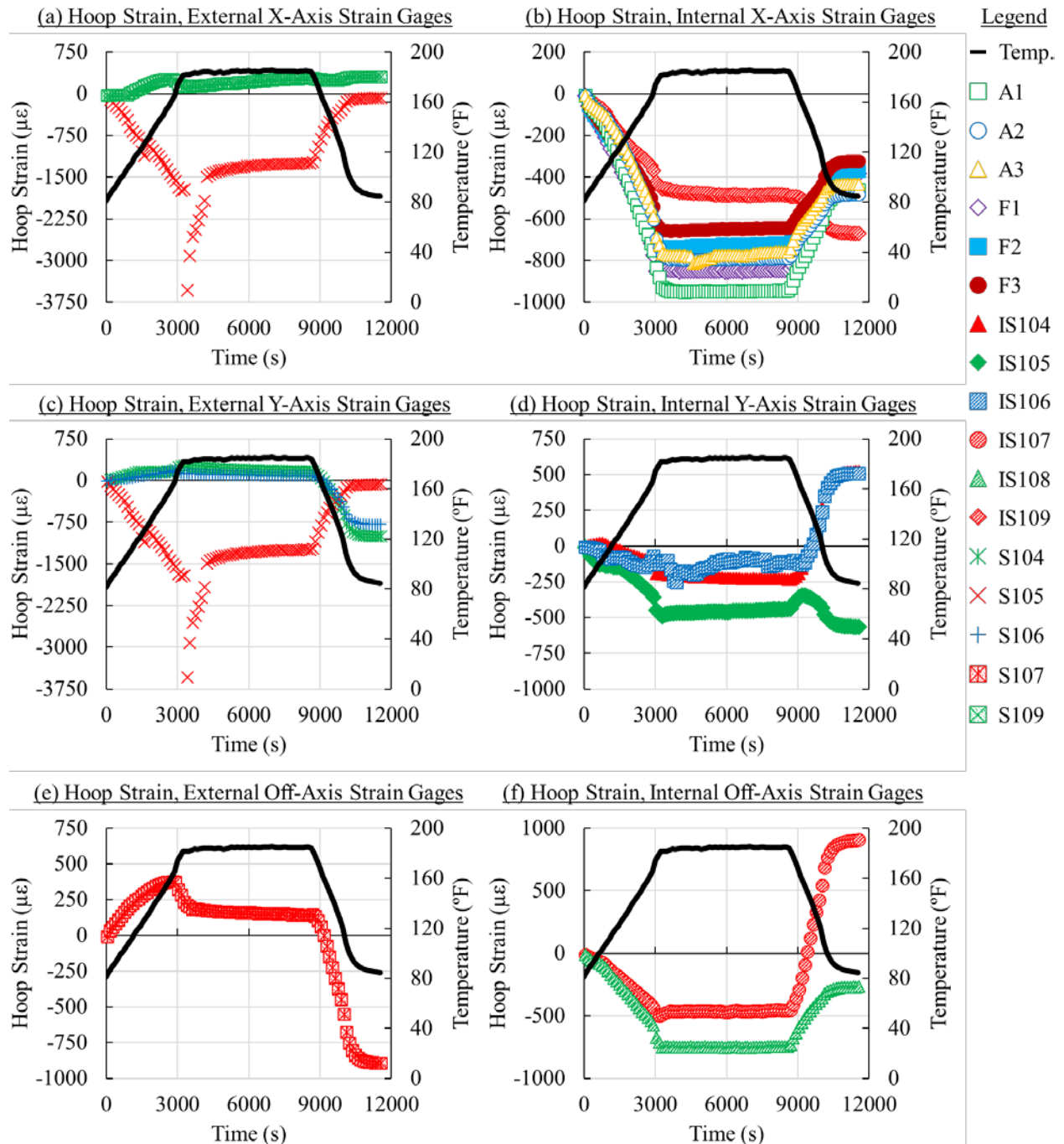


Figure D-7. Hoop strain response measured during curing process for repair patch UDB: (a) hoop strain, external X-axis strain gauges, (b) hoop strain, internal X-axis strain gauges, (c) hoop strain, external Y-axis strain gauges, (d) hoop strain, external Y-axis strain gauges, (e) hoop strain, external off-axis strain gauges, and (f) hoop strain, internal off-axis strain gauges

D.3.8 Repair Patch UDBC

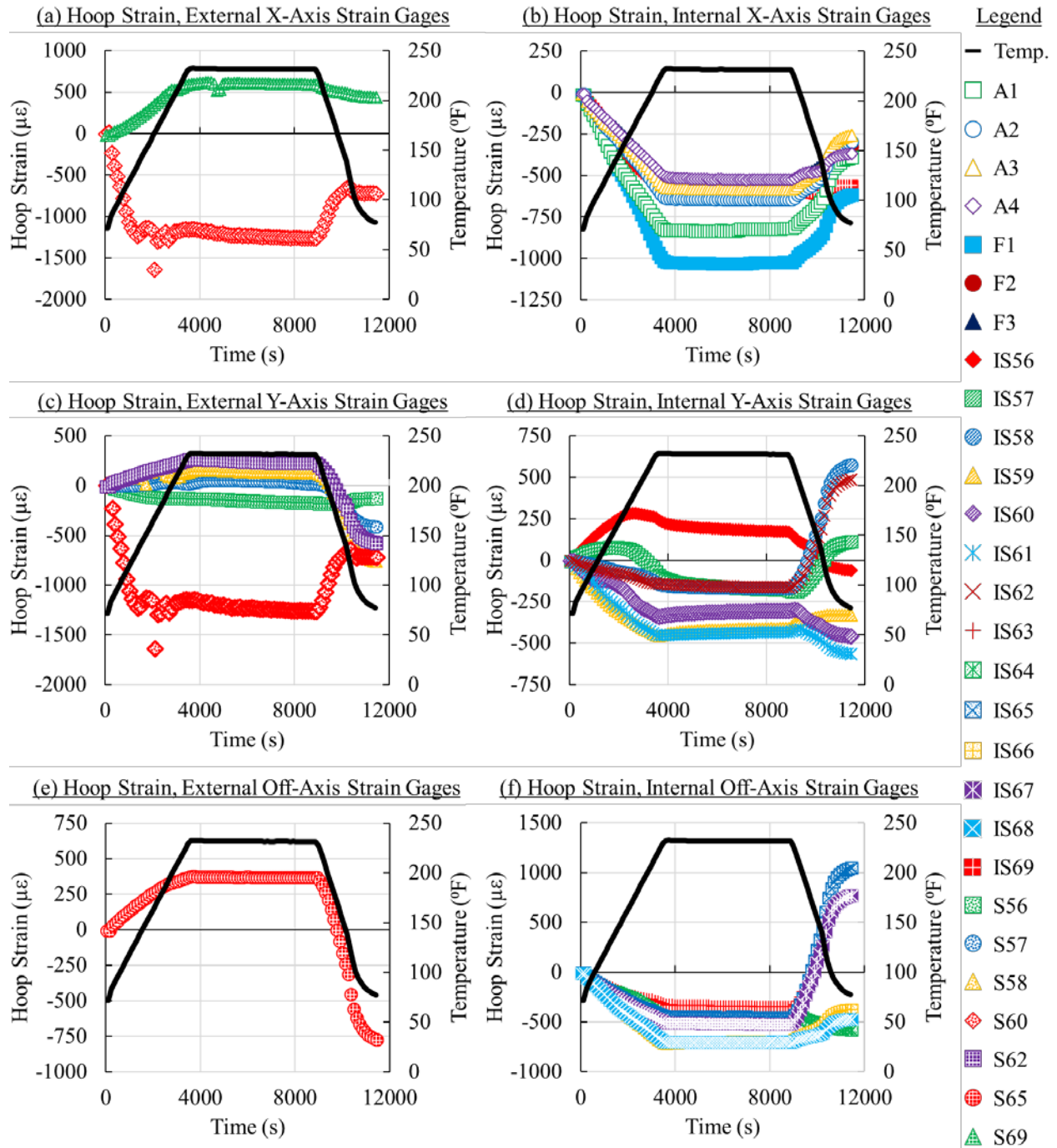


Figure D-8. Hoop strain response measured during curing process for repair patch UDBC: (a) hoop strain, external X-axis strain gauges, (b) hoop strain, internal X-axis strain gauges, (c) hoop strain, external Y-axis strain gauges, (d) hoop strain, external Y-axis strain gauges, (e) hoop strain, external off-axis strain gauges, and (f) hoop strain, internal off-axis strain gauges

APPENDIX E—STRAIN GAUGE RESPONSE DURING HOT-WET CONDITIONING

E.1 INTRODUCTION

During the 4-week period of hot-wet conditioning, strain gauges installed on the internal and external fuselage panel surfaces in the vicinity of each repair patch and the top of each repair patch were used to monitor the distribution of strain, whereas thermocouples installed on the internal and external fuselage panel surfaces in the vicinity of each repair patch and the top of each repair patch were used to monitor the distribution of temperature. Provided in section E-2 is an overview of the reduction procedure applied to the raw dataset. Provided in section E-3 are plots displaying the reduced time-dependent strain and temperature measurements obtained during the hot-wet conditioning period for each adhesively bonded repair patch installed at the onset of the test (i.e., RAC, RBC, UAC, UBC, UDAC, and UDBC). For each point, measured strains are provided in units of $\mu\epsilon$, whereas measured temperatures are provided in $^{\circ}\text{F}$.

E.2 REDUCTION PROCEDURE

During acquisition, measurements by strain gauges and thermocouples were captured and stored every 100 seconds, resulting in prohibitively large data file sizes. To remedy this issue, the frequency of the dataset was reduced to 1 data point for every 1 hour of acquisition. This reduced frequency was specifically chosen because it reduced the overall size of the dataset while simultaneously maintaining the accuracy of the measured responses.

E.3 RAW STRAIN GAUGE RESPONSE DURING HOT-WET CONDITIONING, GRAPHED

E.3.1 Repair Patch RAC

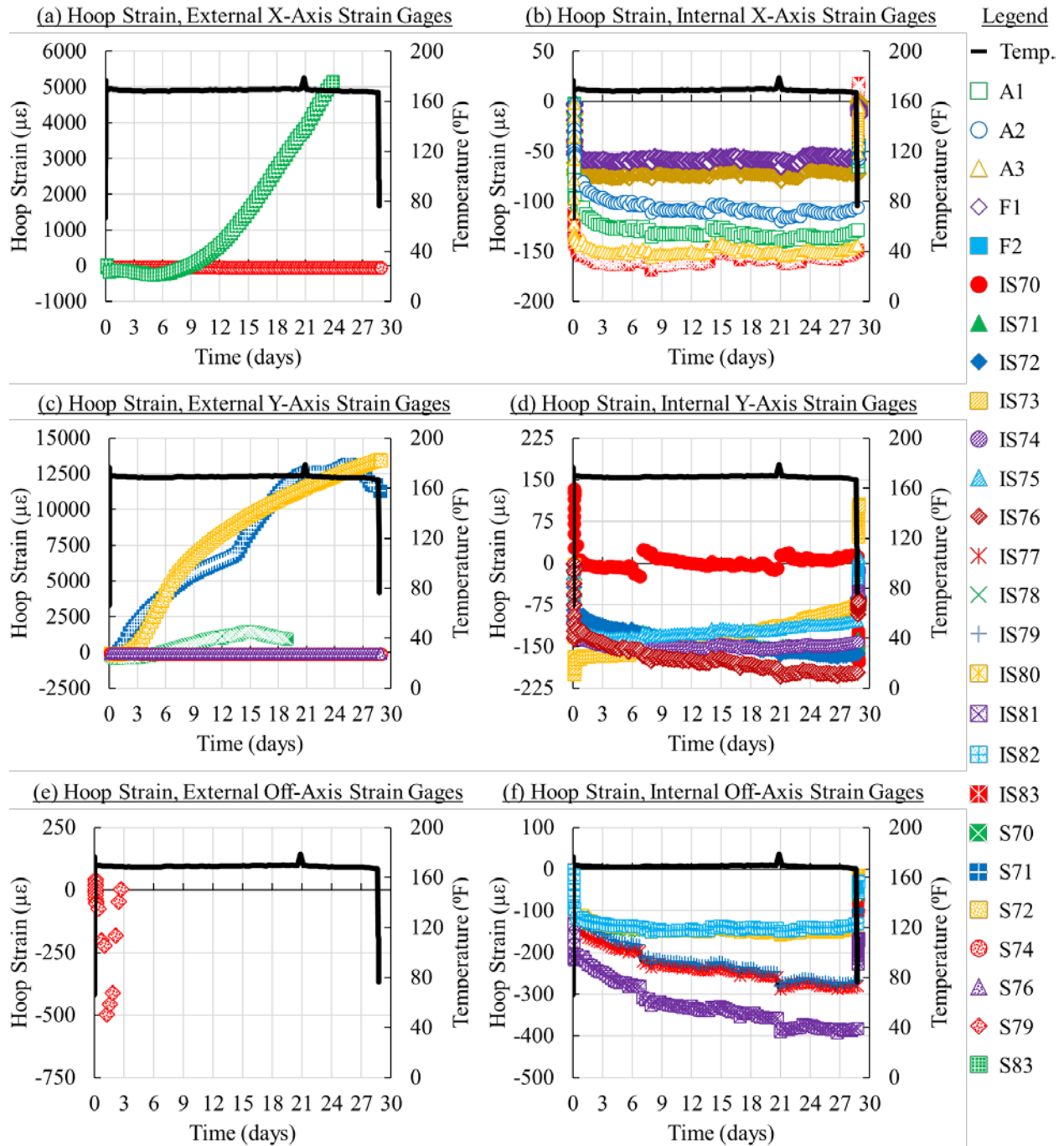


Figure E-1. Hoop strain response measured during hot-wet conditioning for repair patch RAC: (a) hoop strain, external X-axis strain gauges, (b) hoop strain, internal X-axis strain gauges, (c) hoop strain, external Y-axis strain gauges, (d) hoop strain, external Y-axis strain gauges, (e) hoop strain, external off-axis strain gauges, and (f) hoop strain, internal off-axis strain gauges

E.3.2 Repair Patch RBC

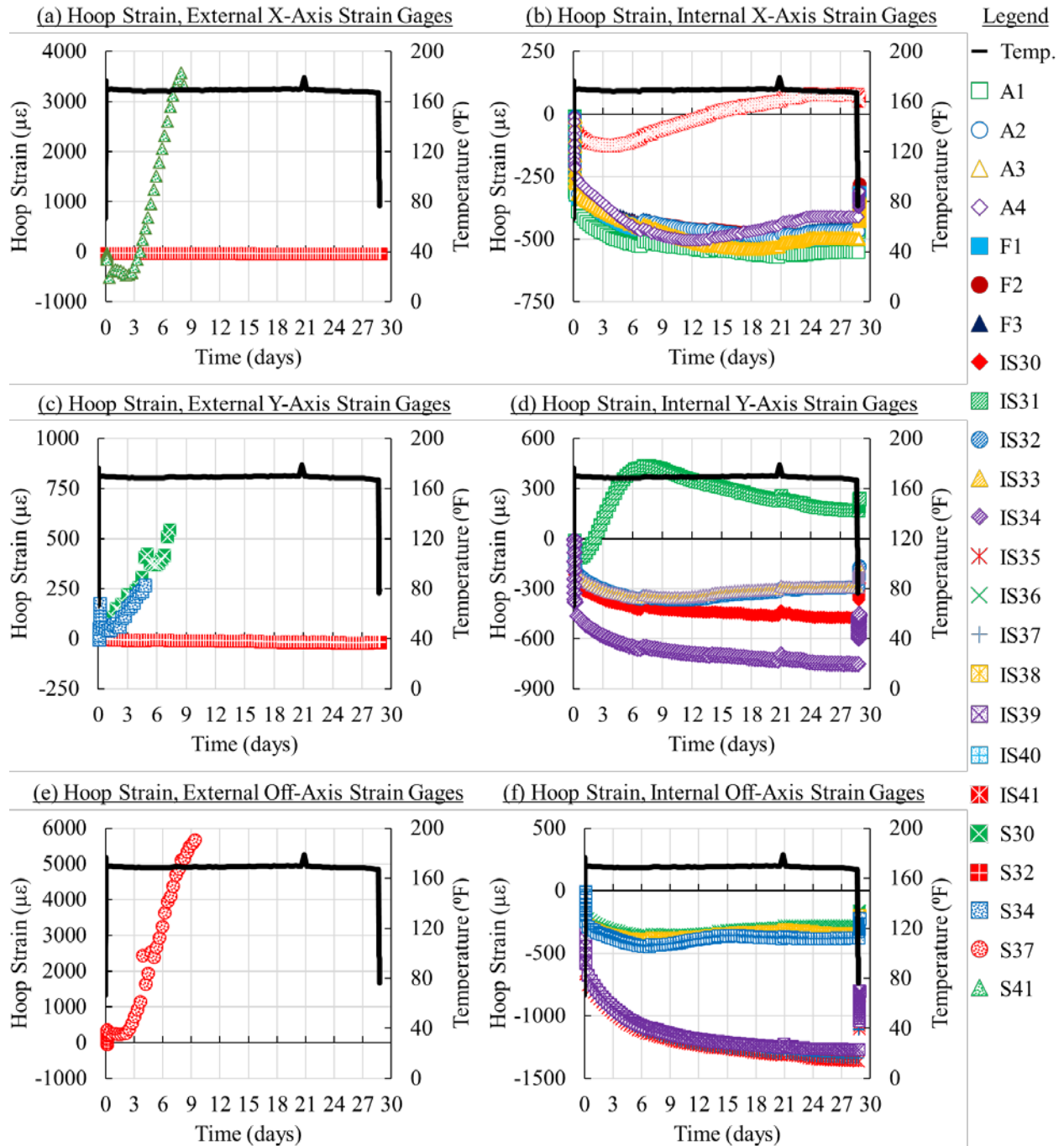


Figure E-2. Hoop strain response measured during hot-wet conditioning for repair patch RBC: (a) hoop strain, external X-axis strain gauges, (b) hoop strain, internal X-axis strain gauges, (c) hoop strain, external Y-axis strain gauges, (d) hoop strain, external Y-axis strain gauges, (e) hoop strain, external off-axis strain gauges, and (f) hoop strain, internal off-axis strain gauges

E.3.3 Repair Patch UAC

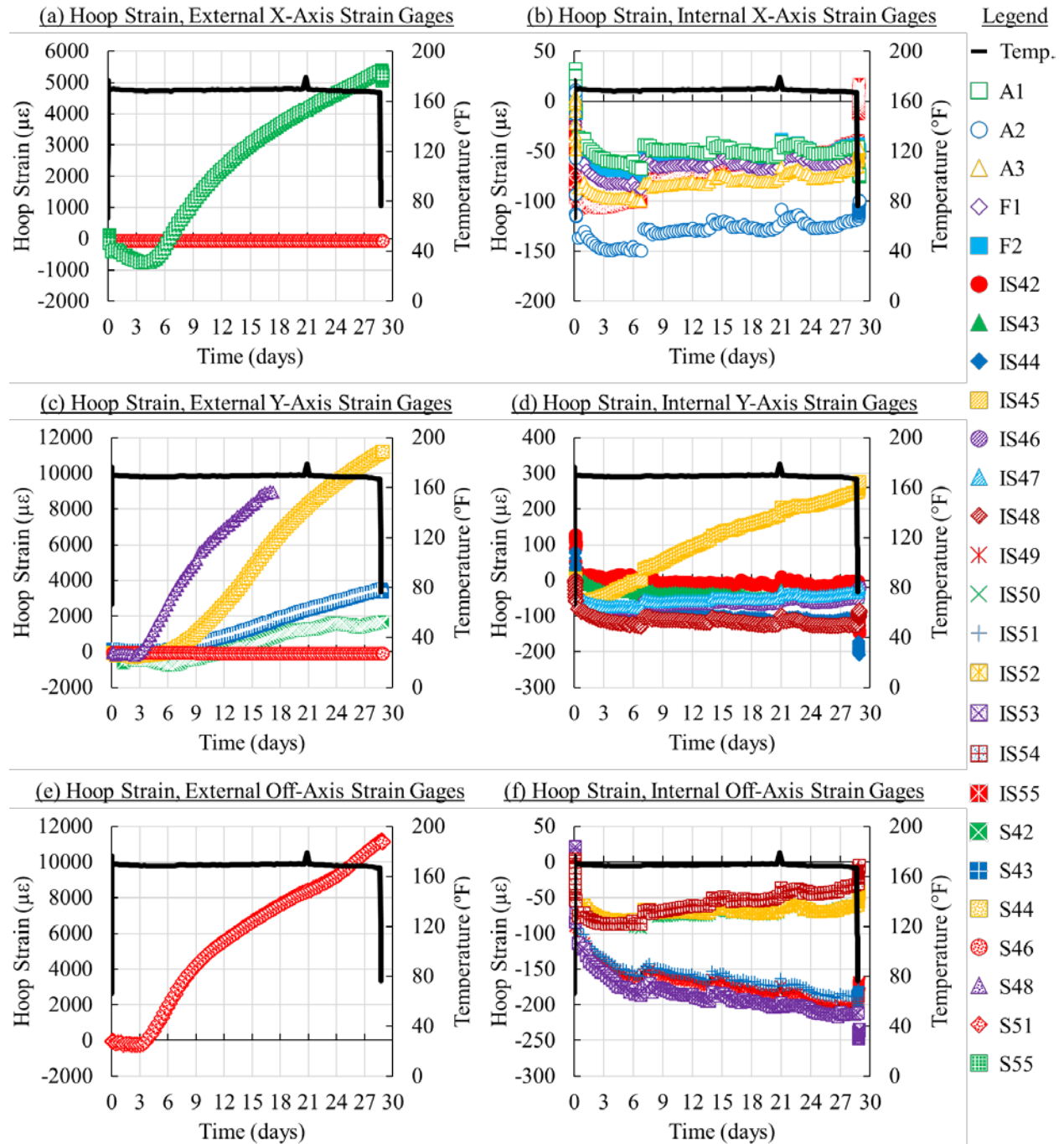


Figure E-3. Hoop strain response measured during hot-wet conditioning for repair patch UAC: (a) hoop strain, external X-axis strain gauges, (b) hoop strain, internal X-axis strain gauges, (c) hoop strain, external Y-axis strain gauges, (d) hoop strain, external Y-axis strain gauges, (e) hoop strain, external off-axis strain gauges, and (f) hoop strain, internal off-axis strain gauges

E.3.4 Repair Patch UBC

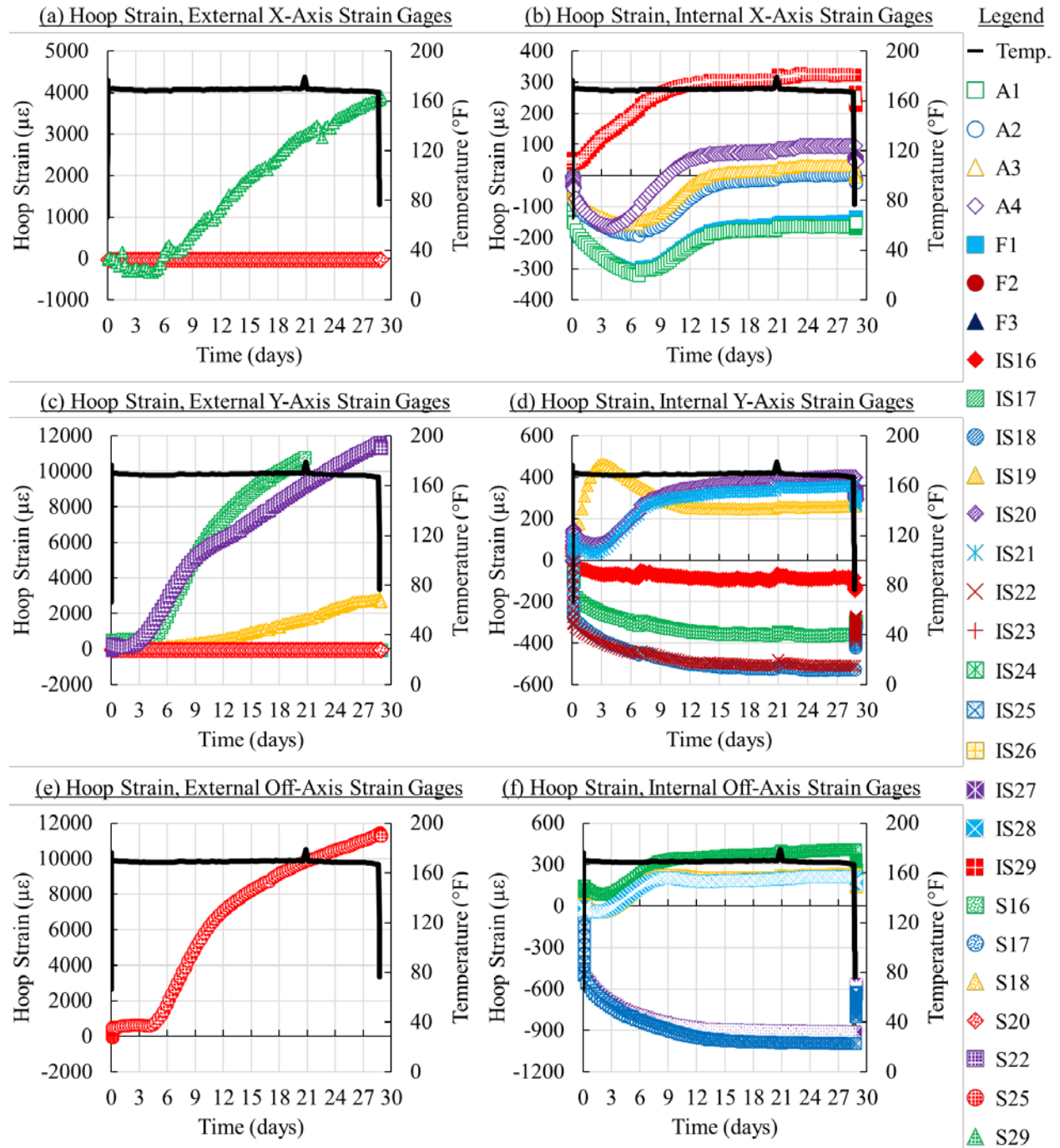


Figure E-4. Hoop strain response measured during hot-wet conditioning for repair patch UBC: (a) hoop strain, external X-axis strain gauges, (b) hoop strain, internal X-axis strain gauges, (c) hoop strain, external Y-axis strain gauges, (d) hoop strain, external Y-axis strain gauges, (e) hoop strain, external off-axis strain gauges, and (f) hoop strain, internal off-axis strain gauges

E.3.5 Repair Patch UDAC

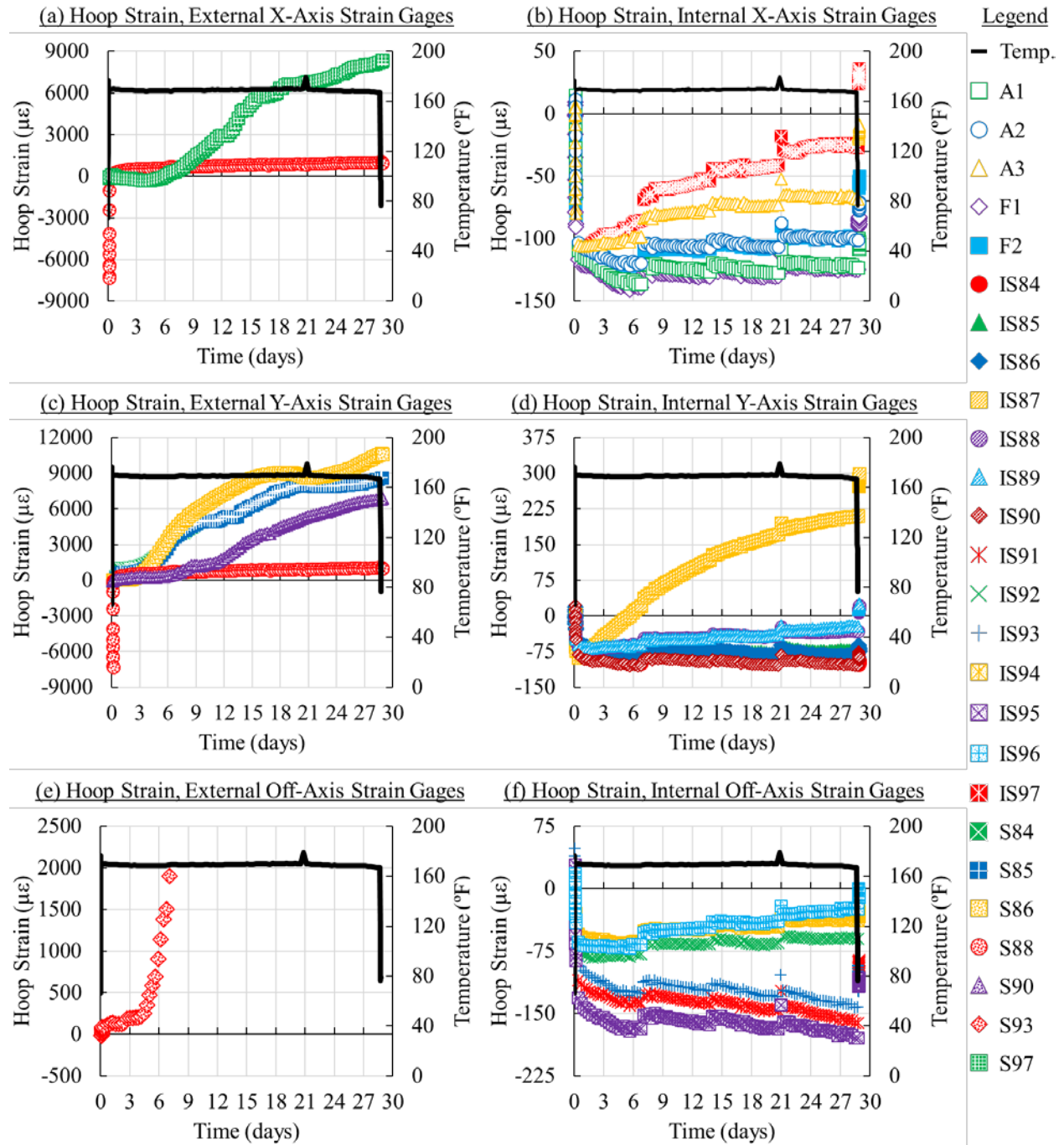


Figure E-5. Hoop strain response measured during hot-wet conditioning for repair patch UDAC: (a) hoop strain, external X-axis strain gauges, (b) hoop strain, internal X-axis strain gauges, (c) hoop strain, external Y-axis strain gauges, (d) hoop strain, external Y-axis strain gauges, (e) hoop strain, external off-axis strain gauges, and (f) hoop strain, internal off-axis strain gauges

E.3.6 Repair Patch UDBC

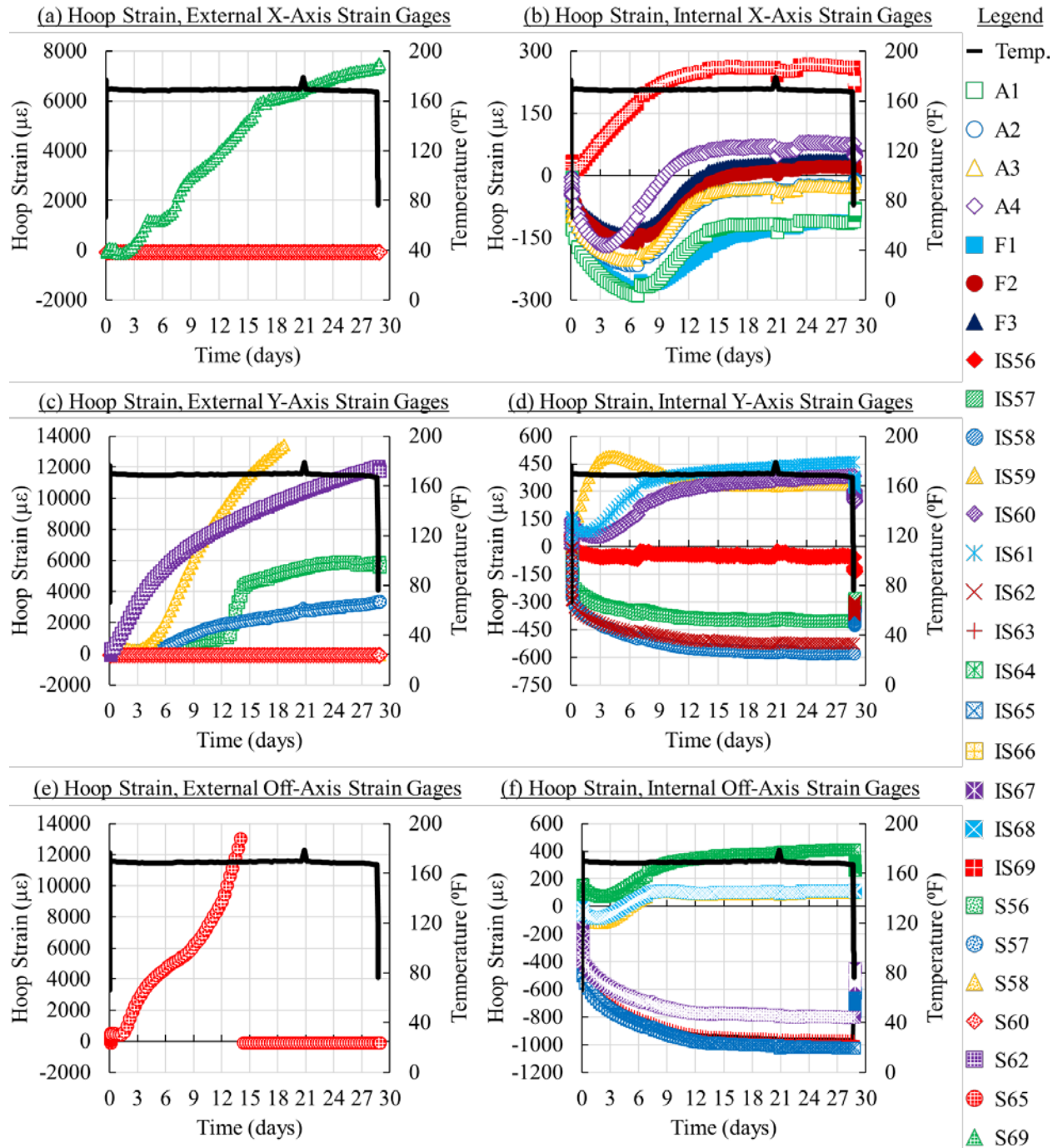


Figure E-6. Hoop strain response measured during hot-wet conditioning for repair patch UDBC: (a) hoop strain, external X-axis strain gauges, (b) hoop strain, internal X-axis strain gauges, (c) hoop strain, external Y-axis strain gauges, (d) hoop strain, external Y-axis strain gauges, (e) hoop strain, external off-axis strain gauges, and (f) hoop strain, internal off-axis strain gauges

APPENDIX F—STRAIN GAUGE RESPONSE DURING STRAIN SURVEYS

F.1 INTRODUCTION

Throughout the duration of the test, the fuselage panel was intermittently subjected to a quasistatic load spectrum for the purpose of monitoring the distribution of strain in the test section. During these strain surveys, which were conducted in a variety of environmental conditions, the applied loads (i.e., pressure, hoop, frame, and longitudinal loads) were incrementally increased from 0%–75% of SSL conditions. A summary of the mechanical and environmental conditions applied during strain surveys is provided in table F-1.

Table F-1. Mechanical and environmental loads considered during strain surveys

Strain Survey	Maximum Mechanical Load				Environmental Load	
	Pressure (psi)	Hoop (lbf)	Frame (lbf)	Longitudinal (lbf)	Temperature (°F)	Relative Humidity (%)
Ambient	6.7	7140	1133	6675	80	60
Cold-Dry	6.7	7140	1133	6675	-25	-
Hot-Wet	6.7	7140	1133	6675	165	85

F.2 RAW STRAIN GAUGE RESPONSE DURING STRAIN SURVEYS, TABULATED

The inspection periods during which strain surveys were conducted were strategically chosen to ensure the ability to evaluate the effect that some event (e.g., the accumulation of fatigue cycles) had on the distribution of strain. A summary of the inspection periods during which strain surveys were conducted and the applied loads during said surveys are provided in table F-2.

Table F-2. Summary of strain surveys conducted with strain gauges

Inspection Period	Maximum Mechanical Load	Environmental Load
Before Phase I Notch Cutting	75% of SSL Conditions	Ambient
After Phase I Notch Cutting	75% of SSL Conditions	Ambient
After Phase I Pre-Cracking	75% of SSL Conditions	Ambient
After Phase I Patch Installation	75% of SSL Conditions	Ambient
After Hot-Wet Conditioning	75% of SSL Conditions	Ambient, Cold-Dry, Hot-Wet
After 10,000 Cycles	75% of SSL Conditions	Ambient, Cold-Dry, Hot-Wet
After 20,000 Cycles	75% of SSL Conditions	Ambient, Cold-Dry, Hot-Wet
After 30,000 Cycles	75% of SSL Conditions	Ambient, Cold-Dry, Hot-Wet
After 40,000 Cycles	75% of SSL Conditions	Ambient, Cold-Dry, Hot-Wet
After 50,000 Cycles	75% of SSL Conditions	Ambient, Cold-Dry
After 60,000 Cycles	75% of SSL Conditions	Ambient, Cold-Dry
After 70,000 Cycles	75% of SSL Conditions	Ambient, Cold-Dry
After 80,000 Cycles	75% of SSL Conditions	Ambient, Cold-Dry
After 90,000 Cycles	75% of SSL Conditions	Ambient, Cold-Dry

During each strain survey, the quasistatic load spectrum, which featured load steps at 0%, 7.5%, 15%, 22.5%, 30%, 37.5%, 45%, 52.5%, 60%, 67.5%, and 75% of SSL conditions, was applied three times, in succession, for the purpose of evaluating and verifying the repeatability of results. During load application, strain gauges installed on the fuselage panel skin, frames, stringers, and in the vicinity of each adhesively bonded repair patch were used to measure the strain at each load step; therefore, 33 data points were captured during each strain survey. Provided in the subsequent sections are representative results of the strain surveys outlined in table F-2.

Table F-3. Summary of raw strain survey results provided in section F.2

Inspection Period	Maximum Mechanical Load	Environmental Load
After Phase I Patch Installation	75% of SSL Conditions	Ambient
After Hot-Wet Conditioning	75% of SSL Conditions	Ambient, Cold-Dry, Hot-Wet
After 30,000 Cycles	75% of SSL Conditions	Ambient, Cold-Dry, Hot-Wet
After 60,000 Cycles	75% of SSL Conditions	Ambient, Cold-Dry
After 90,000 Cycles	75% of SSL Conditions	Ambient, Cold-Dry

Raw strain survey results for select inspections (outlined in table F-3) are provided in table form in section F-2 of this appendix. Additionally, the post-processing procedure applied to all raw strain survey results is outlined in section F-3.

F.2.1 Ambient Environmental Conditions

F.2.1.1 After Phase I Patch Installation

Representative strain survey results for a single inspection following the application of this post-processing procedure is provided via graphs in section F-4. In each case, the applied pressure is provided in units of psi; the frame, hoop, and longitudinal loads are provided in units of lbf, and the measured strains are provided in units of $\mu\epsilon$.

Table F-4. Raw data, strain survey conducted after phase I patch installation, ambient environmental conditions (Run 1)

Load Step	0	1	2	3	4	5	6	7	8	9	10
Pressure (psi)	-0.07	0.65	1.33	2.01	2.66	3.34	3.99	4.68	5.30	6.00	6.65
Frame-1 (lbf)	-1	130	241	349	464	557	664	795	935	1035	1137
Frame-2 (lbf)	37	106	236	332	458	554	658	793	908	1016	1134
Frame-3 (lbf)	1	106	236	341	450	567	682	790	908	1021	1131
Frame-4 (lbf)	44	125	226	324	452	569	679	794	907	1020	1134
Frame-5 (lbf)	2	124	210	347	446	565	682	792	903	1026	1128
Frame-6 (lbf)	13	115	218	354	447	567	677	793	912	1024	1124
Frame-7 (lbf)	-3	112	225	345	447	568	677	788	906	1020	1135
Frame-8 (lbf)	-6	122	221	338	453	565	684	796	904	1021	1138
Frame-9 (lbf)	22	111	224	342	455	568	682	793	906	1019	1131
Frame-10 (lbf)	-1	111	228	343	454	566	686	796	905	1019	1134
Frame-11 (lbf)	-4	118	228	340	454	564	681	801	904	1017	1130
Frame-12 (lbf)	17	122	225	344	453	567	679	794	908	1021	1133
Hoop-1 (lbf)	10	706	1442	2145	2846	3571	4295	4983	5700	6420	7152
Hoop-2 (lbf)	176	713	1416	2102	2830	3579	4302	4977	5711	6422	7139
Hoop-3 (lbf)	50	721	1436	2154	2859	3570	4273	4994	5720	6427	7138

**Table F-4. Raw data, strain survey conducted after phase I patch installation, ambient environmental conditions (Run 1)
(continued)**

Load Step	0	1	2	3	4	5	6	7	8	9	10
Pressure (psi)	-0.07	0.65	1.33	2.01	2.66	3.34	3.99	4.68	5.30	6.00	6.65
Hoop-4 (lb _f)	30	701	1428	2149	2842	3573	4283	5010	5743	6425	7125
Hoop-5 (lb _f)	20	687	1418	2149	2863	3583	4299	5005	5722	6419	7110
Hoop-6 (lb _f)	-11	713	1428	2135	2865	3575	4271	4984	5704	6412	7170
Hoop-7 (lb _f)	1	717	1434	2147	2855	3568	4272	4990	5717	6409	7133
Hoop-8 (lb _f)	40	715	1408	2143	2850	3587	4277	4990	5727	6421	7141
Hoop-9 (lb _f)	-1	722	1423	2118	2866	3580	4289	5010	5719	6425	7147
Hoop-10 (lb _f)	-15	710	1444	2135	2847	3577	4271	5002	5715	6418	7134
Hoop-11 (lb _f)	56	700	1394	2138	2855	3579	4289	5002	5715	6413	7151
Hoop-12 (lb _f)	93	737	1454	2131	2859	3580	4277	5005	5726	6429	7141
Hoop-13 (lb _f)	17	714	1433	2131	2849	3579	4278	4993	5709	6429	7140
Hoop-14 (lb _f)	1	724	1426	2133	2862	3565	4289	4996	5703	6428	7137
Long-1 (lb _f)	10	650	1312	2004	2653	3303	4012	4638	5310	5966	6710
Long-2 (lb _f)	6	675	1333	1997	2681	3335	4021	4671	5347	6013	6677
Long-3 (lb _f)	7	665	1336	2007	2668	3328	4018	4676	5333	6006	6676
Long-4 (lb _f)	16	682	1359	2010	2670	3335	4006	4672	5345	6004	6673
Long-5 (lb _f)	4	674	1334	1992	2669	3340	4004	4670	5335	6008	6676
Long-6 (lb _f)	2	672	1341	2000	2685	3322	4013	4674	5364	6012	6673
Long-7 (lb _f)	-1	628	1316	1998	2683	3326	4007	4674	5330	6034	6665
Long-8 (lb _f)	4	673	1337	2009	2658	3333	4007	4669	5337	6018	6701
F01 (μ ϵ)	11	4	52	87	147	187	238	280	326	369	414

**Table F-4. Raw data, strain survey conducted after phase I patch installation, ambient environmental conditions (Run 1)
(continued)**

Load Step	0	1	2	3	4	5	6	7	8	9	10
Pressure (psi)	-0.07	0.65	1.33	2.01	2.66	3.34	3.99	4.68	5.30	6.00	6.65
F02 ($\mu\epsilon$)	-23	73	108	171	204	266	309	363	408	463	511
F03 ($\mu\epsilon$)	61	-28	26	42	102	131	172	203	245	278	311
F04 ($\mu\epsilon$)	-23	100	143	214	255	326	377	437	493	559	613
F05 ($\mu\epsilon$)	-	-	-	-	-	-	-	-	-	-	-
F06 ($\mu\epsilon$)	-48	96	133	202	233	294	336	389	435	495	547
F07 ($\mu\epsilon$)	35	-38	31	47	115	137	182	222	264	300	339
F08 ($\mu\epsilon$)	-28	96	125	182	214	272	314	367	414	468	518
IS16 ($\mu\epsilon$)	-30	37	98	155	214	276	336	401	464	530	598
IS17 ($\mu\epsilon$)	-47	-109	-131	-135	-119	-93	-58	-14	32	83	140
IS18 ($\mu\epsilon$)	-55	-132	-171	-189	-187	-174	-153	-122	-86	-45	2
IS19 ($\mu\epsilon$)	-54	43	125	200	271	340	405	472	534	598	662
IS20 ($\mu\epsilon$)	-66	46	143	231	312	390	462	534	601	666	731
IS21 ($\mu\epsilon$)	-60	44	135	217	294	368	435	503	565	626	686
IS22 ($\mu\epsilon$)	-43	-128	-170	-198	-203	-199	-184	-159	-128	-91	-46
IS23 ($\mu\epsilon$)	-50	-94	-129	-155	-169	-179	-182	-178	-171	-159	-141
IS24 ($\mu\epsilon$)	-53	77	184	283	372	458	536	613	684	753	821
IS25 ($\mu\epsilon$)	70	31	-2	-27	-41	-51	-54	-50	-42	-30	-11
IS26 ($\mu\epsilon$)	38	243	401	550	681	808	920	1032	1133	1231	1326
IS27 ($\mu\epsilon$)	-56	-87	-109	-125	-128	-126	-119	-103	-84	-61	-31
IS28 ($\mu\epsilon$)	21	219	372	516	642	765	874	983	1082	1177	1271

**Table F-4. Raw data, strain survey conducted after phase I patch installation, ambient environmental conditions (Run 1)
(continued)**

Load Step	0	1	2	3	4	5	6	7	8	9	10
Pressure (psi)	-0.07	0.65	1.33	2.01	2.66	3.34	3.99	4.68	5.30	6.00	6.65
IS29 ($\mu\epsilon$)	9	189	329	458	572	682	778	876	966	1052	1137
IS30 ($\mu\epsilon$)	19	-49	-73	-89	-86	-75	-54	-24	10	50	97
IS31 ($\mu\epsilon$)	-9	122	225	326	417	508	590	675	753	830	907
IS32 ($\mu\epsilon$)	-18	95	185	268	343	416	479	543	601	657	712
IS33 ($\mu\epsilon$)	-10	110	204	292	370	447	513	580	641	701	759
IS34 ($\mu\epsilon$)	-55	-122	-160	-187	-194	-192	-182	-161	-136	-105	-67
IS35 ($\mu\epsilon$)	-77	-157	-226	-282	-322	-356	-380	-396	-407	-411	-409
IS36 ($\mu\epsilon$)	-18	102	195	283	361	437	503	570	630	688	745
IS37 ($\mu\epsilon$)	-50	-153	-233	-302	-351	-392	-422	-443	-458	-466	-466
IS38 ($\mu\epsilon$)	3	140	246	347	436	522	598	675	744	810	875
IS39 ($\mu\epsilon$)	-49	-164	-240	-302	-342	-373	-393	-402	-405	-401	-389
IS40 ($\mu\epsilon$)	2	134	239	338	427	515	592	670	741	810	878
IS41 ($\mu\epsilon$)	7	158	275	387	487	586	673	762	843	923	1002
IS42 ($\mu\epsilon$)	-28	49	117	185	251	320	386	457	524	593	664
IS43 ($\mu\epsilon$)	-31	-11	23	66	117	174	233	297	361	428	498
IS44 ($\mu\epsilon$)	-61	-84	-83	-70	-45	-12	27	73	120	172	228
IS45 ($\mu\epsilon$)	-11	99	193	279	357	434	504	575	640	705	769
IS46 ($\mu\epsilon$)	-11	88	175	255	328	399	463	527	587	645	702
IS47 ($\mu\epsilon$)	-11	84	167	244	314	383	445	508	566	624	680
IS48 ($\mu\epsilon$)	-26	-30	-8	20	58	102	150	205	261	320	384

**Table F-4. Raw data, strain survey conducted after phase I patch installation, ambient environmental conditions (Run 1)
(continued)**

Load Step	0	1	2	3	4	5	6	7	8	9	10
Pressure (psi)	-0.07	0.65	1.33	2.01	2.66	3.34	3.99	4.68	5.30	6.00	6.65
IS49 ($\mu\epsilon$)	-69	-58	-52	-45	-33	-18	0	23	47	74	106
IS50 ($\mu\epsilon$)	-7	104	198	285	362	438	506	575	638	699	760
IS51 ($\mu\epsilon$)	-48	-23	-9	6	24	44	67	94	122	152	187
IS52 ($\mu\epsilon$)	16	159	278	391	492	591	680	769	851	932	1011
IS53 ($\mu\epsilon$)	-67	-45	-30	-11	12	40	72	108	146	186	231
IS54 ($\mu\epsilon$)	4	142	257	365	461	555	640	726	805	882	958
IS55 ($\mu\epsilon$)	-8	123	232	330	419	505	583	663	735	808	880
IS56 ($\mu\epsilon$)	-11	41	91	138	189	244	298	356	414	474	537
IS57 ($\mu\epsilon$)	-57	-145	-184	-201	-196	-179	-154	-119	-80	-35	14
IS58 ($\mu\epsilon$)	0	-121	-185	-224	-237	-236	-225	-203	-174	-139	-97
IS59 ($\mu\epsilon$)	-18	70	145	216	283	349	411	476	538	601	665
IS60 ($\mu\epsilon$)	-28	72	158	236	307	377	440	504	564	624	683
IS61 ($\mu\epsilon$)	-31	68	153	230	301	370	432	496	555	615	672
IS62 ($\mu\epsilon$)	-48	-137	-178	-201	-203	-194	-177	-149	-116	-76	-31
IS63 ($\mu\epsilon$)	-65	-125	-165	-195	-215	-230	-238	-241	-239	-232	-220
IS64 ($\mu\epsilon$)	16	144	249	345	431	515	589	663	731	798	863
IS65 ($\mu\epsilon$)	-60	-97	-117	-132	-138	-140	-136	-128	-115	-99	-77
IS66 ($\mu\epsilon$)	20	232	401	562	700	835	952	1068	1174	1275	1373
IS67 ($\mu\epsilon$)	39	14	8	6	13	24	40	61	86	116	150
IS68 ($\mu\epsilon$)	14	206	360	508	635	762	871	980	1080	1177	1270

**Table F-4. Raw data, strain survey conducted after phase I patch installation, ambient environmental conditions (Run 1)
(continued)**

Load Step	0	1	2	3	4	5	6	7	8	9	10
Pressure (psi)	-0.07	0.65	1.33	2.01	2.66	3.34	3.99	4.68	5.30	6.00	6.65
IS69 ($\mu\epsilon$)	8	189	330	464	578	691	788	885	975	1062	1147
IS70 ($\mu\epsilon$)	-11	25	74	118	170	223	278	336	392	452	513
IS71 ($\mu\epsilon$)	-23	-54	-47	-23	14	59	108	163	220	280	343
IS72 ($\mu\epsilon$)	-26	-67	-69	-52	-23	17	60	111	163	220	281
IS73 ($\mu\epsilon$)	26	122	205	291	367	445	512	582	647	711	772
IS74 ($\mu\epsilon$)	8	101	183	265	338	413	479	547	609	670	729
IS75 ($\mu\epsilon$)	13	108	191	273	347	422	488	556	619	680	740
IS76 ($\mu\epsilon$)	-15	4	32	71	117	170	224	284	345	409	476
IS77 ($\mu\epsilon$)	-30	-54	-59	-48	-32	-10	14	43	74	107	144
IS78 ($\mu\epsilon$)	11	111	200	288	367	447	517	589	655	720	783
IS79 ($\mu\epsilon$)	-54	-85	-94	-85	-73	-53	-33	-7	19	49	82
IS80 ($\mu\epsilon$)	11	130	232	337	428	523	607	691	769	847	922
IS81 ($\mu\epsilon$)	-49	-96	-110	-107	-97	-78	-58	-31	-3	28	63
IS82 ($\mu\epsilon$)	-4	105	198	294	379	467	544	624	697	770	842
IS83 ($\mu\epsilon$)	-16	90	178	265	343	422	493	565	633	700	767
IS84 ($\mu\epsilon$)	-29	9	65	121	180	241	301	366	428	493	559
IS85 ($\mu\epsilon$)	-27	-31	-5	34	83	138	195	259	322	389	459
IS86 ($\mu\epsilon$)	-35	-51	-43	-20	15	57	102	155	209	267	330
IS87 ($\mu\epsilon$)	-10	88	166	238	303	366	424	483	537	591	646
IS88 ($\mu\epsilon$)	-10	78	150	217	277	335	387	439	487	534	581

**Table F-4. Raw data, strain survey conducted after phase I patch installation, ambient environmental conditions (Run 1)
(continued)**

Load Step	0	1	2	3	4	5	6	7	8	9	10
Pressure (psi)	-0.07	0.65	1.33	2.01	2.66	3.34	3.99	4.68	5.30	6.00	6.65
IS89 ($\mu\epsilon$)	-16	70	141	206	265	323	374	427	475	522	570
IS90 ($\mu\epsilon$)	-20	-19	-3	25	65	112	162	219	277	339	404
IS91 ($\mu\epsilon$)	-56	-33	-21	-8	9	29	51	79	107	139	175
IS92 ($\mu\epsilon$)	-16	83	164	238	303	368	425	482	535	587	637
IS93 ($\mu\epsilon$)	-59	-22	-1	21	46	74	104	138	173	211	253
IS94 ($\mu\epsilon$)	13	159	276	388	487	585	673	762	843	924	1003
IS95 ($\mu\epsilon$)	-54	-14	14	46	80	118	155	198	240	286	335
IS96 ($\mu\epsilon$)	1	137	244	346	437	527	607	689	764	838	913
IS97 ($\mu\epsilon$)	-3	131	232	326	410	492	567	643	712	782	852
L01 ($\mu\epsilon$)	-	-	-	-	-	-	-	-	-	-	-
L02 ($\mu\epsilon$)	-16	7	11	22	28	39	49	60	73	86	99
L03 ($\mu\epsilon$)	-18	-7	-12	-4	-3	8	18	30	44	60	77
L04 ($\mu\epsilon$)	-15	14	22	40	51	70	86	104	123	142	163
L05 ($\mu\epsilon$)	-8	9	16	27	33	43	52	61	72	82	93
L06 ($\mu\epsilon$)	-12	11	20	25	34	40	49	58	64	72	80
L07 ($\mu\epsilon$)	-	-	-	-	-	-	-	-	-	-	-
L08 ($\mu\epsilon$)	-10	48	74	102	122	146	167	189	211	233	255
L09 ($\mu\epsilon$)	-9	54	86	123	148	181	206	231	257	282	309
L10 ($\mu\epsilon$)	-	-	-	-	-	-	-	-	-	-	-

**Table F-4. Raw data, strain survey conducted after phase I patch installation, ambient environmental conditions (Run 1)
(continued)**

Load Step	0	1	2	3	4	5	6	7	8	9	10
Pressure (psi)	-0.07	0.65	1.33	2.01	2.66	3.34	3.99	4.68	5.30	6.00	6.65
RAC-A1 ($\mu\epsilon$)	11	130	232	338	433	532	620	711	795	878	960
RAC-A2 ($\mu\epsilon$)	6	117	212	309	394	484	563	643	718	793	865
RAC-A3 ($\mu\epsilon$)	-4	96	179	263	337	412	479	547	610	672	733
RAC-F1 ($\mu\epsilon$)	17	134	233	335	427	521	605	691	771	849	927
RAC-F2 ($\mu\epsilon$)	4	116	210	305	390	477	554	633	706	778	849
RBC-A1 ($\mu\epsilon$)	29	212	344	469	574	675	761	846	921	992	1060
RBC-A2 ($\mu\epsilon$)	17	178	295	404	496	585	661	736	802	865	925
RBC-A3 ($\mu\epsilon$)	17	165	273	375	462	546	618	690	755	816	876
RBC-A4 ($\mu\epsilon$)	4	136	237	332	416	497	569	641	706	768	829
RBC-F1 ($\mu\epsilon$)	24	209	339	461	563	660	745	826	899	967	1032
RBC-F2 ($\mu\epsilon$)	11	181	300	411	504	593	669	744	810	872	932
RBC-F3 ($\mu\epsilon$)	-1	164	278	385	474	560	634	706	771	832	891
S16 ($\mu\epsilon$)	81	283	448	588	709	822	922	1019	1108	1196	1282
S17 ($\mu\epsilon$)	-	-	-	-	-	-	-	-	-	-	-
S18 ($\mu\epsilon$)	47	117	189	261	331	401	469	539	606	674	744
S20 ($\mu\epsilon$)	-276	-731	-1059	-1369	-1623	-1866	-2073	-2270	-2442	-2600	-2748
S22 ($\mu\epsilon$)	55	216	354	477	586	688	778	867	949	1029	1108
S25 ($\mu\epsilon$)	107	280	441	594	736	877	1005	1135	1256	1376	1494
S29 ($\mu\epsilon$)	10	22	61	111	166	227	287	350	413	477	542
S30 ($\mu\epsilon$)	38	232	395	541	670	791	897	1002	1097	1189	1279

**Table F-4. Raw data, strain survey conducted after phase I patch installation, ambient environmental conditions (Run 1)
(continued)**

Load Step	0	1	2	3	4	5	6	7	8	9	10
Pressure (psi)	-0.07	0.65	1.33	2.01	2.66	3.34	3.99	4.68	5.30	6.00	6.65
S32 ($\mu\epsilon$)	-164	-355	-478	-598	-691	-782	-858	-930	-993	-1051	-1103
S34 ($\mu\epsilon$)	84	260	414	554	677	796	901	1005	1100	1194	1286
S37 ($\mu\epsilon$)	80	272	457	627	784	938	1078	1218	1349	1478	1605
S41 ($\mu\epsilon$)	-8	35	92	157	221	290	356	424	489	554	620
S42 ($\mu\epsilon$)	35	112	191	268	344	420	492	567	639	712	786
S43 ($\mu\epsilon$)	64	193	305	407	498	588	668	750	826	903	980
S44 ($\mu\epsilon$)	50	198	329	448	554	657	750	842	929	1014	1099
S46 ($\mu\epsilon$)	-112	-440	-699	-948	-1160	-1369	-1551	-1728	-1889	-2043	-2189
S48 ($\mu\epsilon$)	53	177	288	394	488	581	665	749	827	906	983
S51 ($\mu\epsilon$)	75	210	352	491	621	752	873	995	1111	1226	1340
S55 ($\mu\epsilon$)	-2	40	94	154	213	275	335	397	455	515	574
S56 ($\mu\epsilon$)	28	112	192	270	344	419	489	562	632	704	776
S57 ($\mu\epsilon$)	107	311	466	597	707	811	901	990	1072	1154	1233
S58 ($\mu\epsilon$)	102	348	534	689	819	941	1046	1148	1241	1332	1420
S60 ($\mu\epsilon$)	133	-415	-815	-1186	-1486	-1774	-2018	-2247	-2449	-2631	-2797
S62 ($\mu\epsilon$)	89	273	416	540	646	746	833	919	997	1075	1150
S65 ($\mu\epsilon$)	107	315	488	654	803	953	1089	1226	1353	1481	1604
S69 ($\mu\epsilon$)	18	53	103	162	223	289	353	421	487	555	622
S70 ($\mu\epsilon$)	31	104	176	249	320	392	459	530	598	668	738
S71 ($\mu\epsilon$)	32	167	278	375	462	547	623	701	773	847	920

**Table F-4. Raw data, strain survey conducted after phase I patch installation, ambient environmental conditions (Run 1)
(continued)**

Load Step	0	1	2	3	4	5	6	7	8	9	10
Pressure (psi)	-0.07	0.65	1.33	2.01	2.66	3.34	3.99	4.68	5.30	6.00	6.65
S72 ($\mu\epsilon$)	55	219	352	466	568	666	754	842	924	1006	1086
S74 ($\mu\epsilon$)	-68	-241	-379	-526	-649	-781	-894	-1009	-1116	-1219	-1319
S76 ($\mu\epsilon$)	26	144	256	356	448	538	619	702	779	857	933
S79 ($\mu\epsilon$)	86	269	425	564	693	820	937	1056	1167	1279	1388
S83 ($\mu\epsilon$)	9	89	157	223	286	352	413	477	537	600	661
S84 ($\mu\epsilon$)	63	153	234	312	387	463	534	608	678	750	823
S85 ($\mu\epsilon$)	60	187	292	386	470	551	625	700	771	842	913
S86 ($\mu\epsilon$)	72	220	347	460	559	656	741	827	906	985	1063
S88 ($\mu\epsilon$)	-4	-154	-248	-332	-394	-452	-497	-537	-568	-595	-615
S90 ($\mu\epsilon$)	45	173	287	390	481	570	648	728	802	875	948
S93 ($\mu\epsilon$)	116	250	389	526	652	779	895	1012	1123	1232	1340
S97 ($\mu\epsilon$)	17	71	132	197	260	325	387	452	513	575	638
UAC-A1 ($\mu\epsilon$)	21	182	318	447	562	673	773	873	963	1052	1138
UAC-A2 ($\mu\epsilon$)	4	153	277	393	495	596	685	773	853	930	1006
UAC-A3 ($\mu\epsilon$)	-3	132	243	344	434	520	598	675	746	815	883
UAC-F1 ($\mu\epsilon$)	38	193	325	452	565	676	776	875	966	1056	1143
UAC-F2 ($\mu\epsilon$)	12	152	272	384	483	581	668	755	834	911	987
UBC-A1 ($\mu\epsilon$)	81	348	552	742	905	1063	1199	1333	1452	1566	1675
UBC-A2 ($\mu\epsilon$)	43	275	452	616	757	893	1010	1126	1229	1327	1422
UBC-A3 ($\mu\epsilon$)	49	265	429	581	712	839	948	1056	1153	1245	1334

**Table F-4. Raw data, strain survey conducted after phase I patch installation, ambient environmental conditions (Run 1)
(continued)**

Load Step	0	1	2	3	4	5	6	7	8	9	10
Pressure (psi)	-0.07	0.65	1.33	2.01	2.66	3.34	3.99	4.68	5.30	6.00	6.65
UBC-A4 ($\mu\epsilon$)	18	211	359	498	619	736	838	940	1032	1119	1205
UBC-F1 ($\mu\epsilon$)	86	356	559	750	913	1070	1206	1339	1458	1570	1678
UBC-F2 ($\mu\epsilon$)	29	265	442	607	748	884	1001	1116	1219	1316	1410
UBC-F3 ($\mu\epsilon$)	13	235	401	555	688	815	925	1034	1131	1223	1312
UDAC-A1 ($\mu\epsilon$)	19	180	308	431	540	646	740	834	920	1004	1087
UDAC-A2 ($\mu\epsilon$)	8	155	271	380	476	570	653	737	812	886	959
UDAC-A3 ($\mu\epsilon$)	-1	129	229	323	407	487	560	633	699	764	830
UDAC-F1 ($\mu\epsilon$)	16	174	305	431	542	651	748	844	932	1019	1102
UDAC-F2 ($\mu\epsilon$)	7	147	260	368	464	558	641	724	800	874	948
UDBC-A1 ($\mu\epsilon$)	55	324	531	728	891	1052	1187	1319	1437	1549	1654
UDBC-A2 ($\mu\epsilon$)	33	267	448	620	764	905	1025	1142	1247	1346	1441
UDBC-A3 ($\mu\epsilon$)	15	235	405	567	703	836	949	1059	1159	1253	1342
UDBC-A4 ($\mu\epsilon$)	8	202	355	501	624	745	849	952	1045	1135	1220
UDBC-F1 ($\mu\epsilon$)	67	362	587	798	974	1146	1291	1433	1559	1678	1791
UDBC-F2 ($\mu\epsilon$)	36	287	477	656	806	952	1075	1196	1304	1406	1502
UDBC-F3 ($\mu\epsilon$)	16	251	429	596	737	874	990	1104	1205	1301	1393

Table F-5. Raw data, strain survey conducted after phase I patch installation, ambient environmental conditions (Run 2)

Load Step	0	1	2	3	4	5	6	7	8	9	10
Pressure (psi)	-0.05	0.64	1.34	1.99	2.66	3.34	4.00	4.66	5.33	6.00	6.69
Frame-1 (lbf)	0	82	215	315	457	573	669	788	940	1005	1132
Frame-2 (lbf)	50	56	210	343	452	567	680	795	906	1020	1133
Frame-3 (lbf)	0	103	230	342	454	562	679	794	903	1019	1137
Frame-4 (lbf)	28	27	229	342	453	569	680	795	908	1019	1132
Frame-5 (lbf)	4	115	222	336	461	565	677	791	907	1014	1124
Frame-6 (lbf)	16	116	218	341	452	573	683	799	900	1023	1139
Frame-7 (lbf)	0	111	229	337	457	563	676	790	907	1019	1133
Frame-8 (lbf)	2	121	228	341	455	567	681	791	910	1018	1132
Frame-9 (lbf)	31	115	224	332	454	570	679	794	905	1019	1132
Frame-10 (lbf)	-1	114	230	343	463	558	680	788	905	1020	1134
Frame-11 (lbf)	-3	112	224	340	454	571	685	788	907	1018	1138
Frame-12 (lbf)	14	115	227	338	457	564	677	793	907	1020	1136
Hoop-1 (lbf)	19	710	1432	2152	2860	3571	4286	4994	5716	6431	7130
Hoop-2 (lbf)	168	683	1438	2156	2858	3560	4271	4997	5706	6420	7169
Hoop-3 (lbf)	42	714	1397	2140	2861	3581	4276	5001	5690	6444	7151
Hoop-4 (lbf)	6	718	1426	2147	2886	3554	4296	5004	5704	6419	7160
Hoop-5 (lbf)	25	752	1433	2149	2867	3568	4275	5006	5718	6425	7135
Hoop-6 (lbf)	3	713	1428	2135	2867	3568	4285	4998	5702	6435	7160
Hoop-7 (lbf)	17	715	1429	2150	2855	3564	4273	4991	5709	6421	7149
Hoop-8 (lbf)	86	715	1424	2142	2863	3563	4279	4991	5705	6425	7143
Hoop-9 (lbf)	23	727	1455	2172	2866	3573	4292	4995	5720	6432	7149

**Table F-5. Raw data, strain survey conducted after phase I patch installation, ambient environmental conditions (Run 2)
(continued)**

Load Step	0	1	2	3	4	5	6	7	8	9	10
Pressure (psi)	-0.05	0.64	1.34	1.99	2.66	3.34	4.00	4.66	5.33	6.00	6.69
Hoop-10 (lb _f)	-6	700	1420	2143	2887	3568	4286	4999	5718	6433	7154
Hoop-11 (lb _f)	0	697	1436	2117	2857	3562	4303	4989	5711	6419	7136
Hoop-12 (lb _f)	112	706	1403	2134	2857	3564	4281	5004	5710	6424	7151
Hoop-13 (lb _f)	11	694	1421	2166	2859	3574	4287	5006	5712	6423	7156
Hoop-14 (lb _f)	2	712	1430	2133	2863	3566	4281	4995	5707	6422	7157
Long-1 (lb _f)	1	676	1349	2010	2671	3339	3994	4673	5386	6027	6624
Long-2 (lb _f)	9	664	1348	2002	2671	3342	4028	4673	5352	6015	6681
Long-3 (lb _f)	-8	662	1333	2003	2666	3334	4001	4674	5348	6007	6623
Long-4 (lb _f)	9	654	1330	2009	2672	3334	4003	4672	5338	6001	6681
Long-5 (lb _f)	2	636	1336	2005	2667	3339	4014	4683	5336	6029	6654
Long-6 (lb _f)	9	668	1345	2008	2661	3341	4016	4667	5338	6035	6705
Long-7 (lb _f)	-9	699	1368	2001	2657	3351	4009	4686	5343	6021	6636
Long-8 (lb _f)	-1	649	1328	2000	2671	3335	4006	4673	5343	6003	6656
F01 (μ ϵ)	-6	-8	35	87	148	182	232	279	313	365	405
F02 (μ ϵ)	-1	80	123	168	220	273	316	365	421	470	524
F03 (μ ϵ)	20	-69	7	50	95	131	169	206	235	277	306
F04 (μ ϵ)	9	96	157	210	261	329	377	436	503	560	626
F05 (μ ϵ)	-	-	-	-	-	-	-	-	-	-	-
F06 (μ ϵ)	0	103	146	185	235	289	332	378	440	492	551
F07 (μ ϵ)	-12	-59	14	62	109	143	187	228	257	304	334

**Table F-5. Raw data, strain survey conducted after phase I patch installation, ambient environmental conditions (Run 2)
(continued)**

Load Step	0	1	2	3	4	5	6	7	8	9	10
Pressure (psi)	-0.05	0.64	1.34	1.99	2.66	3.34	4.00	4.66	5.33	6.00	6.69
F08 ($\mu\epsilon$)	18	88	127	169	217	270	312	360	417	468	523
IS16 ($\mu\epsilon$)	-29	39	94	151	214	271	335	398	463	527	597
IS17 ($\mu\epsilon$)	-50	-107	-136	-137	-120	-97	-59	-17	30	80	138
IS18 ($\mu\epsilon$)	-62	-132	-176	-191	-189	-178	-155	-124	-89	-48	-1
IS19 ($\mu\epsilon$)	-58	41	121	196	269	334	402	468	532	594	660
IS20 ($\mu\epsilon$)	-69	43	140	226	311	384	459	530	597	662	729
IS21 ($\mu\epsilon$)	-65	40	132	213	293	362	433	499	562	622	684
IS22 ($\mu\epsilon$)	-55	-135	-175	-198	-205	-203	-186	-161	-131	-93	-48
IS23 ($\mu\epsilon$)	-57	-94	-134	-158	-173	-183	-184	-181	-174	-162	-144
IS24 ($\mu\epsilon$)	-55	75	183	279	371	452	533	609	681	749	818
IS25 ($\mu\epsilon$)	65	31	-6	-29	-43	-54	-55	-51	-44	-32	-14
IS26 ($\mu\epsilon$)	43	246	406	548	685	805	922	1031	1134	1230	1327
IS27 ($\mu\epsilon$)	-62	-88	-113	-126	-129	-130	-119	-105	-86	-63	-34
IS28 ($\mu\epsilon$)	24	221	376	513	646	762	875	981	1082	1176	1272
IS29 ($\mu\epsilon$)	9	189	331	455	574	677	779	875	965	1050	1137
IS30 ($\mu\epsilon$)	8	-52	-82	-92	-89	-81	-56	-28	6	47	94
IS31 ($\mu\epsilon$)	-7	123	225	322	417	502	589	672	751	828	906
IS32 ($\mu\epsilon$)	-18	96	183	265	343	410	478	540	599	654	710
IS33 ($\mu\epsilon$)	-8	111	203	288	371	440	512	578	639	698	757
IS34 ($\mu\epsilon$)	-64	-131	-167	-188	-196	-197	-184	-164	-140	-108	-70

**Table F-5. Raw data, strain survey conducted after phase I patch installation, ambient environmental conditions (Run 2)
(continued)**

Load Step	0	1	2	3	4	5	6	7	8	9	10
Pressure (psi)	-0.05	0.64	1.34	1.99	2.66	3.34	4.00	4.66	5.33	6.00	6.69
IS35 ($\mu\epsilon$)	-83	-157	-234	-286	-327	-361	-383	-399	-411	-414	-413
IS36 ($\mu\epsilon$)	-17	102	194	279	361	431	502	567	627	685	742
IS37 ($\mu\epsilon$)	-56	-153	-241	-304	-354	-396	-424	-445	-461	-469	-470
IS38 ($\mu\epsilon$)	5	141	247	344	437	518	598	672	742	808	874
IS39 ($\mu\epsilon$)	-58	-166	-248	-304	-345	-378	-395	-404	-409	-404	-394
IS40 ($\mu\epsilon$)	4	135	238	335	428	510	591	668	739	808	877
IS41 ($\mu\epsilon$)	10	158	276	384	489	582	673	761	843	921	1001
IS42 ($\mu\epsilon$)	-28	51	114	181	250	315	385	453	522	591	663
IS43 ($\mu\epsilon$)	-31	-7	22	65	117	170	232	295	361	427	498
IS44 ($\mu\epsilon$)	-62	-78	-86	-72	-47	-16	26	70	119	170	227
IS45 ($\mu\epsilon$)	-10	103	193	277	358	430	504	572	640	704	769
IS46 ($\mu\epsilon$)	-11	90	175	253	328	394	462	524	586	643	702
IS47 ($\mu\epsilon$)	-11	85	167	242	314	379	445	505	565	622	679
IS48 ($\mu\epsilon$)	-34	-33	-11	19	57	97	149	202	259	318	383
IS49 ($\mu\epsilon$)	-67	-48	-53	-45	-34	-21	0	21	46	73	106
IS50 ($\mu\epsilon$)	-6	107	199	283	363	434	506	572	637	698	760
IS51 ($\mu\epsilon$)	-44	-11	-8	6	24	42	67	93	122	152	187
IS52 ($\mu\epsilon$)	19	165	282	390	494	588	681	767	853	932	1013
IS53 ($\mu\epsilon$)	-63	-34	-30	-11	13	38	72	107	145	185	231
IS54 ($\mu\epsilon$)	7	149	260	363	463	552	641	724	805	881	959

**Table F-5. Raw data, strain survey conducted after phase I patch installation, ambient environmental conditions (Run 2)
(continued)**

Load Step	0	1	2	3	4	5	6	7	8	9	10
Pressure (psi)	-0.05	0.64	1.34	1.99	2.66	3.34	4.00	4.66	5.33	6.00	6.69
IS55 ($\mu\epsilon$)	-7	129	232	328	420	500	583	659	734	806	880
IS56 ($\mu\epsilon$)	-12	40	89	137	190	240	297	354	412	472	537
IS57 ($\mu\epsilon$)	-65	-148	-188	-202	-197	-183	-156	-121	-82	-39	13
IS58 ($\mu\epsilon$)	-10	-123	-190	-225	-239	-240	-227	-204	-176	-141	-98
IS59 ($\mu\epsilon$)	-21	66	145	214	283	345	410	473	536	597	664
IS60 ($\mu\epsilon$)	-31	69	157	233	307	372	438	502	562	620	681
IS61 ($\mu\epsilon$)	-34	64	152	228	301	365	430	493	553	610	670
IS62 ($\mu\epsilon$)	-58	-142	-183	-202	-205	-199	-179	-151	-119	-80	-33
IS63 ($\mu\epsilon$)	-78	-125	-168	-197	-218	-233	-240	-243	-241	-235	-223
IS64 ($\mu\epsilon$)	15	143	251	344	433	511	588	661	730	795	863
IS65 ($\mu\epsilon$)	-74	-96	-119	-133	-139	-143	-138	-130	-118	-102	-79
IS66 ($\mu\epsilon$)	20	235	409	560	704	831	953	1067	1174	1273	1374
IS67 ($\mu\epsilon$)	27	17	8	7	14	22	40	62	86	115	150
IS68 ($\mu\epsilon$)	14	211	368	507	640	758	872	979	1081	1175	1272
IS69 ($\mu\epsilon$)	8	194	337	463	582	686	788	884	975	1060	1148
IS70 ($\mu\epsilon$)	-18	23	70	117	169	219	276	333	391	449	512
IS71 ($\mu\epsilon$)	-32	-57	-50	-25	13	54	106	161	218	276	341
IS72 ($\mu\epsilon$)	-34	-69	-71	-54	-23	12	58	108	162	217	279
IS73 ($\mu\epsilon$)	23	119	206	287	366	439	509	578	644	704	768
IS74 ($\mu\epsilon$)	7	99	184	262	339	410	479	545	609	668	729

**Table F-5. Raw data, strain survey conducted after phase I patch installation, ambient environmental conditions (Run 2)
(continued)**

Load Step	0	1	2	3	4	5	6	7	8	9	10
Pressure (psi)	-0.05	0.64	1.34	1.99	2.66	3.34	4.00	4.66	5.33	6.00	6.69
IS75 ($\mu\epsilon$)	12	106	191	270	348	418	487	554	618	678	739
IS76 ($\mu\epsilon$)	-18	0	30	69	116	165	222	282	343	405	474
IS77 ($\mu\epsilon$)	-38	-53	-58	-50	-32	-13	13	42	73	105	143
IS78 ($\mu\epsilon$)	10	110	202	285	368	443	516	587	655	718	783
IS79 ($\mu\epsilon$)	-62	-82	-92	-87	-73	-56	-34	-8	19	47	81
IS80 ($\mu\epsilon$)	11	131	236	334	431	520	606	690	771	845	923
IS81 ($\mu\epsilon$)	-60	-94	-111	-110	-97	-82	-60	-34	-5	25	61
IS82 ($\mu\epsilon$)	-4	106	202	291	381	463	544	622	698	769	842
IS83 ($\mu\epsilon$)	-19	90	179	261	343	416	490	561	630	695	764
IS84 ($\mu\epsilon$)	-32	11	62	118	180	236	301	363	427	490	558
IS85 ($\mu\epsilon$)	-30	-26	-7	32	82	132	194	256	321	387	458
IS86 ($\mu\epsilon$)	-36	-45	-45	-22	14	52	102	153	207	265	328
IS87 ($\mu\epsilon$)	-10	91	165	235	302	361	423	479	535	589	644
IS88 ($\mu\epsilon$)	-10	78	149	214	276	330	385	436	485	532	579
IS89 ($\mu\epsilon$)	-16	70	138	202	265	317	373	424	472	521	569
IS90 ($\mu\epsilon$)	-22	-19	-6	23	64	106	160	216	275	336	402
IS91 ($\mu\epsilon$)	-53	-22	-23	-10	8	25	51	77	105	137	173
IS92 ($\mu\epsilon$)	-16	85	163	234	303	362	423	479	533	584	636
IS93 ($\mu\epsilon$)	-53	-8	-2	20	46	70	104	137	172	209	252
IS94 ($\mu\epsilon$)	20	167	280	387	491	582	675	761	844	923	1004

**Table F-5. Raw data, strain survey conducted after phase I patch installation, ambient environmental conditions (Run 2)
(continued)**

Load Step	0	1	2	3	4	5	6	7	8	9	10
Pressure (psi)	-0.05	0.64	1.34	1.99	2.66	3.34	4.00	4.66	5.33	6.00	6.69
IS95 ($\mu\epsilon$)	-49	-3	13	44	81	113	155	197	239	285	334
IS96 ($\mu\epsilon$)	7	146	247	344	440	523	609	688	764	838	913
IS97 ($\mu\epsilon$)	0	138	232	322	411	486	566	639	710	779	850
L01 ($\mu\epsilon$)	-	-	-	-	-	-	-	-	-	-	-
L02 ($\mu\epsilon$)	-8	15	15	21	27	41	49	61	76	89	101
L03 ($\mu\epsilon$)	-11	5	-5	-5	-1	13	21	34	51	66	82
L04 ($\mu\epsilon$)	-7	22	30	42	55	75	90	109	130	149	169
L05 ($\mu\epsilon$)	-3	12	22	30	37	48	56	66	76	87	97
L06 ($\mu\epsilon$)	-9	14	20	28	36	42	52	60	65	72	78
L07 ($\mu\epsilon$)	-	-	-	-	-	-	-	-	-	-	-
L08 ($\mu\epsilon$)	-2	54	77	100	121	148	167	189	214	235	256
L09 ($\mu\epsilon$)	-2	69	93	126	155	185	212	239	263	293	316
L10 ($\mu\epsilon$)	-	-	-	-	-	-	-	-	-	-	-
RAC-A1 ($\mu\epsilon$)	12	131	236	336	436	529	621	710	796	877	962
RAC-A2 ($\mu\epsilon$)	6	118	215	306	396	480	562	642	719	791	866
RAC-A3 ($\mu\epsilon$)	-5	96	181	259	337	407	477	544	608	668	731
RAC-F1 ($\mu\epsilon$)	19	134	237	334	430	519	606	691	772	849	929
RAC-F2 ($\mu\epsilon$)	4	114	212	303	392	474	554	632	706	777	849
RBC-A1 ($\mu\epsilon$)	35	215	347	465	576	670	761	844	920	990	1059
RBC-A2 ($\mu\epsilon$)	21	180	296	400	497	580	660	734	801	863	924

**Table F-5. Raw data, strain survey conducted after phase I patch installation, ambient environmental conditions (Run 2)
(continued)**

Load Step	0	1	2	3	4	5	6	7	8	9	10
Pressure (psi)	-0.05	0.64	1.34	1.99	2.66	3.34	4.00	4.66	5.33	6.00	6.69
RBC-A3 ($\mu\epsilon$)	20	166	274	371	463	541	618	688	753	814	874
RBC-A4 ($\mu\epsilon$)	6	136	237	329	417	493	568	639	704	766	828
RBC-F1 ($\mu\epsilon$)	31	215	342	457	565	656	745	825	898	966	1032
RBC-F2 ($\mu\epsilon$)	18	188	302	408	506	589	669	742	809	870	931
RBC-F3 ($\mu\epsilon$)	5	170	279	381	475	555	633	704	769	830	890
S16 ($\mu\epsilon$)	84	278	452	588	714	819	924	1018	1109	1196	1284
S17 ($\mu\epsilon$)	-	-	-	-	-	-	-	-	-	-	-
S18 ($\mu\epsilon$)	45	112	194	262	335	401	472	539	607	674	745
S20 ($\mu\epsilon$)	-304	-756	-1086	-1371	-1640	-1874	-2088	-2277	-2453	-2608	-2756
S22 ($\mu\epsilon$)	60	215	357	476	589	684	779	865	949	1028	1109
S25 ($\mu\epsilon$)	112	277	447	594	741	873	1008	1134	1258	1376	1497
S29 ($\mu\epsilon$)	12	22	63	111	168	226	288	350	414	477	543
S30 ($\mu\epsilon$)	40	226	398	541	673	787	897	999	1096	1187	1280
S32 ($\mu\epsilon$)	-184	-372	-493	-602	-702	-790	-867	-937	-1002	-1057	-1111
S34 ($\mu\epsilon$)	89	266	417	552	681	792	902	1003	1100	1192	1287
S37 ($\mu\epsilon$)	79	266	459	626	788	932	1078	1215	1348	1476	1607
S41 ($\mu\epsilon$)	-8	34	93	155	223	288	356	422	489	553	620
S42 ($\mu\epsilon$)	33	107	194	270	346	417	493	566	640	712	788
S43 ($\mu\epsilon$)	64	187	309	407	502	585	670	749	828	904	983
S44 ($\mu\epsilon$)	48	191	331	447	557	654	750	840	929	1014	1100

**Table F-5. Raw data, strain survey conducted after phase I patch installation, ambient environmental conditions (Run 2)
(continued)**

Load Step	0	1	2	3	4	5	6	7	8	9	10
Pressure (psi)	-0.05	0.64	1.34	1.99	2.66	3.34	4.00	4.66	5.33	6.00	6.69
S46 ($\mu\epsilon$)	-133	-463	-718	-950	-1172	-1373	-1560	-1733	-1900	-2049	-2199
S48 ($\mu\epsilon$)	56	176	290	392	491	578	665	747	828	904	984
S51 ($\mu\epsilon$)	71	200	353	488	624	748	873	992	1112	1225	1342
S55 ($\mu\epsilon$)	-4	35	93	150	212	271	333	393	453	512	574
S56 ($\mu\epsilon$)	29	110	196	271	348	418	492	562	633	703	778
S57 ($\mu\epsilon$)	115	310	472	597	712	809	904	990	1074	1154	1236
S58 ($\mu\epsilon$)	112	345	539	689	825	938	1048	1147	1242	1331	1423
S60 ($\mu\epsilon$)	130	-419	-827	-1171	-1493	-1768	-2019	-2241	-2448	-2627	-2796
S62 ($\mu\epsilon$)	96	271	420	539	650	742	834	917	997	1073	1151
S65 ($\mu\epsilon$)	119	312	495	653	810	951	1092	1225	1356	1480	1608
S69 ($\mu\epsilon$)	23	53	105	162	226	289	355	421	489	555	625
S70 ($\mu\epsilon$)	33	100	178	248	321	388	459	528	597	665	738
S71 ($\mu\epsilon$)	35	163	279	374	464	543	622	698	772	844	920
S72 ($\mu\epsilon$)	60	213	352	465	570	662	753	840	924	1003	1087
S74 ($\mu\epsilon$)	-77	-250	-393	-527	-659	-785	-901	-1015	-1125	-1226	-1329
S76 ($\mu\epsilon$)	27	141	256	354	449	533	618	699	778	853	932
S79 ($\mu\epsilon$)	91	261	423	561	695	815	936	1052	1166	1275	1389
S83 ($\mu\epsilon$)	15	89	158	222	288	349	412	475	537	597	660
S84 ($\mu\epsilon$)	64	150	236	311	389	459	534	605	678	749	824
S85 ($\mu\epsilon$)	62	181	295	386	473	548	627	699	771	842	915

**Table F-5. Raw data, strain survey conducted after phase I patch installation, ambient environmental conditions (Run 2)
(continued)**

Load Step	0	1	2	3	4	5	6	7	8	9	10
Pressure (psi)	-0.05	0.64	1.34	1.99	2.66	3.34	4.00	4.66	5.33	6.00	6.69
S86 ($\mu\epsilon$)	71	210	349	459	563	652	742	825	907	985	1066
S88 ($\mu\epsilon$)	-15	-166	-255	-331	-398	-454	-499	-538	-571	-595	-615
S90 ($\mu\epsilon$)	46	169	289	389	484	566	649	726	802	875	950
S93 ($\mu\epsilon$)	113	237	392	524	656	775	896	1010	1124	1232	1344
S97 ($\mu\epsilon$)	19	70	135	197	263	324	389	451	514	575	640
UAC-A1 ($\mu\epsilon$)	25	190	323	446	565	670	775	871	965	1052	1140
UAC-A2 ($\mu\epsilon$)	6	159	279	391	497	591	685	770	853	929	1007
UAC-A3 ($\mu\epsilon$)	0	138	244	342	435	516	598	673	746	814	883
UAC-F1 ($\mu\epsilon$)	45	200	332	453	570	675	779	876	970	1057	1146
UAC-F2 ($\mu\epsilon$)	17	158	276	384	486	579	670	754	836	912	989
UBC-A1 ($\mu\epsilon$)	89	353	559	740	911	1060	1201	1332	1453	1565	1675
UBC-A2 ($\mu\epsilon$)	48	278	456	612	760	888	1011	1124	1229	1325	1422
UBC-A3 ($\mu\epsilon$)	53	267	433	578	715	834	949	1055	1153	1243	1334
UBC-A4 ($\mu\epsilon$)	19	211	362	495	621	731	838	938	1031	1117	1204
UBC-F1 ($\mu\epsilon$)	95	364	567	747	919	1066	1208	1338	1459	1569	1679
UBC-F2 ($\mu\epsilon$)	36	273	447	604	752	879	1002	1114	1219	1315	1411
UBC-F3 ($\mu\epsilon$)	19	242	405	552	691	810	926	1031	1131	1221	1312
UDAC-A1 ($\mu\epsilon$)	28	190	313	430	544	643	742	833	921	1004	1087
UDAC-A2 ($\mu\epsilon$)	15	164	274	378	479	566	654	735	812	886	960
UDAC-A3 ($\mu\epsilon$)	4	136	231	321	409	483	560	630	698	763	829

**Table F-5. Raw data, strain survey conducted after phase I patch installation, ambient environmental conditions (Run 2)
(continued)**

Load Step	0	1	2	3	4	5	6	7	8	9	10
Pressure (psi)	-0.05	0.64	1.34	1.99	2.66	3.34	4.00	4.66	5.33	6.00	6.69
UDAC-F1 ($\mu\epsilon$)	24	182	311	430	545	648	749	843	934	1018	1104
UDAC-F2 ($\mu\epsilon$)	14	153	264	367	467	554	642	723	800	874	948
UDBC-A1 ($\mu\epsilon$)	58	328	541	726	897	1048	1188	1318	1439	1547	1656
UDBC-A2 ($\mu\epsilon$)	35	271	457	618	769	902	1026	1141	1248	1345	1442
UDBC-A3 ($\mu\epsilon$)	16	239	414	565	707	832	949	1058	1159	1251	1343
UDBC-A4 ($\mu\epsilon$)	8	207	363	499	628	742	850	951	1046	1133	1221
UDBC-F1 ($\mu\epsilon$)	71	364	597	795	980	1142	1293	1432	1561	1677	1793
UDBC-F2 ($\mu\epsilon$)	39	288	485	653	811	948	1076	1195	1305	1404	1504
UDBC-F3 ($\mu\epsilon$)	18	252	436	593	741	870	990	1102	1205	1300	1394

Table F-6. Raw data, strain survey conducted after phase I patch installation, ambient environmental conditions (Run 3)

Load Step	0	1	2	3	4	5	6	7	8	9	10
Pressure (psi)	-0.02	0.67	1.33	2.00	2.67	3.32	4.00	4.66	5.40	5.99	6.70
Frame-1 (lbf)	-1	129	272	325	470	544	677	756	896	1006	1149
Frame-2 (lbf)	39	36	241	325	454	561	681	792	907	1021	1131
Frame-3 (lbf)	0	109	235	348	449	568	681	792	908	1021	1133
Frame-4 (lbf)	29	105	226	343	452	570	681	795	905	1020	1136
Frame-5 (lbf)	2	119	232	328	453	564	683	787	903	1026	1127
Frame-6 (lbf)	16	109	222	349	448	571	689	791	910	1027	1128
Frame-7 (lbf)	3	104	225	345	460	568	683	792	903	1025	1128
Frame-8 (lbf)	-3	115	229	338	448	571	683	791	906	1016	1132
Frame-9 (lbf)	24	115	229	335	458	567	671	792	907	1020	1132
Frame-10 (lbf)	0	118	232	349	443	576	694	781	901	1021	1134
Frame-11 (lbf)	-4	113	223	335	453	562	685	786	906	1021	1130
Frame-12 (lbf)	25	112	224	346	446	567	681	791	904	1020	1133
Hoop-1 (lbf)	19	692	1410	2148	2862	3577	4278	5005	5724	6451	7114
Hoop-2 (lbf)	187	714	1441	2137	2851	3573	4284	5014	5717	6415	7156
Hoop-3 (lbf)	40	732	1447	2148	2859	3568	4278	5006	5722	6426	7127
Hoop-4 (lbf)	13	706	1415	2151	2861	3578	4283	5003	5718	6436	7137
Hoop-5 (lbf)	25	738	1436	2143	2852	3571	4286	4997	5725	6442	7135
Hoop-6 (lbf)	10	710	1428	2150	2871	3559	4283	5001	5708	6437	7130
Hoop-7 (lbf)	10	717	1430	2113	2855	3560	4281	5003	5708	6420	7146
Hoop-8 (lbf)	87	712	1426	2141	2866	3570	4292	5000	5713	6423	7152
Hoop-9 (lbf)	38	717	1459	2126	2857	3540	4282	5000	5718	6422	7131

**Table F-6. Raw data, strain survey conducted after phase I patch installation, ambient environmental conditions (Run 3)
(continued)**

Load Step	0	1	2	3	4	5	6	7	8	9	10
Pressure (psi)	-0.02	0.67	1.33	2.00	2.67	3.32	4.00	4.66	5.40	5.99	6.70
Hoop-10 (lb _f)	0	713	1426	2128	2856	3586	4282	4999	5715	6425	7144
Hoop-11 (lb _f)	10	732	1417	2149	2874	3571	4269	5000	5703	6440	7144
Hoop-12 (lb _f)	139	741	1439	2134	2859	3560	4284	4998	5734	6424	7145
Hoop-13 (lb _f)	27	686	1427	2164	2862	3600	4272	5005	5724	6414	7130
Hoop-14 (lb _f)	-3	740	1429	2145	2855	3574	4292	4993	5706	6430	7138
Long-1 (lb _f)	-48	677	1365	1977	2678	3311	3998	4702	5347	6054	6634
Long-2 (lb _f)	-11	683	1320	2008	2667	3338	4024	4678	5346	6008	6672
Long-3 (lb _f)	-6	661	1338	1999	2669	3340	4011	4670	5345	6007	6666
Long-4 (lb _f)	-5	668	1319	2011	2670	3332	4003	4680	5334	6007	6679
Long-5 (lb _f)	1	657	1337	2004	2670	3338	4033	4674	5325	6013	6682
Long-6 (lb _f)	-5	683	1340	1997	2670	3334	4008	4675	5356	6015	6680
Long-7 (lb _f)	-73	663	1334	2005	2658	3343	3970	4660	5359	6007	6680
Long-8 (lb _f)	1	693	1333	2002	2679	3341	4010	4694	5337	6041	6672
F01 (μ ϵ)	-32	-21	40	85	136	183	227	270	293	357	395
F02 (μ ϵ)	17	80	124	173	219	266	322	368	444	470	532
F03 (μ ϵ)	-14	-47	16	48	96	135	161	200	213	271	299
F04 (μ ϵ)	37	111	155	209	264	318	382	440	532	560	631
F05 (μ ϵ)	-	-	-	-	-	-	-	-	-	-	-
F06 (μ ϵ)	30	108	141	191	233	278	341	381	473	492	561
F07 (μ ϵ)	-45	-68	23	63	99	145	181	220	235	294	327

**Table F-6. Raw data, strain survey conducted after phase I patch installation, ambient environmental conditions (Run 3)
(continued)**

Load Step	0	1	2	3	4	5	6	7	8	9	10
Pressure (psi)	-0.02	0.67	1.33	2.00	2.67	3.32	4.00	4.66	5.40	5.99	6.70
F08 ($\mu\epsilon$)	42	78	129	168	218	262	319	366	443	469	530
IS16 ($\mu\epsilon$)	-28	35	94	152	211	271	332	397	462	528	595
IS17 ($\mu\epsilon$)	-57	-114	-137	-137	-122	-96	-62	-18	28	81	136
IS18 ($\mu\epsilon$)	-69	-139	-177	-192	-191	-178	-157	-126	-91	-48	-2
IS19 ($\mu\epsilon$)	-56	38	121	195	266	333	398	466	529	593	657
IS20 ($\mu\epsilon$)	-67	42	139	225	307	383	455	528	595	661	726
IS21 ($\mu\epsilon$)	-63	39	132	212	289	361	428	497	560	621	681
IS22 ($\mu\epsilon$)	-64	-137	-176	-200	-207	-202	-189	-163	-134	-93	-50
IS23 ($\mu\epsilon$)	-61	-102	-136	-160	-174	-183	-187	-183	-178	-162	-147
IS24 ($\mu\epsilon$)	-50	75	183	278	368	451	529	607	679	748	815
IS25 ($\mu\epsilon$)	61	24	-7	-30	-44	-53	-57	-53	-48	-32	-15
IS26 ($\mu\epsilon$)	56	248	409	551	685	806	920	1031	1136	1232	1326
IS27 ($\mu\epsilon$)	-65	-94	-114	-127	-131	-129	-122	-106	-91	-63	-35
IS28 ($\mu\epsilon$)	36	223	378	515	645	762	873	982	1084	1178	1271
IS29 ($\mu\epsilon$)	19	192	333	456	573	678	776	874	964	1051	1135
IS30 ($\mu\epsilon$)	-3	-58	-82	-93	-92	-79	-60	-30	3	46	91
IS31 ($\mu\epsilon$)	-2	119	225	322	415	502	586	671	751	828	904
IS32 ($\mu\epsilon$)	-14	92	184	264	340	410	475	539	597	654	707
IS33 ($\mu\epsilon$)	-4	107	204	288	367	440	509	576	638	697	754
IS34 ($\mu\epsilon$)	-72	-132	-168	-190	-199	-197	-187	-166	-143	-109	-73

**Table F-6. Raw data, strain survey conducted after phase I patch installation, ambient environmental conditions (Run 3)
(continued)**

Load Step	0	1	2	3	4	5	6	7	8	9	10
Pressure (psi)	-0.02	0.67	1.33	2.00	2.67	3.32	4.00	4.66	5.40	5.99	6.70
IS35 ($\mu\epsilon$)	-90	-170	-236	-288	-330	-361	-386	-402	-416	-417	-417
IS36 ($\mu\epsilon$)	-13	98	194	279	358	431	498	565	626	684	740
IS37 ($\mu\epsilon$)	-64	-165	-242	-306	-356	-395	-427	-448	-467	-470	-472
IS38 ($\mu\epsilon$)	12	139	248	344	435	518	595	672	742	808	872
IS39 ($\mu\epsilon$)	-69	-177	-249	-306	-348	-377	-398	-407	-415	-406	-396
IS40 ($\mu\epsilon$)	10	132	239	335	426	510	588	667	739	808	875
IS41 ($\mu\epsilon$)	18	158	278	385	488	582	670	761	843	922	999
IS42 ($\mu\epsilon$)	-29	46	113	181	248	314	381	452	522	591	662
IS43 ($\mu\epsilon$)	-32	-12	22	65	115	171	230	294	361	428	498
IS44 ($\mu\epsilon$)	-65	-86	-87	-73	-49	-16	22	68	117	170	225
IS45 ($\mu\epsilon$)	-4	101	194	277	355	430	501	571	640	704	768
IS46 ($\mu\epsilon$)	-7	89	175	253	326	394	460	524	586	643	700
IS47 ($\mu\epsilon$)	-7	84	167	242	312	378	442	505	566	622	678
IS48 ($\mu\epsilon$)	-37	-33	-11	18	55	98	146	201	258	318	382
IS49 ($\mu\epsilon$)	-64	-57	-54	-46	-35	-20	-3	20	44	74	104
IS50 ($\mu\epsilon$)	0	106	199	283	361	434	504	572	638	698	759
IS51 ($\mu\epsilon$)	-39	-21	-9	6	22	43	66	92	120	152	186
IS52 ($\mu\epsilon$)	28	163	283	391	493	588	680	768	855	933	1013
IS53 ($\mu\epsilon$)	-58	-45	-30	-11	11	39	70	106	143	186	230
IS54 ($\mu\epsilon$)	15	146	261	364	461	552	639	724	807	882	958

**Table F-6. Raw data, strain survey conducted after phase I patch installation, ambient environmental conditions (Run 3)
(continued)**

Load Step	0	1	2	3	4	5	6	7	8	9	10
Pressure (psi)	-0.02	0.67	1.33	2.00	2.67	3.32	4.00	4.66	5.40	5.99	6.70
IS55 ($\mu\epsilon$)	-1	126	233	328	417	501	580	659	734	807	878
IS56 ($\mu\epsilon$)	-12	41	89	138	187	240	294	353	412	471	535
IS57 ($\mu\epsilon$)	-74	-149	-189	-202	-200	-183	-159	-123	-84	-39	11
IS58 ($\mu\epsilon$)	-20	-125	-191	-225	-240	-239	-229	-206	-179	-142	-100
IS59 ($\mu\epsilon$)	-19	71	145	214	280	344	406	472	535	597	661
IS60 ($\mu\epsilon$)	-28	73	158	234	305	372	435	500	561	620	679
IS61 ($\mu\epsilon$)	-32	68	152	228	298	364	426	491	551	609	667
IS62 ($\mu\epsilon$)	-68	-144	-184	-203	-207	-198	-182	-153	-121	-81	-36
IS63 ($\mu\epsilon$)	-84	-124	-171	-199	-219	-233	-243	-245	-246	-236	-225
IS64 ($\mu\epsilon$)	21	150	252	345	431	511	585	660	730	795	861
IS65 ($\mu\epsilon$)	-80	-94	-123	-134	-141	-142	-141	-132	-122	-102	-81
IS66 ($\mu\epsilon$)	31	246	409	562	703	831	950	1066	1176	1274	1372
IS67 ($\mu\epsilon$)	22	20	7	8	13	25	38	60	84	115	149
IS68 ($\mu\epsilon$)	24	221	367	508	639	758	869	979	1083	1176	1271
IS69 ($\mu\epsilon$)	18	204	337	465	581	687	785	883	976	1060	1146
IS70 ($\mu\epsilon$)	-22	25	71	119	168	221	274	333	389	449	510
IS71 ($\mu\epsilon$)	-38	-54	-49	-24	11	55	103	160	216	276	339
IS72 ($\mu\epsilon$)	-39	-66	-71	-54	-24	13	56	108	160	217	277
IS73 ($\mu\epsilon$)	25	124	207	289	368	441	510	581	647	709	770
IS74 ($\mu\epsilon$)	11	104	185	263	339	410	477	545	610	669	728

**Table F-6. Raw data, strain survey conducted after phase I patch installation, ambient environmental conditions (Run 3)
(continued)**

Load Step	0	1	2	3	4	5	6	7	8	9	10
Pressure (psi)	-0.02	0.67	1.33	2.00	2.67	3.32	4.00	4.66	5.40	5.99	6.70
IS75 ($\mu\epsilon$)	16	110	192	271	347	418	485	554	619	678	738
IS76 ($\mu\epsilon$)	-18	3	30	69	115	166	219	281	342	406	472
IS77 ($\mu\epsilon$)	-39	-48	-59	-49	-32	-12	11	41	70	105	141
IS78 ($\mu\epsilon$)	14	116	202	286	367	442	515	587	655	718	781
IS79 ($\mu\epsilon$)	-64	-77	-94	-86	-72	-55	-36	-10	16	47	79
IS80 ($\mu\epsilon$)	17	139	237	335	431	519	605	690	772	847	922
IS81 ($\mu\epsilon$)	-65	-90	-113	-109	-98	-82	-62	-35	-8	25	59
IS82 ($\mu\epsilon$)	1	113	202	293	381	463	542	622	699	770	841
IS83 ($\mu\epsilon$)	-14	96	179	262	341	416	487	561	629	696	762
IS84 ($\mu\epsilon$)	-37	6	62	120	177	237	298	363	427	491	557
IS85 ($\mu\epsilon$)	-36	-34	-8	32	79	134	192	256	321	387	455
IS86 ($\mu\epsilon$)	-39	-53	-45	-21	11	53	99	152	207	265	326
IS87 ($\mu\epsilon$)	-6	87	164	234	299	360	420	478	535	588	642
IS88 ($\mu\epsilon$)	-8	76	148	213	273	329	382	435	485	531	577
IS89 ($\mu\epsilon$)	-14	67	138	202	260	316	370	422	472	519	566
IS90 ($\mu\epsilon$)	-23	-22	-6	23	60	107	158	215	274	336	400
IS91 ($\mu\epsilon$)	-50	-32	-24	-10	5	26	48	75	103	136	171
IS92 ($\mu\epsilon$)	-12	82	163	234	300	361	420	478	533	583	634
IS93 ($\mu\epsilon$)	-48	-19	-2	21	44	72	102	136	170	209	250
IS94 ($\mu\epsilon$)	29	165	281	389	488	583	674	762	847	925	1003

**Table F-6. Raw data, strain survey conducted after phase I patch installation, ambient environmental conditions (Run 3)
(continued)**

Load Step	0	1	2	3	4	5	6	7	8	9	10
Pressure (psi)	-0.02	0.67	1.33	2.00	2.67	3.32	4.00	4.66	5.40	5.99	6.70
IS95 ($\mu\epsilon$)	-47	-14	14	46	77	114	154	195	238	284	331
IS96 ($\mu\epsilon$)	15	142	248	346	437	524	608	687	766	838	911
IS97 ($\mu\epsilon$)	7	132	232	324	407	487	563	639	710	779	848
L01 ($\mu\epsilon$)	-	-	-	-	-	-	-	-	-	-	-
L02 ($\mu\epsilon$)	-4	15	12	21	30	39	53	63	80	90	104
L03 ($\mu\epsilon$)	-7	5	-8	-5	3	11	25	35	57	67	85
L04 ($\mu\epsilon$)	-1	24	28	42	58	74	94	110	136	151	172
L05 ($\mu\epsilon$)	0	17	21	30	39	48	59	67	80	88	98
L06 ($\mu\epsilon$)	-4	10	22	28	35	44	52	59	61	72	76
L07 ($\mu\epsilon$)	-	-	-	-	-	-	-	-	-	-	-
L08 ($\mu\epsilon$)	4	53	76	100	124	146	170	191	218	236	259
L09 ($\mu\epsilon$)	2	59	90	126	155	184	216	239	271	293	317
L10 ($\mu\epsilon$)	-	-	-	-	-	-	-	-	-	-	-
RAC-A1 ($\mu\epsilon$)	18	138	237	337	436	529	619	710	799	879	961
RAC-A2 ($\mu\epsilon$)	12	124	215	307	396	479	560	642	720	792	865
RAC-A3 ($\mu\epsilon$)	0	102	181	261	336	407	475	544	608	669	730
RAC-F1 ($\mu\epsilon$)	26	140	239	335	430	519	605	691	775	851	929
RAC-F2 ($\mu\epsilon$)	10	120	213	304	392	474	552	632	708	778	848
RBC-A1 ($\mu\epsilon$)	46	212	348	466	574	670	759	844	921	991	1057
RBC-A2 ($\mu\epsilon$)	31	177	297	401	496	580	658	733	800	863	922

**Table F-6. Raw data, strain survey conducted after phase I patch installation, ambient environmental conditions (Run 3)
(continued)**

Load Step	0	1	2	3	4	5	6	7	8	9	10
Pressure (psi)	-0.02	0.67	1.33	2.00	2.67	3.32	4.00	4.66	5.40	5.99	6.70
RBC-A3 ($\mu\epsilon$)	28	163	275	371	461	541	615	687	753	814	872
RBC-A4 ($\mu\epsilon$)	12	134	239	329	415	493	565	638	703	766	826
RBC-F1 ($\mu\epsilon$)	43	210	343	459	564	657	743	825	899	966	1031
RBC-F2 ($\mu\epsilon$)	28	182	303	409	504	589	667	741	809	871	929
RBC-F3 ($\mu\epsilon$)	14	163	280	382	473	555	631	703	769	830	888
S16 ($\mu\epsilon$)	94	287	454	591	711	820	920	1019	1111	1196	1283
S17 ($\mu\epsilon$)	-	-	-	-	-	-	-	-	-	-	-
S18 ($\mu\epsilon$)	48	118	193	264	333	401	468	539	608	675	744
S20 ($\mu\epsilon$)	-344	-766	-1094	-1383	-1648	-1878	-2092	-2286	-2468	-2617	-2763
S22 ($\mu\epsilon$)	68	220	359	478	586	685	775	866	950	1028	1107
S25 ($\mu\epsilon$)	120	287	449	597	739	874	1005	1135	1262	1377	1496
S29 ($\mu\epsilon$)	11	24	64	112	167	226	286	351	416	477	542
S30 ($\mu\epsilon$)	49	234	401	542	671	787	895	1000	1098	1188	1279
S32 ($\mu\epsilon$)	-206	-373	-500	-609	-708	-793	-872	-943	-1010	-1063	-1115
S34 ($\mu\epsilon$)	96	265	419	555	679	793	899	1004	1102	1193	1285
S37 ($\mu\epsilon$)	85	278	463	629	785	934	1075	1216	1352	1478	1606
S41 ($\mu\epsilon$)	-7	36	94	156	222	288	354	423	490	554	619
S42 ($\mu\epsilon$)	37	113	195	270	345	418	492	566	642	713	788
S43 ($\mu\epsilon$)	69	194	309	408	500	585	668	749	830	904	982
S44 ($\mu\epsilon$)	53	198	333	448	555	653	748	841	933	1015	1100

**Table F-6. Raw data, strain survey conducted after phase I patch installation, ambient environmental conditions (Run 3)
(continued)**

Load Step	0	1	2	3	4	5	6	7	8	9	10
Pressure (psi)	-0.02	0.67	1.33	2.00	2.67	3.32	4.00	4.66	5.40	5.99	6.70
S46 ($\mu\epsilon$)	-159	-466	-723	-958	-1176	-1375	-1565	-1740	-1914	-2056	-2204
S48 ($\mu\epsilon$)	60	178	292	393	489	577	663	747	830	905	983
S51 ($\mu\epsilon$)	72	210	355	490	622	747	871	994	1117	1227	1342
S55 ($\mu\epsilon$)	-5	38	93	150	210	270	330	392	454	512	572
S56 ($\mu\epsilon$)	34	114	196	273	346	418	488	562	635	704	776
S57 ($\mu\epsilon$)	127	316	474	600	710	809	900	990	1076	1154	1234
S58 ($\mu\epsilon$)	125	352	542	692	822	938	1044	1147	1244	1332	1421
S60 ($\mu\epsilon$)	98	-432	-821	-1172	-1486	-1758	-2009	-2240	-2455	-2627	-2794
S62 ($\mu\epsilon$)	107	277	422	541	647	743	830	918	998	1073	1149
S65 ($\mu\epsilon$)	131	320	498	657	807	950	1088	1226	1362	1481	1607
S69 ($\mu\epsilon$)	24	54	106	163	225	288	353	421	491	555	624
S70 ($\mu\epsilon$)	37	104	179	249	320	389	456	528	598	665	736
S71 ($\mu\epsilon$)	41	166	281	375	461	543	620	698	773	844	918
S72 ($\mu\epsilon$)	65	216	355	466	567	662	751	840	925	1004	1086
S74 ($\mu\epsilon$)	-92	-261	-396	-531	-665	-786	-905	-1020	-1136	-1232	-1334
S76 ($\mu\epsilon$)	28	143	258	355	447	534	616	699	779	854	931
S79 ($\mu\epsilon$)	97	263	427	563	691	814	933	1052	1170	1276	1388
S83 ($\mu\epsilon$)	20	90	159	223	287	349	411	475	538	597	659
S84 ($\mu\epsilon$)	70	155	237	312	387	460	532	606	679	749	822
S85 ($\mu\epsilon$)	69	188	296	387	471	549	624	699	773	842	914

**Table F-6. Raw data, strain survey conducted after phase I patch installation, ambient environmental conditions (Run 3)
(continued)**

Load Step	0	1	2	3	4	5	6	7	8	9	10
Pressure (psi)	-0.02	0.67	1.33	2.00	2.67	3.32	4.00	4.66	5.40	5.99	6.70
S86 ($\mu\epsilon$)	76	219	349	459	559	651	739	825	908	985	1064
S88 ($\mu\epsilon$)	-30	-167	-258	-334	-401	-454	-502	-540	-575	-597	-618
S90 ($\mu\epsilon$)	48	173	289	390	481	566	646	726	803	875	948
S93 ($\mu\epsilon$)	114	248	393	525	653	775	893	1011	1128	1233	1342
S97 ($\mu\epsilon$)	22	74	135	197	261	324	386	451	514	576	638
UAC-A1 ($\mu\epsilon$)	36	189	325	448	564	672	774	873	968	1054	1140
UAC-A2 ($\mu\epsilon$)	13	157	280	392	495	591	683	771	855	931	1006
UAC-A3 ($\mu\epsilon$)	7	135	246	343	433	517	596	673	746	815	882
UAC-F1 ($\mu\epsilon$)	56	203	335	456	570	677	779	878	975	1060	1148
UAC-F2 ($\mu\epsilon$)	26	160	278	385	486	579	669	755	839	914	990
UBC-A1 ($\mu\epsilon$)	106	357	562	743	911	1061	1200	1333	1457	1568	1676
UBC-A2 ($\mu\epsilon$)	62	280	459	614	759	889	1009	1124	1231	1327	1421
UBC-A3 ($\mu\epsilon$)	66	270	435	580	714	835	947	1055	1154	1245	1333
UBC-A4 ($\mu\epsilon$)	30	214	364	496	620	731	835	937	1031	1118	1203
UBC-F1 ($\mu\epsilon$)	112	364	570	751	918	1067	1207	1339	1462	1572	1680
UBC-F2 ($\mu\epsilon$)	50	271	449	606	750	880	1000	1115	1221	1317	1410
UBC-F3 ($\mu\epsilon$)	32	240	407	554	689	811	924	1032	1132	1223	1311
UDAC-A1 ($\mu\epsilon$)	38	188	315	433	542	644	742	834	925	1005	1087
UDAC-A2 ($\mu\epsilon$)	24	161	275	380	476	567	653	735	815	886	958
UDAC-A3 ($\mu\epsilon$)	11	132	232	323	405	484	558	630	699	763	827

**Table F-6. Raw data, strain survey conducted after phase I patch installation, ambient environmental conditions (Run 3)
(continued)**

Load Step	0	1	2	3	4	5	6	7	8	9	10
Pressure (psi)	-0.02	0.67	1.33	2.00	2.67	3.32	4.00	4.66	5.40	5.99	6.70
UDAC-F1 ($\mu\epsilon$)	34	183	313	433	544	649	749	844	938	1020	1103
UDAC-F2 ($\mu\epsilon$)	23	153	266	369	465	555	641	723	804	874	947
UDBC-A1 ($\mu\epsilon$)	74	342	543	728	897	1048	1186	1318	1442	1549	1655
UDBC-A2 ($\mu\epsilon$)	50	284	458	620	769	901	1023	1141	1250	1346	1441
UDBC-A3 ($\mu\epsilon$)	29	251	414	567	707	832	947	1057	1161	1252	1342
UDBC-A4 ($\mu\epsilon$)	19	218	363	501	628	742	847	950	1047	1133	1220
UDBC-F1 ($\mu\epsilon$)	89	378	599	798	981	1142	1290	1432	1564	1679	1792
UDBC-F2 ($\mu\epsilon$)	54	299	486	655	811	948	1074	1195	1307	1406	1503
UDBC-F3 ($\mu\epsilon$)	32	262	437	595	741	870	988	1102	1207	1301	1392

F.2.1.2 After Hot-Wet Conditioning

Table F-7. Raw data, strain survey conducted after hot-wet conditioning, ambient environmental conditions (Run 1)

Load Step	0	1	2	3	4	5	6	7	8	9	10
Pressure (psi)	-0.04	0.68	1.34	2.01	2.66	3.32	4.00	4.66	5.34	6.00	6.66
Frame-1 (lbf)	3	110	246	310	517	557	697	828	898	1041	1099
Frame-2 (lbf)	41	114	227	352	448	572	682	791	907	1017	1130
Frame-3 (lbf)	0	121	218	336	456	568	679	794	905	1021	1137
Frame-4 (lbf)	24	114	213	336	458	563	680	794	902	1020	1137
Frame-5 (lbf)	3	115	225	349	455	563	685	799	908	1016	1133
Frame-6 (lbf)	1	121	229	347	446	564	675	798	908	1006	1122
Frame-7 (lbf)	5	110	226	335	454	568	680	790	905	1016	1137
Frame-8 (lbf)	13	122	226	339	460	564	679	790	904	1024	1134
Frame-9 (lbf)	3	111	226	339	450	569	680	793	907	1019	1132
Frame-10 (lbf)	1	119	211	349	450	572	680	796	904	1020	1134
Frame-11 (lbf)	-4	121	228	336	449	578	677	798	907	1021	1137
Frame-12 (lbf)	0	114	227	344	456	562	684	796	905	1020	1134
Hoop-1 (lbf)	11	713	1451	2164	2826	3575	4263	4987	5711	6413	7139
Hoop-2 (lbf)	81	723	1364	2130	2873	3565	4278	4985	5728	6420	7148
Hoop-3 (lbf)	10	721	1437	2145	2862	3571	4281	5000	5707	6434	7163
Hoop-4 (lbf)	8	710	1434	2157	2855	3574	4275	4992	5724	6415	7154
Hoop-5 (lbf)	15	709	1424	2136	2847	3582	4279	4982	5726	6451	7121
Hoop-6 (lbf)	13	711	1432	2135	2851	3575	4292	4988	5711	6410	7141
Hoop-7 (lbf)	11	711	1434	2143	2870	3580	4282	5005	5713	6431	7151
Hoop-8 (lbf)	22	710	1422	2143	2860	3570	4284	5004	5713	6429	7145

**Table F-7. Raw data, strain survey conducted after hot-wet conditioning, ambient environmental conditions (Run 1)
(continued)**

Load Step	0	1	2	3	4	5	6	7	8	9	10
Pressure (psi)	-0.04	0.68	1.34	2.01	2.66	3.32	4.00	4.66	5.34	6.00	6.66
Hoop-9 (lbf)	14	733	1462	2148	2858	3578	4282	4996	5708	6435	7145
Hoop-10 (lbf)	5	725	1434	2149	2868	3573	4243	4998	5712	6430	7144
Hoop-11 (lbf)	23	711	1443	2150	2851	3570	4291	5010	5733	6408	7137
Hoop-12 (lbf)	28	684	1436	2144	2852	3577	4284	4999	5720	6425	7148
Hoop-13 (lbf)	19	710	1482	2168	2867	3538	4290	4994	5698	6427	7142
Hoop-14 (lbf)	9	704	1427	2126	2864	3583	4288	4995	5713	6423	7144
Long-1 (lbf)	-1	669	1341	2002	2630	3354	4023	4700	5380	6016	6621
Long-2 (lbf)	0	664	1341	2006	2676	3335	3992	4683	5344	6010	6676
Long-3 (lbf)	0	668	1333	2005	2675	3335	4009	4672	5331	6007	6668
Long-4 (lbf)	11	677	1334	2009	2666	3335	4002	4674	5335	6007	6676
Long-5 (lbf)	-10	672	1339	2008	2667	3338	4000	4669	5344	6011	6676
Long-6 (lbf)	5	688	1335	2001	2678	3355	4007	4681	5366	5981	6698
Long-7 (lbf)	-14	694	1371	2008	2675	3346	4007	4671	5342	5946	6663
Long-8 (lbf)	-3	666	1324	1989	2666	3339	3993	4672	5346	6000	6674
F01 ($\mu\epsilon$)	6	33	87	130	181	220	261	303	346	390	435
F02 ($\mu\epsilon$)	-4	54	91	141	197	248	310	363	416	471	524
F03 ($\mu\epsilon$)	17	13	70	108	146	178	197	225	255	285	322
F04 ($\mu\epsilon$)	-2	79	118	175	238	306	380	442	507	571	632
F05 ($\mu\epsilon$)	-	-	-	-	-	-	-	-	-	-	-
F06 ($\mu\epsilon$)	-15	70	106	157	205	261	325	379	433	492	544

**Table F-7. Raw data, strain survey conducted after hot-wet conditioning, ambient environmental conditions (Run 1)
(continued)**

Load Step	0	1	2	3	4	5	6	7	8	9	10
Pressure (psi)	-0.04	0.68	1.34	2.01	2.66	3.32	4.00	4.66	5.34	6.00	6.66
F07 ($\mu\epsilon$)	22	1	68	111	151	189	217	249	282	316	354
F08 ($\mu\epsilon$)	-4	79	106	151	196	254	314	368	424	480	533
IS16 ($\mu\epsilon$)	-3	106	188	261	330	398	464	533	590	660	733
IS17 ($\mu\epsilon$)	-4	-2	15	41	77	120	168	223	277	339	404
IS18 ($\mu\epsilon$)	-3	-37	-41	-33	-11	18	56	100	149	202	261
IS19 ($\mu\epsilon$)	-3	39	89	130	172	213	255	299	344	390	437
IS20 ($\mu\epsilon$)	-2	57	118	168	216	261	305	348	392	434	478
IS21 ($\mu\epsilon$)	-2	51	108	154	197	238	277	315	353	390	428
IS22 ($\mu\epsilon$)	0	-59	-73	-78	-67	-47	-16	23	68	118	174
IS23 ($\mu\epsilon$)	-3	-57	-83	-101	-105	-104	-95	-79	-57	-32	-1
IS24 ($\mu\epsilon$)	-2	80	160	227	291	349	405	460	514	565	616
IS25 ($\mu\epsilon$)	-3	-47	-60	-65	-56	-40	-17	13	47	85	128
IS26 ($\mu\epsilon$)	-2	148	286	404	517	620	718	812	900	984	1065
IS27 ($\mu\epsilon$)	-3	-42	-44	-39	-19	7	40	79	121	169	221
IS28 ($\mu\epsilon$)	-2	141	273	384	492	590	685	774	858	939	1019
IS29 ($\mu\epsilon$)	-2	132	255	355	453	542	628	711	789	867	943
IS30 ($\mu\epsilon$)	-3	-11	2	20	41	71	109	155	205	260	319
IS31 ($\mu\epsilon$)	-4	69	146	213	282	347	411	474	536	596	657
IS32 ($\mu\epsilon$)	-3	67	136	195	253	304	355	403	449	493	536
IS33 ($\mu\epsilon$)	-3	74	146	207	269	322	376	427	475	523	568

**Table F-7. Raw data, strain survey conducted after hot-wet conditioning, ambient environmental conditions (Run 1)
(continued)**

Load Step	0	1	2	3	4	5	6	7	8	9	10
Pressure (psi)	-0.04	0.68	1.34	2.01	2.66	3.32	4.00	4.66	5.34	6.00	6.66
IS34 ($\mu\epsilon$)	1	-1	9	22	44	69	100	128	170	217	267
IS35 ($\mu\epsilon$)	-2	-80	-129	-164	-184	-197	-199	-195	-186	-170	-150
IS36 ($\mu\epsilon$)	-3	73	147	210	271	327	380	432	480	527	572
IS37 ($\mu\epsilon$)	-2	-89	-138	-171	-188	-196	-193	-182	-165	-142	-113
IS38 ($\mu\epsilon$)	-3	88	177	252	326	394	459	522	580	637	692
IS39 ($\mu\epsilon$)	-1	-93	-138	-166	-174	-172	-160	-139	-112	-79	-40
IS40 ($\mu\epsilon$)	-2	94	187	267	347	419	490	557	620	681	741
IS41 ($\mu\epsilon$)	-2	111	217	308	397	478	557	632	704	775	844
IS42 ($\mu\epsilon$)	-6	103	183	256	325	394	462	533	603	673	745
IS43 ($\mu\epsilon$)	-5	22	63	112	166	225	287	353	421	491	564
IS44 ($\mu\epsilon$)	-5	-35	-33	-15	13	50	93	142	195	251	310
IS45 ($\mu\epsilon$)	-3	72	149	219	285	349	410	470	529	586	643
IS46 ($\mu\epsilon$)	-3	80	160	232	299	363	424	483	540	595	650
IS47 ($\mu\epsilon$)	-2	77	154	224	289	351	410	467	523	577	631
IS48 ($\mu\epsilon$)	1	3	34	68	109	156	208	265	326	389	456
IS49 ($\mu\epsilon$)	-4	-48	-63	-67	-64	-53	-38	-18	6	34	66
IS50 ($\mu\epsilon$)	-2	90	176	254	327	395	460	523	584	643	700
IS51 ($\mu\epsilon$)	-5	-39	-47	-44	-33	-16	4	30	58	90	125
IS52 ($\mu\epsilon$)	-3	120	234	339	438	531	620	706	789	868	946
IS53 ($\mu\epsilon$)	-5	-37	-40	-27	-7	20	52	89	130	174	222

**Table F-7. Raw data, strain survey conducted after hot-wet conditioning, ambient environmental conditions (Run 1)
(continued)**

Load Step	0	1	2	3	4	5	6	7	8	9	10
Pressure (psi)	-0.04	0.68	1.34	2.01	2.66	3.32	4.00	4.66	5.34	6.00	6.66
IS54 ($\mu\epsilon$)	-3	113	221	321	413	501	585	667	745	820	894
IS55 ($\mu\epsilon$)	-4	106	209	301	384	463	539	613	685	755	825
IS56 ($\mu\epsilon$)	-3	77	143	201	259	316	376	437	499	563	629
IS57 ($\mu\epsilon$)	-3	-21	-13	5	36	71	115	164	216	273	333
IS58 ($\mu\epsilon$)	-3	-59	-77	-80	-66	-45	-14	23	66	114	167
IS59 ($\mu\epsilon$)	-3	45	97	141	185	226	270	313	358	405	453
IS60 ($\mu\epsilon$)	-2	60	122	172	220	262	305	347	388	430	472
IS61 ($\mu\epsilon$)	-2	59	119	167	214	255	296	336	375	414	454
IS62 ($\mu\epsilon$)	0	-52	-64	-67	-53	-34	-3	34	75	124	176
IS63 ($\mu\epsilon$)	-3	-59	-86	-106	-113	-117	-113	-104	-91	-71	-47
IS64 ($\mu\epsilon$)	-2	85	168	236	302	360	417	472	524	575	626
IS65 ($\mu\epsilon$)	-4	-26	-22	-12	10	33	63	98	136	179	226
IS66 ($\mu\epsilon$)	-4	157	302	427	548	655	759	857	948	1036	1120
IS67 ($\mu\epsilon$)	-4	-18	-3	16	48	81	121	166	213	265	320
IS68 ($\mu\epsilon$)	-3	143	276	391	503	603	700	791	876	960	1040
IS69 ($\mu\epsilon$)	-5	130	250	350	449	537	625	707	785	864	940
IS70 ($\mu\epsilon$)	-5	64	128	183	237	287	344	402	461	523	586
IS71 ($\mu\epsilon$)	-6	-22	2	35	80	127	183	242	303	367	434
IS72 ($\mu\epsilon$)	-6	-45	-35	-11	27	68	119	174	232	294	358
IS73 ($\mu\epsilon$)	-4	75	156	229	302	368	435	497	557	616	673

**Table F-7. Raw data, strain survey conducted after hot-wet conditioning, ambient environmental conditions (Run 1)
(continued)**

Load Step	0	1	2	3	4	5	6	7	8	9	10
Pressure (psi)	-0.04	0.68	1.34	2.01	2.66	3.32	4.00	4.66	5.34	6.00	6.66
IS74 ($\mu\epsilon$)	-3	79	161	233	305	371	437	499	558	616	672
IS75 ($\mu\epsilon$)	-3	80	163	236	309	376	442	504	564	623	680
IS76 ($\mu\epsilon$)	-2	13	52	94	149	202	263	325	390	458	527
IS77 ($\mu\epsilon$)	-7	-61	-69	-66	-49	-29	-3	27	60	97	136
IS78 ($\mu\epsilon$)	-4	86	175	254	332	403	473	540	604	666	726
IS79 ($\mu\epsilon$)	-8	-62	-68	-64	-45	-23	4	35	67	104	143
IS80 ($\mu\epsilon$)	-4	101	203	296	391	477	562	643	720	796	869
IS81 ($\mu\epsilon$)	-8	-75	-89	-90	-75	-58	-34	-6	24	59	97
IS82 ($\mu\epsilon$)	-5	89	183	269	357	436	514	591	663	734	803
IS83 ($\mu\epsilon$)	-6	90	183	263	344	415	485	554	619	685	749
IS84 ($\mu\epsilon$)	-5	75	145	207	269	331	395	459	525	592	659
IS85 ($\mu\epsilon$)	-6	6	44	90	144	203	267	334	404	475	548
IS86 ($\mu\epsilon$)	-5	-24	-11	18	57	102	155	210	270	333	398
IS87 ($\mu\epsilon$)	-3	61	122	177	228	277	325	372	419	465	512
IS88 ($\mu\epsilon$)	-2	69	133	189	241	289	336	381	425	468	510
IS89 ($\mu\epsilon$)	-2	68	128	181	232	278	324	367	410	453	495
IS90 ($\mu\epsilon$)	-1	-10	10	40	81	127	180	236	296	359	425
IS91 ($\mu\epsilon$)	-5	-42	-54	-52	-44	-30	-10	14	42	75	110
IS92 ($\mu\epsilon$)	-2	80	153	218	277	331	384	434	483	531	577
IS93 ($\mu\epsilon$)	-6	-24	-18	3	29	60	98	138	181	228	278

**Table F-7. Raw data, strain survey conducted after hot-wet conditioning, ambient environmental conditions (Run 1)
(continued)**

Load Step	0	1	2	3	4	5	6	7	8	9	10
Pressure (psi)	-0.04	0.68	1.34	2.01	2.66	3.32	4.00	4.66	5.34	6.00	6.66
IS94 ($\mu\epsilon$)	-3	120	232	337	436	528	619	703	785	864	941
IS95 ($\mu\epsilon$)	-6	-14	2	29	63	99	141	184	230	279	330
IS96 ($\mu\epsilon$)	-3	107	207	301	389	471	553	629	704	777	848
IS97 ($\mu\epsilon$)	-5	101	197	284	364	440	514	587	657	726	794
L01 ($\mu\epsilon$)	-	-	-	-	-	-	-	-	-	-	-
L02 ($\mu\epsilon$)	2	36	43	56	69	82	98	114	134	150	164
L03 ($\mu\epsilon$)	2	18	15	25	40	53	72	91	110	131	150
L04 ($\mu\epsilon$)	4	43	57	78	100	121	147	176	201	225	248
L05 ($\mu\epsilon$)	6	23	25	34	43	50	61	70	80	90	99
L06 ($\mu\epsilon$)	7	44	56	69	85	97	110	120	131	141	149
L07 ($\mu\epsilon$)	-	-	-	-	-	-	-	-	-	-	-
L08 ($\mu\epsilon$)	4	50	69	92	116	140	166	190	213	236	257
L09 ($\mu\epsilon$)	3	64	90	118	144	173	202	228	252	279	300
L10 ($\mu\epsilon$)	-	-	-	-	-	-	-	-	-	-	-
RAC-A1 ($\mu\epsilon$)	-4	107	213	312	412	506	599	688	774	858	940
RAC-A2 ($\mu\epsilon$)	-4	97	195	284	375	458	540	619	695	769	841
RAC-A3 ($\mu\epsilon$)	-4	87	174	252	330	399	467	533	595	657	717
RAC-F1 ($\mu\epsilon$)	-3	104	208	301	398	485	574	658	738	818	894
RAC-F2 ($\mu\epsilon$)	-3	98	195	281	370	450	530	607	679	752	821
RBC-A1 ($\mu\epsilon$)	-3	118	228	321	410	490	566	637	703	764	823

**Table F-7. Raw data, strain survey conducted after hot-wet conditioning, ambient environmental conditions (Run 1)
(continued)**

Load Step	0	1	2	3	4	5	6	7	8	9	10
Pressure (psi)	-0.04	0.68	1.34	2.01	2.66	3.32	4.00	4.66	5.34	6.00	6.66
RBC-A2 ($\mu\epsilon$)	-3	103	199	280	358	427	494	556	612	666	717
RBC-A3 ($\mu\epsilon$)	-3	100	194	274	351	419	486	547	604	659	712
RBC-A4 ($\mu\epsilon$)	-2	99	194	274	352	422	490	554	614	671	727
RBC-F1 ($\mu\epsilon$)	-4	117	224	314	402	478	552	621	683	742	798
RBC-F2 ($\mu\epsilon$)	-4	106	202	284	363	431	497	559	616	669	719
RBC-F3 ($\mu\epsilon$)	-4	106	201	281	359	427	493	554	611	664	714
S16 ($\mu\epsilon$)	5	58	135	204	274	341	408	477	556	625	696
S17 ($\mu\epsilon$)	-	-	-	-	-	-	-	-	-	-	-
S18 ($\mu\epsilon$)	5	164	304	417	516	607	691	773	853	930	1006
S20 ($\mu\epsilon$)	8	-333	-625	-874	-1101	-1304	-1487	-1646	-1788	-1914	-2024
S22 ($\mu\epsilon$)	2	147	271	377	471	558	637	714	788	861	932
S25 ($\mu\epsilon$)	4	195	364	513	651	782	907	1027	1144	1257	1367
S29 ($\mu\epsilon$)	0	60	122	186	251	316	381	447	512	578	644
S30 ($\mu\epsilon$)	-1	147	284	401	512	610	700	787	870	951	1032
S32 ($\mu\epsilon$)	1	-129	-234	-326	-413	-489	-562	-627	-684	-735	-780
S34 ($\mu\epsilon$)	-6	105	219	321	418	510	599	699	783	867	950
S37 ($\mu\epsilon$)	-2	206	389	546	689	822	946	1064	1177	1287	1395
S41 ($\mu\epsilon$)	1	80	155	229	303	373	443	511	577	643	708
S42 ($\mu\epsilon$)	2	58	134	207	280	352	423	495	566	637	710
S43 ($\mu\epsilon$)	6	124	233	326	412	491	566	640	713	785	856

**Table F-7. Raw data, strain survey conducted after hot-wet conditioning, ambient environmental conditions (Run 1)
(continued)**

Load Step	0	1	2	3	4	5	6	7	8	9	10
Pressure (psi)	-0.04	0.68	1.34	2.01	2.66	3.32	4.00	4.66	5.34	6.00	6.66
S44 ($\mu\epsilon$)	1	162	299	415	521	618	710	799	885	969	1051
S46 ($\mu\epsilon$)	7	-290	-553	-796	-1023	-1233	-1432	-1616	-1787	-1947	-2097
S48 ($\mu\epsilon$)	-5	126	240	344	438	527	610	691	769	846	922
S51 ($\mu\epsilon$)	1	188	355	503	640	770	896	1018	1136	1252	1366
S55 ($\mu\epsilon$)	1	67	134	203	271	340	408	475	542	608	675
S56 ($\mu\epsilon$)	5	76	157	230	301	369	438	505	573	642	710
S57 ($\mu\epsilon$)	-	-	-	-	-	-	-	-	-	-	-
S58 ($\mu\epsilon$)	5	193	342	463	566	659	746	829	908	987	1063
S60 ($\mu\epsilon$)	9	-391	-734	-1027	-1304	-1547	-1775	-1980	-2166	-2338	-2493
S62 ($\mu\epsilon$)	-1	152	278	383	478	563	643	718	792	864	935
S65 ($\mu\epsilon$)	1	191	352	495	630	757	882	999	1115	1226	1335
S69 ($\mu\epsilon$)	4	78	146	215	283	351	418	485	552	618	685
S70 ($\mu\epsilon$)	0	71	151	225	302	379	453	525	597	670	743
S71 ($\mu\epsilon$)	-	-	-	-	-	-	-	-	-	-	-
S72 ($\mu\epsilon$)	2	192	334	450	553	648	735	819	899	978	1056
S74 ($\mu\epsilon$)	3	-172	-330	-478	-627	-765	-904	-1034	-1156	-1275	-1388
S76 ($\mu\epsilon$)	-1	138	259	364	459	548	633	715	796	874	952
S79 ($\mu\epsilon$)	3	215	383	527	659	781	900	1014	1124	1233	1338
S83 ($\mu\epsilon$)	2	91	165	234	302	366	429	492	553	614	675
S84 ($\mu\epsilon$)	5	69	146	221	295	367	437	508	580	652	724

**Table F-7. Raw data, strain survey conducted after hot-wet conditioning, ambient environmental conditions (Run 1)
(continued)**

Load Step	0	1	2	3	4	5	6	7	8	9	10
Pressure (psi)	-0.04	0.68	1.34	2.01	2.66	3.32	4.00	4.66	5.34	6.00	6.66
S85 ($\mu\epsilon$)	-	-	-	-	-	-	-	-	-	-	-
S86 ($\mu\epsilon$)	6	170	302	410	506	594	676	754	831	906	980
S88 ($\mu\epsilon$)	6	-104	-187	-260	-324	-378	-425	-462	-491	-515	-532
S90 ($\mu\epsilon$)	2	154	278	382	475	560	643	721	798	872	945
S93 ($\mu\epsilon$)	7	194	353	492	618	739	853	963	1071	1175	1277
S97 ($\mu\epsilon$)	6	85	156	225	293	359	424	489	553	616	680
UAC-A1 ($\mu\epsilon$)	-3	142	278	403	519	628	731	831	924	1014	1102
UAC-A2 ($\mu\epsilon$)	-3	130	254	365	468	564	656	744	826	906	983
UAC-A3 ($\mu\epsilon$)	-3	115	223	319	407	488	566	641	712	781	848
UAC-F1 ($\mu\epsilon$)	-3	139	272	396	512	623	728	829	925	1017	1105
UAC-F2 ($\mu\epsilon$)	-3	122	239	346	446	541	630	716	798	876	952
UBC-A1 ($\mu\epsilon$)	-3	199	381	535	680	811	934	1048	1154	1253	1347
UBC-A2 ($\mu\epsilon$)	-3	165	315	441	559	666	767	860	946	1028	1106
UBC-A3 ($\mu\epsilon$)	-2	152	292	406	516	613	706	792	871	947	1019
UBC-A4 ($\mu\epsilon$)	-2	144	274	382	485	577	666	748	825	900	972
UBC-F1 ($\mu\epsilon$)	-4	198	377	530	674	802	923	1036	1141	1239	1331
UBC-F2 ($\mu\epsilon$)	-4	166	316	442	561	666	765	858	945	1025	1102
UBC-F3 ($\mu\epsilon$)	-4	154	294	411	522	619	711	797	879	955	1027
UDAC-A1 ($\mu\epsilon$)	-3	138	264	383	495	598	699	791	881	967	1049
UDAC-A2 ($\mu\epsilon$)	-4	122	234	337	434	523	611	691	769	844	916

**Table F-7. Raw data, strain survey conducted after hot-wet conditioning, ambient environmental conditions (Run 1)
(continued)**

Load Step	0	1	2	3	4	5	6	7	8	9	10
Pressure (psi)	-0.04	0.68	1.34	2.01	2.66	3.32	4.00	4.66	5.34	6.00	6.66
UDAC-A3 ($\mu\epsilon$)	-4	105	202	289	371	446	520	589	656	721	784
UDAC-F1 ($\mu\epsilon$)	-3	138	267	389	502	609	710	806	898	985	1069
UDAC-F2 ($\mu\epsilon$)	-2	119	228	332	428	517	604	685	763	838	910
UDBC-A1 ($\mu\epsilon$)	-4	195	372	522	666	790	909	1018	1119	1214	1303
UDBC-A2 ($\mu\epsilon$)	-4	166	316	443	565	670	772	864	949	1031	1107
UDBC-A3 ($\mu\epsilon$)	-4	156	296	414	528	627	721	808	887	964	1036
UDBC-A4 ($\mu\epsilon$)	-4	144	273	381	486	577	665	747	823	897	967
UDBC-F1 ($\mu\epsilon$)	-3	210	400	560	713	846	974	1090	1198	1300	1396
UDBC-F2 ($\mu\epsilon$)	-3	174	331	462	588	697	801	897	985	1069	1147
UDBC-F3 ($\mu\epsilon$)	-3	162	308	429	546	647	744	833	915	993	1067

Table F-8. Raw data, strain survey conducted after hot-wet conditioning, ambient environmental conditions (Run 2)

Load Step	0	1	2	3	4	5	6	7	8	9	10
Pressure (psi)	-0.03	0.68	1.32	2.02	2.67	3.31	4.00	4.67	5.34	6.02	6.69
Frame-1 (lbf)	4	133	243	336	424	557	692	815	847	1049	1111
Frame-2 (lbf)	46	110	221	355	458	568	681	792	905	1021	1133
Frame-3 (lbf)	1	120	228	337	451	569	678	791	906	1021	1133
Frame-4 (lbf)	23	126	224	339	449	569	679	793	907	1021	1132
Frame-5 (lbf)	7	102	218	320	459	564	675	792	909	1029	1144
Frame-6 (lbf)	7	122	233	343	464	562	676	784	918	1029	1131
Frame-7 (lbf)	5	106	222	342	448	562	681	792	905	1020	1137
Frame-8 (lbf)	12	104	224	337	455	573	672	793	905	1019	1132
Frame-9 (lbf)	18	116	225	344	453	568	683	790	909	1020	1133
Frame-10 (lbf)	1	121	238	342	449	566	677	793	910	1019	1133
Frame-11 (lbf)	-1	113	220	339	446	565	676	796	907	1014	1135
Frame-12 (lbf)	-1	117	232	345	449	569	684	794	905	1019	1129
Hoop-1 (lbf)	2	704	1432	2136	2859	3569	4294	4990	5726	6409	7154
Hoop-2 (lbf)	134	743	1441	2160	2879	3575	4269	5013	5724	6415	7161
Hoop-3 (lbf)	47	718	1418	2140	2857	3572	4291	4995	5726	6429	7159
Hoop-4 (lbf)	10	717	1422	2143	2867	3573	4283	5004	5709	6407	7143
Hoop-5 (lbf)	10	714	1433	2139	2863	3561	4295	4981	5734	6426	7137
Hoop-6 (lbf)	-9	712	1443	2146	2864	3566	4272	5010	5714	6430	7157
Hoop-7 (lbf)	-8	709	1413	2142	2847	3564	4288	5001	5720	6434	7138
Hoop-8 (lbf)	130	700	1425	2149	2851	3562	4287	5003	5714	6426	7145
Hoop-9 (lbf)	67	710	1434	2112	2853	3576	4285	5002	5713	6430	7147

**Table F-8. Raw data, strain survey conducted after hot-wet conditioning, ambient environmental conditions (Run 2)
(continued)**

Load Step	0	1	2	3	4	5	6	7	8	9	10
Pressure (psi)	-0.03	0.68	1.32	2.02	2.67	3.31	4.00	4.67	5.34	6.02	6.69
Hoop-10 (lb _f)	3	720	1438	2146	2869	3566	4290	5003	5724	6426	7149
Hoop-11 (lb _f)	37	728	1439	2143	2841	3556	4282	4984	5719	6411	7138
Hoop-12 (lb _f)	95	722	1418	2138	2866	3569	4287	4999	5710	6432	7138
Hoop-13 (lb _f)	41	715	1420	2129	2874	3591	4278	5007	5712	6433	7141
Hoop-14 (lb _f)	19	731	1429	2149	2845	3563	4295	5004	5719	6424	7159
Long-1 (lb _f)	-7	676	1338	2017	2688	3339	3982	4712	5316	6039	6681
Long-2 (lb _f)	14	683	1336	2002	2669	3346	4006	4687	5316	5986	6699
Long-3 (lb _f)	9	678	1330	2009	2670	3334	4011	4670	5336	6010	6668
Long-4 (lb _f)	-13	669	1373	2019	2664	3338	4005	4673	5338	6008	6672
Long-5 (lb _f)	2	674	1335	2004	2661	3352	4011	4697	5356	6005	6663
Long-6 (lb _f)	-6	644	1351	2004	2688	3332	4006	4689	5326	6032	6675
Long-7 (lb _f)	56	669	1311	2031	2677	3345	4009	4674	5322	5960	6668
Long-8 (lb _f)	3	691	1337	2012	2671	3333	4006	4671	5343	6000	6676
F01 (μ ϵ)	33	42	79	110	175	211	248	297	339	381	429
F02 (μ ϵ)	-22	35	88	143	203	253	308	366	419	478	528
F03 (μ ϵ)	67	47	74	104	140	170	197	227	256	285	324
F04 (μ ϵ)	-37	55	111	181	243	306	373	437	504	569	627
F05 (μ ϵ)	-	-	-	-	-	-	-	-	-	-	-
F06 (μ ϵ)	-33	41	99	159	208	264	324	378	436	498	550
F07 (μ ϵ)	40	30	67	106	143	180	210	243	276	309	347

**Table F-8. Raw data, strain survey conducted after hot-wet conditioning, ambient environmental conditions (Run 2)
(continued)**

Load Step	0	1	2	3	4	5	6	7	8	9	10
Pressure (psi)	-0.03	0.68	1.32	2.02	2.67	3.31	4.00	4.67	5.34	6.02	6.69
F08 ($\mu\epsilon$)	-17	48	98	156	207	257	314	370	429	487	539
IS16 ($\mu\epsilon$)	-17	86	165	238	308	376	445	515	586	658	731
IS17 ($\mu\epsilon$)	-20	-17	1	28	66	110	161	216	275	337	403
IS18 ($\mu\epsilon$)	-14	-44	-48	-39	-16	15	54	98	148	201	260
IS19 ($\mu\epsilon$)	-7	36	81	122	165	207	251	294	340	386	435
IS20 ($\mu\epsilon$)	-7	52	108	157	206	252	298	342	387	430	475
IS21 ($\mu\epsilon$)	-9	44	96	141	186	227	268	308	347	386	425
IS22 ($\mu\epsilon$)	-7	-62	-81	-85	-72	-50	-19	20	66	117	173
IS23 ($\mu\epsilon$)	-27	-78	-101	-116	-117	-113	-101	-84	-61	-33	-1
IS24 ($\mu\epsilon$)	-4	78	154	220	285	344	401	456	511	563	614
IS25 ($\mu\epsilon$)	-10	-52	-63	-66	-55	-39	-15	14	48	86	129
IS26 ($\mu\epsilon$)	6	155	289	408	520	623	721	813	902	986	1067
IS27 ($\mu\epsilon$)	-18	-53	-55	-48	-25	2	37	76	121	170	223
IS28 ($\mu\epsilon$)	5	146	273	386	493	591	685	774	859	941	1020
IS29 ($\mu\epsilon$)	4	134	250	350	447	537	624	706	787	866	944
IS30 ($\mu\epsilon$)	-5	-15	-8	7	34	67	107	152	204	258	318
IS31 ($\mu\epsilon$)	0	73	146	213	281	346	410	473	535	596	656
IS32 ($\mu\epsilon$)	0	70	136	194	251	303	354	402	448	492	535
IS33 ($\mu\epsilon$)	-1	76	145	206	266	321	374	425	474	522	567
IS34 ($\mu\epsilon$)	-9	-6	1	13	29	54	87	125	168	215	266

**Table F-8. Raw data, strain survey conducted after hot-wet conditioning, ambient environmental conditions (Run 2)
(continued)**

Load Step	0	1	2	3	4	5	6	7	8	9	10
Pressure (psi)	-0.03	0.68	1.32	2.02	2.67	3.31	4.00	4.67	5.34	6.02	6.69
IS35 ($\mu\epsilon$)	-23	-99	-145	-178	-195	-204	-205	-199	-188	-171	-149
IS36 ($\mu\epsilon$)	1	76	147	209	270	326	380	431	480	527	572
IS37 ($\mu\epsilon$)	-11	-96	-144	-176	-191	-197	-193	-182	-165	-142	-113
IS38 ($\mu\epsilon$)	2	92	177	253	327	395	460	522	581	638	692
IS39 ($\mu\epsilon$)	-13	-103	-147	-173	-179	-175	-162	-140	-112	-79	-39
IS40 ($\mu\epsilon$)	1	96	186	267	346	419	490	556	620	682	741
IS41 ($\mu\epsilon$)	1	113	215	307	395	477	556	631	704	775	844
IS42 ($\mu\epsilon$)	-12	91	173	246	318	388	460	530	602	673	746
IS43 ($\mu\epsilon$)	-8	21	63	111	166	225	289	354	424	494	566
IS44 ($\mu\epsilon$)	-23	-47	-42	-23	7	45	91	140	195	251	312
IS45 ($\mu\epsilon$)	-2	76	151	220	285	348	411	470	530	587	644
IS46 ($\mu\epsilon$)	-2	82	159	231	297	361	423	482	540	596	650
IS47 ($\mu\epsilon$)	-1	80	155	223	287	349	409	467	523	578	631
IS48 ($\mu\epsilon$)	-13	-1	27	62	104	152	206	264	326	389	456
IS49 ($\mu\epsilon$)	-29	-64	-76	-79	-73	-61	-42	-21	6	35	68
IS50 ($\mu\epsilon$)	0	93	178	254	326	395	461	524	585	644	701
IS51 ($\mu\epsilon$)	-29	-54	-58	-54	-41	-22	1	27	58	91	127
IS52 ($\mu\epsilon$)	2	126	238	342	440	533	623	708	792	872	949
IS53 ($\mu\epsilon$)	-36	-59	-55	-42	-18	12	48	86	129	175	224
IS54 ($\mu\epsilon$)	2	118	225	323	415	502	588	668	747	823	897

**Table F-8. Raw data, strain survey conducted after hot-wet conditioning, ambient environmental conditions (Run 2)
(continued)**

Load Step	0	1	2	3	4	5	6	7	8	9	10
Pressure (psi)	-0.03	0.68	1.32	2.02	2.67	3.31	4.00	4.67	5.34	6.02	6.69
IS55 ($\mu\epsilon$)	3	113	212	300	383	462	539	613	686	756	826
IS56 ($\mu\epsilon$)	-18	68	131	190	249	309	370	432	496	561	628
IS57 ($\mu\epsilon$)	-16	-25	-19	1	31	69	113	162	215	272	332
IS58 ($\mu\epsilon$)	-13	-60	-79	-81	-67	-45	-14	22	66	114	167
IS59 ($\mu\epsilon$)	-3	49	95	137	180	223	266	310	355	402	450
IS60 ($\mu\epsilon$)	-2	64	119	167	214	258	301	343	386	428	470
IS61 ($\mu\epsilon$)	-2	62	115	162	207	250	291	332	372	411	452
IS62 ($\mu\epsilon$)	-5	-53	-70	-72	-59	-37	-6	31	74	123	176
IS63 ($\mu\epsilon$)	-32	-81	-106	-123	-128	-128	-122	-110	-93	-72	-46
IS64 ($\mu\epsilon$)	0	90	166	233	298	357	415	469	522	574	624
IS65 ($\mu\epsilon$)	-10	-26	-23	-13	8	33	63	98	137	181	228
IS66 ($\mu\epsilon$)	5	167	306	431	550	658	762	858	950	1038	1121
IS67 ($\mu\epsilon$)	-1	-8	2	21	51	85	124	168	216	268	322
IS68 ($\mu\epsilon$)	4	152	279	394	504	604	701	791	878	962	1041
IS69 ($\mu\epsilon$)	2	137	249	350	447	536	623	705	785	864	941
IS70 ($\mu\epsilon$)	-22	52	109	162	219	277	337	397	459	521	585
IS71 ($\mu\epsilon$)	-19	-27	-8	25	71	123	180	239	302	367	433
IS72 ($\mu\epsilon$)	-12	-44	-38	-14	24	68	120	174	233	295	359
IS73 ($\mu\epsilon$)	-2	79	156	230	302	369	435	497	558	617	673
IS74 ($\mu\epsilon$)	-1	83	160	233	305	371	437	498	559	617	673

**Table F-8. Raw data, strain survey conducted after hot-wet conditioning, ambient environmental conditions (Run 2)
(continued)**

Load Step	0	1	2	3	4	5	6	7	8	9	10
Pressure (psi)	-0.03	0.68	1.32	2.02	2.67	3.31	4.00	4.67	5.34	6.02	6.69
IS75 ($\mu\epsilon$)	-2	85	162	236	308	376	442	504	565	624	681
IS76 ($\mu\epsilon$)	-6	15	50	93	146	202	263	325	391	458	528
IS77 ($\mu\epsilon$)	-20	-68	-78	-72	-54	-33	-5	25	59	97	137
IS78 ($\mu\epsilon$)	-2	90	174	254	331	403	474	540	605	667	727
IS79 ($\mu\epsilon$)	-16	-62	-71	-65	-47	-24	4	33	67	104	144
IS80 ($\mu\epsilon$)	-2	106	205	300	392	478	564	644	722	798	871
IS81 ($\mu\epsilon$)	-21	-79	-96	-96	-82	-62	-37	-9	23	59	97
IS82 ($\mu\epsilon$)	-2	96	186	272	357	437	516	591	665	736	806
IS83 ($\mu\epsilon$)	0	101	185	264	342	414	485	552	619	685	749
IS84 ($\mu\epsilon$)	-5	67	135	198	262	326	392	456	524	591	659
IS85 ($\mu\epsilon$)	-11	1	38	85	139	200	266	332	404	475	549
IS86 ($\mu\epsilon$)	-10	-27	-12	16	53	100	153	209	270	333	398
IS87 ($\mu\epsilon$)	-5	61	121	175	224	274	323	370	418	465	511
IS88 ($\mu\epsilon$)	-4	68	130	185	235	284	332	377	423	466	509
IS89 ($\mu\epsilon$)	-3	66	125	177	225	272	319	363	408	452	494
IS90 ($\mu\epsilon$)	-10	-11	7	37	74	122	176	233	295	358	424
IS91 ($\mu\epsilon$)	-17	-47	-57	-56	-50	-34	-13	12	41	74	111
IS92 ($\mu\epsilon$)	-3	80	152	215	272	328	381	432	482	530	577
IS93 ($\mu\epsilon$)	-12	-23	-14	4	28	61	98	138	182	229	278
IS94 ($\mu\epsilon$)	0	126	237	342	437	530	619	704	787	866	943

**Table F-8. Raw data, strain survey conducted after hot-wet conditioning, ambient environmental conditions (Run 2)
(continued)**

Load Step	0	1	2	3	4	5	6	7	8	9	10
Pressure (psi)	-0.03	0.68	1.32	2.02	2.67	3.31	4.00	4.67	5.34	6.02	6.69
IS95 ($\mu\epsilon$)	-11	-13	4	29	60	98	140	183	230	280	330
IS96 ($\mu\epsilon$)	-1	111	211	303	388	472	552	629	705	778	848
IS97 ($\mu\epsilon$)	-3	104	197	281	361	438	513	585	656	725	794
L01 ($\mu\epsilon$)	-	-	-	-	-	-	-	-	-	-	-
L02 ($\mu\epsilon$)	12	40	54	68	80	94	110	126	140	157	171
L03 ($\mu\epsilon$)	5	19	25	36	47	62	79	98	116	138	156
L04 ($\mu\epsilon$)	8	44	66	88	111	135	159	184	208	232	254
L05 ($\mu\epsilon$)	8	24	33	41	47	56	65	75	84	94	102
L06 ($\mu\epsilon$)	12	45	60	73	86	100	112	124	134	142	151
L07 ($\mu\epsilon$)	-	-	-	-	-	-	-	-	-	-	-
L08 ($\mu\epsilon$)	14	54	79	105	128	151	175	199	220	245	265
L09 ($\mu\epsilon$)	12	63	93	124	155	181	208	231	258	283	308
L10 ($\mu\epsilon$)	-	-	-	-	-	-	-	-	-	-	-
RAC-A1 ($\mu\epsilon$)	0	113	216	316	414	508	602	690	776	861	942
RAC-A2 ($\mu\epsilon$)	-1	103	196	287	375	459	541	619	696	770	842
RAC-A3 ($\mu\epsilon$)	-1	94	176	253	328	399	467	532	596	657	717
RAC-F1 ($\mu\epsilon$)	1	109	209	304	398	487	575	659	740	820	897
RAC-F2 ($\mu\epsilon$)	1	102	195	283	370	451	530	607	681	753	823
RBC-A1 ($\mu\epsilon$)	2	122	229	323	412	492	568	639	704	766	824
RBC-A2 ($\mu\epsilon$)	1	106	199	281	358	429	495	556	613	667	718

**Table F-8. Raw data, strain survey conducted after hot-wet conditioning, ambient environmental conditions (Run 2)
(continued)**

Load Step	0	1	2	3	4	5	6	7	8	9	10
Pressure (psi)	-0.03	0.68	1.32	2.02	2.67	3.31	4.00	4.67	5.34	6.02	6.69
RBC-A3 ($\mu\epsilon$)	1	103	194	274	350	420	486	547	605	660	713
RBC-A4 ($\mu\epsilon$)	1	101	192	274	351	422	490	554	614	672	728
RBC-F1 ($\mu\epsilon$)	1	122	226	318	405	482	555	623	685	745	800
RBC-F2 ($\mu\epsilon$)	0	109	204	287	365	434	500	560	617	670	720
RBC-F3 ($\mu\epsilon$)	0	108	202	284	361	429	495	555	612	665	716
S16 ($\mu\epsilon$)	33	89	156	224	291	359	427	494	564	632	703
S17 ($\mu\epsilon$)	-	-	-	-	-	-	-	-	-	-	-
S18 ($\mu\epsilon$)	33	188	314	423	522	612	698	779	859	935	1012
S20 ($\mu\epsilon$)	41	-296	-583	-838	-1064	-1268	-1455	-1619	-1767	-1901	-2016
S22 ($\mu\epsilon$)	17	160	278	380	474	560	641	717	793	865	938
S25 ($\mu\epsilon$)	25	213	372	518	656	786	912	1032	1150	1262	1374
S29 ($\mu\epsilon$)	-2	60	121	185	250	315	381	446	512	577	644
S30 ($\mu\epsilon$)	10	162	292	407	512	608	699	785	870	952	1033
S32 ($\mu\epsilon$)	3	-122	-230	-324	-412	-488	-559	-624	-680	-733	-778
S34 ($\mu\epsilon$)	8	117	224	324	428	521	611	697	783	866	950
S37 ($\mu\epsilon$)	13	223	396	549	689	819	943	1061	1176	1285	1393
S41 ($\mu\epsilon$)	1	80	154	228	301	371	441	508	575	641	706
S42 ($\mu\epsilon$)	11	70	142	212	283	354	426	497	569	641	713
S43 ($\mu\epsilon$)	15	132	235	327	412	492	569	644	719	791	864
S44 ($\mu\epsilon$)	28	184	314	427	529	624	716	803	889	972	1053

**Table F-8. Raw data, strain survey conducted after hot-wet conditioning, ambient environmental conditions (Run 2)
(continued)**

Load Step	0	1	2	3	4	5	6	7	8	9	10
Pressure (psi)	-0.03	0.68	1.32	2.02	2.67	3.31	4.00	4.67	5.34	6.02	6.69
S46 ($\mu\epsilon$)	-5	-306	-570	-816	-1037	-1245	-1442	-1623	-1794	-1953	-2099
S48 ($\mu\epsilon$)	13	136	245	346	439	525	610	690	770	846	922
S51 ($\mu\epsilon$)	42	222	379	523	657	784	907	1026	1143	1255	1366
S55 ($\mu\epsilon$)	-2	64	131	199	268	336	405	473	541	608	675
S56 ($\mu\epsilon$)	30	100	172	242	312	378	446	512	581	647	716
S57 ($\mu\epsilon$)	-	-	-	-	-	-	-	-	-	-	-
S58 ($\mu\epsilon$)	26	209	348	464	568	660	750	832	915	991	1069
S60 ($\mu\epsilon$)	2	-396	-729	-1029	-1300	-1543	-1771	-1974	-2165	-2338	-2494
S62 ($\mu\epsilon$)	15	168	286	389	482	566	646	721	797	868	940
S65 ($\mu\epsilon$)	27	211	365	507	640	767	890	1007	1122	1232	1340
S69 ($\mu\epsilon$)	10	82	151	219	288	356	424	491	559	625	692
S70 ($\mu\epsilon$)	17	89	164	237	311	382	455	526	598	670	743
S71 ($\mu\epsilon$)	-	-	-	-	-	-	-	-	-	-	-
S72 ($\mu\epsilon$)	14	202	337	451	552	645	733	817	899	978	1056
S74 ($\mu\epsilon$)	-6	-181	-339	-491	-639	-778	-914	-1043	-1166	-1285	-1396
S76 ($\mu\epsilon$)	7	147	260	363	458	547	633	715	796	875	953
S79 ($\mu\epsilon$)	13	224	384	526	656	779	898	1012	1124	1233	1339
S83 ($\mu\epsilon$)	-1	88	162	232	298	363	427	490	552	614	675
S84 ($\mu\epsilon$)	21	91	162	234	304	375	446	517	590	660	733
S85 ($\mu\epsilon$)	-	-	-	-	-	-	-	-	-	-	-

**Table F-8. Raw data, strain survey conducted after hot-wet conditioning, ambient environmental conditions (Run 2)
(continued)**

Load Step	0	1	2	3	4	5	6	7	8	9	10
Pressure (psi)	-0.03	0.68	1.32	2.02	2.67	3.31	4.00	4.67	5.34	6.02	6.69
S86 ($\mu\epsilon$)	25	184	308	414	510	597	680	760	839	913	988
S88 ($\mu\epsilon$)	10	-105	-191	-266	-326	-378	-422	-458	-487	-510	-526
S90 ($\mu\epsilon$)	22	167	285	388	481	567	650	728	806	880	955
S93 ($\mu\epsilon$)	19	196	348	485	613	733	848	958	1067	1171	1274
S97 ($\mu\epsilon$)	16	92	162	231	298	365	431	496	561	625	689
UAC-A1 ($\mu\epsilon$)	3	150	284	407	522	630	735	833	928	1018	1105
UAC-A2 ($\mu\epsilon$)	2	136	258	367	469	566	658	745	829	909	986
UAC-A3 ($\mu\epsilon$)	2	120	225	319	406	488	567	641	713	782	850
UAC-F1 ($\mu\epsilon$)	3	147	278	402	516	627	733	833	929	1021	1109
UAC-F2 ($\mu\epsilon$)	1	128	242	350	448	542	633	718	800	879	955
UBC-A1 ($\mu\epsilon$)	11	212	388	544	688	817	939	1052	1157	1256	1349
UBC-A2 ($\mu\epsilon$)	7	172	317	445	563	669	769	861	948	1030	1107
UBC-A3 ($\mu\epsilon$)	6	159	293	409	517	615	707	792	872	948	1020
UBC-A4 ($\mu\epsilon$)	6	149	274	382	484	577	665	747	825	900	972
UBC-F1 ($\mu\epsilon$)	9	209	384	538	680	808	929	1040	1144	1242	1334
UBC-F2 ($\mu\epsilon$)	5	172	318	445	563	668	768	859	946	1027	1104
UBC-F3 ($\mu\epsilon$)	4	160	295	413	522	620	713	799	880	957	1029
UDAC-A1 ($\mu\epsilon$)	2	146	272	390	498	601	700	793	883	969	1050
UDAC-A2 ($\mu\epsilon$)	0	128	239	342	435	525	611	692	770	845	917
UDAC-A3 ($\mu\epsilon$)	-1	109	204	289	369	445	519	588	656	721	784

**Table F-8. Raw data, strain survey conducted after hot-wet conditioning, ambient environmental conditions (Run 2)
(continued)**

Load Step	0	1	2	3	4	5	6	7	8	9	10
Pressure (psi)	-0.03	0.68	1.32	2.02	2.67	3.31	4.00	4.67	5.34	6.02	6.69
UDAC-F1 ($\mu\epsilon$)	1	146	275	396	504	612	714	808	900	988	1071
UDAC-F2 ($\mu\epsilon$)	0	125	234	336	427	518	605	686	765	840	912
UDBC-A1 ($\mu\epsilon$)	7	208	378	529	669	795	913	1021	1122	1218	1305
UDBC-A2 ($\mu\epsilon$)	5	176	320	448	566	673	774	865	952	1033	1109
UDBC-A3 ($\mu\epsilon$)	5	165	299	419	529	629	722	808	889	966	1037
UDBC-A4 ($\mu\epsilon$)	5	152	275	384	486	578	666	747	824	898	968
UDBC-F1 ($\mu\epsilon$)	6	222	405	567	717	851	978	1093	1202	1304	1399
UDBC-F2 ($\mu\epsilon$)	3	181	332	465	589	699	803	898	987	1071	1149
UDBC-F3 ($\mu\epsilon$)	2	167	308	431	546	648	745	833	916	995	1069

Table F-9. Raw data, strain survey conducted after hot-wet conditioning, ambient environmental conditions (Run 3)

Load Step	0	1	2	3	4	5	6	7	8	9	10
Pressure (psi)	-0.06	0.66	1.34	2.00	2.67	3.33	4.02	4.67	5.32	6.00	6.67
Frame-1 (lbf)	2	140	192	350	466	536	677	757	876	982	1126
Frame-2 (lbf)	46	110	223	331	461	553	679	792	904	1020	1134
Frame-3 (lbf)	1	110	220	336	456	567	682	793	906	1022	1128
Frame-4 (lbf)	25	113	229	331	449	567	681	792	906	1023	1132
Frame-5 (lbf)	6	105	224	342	443	564	692	788	909	1021	1130
Frame-6 (lbf)	2	108	224	341	446	571	686	803	900	1014	1135
Frame-7 (lbf)	8	114	230	341	451	567	682	793	908	1019	1133
Frame-8 (lbf)	14	118	219	337	452	567	677	792	905	1019	1129
Frame-9 (lbf)	21	112	228	346	457	566	680	794	906	1021	1133
Frame-10 (lbf)	1	108	233	339	462	570	674	794	909	1017	1132
Frame-11 (lbf)	0	115	225	349	447	561	681	797	907	1015	1133
Frame-12 (lbf)	0	110	230	341	457	567	673	788	909	1020	1131
Hoop-1 (lbf)	8	714	1428	2142	2854	3589	4296	5007	5709	6432	7153
Hoop-2 (lbf)	119	704	1469	2125	2874	3563	4276	4999	5715	6445	7137
Hoop-3 (lbf)	62	695	1419	2136	2846	3572	4291	4993	5719	6412	7140
Hoop-4 (lbf)	19	732	1436	2163	2851	3568	4285	5005	5705	6422	7154
Hoop-5 (lbf)	24	723	1431	2144	2866	3572	4278	5013	5727	6412	7142
Hoop-6 (lbf)	0	715	1427	2137	2853	3580	4291	4999	5704	6424	7141
Hoop-7 (lbf)	10	699	1432	2144	2855	3562	4277	5004	5718	6429	7133
Hoop-8 (lbf)	149	714	1432	2140	2851	3572	4288	4993	5706	6429	7134
Hoop-9 (lbf)	51	704	1432	2147	2853	3568	4284	4993	5716	6417	7131

**Table F-9. Raw data, strain survey conducted after hot-wet conditioning, ambient environmental conditions (Run 3)
(continued)**

Load Step	0	1	2	3	4	5	6	7	8	9	10
Pressure (psi)	-0.06	0.66	1.34	2.00	2.67	3.33	4.02	4.67	5.32	6.00	6.67
Hoop-10 (lb _f)	2	736	1425	2126	2875	3569	4296	5001	5706	6421	7145
Hoop-11 (lb _f)	43	692	1412	2137	2860	3564	4277	4999	5717	6417	7152
Hoop-12 (lb _f)	108	709	1436	2142	2851	3563	4295	5004	5724	6430	7142
Hoop-13 (lb _f)	37	684	1449	2160	2842	3582	4279	4987	5708	6421	7141
Hoop-14 (lb _f)	20	719	1417	2131	2861	3571	4288	5013	5708	6419	7134
Long-1 (lb _f)	1	643	1349	2007	2657	3325	4014	4685	5337	5997	6698
Long-2 (lb _f)	16	671	1339	2005	2671	3340	3993	4672	5319	6010	6674
Long-3 (lb _f)	-8	677	1335	2002	2680	3338	4004	4673	5338	6007	6672
Long-4 (lb _f)	7	672	1339	1994	2670	3336	3999	4674	5340	6011	6675
Long-5 (lb _f)	-1	670	1338	2004	2670	3332	4008	4685	5340	6014	6670
Long-6 (lb _f)	-7	673	1338	2000	2679	3346	4015	4675	5330	6031	6699
Long-7 (lb _f)	4	667	1342	2000	2631	3349	4010	4669	5340	6011	6680
Long-8 (lb _f)	-1	669	1336	1994	2672	3338	4004	4673	5344	6003	6661
F01 (μ ϵ)	30	30	64	121	159	204	246	289	334	373	416
F02 (μ ϵ)	-25	52	96	151	206	259	316	372	423	478	531
F03 (μ ϵ)	68	13	56	96	127	158	186	211	246	280	314
F04 (μ ϵ)	-35	76	132	186	253	318	383	450	508	573	634
F05 (μ ϵ)	-	-	-	-	-	-	-	-	-	-	-
F06 (μ ϵ)	-36	56	113	162	220	272	329	389	440	497	553
F07 (μ ϵ)	38	3	45	93	130	163	196	226	263	297	333

**Table F-9. Raw data, strain survey conducted after hot-wet conditioning, ambient environmental conditions (Run 3)
(continued)**

Load Step	0	1	2	3	4	5	6	7	8	9	10
Pressure (psi)	-0.06	0.66	1.34	2.00	2.67	3.33	4.02	4.67	5.32	6.00	6.67
F08 ($\mu\epsilon$)	-17	75	117	161	216	268	326	383	434	492	545
IS16 ($\mu\epsilon$)	-18	81	164	237	307	375	443	512	583	655	729
IS17 ($\mu\epsilon$)	-22	-20	-1	28	65	109	160	213	273	335	401
IS18 ($\mu\epsilon$)	-16	-46	-50	-38	-17	14	52	96	146	199	258
IS19 ($\mu\epsilon$)	-9	34	78	121	162	204	248	291	337	383	432
IS20 ($\mu\epsilon$)	-8	50	106	156	204	249	295	339	384	427	473
IS21 ($\mu\epsilon$)	-11	41	93	140	183	224	265	304	344	383	422
IS22 ($\mu\epsilon$)	-8	-65	-85	-85	-75	-53	-21	18	64	114	171
IS23 ($\mu\epsilon$)	-30	-77	-104	-116	-120	-115	-103	-86	-62	-35	-2
IS24 ($\mu\epsilon$)	-4	78	153	221	283	343	400	455	508	560	612
IS25 ($\mu\epsilon$)	-12	-49	-65	-65	-56	-40	-16	12	47	85	128
IS26 ($\mu\epsilon$)	7	161	291	410	520	623	722	813	900	983	1066
IS27 ($\mu\epsilon$)	-20	-51	-58	-47	-27	0	36	75	120	169	222
IS28 ($\mu\epsilon$)	5	152	274	388	493	591	686	773	858	939	1019
IS29 ($\mu\epsilon$)	4	138	250	352	446	536	623	705	785	864	942
IS30 ($\mu\epsilon$)	-6	-24	-13	6	31	64	104	149	201	254	315
IS31 ($\mu\epsilon$)	-1	74	144	213	279	344	409	471	532	592	654
IS32 ($\mu\epsilon$)	-1	70	134	194	250	302	352	400	446	489	533
IS33 ($\mu\epsilon$)	-3	75	143	206	264	319	373	423	472	517	564
IS34 ($\mu\epsilon$)	-11	-10	-2	12	27	53	85	123	166	212	263

**Table F-9. Raw data, strain survey conducted after hot-wet conditioning, ambient environmental conditions (Run 3)
(continued)**

Load Step	0	1	2	3	4	5	6	7	8	9	10
Pressure (psi)	-0.06	0.66	1.34	2.00	2.67	3.33	4.02	4.67	5.32	6.00	6.67
IS35 ($\mu\epsilon$)	-27	-101	-149	-178	-198	-206	-207	-202	-189	-173	-151
IS36 ($\mu\epsilon$)	0	77	145	209	269	324	378	429	477	523	569
IS37 ($\mu\epsilon$)	-13	-96	-148	-176	-193	-199	-195	-185	-167	-144	-114
IS38 ($\mu\epsilon$)	2	95	176	254	326	394	459	520	579	635	690
IS39 ($\mu\epsilon$)	-16	-104	-152	-173	-182	-177	-163	-143	-114	-81	-41
IS40 ($\mu\epsilon$)	1	99	185	268	345	418	489	555	619	679	740
IS41 ($\mu\epsilon$)	1	117	215	308	393	476	555	630	702	772	842
IS42 ($\mu\epsilon$)	-15	89	170	245	316	386	457	527	599	671	744
IS43 ($\mu\epsilon$)	-10	18	61	110	165	224	287	353	421	491	564
IS44 ($\mu\epsilon$)	-26	-51	-44	-25	6	44	89	138	193	249	310
IS45 ($\mu\epsilon$)	-4	75	150	218	285	348	410	469	528	585	643
IS46 ($\mu\epsilon$)	-3	80	159	230	298	361	423	481	539	594	649
IS47 ($\mu\epsilon$)	-2	79	154	222	288	349	409	466	522	576	630
IS48 ($\mu\epsilon$)	-14	-4	26	61	104	151	205	262	324	387	455
IS49 ($\mu\epsilon$)	-32	-65	-78	-80	-73	-61	-43	-22	5	34	67
IS50 ($\mu\epsilon$)	-1	93	178	254	327	394	460	523	584	642	700
IS51 ($\mu\epsilon$)	-31	-54	-59	-54	-40	-23	1	27	57	90	126
IS52 ($\mu\epsilon$)	2	127	240	342	442	533	623	709	791	870	948
IS53 ($\mu\epsilon$)	-39	-59	-57	-42	-18	11	47	85	128	173	222
IS54 ($\mu\epsilon$)	1	119	225	323	416	502	587	668	746	821	896

**Table F-9. Raw data, strain survey conducted after hot-wet conditioning, ambient environmental conditions (Run 3)
(continued)**

Load Step	0	1	2	3	4	5	6	7	8	9	10
Pressure (psi)	-0.06	0.66	1.34	2.00	2.67	3.33	4.02	4.67	5.32	6.00	6.67
IS55 ($\mu\epsilon$)	2	112	211	299	383	461	538	611	683	753	823
IS56 ($\mu\epsilon$)	-19	64	130	189	248	307	368	430	494	558	626
IS57 ($\mu\epsilon$)	-17	-29	-21	0	30	68	112	160	214	270	330
IS58 ($\mu\epsilon$)	-14	-63	-82	-81	-69	-47	-16	21	64	111	165
IS59 ($\mu\epsilon$)	-4	46	92	136	178	220	263	307	352	398	447
IS60 ($\mu\epsilon$)	-2	61	117	166	212	256	299	341	383	425	468
IS61 ($\mu\epsilon$)	-1	60	114	162	206	248	290	329	370	409	450
IS62 ($\mu\epsilon$)	-5	-57	-73	-73	-61	-39	-8	29	72	120	173
IS63 ($\mu\epsilon$)	-34	-83	-110	-124	-131	-130	-124	-113	-96	-74	-48
IS64 ($\mu\epsilon$)	1	89	165	234	297	356	414	467	520	572	623
IS65 ($\mu\epsilon$)	-11	-29	-27	-14	5	31	62	96	136	178	226
IS66 ($\mu\epsilon$)	7	169	307	433	550	658	761	857	948	1035	1120
IS67 ($\mu\epsilon$)	-1	-11	-1	22	49	84	124	167	214	266	321
IS68 ($\mu\epsilon$)	6	153	279	396	504	604	701	790	876	959	1040
IS69 ($\mu\epsilon$)	4	137	249	351	446	536	622	705	784	861	939
IS70 ($\mu\epsilon$)	-23	46	106	161	218	275	334	393	456	518	583
IS71 ($\mu\epsilon$)	-20	-31	-10	25	70	121	178	236	299	364	432
IS72 ($\mu\epsilon$)	-12	-47	-40	-14	22	67	118	172	231	292	357
IS73 ($\mu\epsilon$)	-2	79	156	230	300	368	434	495	556	614	672
IS74 ($\mu\epsilon$)	-1	83	160	233	303	370	436	497	557	614	672

**Table F-9. Raw data, strain survey conducted after hot-wet conditioning, ambient environmental conditions (Run 3)
(continued)**

Load Step	0	1	2	3	4	5	6	7	8	9	10
Pressure (psi)	-0.06	0.66	1.34	2.00	2.67	3.33	4.02	4.67	5.32	6.00	6.67
IS75 ($\mu\epsilon$)	-1	84	162	236	307	374	440	502	563	622	680
IS76 ($\mu\epsilon$)	-5	15	49	93	144	200	260	322	388	456	527
IS77 ($\mu\epsilon$)	-21	-68	-79	-72	-56	-34	-7	23	57	95	136
IS78 ($\mu\epsilon$)	-2	90	174	254	330	402	472	538	603	665	726
IS79 ($\mu\epsilon$)	-16	-63	-73	-64	-48	-25	2	31	65	102	143
IS80 ($\mu\epsilon$)	-1	107	206	300	391	478	563	643	720	795	870
IS81 ($\mu\epsilon$)	-21	-81	-98	-95	-83	-64	-39	-11	21	57	96
IS82 ($\mu\epsilon$)	-1	97	186	273	357	437	515	590	663	734	805
IS83 ($\mu\epsilon$)	1	99	184	264	340	412	483	550	616	681	748
IS84 ($\mu\epsilon$)	-6	63	132	197	261	324	390	455	522	588	657
IS85 ($\mu\epsilon$)	-13	-3	36	84	139	199	264	332	402	472	546
IS86 ($\mu\epsilon$)	-13	-30	-14	16	54	100	152	209	269	330	396
IS87 ($\mu\epsilon$)	-6	60	120	173	224	273	321	369	416	462	509
IS88 ($\mu\epsilon$)	-4	67	130	184	235	283	331	376	421	463	507
IS89 ($\mu\epsilon$)	-5	64	124	177	226	271	317	362	407	448	491
IS90 ($\mu\epsilon$)	-11	-14	6	36	75	121	174	232	293	354	421
IS91 ($\mu\epsilon$)	-19	-48	-57	-57	-48	-34	-14	11	41	72	109
IS92 ($\mu\epsilon$)	-4	80	152	214	273	327	380	431	481	527	575
IS93 ($\mu\epsilon$)	-13	-23	-15	4	30	61	97	137	181	226	277
IS94 ($\mu\epsilon$)	1	129	239	342	440	531	620	705	786	864	942

**Table F-9. Raw data, strain survey conducted after hot-wet conditioning, ambient environmental conditions (Run 3)
(continued)**

Load Step	0	1	2	3	4	5	6	7	8	9	10
Pressure (psi)	-0.06	0.66	1.34	2.00	2.67	3.33	4.02	4.67	5.32	6.00	6.67
IS95 ($\mu\epsilon$)	-12	-13	3	30	62	98	139	183	230	276	328
IS96 ($\mu\epsilon$)	-1	112	212	304	391	472	553	630	704	775	847
IS97 ($\mu\epsilon$)	-4	104	197	282	362	438	512	584	655	722	791
L01 ($\mu\epsilon$)	-	-	-	-	-	-	-	-	-	-	-
L02 ($\mu\epsilon$)	14	45	58	70	84	98	113	130	145	161	175
L03 ($\mu\epsilon$)	6	22	30	39	51	66	83	103	121	141	161
L04 ($\mu\epsilon$)	9	50	71	91	116	140	164	189	212	235	258
L05 ($\mu\epsilon$)	8	27	36	43	50	59	68	78	87	96	105
L06 ($\mu\epsilon$)	11	47	61	75	88	101	113	125	135	143	151
L07 ($\mu\epsilon$)	-	-	-	-	-	-	-	-	-	-	-
L08 ($\mu\epsilon$)	16	60	84	108	132	155	179	203	225	249	270
L09 ($\mu\epsilon$)	12	67	98	127	154	184	212	242	262	288	310
L10 ($\mu\epsilon$)	-	-	-	-	-	-	-	-	-	-	-
RAC-A1 ($\mu\epsilon$)	0	114	217	316	414	508	601	689	775	859	942
RAC-A2 ($\mu\epsilon$)	-1	104	198	287	375	459	541	619	695	769	842
RAC-A3 ($\mu\epsilon$)	0	93	175	253	327	397	466	530	593	655	716
RAC-F1 ($\mu\epsilon$)	2	112	210	305	398	488	576	659	739	819	897
RAC-F2 ($\mu\epsilon$)	1	104	196	284	369	451	531	607	680	752	822
RBC-A1 ($\mu\epsilon$)	2	126	229	324	411	492	568	637	702	763	822
RBC-A2 ($\mu\epsilon$)	1	110	199	282	358	428	494	554	611	664	716

**Table F-9. Raw data, strain survey conducted after hot-wet conditioning, ambient environmental conditions (Run 3)
(continued)**

Load Step	0	1	2	3	4	5	6	7	8	9	10
Pressure (psi)	-0.06	0.66	1.34	2.00	2.67	3.33	4.02	4.67	5.32	6.00	6.67
RBC-A3 ($\mu\epsilon$)	1	106	194	275	349	419	485	546	603	658	711
RBC-A4 ($\mu\epsilon$)	1	105	193	275	350	421	489	552	612	670	726
RBC-F1 ($\mu\epsilon$)	1	126	227	319	404	482	555	622	684	742	798
RBC-F2 ($\mu\epsilon$)	-1	113	204	287	364	433	499	559	615	667	718
RBC-F3 ($\mu\epsilon$)	-1	112	202	284	360	428	494	554	610	662	714
S16 ($\mu\epsilon$)	39	94	162	227	295	361	430	497	565	633	704
S17 ($\mu\epsilon$)	-	-	-	-	-	-	-	-	-	-	-
S18 ($\mu\epsilon$)	40	190	319	427	525	615	700	781	859	936	1013
S20 ($\mu\epsilon$)	53	-298	-582	-830	-1058	-1260	-1446	-1613	-1760	-1892	-2012
S22 ($\mu\epsilon$)	21	162	281	383	477	562	642	719	792	864	938
S25 ($\mu\epsilon$)	31	216	378	523	661	790	915	1035	1150	1263	1374
S29 ($\mu\epsilon$)	-3	59	121	185	250	314	380	445	511	576	642
S30 ($\mu\epsilon$)	12	164	294	408	513	608	699	785	869	950	1031
S32 ($\mu\epsilon$)	7	-127	-229	-322	-408	-484	-556	-619	-675	-726	-773
S34 ($\mu\epsilon$)	8	116	223	324	428	519	609	695	780	863	947
S37 ($\mu\epsilon$)	16	220	397	549	689	818	942	1059	1172	1281	1390
S41 ($\mu\epsilon$)	-4	78	153	225	297	368	437	506	572	637	702
S42 ($\mu\epsilon$)	14	72	144	213	285	355	427	498	569	640	713
S43 ($\mu\epsilon$)	20	136	240	330	415	494	571	646	718	791	864
S44 ($\mu\epsilon$)	30	185	314	427	530	625	716	802	887	969	1051

**Table F-9. Raw data, strain survey conducted after hot-wet conditioning, ambient environmental conditions (Run 3)
(continued)**

Load Step	0	1	2	3	4	5	6	7	8	9	10
Pressure (psi)	-0.06	0.66	1.34	2.00	2.67	3.33	4.02	4.67	5.32	6.00	6.67
S46 ($\mu\epsilon$)	-1	-310	-575	-813	-1041	-1248	-1444	-1626	-1793	-1951	-2100
S48 ($\mu\epsilon$)	12	135	244	345	438	525	609	689	767	843	920
S51 ($\mu\epsilon$)	44	221	380	522	656	783	906	1024	1139	1251	1363
S55 ($\mu\epsilon$)	-2	64	131	199	268	335	404	471	539	605	673
S56 ($\mu\epsilon$)	36	104	178	247	315	381	448	515	581	648	717
S57 ($\mu\epsilon$)	-	-	-	-	-	-	-	-	-	-	-
S58 ($\mu\epsilon$)	33	214	353	471	574	666	754	835	916	992	1071
S60 ($\mu\epsilon$)	4	-399	-735	-1028	-1297	-1541	-1767	-1976	-2161	-2333	-2492
S62 ($\mu\epsilon$)	19	172	291	392	485	568	647	723	797	868	939
S65 ($\mu\epsilon$)	33	218	374	513	646	773	894	1012	1124	1233	1341
S69 ($\mu\epsilon$)	13	88	156	224	292	360	427	495	561	627	694
S70 ($\mu\epsilon$)	19	91	164	238	310	382	454	525	596	668	742
S71 ($\mu\epsilon$)	-	-	-	-	-	-	-	-	-	-	-
S72 ($\mu\epsilon$)	15	200	337	450	552	643	732	815	896	975	1054
S74 ($\mu\epsilon$)	-9	-190	-345	-496	-642	-783	-919	-1047	-1168	-1286	-1399
S76 ($\mu\epsilon$)	7	143	260	362	458	546	631	713	793	872	951
S79 ($\mu\epsilon$)	13	220	384	524	655	777	896	1010	1120	1228	1336
S83 ($\mu\epsilon$)	-1	88	163	231	298	362	426	488	550	611	673
S84 ($\mu\epsilon$)	27	97	169	238	310	380	450	521	591	662	735
S85 ($\mu\epsilon$)	-	-	-	-	-	-	-	-	-	-	-

**Table F-9. Raw data, strain survey conducted after hot-wet conditioning, ambient environmental conditions (Run 3)
(continued)**

Load Step	0	1	2	3	4	5	6	7	8	9	10
Pressure (psi)	-0.06	0.66	1.34	2.00	2.67	3.33	4.02	4.67	5.32	6.00	6.67
S86 ($\mu\epsilon$)	32	189	313	419	514	601	684	763	839	914	990
S88 ($\mu\epsilon$)	14	-105	-191	-262	-325	-377	-421	-457	-485	-508	-525
S90 ($\mu\epsilon$)	28	172	291	393	486	572	654	732	807	882	957
S93 ($\mu\epsilon$)	8	182	336	472	600	719	835	946	1053	1157	1260
S97 ($\mu\epsilon$)	22	98	168	235	303	369	434	499	563	626	691
UAC-A1 ($\mu\epsilon$)	3	151	285	407	524	631	735	833	927	1016	1104
UAC-A2 ($\mu\epsilon$)	1	137	258	367	471	566	658	744	828	907	985
UAC-A3 ($\mu\epsilon$)	1	120	225	318	407	488	566	640	712	780	848
UAC-F1 ($\mu\epsilon$)	3	148	281	401	520	628	734	833	929	1020	1109
UAC-F2 ($\mu\epsilon$)	1	128	245	349	450	543	633	718	800	878	954
UBC-A1 ($\mu\epsilon$)	12	219	390	546	688	817	940	1051	1156	1254	1349
UBC-A2 ($\mu\epsilon$)	7	178	319	447	562	668	769	860	946	1027	1106
UBC-A3 ($\mu\epsilon$)	7	165	294	411	517	614	707	791	871	946	1019
UBC-A4 ($\mu\epsilon$)	6	154	275	384	484	576	665	746	824	898	971
UBC-F1 ($\mu\epsilon$)	10	216	386	540	680	808	930	1040	1143	1239	1332
UBC-F2 ($\mu\epsilon$)	5	177	319	447	562	668	768	859	944	1024	1102
UBC-F3 ($\mu\epsilon$)	4	165	296	414	522	620	713	798	878	954	1028
UDAC-A1 ($\mu\epsilon$)	2	147	274	391	501	603	701	794	883	966	1049
UDAC-A2 ($\mu\epsilon$)	0	129	241	342	438	526	611	692	770	842	915
UDAC-A3 ($\mu\epsilon$)	-2	110	204	290	370	445	518	588	655	718	782

**Table F-9. Raw data, strain survey conducted after hot-wet conditioning, ambient environmental conditions (Run 3)
(continued)**

Load Step	0	1	2	3	4	5	6	7	8	9	10
Pressure (psi)	-0.06	0.66	1.34	2.00	2.67	3.33	4.02	4.67	5.32	6.00	6.67
UDAC-F1 ($\mu\epsilon$)	2	147	278	395	508	613	714	809	900	985	1070
UDAC-F2 ($\mu\epsilon$)	0	125	236	335	431	519	605	686	764	837	910
UDBC-A1 ($\mu\epsilon$)	9	211	379	531	669	795	912	1020	1120	1214	1304
UDBC-A2 ($\mu\epsilon$)	7	178	321	449	566	673	773	864	950	1030	1108
UDBC-A3 ($\mu\epsilon$)	7	167	301	420	529	629	722	807	888	963	1036
UDBC-A4 ($\mu\epsilon$)	6	154	276	386	486	578	665	746	822	895	967
UDBC-F1 ($\mu\epsilon$)	8	226	407	569	716	851	978	1093	1200	1301	1398
UDBC-F2 ($\mu\epsilon$)	4	185	333	467	588	699	803	897	985	1068	1148
UDBC-F3 ($\mu\epsilon$)	3	171	309	433	545	648	745	832	915	992	1068

F.2.1.3 After 30,000 Cycles

Table F-10. Raw data, strain survey conducted after 30,000 cycles, ambient environmental conditions (Run 1)

Load Step	0	1	2	3	4	5	6	7	8	9	10
Pressure (psi)	-0.01	0.68	1.34	2.00	2.67	3.32	4.00	4.67	5.33	6.02	6.66
Frame-1 (lb _f)	6	135	264	328	460	566	688	821	922	1033	1114
Frame-2 (lb _f)	56	59	227	348	443	567	681	792	905	1021	1130
Frame-3 (lb _f)	1	109	230	344	453	567	681	792	905	1020	1132
Frame-4 (lb _f)	32	30	226	339	458	568	679	792	906	1020	1132
Frame-5 (lb _f)	1	103	232	336	456	563	659	795	903	1020	1114
Frame-6 (lb _f)	-2	116	239	345	435	569	691	776	912	1020	1125
Frame-7 (lb _f)	1	115	235	343	453	570	682	795	909	1020	1137
Frame-8 (lb _f)	-4	115	229	335	449	568	674	797	909	1021	1129
Frame-9 (lb _f)	27	31	227	344	449	556	680	793	908	1018	1132
Frame-10 (lb _f)	1	116	221	336	455	567	664	793	906	1020	1133
Frame-11 (lb _f)	-7	116	227	343	453	567	674	798	900	1018	1131
Frame-12 (lb _f)	-1	113	231	343	450	568	677	782	905	1023	1130
Hoop-1 (lb _f)	23	705	1386	2127	2858	3577	4274	4996	5708	6420	7139
Hoop-2 (lb _f)	70	707	1469	2156	2836	3577	4292	5012	5710	6445	7148
Hoop-3 (lb _f)	29	724	1426	2149	2858	3564	4281	4994	5714	6443	7143
Hoop-4 (lb _f)	-4	723	1433	2133	2868	3568	4296	4992	5712	6416	7149
Hoop-5 (lb _f)	31	743	1414	2148	2850	3555	4293	5003	5723	6426	7127
Hoop-6 (lb _f)	27	725	1417	2150	2859	3568	4286	4999	5700	6430	7145
Hoop-7 (lb _f)	24	692	1422	2141	2856	3572	4291	4998	5707	6436	7138
Hoop-8 (lb _f)	124	715	1415	2145	2856	3581	4288	4996	5713	6425	7140

Table F-10. Raw data, strain survey conducted after 30,000 cycles, ambient environmental conditions (Run 1) (continued)

Load Step	0	1	2	3	4	5	6	7	8	9	10
Pressure (psi)	-0.01	0.68	1.34	2.00	2.67	3.32	4.00	4.67	5.33	6.02	6.66
Hoop-9 (lbf)	-3	723	1410	2145	2852	3575	4280	4998	5719	6435	7138
Hoop-10 (lbf)	5	708	1430	2147	2849	3566	4288	5003	5712	6422	7146
Hoop-11 (lbf)	8	725	1433	2158	2859	3560	4291	4991	5714	6432	7145
Hoop-12 (lbf)	103	721	1425	2142	2858	3555	4288	4988	5705	6434	7129
Hoop-13 (lbf)	43	721	1439	2117	2855	3572	4315	5001	5713	6434	7135
Hoop-14 (lbf)	9	690	1427	2134	2862	3580	4273	4993	5707	6426	7141
Long-1 (lbf)	-6	675	1359	1983	2666	3320	4027	4647	5336	5972	6716
Long-2 (lbf)	13	652	1334	1997	2671	3342	4007	4667	5356	6013	6667
Long-3 (lbf)	-9	659	1336	2010	2669	3356	4009	4673	5336	5962	6707
Long-4 (lbf)	3	705	1330	2007	2671	3335	4004	4669	5334	6010	6677
Long-5 (lbf)	4	664	1318	2000	2668	3345	4013	4665	5339	6008	6682
Long-6 (lbf)	10	660	1345	1995	2673	3340	4016	4675	5326	6003	6673
Long-7 (lbf)	-19	693	1385	2002	2676	3327	4019	4684	5326	6000	6672
Long-8 (lbf)	-4	669	1329	2002	2667	3340	4007	4662	5328	5999	6661
F01 ($\mu\epsilon$)	4	12	80	104	147	172	198	246	283	319	356
F02 ($\mu\epsilon$)	-2	57	98	152	212	265	317	377	435	490	542
F03 ($\mu\epsilon$)	25	-85	48	81	104	131	162	192	220	246	282
F04 ($\mu\epsilon$)	15	52	131	197	260	323	393	459	528	593	656
F05 ($\mu\epsilon$)	-	-	-	-	-	-	-	-	-	-	-
F06 ($\mu\epsilon$)	7	88	115	173	231	287	347	404	469	530	585
F07 ($\mu\epsilon$)	4	-18	49	80	110	142	172	204	232	267	303

Table F-10. Raw data, strain survey conducted after 30,000 cycles, ambient environmental conditions (Run 1) (continued)

Load Step	0	1	2	3	4	5	6	7	8	9	10
Pressure (psi)	-0.01	0.68	1.34	2.00	2.67	3.32	4.00	4.67	5.33	6.02	6.66
F08 ($\mu\epsilon$)	21	68	125	184	237	294	350	404	461	517	570
IS16 ($\mu\epsilon$)	-9	78	158	225	288	351	417	483	550	620	689
IS17 ($\mu\epsilon$)	-12	-14	-3	19	51	91	138	189	245	305	367
IS18 ($\mu\epsilon$)	-9	-39	-55	-50	-34	-8	27	66	113	164	219
IS19 ($\mu\epsilon$)	-12	33	63	97	130	165	202	240	280	323	366
IS20 ($\mu\epsilon$)	-10	48	93	135	174	213	253	291	330	370	410
IS21 ($\mu\epsilon$)	-10	44	88	129	167	204	242	278	315	353	389
IS22 ($\mu\epsilon$)	-15	-72	-105	-117	-115	-100	-75	-43	-3	44	94
IS23 ($\mu\epsilon$)	-8	-51	-93	-113	-122	-122	-114	-101	-82	-56	-27
IS24 ($\mu\epsilon$)	-8	69	127	183	234	283	332	378	423	469	513
IS25 ($\mu\epsilon$)	-5	-32	-58	-61	-55	-40	-18	8	41	79	120
IS26 ($\mu\epsilon$)	0	164	283	402	510	612	709	798	884	966	1043
IS27 ($\mu\epsilon$)	-6	-22	-32	-21	-2	26	61	100	144	193	244
IS28 ($\mu\epsilon$)	2	163	280	399	507	610	708	798	885	970	1049
IS29 ($\mu\epsilon$)	-2	143	248	353	448	539	628	711	792	872	948
IS30 ($\mu\epsilon$)	-17	-35	-26	-15	4	31	67	107	153	204	258
IS31 ($\mu\epsilon$)	-8	84	146	215	282	349	415	478	541	604	666
IS32 ($\mu\epsilon$)	-8	75	131	189	244	297	347	394	440	484	527
IS33 ($\mu\epsilon$)	-7	83	142	204	262	318	372	421	470	518	563
IS34 ($\mu\epsilon$)	-14	-17	-19	-16	-4	17	44	75	113	155	201
IS35 ($\mu\epsilon$)	-12	-73	-130	-162	-182	-192	-195	-192	-182	-167	-148

Table F-10. Raw data, strain survey conducted after 30,000 cycles, ambient environmental conditions (Run 1) (continued)

Load Step	0	1	2	3	4	5	6	7	8	9	10
Pressure (psi)	-0.01	0.68	1.34	2.00	2.67	3.32	4.00	4.67	5.33	6.02	6.66
IS36 ($\mu\epsilon$)	-8	80	140	202	259	314	367	416	463	510	553
IS37 ($\mu\epsilon$)	-9	-81	-138	-171	-189	-196	-195	-186	-171	-149	-123
IS38 ($\mu\epsilon$)	-5	100	173	249	321	389	454	515	575	632	686
IS39 ($\mu\epsilon$)	-9	-87	-137	-162	-171	-168	-156	-137	-111	-78	-42
IS40 ($\mu\epsilon$)	-3	106	185	267	345	419	491	557	622	685	745
IS41 ($\mu\epsilon$)	1	131	226	323	413	498	581	658	733	807	876
IS42 ($\mu\epsilon$)	-16	69	156	229	297	367	438	506	576	646	716
IS43 ($\mu\epsilon$)	-13	15	51	99	151	210	273	337	404	473	543
IS44 ($\mu\epsilon$)	-13	-30	-36	-17	11	50	95	142	195	252	310
IS45 ($\mu\epsilon$)	-8	84	143	212	274	336	396	452	508	564	618
IS46 ($\mu\epsilon$)	-7	80	142	209	268	326	382	434	485	535	583
IS47 ($\mu\epsilon$)	-6	81	141	207	266	324	379	432	483	534	583
IS48 ($\mu\epsilon$)	-13	7	18	50	88	135	187	241	300	362	426
IS49 ($\mu\epsilon$)	-7	-15	-48	-46	-39	-24	-6	16	42	72	105
IS50 ($\mu\epsilon$)	-5	100	170	247	316	383	447	507	565	621	676
IS51 ($\mu\epsilon$)	-8	2	-24	-12	4	27	52	79	111	146	183
IS52 ($\mu\epsilon$)	-2	143	240	348	447	542	634	719	802	882	959
IS53 ($\mu\epsilon$)	-10	6	-14	6	33	67	103	143	186	233	282
IS54 ($\mu\epsilon$)	-4	135	224	325	418	508	593	673	752	829	902
IS55 ($\mu\epsilon$)	-8	126	205	297	380	461	539	612	684	755	824
IS56 ($\mu\epsilon$)	-15	62	116	166	216	268	323	379	438	499	559

Table F-10. Raw data, strain survey conducted after 30,000 cycles, ambient environmental conditions (Run 1) (continued)

Load Step	0	1	2	3	4	5	6	7	8	9	10
Pressure (psi)	-0.01	0.68	1.34	2.00	2.67	3.32	4.00	4.67	5.33	6.02	6.66
IS57 ($\mu\epsilon$)	-15	-27	-28	-17	5	35	74	116	163	215	269
IS58 ($\mu\epsilon$)	-12	-55	-78	-85	-77	-60	-33	-1	39	85	133
IS59 ($\mu\epsilon$)	-9	37	73	105	136	169	205	240	278	317	358
IS60 ($\mu\epsilon$)	-7	52	99	140	177	214	251	286	323	360	396
IS61 ($\mu\epsilon$)	-8	53	104	147	186	225	265	303	341	380	418
IS62 ($\mu\epsilon$)	-8	-56	-73	-79	-72	-55	-28	4	43	88	136
IS63 ($\mu\epsilon$)	-7	-56	-91	-114	-127	-132	-130	-122	-109	-89	-66
IS64 ($\mu\epsilon$)	-6	65	121	170	215	258	301	341	381	421	460
IS65 ($\mu\epsilon$)	-5	-18	-21	-14	1	21	49	80	117	157	200
IS66 ($\mu\epsilon$)	4	158	286	402	508	606	700	786	869	947	1020
IS67 ($\mu\epsilon$)	-5	-4	8	29	57	90	130	172	219	270	322
IS68 ($\mu\epsilon$)	6	164	296	419	533	639	740	833	923	1009	1090
IS69 ($\mu\epsilon$)	4	154	271	378	479	571	662	745	826	905	980
IS70 ($\mu\epsilon$)	-27	45	98	146	197	249	305	362	420	480	541
IS71 ($\mu\epsilon$)	-23	-23	-4	28	70	118	174	231	291	355	418
IS72 ($\mu\epsilon$)	-15	-36	-27	-3	33	77	127	180	238	298	360
IS73 ($\mu\epsilon$)	-5	78	151	221	288	351	414	472	529	584	637
IS74 ($\mu\epsilon$)	-5	77	149	216	281	342	402	458	513	565	616
IS75 ($\mu\epsilon$)	-6	78	152	220	285	346	407	464	519	573	624
IS76 ($\mu\epsilon$)	-3	21	58	102	153	209	270	332	397	464	532
IS77 ($\mu\epsilon$)	-10	-41	-48	-41	-23	-1	26	56	89	126	165

Table F-10. Raw data, strain survey conducted after 30,000 cycles, ambient environmental conditions (Run 1) (continued)

Load Step	0	1	2	3	4	5	6	7	8	9	10
Pressure (psi)	-0.01	0.68	1.34	2.00	2.67	3.32	4.00	4.67	5.33	6.02	6.66
IS78 ($\mu\epsilon$)	-4	87	166	240	310	377	442	504	563	621	675
IS79 ($\mu\epsilon$)	-10	-40	-46	-37	-18	5	32	62	95	131	169
IS80 ($\mu\epsilon$)	-2	111	209	304	395	481	566	645	722	797	869
IS81 ($\mu\epsilon$)	-15	-57	-71	-67	-53	-33	-8	20	52	87	124
IS82 ($\mu\epsilon$)	-3	99	188	275	358	438	516	590	663	733	801
IS83 ($\mu\epsilon$)	-6	96	182	261	336	408	479	546	611	676	739
IS84 ($\mu\epsilon$)	-10	53	119	179	238	300	363	424	488	553	618
IS85 ($\mu\epsilon$)	-16	-11	8	50	99	157	220	282	350	420	490
IS86 ($\mu\epsilon$)	-15	-33	-40	-17	16	60	111	161	219	280	341
IS87 ($\mu\epsilon$)	-7	60	97	143	186	229	271	310	350	390	430
IS88 ($\mu\epsilon$)	-6	53	92	134	171	208	243	275	307	339	370
IS89 ($\mu\epsilon$)	-5	52	90	130	166	202	237	268	301	333	364
IS90 ($\mu\epsilon$)	-11	-3	-3	25	61	107	159	211	270	332	395
IS91 ($\mu\epsilon$)	-11	-24	-62	-64	-59	-44	-26	-5	22	53	87
IS92 ($\mu\epsilon$)	-6	78	129	185	234	282	328	369	410	450	488
IS93 ($\mu\epsilon$)	-14	7	-12	9	37	72	111	150	195	243	292
IS94 ($\mu\epsilon$)	-3	155	255	366	469	567	662	748	834	916	994
IS95 ($\mu\epsilon$)	-14	17	8	37	71	112	156	199	247	298	349
IS96 ($\mu\epsilon$)	-6	134	216	313	402	489	573	649	726	801	871
IS97 ($\mu\epsilon$)	-11	125	197	284	365	444	520	591	663	732	800
L01 ($\mu\epsilon$)	-	-	-	-	-	-	-	-	-	-	-

Table F-10. Raw data, strain survey conducted after 30,000 cycles, ambient environmental conditions (Run 1) (continued)

Load Step	0	1	2	3	4	5	6	7	8	9	10
Pressure (psi)	-0.01	0.68	1.34	2.00	2.67	3.32	4.00	4.67	5.33	6.02	6.66
L02 ($\mu\epsilon$)	24	38	43	52	63	76	89	100	114	129	143
L03 ($\mu\epsilon$)	17	22	18	25	37	51	67	82	101	120	139
L04 ($\mu\epsilon$)	24	50	60	79	102	124	147	168	192	215	236
L05 ($\mu\epsilon$)	22	29	30	37	45	54	63	71	81	91	102
L06 ($\mu\epsilon$)	14	46	61	80	99	116	130	142	153	162	172
L07 ($\mu\epsilon$)	-	-	-	-	-	-	-	-	-	-	-
L08 ($\mu\epsilon$)	27	50	69	89	112	134	157	177	199	222	243
L09 ($\mu\epsilon$)	24	73	87	114	140	167	193	214	240	265	288
L10 ($\mu\epsilon$)	-	-	-	-	-	-	-	-	-	-	-
RAC-A1 ($\mu\epsilon$)	-2	120	228	333	434	532	628	719	808	894	977
RAC-A2 ($\mu\epsilon$)	-3	106	201	293	381	465	548	626	703	777	848
RAC-A3 ($\mu\epsilon$)	-4	93	176	253	327	397	465	530	592	653	712
RAC-F1 ($\mu\epsilon$)	2	117	219	319	414	505	596	681	764	845	923
RAC-F2 ($\mu\epsilon$)	1	107	200	290	375	458	539	614	688	761	829
RBC-A1 ($\mu\epsilon$)	-4	140	232	332	425	513	594	669	740	807	869
RBC-A2 ($\mu\epsilon$)	-4	118	197	280	357	429	496	558	616	672	723
RBC-A3 ($\mu\epsilon$)	-4	113	190	270	345	416	482	543	601	658	710
RBC-A4 ($\mu\epsilon$)	-2	113	192	275	351	424	493	557	618	677	733
RBC-F1 ($\mu\epsilon$)	-5	143	228	324	414	497	574	644	711	773	831
RBC-F2 ($\mu\epsilon$)	-5	128	202	285	362	434	501	561	619	673	724
RBC-F3 ($\mu\epsilon$)	-6	127	198	280	355	426	492	551	608	663	713

Table F-10. Raw data, strain survey conducted after 30,000 cycles, ambient environmental conditions (Run 1) (continued)

Load Step	0	1	2	3	4	5	6	7	8	9	10
Pressure (psi)	-0.01	0.68	1.34	2.00	2.67	3.32	4.00	4.67	5.33	6.02	6.66
S16 ($\mu\epsilon$)	-40	27	77	130	180	226	272	314	357	400	441
S17 ($\mu\epsilon$)	-	-	-	-	-	-	-	-	-	-	-
S18 ($\mu\epsilon$)	-16	150	292	412	516	612	705	790	875	957	1038
S20 ($\mu\epsilon$)	-93	-391	-585	-795	-963	-1109	-1248	-1360	-1458	-1534	-1612
S22 ($\mu\epsilon$)	5	148	276	383	477	563	646	724	801	877	951
S25 ($\mu\epsilon$)	-4	170	329	470	601	727	849	964	1077	1187	1293
S29 ($\mu\epsilon$)	5	77	149	222	292	362	432	501	570	638	705
S30 ($\mu\epsilon$)	-3	146	266	376	473	564	652	734	815	894	970
S32 ($\mu\epsilon$)	41	-98	-173	-260	-340	-414	-480	-539	-594	-643	-686
S34 ($\mu\epsilon$)	-2319	-2434	-1456	-2017	-1498	-1903	-1421	-611	-1106	-1758	-1394
S37 ($\mu\epsilon$)	-3	202	376	527	662	788	911	1025	1137	1245	1349
S41 ($\mu\epsilon$)	11	97	179	261	339	416	492	564	636	706	773
S42 ($\mu\epsilon$)	0	0	0	0	0	0	0	0	0	0	0
S43 ($\mu\epsilon$)	-2	110	199	280	350	415	478	537	596	654	710
S44 ($\mu\epsilon$)	-11	153	289	409	516	611	700	784	869	948	1025
S46 ($\mu\epsilon$)	50	-278	-493	-723	-928	-1119	-1297	-1453	-1602	-1739	-1862
S48 ($\mu\epsilon$)	-1	122	240	343	434	521	605	684	761	837	911
S51 ($\mu\epsilon$)	-13	150	314	452	579	700	820	933	1044	1153	1257
S55 ($\mu\epsilon$)	0	59	130	198	265	333	401	467	534	600	665
S56 ($\mu\epsilon$)	12	78	148	214	275	336	397	456	517	578	639
S57 ($\mu\epsilon$)	-	-	-	-	-	-	-	-	-	-	-

Table F-10. Raw data, strain survey conducted after 30,000 cycles, ambient environmental conditions (Run 1) (continued)

Load Step	0	1	2	3	4	5	6	7	8	9	10
Pressure (psi)	-0.01	0.68	1.34	2.00	2.67	3.32	4.00	4.67	5.33	6.02	6.66
S58 ($\mu\epsilon$)	5	173	309	419	516	603	687	765	841	915	987
S60 ($\mu\epsilon$)	-36	-298	-531	-714	-877	-1015	-1124	-1220	-1344	-1425	-1451
S62 ($\mu\epsilon$)	1	148	264	361	448	527	603	675	746	815	882
S65 ($\mu\epsilon$)	-4	209	383	537	677	806	930	1044	1155	1262	1363
S69 ($\mu\epsilon$)	3	57	110	161	210	257	304	349	395	441	484
S70 ($\mu\epsilon$)	-4	67	145	218	288	356	426	493	562	630	698
S71 ($\mu\epsilon$)	-	-	-	-	-	-	-	-	-	-	-
S72 ($\mu\epsilon$)	1	176	312	422	518	607	692	772	851	927	1001
S74 ($\mu\epsilon$)	18	-171	-331	-489	-639	-781	-919	-1047	-1170	-1287	-1396
S76 ($\mu\epsilon$)	-8	133	249	350	441	527	611	691	769	846	920
S79 ($\mu\epsilon$)	-10	183	339	472	593	708	821	928	1032	1135	1234
S83 ($\mu\epsilon$)	16	105	183	257	327	395	463	528	593	657	719
S84 ($\mu\epsilon$)	6	90	157	235	310	386	461	535	610	686	762
S85 ($\mu\epsilon$)	-	-	-	-	-	-	-	-	-	-	-
S86 ($\mu\epsilon$)	-30	42	101	144	179	211	240	268	284	314	327
S88 ($\mu\epsilon$)	3	-168	-257	-351	-429	-495	-552	-594	-629	-655	-673
S90 ($\mu\epsilon$)	9	146	272	375	465	549	630	706	781	855	927
S93 ($\mu\epsilon$)	12	181	351	491	617	737	854	964	1073	1178	1280
S97 ($\mu\epsilon$)	17	86	158	227	293	359	424	488	552	615	677
UAC-A1 ($\mu\epsilon$)	-2	172	291	421	539	653	760	859	956	1048	1136
UAC-A2 ($\mu\epsilon$)	-4	154	257	371	474	572	666	752	836	916	993

Table F-10. Raw data, strain survey conducted after 30,000 cycles, ambient environmental conditions (Run 1) (continued)

Load Step	0	1	2	3	4	5	6	7	8	9	10
Pressure (psi)	-0.01	0.68	1.34	2.00	2.67	3.32	4.00	4.67	5.33	6.02	6.66
UAC-A3 ($\mu\epsilon$)	-5	135	221	318	405	489	569	642	714	784	850
UAC-F1 ($\mu\epsilon$)	2	170	292	426	547	664	776	877	977	1073	1163
UAC-F2 ($\mu\epsilon$)	0	145	248	361	462	560	653	738	821	901	977
UBC-A1 ($\mu\epsilon$)	-	-	-	-	-	-	-	-	-	-	-
UBC-A2 ($\mu\epsilon$)	-1	198	341	483	612	730	840	939	1034	1123	1204
UBC-A3 ($\mu\epsilon$)	0	175	298	422	533	635	733	820	903	982	1055
UBC-A4 ($\mu\epsilon$)	0	160	273	386	488	583	674	756	835	912	984
UBC-F1 ($\mu\epsilon$)	-	-	-	-	-	-	-	-	-	-	-
UBC-F2 ($\mu\epsilon$)	-1	210	347	490	618	737	847	946	1040	1128	1209
UBC-F3 ($\mu\epsilon$)	-2	188	307	433	547	652	749	837	922	1001	1074
UDAC-A1 ($\mu\epsilon$)	-4	183	300	430	549	663	771	867	964	1056	1142
UDAC-A2 ($\mu\epsilon$)	-5	157	254	363	463	559	650	731	813	891	963
UDAC-A3 ($\mu\epsilon$)	-6	129	206	295	377	456	531	600	668	735	797
UDAC-F1 ($\mu\epsilon$)	0	176	297	428	546	661	769	866	962	1055	1141
UDAC-F2 ($\mu\epsilon$)	0	147	245	354	452	547	638	718	799	876	949
UDBC-A1 ($\mu\epsilon$)	-	-	-	-	-	-	-	-	-	-	-
UDBC-A2 ($\mu\epsilon$)	6	206	371	522	659	784	902	1006	1105	1197	1281
UDBC-A3 ($\mu\epsilon$)	7	183	326	456	574	681	782	873	959	1038	1112
UDBC-A4 ($\mu\epsilon$)	7	167	295	413	519	617	710	794	874	950	1021
UDBC-F1 ($\mu\epsilon$)	-	-	-	-	-	-	-	-	-	-	-
UDBC-F2 ($\mu\epsilon$)	6	218	395	556	701	834	959	1070	1174	1272	1361

Table F-10. Raw data, strain survey conducted after 30,000 cycles, ambient environmental conditions (Run 1) (continued)

Load Step	0	1	2	3	4	5	6	7	8	9	10
Pressure (psi)	-0.01	0.68	1.34	2.00	2.67	3.32	4.00	4.67	5.33	6.02	6.66
UDBC-F3 ($\mu\epsilon$)	5	185	333	467	588	698	803	895	983	1066	1141

Table F-11. Raw data, strain survey conducted after 30,000 cycles, ambient environmental conditions (Run 2)

Load Step	0	1	2	3	4	5	6	7	8	9	10
Pressure (psi)	0.01	0.67	1.33	2.01	2.66	3.34	4.00	4.67	5.34	6.01	6.67
Frame-1 (lbf)	2	126	214	329	458	551	661	794	909	1046	1133
Frame-2 (lbf)	55	111	219	347	453	567	680	792	906	1020	1133
Frame-3 (lbf)	1	106	231	343	451	568	682	791	906	1021	1132
Frame-4 (lbf)	40	113	229	334	446	567	682	792	907	1020	1133
Frame-5 (lbf)	2	107	218	353	444	570	677	793	905	1018	1132
Frame-6 (lbf)	-12	120	227	345	455	556	684	782	911	1019	1128
Frame-7 (lbf)	8	110	227	342	454	567	685	793	908	1023	1129
Frame-8 (lbf)	-1	112	231	333	454	570	675	798	907	1013	1131
Frame-9 (lbf)	31	112	227	344	445	566	680	798	906	1018	1132
Frame-10 (lbf)	0	118	216	343	442	563	665	793	905	1018	1132
Frame-11 (lbf)	-6	116	230	348	459	573	684	795	907	1022	1136
Frame-12 (lbf)	-1	105	229	341	445	568	684	793	906	1022	1131
Hoop-1 (lbf)	29	716	1403	2151	2861	3572	4284	4985	5704	6410	7130
Hoop-2 (lbf)	48	694	1482	2113	2836	3600	4273	4987	5717	6441	7123
Hoop-3 (lbf)	31	724	1429	2145	2866	3570	4292	5007	5708	6422	7139
Hoop-4 (lbf)	-9	714	1414	2139	2851	3565	4282	5004	5709	6410	7151
Hoop-5 (lbf)	31	743	1427	2145	2861	3571	4284	4996	5731	6414	7134
Hoop-6 (lbf)	41	707	1428	2143	2854	3571	4288	5012	5709	6429	7140
Hoop-7 (lbf)	33	712	1433	2144	2863	3574	4292	5009	5714	6445	7140
Hoop-8 (lbf)	137	714	1425	2146	2856	3570	4286	5003	5714	6428	7142
Hoop-9 (lbf)	4	715	1411	2139	2851	3581	4286	4979	5722	6434	7144

Table F-11. Raw data, strain survey conducted after 30,000 cycles, ambient environmental conditions (Run 2) (continued)

Load Step	0	1	2	3	4	5	6	7	8	9	10
Pressure (psi)	0.01	0.67	1.33	2.01	2.66	3.34	4.00	4.67	5.34	6.01	6.67
Hoop-10 (lbf)	-6	707	1446	2137	2872	3577	4285	5002	5713	6421	7139
Hoop-11 (lbf)	27	709	1443	2143	2877	3585	4281	5016	5712	6429	7154
Hoop-12 (lbf)	113	721	1423	2152	2850	3563	4280	5002	5716	6418	7138
Hoop-13 (lbf)	44	730	1419	2123	2858	3576	4282	4999	5708	6429	7138
Hoop-14 (lbf)	12	712	1430	2155	2851	3564	4288	5000	5701	6442	7136
Long-1 (lbf)	-6	646	1359	2009	2677	3319	4019	4699	5364	5994	6693
Long-2 (lbf)	-1	669	1334	2006	2680	3334	4005	4674	5342	6003	6675
Long-3 (lbf)	0	668	1338	2006	2664	3339	4002	4672	5340	6006	6675
Long-4 (lbf)	-27	636	1303	2008	2670	3340	4004	4670	5339	6012	6667
Long-5 (lbf)	-1	670	1334	2003	2672	3332	4004	4671	5346	6007	6692
Long-6 (lbf)	-15	663	1330	2013	2671	3337	4008	4660	5324	6009	6657
Long-7 (lbf)	-24	659	1317	2001	2667	3332	3963	4670	5323	6016	6693
Long-8 (lbf)	12	680	1340	1991	2673	3336	4004	4678	5351	6010	6680
F01 ($\mu\epsilon$)	-4	36	73	109	132	170	204	245	279	316	354
F02 ($\mu\epsilon$)	3	38	96	157	210	270	321	379	435	492	544
F03 ($\mu\epsilon$)	16	11	47	74	97	128	158	186	211	241	275
F04 ($\mu\epsilon$)	25	76	132	201	261	333	398	468	534	599	663
F05 ($\mu\epsilon$)	-	-	-	-	-	-	-	-	-	-	-
F06 ($\mu\epsilon$)	18	59	114	183	231	294	346	411	474	535	590
F07 ($\mu\epsilon$)	-8	9	41	74	102	133	166	196	228	261	299
F08 ($\mu\epsilon$)	31	68	124	185	239	298	354	409	467	521	575

Table F-11. Raw data, strain survey conducted after 30,000 cycles, ambient environmental conditions (Run 2) (continued)

Load Step	0	1	2	3	4	5	6	7	8	9	10
Pressure (psi)	0.01	0.67	1.33	2.01	2.66	3.34	4.00	4.67	5.34	6.01	6.67
IS16 ($\mu\epsilon$)	-9	82	156	222	286	351	415	481	549	618	688
IS17 ($\mu\epsilon$)	-15	-17	-5	17	49	90	136	187	244	304	366
IS18 ($\mu\epsilon$)	-13	-45	-55	-52	-35	-9	25	65	112	163	218
IS19 ($\mu\epsilon$)	-14	25	62	94	128	163	200	238	278	321	365
IS20 ($\mu\epsilon$)	-10	44	92	132	173	211	251	289	328	368	409
IS21 ($\mu\epsilon$)	-11	40	87	126	165	203	240	276	313	351	388
IS22 ($\mu\epsilon$)	-19	-75	-104	-119	-116	-102	-77	-44	-4	42	93
IS23 ($\mu\epsilon$)	-11	-62	-93	-114	-122	-123	-115	-102	-83	-58	-28
IS24 ($\mu\epsilon$)	-8	63	127	180	233	282	330	376	422	467	512
IS25 ($\mu\epsilon$)	-7	-43	-57	-63	-54	-41	-19	7	40	77	119
IS26 ($\mu\epsilon$)	5	152	285	401	512	613	709	798	884	966	1044
IS27 ($\mu\epsilon$)	-9	-31	-30	-23	-1	25	60	99	144	192	244
IS28 ($\mu\epsilon$)	7	150	283	398	510	611	708	798	886	969	1049
IS29 ($\mu\epsilon$)	1	133	251	351	450	540	628	711	792	871	948
IS30 ($\mu\epsilon$)	-22	-31	-28	-17	1	30	64	105	151	201	256
IS31 ($\mu\epsilon$)	-8	73	147	214	283	349	414	478	541	603	665
IS32 ($\mu\epsilon$)	-8	66	131	188	244	296	346	393	439	483	525
IS33 ($\mu\epsilon$)	-6	73	143	204	262	318	370	420	470	516	561
IS34 ($\mu\epsilon$)	-16	-19	-19	-18	-5	15	42	73	111	153	199
IS35 ($\mu\epsilon$)	-17	-84	-130	-164	-182	-193	-196	-193	-184	-169	-150
IS36 ($\mu\epsilon$)	-7	71	140	200	259	314	366	415	462	508	552

Table F-11. Raw data, strain survey conducted after 30,000 cycles, ambient environmental conditions (Run 2) (continued)

Load Step	0	1	2	3	4	5	6	7	8	9	10
Pressure (psi)	0.01	0.67	1.33	2.01	2.66	3.34	4.00	4.67	5.34	6.01	6.67
IS37 ($\mu\epsilon$)	-14	-90	-138	-173	-189	-197	-196	-188	-172	-151	-125
IS38 ($\mu\epsilon$)	-3	90	174	248	321	389	454	515	574	631	685
IS39 ($\mu\epsilon$)	-14	-93	-136	-163	-171	-169	-157	-138	-112	-80	-43
IS40 ($\mu\epsilon$)	-1	96	187	267	346	420	490	557	622	684	744
IS41 ($\mu\epsilon$)	4	121	228	322	414	499	581	658	733	805	876
IS42 ($\mu\epsilon$)	-16	76	155	226	296	367	436	505	574	645	715
IS43 ($\mu\epsilon$)	-15	11	51	96	151	209	271	335	403	472	543
IS44 ($\mu\epsilon$)	-15	-39	-36	-19	11	49	92	141	194	250	309
IS45 ($\mu\epsilon$)	-7	71	144	210	274	336	394	451	508	563	618
IS46 ($\mu\epsilon$)	-6	71	143	207	268	326	380	433	484	534	582
IS47 ($\mu\epsilon$)	-5	72	142	205	266	323	378	431	483	533	582
IS48 ($\mu\epsilon$)	-14	-4	19	48	88	134	185	240	299	361	425
IS49 ($\mu\epsilon$)	-9	-36	-46	-48	-38	-25	-7	15	41	71	104
IS50 ($\mu\epsilon$)	-3	89	172	245	317	383	446	506	565	621	675
IS51 ($\mu\epsilon$)	-9	-23	-22	-14	5	25	50	78	110	144	182
IS52 ($\mu\epsilon$)	2	127	242	347	448	543	633	719	802	882	959
IS53 ($\mu\epsilon$)	-11	-20	-13	5	34	65	101	141	185	232	281
IS54 ($\mu\epsilon$)	0	117	226	324	419	508	592	673	752	828	902
IS55 ($\mu\epsilon$)	-7	106	207	295	380	460	537	610	683	753	823
IS56 ($\mu\epsilon$)	-14	60	114	164	214	268	322	379	437	497	559
IS57 ($\mu\epsilon$)	-18	-29	-29	-18	4	35	72	115	162	214	269

Table F-11. Raw data, strain survey conducted after 30,000 cycles, ambient environmental conditions (Run 2) (continued)

Load Step	0	1	2	3	4	5	6	7	8	9	10
Pressure (psi)	0.01	0.67	1.33	2.01	2.66	3.34	4.00	4.67	5.34	6.01	6.67
IS58 ($\mu\epsilon$)	-16	-57	-79	-86	-78	-61	-35	-1	38	83	132
IS59 ($\mu\epsilon$)	-9	35	72	103	135	168	203	239	276	316	357
IS60 ($\mu\epsilon$)	-7	51	99	138	176	213	249	285	322	359	396
IS61 ($\mu\epsilon$)	-8	53	104	145	186	225	263	301	340	379	418
IS62 ($\mu\epsilon$)	-12	-55	-73	-80	-73	-56	-31	2	42	86	135
IS63 ($\mu\epsilon$)	-10	-58	-91	-115	-127	-133	-131	-123	-110	-90	-67
IS64 ($\mu\epsilon$)	-4	64	121	168	214	257	299	340	380	420	459
IS65 ($\mu\epsilon$)	-8	-20	-20	-15	1	22	48	80	116	156	200
IS66 ($\mu\epsilon$)	9	157	287	402	509	608	700	787	868	947	1021
IS67 ($\mu\epsilon$)	-8	-5	9	28	57	91	129	172	219	269	321
IS68 ($\mu\epsilon$)	12	162	298	419	534	641	740	835	924	1009	1090
IS69 ($\mu\epsilon$)	9	149	272	379	479	572	660	745	826	905	980
IS70 ($\mu\epsilon$)	-28	44	96	144	195	248	303	360	418	479	540
IS71 ($\mu\epsilon$)	-26	-24	-5	25	68	117	171	229	290	353	418
IS72 ($\mu\epsilon$)	-19	-36	-27	-4	33	76	126	179	236	297	359
IS73 ($\mu\epsilon$)	-4	77	153	220	288	352	413	472	528	584	637
IS74 ($\mu\epsilon$)	-3	76	150	216	281	342	401	458	512	565	616
IS75 ($\mu\epsilon$)	-4	78	152	219	285	347	406	464	518	572	624
IS76 ($\mu\epsilon$)	-2	21	59	101	153	209	268	331	395	463	531
IS77 ($\mu\epsilon$)	-12	-43	-47	-42	-23	-1	25	55	88	125	164
IS78 ($\mu\epsilon$)	-2	85	167	239	310	378	442	503	562	620	675

Table F-11. Raw data, strain survey conducted after 30,000 cycles, ambient environmental conditions (Run 2) (continued)

Load Step	0	1	2	3	4	5	6	7	8	9	10
Pressure (psi)	0.01	0.67	1.33	2.01	2.66	3.34	4.00	4.67	5.34	6.01	6.67
IS79 ($\mu\epsilon$)	-12	-42	-45	-38	-18	4	31	61	93	130	168
IS80 ($\mu\epsilon$)	2	110	211	304	395	482	565	645	722	797	869
IS81 ($\mu\epsilon$)	-18	-59	-70	-68	-53	-34	-10	19	50	86	123
IS82 ($\mu\epsilon$)	0	97	189	274	358	439	515	590	661	732	801
IS83 ($\mu\epsilon$)	-4	95	183	260	336	408	477	544	609	674	738
IS84 ($\mu\epsilon$)	-11	55	119	177	237	299	361	423	487	551	616
IS85 ($\mu\epsilon$)	-19	-18	9	48	99	156	217	282	349	418	488
IS86 ($\mu\epsilon$)	-19	-46	-40	-19	16	59	107	160	218	278	339
IS87 ($\mu\epsilon$)	-7	49	98	143	186	228	269	309	350	389	429
IS88 ($\mu\epsilon$)	-6	47	93	133	171	207	241	274	306	338	368
IS89 ($\mu\epsilon$)	-5	46	91	130	165	201	234	267	300	331	362
IS90 ($\mu\epsilon$)	-12	-15	-2	24	60	105	156	211	270	330	392
IS91 ($\mu\epsilon$)	-13	-45	-61	-65	-58	-46	-28	-5	22	52	86
IS92 ($\mu\epsilon$)	-5	68	131	184	234	281	326	368	410	449	486
IS93 ($\mu\epsilon$)	-16	-20	-11	9	38	71	108	149	195	242	291
IS94 ($\mu\epsilon$)	0	136	257	366	470	568	660	749	834	916	994
IS95 ($\mu\epsilon$)	-16	-10	10	37	71	111	153	198	247	297	347
IS96 ($\mu\epsilon$)	-3	113	218	313	403	489	570	649	726	800	870
IS97 ($\mu\epsilon$)	-9	102	197	283	365	443	518	590	661	731	798
L01 ($\mu\epsilon$)	-	-	-	-	-	-	-	-	-	-	-
L02 ($\mu\epsilon$)	27	37	45	56	68	79	92	105	119	133	146

Table F-11. Raw data, strain survey conducted after 30,000 cycles, ambient environmental conditions (Run 2) (continued)

Load Step	0	1	2	3	4	5	6	7	8	9	10
Pressure (psi)	0.01	0.67	1.33	2.01	2.66	3.34	4.00	4.67	5.34	6.01	6.67
L03 ($\mu\epsilon$)	19	18	19	30	41	54	69	86	105	124	142
L04 ($\mu\epsilon$)	27	44	62	84	105	128	150	172	196	218	239
L05 ($\mu\epsilon$)	24	28	33	40	48	56	65	74	84	94	103
L06 ($\mu\epsilon$)	13	41	62	81	97	113	128	140	151	160	169
L07 ($\mu\epsilon$)	-	-	-	-	-	-	-	-	-	-	-
L08 ($\mu\epsilon$)	30	49	71	93	117	138	160	182	204	226	247
L09 ($\mu\epsilon$)	26	62	92	121	143	170	195	218	245	267	286
L10 ($\mu\epsilon$)	-	-	-	-	-	-	-	-	-	-	-
RAC-A1 ($\mu\epsilon$)	2	118	229	333	435	534	628	719	807	894	977
RAC-A2 ($\mu\epsilon$)	0	105	203	293	382	467	548	627	702	777	848
RAC-A3 ($\mu\epsilon$)	-1	92	177	253	327	397	464	529	591	652	711
RAC-F1 ($\mu\epsilon$)	6	116	222	319	415	508	596	682	765	845	923
RAC-F2 ($\mu\epsilon$)	4	106	203	290	377	459	538	615	689	760	830
RBC-A1 ($\mu\epsilon$)	-1	124	235	332	427	514	595	670	740	807	869
RBC-A2 ($\mu\epsilon$)	-2	105	199	279	358	429	496	558	616	671	723
RBC-A3 ($\mu\epsilon$)	-2	101	192	270	346	416	482	543	602	657	709
RBC-A4 ($\mu\epsilon$)	0	102	194	274	352	424	493	557	618	676	733
RBC-F1 ($\mu\epsilon$)	-1	123	230	325	416	498	574	645	711	773	832
RBC-F2 ($\mu\epsilon$)	-3	109	203	285	364	435	501	561	619	673	723
RBC-F3 ($\mu\epsilon$)	-4	107	200	280	357	427	492	552	609	662	713
S16 ($\mu\epsilon$)	-50	17	75	126	177	224	269	313	355	397	439

Table F-11. Raw data, strain survey conducted after 30,000 cycles, ambient environmental conditions (Run 2) (continued)

Load Step	0	1	2	3	4	5	6	7	8	9	10
Pressure (psi)	0.01	0.67	1.33	2.01	2.66	3.34	4.00	4.67	5.34	6.01	6.67
S17 ($\mu\epsilon$)	-	-	-	-	-	-	-	-	-	-	-
S18 ($\mu\epsilon$)	-17	153	294	410	514	612	703	791	874	956	1037
S20 ($\mu\epsilon$)	-85	-320	-541	-762	-938	-1087	-1224	-1347	-1453	-1531	-1597
S22 ($\mu\epsilon$)	10	155	278	383	476	565	647	726	802	878	952
S25 ($\mu\epsilon$)	3	174	330	471	601	729	850	966	1078	1187	1294
S29 ($\mu\epsilon$)	7	77	149	221	291	362	431	500	568	637	704
S30 ($\mu\epsilon$)	1	144	268	374	473	565	651	734	814	893	970
S32 ($\mu\epsilon$)	24	-89	-187	-274	-356	-428	-495	-554	-608	-657	-701
S34 ($\mu\epsilon$)	-2557	-1697	-1888	-2071	-1629	-1637	-1700	-1669	-1944	-2202	-1994
S37 ($\mu\epsilon$)	3	206	377	526	661	789	909	1025	1136	1244	1350
S41 ($\mu\epsilon$)	15	96	180	261	340	418	492	565	636	706	774
S42 ($\mu\epsilon$)	0	0	0	0	0	0	0	0	0	0	0
S43 ($\mu\epsilon$)	-1	109	202	280	351	417	478	538	597	654	710
S44 ($\mu\epsilon$)	1	162	302	422	532	625	715	800	883	963	1040
S46 ($\mu\epsilon$)	55	-226	-482	-710	-920	-1108	-1280	-1442	-1591	-1728	-1853
S48 ($\mu\epsilon$)	2	127	241	342	434	522	604	684	761	837	911
S51 ($\mu\epsilon$)	-13	158	312	448	575	699	816	931	1041	1149	1255
S55 ($\mu\epsilon$)	1	62	129	197	264	333	399	466	533	598	664
S56 ($\mu\epsilon$)	16	83	152	215	277	339	399	459	519	580	640
S57 ($\mu\epsilon$)	-	-	-	-	-	-	-	-	-	-	-
S58 ($\mu\epsilon$)	12	177	311	420	516	606	687	767	842	916	988

Table F-11. Raw data, strain survey conducted after 30,000 cycles, ambient environmental conditions (Run 2) (continued)

Load Step	0	1	2	3	4	5	6	7	8	9	10
Pressure (psi)	0.01	0.67	1.33	2.01	2.66	3.34	4.00	4.67	5.34	6.01	6.67
S60 ($\mu\epsilon$)	-70	-294	-531	-719	-883	-1020	-1102	-1254	-1339	-1420	-1482
S62 ($\mu\epsilon$)	7	151	266	363	448	529	604	677	747	816	884
S65 ($\mu\epsilon$)	-5	198	375	529	668	800	922	1039	1149	1256	1357
S69 ($\mu\epsilon$)	5	60	113	164	212	260	306	352	395	441	484
S70 ($\mu\epsilon$)	-11	67	144	215	286	355	423	492	560	628	697
S71 ($\mu\epsilon$)	-	-	-	-	-	-	-	-	-	-	-
S72 ($\mu\epsilon$)	5	178	311	421	517	607	691	772	849	926	1001
S74 ($\mu\epsilon$)	14	-163	-332	-488	-640	-783	-919	-1048	-1170	-1286	-1396
S76 ($\mu\epsilon$)	-7	134	250	350	440	528	611	691	769	846	921
S79 ($\mu\epsilon$)	-9	181	336	468	589	707	818	926	1030	1133	1232
S83 ($\mu\epsilon$)	18	104	185	264	333	401	466	532	596	659	723
S84 ($\mu\epsilon$)	10	85	161	237	312	388	463	538	612	688	763
S85 ($\mu\epsilon$)	-	-	-	-	-	-	-	-	-	-	-
S86 ($\mu\epsilon$)	-52	25	80	120	154	186	215	243	269	295	321
S88 ($\mu\epsilon$)	-1	-143	-255	-349	-429	-494	-548	-592	-628	-654	-673
S90 ($\mu\epsilon$)	14	157	277	377	468	554	633	710	784	857	930
S93 ($\mu\epsilon$)	19	199	356	492	619	741	856	968	1075	1180	1282
S97 ($\mu\epsilon$)	22	91	162	229	296	363	427	491	554	617	679
UAC-A1 ($\mu\epsilon$)	3	153	293	421	542	654	759	860	956	1048	1136
UAC-A2 ($\mu\epsilon$)	-1	135	259	369	475	573	664	752	836	916	992
UAC-A3 ($\mu\epsilon$)	-2	116	222	316	406	489	567	642	714	783	849

Table F-11. Raw data, strain survey conducted after 30,000 cycles, ambient environmental conditions (Run 2) (continued)

Load Step	0	1	2	3	4	5	6	7	8	9	10
Pressure (psi)	0.01	0.67	1.33	2.01	2.66	3.34	4.00	4.67	5.34	6.01	6.67
UAC-F1 ($\mu\epsilon$)	8	156	296	425	550	666	774	878	978	1073	1164
UAC-F2 ($\mu\epsilon$)	4	132	251	360	464	561	652	738	822	901	977
UBC-A1 ($\mu\epsilon$)	-	-	-	-	-	-	-	-	-	-	-
UBC-A2 ($\mu\epsilon$)	4	183	344	483	614	731	840	940	1034	1122	1204
UBC-A3 ($\mu\epsilon$)	4	161	301	421	535	637	732	820	903	981	1055
UBC-A4 ($\mu\epsilon$)	3	147	275	384	489	583	673	756	835	911	984
UBC-F1 ($\mu\epsilon$)	-	-	-	-	-	-	-	-	-	-	-
UBC-F2 ($\mu\epsilon$)	5	187	350	490	621	739	847	947	1040	1128	1210
UBC-F3 ($\mu\epsilon$)	3	166	309	433	549	653	749	838	921	1000	1074
UDAC-A1 ($\mu\epsilon$)	0	159	303	431	550	663	768	868	965	1055	1141
UDAC-A2 ($\mu\epsilon$)	-2	135	256	364	464	559	648	732	813	890	962
UDAC-A3 ($\mu\epsilon$)	-4	110	208	295	378	456	529	600	668	734	796
UDAC-F1 ($\mu\epsilon$)	5	159	300	428	549	662	767	867	963	1054	1141
UDAC-F2 ($\mu\epsilon$)	4	132	248	354	454	548	636	719	800	876	948
UDBC-A1 ($\mu\epsilon$)	-	-	-	-	-	-	-	-	-	-	-
UDBC-A2 ($\mu\epsilon$)	13	203	373	522	661	787	902	1008	1105	1197	1281
UDBC-A3 ($\mu\epsilon$)	13	180	328	456	576	684	783	874	959	1038	1112
UDBC-A4 ($\mu\epsilon$)	13	164	297	413	520	618	709	794	874	950	1021
UDBC-F1 ($\mu\epsilon$)	-	-	-	-	-	-	-	-	-	-	-
UDBC-F2 ($\mu\epsilon$)	13	216	399	556	704	837	959	1072	1175	1272	1362
UDBC-F3 ($\mu\epsilon$)	11	183	336	467	590	701	803	897	984	1065	1142

Table F-12. Raw data, strain survey conducted after 30,000 cycles, ambient environmental conditions (Run 3)

Load Step	0	1	2	3	4	5	6	7	8	9	10
Pressure (psi)	-0.05	0.66	1.34	2.00	2.68	3.35	4.00	4.66	5.34	6.01	6.70
Frame-1 (lbf)	4	108	256	335	455	544	673	773	921	1022	1126
Frame-2 (lbf)	58	55	224	339	457	566	678	792	909	1018	1132
Frame-3 (lbf)	2	111	225	342	455	566	677	793	905	1020	1132
Frame-4 (lbf)	36	36	225	343	464	566	682	796	905	1020	1137
Frame-5 (lbf)	2	114	226	344	452	572	678	795	904	1021	1131
Frame-6 (lbf)	0	108	239	330	461	567	686	802	909	1019	1130
Frame-7 (lbf)	8	114	228	343	457	567	678	796	910	1012	1133
Frame-8 (lbf)	5	109	220	350	440	563	683	793	905	1020	1127
Frame-9 (lbf)	34	31	227	340	444	566	678	793	908	1019	1132
Frame-10 (lbf)	1	109	232	344	459	570	689	794	907	1019	1134
Frame-11 (lbf)	3	118	228	339	459	568	677	791	902	1023	1138
Frame-12 (lbf)	1	109	224	336	457	557	678	794	908	1019	1134
Hoop-1 (lbf)	20	712	1427	2139	2855	3582	4284	5004	5706	6438	7156
Hoop-2 (lbf)	64	692	1387	2168	2840	3573	4279	5007	5714	6443	7121
Hoop-3 (lbf)	31	720	1425	2128	2851	3576	4289	4994	5705	6428	7136
Hoop-4 (lbf)	-16	706	1442	2143	2856	3575	4284	4998	5721	6433	7132
Hoop-5 (lbf)	35	707	1424	2134	2862	3562	4270	5008	5715	6436	7158
Hoop-6 (lbf)	34	723	1428	2145	2846	3576	4282	5006	5712	6419	7140
Hoop-7 (lbf)	61	722	1422	2141	2853	3566	4279	4996	5713	6422	7148
Hoop-8 (lbf)	146	715	1426	2152	2854	3572	4288	4999	5707	6435	7146
Hoop-9 (lbf)	2	736	1432	2101	2859	3572	4296	4998	5721	6427	7146

Table F-12. Raw data, strain survey conducted after 30,000 cycles, ambient environmental conditions (Run 3) (continued)

Load Step	0	1	2	3	4	5	6	7	8	9	10
Pressure (psi)	-0.05	0.66	1.34	2.00	2.68	3.35	4.00	4.66	5.34	6.01	6.70
Hoop-10 (lbf)	4	717	1418	2144	2843	3577	4272	5005	5713	6421	7141
Hoop-11 (lbf)	16	696	1429	2145	2845	3587	4296	4999	5734	6411	7138
Hoop-12 (lbf)	118	716	1423	2141	2871	3568	4274	5010	5708	6426	7147
Hoop-13 (lbf)	45	716	1452	2137	2865	3571	4274	4993	5721	6429	7131
Hoop-14 (lbf)	6	708	1432	2156	2851	3569	4286	5001	5705	6446	7141
Long-1 (lbf)	0	672	1348	1960	2632	3365	3982	4650	5337	6013	6698
Long-2 (lbf)	-3	666	1325	2005	2675	3336	4012	4677	5340	6006	6670
Long-3 (lbf)	-6	671	1342	2000	2668	3339	4006	4679	5343	6007	6676
Long-4 (lbf)	8	646	1321	2002	2666	3339	4004	4673	5342	6008	6685
Long-5 (lbf)	-5	675	1312	2002	2670	3333	4008	4673	5341	5996	6667
Long-6 (lbf)	-6	682	1343	1996	2657	3336	4012	4671	5341	6008	6671
Long-7 (lbf)	5	687	1330	2020	2656	3344	4009	4713	5342	6000	6670
Long-8 (lbf)	1	677	1309	1997	2670	3329	4001	4679	5348	6015	6681
F01 ($\mu\epsilon$)	24	7	65	106	126	170	203	242	273	311	345
F02 ($\mu\epsilon$)	-19	67	101	164	213	275	327	377	439	496	549
F03 ($\mu\epsilon$)	55	-101	34	62	87	119	149	181	205	232	264
F04 ($\mu\epsilon$)	-4	73	145	212	272	341	403	467	540	608	672
F05 ($\mu\epsilon$)	-	-	-	-	-	-	-	-	-	-	-
F06 ($\mu\epsilon$)	-13	105	128	191	246	305	361	415	482	541	600
F07 ($\mu\epsilon$)	25	-41	28	58	92	122	154	189	215	246	281
F08 ($\mu\epsilon$)	11	93	141	202	255	313	365	417	476	533	588

Table F-12. Raw data, strain survey conducted after 30,000 cycles, ambient environmental conditions (Run 3) (continued)

Load Step	0	1	2	3	4	5	6	7	8	9	10
Pressure (psi)	-0.05	0.66	1.34	2.00	2.68	3.35	4.00	4.66	5.34	6.01	6.70
IS16 ($\mu\epsilon$)	-13	72	155	221	284	349	414	479	547	616	686
IS17 ($\mu\epsilon$)	-14	-19	-7	15	48	88	135	186	242	301	365
IS18 ($\mu\epsilon$)	-10	-42	-57	-53	-36	-10	24	65	111	161	216
IS19 ($\mu\epsilon$)	-13	28	60	93	127	162	199	237	277	319	363
IS20 ($\mu\epsilon$)	-10	43	90	132	172	211	250	289	328	367	407
IS21 ($\mu\epsilon$)	-10	39	85	126	164	202	239	276	313	349	387
IS22 ($\mu\epsilon$)	-12	-76	-108	-121	-118	-103	-78	-45	-5	40	92
IS23 ($\mu\epsilon$)	-9	-53	-95	-116	-124	-125	-117	-103	-84	-59	-29
IS24 ($\mu\epsilon$)	-9	65	125	180	232	281	329	375	421	465	510
IS25 ($\mu\epsilon$)	-6	-35	-60	-64	-57	-43	-21	6	39	75	117
IS26 ($\mu\epsilon$)	-1	162	284	402	511	613	708	797	883	964	1043
IS27 ($\mu\epsilon$)	-6	-25	-34	-24	-4	24	59	98	142	190	242
IS28 ($\mu\epsilon$)	1	162	282	399	508	611	707	797	885	968	1048
IS29 ($\mu\epsilon$)	-3	141	248	351	448	539	626	709	791	869	947
IS30 ($\mu\epsilon$)	-16	-41	-30	-19	0	28	63	103	149	199	254
IS31 ($\mu\epsilon$)	-8	81	145	214	282	348	413	476	540	602	664
IS32 ($\mu\epsilon$)	-9	72	129	188	243	295	345	392	438	482	524
IS33 ($\mu\epsilon$)	-8	80	140	203	261	318	370	420	468	515	559
IS34 ($\mu\epsilon$)	-14	-22	-22	-20	-7	13	41	72	110	151	197
IS35 ($\mu\epsilon$)	-13	-75	-132	-165	-185	-195	-198	-194	-185	-171	-151
IS36 ($\mu\epsilon$)	-8	77	138	200	258	313	365	414	461	507	551

Table F-12. Raw data, strain survey conducted after 30,000 cycles, ambient environmental conditions (Run 3) (continued)

Load Step	0	1	2	3	4	5	6	7	8	9	10
Pressure (psi)	-0.05	0.66	1.34	2.00	2.68	3.35	4.00	4.66	5.34	6.01	6.70
IS37 ($\mu\epsilon$)	-9	-85	-141	-174	-192	-199	-197	-189	-174	-153	-127
IS38 ($\mu\epsilon$)	-6	98	172	248	320	388	453	513	573	629	684
IS39 ($\mu\epsilon$)	-7	-92	-139	-165	-174	-171	-159	-139	-113	-81	-45
IS40 ($\mu\epsilon$)	-4	105	184	267	344	419	489	556	621	683	743
IS41 ($\mu\epsilon$)	-1	130	226	322	412	498	579	656	732	804	875
IS42 ($\mu\epsilon$)	-20	65	154	225	294	365	435	504	573	643	714
IS43 ($\mu\epsilon$)	-15	11	48	95	149	208	271	335	402	471	542
IS44 ($\mu\epsilon$)	-14	-35	-38	-21	10	47	92	140	193	249	308
IS45 ($\mu\epsilon$)	-10	80	142	209	274	335	394	451	507	562	617
IS46 ($\mu\epsilon$)	-9	77	142	206	268	325	380	433	484	533	582
IS47 ($\mu\epsilon$)	-8	78	141	204	265	323	378	430	482	532	582
IS48 ($\mu\epsilon$)	-11	3	16	47	88	133	185	239	298	360	425
IS49 ($\mu\epsilon$)	-9	-18	-47	-49	-39	-26	-7	15	41	71	104
IS50 ($\mu\epsilon$)	-7	97	170	245	316	383	446	506	564	620	675
IS51 ($\mu\epsilon$)	-11	-1	-23	-15	4	24	50	78	109	144	181
IS52 ($\mu\epsilon$)	-4	141	241	347	448	543	633	718	802	882	960
IS53 ($\mu\epsilon$)	-13	1	-14	4	32	64	102	141	185	231	280
IS54 ($\mu\epsilon$)	-7	132	225	324	419	507	592	673	752	827	901
IS55 ($\mu\epsilon$)	-11	121	204	294	380	460	537	610	682	752	822
IS56 ($\mu\epsilon$)	-17	58	114	165	215	267	322	377	437	496	558
IS57 ($\mu\epsilon$)	-16	-30	-30	-19	3	34	71	114	162	213	268

Table F-12. Raw data, strain survey conducted after 30,000 cycles, ambient environmental conditions (Run 3) (continued)

Load Step	0	1	2	3	4	5	6	7	8	9	10
Pressure (psi)	-0.05	0.66	1.34	2.00	2.68	3.35	4.00	4.66	5.34	6.01	6.70
IS58 ($\mu\epsilon$)	-11	-58	-80	-86	-79	-62	-35	-2	38	82	131
IS59 ($\mu\epsilon$)	-9	33	71	103	135	168	202	238	276	315	356
IS60 ($\mu\epsilon$)	-8	48	98	138	175	212	249	285	321	358	395
IS61 ($\mu\epsilon$)	-8	49	102	145	185	224	263	301	339	378	417
IS62 ($\mu\epsilon$)	-6	-60	-76	-82	-75	-57	-31	1	41	85	133
IS63 ($\mu\epsilon$)	-5	-58	-93	-116	-129	-134	-132	-124	-110	-92	-68
IS64 ($\mu\epsilon$)	-6	61	120	168	213	257	298	339	379	419	458
IS65 ($\mu\epsilon$)	-4	-22	-22	-16	-1	20	47	79	115	155	198
IS66 ($\mu\epsilon$)	3	157	287	402	508	607	700	785	868	945	1020
IS67 ($\mu\epsilon$)	-3	-8	8	27	56	89	129	171	218	267	320
IS68 ($\mu\epsilon$)	6	164	299	421	534	641	740	834	924	1008	1090
IS69 ($\mu\epsilon$)	5	152	273	380	479	573	661	744	826	904	980
IS70 ($\mu\epsilon$)	-26	39	95	144	194	247	303	359	418	477	538
IS71 ($\mu\epsilon$)	-22	-28	-7	25	67	116	171	228	289	351	416
IS72 ($\mu\epsilon$)	-15	-39	-29	-4	32	75	125	178	236	296	358
IS73 ($\mu\epsilon$)	-6	75	151	221	287	351	412	471	528	583	636
IS74 ($\mu\epsilon$)	-6	74	148	216	280	341	400	457	511	564	615
IS75 ($\mu\epsilon$)	-7	75	151	219	283	346	405	462	518	571	623
IS76 ($\mu\epsilon$)	-3	18	56	101	151	207	267	329	395	461	530
IS77 ($\mu\epsilon$)	-10	-43	-49	-42	-25	-3	24	54	87	124	163
IS78 ($\mu\epsilon$)	-6	84	165	239	309	376	441	502	562	619	674

Table F-12. Raw data, strain survey conducted after 30,000 cycles, ambient environmental conditions (Run 3) (continued)

Load Step	0	1	2	3	4	5	6	7	8	9	10
Pressure (psi)	-0.05	0.66	1.34	2.00	2.68	3.35	4.00	4.66	5.34	6.01	6.70
IS79 ($\mu\epsilon$)	-11	-43	-47	-39	-21	2	30	60	93	128	167
IS80 ($\mu\epsilon$)	-4	109	210	304	394	481	565	644	722	796	868
IS81 ($\mu\epsilon$)	-15	-62	-72	-69	-56	-36	-10	18	50	84	122
IS82 ($\mu\epsilon$)	-5	95	188	274	357	437	514	589	661	731	800
IS83 ($\mu\epsilon$)	-8	92	181	260	334	406	476	543	609	673	736
IS84 ($\mu\epsilon$)	-9	49	117	176	237	299	361	423	487	551	616
IS85 ($\mu\epsilon$)	-15	-15	6	47	99	156	218	282	349	418	488
IS86 ($\mu\epsilon$)	-15	-37	-42	-20	16	59	108	161	218	277	339
IS87 ($\mu\epsilon$)	-9	57	97	142	187	229	270	309	349	389	428
IS88 ($\mu\epsilon$)	-7	51	91	132	171	207	241	274	306	337	368
IS89 ($\mu\epsilon$)	-6	50	89	129	166	202	236	268	300	331	361
IS90 ($\mu\epsilon$)	-11	-7	-5	23	61	106	157	211	269	330	392
IS91 ($\mu\epsilon$)	-13	-27	-62	-66	-57	-45	-27	-5	22	52	86
IS92 ($\mu\epsilon$)	-8	75	129	183	234	282	326	368	409	448	486
IS93 ($\mu\epsilon$)	-17	3	-12	8	38	71	109	150	194	241	290
IS94 ($\mu\epsilon$)	-6	153	256	367	471	569	662	749	835	916	995
IS95 ($\mu\epsilon$)	-16	13	7	36	72	112	155	199	247	296	346
IS96 ($\mu\epsilon$)	-9	131	216	312	404	490	572	649	726	799	870
IS97 ($\mu\epsilon$)	-14	121	196	282	365	444	519	590	661	730	798
L01 ($\mu\epsilon$)	-	-	-	-	-	-	-	-	-	-	-
L02 ($\mu\epsilon$)	24	44	49	57	69	80	92	106	120	134	148

Table F-12. Raw data, strain survey conducted after 30,000 cycles, ambient environmental conditions (Run 3) (continued)

Load Step	0	1	2	3	4	5	6	7	8	9	10
Pressure (psi)	-0.05	0.66	1.34	2.00	2.68	3.35	4.00	4.66	5.34	6.01	6.70
L03 ($\mu\epsilon$)	15	28	23	31	42	56	71	87	106	125	144
L04 ($\mu\epsilon$)	22	56	64	86	107	130	151	173	197	220	241
L05 ($\mu\epsilon$)	22	34	33	41	49	58	67	76	86	97	105
L06 ($\mu\epsilon$)	10	42	56	77	95	112	126	139	149	159	166
L07 ($\mu\epsilon$)	-	-	-	-	-	-	-	-	-	-	-
L08 ($\mu\epsilon$)	25	57	75	95	118	140	161	183	206	229	250
L09 ($\mu\epsilon$)	23	81	90	121	145	175	199	223	247	271	289
L10 ($\mu\epsilon$)	-	-	-	-	-	-	-	-	-	-	-
RAC-A1 ($\mu\epsilon$)	-4	118	229	333	434	533	627	718	807	893	977
RAC-A2 ($\mu\epsilon$)	-5	104	202	293	381	466	547	625	702	776	848
RAC-A3 ($\mu\epsilon$)	-6	90	175	252	325	396	463	528	590	651	710
RAC-F1 ($\mu\epsilon$)	2	117	221	320	415	508	596	681	765	845	923
RAC-F2 ($\mu\epsilon$)	0	106	201	290	376	459	538	613	688	760	829
RBC-A1 ($\mu\epsilon$)	-6	138	233	332	426	513	593	668	739	806	868
RBC-A2 ($\mu\epsilon$)	-5	116	196	279	356	428	495	556	615	670	722
RBC-A3 ($\mu\epsilon$)	-5	111	190	270	345	415	481	542	601	656	708
RBC-A4 ($\mu\epsilon$)	-4	111	192	274	351	423	491	555	617	675	731
RBC-F1 ($\mu\epsilon$)	-7	141	229	325	414	497	573	643	710	772	831
RBC-F2 ($\mu\epsilon$)	-8	126	202	286	363	434	500	560	618	672	723
RBC-F3 ($\mu\epsilon$)	-9	125	198	280	356	426	491	550	608	661	712
S16 ($\mu\epsilon$)	-39	23	70	123	171	219	264	308	350	392	435

Table F-12. Raw data, strain survey conducted after 30,000 cycles, ambient environmental conditions (Run 3) (continued)

Load Step	0	1	2	3	4	5	6	7	8	9	10
Pressure (psi)	-0.05	0.66	1.34	2.00	2.68	3.35	4.00	4.66	5.34	6.01	6.70
S17 ($\mu\epsilon$)	-	-	-	-	-	-	-	-	-	-	-
S18 ($\mu\epsilon$)	-14	148	291	410	513	610	702	789	873	955	1037
S20 ($\mu\epsilon$)	-12	-308	-506	-709	-881	-1036	-1166	-1283	-1391	-1478	-1563
S22 ($\mu\epsilon$)	8	149	278	384	478	566	649	728	804	879	954
S25 ($\mu\epsilon$)	-1	172	330	472	603	730	850	966	1079	1188	1295
S29 ($\mu\epsilon$)	2	76	149	221	291	361	430	499	568	635	703
S30 ($\mu\epsilon$)	-2	143	265	374	473	565	652	734	815	893	970
S32 ($\mu\epsilon$)	13	-133	-209	-298	-380	-454	-520	-581	-639	-690	-741
S34 ($\mu\epsilon$)	-2751	-1821	-2595	-1842	-1552	-1902	-563	-301	-2150	-1913	69
S37 ($\mu\epsilon$)	-1	200	376	527	662	790	910	1025	1136	1244	1350
S41 ($\mu\epsilon$)	10	99	181	262	341	418	492	564	636	705	773
S42 ($\mu\epsilon$)	0	0	0	0	0	0	0	0	0	0	0
S43 ($\mu\epsilon$)	2	113	201	281	352	418	480	539	598	655	712
S44 ($\mu\epsilon$)	10	174	314	434	547	641	729	814	896	975	1052
S46 ($\mu\epsilon$)	84	-251	-476	-703	-912	-1102	-1274	-1433	-1584	-1720	-1847
S48 ($\mu\epsilon$)	-2	121	240	343	435	523	605	684	761	837	911
S51 ($\mu\epsilon$)	-15	144	309	447	574	698	815	928	1040	1147	1253
S55 ($\mu\epsilon$)	-2	58	129	197	264	332	399	465	532	597	663
S56 ($\mu\epsilon$)	16	81	151	216	278	339	400	460	520	580	642
S57 ($\mu\epsilon$)	-	-	-	-	-	-	-	-	-	-	-
S58 ($\mu\epsilon$)	5	172	310	421	517	606	689	767	843	916	989

Table F-12. Raw data, strain survey conducted after 30,000 cycles, ambient environmental conditions (Run 3) (continued)

Load Step	0	1	2	3	4	5	6	7	8	9	10
Pressure (psi)	-0.05	0.66	1.34	2.00	2.68	3.35	4.00	4.66	5.34	6.01	6.70
S60 ($\mu\epsilon$)	-84	-362	-537	-753	-890	-1047	-1155	-1283	-1392	-1474	-1546
S62 ($\mu\epsilon$)	3	149	268	364	450	530	606	679	748	817	886
S65 ($\mu\epsilon$)	-20	197	372	528	667	797	919	1034	1145	1252	1355
S69 ($\mu\epsilon$)	10	62	113	163	211	259	305	351	395	439	484
S70 ($\mu\epsilon$)	-14	56	135	208	278	348	416	484	553	621	690
S71 ($\mu\epsilon$)	-	-	-	-	-	-	-	-	-	-	-
S72 ($\mu\epsilon$)	0	172	311	421	517	607	691	770	849	925	1001
S74 ($\mu\epsilon$)	25	-169	-331	-488	-638	-782	-917	-1043	-1169	-1285	-1396
S76 ($\mu\epsilon$)	-7	130	249	350	442	529	611	691	769	846	922
S79 ($\mu\epsilon$)	-14	176	334	468	589	706	817	923	1029	1131	1230
S83 ($\mu\epsilon$)	15	101	176	252	324	395	461	525	590	653	716
S84 ($\mu\epsilon$)	9	94	161	239	314	390	465	540	614	690	766
S85 ($\mu\epsilon$)	-	-	-	-	-	-	-	-	-	-	-
S86 ($\mu\epsilon$)	-39	28	84	125	159	191	219	247	273	299	325
S88 ($\mu\epsilon$)	13	-164	-257	-349	-428	-493	-546	-590	-626	-652	-670
S90 ($\mu\epsilon$)	15	151	277	379	469	555	635	712	786	860	933
S93 ($\mu\epsilon$)	17	185	355	494	620	742	858	969	1077	1182	1285
S97 ($\mu\epsilon$)	22	92	163	231	298	364	429	493	556	619	682
UAC-A1 ($\mu\epsilon$)	-5	170	293	420	542	654	760	859	956	1048	1136
UAC-A2 ($\mu\epsilon$)	-7	151	258	369	475	572	665	751	835	915	992
UAC-A3 ($\mu\epsilon$)	-8	131	221	316	405	489	567	641	713	782	849

Table F-12. Raw data, strain survey conducted after 30,000 cycles, ambient environmental conditions (Run 3) (continued)

Load Step	0	1	2	3	4	5	6	7	8	9	10
Pressure (psi)	-0.05	0.66	1.34	2.00	2.68	3.35	4.00	4.66	5.34	6.01	6.70
UAC-F1 ($\mu\epsilon$)	0	168	296	425	550	666	775	878	978	1072	1164
UAC-F2 ($\mu\epsilon$)	-3	142	250	359	464	561	652	738	821	900	977
UBC-A1 ($\mu\epsilon$)	-	-	-	-	-	-	-	-	-	-	-
UBC-A2 ($\mu\epsilon$)	-4	197	342	483	612	730	839	938	1033	1121	1203
UBC-A3 ($\mu\epsilon$)	-3	173	299	421	533	636	730	818	902	980	1054
UBC-A4 ($\mu\epsilon$)	-3	158	273	384	487	582	671	754	834	910	983
UBC-F1 ($\mu\epsilon$)	-	-	-	-	-	-	-	-	-	-	-
UBC-F2 ($\mu\epsilon$)	-4	209	348	490	620	739	847	946	1040	1127	1209
UBC-F3 ($\mu\epsilon$)	-5	187	308	433	547	652	748	836	921	999	1073
UDAC-A1 ($\mu\epsilon$)	-8	180	301	431	552	665	770	868	965	1055	1141
UDAC-A2 ($\mu\epsilon$)	-9	154	255	364	466	561	649	732	813	890	962
UDAC-A3 ($\mu\epsilon$)	-9	126	206	295	378	457	530	600	668	733	796
UDAC-F1 ($\mu\epsilon$)	-4	175	300	429	551	663	769	867	964	1055	1142
UDAC-F2 ($\mu\epsilon$)	-3	145	247	354	455	549	637	719	800	876	949
UDBC-A1 ($\mu\epsilon$)	-	-	-	-	-	-	-	-	-	-	-
UDBC-A2 ($\mu\epsilon$)	6	206	374	524	661	787	901	1006	1106	1196	1281
UDBC-A3 ($\mu\epsilon$)	7	183	329	457	576	684	782	873	959	1037	1112
UDBC-A4 ($\mu\epsilon$)	7	167	298	414	520	619	709	793	874	949	1020
UDBC-F1 ($\mu\epsilon$)	-	-	-	-	-	-	-	-	-	-	-
UDBC-F2 ($\mu\epsilon$)	5	219	398	557	703	837	959	1070	1176	1271	1362
UDBC-F3 ($\mu\epsilon$)	4	185	335	468	589	700	802	895	984	1064	1141

F.2.1.4 After 60,000 Cycles

Table F-13. Raw data, strain survey conducted after 60,000 cycles, ambient environmental conditions (Run 1)

Load Step	0	1	2	3	4	5	6	7	8	9	10
Pressure (psi)	0.00	0.66	1.24	1.95	2.65	3.29	3.99	4.67	5.35	5.96	6.61
Frame-1 (lbf)	8	107	212	286	415	550	640	802	875	1017	1073
Frame-2 (lbf)	51	128	244	338	432	574	692	796	882	1014	1135
Frame-3 (lbf)	0	114	218	325	458	570	668	793	907	1019	1133
Frame-4 (lbf)	38	115	223	323	439	568	675	796	895	1019	1133
Frame-5 (lbf)	5	118	235	331	439	560	687	788	918	1020	1125
Frame-6 (lbf)	-1	97	217	352	477	543	692	805	910	1015	1124
Frame-7 (lbf)	3	112	217	341	469	560	677	791	899	1020	1133
Frame-8 (lbf)	-1	119	224	341	466	566	689	790	922	1018	1134
Frame-9 (lbf)	36	115	232	339	439	566	679	793	899	1019	1136
Frame-10 (lbf)	0	121	234	332	455	558	669	785	885	1013	1132
Frame-11 (lbf)	-10	113	218	331	447	571	681	790	905	1027	1130
Frame-12 (lbf)	21	114	231	351	451	571	685	802	914	1031	1146
Hoop-1 (lbf)	5	697	1435	2150	2881	3567	4279	5010	5735	6410	7160
Hoop-2 (lbf)	36	788	1383	2145	2868	3559	4269	5004	5712	6428	7159
Hoop-3 (lbf)	-2	721	1419	2151	2878	3564	4278	4999	5723	6410	7153
Hoop-4 (lbf)	7	721	1431	2126	2858	3562	4294	5004	5719	6426	7142
Hoop-5 (lbf)	-9	716	1431	2139	2889	3563	4285	4997	5726	6415	7140
Hoop-6 (lbf)	-15	720	1425	2132	2874	3561	4290	5011	5725	6425	7143
Hoop-7 (lbf)	-4	705	1438	2136	2839	3568	4283	5002	5707	6412	7134
Hoop-8 (lbf)	129	721	1438	2144	2867	3566	4290	5005	5726	6430	7141

F-100

Table F-13. Raw data, strain survey conducted after 60,000 cycles, ambient environmental conditions (Run 1) (continued)

Load Step	0	1	2	3	4	5	6	7	8	9	10
Pressure (psi)	0.00	0.66	1.24	1.95	2.65	3.29	3.99	4.67	5.35	5.96	6.61
Hoop-9 (lbf)	5	742	1441	2160	2828	3550	4287	4999	5721	6407	7144
Hoop-10 (lbf)	-8	703	1359	2124	2855	3564	4289	5028	5742	6411	7150
Hoop-11 (lbf)	8	702	1431	2127	2867	3578	4306	5013	5702	6407	7135
Hoop-12 (lbf)	83	719	1425	2152	2899	3569	4292	5011	5715	6422	7146
Hoop-13 (lbf)	76	731	1445	2092	2856	3554	4300	4997	5738	6423	7151
Hoop-14 (lbf)	6	712	1417	2142	2865	3569	4284	4996	5715	6428	7156
Long-1 (lbf)	22	654	1288	2057	2728	3318	4027	4723	5346	6008	6709
Long-2 (lbf)	-10	677	1328	1988	2667	3335	4008	4657	5335	6009	6673
Long-3 (lbf)	-13	675	1340	2000	2659	3344	4009	4665	5332	6011	6675
Long-4 (lbf)	-21	669	1348	2000	2646	3345	4003	4676	5319	6017	6676
Long-5 (lbf)	0	655	1335	2012	2670	3338	4010	4657	5336	6028	6687
Long-6 (lbf)	1	683	1339	1980	2664	3352	4030	4683	5323	6013	6670
Long-7 (lbf)	-41	656	1332	1983	2670	3346	4020	4695	5335	5991	6677
Long-8 (lbf)	3	652	1340	2003	2670	3340	4004	4671	5335	6017	6669
F01 ($\mu\epsilon$)	-	-	-	-	-	-	-	-	-	-	-
F02 ($\mu\epsilon$)	-	-	-	-	-	-	-	-	-	-	-
F03 ($\mu\epsilon$)	-	-	-	-	-	-	-	-	-	-	-
F04 ($\mu\epsilon$)	-	-	-	-	-	-	-	-	-	-	-
F05 ($\mu\epsilon$)	-	-	-	-	-	-	-	-	-	-	-
F06 ($\mu\epsilon$)	-	-	-	-	-	-	-	-	-	-	-
F07 ($\mu\epsilon$)	-	-	-	-	-	-	-	-	-	-	-

F-101

Table F-13. Raw data, strain survey conducted after 60,000 cycles, ambient environmental conditions (Run 1) (continued)

Load Step	0	1	2	3	4	5	6	7	8	9	10
Pressure (psi)	0.00	0.66	1.24	1.95	2.65	3.29	3.99	4.67	5.35	5.96	6.61
F08 ($\mu\epsilon$)	-	-	-	-	-	-	-	-	-	-	-
IS18 ($\mu\epsilon$)	-14	-77	-104	-116	-109	-90	-57	-20	26	74	131
IS20 ($\mu\epsilon$)	9	47	81	109	143	173	208	240	276	309	348
IS22 ($\mu\epsilon$)	-6	-74	-106	-127	-128	-115	-87	-53	-9	36	92
IS25 ($\mu\epsilon$)	-25	-109	-146	-167	-174	-168	-150	-127	-95	-61	-18
IS26 ($\mu\epsilon$)	5	119	214	313	410	489	571	644	715	779	844
IS27 ($\mu\epsilon$)	-8	-78	-97	-98	-86	-61	-25	14	61	110	165
IS28 ($\mu\epsilon$)	8	139	255	380	503	603	707	800	890	970	1052
IS29 ($\mu\epsilon$)	3	112	209	312	414	500	592	675	758	833	912
IS30 ($\mu\epsilon$)	-25	-36	-33	-34	-18	7	46	86	135	184	243
IS32 ($\mu\epsilon$)	0	76	135	195	256	305	358	404	452	493	538
IS34 ($\mu\epsilon$)	-19	-28	-31	-31	-19	2	34	68	111	155	207
IS37 ($\mu\epsilon$)	-40	-138	-199	-246	-277	-289	-289	-284	-266	-245	-215
IS38 ($\mu\epsilon$)	-152	-57	69	170	289	314	478	466	635	611	701
IS39 ($\mu\epsilon$)	-50	-146	-199	-236	-256	-256	-242	-224	-194	-162	-121
IS40 ($\mu\epsilon$)	-2	101	183	273	362	434	512	581	649	709	772
IS41 ($\mu\epsilon$)	2	112	202	297	391	469	552	627	701	767	837
IS44 ($\mu\epsilon$)	-15	-64	-81	-77	-57	-31	7	49	97	146	202
IS46 ($\mu\epsilon$)	-3	63	118	179	241	291	346	396	446	491	539
IS48 ($\mu\epsilon$)	-11	-18	-8	12	47	83	133	184	239	295	358
IS51 ($\mu\epsilon$)	-24	-58	-71	-61	-43	-27	-1	28	60	95	135

Table F-13. Raw data, strain survey conducted after 60,000 cycles, ambient environmental conditions (Run 1) (continued)

Load Step	0	1	2	3	4	5	6	7	8	9	10
Pressure (psi)	0.00	0.66	1.24	1.95	2.65	3.29	3.99	4.67	5.35	5.96	6.61
IS52 ($\mu\epsilon$)	250	366	462	572	685	773	868	957	1042	1120	1200
IS55 ($\mu\epsilon$)	-9	94	179	269	362	434	515	589	662	729	801
IS58 ($\mu\epsilon$)	-29	-101	-135	-153	-151	-137	-108	-74	-31	14	68
IS60 ($\mu\epsilon$)	7	51	85	114	148	174	207	236	269	298	332
IS62 ($\mu\epsilon$)	-9	-66	-91	-105	-102	-88	-59	-25	17	62	115
IS65 ($\mu\epsilon$)	-18	-73	-91	-99	-96	-82	-58	-29	7	45	91
IS66 ($\mu\epsilon$)	10	120	209	301	391	462	537	605	671	728	788
IS67 ($\mu\epsilon$)	-14	-41	-36	-20	8	40	84	130	182	234	292
IS68 ($\mu\epsilon$)	8	160	290	428	563	669	779	878	973	1057	1142
IS69 ($\mu\epsilon$)	-1	129	234	347	458	544	638	723	807	883	962
IS72 ($\mu\epsilon$)	-11	-41	-39	-19	16	55	107	159	219	276	340
IS74 ($\mu\epsilon$)	2	77	140	210	280	339	402	458	516	566	619
IS76 ($\mu\epsilon$)	-1	17	47	87	138	187	249	310	377	440	511
IS79 ($\mu\epsilon$)	-43	-79	-81	-65	-44	-21	11	42	81	118	161
IS80 ($\mu\epsilon$)	-1	104	196	299	403	488	579	664	746	820	896
IS83 ($\mu\epsilon$)	-1	97	177	263	350	418	494	563	633	696	764
IS86 ($\mu\epsilon$)	-14	-44	-50	-32	3	40	91	142	200	256	320
IS88 ($\mu\epsilon$)	-3	50	88	129	169	201	237	269	302	330	362
IS90 ($\mu\epsilon$)	-15	-21	-17	4	41	79	131	182	241	297	361
IS93 ($\mu\epsilon$)	-28	-23	-19	8	43	72	114	155	203	250	303
IS94 ($\mu\epsilon$)	-5	132	236	354	473	564	662	753	840	918	1000

Table F-13. Raw data, strain survey conducted after 60,000 cycles, ambient environmental conditions (Run 1) (continued)

Load Step	0	1	2	3	4	5	6	7	8	9	10
Pressure (psi)	0.00	0.66	1.24	1.95	2.65	3.29	3.99	4.67	5.35	5.96	6.61
IS95 ($\mu\epsilon$)	-26	-11	1	33	74	108	155	199	251	298	354
IS96 ($\mu\epsilon$)	-10	109	198	299	402	481	568	648	726	797	871
IS97 ($\mu\epsilon$)	-11	102	184	273	364	435	515	586	659	725	796
IS104 ($\mu\epsilon$)	-11	-82	-121	-138	-143	-135	-118	-95	-66	-33	7
IS105 ($\mu\epsilon$)	3	65	109	152	193	228	265	298	331	361	397
IS106 ($\mu\epsilon$)	-18	-134	-202	-255	-289	-303	-306	-302	-288	-270	-243
IS107 ($\mu\epsilon$)	-15	-24	-39	-37	-30	-16	8	37	73	112	158
IS108 ($\mu\epsilon$)	6	217	370	530	679	798	919	1028	1131	1224	1317
IS109 ($\mu\epsilon$)	-	-	-	-	-	-	-	-	-	-	-
IS110 ($\mu\epsilon$)	-17	-74	-102	-116	-115	-99	-71	-39	4	47	101
IS111 ($\mu\epsilon$)	8	74	129	182	238	285	338	385	435	481	531
IS112 ($\mu\epsilon$)	-15	-107	-156	-190	-205	-201	-184	-161	-127	-90	-44
IS113 ($\mu\epsilon$)	-1	-17	-23	-25	-24	-10	11	33	65	99	140
IS114 ($\mu\epsilon$)	19	211	365	520	667	786	908	1015	1120	1212	1305
IS115 ($\mu\epsilon$)	-	-	-	-	-	-	-	-	-	-	-
L01 ($\mu\epsilon$)	-	-	-	-	-	-	-	-	-	-	-
L02 ($\mu\epsilon$)	-	-	-	-	-	-	-	-	-	-	-
L03 ($\mu\epsilon$)	-	-	-	-	-	-	-	-	-	-	-
L04 ($\mu\epsilon$)	-	-	-	-	-	-	-	-	-	-	-
L05 ($\mu\epsilon$)	-	-	-	-	-	-	-	-	-	-	-
L06 ($\mu\epsilon$)	-	-	-	-	-	-	-	-	-	-	-

Table F-13. Raw data, strain survey conducted after 60,000 cycles, ambient environmental conditions (Run 1) (continued)

Load Step	0	1	2	3	4	5	6	7	8	9	10
Pressure (psi)	0.00	0.66	1.24	1.95	2.65	3.29	3.99	4.67	5.35	5.96	6.61
L07 ($\mu\epsilon$)	-	-	-	-	-	-	-	-	-	-	-
L08 ($\mu\epsilon$)	-	-	-	-	-	-	-	-	-	-	-
L09 ($\mu\epsilon$)	-	-	-	-	-	-	-	-	-	-	-
L10 ($\mu\epsilon$)	-	-	-	-	-	-	-	-	-	-	-
RAC-A1 ($\mu\epsilon$)	-2	111	211	323	439	534	636	733	826	910	998
RAC-F1 ($\mu\epsilon$)	11	116	207	312	418	507	603	691	779	857	938
RBC-A1 ($\mu\epsilon$)	8	158	271	394	514	609	709	795	878	950	1022
RBC-A2 ($\mu\epsilon$)	-1	119	210	306	399	471	548	613	676	731	786
RBC-A3 ($\mu\epsilon$)	-4	110	196	287	375	445	519	582	645	698	754
RBC-F1 ($\mu\epsilon$)	-6	143	254	372	487	574	665	744	819	884	950
RBC-F2 ($\mu\epsilon$)	-7	119	211	308	402	472	547	611	672	726	779
RBC-F3 ($\mu\epsilon$)	-7	117	205	300	391	459	531	594	654	706	760
S18 ($\mu\epsilon$)	34	195	310	407	503	579	660	733	806	871	943
S20 ($\mu\epsilon$)	11	-173	-309	-450	-581	-673	-757	-827	-883	-925	-958
S22 ($\mu\epsilon$)	-5	148	263	363	462	537	617	689	759	821	891
S25 ($\mu\epsilon$)	25	218	366	510	659	780	906	1025	1138	1240	1348
S29 ($\mu\epsilon$)	-4	60	117	181	251	313	382	448	514	576	642
S30 ($\mu\epsilon$)	48	205	329	450	567	660	757	845	931	1008	1091
S32 ($\mu\epsilon$)	10	-123	-220	-330	-435	-510	-585	-650	-707	-756	-799
S34 ($\mu\epsilon$)	5	99	178	258	342	406	481	547	614	674	740
S37 ($\mu\epsilon$)	55	278	450	613	774	902	1037	1159	1276	1381	1491

Table F-13. Raw data, strain survey conducted after 60,000 cycles, ambient environmental conditions (Run 1) (continued)

Load Step	0	1	2	3	4	5	6	7	8	9	10
Pressure (psi)	0.00	0.66	1.24	1.95	2.65	3.29	3.99	4.67	5.35	5.96	6.61
S41 ($\mu\epsilon$)	-2	69	135	211	292	360	435	504	574	637	705
S42 ($\mu\epsilon$)	-	-	-	-	-	-	-	-	-	-	-
S43 ($\mu\epsilon$)	-	-	-	-	-	-	-	-	-	-	-
S44 ($\mu\epsilon$)	12	169	286	394	500	586	677	759	839	912	990
S46 ($\mu\epsilon$)	5	-65	-118	-184	-243	-287	-324	-356	-382	-401	-413
S48 ($\mu\epsilon$)	-96	11	95	174	255	317	385	444	506	559	618
S51 ($\mu\epsilon$)	13	192	334	470	610	726	851	967	1080	1182	1290
S55 ($\mu\epsilon$)	-1	65	127	198	274	339	411	481	549	613	682
S58 ($\mu\epsilon$)	2	81	149	204	265	310	360	406	451	493	541
S60 ($\mu\epsilon$)	-9	-229	-395	-561	-713	-820	-919	-1001	-1066	-1119	-1158
S62 ($\mu\epsilon$)	-12	158	279	385	493	573	658	736	811	878	952
S65 ($\mu\epsilon$)	29	219	362	507	660	781	909	1029	1142	1245	1353
S69 ($\mu\epsilon$)	-16	41	96	152	215	267	326	381	437	488	544
S72 ($\mu\epsilon$)	39	212	330	437	543	626	713	794	873	944	1020
S74 ($\mu\epsilon$)	0	-116	-220	-343	-464	-561	-662	-756	-842	-920	-994
S76 ($\mu\epsilon$)	16	137	229	317	412	488	571	649	726	795	871
S79 ($\mu\epsilon$)	45	235	371	503	641	753	873	986	1096	1195	1300
S83 ($\mu\epsilon$)	1	88	160	237	316	382	453	520	587	648	714
S86 ($\mu\epsilon$)	21	180	299	402	504	583	667	744	818	884	956
S88 ($\mu\epsilon$)	12	-129	-217	-315	-397	-451	-496	-531	-556	-571	-577
S90 ($\mu\epsilon$)	46	186	297	399	501	582	669	748	825	895	970

Table F-13. Raw data, strain survey conducted after 60,000 cycles, ambient environmental conditions (Run 1) (continued)

Load Step	0	1	2	3	4	5	6	7	8	9	10
Pressure (psi)	0.00	0.66	1.24	1.95	2.65	3.29	3.99	4.67	5.35	5.96	6.61
S93 ($\mu\epsilon$)	31	200	341	473	611	721	840	950	1056	1152	1254
S97 ($\mu\epsilon$)	6	73	136	204	279	341	410	474	539	598	662
S104 ($\mu\epsilon$)	18	194	325	444	558	649	742	826	906	978	1056
S105 ($\mu\epsilon$)	-8	-323	-530	-740	-939	-1081	-1229	-1357	-1470	-1566	-1660
S106 ($\mu\epsilon$)	32	251	410	559	698	805	915	1014	1106	1189	1278
S107 ($\mu\epsilon$)	38	207	362	522	688	827	972	1110	1240	1359	1483
S109 ($\mu\epsilon$)	-4	19	67	137	218	289	369	448	525	598	675
S110 ($\mu\epsilon$)	38	203	333	458	581	677	777	870	958	1038	1123
S111 ($\mu\epsilon$)	-25	-297	-495	-683	-851	-973	-1087	-1179	-1256	-1316	-1365
S112 ($\mu\epsilon$)	43	232	369	496	618	711	808	896	980	1056	1137
S113 ($\mu\epsilon$)	35	209	358	515	681	814	956	1088	1215	1331	1451
S115 ($\mu\epsilon$)	-25	22	78	153	236	308	389	468	547	621	698
UAC-A1 ($\mu\epsilon$)	-6	134	252	385	520	624	736	839	937	1026	1117
UAC-F1 ($\mu\epsilon$)	-7	129	244	380	519	627	742	850	950	1043	1138
UB-A1 ($\mu\epsilon$)	-	-	-	-	-	-	-	-	-	-	-
UB-A2 ($\mu\epsilon$)	29	263	454	645	826	971	1115	1243	1362	1467	1571
UB-A3 ($\mu\epsilon$)	26	233	401	570	728	855	983	1097	1204	1298	1392
UB-F1 ($\mu\epsilon$)	-	-	-	-	-	-	-	-	-	-	-
UB-F2 ($\mu\epsilon$)	-32	139	273	408	537	640	746	838	927	1003	1081
UB-F3 ($\mu\epsilon$)	-333	-260	-206	-158	-110	-76	-37	-6	25	48	75
UBC-A1 ($\mu\epsilon$)	-	-	-	-	-	-	-	-	-	-	-

Table F-13. Raw data, strain survey conducted after 60,000 cycles, ambient environmental conditions (Run 1) (continued)

Load Step	0	1	2	3	4	5	6	7	8	9	10
Pressure (psi)	0.00	0.66	1.24	1.95	2.65	3.29	3.99	4.67	5.35	5.96	6.61
UBC-A2 ($\mu\epsilon$)	24	224	399	588	771	915	1060	1188	1307	1410	1512
UBC-A3 ($\mu\epsilon$)	6	160	290	429	562	667	775	869	957	1035	1113
UBC-F1 ($\mu\epsilon$)	-	-	-	-	-	-	-	-	-	-	-
UBC-F2 ($\mu\epsilon$)	12	216	393	584	769	912	1058	1185	1305	1408	1510
UBC-F3 ($\mu\epsilon$)	-1	161	293	436	573	678	787	881	971	1049	1127
UDAC-A1 ($\mu\epsilon$)	-7	155	277	416	556	661	775	876	976	1062	1153
UDAC-F1 ($\mu\epsilon$)	-6	150	271	412	552	659	772	876	974	1063	1154
UDB-A1 ($\mu\epsilon$)	-	-	-	-	-	-	-	-	-	-	-
UDB-A2 ($\mu\epsilon$)	-172	-8	113	236	354	444	536	618	693	758	823
UDB-A3 ($\mu\epsilon$)	-2	232	407	584	748	877	1006	1122	1229	1324	1419
UDB-F1 ($\mu\epsilon$)	-	-	-	-	-	-	-	-	-	-	-
UDB-F2 ($\mu\epsilon$)	13	307	533	770	991	1164	1335	1489	1628	1752	1875
UDB-F3 ($\mu\epsilon$)	3	244	423	614	792	929	1067	1193	1306	1406	1507
UDBC-A1 ($\mu\epsilon$)	-	-	-	-	-	-	-	-	-	-	-
UDBC-A2 ($\mu\epsilon$)	-	-	-	-	-	-	-	-	-	-	-
UDBC-A3 ($\mu\epsilon$)	6	191	344	504	655	771	888	991	1086	1168	1249
UDBC-F1 ($\mu\epsilon$)	-	-	-	-	-	-	-	-	-	-	-
UDBC-F2 ($\mu\epsilon$)	-	-	-	-	-	-	-	-	-	-	-
UDBC-F3 ($\mu\epsilon$)	10	200	361	528	684	807	929	1036	1135	1220	1303

Table F-14. Raw data, strain survey conducted after 60,000 cycles, ambient environmental conditions (Run 2)

Load Step	0	1	2	3	4	5	6	7	8	9	10
Pressure (psi)	-0.01	0.66	1.35	2.00	2.66	3.31	4.00	4.68	5.28	5.99	6.69
Frame-1 (lbf)	-1	91	248	346	461	550	611	834	942	945	1138
Frame-2 (lbf)	76	108	224	322	451	552	684	791	916	1019	1130
Frame-3 (lbf)	0	105	257	334	462	552	682	798	902	1007	1133
Frame-4 (lbf)	36	139	226	338	452	568	671	781	908	1028	1130
Frame-5 (lbf)	4	117	211	346	457	562	670	793	902	1027	1138
Frame-6 (lbf)	-1	116	217	354	449	557	669	800	903	1027	1134
Frame-7 (lbf)	0	116	218	345	461	567	679	796	907	1016	1132
Frame-8 (lbf)	1	114	228	350	447	564	685	783	907	1029	1133
Frame-9 (lbf)	31	124	230	330	449	565	685	798	912	1023	1132
Frame-10 (lbf)	0	95	227	314	450	584	686	794	915	1016	1135
Frame-11 (lbf)	-1	105	229	328	461	575	679	795	908	1020	1134
Frame-12 (lbf)	0	124	227	351	453	564	678	803	901	1031	1135
Hoop-1 (lbf)	-14	722	1417	2161	2845	3601	4311	4997	5696	6437	7151
Hoop-2 (lbf)	17	635	1390	2091	2855	3574	4329	4995	5712	6437	7148
Hoop-3 (lbf)	-9	737	1432	2145	2846	3556	4293	5000	5688	6425	7147
Hoop-4 (lbf)	3	738	1441	2149	2848	3597	4302	5018	5692	6424	7153
Hoop-5 (lbf)	-13	713	1412	2151	2841	3577	4304	5011	5726	6411	7155
Hoop-6 (lbf)	-13	725	1442	2139	2834	3597	4299	5010	5697	6433	7151
Hoop-7 (lbf)	0	712	1441	2150	2846	3575	4294	5012	5705	6411	7157
Hoop-8 (lbf)	129	724	1430	2136	2842	3584	4300	5007	5708	6415	7168
Hoop-9 (lbf)	34	732	1500	2118	2843	3577	4289	5007	5695	6420	7149

Table F-14. Raw data, strain survey conducted after 60,000 cycles, ambient environmental conditions (Run 2) (continued)

Load Step	0	1	2	3	4	5	6	7	8	9	10
Pressure (psi)	-0.01	0.66	1.35	2.00	2.66	3.31	4.00	4.68	5.28	5.99	6.69
Hoop-10 (lbf)	-2	741	1413	2177	2822	3598	4331	5024	5696	6415	7163
Hoop-11 (lbf)	14	700	1450	2136	2855	3575	4305	5024	5716	6407	7153
Hoop-12 (lbf)	108	720	1406	2156	2847	3562	4287	4994	5695	6438	7152
Hoop-13 (lbf)	96	734	1451	2175	2871	3608	4304	5024	5730	6424	7150
Hoop-14 (lbf)	14	682	1409	2147	2838	3578	4288	5001	5696	6444	7154
Long-1 (lbf)	-7	697	1347	1996	2733	3333	3966	4681	5343	6048	6660
Long-2 (lbf)	4	669	1336	2021	2675	3330	3998	4661	5336	5998	6672
Long-3 (lbf)	-12	696	1348	2011	2674	3332	4013	4658	5351	6007	6665
Long-4 (lbf)	-38	703	1354	2002	2671	3329	4002	4664	5341	6003	6677
Long-5 (lbf)	-1	674	1329	2004	2674	3352	4014	4677	5341	6025	6693
Long-6 (lbf)	-7	672	1357	1999	2653	3334	3996	4682	5356	5969	6662
Long-7 (lbf)	5	629	1344	2016	2673	3375	3988	4676	5341	6011	6663
Long-8 (lbf)	2	685	1327	1994	2666	3334	4005	4672	5344	6015	6683
F01 ($\mu\epsilon$)	-	-	-	-	-	-	-	-	-	-	-
F02 ($\mu\epsilon$)	-	-	-	-	-	-	-	-	-	-	-
F03 ($\mu\epsilon$)	-	-	-	-	-	-	-	-	-	-	-
F04 ($\mu\epsilon$)	-	-	-	-	-	-	-	-	-	-	-
F05 ($\mu\epsilon$)	-	-	-	-	-	-	-	-	-	-	-
F06 ($\mu\epsilon$)	-	-	-	-	-	-	-	-	-	-	-
F07 ($\mu\epsilon$)	-	-	-	-	-	-	-	-	-	-	-
F08 ($\mu\epsilon$)	-	-	-	-	-	-	-	-	-	-	-

Table F-14. Raw data, strain survey conducted after 60,000 cycles, ambient environmental conditions (Run 2) (continued)

Load Step	0	1	2	3	4	5	6	7	8	9	10
Pressure (psi)	-0.01	0.66	1.35	2.00	2.66	3.31	4.00	4.68	5.28	5.99	6.69
IS18 ($\mu\epsilon$)	-13	-79	-112	-118	-113	-90	-58	-22	22	73	132
IS20 ($\mu\epsilon$)	6	44	76	109	138	173	208	239	273	309	348
IS22 ($\mu\epsilon$)	-6	-74	-116	-130	-133	-115	-88	-55	-14	35	93
IS25 ($\mu\epsilon$)	-23	-106	-151	-167	-176	-167	-150	-128	-97	-61	-17
IS26 ($\mu\epsilon$)	6	121	225	321	406	489	571	643	709	777	846
IS27 ($\mu\epsilon$)	-5	-73	-99	-95	-86	-59	-24	15	60	110	169
IS28 ($\mu\epsilon$)	9	143	271	392	498	602	707	799	882	969	1055
IS29 ($\mu\epsilon$)	3	116	219	321	409	500	591	674	750	831	914
IS30 ($\mu\epsilon$)	-26	-42	-49	-40	-24	8	44	83	130	183	243
IS32 ($\mu\epsilon$)	-2	74	137	197	249	303	356	402	445	491	537
IS34 ($\mu\epsilon$)	-18	-28	-37	-33	-22	3	33	67	107	154	208
IS37 ($\mu\epsilon$)	-39	-138	-208	-249	-278	-288	-290	-283	-267	-245	-215
IS38 ($\mu\epsilon$)	63	220	351	454	458	604	246	333	456	421	489
IS39 ($\mu\epsilon$)	-50	-146	-209	-240	-258	-256	-244	-225	-197	-163	-121
IS40 ($\mu\epsilon$)	-1	103	193	280	358	434	512	581	643	708	773
IS41 ($\mu\epsilon$)	1	114	211	305	387	469	552	626	694	766	839
IS44 ($\mu\epsilon$)	-18	-67	-84	-80	-62	-34	7	47	91	143	202
IS46 ($\mu\epsilon$)	-4	61	125	182	237	290	347	396	441	490	541
IS48 ($\mu\epsilon$)	-12	-20	-11	12	42	83	134	182	234	294	359
IS51 ($\mu\epsilon$)	-25	-59	-64	-60	-47	-28	0	27	57	93	135
IS52 ($\mu\epsilon$)	251	366	480	581	681	773	872	958	1035	1120	1204

Table F-14. Raw data, strain survey conducted after 60,000 cycles, ambient environmental conditions (Run 2) (continued)

Load Step	0	1	2	3	4	5	6	7	8	9	10
Pressure (psi)	-0.01	0.66	1.35	2.00	2.66	3.31	4.00	4.68	5.28	5.99	6.69
IS55 ($\mu\epsilon$)	-9	92	188	273	355	433	516	587	655	727	802
IS58 ($\mu\epsilon$)	-29	-100	-142	-154	-154	-135	-109	-76	-35	13	69
IS60 ($\mu\epsilon$)	4	50	83	115	143	175	207	235	265	297	332
IS62 ($\mu\epsilon$)	-9	-66	-98	-107	-106	-87	-59	-27	13	60	116
IS65 ($\mu\epsilon$)	-17	-67	-95	-99	-98	-80	-58	-30	6	45	93
IS66 ($\mu\epsilon$)	9	123	220	309	387	463	538	604	665	727	790
IS67 ($\mu\epsilon$)	-12	-35	-37	-17	6	44	86	131	180	234	295
IS68 ($\mu\epsilon$)	7	167	309	440	558	670	780	878	965	1056	1145
IS69 ($\mu\epsilon$)	-4	134	250	357	453	547	640	724	801	882	965
IS72 ($\mu\epsilon$)	-13	-39	-42	-17	12	57	107	159	214	275	343
IS74 ($\mu\epsilon$)	1	78	147	215	277	340	402	458	511	566	621
IS76 ($\mu\epsilon$)	-3	20	48	90	134	189	249	309	371	440	514
IS79 ($\mu\epsilon$)	-48	-74	-80	-64	-48	-20	8	41	77	116	161
IS80 ($\mu\epsilon$)	-3	109	210	308	400	491	581	664	739	819	900
IS83 ($\mu\epsilon$)	-4	99	187	269	344	421	495	562	628	695	765
IS86 ($\mu\epsilon$)	-15	-46	-49	-32	-2	39	91	141	193	256	322
IS88 ($\mu\epsilon$)	-3	49	92	130	166	201	238	268	298	330	362
IS90 ($\mu\epsilon$)	-15	-21	-17	4	36	79	131	181	234	297	364
IS93 ($\mu\epsilon$)	-26	-24	-10	10	39	73	116	157	199	250	306
IS94 ($\mu\epsilon$)	-4	133	257	364	469	565	667	756	833	920	1005
IS95 ($\mu\epsilon$)	-25	-13	9	35	70	110	157	200	246	299	356

Table F-14. Raw data, strain survey conducted after 60,000 cycles, ambient environmental conditions (Run 2) (continued)

Load Step	0	1	2	3	4	5	6	7	8	9	10
Pressure (psi)	-0.01	0.66	1.35	2.00	2.66	3.31	4.00	4.68	5.28	5.99	6.69
IS96 ($\mu\epsilon$)	-9	109	214	307	397	482	572	649	719	798	875
IS97 ($\mu\epsilon$)	-11	100	194	278	357	436	516	586	652	724	798
IS104 ($\mu\epsilon$)	-6	-82	-122	-140	-145	-136	-117	-97	-69	-35	7
IS105 ($\mu\epsilon$)	0	62	112	154	190	228	267	297	327	361	398
IS106 ($\mu\epsilon$)	-19	-135	-214	-261	-291	-303	-306	-303	-291	-271	-243
IS107 ($\mu\epsilon$)	-7	-24	-33	-37	-32	-17	9	37	70	111	159
IS108 ($\mu\epsilon$)	10	218	395	541	674	797	923	1028	1122	1223	1320
IS109 ($\mu\epsilon$)	-	-	-	-	-	-	-	-	-	-	-
IS110 ($\mu\epsilon$)	-13	-73	-108	-118	-117	-99	-71	-40	1	48	103
IS111 ($\mu\epsilon$)	5	73	131	185	233	285	338	383	430	480	532
IS112 ($\mu\epsilon$)	-15	-108	-167	-194	-208	-202	-185	-163	-130	-91	-43
IS113 ($\mu\epsilon$)	4	-12	-27	-27	-27	-11	9	31	63	98	141
IS114 ($\mu\epsilon$)	22	217	383	532	661	786	908	1014	1111	1211	1309
IS115 ($\mu\epsilon$)	-	-	-	-	-	-	-	-	-	-	-
L01 ($\mu\epsilon$)	-	-	-	-	-	-	-	-	-	-	-
L02 ($\mu\epsilon$)	-	-	-	-	-	-	-	-	-	-	-
L03 ($\mu\epsilon$)	-	-	-	-	-	-	-	-	-	-	-
L04 ($\mu\epsilon$)	-	-	-	-	-	-	-	-	-	-	-
L05 ($\mu\epsilon$)	-	-	-	-	-	-	-	-	-	-	-
L06 ($\mu\epsilon$)	-	-	-	-	-	-	-	-	-	-	-
L07 ($\mu\epsilon$)	-	-	-	-	-	-	-	-	-	-	-

Table F-14. Raw data, strain survey conducted after 60,000 cycles, ambient environmental conditions (Run 2) (continued)

Load Step	0	1	2	3	4	5	6	7	8	9	10
Pressure (psi)	-0.01	0.66	1.35	2.00	2.66	3.31	4.00	4.68	5.28	5.99	6.69
L08 ($\mu\epsilon$)	-	-	-	-	-	-	-	-	-	-	-
L09 ($\mu\epsilon$)	-	-	-	-	-	-	-	-	-	-	-
L10 ($\mu\epsilon$)	-	-	-	-	-	-	-	-	-	-	-
RAC-A1 ($\mu\epsilon$)	-4	113	225	333	435	536	638	733	818	910	1001
RAC-F1 ($\mu\epsilon$)	10	121	221	322	416	510	605	693	772	858	944
RBC-A1 ($\mu\epsilon$)	11	163	289	406	511	611	710	797	871	949	1025
RBC-A2 ($\mu\epsilon$)	1	122	222	315	395	472	547	613	669	729	787
RBC-A3 ($\mu\epsilon$)	-2	113	207	296	372	446	519	582	638	697	755
RBC-F1 ($\mu\epsilon$)	-3	147	272	384	483	575	666	746	813	884	953
RBC-F2 ($\mu\epsilon$)	-5	121	225	316	397	473	547	611	667	724	781
RBC-F3 ($\mu\epsilon$)	-4	118	220	308	387	460	532	594	648	705	761
S18 ($\mu\epsilon$)	35	194	314	412	499	583	663	732	799	872	945
S20 ($\mu\epsilon$)	14	-169	-332	-462	-579	-676	-765	-834	-880	-929	-965
S22 ($\mu\epsilon$)	-13	137	259	359	448	536	614	682	747	818	889
S25 ($\mu\epsilon$)	24	217	380	520	654	785	911	1024	1128	1241	1352
S29 ($\mu\epsilon$)	-5	59	123	185	249	313	383	447	508	575	645
S30 ($\mu\epsilon$)	49	208	343	459	562	661	760	844	924	1008	1094
S32 ($\mu\epsilon$)	10	-127	-244	-345	-434	-510	-587	-655	-704	-758	-805
S34 ($\mu\epsilon$)	-1	93	177	258	332	405	480	545	606	673	741
S37 ($\mu\epsilon$)	54	276	463	622	767	904	1040	1158	1266	1381	1496
S41 ($\mu\epsilon$)	-3	69	144	216	289	361	436	504	568	638	708

Table F-14. Raw data, strain survey conducted after 60,000 cycles, ambient environmental conditions (Run 2) (continued)

Load Step	0	1	2	3	4	5	6	7	8	9	10
Pressure (psi)	-0.01	0.66	1.35	2.00	2.66	3.31	4.00	4.68	5.28	5.99	6.69
S42 ($\mu\epsilon$)	-	-	-	-	-	-	-	-	-	-	-
S43 ($\mu\epsilon$)	-	-	-	-	-	-	-	-	-	-	-
S44 ($\mu\epsilon$)	12	168	295	401	497	588	680	759	832	912	994
S46 ($\mu\epsilon$)	0	-69	-140	-195	-247	-288	-328	-360	-382	-402	-416
S48 ($\mu\epsilon$)	-115	-8	79	158	231	301	370	429	483	545	606
S51 ($\mu\epsilon$)	12	190	342	477	604	727	854	966	1068	1182	1295
S55 ($\mu\epsilon$)	-2	66	135	202	271	339	413	480	543	613	684
S58 ($\mu\epsilon$)	-9	72	141	199	252	307	357	399	441	489	540
S60 ($\mu\epsilon$)	-6	-234	-418	-574	-709	-823	-926	-1008	-1065	-1122	-1164
S62 ($\mu\epsilon$)	-18	151	285	388	484	574	660	732	801	877	953
S65 ($\mu\epsilon$)	29	217	383	521	657	786	915	1030	1132	1247	1359
S69 ($\mu\epsilon$)	-22	34	95	150	208	267	325	377	428	485	544
S72 ($\mu\epsilon$)	40	208	340	444	539	627	716	794	866	945	1024
S74 ($\mu\epsilon$)	0	-123	-242	-356	-463	-562	-665	-759	-835	-920	-1000
S76 ($\mu\epsilon$)	17	132	234	323	408	491	574	649	720	797	875
S79 ($\mu\epsilon$)	47	230	384	513	638	756	878	987	1087	1196	1306
S83 ($\mu\epsilon$)	2	88	170	243	314	383	455	520	582	649	717
S86 ($\mu\epsilon$)	21	182	305	408	499	586	670	742	810	884	959
S88 ($\mu\epsilon$)	10	-128	-243	-324	-398	-451	-500	-535	-555	-572	-581
S90 ($\mu\epsilon$)	48	188	308	409	499	588	674	749	820	898	975
S93 ($\mu\epsilon$)	30	202	349	481	604	725	844	949	1046	1153	1258

Table F-14. Raw data, strain survey conducted after 60,000 cycles, ambient environmental conditions (Run 2) (continued)

Load Step	0	1	2	3	4	5	6	7	8	9	10
Pressure (psi)	-0.01	0.66	1.35	2.00	2.66	3.31	4.00	4.68	5.28	5.99	6.69
S97 ($\mu\epsilon$)	4	74	144	210	276	343	412	473	532	598	663
S104 ($\mu\epsilon$)	10	192	336	454	556	651	747	826	899	979	1060
S105 ($\mu\epsilon$)	-8	-320	-565	-758	-930	-1081	-1235	-1359	-1461	-1568	-1667
S106 ($\mu\epsilon$)	29	249	427	569	693	807	920	1013	1097	1189	1281
S107 ($\mu\epsilon$)	32	208	379	535	686	829	979	1111	1230	1361	1490
S109 ($\mu\epsilon$)	-7	19	76	142	215	289	372	448	518	597	679
S110 ($\mu\epsilon$)	32	202	348	468	578	678	782	870	951	1039	1128
S111 ($\mu\epsilon$)	-26	-302	-519	-699	-846	-974	-1089	-1182	-1253	-1318	-1371
S112 ($\mu\epsilon$)	42	231	385	506	615	713	812	896	973	1057	1141
S113 ($\mu\epsilon$)	32	208	380	532	679	817	963	1091	1208	1335	1460
S115 ($\mu\epsilon$)	-23	19	87	157	231	305	388	465	538	620	701
UAC-A1 ($\mu\epsilon$)	-4	135	273	396	515	623	740	840	929	1026	1121
UAC-F1 ($\mu\epsilon$)	-5	131	268	392	515	626	748	852	943	1043	1142
UB-A1 ($\mu\epsilon$)	-	-	-	-	-	-	-	-	-	-	-
UB-A2 ($\mu\epsilon$)	35	272	478	662	821	971	1116	1242	1354	1467	1575
UB-A3 ($\mu\epsilon$)	31	241	421	584	723	855	984	1096	1196	1297	1395
UB-F1 ($\mu\epsilon$)	-	-	-	-	-	-	-	-	-	-	-
UB-F2 ($\mu\epsilon$)	-41	132	278	408	521	630	737	829	911	995	1077
UB-F3 ($\mu\epsilon$)	-384	-305	-251	-204	-166	-124	-85	-54	-25	5	38
UBC-A1 ($\mu\epsilon$)	-	-	-	-	-	-	-	-	-	-	-
UBC-A2 ($\mu\epsilon$)	29	232	427	608	768	916	1063	1190	1298	1410	1518

Table F-14. Raw data, strain survey conducted after 60,000 cycles, ambient environmental conditions (Run 2) (continued)

Load Step	0	1	2	3	4	5	6	7	8	9	10
Pressure (psi)	-0.01	0.66	1.35	2.00	2.66	3.31	4.00	4.68	5.28	5.99	6.69
UBC-A3 ($\mu\epsilon$)	9	165	309	442	558	667	775	868	950	1034	1115
UBC-F1 ($\mu\epsilon$)	-	-	-	-	-	-	-	-	-	-	-
UBC-F2 ($\mu\epsilon$)	16	220	421	602	764	913	1060	1187	1295	1407	1515
UBC-F3 ($\mu\epsilon$)	1	162	313	448	567	677	787	880	962	1047	1129
UDAC-A1 ($\mu\epsilon$)	-6	156	302	428	550	662	778	878	966	1064	1159
UDAC-F1 ($\mu\epsilon$)	-5	152	298	425	548	659	778	879	966	1064	1160
UDB-A1 ($\mu\epsilon$)	-	-	-	-	-	-	-	-	-	-	-
UDB-A2 ($\mu\epsilon$)	-196	-32	108	222	325	417	512	590	657	729	796
UDB-A3 ($\mu\epsilon$)	0	231	430	594	741	874	1007	1119	1218	1321	1420
UDB-F1 ($\mu\epsilon$)	-	-	-	-	-	-	-	-	-	-	-
UDB-F2 ($\mu\epsilon$)	20	310	572	789	987	1162	1341	1488	1617	1751	1878
UDB-F3 ($\mu\epsilon$)	8	247	457	629	789	927	1072	1193	1295	1405	1510
UDBC-A1 ($\mu\epsilon$)	-	-	-	-	-	-	-	-	-	-	-
UDBC-A2 ($\mu\epsilon$)	-	-	-	-	-	-	-	-	-	-	-
UDBC-A3 ($\mu\epsilon$)	6	199	368	518	650	773	889	990	1078	1166	1251
UDBC-F1 ($\mu\epsilon$)	-	-	-	-	-	-	-	-	-	-	-
UDBC-F2 ($\mu\epsilon$)	-	-	-	-	-	-	-	-	-	-	-
UDBC-F3 ($\mu\epsilon$)	11	210	384	543	680	808	930	1035	1126	1218	1306

Table F-15. Raw data, strain survey conducted after 60,000 cycles, ambient environmental conditions (Run 3)

Load Step	0	1	2	3	4	5	6	7	8	9	10
Pressure (psi)	0.02	0.68	1.33	1.96	2.64	3.31	3.98	4.63	5.30	5.97	6.62
Frame-1 (lbf)	0	101	222	389	447	533	661	862	908	982	1140
Frame-2 (lbf)	48	71	209	326	446	566	703	778	906	1019	1129
Frame-3 (lbf)	0	116	210	340	452	554	688	801	903	1020	1138
Frame-4 (lbf)	36	96	228	355	459	574	679	788	909	1024	1130
Frame-5 (lbf)	3	105	216	343	435	559	679	787	894	1020	1146
Frame-6 (lbf)	1	131	211	318	451	585	702	804	920	1005	1119
Frame-7 (lbf)	0	109	226	332	454	574	680	796	910	1017	1133
Frame-8 (lbf)	0	110	252	329	443	576	674	787	910	1032	1124
Frame-9 (lbf)	35	104	222	331	452	568	679	795	904	1021	1133
Frame-10 (lbf)	0	104	215	348	470	561	672	805	900	1017	1139
Frame-11 (lbf)	0	110	223	337	457	561	678	793	911	1022	1134
Frame-12 (lbf)	0	113	220	362	453	564	682	790	911	1031	1155
Hoop-1 (lbf)	-17	740	1447	2153	2875	3554	4286	4962	5715	6433	7136
Hoop-2 (lbf)	35	663	1442	2100	2873	3555	4283	5001	5707	6425	7138
Hoop-3 (lbf)	0	701	1439	2168	2845	3559	4278	4978	5703	6426	7137
Hoop-4 (lbf)	-1	720	1420	2137	2857	3560	4286	4991	5719	6422	7137
Hoop-5 (lbf)	-3	693	1446	2148	2849	3550	4269	4970	5702	6436	7121
Hoop-6 (lbf)	0	713	1419	2128	2853	3558	4277	4994	5714	6408	7130
Hoop-7 (lbf)	9	718	1440	2144	2851	3565	4267	4992	5700	6421	7137
Hoop-8 (lbf)	23	708	1434	2137	2857	3558	4264	4981	5702	6419	7135
Hoop-9 (lbf)	68	709	1432	2133	2867	3540	4291	4995	5716	6420	7123

Table F-15. Raw data, strain survey conducted after 60,000 cycles, ambient environmental conditions (Run 3) (continued)

Load Step	0	1	2	3	4	5	6	7	8	9	10
Pressure (psi)	0.02	0.68	1.33	1.96	2.64	3.31	3.98	4.63	5.30	5.97	6.62
Hoop-10 (lbf)	34	697	1384	2138	2858	3548	4272	4995	5713	6413	7134
Hoop-11 (lbf)	11	745	1439	2145	2845	3552	4289	5023	5688	6409	7160
Hoop-12 (lbf)	97	743	1477	2119	2847	3573	4273	4993	5721	6428	7134
Hoop-13 (lbf)	67	706	1399	2139	2861	3565	4308	4973	5716	6437	7138
Hoop-14 (lbf)	14	723	1440	2138	2851	3553	4274	4977	5707	6435	7126
Long-1 (lbf)	-22	638	1328	2034	2694	3306	4005	4676	5330	6048	6673
Long-2 (lbf)	-13	671	1304	1997	2667	3346	4006	4671	5348	6003	6673
Long-3 (lbf)	-10	670	1342	2002	2667	3344	4002	4677	5345	6004	6677
Long-4 (lbf)	13	664	1365	2002	2661	3334	4008	4667	5345	6008	6673
Long-5 (lbf)	-6	682	1338	2002	2671	3345	3991	4666	5343	6022	6676
Long-6 (lbf)	-7	690	1351	1997	2642	3338	3999	4685	5344	6005	6677
Long-7 (lbf)	-21	695	1357	1998	2629	3330	4003	4674	5362	6010	6667
Long-8 (lbf)	5	640	1335	2004	2672	3341	4001	4678	5340	6014	6676
F01 ($\mu\epsilon$)	-	-	-	-	-	-	-	-	-	-	-
F02 ($\mu\epsilon$)	-	-	-	-	-	-	-	-	-	-	-
F03 ($\mu\epsilon$)	-	-	-	-	-	-	-	-	-	-	-
F04 ($\mu\epsilon$)	-	-	-	-	-	-	-	-	-	-	-
F05 ($\mu\epsilon$)	-	-	-	-	-	-	-	-	-	-	-
F06 ($\mu\epsilon$)	-	-	-	-	-	-	-	-	-	-	-
F07 ($\mu\epsilon$)	-	-	-	-	-	-	-	-	-	-	-
F08 ($\mu\epsilon$)	-	-	-	-	-	-	-	-	-	-	-

Table F-15. Raw data, strain survey conducted after 60,000 cycles, ambient environmental conditions (Run 3) (continued)

Load Step	0	1	2	3	4	5	6	7	8	9	10
Pressure (psi)	0.02	0.68	1.33	1.96	2.64	3.31	3.98	4.63	5.30	5.97	6.62
IS18 ($\mu\epsilon$)	-16	-80	-108	-118	-109	-90	-59	-19	24	75	129
IS20 ($\mu\epsilon$)	7	41	79	107	141	171	205	241	274	310	345
IS22 ($\mu\epsilon$)	-9	-80	-112	-130	-128	-116	-89	-53	-12	37	89
IS25 ($\mu\epsilon$)	-25	-107	-145	-169	-171	-167	-149	-124	-94	-58	-18
IS26 ($\mu\epsilon$)	9	123	228	316	406	488	567	641	711	779	842
IS27 ($\mu\epsilon$)	-6	-73	-91	-97	-80	-58	-23	18	64	114	167
IS28 ($\mu\epsilon$)	13	147	275	384	499	602	703	795	885	970	1051
IS29 ($\mu\epsilon$)	5	116	224	313	411	499	587	671	754	833	909
IS30 ($\mu\epsilon$)	-29	-46	-46	-39	-19	6	42	87	131	185	239
IS32 ($\mu\epsilon$)	-2	74	139	192	250	302	353	402	447	492	533
IS34 ($\mu\epsilon$)	-20	-32	-35	-33	-19	2	32	69	109	156	204
IS37 ($\mu\epsilon$)	-44	-139	-203	-249	-272	-287	-287	-278	-264	-242	-215
IS38 ($\mu\epsilon$)	-165	-34	44	126	222	361	458	531	583	626	606
IS39 ($\mu\epsilon$)	-56	-150	-204	-240	-252	-256	-242	-221	-194	-160	-122
IS40 ($\mu\epsilon$)	0	104	197	274	359	434	509	579	646	710	770
IS41 ($\mu\epsilon$)	1	114	215	298	388	468	548	623	697	768	835
IS44 ($\mu\epsilon$)	-19	-68	-84	-80	-61	-35	3	47	93	144	198
IS46 ($\mu\epsilon$)	-3	62	124	180	237	290	343	395	443	491	538
IS48 ($\mu\epsilon$)	-14	-23	-10	12	44	82	129	183	237	295	355
IS51 ($\mu\epsilon$)	-25	-54	-65	-61	-47	-29	-3	28	59	94	133
IS52 ($\mu\epsilon$)	254	371	479	579	678	773	865	954	1039	1121	1200

Table F-15. Raw data, strain survey conducted after 60,000 cycles, ambient environmental conditions (Run 3) (continued)

Load Step	0	1	2	3	4	5	6	7	8	9	10
Pressure (psi)	0.02	0.68	1.33	1.96	2.64	3.31	3.98	4.63	5.30	5.97	6.62
IS55 ($\mu\epsilon$)	-8	95	188	271	354	432	510	587	658	729	797
IS58 ($\mu\epsilon$)	-32	-101	-139	-154	-150	-136	-110	-74	-34	15	65
IS60 ($\mu\epsilon$)	4	47	85	113	145	174	203	236	265	298	329
IS62 ($\mu\epsilon$)	-13	-71	-95	-108	-102	-87	-61	-25	15	63	112
IS65 ($\mu\epsilon$)	-17	-67	-89	-98	-91	-79	-57	-25	8	49	92
IS66 ($\mu\epsilon$)	12	125	223	305	388	463	534	604	667	729	786
IS67 ($\mu\epsilon$)	-11	-33	-29	-16	12	45	86	135	184	238	294
IS68 ($\mu\epsilon$)	11	171	312	434	558	670	775	876	968	1057	1140
IS69 ($\mu\epsilon$)	-1	139	253	352	454	547	635	723	804	885	961
IS72 ($\mu\epsilon$)	-13	-39	-37	-19	17	57	105	161	216	278	339
IS74 ($\mu\epsilon$)	2	79	150	212	279	340	400	459	513	567	618
IS76 ($\mu\epsilon$)	-4	17	52	88	138	189	247	311	374	443	510
IS79 ($\mu\epsilon$)	-47	-71	-75	-66	-44	-21	9	45	78	118	159
IS80 ($\mu\epsilon$)	1	112	213	305	402	491	578	663	743	821	896
IS83 ($\mu\epsilon$)	-2	103	190	267	348	420	492	566	630	698	762
IS86 ($\mu\epsilon$)	-16	-45	-48	-33	0	40	88	142	196	256	318
IS88 ($\mu\epsilon$)	-2	49	92	129	167	202	235	269	299	330	360
IS90 ($\mu\epsilon$)	-15	-22	-16	3	38	79	128	183	236	296	358
IS93 ($\mu\epsilon$)	-25	-17	-10	10	40	74	114	158	202	251	303
IS94 ($\mu\epsilon$)	0	140	256	362	467	566	661	752	837	920	1000
IS95 ($\mu\epsilon$)	-24	-6	9	35	71	111	155	203	248	300	353

Table F-15. Raw data, strain survey conducted after 60,000 cycles, ambient environmental conditions (Run 3) (continued)

Load Step	0	1	2	3	4	5	6	7	8	9	10
Pressure (psi)	0.02	0.68	1.33	1.96	2.64	3.31	3.98	4.63	5.30	5.97	6.62
IS96 ($\mu\epsilon$)	-6	115	214	304	396	483	567	647	723	797	870
IS97 ($\mu\epsilon$)	-9	105	194	274	357	435	512	587	655	725	793
IS104 ($\mu\epsilon$)	-4	-80	-122	-140	-143	-137	-119	-95	-67	-34	4
IS105 ($\mu\epsilon$)	2	60	109	151	191	225	261	296	328	361	394
IS106 ($\mu\epsilon$)	-25	-141	-213	-259	-287	-304	-306	-299	-289	-270	-245
IS107 ($\mu\epsilon$)	-3	-19	-34	-37	-29	-16	8	39	73	113	159
IS108 ($\mu\epsilon$)	19	224	392	537	674	796	915	1025	1127	1223	1316
IS109 ($\mu\epsilon$)	-	-	-	-	-	-	-	-	-	-	-
IS110 ($\mu\epsilon$)	-12	-72	-104	-118	-113	-98	-72	-36	3	49	101
IS111 ($\mu\epsilon$)	7	71	132	181	233	283	333	383	431	480	529
IS112 ($\mu\epsilon$)	-19	-113	-163	-193	-203	-201	-186	-160	-129	-89	-45
IS113 ($\mu\epsilon$)	9	-13	-22	-28	-21	-10	10	37	65	101	141
IS114 ($\mu\epsilon$)	30	221	389	525	662	786	903	1013	1115	1212	1305
IS115 ($\mu\epsilon$)	-	-	-	-	-	-	-	-	-	-	-
L01 ($\mu\epsilon$)	-	-	-	-	-	-	-	-	-	-	-
L02 ($\mu\epsilon$)	-	-	-	-	-	-	-	-	-	-	-
L03 ($\mu\epsilon$)	-	-	-	-	-	-	-	-	-	-	-
L04 ($\mu\epsilon$)	-	-	-	-	-	-	-	-	-	-	-
L05 ($\mu\epsilon$)	-	-	-	-	-	-	-	-	-	-	-
L06 ($\mu\epsilon$)	-	-	-	-	-	-	-	-	-	-	-
L07 ($\mu\epsilon$)	-	-	-	-	-	-	-	-	-	-	-

Table F-15. Raw data, strain survey conducted after 60,000 cycles, ambient environmental conditions (Run 3) (continued)

Load Step	0	1	2	3	4	5	6	7	8	9	10
Pressure (psi)	0.02	0.68	1.33	1.96	2.64	3.31	3.98	4.63	5.30	5.97	6.62
L08 ($\mu\epsilon$)	-	-	-	-	-	-	-	-	-	-	-
L09 ($\mu\epsilon$)	-	-	-	-	-	-	-	-	-	-	-
L10 ($\mu\epsilon$)	-	-	-	-	-	-	-	-	-	-	-
RAC-A1 ($\mu\epsilon$)	-2	116	227	329	435	536	633	730	822	912	997
RAC-F1 ($\mu\epsilon$)	14	123	226	318	418	512	603	691	776	859	940
RBC-A1 ($\mu\epsilon$)	15	167	293	399	511	612	707	793	876	951	1022
RBC-A2 ($\mu\epsilon$)	3	125	226	308	395	472	544	610	673	730	783
RBC-A3 ($\mu\epsilon$)	-1	116	211	289	373	446	517	581	642	699	752
RBC-F1 ($\mu\epsilon$)	1	154	276	377	482	576	664	742	818	886	950
RBC-F2 ($\mu\epsilon$)	-2	127	227	310	396	473	544	609	670	726	778
RBC-F3 ($\mu\epsilon$)	-1	125	222	303	386	460	530	593	652	707	759
S18 ($\mu\epsilon$)	38	190	312	408	496	577	653	728	799	870	937
S20 ($\mu\epsilon$)	10	-174	-332	-460	-574	-675	-759	-824	-884	-927	-963
S22 ($\mu\epsilon$)	-17	137	253	353	444	525	601	675	744	814	877
S25 ($\mu\epsilon$)	29	219	375	514	649	777	899	1015	1129	1238	1342
S29 ($\mu\epsilon$)	-6	59	122	183	248	313	379	445	510	577	640
S30 ($\mu\epsilon$)	53	207	345	456	564	662	754	843	927	1010	1088
S32 ($\mu\epsilon$)	4	-138	-245	-336	-428	-511	-584	-645	-707	-756	-803
S34 ($\mu\epsilon$)	-4	93	180	253	332	403	473	542	607	673	734
S37 ($\mu\epsilon$)	60	276	463	619	767	903	1031	1153	1269	1382	1487
S41 ($\mu\epsilon$)	-3	69	143	214	288	360	432	502	570	638	703

Table F-15. Raw data, strain survey conducted after 60,000 cycles, ambient environmental conditions (Run 3) (continued)

Load Step	0	1	2	3	4	5	6	7	8	9	10
Pressure (psi)	0.02	0.68	1.33	1.96	2.64	3.31	3.98	4.63	5.30	5.97	6.62
S42 ($\mu\epsilon$)	-	-	-	-	-	-	-	-	-	-	-
S43 ($\mu\epsilon$)	-	-	-	-	-	-	-	-	-	-	-
S44 ($\mu\epsilon$)	15	166	294	398	497	587	673	756	835	913	988
S46 ($\mu\epsilon$)	-4	-77	-141	-198	-247	-293	-331	-360	-385	-404	-418
S48 ($\mu\epsilon$)	-124	-19	74	151	226	293	358	420	479	539	593
S51 ($\mu\epsilon$)	15	186	341	473	603	726	845	960	1073	1182	1288
S55 ($\mu\epsilon$)	-1	65	134	200	270	339	408	477	546	614	680
S58 ($\mu\epsilon$)	-17	64	139	195	250	301	347	395	441	487	531
S60 ($\mu\epsilon$)	-12	-240	-421	-573	-705	-824	-922	-1001	-1070	-1122	-1164
S62 ($\mu\epsilon$)	-17	152	278	383	479	565	646	726	800	874	943
S65 ($\mu\epsilon$)	32	219	377	515	650	781	902	1020	1135	1244	1348
S69 ($\mu\epsilon$)	-29	28	88	145	203	259	314	372	427	482	535
S72 ($\mu\epsilon$)	39	204	339	442	538	626	710	791	868	946	1019
S74 ($\mu\epsilon$)	-3	-129	-243	-350	-460	-563	-660	-750	-839	-919	-997
S76 ($\mu\epsilon$)	18	130	234	323	408	490	569	647	722	799	870
S79 ($\mu\epsilon$)	47	227	383	511	636	755	870	982	1090	1198	1300
S83 ($\mu\epsilon$)	3	89	169	241	313	383	451	520	584	651	713
S86 ($\mu\epsilon$)	21	177	302	403	496	580	660	737	811	883	951
S88 ($\mu\epsilon$)	8	-138	-242	-327	-396	-455	-501	-533	-558	-574	-583
S90 ($\mu\epsilon$)	52	189	305	403	497	584	665	745	821	897	968
S93 ($\mu\epsilon$)	32	198	346	475	600	719	832	941	1047	1151	1248

Table F-15. Raw data, strain survey conducted after 60,000 cycles, ambient environmental conditions (Run 3) (continued)

Load Step	0	1	2	3	4	5	6	7	8	9	10
Pressure (psi)	0.02	0.68	1.33	1.96	2.64	3.31	3.98	4.63	5.30	5.97	6.62
S97 ($\mu\epsilon$)	5	73	139	205	272	339	403	468	532	596	656
S104 ($\mu\epsilon$)	11	186	332	449	554	649	738	821	901	979	1054
S105 ($\mu\epsilon$)	-21	-326	-559	-752	-925	-1079	-1223	-1352	-1467	-1568	-1661
S106 ($\mu\epsilon$)	37	251	423	563	691	805	909	1007	1100	1189	1274
S107 ($\mu\epsilon$)	35	207	377	531	683	828	969	1104	1234	1361	1483
S109 ($\mu\epsilon$)	-10	19	74	139	212	288	366	443	521	598	674
S110 ($\mu\epsilon$)	33	200	346	465	575	678	773	866	953	1039	1122
S111 ($\mu\epsilon$)	-38	-308	-523	-690	-843	-972	-1084	-1176	-1255	-1318	-1369
S112 ($\mu\epsilon$)	48	234	383	503	613	712	804	892	975	1057	1135
S113 ($\mu\epsilon$)	34	212	380	528	675	818	953	1085	1212	1335	1453
S115 ($\mu\epsilon$)	-30	18	82	151	226	304	382	461	540	619	696
UAC-A1 ($\mu\epsilon$)	-1	140	272	392	512	623	732	835	933	1026	1116
UAC-F1 ($\mu\epsilon$)	-1	136	267	390	512	627	740	846	947	1044	1137
UB-A1 ($\mu\epsilon$)	-	-	-	-	-	-	-	-	-	-	-
UB-A2 ($\mu\epsilon$)	45	277	486	654	822	972	1112	1239	1359	1469	1571
UB-A3 ($\mu\epsilon$)	40	246	429	576	723	856	979	1093	1200	1299	1391
UB-F1 ($\mu\epsilon$)	-	-	-	-	-	-	-	-	-	-	-
UB-F2 ($\mu\epsilon$)	-43	128	274	395	515	624	727	822	909	991	1068
UB-F3 ($\mu\epsilon$)	-422	-340	-281	-238	-194	-156	-118	-83	-51	-21	9
UBC-A1 ($\mu\epsilon$)	-	-	-	-	-	-	-	-	-	-	-
UBC-A2 ($\mu\epsilon$)	36	240	434	599	768	919	1059	1185	1305	1413	1514

Table F-15. Raw data, strain survey conducted after 60,000 cycles, ambient environmental conditions (Run 3) (continued)

Load Step	0	1	2	3	4	5	6	7	8	9	10
Pressure (psi)	0.02	0.68	1.33	1.96	2.64	3.31	3.98	4.63	5.30	5.97	6.62
UBC-A3 ($\mu\epsilon$)	13	169	313	434	557	668	771	864	954	1035	1111
UBC-F1 ($\mu\epsilon$)	-	-	-	-	-	-	-	-	-	-	-
UBC-F2 ($\mu\epsilon$)	21	230	425	593	762	914	1055	1182	1301	1409	1510
UBC-F3 ($\mu\epsilon$)	5	170	316	440	565	678	782	877	966	1048	1125
UDAC-A1 ($\mu\epsilon$)	-2	164	300	424	548	664	773	875	970	1063	1153
UDAC-F1 ($\mu\epsilon$)	-1	159	296	422	545	661	771	873	970	1063	1154
UDB-A1 ($\mu\epsilon$)	-	-	-	-	-	-	-	-	-	-	-
UDB-A2 ($\mu\epsilon$)	-211	-51	83	196	301	394	484	565	639	707	771
UDB-A3 ($\mu\epsilon$)	8	237	427	589	739	873	1000	1116	1222	1321	1415
UDB-F1 ($\mu\epsilon$)	-	-	-	-	-	-	-	-	-	-	-
UDB-F2 ($\mu\epsilon$)	30	318	568	785	985	1163	1331	1484	1623	1752	1873
UDB-F3 ($\mu\epsilon$)	15	253	452	626	786	929	1064	1186	1300	1406	1505
UDBC-A1 ($\mu\epsilon$)	-	-	-	-	-	-	-	-	-	-	-
UDBC-A2 ($\mu\epsilon$)	-	-	-	-	-	-	-	-	-	-	-
UDBC-A3 ($\mu\epsilon$)	10	205	371	511	650	773	884	988	1081	1168	1247
UDBC-F1 ($\mu\epsilon$)	-	-	-	-	-	-	-	-	-	-	-
UDBC-F2 ($\mu\epsilon$)	-	-	-	-	-	-	-	-	-	-	-
UDBC-F3 ($\mu\epsilon$)	15	213	389	535	681	808	925	1032	1130	1220	1302

F.2.1.5 After 90,000 Cycles

Table F-16. Raw data, strain survey conducted after 90,000 cycles, ambient environmental conditions (Run 1)

Load Step	0	1	2	3	4	5	6	7	8	9	10
Pressure (psi)	-0.01	0.66	1.33	2.01	2.65	3.34	4.00	4.64	5.31	6.02	6.68
Frame-1 (lb _f)	2	129	247	318	506	545	669	840	934	1056	1093
Frame-2 (lb _f)	39	114	212	335	448	564	686	782	906	1021	1132
Frame-3 (lb _f)	0	119	219	353	458	561	680	798	911	1020	1131
Frame-4 (lb _f)	19	105	219	346	451	559	689	786	908	1001	1132
Frame-5 (lb _f)	7	135	213	321	431	577	656	789	901	1030	1129
Frame-6 (lb _f)	1	119	212	368	455	572	677	784	916	1020	1116
Frame-7 (lb _f)	-2	110	219	348	448	568	675	792	905	1017	1124
Frame-8 (lb _f)	8	103	227	338	444	584	676	783	909	1018	1124
Frame-9 (lb _f)	10	112	228	348	451	570	677	788	903	1013	1134
Frame-10 (lb _f)	1	104	223	355	439	579	673	782	914	1019	1144
Frame-11 (lb _f)	5	115	216	340	455	568	677	786	906	1015	1135
Frame-12 (lb _f)	0	121	238	349	452	564	669	781	902	1000	1132
Hoop-1 (lb _f)	10	716	1424	2154	2833	3586	4290	4993	5701	6429	7143
Hoop-2 (lb _f)	63	695	1384	2150	2870	3585	4281	4962	5703	6403	7156
Hoop-3 (lb _f)	9	711	1442	2140	2847	3579	4292	4992	5718	6436	7148
Hoop-4 (lb _f)	0	723	1435	2168	2860	3576	4294	4994	5701	6443	7133
Hoop-5 (lb _f)	3	685	1430	2162	2850	3578	4295	5006	5722	6411	7130
Hoop-6 (lb _f)	0	717	1430	2145	2858	3579	4291	4990	5708	6433	7144
Hoop-7 (lb _f)	5	710	1428	2135	2843	3573	4290	4997	5711	6444	7136
Hoop-8 (lb _f)	-2	718	1413	2144	2859	3575	4286	4996	5707	6435	7142

Table F-16. Raw data, strain survey conducted after 90,000 cycles, ambient environmental conditions (Run 1) (continued)

Load Step	0	1	2	3	4	5	6	7	8	9	10
Pressure (psi)	-0.01	0.66	1.33	2.01	2.65	3.34	4.00	4.64	5.31	6.02	6.68
Hoop-9 (lbf)	3	676	1449	2131	2868	3605	4291	4991	5710	6423	7136
Hoop-10 (lbf)	9	703	1386	2124	2844	3577	4289	4971	5713	6444	7146
Hoop-11 (lbf)	14	739	1436	2106	2865	3583	4286	5009	5723	6420	7130
Hoop-12 (lbf)	6	682	1428	2171	2855	3558	4286	5002	5706	6426	7145
Hoop-13 (lbf)	7	697	1456	2221	2883	3536	4318	5010	5719	6434	7145
Hoop-14 (lbf)	-4	736	1411	2129	2839	3585	4283	4987	5707	6427	7135
Long-1 (lbf)	-4	662	1357	2016	2672	3343	4005	4661	5316	6009	6660
Long-2 (lbf)	10	665	1342	2008	2686	3319	3996	4679	5339	6001	6674
Long-3 (lbf)	11	664	1347	2007	2681	3329	4001	4683	5341	5999	6682
Long-4 (lbf)	-27	665	1318	2001	2671	3308	4006	4673	5340	6009	6676
Long-5 (lbf)	-7	663	1324	2005	2670	3337	4003	4665	5340	6011	6671
Long-6 (lbf)	44	676	1333	2007	2652	3333	3995	4700	5343	6006	6683
Long-7 (lbf)	-1	684	1344	2004	2670	3338	4032	4678	5343	6005	6679
Long-8 (lbf)	2	636	1327	2012	2671	3340	4005	4670	5340	5989	6639
F01 ($\mu\epsilon$)	-	-	-	-	-	-	-	-	-	-	-
F02 ($\mu\epsilon$)	-	-	-	-	-	-	-	-	-	-	-
F03 ($\mu\epsilon$)	-	-	-	-	-	-	-	-	-	-	-
F04 ($\mu\epsilon$)	-	-	-	-	-	-	-	-	-	-	-
F05 ($\mu\epsilon$)	-	-	-	-	-	-	-	-	-	-	-
F06 ($\mu\epsilon$)	-	-	-	-	-	-	-	-	-	-	-
F07 ($\mu\epsilon$)	-	-	-	-	-	-	-	-	-	-	-

Table F-16. Raw data, strain survey conducted after 90,000 cycles, ambient environmental conditions (Run 1) (continued)

Load Step	0	1	2	3	4	5	6	7	8	9	10
Pressure (psi)	-0.01	0.66	1.33	2.01	2.65	3.34	4.00	4.64	5.31	6.02	6.68
F08 ($\mu\epsilon$)	-	-	-	-	-	-	-	-	-	-	-
IS18 ($\mu\epsilon$)	-2	-71	-104	-113	-103	-81	-50	-11	35	87	143
IS20 ($\mu\epsilon$)	5	50	83	116	149	182	215	247	282	317	352
IS22 ($\mu\epsilon$)	4	-66	-106	-123	-118	-104	-77	-42	2	51	106
IS25 ($\mu\epsilon$)	-4	-94	-140	-163	-165	-160	-145	-122	-91	-56	-15
IS26 ($\mu\epsilon$)	3	93	167	237	302	364	421	474	528	579	628
IS27 ($\mu\epsilon$)	-2	-72	-93	-93	-72	-45	-11	29	76	126	180
IS28 ($\mu\epsilon$)	2	145	278	401	516	626	725	817	907	993	1074
IS29 ($\mu\epsilon$)	3	125	234	335	431	524	612	694	776	855	932
IS30 ($\mu\epsilon$)	3	-14	-20	-11	8	36	70	110	157	209	263
IS32 ($\mu\epsilon$)	1	76	139	199	256	310	360	407	453	498	541
IS34 ($\mu\epsilon$)	5	-9	-17	-15	0	22	53	88	129	176	226
IS37 ($\mu\epsilon$)	-	-	-	-	-	-	-	-	-	-	-
IS38 ($\mu\epsilon$)	-	-	-	-	-	-	-	-	-	-	-
IS39 ($\mu\epsilon$)	3	-97	-155	-186	-194	-192	-179	-157	-127	-93	-53
IS40 ($\mu\epsilon$)	1	101	190	274	356	435	508	576	644	708	769
IS41 ($\mu\epsilon$)	1	116	217	311	401	488	568	643	718	791	860
IS44 ($\mu\epsilon$)	0	-53	-69	-63	-44	-16	20	60	108	159	212
IS46 ($\mu\epsilon$)	2	69	130	189	243	297	347	392	441	488	532
IS48 ($\mu\epsilon$)	6	3	13	39	73	113	160	208	265	324	384
IS51 ($\mu\epsilon$)	0	-40	-48	-40	-24	-3	22	50	84	121	159

Table F-16. Raw data, strain survey conducted after 90,000 cycles, ambient environmental conditions (Run 1) (continued)

Load Step	0	1	2	3	4	5	6	7	8	9	10
Pressure (psi)	-0.01	0.66	1.33	2.01	2.65	3.34	4.00	4.64	5.31	6.02	6.68
IS52 ($\mu\epsilon$)	4	121	232	343	445	546	639	724	813	898	977
IS55 ($\mu\epsilon$)	3	107	201	291	375	457	533	604	679	751	819
IS58 ($\mu\epsilon$)	8	-40	-70	-74	-62	-42	-10	29	77	132	197
IS60 ($\mu\epsilon$)	6	61	96	129	159	188	218	247	277	308	339
IS62 ($\mu\epsilon$)	5	-48	-77	-87	-78	-62	-32	3	46	95	148
IS65 ($\mu\epsilon$)	-3	-67	-93	-104	-97	-85	-62	-33	2	42	87
IS66 ($\mu\epsilon$)	3	93	166	233	295	354	411	463	515	565	613
IS67 ($\mu\epsilon$)	0	-32	-29	-13	19	53	96	142	193	248	305
IS68 ($\mu\epsilon$)	1	156	299	426	546	657	760	853	945	1031	1112
IS69 ($\mu\epsilon$)	-1	137	260	368	470	567	659	743	827	909	987
IS72 ($\mu\epsilon$)	-2	-33	-30	-10	26	65	113	165	218	276	335
IS74 ($\mu\epsilon$)	2	79	148	216	282	344	404	461	515	570	621
IS76 ($\mu\epsilon$)	3	23	53	93	144	197	257	318	383	451	520
IS79 ($\mu\epsilon$)	-6	-44	-44	-33	-7	17	49	84	119	159	200
IS80 ($\mu\epsilon$)	0	106	209	307	402	494	582	664	745	824	898
IS83 ($\mu\epsilon$)	-2	96	187	270	351	427	501	570	638	706	771
IS86 ($\mu\epsilon$)	0	-32	-33	-10	24	66	116	168	226	289	350
IS88 ($\mu\epsilon$)	1	54	96	138	175	211	245	276	307	339	368
IS90 ($\mu\epsilon$)	3	-6	-1	25	61	104	154	206	263	325	385
IS93 ($\mu\epsilon$)	-3	-6	6	33	63	99	139	181	228	278	329
IS94 ($\mu\epsilon$)	0	134	255	370	473	575	669	755	844	929	1007

Table F-16. Raw data, strain survey conducted after 90,000 cycles, ambient environmental conditions (Run 1) (continued)

Load Step	0	1	2	3	4	5	6	7	8	9	10
Pressure (psi)	-0.01	0.66	1.33	2.01	2.65	3.34	4.00	4.64	5.31	6.02	6.68
IS95 ($\mu\epsilon$)	-2	4	23	56	93	134	178	224	273	326	378
IS96 ($\mu\epsilon$)	0	116	218	318	408	498	581	658	736	813	883
IS97 ($\mu\epsilon$)	0	108	199	288	370	451	526	597	669	740	806
IS104 ($\mu\epsilon$)	-7	-66	-95	-106	-100	-88	-69	-45	-13	23	62
IS105 ($\mu\epsilon$)	10	87	135	176	213	247	278	307	339	369	399
IS106 ($\mu\epsilon$)	0	-115	-186	-229	-249	-261	-261	-253	-238	-216	-189
IS107 ($\mu\epsilon$)	-8	-29	-42	-46	-35	-20	3	32	70	112	158
IS108 ($\mu\epsilon$)	5	157	277	382	477	567	649	724	800	872	938
IS109 ($\mu\epsilon$)	-	-	-	-	-	-	-	-	-	-	-
IS110 ($\mu\epsilon$)	-3	-56	-87	-96	-88	-69	-41	-4	39	88	141
IS111 ($\mu\epsilon$)	8	87	142	193	240	288	333	378	424	470	515
IS112 ($\mu\epsilon$)	4	-84	-136	-163	-169	-163	-145	-117	-82	-40	7
IS113 ($\mu\epsilon$)	-1	-28	-45	-53	-44	-33	-15	10	40	76	116
IS114 ($\mu\epsilon$)	8	165	289	398	497	591	676	755	832	906	975
IS115 ($\mu\epsilon$)	-	-	-	-	-	-	-	-	-	-	-
L01 ($\mu\epsilon$)	-	-	-	-	-	-	-	-	-	-	-
L02 ($\mu\epsilon$)	-	-	-	-	-	-	-	-	-	-	-
L03 ($\mu\epsilon$)	-	-	-	-	-	-	-	-	-	-	-
L04 ($\mu\epsilon$)	-	-	-	-	-	-	-	-	-	-	-
L05 ($\mu\epsilon$)	-	-	-	-	-	-	-	-	-	-	-
L06 ($\mu\epsilon$)	-	-	-	-	-	-	-	-	-	-	-

Table F-16. Raw data, strain survey conducted after 90,000 cycles, ambient environmental conditions (Run 1) (continued)

Load Step	0	1	2	3	4	5	6	7	8	9	10
Pressure (psi)	-0.01	0.66	1.33	2.01	2.65	3.34	4.00	4.64	5.31	6.02	6.68
L07 ($\mu\epsilon$)	-	-	-	-	-	-	-	-	-	-	-
L08 ($\mu\epsilon$)	-	-	-	-	-	-	-	-	-	-	-
L09 ($\mu\epsilon$)	-	-	-	-	-	-	-	-	-	-	-
L10 ($\mu\epsilon$)	-	-	-	-	-	-	-	-	-	-	-
RAC-A1 ($\mu\epsilon$)	0	115	227	336	441	545	644	736	830	920	1006
RAC-F1 ($\mu\epsilon$)	1	109	211	311	410	505	598	686	771	856	937
RBC-A1 ($\mu\epsilon$)	-	-	-	-	-	-	-	-	-	-	-
RBC-A2 ($\mu\epsilon$)	1	120	221	313	400	481	554	621	685	745	800
RBC-A3 ($\mu\epsilon$)	1	111	204	290	371	447	517	581	642	700	753
RBC-F1 ($\mu\epsilon$)	-	-	-	-	-	-	-	-	-	-	-
RBC-F2 ($\mu\epsilon$)	-1	123	225	318	403	485	556	621	684	742	795
RBC-F3 ($\mu\epsilon$)	-1	117	214	303	384	462	530	592	652	708	759
S18 ($\mu\epsilon$)	16	182	301	401	481	559	630	697	765	833	900
S20 ($\mu\epsilon$)	-	-	-	-	-	-	-	-	-	-	-
S22 ($\mu\epsilon$)	7	153	259	345	410	476	533	584	636	688	739
S25 ($\mu\epsilon$)	12	212	368	510	632	757	871	977	1085	1190	1290
S29 ($\mu\epsilon$)	-1	68	137	205	273	343	411	476	544	611	676
S30 ($\mu\epsilon$)	-1754	22670	-5085	-5436	-5303	-5163	-5041	-4952	-8388	-12185	-14545
S32 ($\mu\epsilon$)	-	-	-	-	-	-	-	-	-	-	-
S34 ($\mu\epsilon$)	-2	89	163	236	300	367	424	477	531	584	634
S37 ($\mu\epsilon$)	5	230	410	571	711	847	971	1085	1201	1312	1417

Table F-16. Raw data, strain survey conducted after 90,000 cycles, ambient environmental conditions (Run 1) (continued)

Load Step	0	1	2	3	4	5	6	7	8	9	10
Pressure (psi)	-0.01	0.66	1.33	2.01	2.65	3.34	4.00	4.64	5.31	6.02	6.68
S41 ($\mu\epsilon$)	1	75	153	231	307	385	458	529	600	671	738
S42 ($\mu\epsilon$)	-	-	-	-	-	-	-	-	-	-	-
S43 ($\mu\epsilon$)	-	-	-	-	-	-	-	-	-	-	-
S44 ($\mu\epsilon$)	4	168	294	402	500	593	677	754	834	913	986
S46 ($\mu\epsilon$)	-	-	-	-	-	-	-	-	-	-	-
S48 ($\mu\epsilon$)	-3	103	191	267	335	401	458	512	569	622	674
S51 ($\mu\epsilon$)	4	192	346	485	613	740	858	968	1082	1193	1297
S55 ($\mu\epsilon$)	-1	68	138	208	277	349	418	484	554	624	690
S58 ($\mu\epsilon$)	9	48	72	93	105	119	132	143	155	166	178
S60 ($\mu\epsilon$)	-	-	-	-	-	-	-	-	-	-	-
S62 ($\mu\epsilon$)	5	173	295	396	483	565	639	707	777	846	912
S65 ($\mu\epsilon$)	8	206	359	498	624	751	867	975	1085	1193	1293
S69 ($\mu\epsilon$)	5	69	131	188	237	290	338	383	431	477	523
S72 ($\mu\epsilon$)	12	191	316	424	516	606	688	764	842	919	991
S74 ($\mu\epsilon$)	-	-	-	-	-	-	-	-	-	-	-
S76 ($\mu\epsilon$)	6	133	232	326	410	493	572	645	722	797	870
S79 ($\mu\epsilon$)	11	209	356	491	613	734	849	955	1066	1173	1275
S83 ($\mu\epsilon$)	1	91	172	248	320	392	461	527	594	661	725
S86 ($\mu\epsilon$)	6	169	293	399	486	571	648	720	790	861	929
S88 ($\mu\epsilon$)	-	-	-	-	-	-	-	-	-	-	-
S90 ($\mu\epsilon$)	5	152	272	378	465	551	632	706	781	855	928

Table F-16. Raw data, strain survey conducted after 90,000 cycles, ambient environmental conditions (Run 1) (continued)

Load Step	0	1	2	3	4	5	6	7	8	9	10
Pressure (psi)	-0.01	0.66	1.33	2.01	2.65	3.34	4.00	4.64	5.31	6.02	6.68
S93 ($\mu\epsilon$)	7	186	335	472	591	712	824	927	1032	1135	1233
S97 ($\mu\epsilon$)	3	72	142	211	273	339	403	464	525	587	648
S104 ($\mu\epsilon$)	22	194	324	431	524	614	694	767	844	920	991
S105 ($\mu\epsilon$)	-	-	-	-	-	-	-	-	-	-	-
S106 ($\mu\epsilon$)	11	242	411	550	667	777	873	961	1051	1137	1218
S107 ($\mu\epsilon$)	16	189	348	500	639	781	913	1035	1162	1285	1399
S109 ($\mu\epsilon$)	-1	27	90	163	241	325	405	482	564	645	722
S110 ($\mu\epsilon$)	15	188	326	444	546	646	737	821	907	991	1071
S111 ($\mu\epsilon$)	-	-	-	-	-	-	-	-	-	-	-
S112 ($\mu\epsilon$)	6	201	344	464	564	661	747	826	907	986	1061
S113 ($\mu\epsilon$)	11	195	358	509	644	784	913	1034	1157	1277	1389
S115 ($\mu\epsilon$)	-3	43	113	191	270	358	441	523	608	699	796
UAC-A1 ($\mu\epsilon$)	2	144	281	415	533	649	756	854	954	1049	1137
UAC-F1 ($\mu\epsilon$)	1	139	274	407	528	647	759	860	964	1063	1155
UB-A1 ($\mu\epsilon$)	-	-	-	-	-	-	-	-	-	-	-
UB-A2 ($\mu\epsilon$)	-	-	-	-	-	-	-	-	-	-	-
UB-A3 ($\mu\epsilon$)	-	-	-	-	-	-	-	-	-	-	-
UB-F1 ($\mu\epsilon$)	-	-	-	-	-	-	-	-	-	-	-
UB-F2 ($\mu\epsilon$)	-	-	-	-	-	-	-	-	-	-	-
UB-F3 ($\mu\epsilon$)	-	-	-	-	-	-	-	-	-	-	-
UBC-A1 ($\mu\epsilon$)	-	-	-	-	-	-	-	-	-	-	-

Table F-16. Raw data, strain survey conducted after 90,000 cycles, ambient environmental conditions (Run 1) (continued)

Load Step	0	1	2	3	4	5	6	7	8	9	10
Pressure (psi)	-0.01	0.66	1.33	2.01	2.65	3.34	4.00	4.64	5.31	6.02	6.68
UBC-A2 ($\mu\epsilon$)	-	-	-	-	-	-	-	-	-	-	-
UBC-A3 ($\mu\epsilon$)	1	186	355	508	648	779	895	998	1098	1190	1274
UBC-F1 ($\mu\epsilon$)	-	-	-	-	-	-	-	-	-	-	-
UBC-F2 ($\mu\epsilon$)	-	-	-	-	-	-	-	-	-	-	-
UBC-F3 ($\mu\epsilon$)	-1	184	359	518	661	796	912	1017	1118	1211	1295
UDAC-A1 ($\mu\epsilon$)	0	158	300	436	556	673	781	879	977	1073	1160
UDAC-F1 ($\mu\epsilon$)	0	154	298	434	553	670	780	878	978	1074	1163
UDB-A1 ($\mu\epsilon$)	-	-	-	-	-	-	-	-	-	-	-
UDB-A2 ($\mu\epsilon$)	-	-	-	-	-	-	-	-	-	-	-
UDB-A3 ($\mu\epsilon$)	5	272	497	690	858	1014	1152	1273	1391	1500	1598
UDB-F1 ($\mu\epsilon$)	-	-	-	-	-	-	-	-	-	-	-
UDB-F2 ($\mu\epsilon$)	-	-	-	-	-	-	-	-	-	-	-
UDB-F3 ($\mu\epsilon$)	0	278	524	738	927	1101	1256	1391	1524	1645	1753
UDBC-A1 ($\mu\epsilon$)	-	-	-	-	-	-	-	-	-	-	-
UDBC-A2 ($\mu\epsilon$)	-	-	-	-	-	-	-	-	-	-	-
UDBC-A3 ($\mu\epsilon$)	1	116	220	307	383	457	519	571	621	666	706
UDBC-F1 ($\mu\epsilon$)	-	-	-	-	-	-	-	-	-	-	-
UDBC-F2 ($\mu\epsilon$)	-	-	-	-	-	-	-	-	-	-	-
UDBC-F3 ($\mu\epsilon$)	-	-	-	-	-	-	-	-	-	-	-

Table F-17. Raw data, strain survey conducted after 90,000 cycles, ambient environmental conditions (Run 2)

Load Step	0	1	2	3	4	5	6	7	8	9	10
Pressure (psi)	0.01	0.67	1.34	2.00	2.66	3.32	3.97	4.65	5.36	6.01	6.67
Frame-1 (lbf)	17	142	259	271	433	513	717	785	871	989	1185
Frame-2 (lbf)	40	107	222	341	453	562	679	798	906	1021	1132
Frame-3 (lbf)	0	112	229	337	457	552	680	796	905	1021	1138
Frame-4 (lbf)	34	117	224	345	451	556	675	804	904	1022	1135
Frame-5 (lbf)	2	102	235	324	427	576	685	831	903	1014	1125
Frame-6 (lbf)	5	122	235	341	437	535	666	794	896	1019	1128
Frame-7 (lbf)	3	113	227	346	456	563	679	789	904	1023	1134
Frame-8 (lbf)	6	104	229	345	442	571	683	791	907	1020	1128
Frame-9 (lbf)	19	116	229	334	452	559	681	801	906	1019	1133
Frame-10 (lbf)	0	103	228	350	446	568	676	795	912	1050	1133
Frame-11 (lbf)	-4	110	221	339	453	565	684	790	909	1028	1128
Frame-12 (lbf)	0	111	221	338	445	567	687	787	893	1026	1131
Hoop-1 (lbf)	49	696	1402	2162	2854	3600	4267	4988	5729	6439	7130
Hoop-2 (lbf)	28	774	1439	2152	2809	3517	4265	4996	5774	6420	7158
Hoop-3 (lbf)	16	689	1437	2127	2849	3570	4270	4999	5732	6447	7144
Hoop-4 (lbf)	11	728	1420	2142	2869	3581	4274	4987	5715	6421	7128
Hoop-5 (lbf)	26	706	1426	2154	2859	3564	4270	4985	5728	6454	7172
Hoop-6 (lbf)	4	701	1425	2151	2850	3582	4277	4979	5718	6431	7158
Hoop-7 (lbf)	56	720	1416	2151	2868	3570	4272	4990	5715	6438	7152
Hoop-8 (lbf)	-2	724	1423	2138	2881	3563	4266	4989	5715	6435	7144
Hoop-9 (lbf)	16	706	1385	2138	2833	3576	4275	4994	5732	6442	7147

Table F-17. Raw data, strain survey conducted after 90,000 cycles, ambient environmental conditions (Run 2) (continued)

Load Step	0	1	2	3	4	5	6	7	8	9	10
Pressure (psi)	0.01	0.67	1.34	2.00	2.66	3.32	3.97	4.65	5.36	6.01	6.67
Hoop-10 (lbf)	5	719	1441	2139	2848	3573	4290	4992	5739	6443	7153
Hoop-11 (lbf)	11	727	1448	2137	2854	3568	4271	5014	5721	6445	7138
Hoop-12 (lbf)	108	713	1411	2159	2864	3592	4287	4986	5712	6426	7137
Hoop-13 (lbf)	-4	759	1427	2121	2849	3575	4290	5004	5721	6431	7153
Hoop-14 (lbf)	18	679	1431	2163	2854	3561	4264	4993	5727	6433	7159
Long-1 (lbf)	-3	709	1344	1981	2670	3374	3994	4603	5367	6015	6702
Long-2 (lbf)	-6	670	1351	2007	2666	3338	4015	4679	5335	6002	6664
Long-3 (lbf)	-5	659	1337	1999	2661	3333	4013	4672	5338	6015	6669
Long-4 (lbf)	-50	700	1335	2015	2657	3347	4010	4669	5340	6012	6674
Long-5 (lbf)	2	667	1332	2011	2664	3345	4004	4676	5346	6011	6675
Long-6 (lbf)	-13	665	1346	2008	2675	3341	4017	4661	5344	6023	6677
Long-7 (lbf)	-10	664	1303	2004	2667	3334	4009	4669	5344	6025	6671
Long-8 (lbf)	5	654	1339	2016	2672	3338	4007	4661	5345	6011	6674
F01 ($\mu\epsilon$)	-	-	-	-	-	-	-	-	-	-	-
F02 ($\mu\epsilon$)	-	-	-	-	-	-	-	-	-	-	-
F03 ($\mu\epsilon$)	-	-	-	-	-	-	-	-	-	-	-
F04 ($\mu\epsilon$)	-	-	-	-	-	-	-	-	-	-	-
F05 ($\mu\epsilon$)	-	-	-	-	-	-	-	-	-	-	-
F06 ($\mu\epsilon$)	-	-	-	-	-	-	-	-	-	-	-
F07 ($\mu\epsilon$)	-	-	-	-	-	-	-	-	-	-	-
F08 ($\mu\epsilon$)	-	-	-	-	-	-	-	-	-	-	-

Table F-17. Raw data, strain survey conducted after 90,000 cycles, ambient environmental conditions (Run 2) (continued)

Load Step	0	1	2	3	4	5	6	7	8	9	10
Pressure (psi)	0.01	0.67	1.34	2.00	2.66	3.32	3.97	4.65	5.36	6.01	6.67
IS18 ($\mu\epsilon$)	-14	-75	-105	-113	-104	-81	-51	-12	35	85	141
IS20 ($\mu\epsilon$)	7	48	81	113	146	180	211	245	280	313	349
IS22 ($\mu\epsilon$)	-3	-68	-108	-123	-122	-105	-79	-43	0	48	103
IS25 ($\mu\epsilon$)	-21	-100	-146	-166	-173	-165	-150	-127	-97	-63	-22
IS26 ($\mu\epsilon$)	8	96	169	238	302	364	419	475	529	577	626
IS27 ($\mu\epsilon$)	-15	-71	-92	-89	-74	-45	-11	30	75	124	177
IS28 ($\mu\epsilon$)	5	152	282	405	518	627	724	819	910	992	1073
IS29 ($\mu\epsilon$)	3	127	232	333	428	522	607	692	775	851	929
IS30 ($\mu\epsilon$)	-6	-22	-25	-18	2	31	65	107	154	204	259
IS32 ($\mu\epsilon$)	-3	75	138	197	253	308	357	405	452	495	538
IS34 ($\mu\epsilon$)	-2	-12	-20	-16	-1	22	52	87	129	174	224
IS37 ($\mu\epsilon$)	-	-	-	-	-	-	-	-	-	-	-
IS38 ($\mu\epsilon$)	-	-	-	-	-	-	-	-	-	-	-
IS39 ($\mu\epsilon$)	-13	-103	-158	-187	-198	-193	-179	-158	-129	-96	-56
IS40 ($\mu\epsilon$)	-5	100	189	273	354	434	505	574	643	705	766
IS41 ($\mu\epsilon$)	-1	117	217	310	399	487	565	642	718	788	858
IS44 ($\mu\epsilon$)	-6	-56	-73	-67	-49	-20	14	56	107	156	209
IS46 ($\mu\epsilon$)	0	69	128	187	241	293	341	390	442	487	531
IS48 ($\mu\epsilon$)	3	3	10	36	68	110	154	205	265	322	382
IS51 ($\mu\epsilon$)	-6	-40	-51	-41	-28	-7	18	47	83	118	157
IS52 ($\mu\epsilon$)	27	149	258	366	465	561	649	737	829	909	987

Table F-17. Raw data, strain survey conducted after 90,000 cycles, ambient environmental conditions (Run 2) (continued)

Load Step	0	1	2	3	4	5	6	7	8	9	10
Pressure (psi)	0.01	0.67	1.34	2.00	2.66	3.32	3.97	4.65	5.36	6.01	6.67
IS55 ($\mu\epsilon$)	-1	107	198	288	370	451	525	601	677	747	816
IS58 ($\mu\epsilon$)	70	14	-2	-5	8	33	66	109	163	235	319
IS60 ($\mu\epsilon$)	11	60	94	124	155	186	215	245	276	305	337
IS62 ($\mu\epsilon$)	-1	-51	-79	-89	-82	-62	-34	1	45	92	146
IS65 ($\mu\epsilon$)	-12	-63	-93	-102	-99	-84	-61	-32	2	41	87
IS66 ($\mu\epsilon$)	8	96	167	232	295	355	410	464	517	565	613
IS67 ($\mu\epsilon$)	-7	-26	-27	-10	18	55	97	143	194	247	305
IS68 ($\mu\epsilon$)	4	163	301	428	547	658	759	855	948	1031	1113
IS69 ($\mu\epsilon$)	1	142	260	367	470	567	656	743	829	907	986
IS72 ($\mu\epsilon$)	-12	-35	-33	-13	22	65	112	163	218	273	333
IS74 ($\mu\epsilon$)	1	79	148	214	280	343	403	459	517	568	620
IS76 ($\mu\epsilon$)	0	22	51	90	140	196	255	317	384	448	518
IS79 ($\mu\epsilon$)	-15	-43	-47	-36	-13	16	48	81	118	155	198
IS80 ($\mu\epsilon$)	-2	108	208	305	401	493	579	662	746	821	897
IS83 ($\mu\epsilon$)	-5	98	185	266	347	425	498	568	638	703	769
IS86 ($\mu\epsilon$)	-5	-32	-33	-11	24	65	114	167	229	287	349
IS88 ($\mu\epsilon$)	0	54	96	136	174	209	242	274	308	337	367
IS90 ($\mu\epsilon$)	0	-8	-4	22	58	100	148	201	263	320	382
IS93 ($\mu\epsilon$)	-9	-6	5	31	61	96	135	178	229	276	328
IS94 ($\mu\epsilon$)	0	137	256	370	475	573	664	754	848	928	1007
IS95 ($\mu\epsilon$)	-7	4	23	56	92	132	176	223	276	324	377

Table F-17. Raw data, strain survey conducted after 90,000 cycles, ambient environmental conditions (Run 2) (continued)

Load Step	0	1	2	3	4	5	6	7	8	9	10
Pressure (psi)	0.01	0.67	1.34	2.00	2.66	3.32	3.97	4.65	5.36	6.01	6.67
IS96 ($\mu\epsilon$)	-2	117	218	317	408	495	575	656	739	811	882
IS97 ($\mu\epsilon$)	-5	107	199	286	368	447	521	594	669	737	804
IS104 ($\mu\epsilon$)	-7	-65	-96	-105	-104	-91	-72	-46	-14	20	60
IS105 ($\mu\epsilon$)	14	81	127	168	205	241	271	303	336	365	396
IS106 ($\mu\epsilon$)	-9	-115	-186	-228	-252	-262	-261	-253	-237	-217	-190
IS107 ($\mu\epsilon$)	-12	-24	-40	-41	-36	-20	3	33	72	112	158
IS108 ($\mu\epsilon$)	8	160	275	381	474	563	644	723	803	871	937
IS109 ($\mu\epsilon$)	-	-	-	-	-	-	-	-	-	-	-
IS110 ($\mu\epsilon$)	-5	-60	-90	-98	-92	-71	-43	-6	38	85	138
IS111 ($\mu\epsilon$)	13	83	137	187	235	283	328	375	422	466	512
IS112 ($\mu\epsilon$)	-5	-87	-141	-166	-174	-167	-149	-122	-87	-47	0
IS113 ($\mu\epsilon$)	-7	-26	-44	-48	-45	-32	-13	11	41	75	114
IS114 ($\mu\epsilon$)	13	165	286	396	494	587	671	753	832	903	972
IS115 ($\mu\epsilon$)	-	-	-	-	-	-	-	-	-	-	-
L01 ($\mu\epsilon$)	-	-	-	-	-	-	-	-	-	-	-
L02 ($\mu\epsilon$)	-	-	-	-	-	-	-	-	-	-	-
L03 ($\mu\epsilon$)	-	-	-	-	-	-	-	-	-	-	-
L04 ($\mu\epsilon$)	-	-	-	-	-	-	-	-	-	-	-
L05 ($\mu\epsilon$)	-	-	-	-	-	-	-	-	-	-	-
L06 ($\mu\epsilon$)	-	-	-	-	-	-	-	-	-	-	-
L07 ($\mu\epsilon$)	-	-	-	-	-	-	-	-	-	-	-

Table F-17. Raw data, strain survey conducted after 90,000 cycles, ambient environmental conditions (Run 2) (continued)

Load Step	0	1	2	3	4	5	6	7	8	9	10
Pressure (psi)	0.01	0.67	1.34	2.00	2.66	3.32	3.97	4.65	5.36	6.01	6.67
L08 ($\mu\epsilon$)	-	-	-	-	-	-	-	-	-	-	-
L09 ($\mu\epsilon$)	-	-	-	-	-	-	-	-	-	-	-
L10 ($\mu\epsilon$)	-	-	-	-	-	-	-	-	-	-	-
RAC-A1 ($\mu\epsilon$)	-1	117	227	335	441	544	640	735	831	918	1005
RAC-F1 ($\mu\epsilon$)	3	112	214	313	412	508	598	686	776	856	937
RBC-A1 ($\mu\epsilon$)	-	-	-	-	-	-	-	-	-	-	-
RBC-A2 ($\mu\epsilon$)	-6	119	220	313	398	480	551	619	684	741	797
RBC-A3 ($\mu\epsilon$)	-6	110	203	289	370	446	514	578	641	696	751
RBC-F1 ($\mu\epsilon$)	-	-	-	-	-	-	-	-	-	-	-
RBC-F2 ($\mu\epsilon$)	-8	122	225	318	403	483	553	620	684	739	793
RBC-F3 ($\mu\epsilon$)	-7	117	215	303	383	460	527	591	652	706	758
S18 ($\mu\epsilon$)	25	185	303	401	486	564	633	706	778	845	911
S20 ($\mu\epsilon$)	-	-	-	-	-	-	-	-	-	-	-
S22 ($\mu\epsilon$)	-7	140	246	331	406	473	528	586	644	696	748
S25 ($\mu\epsilon$)	23	214	370	509	639	761	871	985	1099	1201	1300
S29 ($\mu\epsilon$)	-4	67	137	205	274	343	408	476	546	610	675
S30 ($\mu\epsilon$)	-	-	-	-	-	-	-	-	-	-	-
S32 ($\mu\epsilon$)	-	-	-	-	-	-	-	-	-	-	-
S34 ($\mu\epsilon$)	-10	81	157	225	292	359	414	470	526	577	628
S37 ($\mu\epsilon$)	18	235	412	568	711	845	964	1083	1203	1309	1415
S41 ($\mu\epsilon$)	-2	73	152	230	308	383	455	528	602	669	737

Table F-17. Raw data, strain survey conducted after 90,000 cycles, ambient environmental conditions (Run 2) (continued)

Load Step	0	1	2	3	4	5	6	7	8	9	10
Pressure (psi)	0.01	0.67	1.34	2.00	2.66	3.32	3.97	4.65	5.36	6.01	6.67
S42 ($\mu\epsilon$)	-	-	-	-	-	-	-	-	-	-	-
S43 ($\mu\epsilon$)	-	-	-	-	-	-	-	-	-	-	-
S44 ($\mu\epsilon$)	8	170	295	402	500	590	671	753	836	911	985
S46 ($\mu\epsilon$)	-	-	-	-	-	-	-	-	-	-	-
S48 ($\mu\epsilon$)	-13	97	184	259	329	394	451	508	566	619	671
S51 ($\mu\epsilon$)	8	193	346	482	612	736	849	965	1084	1190	1295
S55 ($\mu\epsilon$)	1	68	138	207	277	347	413	483	556	623	689
S58 ($\mu\epsilon$)	13	45	65	84	100	115	128	142	156	168	180
S60 ($\mu\epsilon$)	-	-	-	-	-	-	-	-	-	-	-
S62 ($\mu\epsilon$)	0	162	286	387	479	561	634	708	783	849	917
S65 ($\mu\epsilon$)	20	203	358	496	628	750	864	978	1094	1197	1298
S69 ($\mu\epsilon$)	-10	58	120	177	234	287	335	386	438	484	531
S72 ($\mu\epsilon$)	20	189	316	420	515	602	682	762	843	916	990
S74 ($\mu\epsilon$)	-	-	-	-	-	-	-	-	-	-	-
S76 ($\mu\epsilon$)	10	130	232	322	409	492	567	645	724	796	870
S79 ($\mu\epsilon$)	19	206	356	487	614	732	842	955	1069	1172	1275
S83 ($\mu\epsilon$)	3	91	172	246	319	391	458	526	595	659	725
S86 ($\mu\epsilon$)	2	166	293	397	489	574	648	725	801	871	939
S88 ($\mu\epsilon$)	-	-	-	-	-	-	-	-	-	-	-
S90 ($\mu\epsilon$)	2	152	275	380	473	560	636	717	798	871	943
S93 ($\mu\epsilon$)	7	185	336	471	597	716	823	934	1046	1146	1244

Table F-17. Raw data, strain survey conducted after 90,000 cycles, ambient environmental conditions (Run 2) (continued)

Load Step	0	1	2	3	4	5	6	7	8	9	10
Pressure (psi)	0.01	0.67	1.34	2.00	2.66	3.32	3.97	4.65	5.36	6.01	6.67
S97 ($\mu\epsilon$)	-4	70	142	211	278	344	405	470	537	598	659
S104 ($\mu\epsilon$)	21	186	316	424	520	609	686	766	845	917	989
S105 ($\mu\epsilon$)	-	-	-	-	-	-	-	-	-	-	-
S106 ($\mu\epsilon$)	23	236	405	543	663	771	865	958	1051	1134	1215
S107 ($\mu\epsilon$)	22	183	342	492	637	775	903	1033	1165	1282	1397
S109 ($\mu\epsilon$)	-5	25	88	162	241	321	399	481	566	644	722
S110 ($\mu\epsilon$)	18	184	321	439	545	642	730	819	908	988	1068
S111 ($\mu\epsilon$)	-	-	-	-	-	-	-	-	-	-	-
S112 ($\mu\epsilon$)	14	195	339	457	561	655	739	823	907	982	1058
S113 ($\mu\epsilon$)	19	189	351	500	642	778	902	1030	1158	1273	1385
S115 ($\mu\epsilon$)	-6	44	114	191	273	357	435	518	604	686	782
UAC-A1 ($\mu\epsilon$)	3	149	282	413	532	645	748	851	956	1048	1136
UAC-F1 ($\mu\epsilon$)	2	143	273	406	528	643	750	856	967	1062	1154
UB-A1 ($\mu\epsilon$)	-	-	-	-	-	-	-	-	-	-	-
UB-A2 ($\mu\epsilon$)	-	-	-	-	-	-	-	-	-	-	-
UB-A3 ($\mu\epsilon$)	-	-	-	-	-	-	-	-	-	-	-
UB-F1 ($\mu\epsilon$)	-	-	-	-	-	-	-	-	-	-	-
UB-F2 ($\mu\epsilon$)	-	-	-	-	-	-	-	-	-	-	-
UB-F3 ($\mu\epsilon$)	-87	-80	-81	-80	-77	-71	-69	-66	-63	-62	-60
UBC-A1 ($\mu\epsilon$)	-	-	-	-	-	-	-	-	-	-	-
UBC-A2 ($\mu\epsilon$)	-	-	-	-	-	-	-	-	-	-	-

Table F-17. Raw data, strain survey conducted after 90,000 cycles, ambient environmental conditions (Run 2) (continued)

Load Step	0	1	2	3	4	5	6	7	8	9	10
Pressure (psi)	0.01	0.67	1.34	2.00	2.66	3.32	3.97	4.65	5.36	6.01	6.67
UBC-A3 ($\mu\epsilon$)	4	193	359	512	650	779	891	998	1099	1187	1271
UBC-F1 ($\mu\epsilon$)	-	-	-	-	-	-	-	-	-	-	-
UBC-F2 ($\mu\epsilon$)	-	-	-	-	-	-	-	-	-	-	-
UBC-F3 ($\mu\epsilon$)	-1	190	363	521	663	794	908	1017	1121	1210	1294
UDAC-A1 ($\mu\epsilon$)	-2	160	300	434	557	669	775	877	982	1071	1159
UDAC-F1 ($\mu\epsilon$)	0	156	296	431	555	667	773	875	983	1073	1163
UDB-A1 ($\mu\epsilon$)	-	-	-	-	-	-	-	-	-	-	-
UDB-A2 ($\mu\epsilon$)	-	-	-	-	-	-	-	-	-	-	-
UDB-A3 ($\mu\epsilon$)	1	274	491	683	849	1001	1135	1263	1386	1490	1588
UDB-F1 ($\mu\epsilon$)	-	-	-	-	-	-	-	-	-	-	-
UDB-F2 ($\mu\epsilon$)	-	-	-	-	-	-	-	-	-	-	-
UDB-F3 ($\mu\epsilon$)	-3	289	524	740	927	1095	1245	1387	1527	1643	1751
UDBC-A1 ($\mu\epsilon$)	-	-	-	-	-	-	-	-	-	-	-
UDBC-A2 ($\mu\epsilon$)	-	-	-	-	-	-	-	-	-	-	-
UDBC-A3 ($\mu\epsilon$)	-66	40	133	216	295	369	431	487	541	586	628
UDBC-F1 ($\mu\epsilon$)	-	-	-	-	-	-	-	-	-	-	-
UDBC-F2 ($\mu\epsilon$)	-	-	-	-	-	-	-	-	-	-	-
UDBC-F3 ($\mu\epsilon$)	-	-	-	-	-	-	-	-	-	-	-

Table F-18. Raw data, strain survey conducted after 90,000 cycles, ambient environmental conditions (Run 3)

Load Step	0	1	2	3	4	5	6	7	8	9	10
Pressure (psi)	0.02	0.67	1.35	1.98	2.65	3.35	3.99	4.69	5.31	6.02	6.70
Frame-1 (lbf)	9	168	225	403	504	540	701	840	866	988	1121
Frame-2 (lbf)	57	85	221	339	458	547	669	792	908	1019	1133
Frame-3 (lbf)	1	111	217	348	466	548	678	796	903	1021	1138
Frame-4 (lbf)	29	106	221	340	462	569	681	792	900	1019	1134
Frame-5 (lbf)	1	123	246	368	456	577	657	793	910	1005	1120
Frame-6 (lbf)	7	99	241	341	442	539	686	790	906	1022	1125
Frame-7 (lbf)	-1	106	232	356	454	570	679	793	907	1014	1134
Frame-8 (lbf)	3	118	224	348	438	555	677	787	912	1017	1130
Frame-9 (lbf)	26	111	230	346	457	567	682	787	906	1019	1136
Frame-10 (lbf)	0	136	227	326	459	567	675	790	921	1025	1113
Frame-11 (lbf)	15	121	227	333	460	562	681	796	906	1018	1137
Frame-12 (lbf)	0	120	223	336	451	556	670	803	895	1028	1137
Hoop-1 (lbf)	37	697	1424	2134	2827	3575	4283	5001	5700	6421	7132
Hoop-2 (lbf)	122	697	1414	2127	2882	3582	4301	4983	5714	6439	7154
Hoop-3 (lbf)	6	670	1429	2155	2858	3591	4298	5007	5698	6425	7160
Hoop-4 (lbf)	16	722	1442	2154	2841	3584	4285	5004	5707	6417	7151
Hoop-5 (lbf)	23	698	1430	2136	2845	3596	4294	4997	5696	6418	7146
Hoop-6 (lbf)	8	710	1416	2140	2851	3580	4297	4992	5696	6428	7146
Hoop-7 (lbf)	37	725	1430	2144	2854	3580	4290	5004	5686	6442	7169
Hoop-8 (lbf)	-2	720	1429	2154	2860	3590	4292	5002	5696	6430	7159
Hoop-9 (lbf)	2	729	1435	2180	2859	3552	4288	5005	5709	6428	7149

Table F-18. Raw data, strain survey conducted after 90,000 cycles, ambient environmental conditions (Run 3) (continued)

Load Step	0	1	2	3	4	5	6	7	8	9	10
Pressure (psi)	0.02	0.67	1.35	1.98	2.65	3.35	3.99	4.69	5.31	6.02	6.70
Hoop-10 (lbf)	1	701	1416	2133	2847	3596	4282	5000	5653	6431	7152
Hoop-11 (lbf)	27	694	1418	2178	2846	3580	4298	4996	5686	6430	7134
Hoop-12 (lbf)	46	713	1428	2109	2854	3595	4280	5005	5717	6416	7152
Hoop-13 (lbf)	5	730	1422	2130	2869	3607	4287	4994	5690	6425	7146
Hoop-14 (lbf)	2	684	1438	2178	2849	3578	4303	5006	5711	6420	7148
Long-1 (lbf)	-1	671	1325	1998	2689	3388	4019	4663	5341	5965	6661
Long-2 (lbf)	-18	669	1341	2008	2675	3327	4006	4675	5340	5998	6689
Long-3 (lbf)	8	686	1334	2014	2678	3332	4006	4669	5347	6006	6677
Long-4 (lbf)	-22	669	1336	2000	2676	3330	4011	4676	5338	6006	6680
Long-5 (lbf)	-2	678	1343	2005	2672	3338	3991	4670	5344	6005	6677
Long-6 (lbf)	-1	692	1358	2003	2686	3336	3999	4670	5361	5989	6696
Long-7 (lbf)	177	685	1341	1990	2659	3348	4005	4692	5345	6002	6704
Long-8 (lbf)	1	665	1351	2002	2667	3333	4026	4655	5347	6006	6677
F01 ($\mu\epsilon$)	-	-	-	-	-	-	-	-	-	-	-
F02 ($\mu\epsilon$)	-	-	-	-	-	-	-	-	-	-	-
F03 ($\mu\epsilon$)	-	-	-	-	-	-	-	-	-	-	-
F04 ($\mu\epsilon$)	-	-	-	-	-	-	-	-	-	-	-
F05 ($\mu\epsilon$)	-	-	-	-	-	-	-	-	-	-	-
F06 ($\mu\epsilon$)	-	-	-	-	-	-	-	-	-	-	-
F07 ($\mu\epsilon$)	-	-	-	-	-	-	-	-	-	-	-
F08 ($\mu\epsilon$)	-	-	-	-	-	-	-	-	-	-	-

Table F-18. Raw data, strain survey conducted after 90,000 cycles, ambient environmental conditions (Run 3) (continued)

Load Step	0	1	2	3	4	5	6	7	8	9	10
Pressure (psi)	0.02	0.67	1.35	1.98	2.65	3.35	3.99	4.69	5.31	6.02	6.70
IS18 ($\mu\epsilon$)	-16	-77	-107	-112	-105	-82	-52	-14	29	83	140
IS20 ($\mu\epsilon$)	5	43	78	113	143	178	210	242	274	311	347
IS22 ($\mu\epsilon$)	-7	-75	-112	-123	-124	-107	-80	-46	-6	45	101
IS25 ($\mu\epsilon$)	-26	-108	-150	-168	-176	-171	-154	-132	-104	-67	-26
IS26 ($\mu\epsilon$)	10	94	170	239	300	365	421	475	524	577	626
IS27 ($\mu\epsilon$)	-15	-76	-93	-87	-74	-47	-12	27	70	122	177
IS28 ($\mu\epsilon$)	9	150	286	406	516	629	727	820	904	992	1074
IS29 ($\mu\epsilon$)	4	121	233	333	425	521	608	690	767	849	928
IS30 ($\mu\epsilon$)	-7	-25	-28	-17	0	30	63	102	147	200	256
IS32 ($\mu\epsilon$)	-3	71	137	197	251	307	356	403	447	492	535
IS34 ($\mu\epsilon$)	-5	-16	-22	-15	-3	22	51	85	125	172	223
IS37 ($\mu\epsilon$)	-	-	-	-	-	-	-	-	-	-	-
IS38 ($\mu\epsilon$)	-	-	-	-	-	-	-	-	-	-	-
IS39 ($\mu\epsilon$)	-13	-108	-160	-185	-198	-195	-181	-161	-133	-98	-59
IS40 ($\mu\epsilon$)	-3	95	189	274	351	433	505	573	637	702	764
IS41 ($\mu\epsilon$)	2	113	218	312	397	486	566	642	713	787	857
IS44 ($\mu\epsilon$)	-10	-60	-76	-71	-52	-21	15	56	99	154	208
IS46 ($\mu\epsilon$)	0	67	128	184	238	294	344	392	435	485	531
IS48 ($\mu\epsilon$)	0	-2	9	33	65	109	156	206	257	320	381
IS51 ($\mu\epsilon$)	-8	-43	-51	-45	-30	-8	19	47	77	116	156
IS52 ($\mu\epsilon$)	35	153	264	364	463	564	655	743	821	909	989

Table F-18. Raw data, strain survey conducted after 90,000 cycles, ambient environmental conditions (Run 3) (continued)

Load Step	0	1	2	3	4	5	6	7	8	9	10
Pressure (psi)	0.02	0.67	1.35	1.98	2.65	3.35	3.99	4.69	5.31	6.02	6.70
IS55 ($\mu\epsilon$)	-2	103	198	285	366	451	527	601	668	744	815
IS58 ($\mu\epsilon$)	183	127	97	92	101	125	160	205	257	326	406
IS60 ($\mu\epsilon$)	10	56	92	125	153	186	215	243	271	304	336
IS62 ($\mu\epsilon$)	-3	-56	-83	-88	-83	-64	-35	-1	38	89	143
IS65 ($\mu\epsilon$)	-16	-63	-94	-99	-98	-85	-62	-35	-2	40	85
IS66 ($\mu\epsilon$)	9	96	168	235	295	357	412	464	513	564	613
IS67 ($\mu\epsilon$)	-10	-26	-28	-7	18	54	96	141	189	245	303
IS68 ($\mu\epsilon$)	5	165	304	431	546	661	761	857	942	1030	1112
IS69 ($\mu\epsilon$)	-1	145	262	370	468	569	657	743	822	906	985
IS72 ($\mu\epsilon$)	-16	-37	-35	-11	21	65	110	160	212	270	329
IS74 ($\mu\epsilon$)	1	78	149	216	279	345	403	459	512	567	619
IS76 ($\mu\epsilon$)	-2	18	50	93	139	197	255	315	377	446	516
IS79 ($\mu\epsilon$)	-21	-42	-47	-31	-12	16	46	79	114	154	195
IS80 ($\mu\epsilon$)	-3	109	210	307	399	495	580	663	740	820	895
IS83 ($\mu\epsilon$)	-7	99	186	270	346	427	498	567	632	700	766
IS86 ($\mu\epsilon$)	-6	-33	-32	-13	22	69	115	168	222	285	348
IS88 ($\mu\epsilon$)	0	52	96	134	172	210	242	274	303	336	366
IS90 ($\mu\epsilon$)	-3	-12	-4	17	54	102	148	201	255	317	379
IS93 ($\mu\epsilon$)	-9	-8	5	26	59	97	136	179	223	274	326
IS94 ($\mu\epsilon$)	2	137	259	365	471	576	668	759	840	926	1007
IS95 ($\mu\epsilon$)	-7	3	25	52	90	135	177	223	270	322	375

Table F-18. Raw data, strain survey conducted after 90,000 cycles, ambient environmental conditions (Run 3) (continued)

Load Step	0	1	2	3	4	5	6	7	8	9	10
Pressure (psi)	0.02	0.67	1.35	1.98	2.65	3.35	3.99	4.69	5.31	6.02	6.70
IS96 ($\mu\epsilon$)	-1	116	221	312	404	497	578	658	730	808	881
IS97 ($\mu\epsilon$)	-6	105	199	282	364	448	521	594	661	733	802
IS104 ($\mu\epsilon$)	-5	-67	-98	-107	-105	-92	-72	-48	-20	18	59
IS105 ($\mu\epsilon$)	12	77	125	167	203	240	272	302	329	363	395
IS106 ($\mu\epsilon$)	-13	-116	-186	-226	-250	-261	-261	-254	-241	-218	-191
IS107 ($\mu\epsilon$)	-8	-24	-38	-41	-35	-20	4	35	67	111	158
IS108 ($\mu\epsilon$)	11	160	279	379	473	566	647	727	795	871	939
IS109 ($\mu\epsilon$)	-	-	-	-	-	-	-	-	-	-	-
IS110 ($\mu\epsilon$)	-5	-63	-93	-99	-93	-73	-45	-9	32	83	137
IS111 ($\mu\epsilon$)	13	79	135	186	233	283	328	374	416	465	511
IS112 ($\mu\epsilon$)	-11	-96	-146	-168	-177	-170	-153	-127	-94	-51	-3
IS113 ($\mu\epsilon$)	-5	-31	-45	-45	-45	-34	-15	9	37	74	113
IS114 ($\mu\epsilon$)	14	161	287	395	491	588	672	753	825	901	972
IS115 ($\mu\epsilon$)	-	-	-	-	-	-	-	-	-	-	-
L01 ($\mu\epsilon$)	-	-	-	-	-	-	-	-	-	-	-
L02 ($\mu\epsilon$)	-	-	-	-	-	-	-	-	-	-	-
L03 ($\mu\epsilon$)	-	-	-	-	-	-	-	-	-	-	-
L04 ($\mu\epsilon$)	-	-	-	-	-	-	-	-	-	-	-
L05 ($\mu\epsilon$)	-	-	-	-	-	-	-	-	-	-	-
L06 ($\mu\epsilon$)	-	-	-	-	-	-	-	-	-	-	-
L07 ($\mu\epsilon$)	-	-	-	-	-	-	-	-	-	-	-

Table F-18. Raw data, strain survey conducted after 90,000 cycles, ambient environmental conditions (Run 3) (continued)

Load Step	0	1	2	3	4	5	6	7	8	9	10
Pressure (psi)	0.02	0.67	1.35	1.98	2.65	3.35	3.99	4.69	5.31	6.02	6.70
L08 ($\mu\epsilon$)	-	-	-	-	-	-	-	-	-	-	-
L09 ($\mu\epsilon$)	-	-	-	-	-	-	-	-	-	-	-
L10 ($\mu\epsilon$)	-	-	-	-	-	-	-	-	-	-	-
RAC-A1 ($\mu\epsilon$)	-1	117	228	336	438	546	642	737	824	917	1005
RAC-F1 ($\mu\epsilon$)	5	114	218	317	412	512	601	689	771	856	937
RBC-A1 ($\mu\epsilon$)	-	-	-	-	-	-	-	-	-	-	-
RBC-A2 ($\mu\epsilon$)	-4	115	221	312	394	478	550	617	677	738	794
RBC-A3 ($\mu\epsilon$)	-4	106	205	289	366	445	513	577	635	694	748
RBC-F1 ($\mu\epsilon$)	-	-	-	-	-	-	-	-	-	-	-
RBC-F2 ($\mu\epsilon$)	-6	120	227	318	399	482	553	619	677	737	791
RBC-F3 ($\mu\epsilon$)	-6	115	217	303	381	460	527	590	646	704	756
S18 ($\mu\epsilon$)	30	177	296	394	477	562	632	702	767	839	907
S20 ($\mu\epsilon$)	-	-	-	-	-	-	-	-	-	-	-
S22 ($\mu\epsilon$)	-8	130	236	323	394	466	523	578	629	686	742
S25 ($\mu\epsilon$)	28	210	366	503	630	761	873	985	1086	1195	1299
S29 ($\mu\epsilon$)	-3	68	138	204	271	344	410	477	539	608	675
S30 ($\mu\epsilon$)	-	-	-	-	-	-	-	-	-	-	-
S32 ($\mu\epsilon$)	-	-	-	-	-	-	-	-	-	-	-
S34 ($\mu\epsilon$)	-13	75	154	226	288	356	413	467	517	571	624
S37 ($\mu\epsilon$)	16	232	411	566	706	847	967	1085	1192	1307	1415
S41 ($\mu\epsilon$)	-2	75	154	229	305	385	457	529	596	667	736

Table F-18. Raw data, strain survey conducted after 90,000 cycles, ambient environmental conditions (Run 3) (continued)

Load Step	0	1	2	3	4	5	6	7	8	9	10
Pressure (psi)	0.02	0.67	1.35	1.98	2.65	3.35	3.99	4.69	5.31	6.02	6.70
S42 ($\mu\epsilon$)	-	-	-	-	-	-	-	-	-	-	-
S43 ($\mu\epsilon$)	-	-	-	-	-	-	-	-	-	-	-
S44 ($\mu\epsilon$)	10	169	296	403	497	592	674	755	828	909	986
S46 ($\mu\epsilon$)	-	-	-	-	-	-	-	-	-	-	-
S48 ($\mu\epsilon$)	-17	91	180	257	325	393	451	507	557	615	669
S51 ($\mu\epsilon$)	9	191	345	481	606	738	852	968	1072	1187	1296
S55 ($\mu\epsilon$)	2	69	139	206	274	348	416	485	549	621	690
S58 ($\mu\epsilon$)	12	37	59	78	94	112	126	138	150	164	176
S60 ($\mu\epsilon$)	-	-	-	-	-	-	-	-	-	-	-
S62 ($\mu\epsilon$)	3	159	280	381	470	559	632	704	770	843	913
S65 ($\mu\epsilon$)	27	202	358	492	620	753	867	981	1083	1194	1299
S69 ($\mu\epsilon$)	-8	52	113	171	225	282	332	380	425	477	526
S72 ($\mu\epsilon$)	22	184	314	417	511	604	684	763	835	914	990
S74 ($\mu\epsilon$)	8	8	7	8	8	8	8	8	8	8	9
S76 ($\mu\epsilon$)	13	128	231	321	406	494	570	646	717	794	870
S79 ($\mu\epsilon$)	23	202	356	486	609	736	846	957	1059	1170	1275
S83 ($\mu\epsilon$)	5	91	173	246	317	392	459	527	589	658	723
S86 ($\mu\epsilon$)	6	163	288	392	480	571	647	722	790	865	935
S88 ($\mu\epsilon$)	-	-	-	-	-	-	-	-	-	-	-
S90 ($\mu\epsilon$)	8	149	271	374	464	558	637	714	787	865	939
S93 ($\mu\epsilon$)	12	183	334	467	588	715	825	933	1033	1141	1242

Table F-18. Raw data, strain survey conducted after 90,000 cycles, ambient environmental conditions (Run 3) (continued)

Load Step	0	1	2	3	4	5	6	7	8	9	10
Pressure (psi)	0.02	0.67	1.35	1.98	2.65	3.35	3.99	4.69	5.31	6.02	6.70
S97 ($\mu\epsilon$)	1	68	138	205	270	342	404	467	527	592	655
S104 ($\mu\epsilon$)	16	182	315	424	516	610	688	767	835	914	989
S105 ($\mu\epsilon$)	-	-	-	-	-	-	-	-	-	-	-
S106 ($\mu\epsilon$)	25	233	404	541	657	772	867	959	1040	1131	1215
S107 ($\mu\epsilon$)	19	181	342	489	632	778	907	1037	1152	1280	1399
S109 ($\mu\epsilon$)	-6	26	90	161	238	323	402	484	558	642	723
S110 ($\mu\epsilon$)	17	182	321	437	540	644	733	820	899	986	1069
S111 ($\mu\epsilon$)	-	-	-	-	-	-	-	-	-	-	-
S112 ($\mu\epsilon$)	16	194	338	454	556	656	741	823	897	979	1057
S113 ($\mu\epsilon$)	18	190	351	496	636	781	907	1033	1146	1270	1387
S115 ($\mu\epsilon$)	-1	49	118	193	272	360	440	521	597	686	783
UAC-A1 ($\mu\epsilon$)	4	148	284	408	527	647	753	856	947	1046	1137
UAC-F1 ($\mu\epsilon$)	3	142	277	399	523	647	756	862	956	1061	1156
UB-A1 ($\mu\epsilon$)	-	-	-	-	-	-	-	-	-	-	-
UB-A2 ($\mu\epsilon$)	-	-	-	-	-	-	-	-	-	-	-
UB-A3 ($\mu\epsilon$)	-	-	-	-	-	-	-	-	-	-	-
UB-F1 ($\mu\epsilon$)	-	-	-	-	-	-	-	-	-	-	-
UB-F2 ($\mu\epsilon$)	-	-	-	-	-	-	-	-	-	-	-
UB-F3 ($\mu\epsilon$)	-180	-170	-165	-155	-149	-143	-139	-136	-133	-129	-126
UBC-A1 ($\mu\epsilon$)	-	-	-	-	-	-	-	-	-	-	-
UBC-A2 ($\mu\epsilon$)	-	-	-	-	-	-	-	-	-	-	-

Table F-18. Raw data, strain survey conducted after 90,000 cycles, ambient environmental conditions (Run 3) (continued)

Load Step	0	1	2	3	4	5	6	7	8	9	10
Pressure (psi)	0.02	0.67	1.35	1.98	2.65	3.35	3.99	4.69	5.31	6.02	6.70
UBC-A3 ($\mu\epsilon$)	6	189	362	511	646	779	892	998	1090	1185	1270
UBC-F1 ($\mu\epsilon$)	-	-	-	-	-	-	-	-	-	-	-
UBC-F2 ($\mu\epsilon$)	-	-	-	-	-	-	-	-	-	-	-
UBC-F3 ($\mu\epsilon$)	2	190	368	521	659	795	911	1019	1112	1208	1294
UDAC-A1 ($\mu\epsilon$)	0	161	305	428	552	675	778	881	973	1069	1159
UDAC-F1 ($\mu\epsilon$)	2	156	300	422	550	673	777	881	973	1072	1164
UDB-A1 ($\mu\epsilon$)	-	-	-	-	-	-	-	-	-	-	-
UDB-A2 ($\mu\epsilon$)	-	-	-	-	-	-	-	-	-	-	-
UDB-A3 ($\mu\epsilon$)	-1	267	488	673	840	999	1134	1261	1369	1483	1583
UDB-F1 ($\mu\epsilon$)	-	-	-	-	-	-	-	-	-	-	-
UDB-F2 ($\mu\epsilon$)	-	-	-	-	-	-	-	-	-	-	-
UDB-F3 ($\mu\epsilon$)	-1	287	530	732	921	1099	1251	1394	1513	1640	1752
UDBC-A1 ($\mu\epsilon$)	-	-	-	-	-	-	-	-	-	-	-
UDBC-A2 ($\mu\epsilon$)	-	-	-	-	-	-	-	-	-	-	-
UDBC-A3 ($\mu\epsilon$)	-140	-27	70	160	238	315	376	433	481	530	573
UDBC-F1 ($\mu\epsilon$)	-	-	-	-	-	-	-	-	-	-	-
UDBC-F2 ($\mu\epsilon$)	-	-	-	-	-	-	-	-	-	-	-
UDBC-F3 ($\mu\epsilon$)	-	-	-	-	-	-	-	-	-	-	-

F.2.2 Cold-Dry Environmental Conditions

F.2.2.1 After Hot-Wet Conditioning

Table F-19. Raw data, strain survey conducted after hot-wet conditioning, cold-dry environmental conditions (Run 1)

Load Step	0	1	2	3	4	5	6	7	8	9	10
Pressure (psi)	0.00	0.67	1.33	2.01	2.65	3.38	3.97	4.66	5.34	6.00	6.65
Frame-1 (lb _f)	4	125	202	370	520	542	650	774	933	1031	1135
Frame-2 (lb _f)	58	107	229	325	451	569	676	795	909	1020	1131
Frame-3 (lb _f)	3	107	223	343	454	567	681	796	905	1019	1134
Frame-4 (lb _f)	53	106	229	338	453	567	681	792	907	1020	1129
Frame-5 (lb _f)	9	107	229	332	457	572	665	793	902	1014	1133
Frame-6 (lb _f)	14	106	225	328	455	569	692	789	904	1015	1129
Frame-7 (lb _f)	22	109	230	337	455	564	683	791	912	1018	1134
Frame-8 (lb _f)	16	115	222	350	460	569	682	790	902	1020	1136
Frame-9 (lb _f)	38	112	221	339	451	566	681	795	906	1021	1135
Frame-10 (lb _f)	0	116	230	332	444	564	677	800	905	1017	1136
Frame-11 (lb _f)	5	110	224	335	455	569	676	797	907	1017	1133
Frame-12 (lb _f)	28	108	228	347	459	563	679	791	911	1021	1133
Hoop-1 (lb _f)	71	705	1434	2125	2845	3575	4297	5005	5709	6413	7130
Hoop-2 (lb _f)	206	746	1441	2210	2813	3576	4304	5001	5716	6435	7132
Hoop-3 (lb _f)	127	718	1442	2128	2853	3579	4289	5005	5714	6436	7140
Hoop-4 (lb _f)	51	714	1436	2139	2840	3595	4288	5000	5702	6426	7141
Hoop-5 (lb _f)	43	718	1421	2138	2855	3556	4285	4995	5724	6426	7148
Hoop-6 (lb _f)	108	718	1427	2149	2854	3590	4274	5010	5723	6426	7144

**Table F-19. Raw data, strain survey conducted after hot-wet conditioning, cold-dry environmental conditions (Run 1)
(continued)**

Load Step	0	1	2	3	4	5	6	7	8	9	10
Pressure (psi)	0.00	0.67	1.33	2.01	2.65	3.38	3.97	4.66	5.34	6.00	6.65
Hoop-7 (lbf)	-7	708	1433	2141	2858	3559	4283	4987	5721	6422	7165
Hoop-8 (lbf)	194	716	1426	2146	2860	3579	4289	4998	5715	6423	7145
Hoop-9 (lbf)	10	704	1429	2162	2856	3569	4282	5007	5711	6419	7149
Hoop-10 (lbf)	-9	730	1435	2130	2850	3595	4282	4998	5730	6423	7146
Hoop-11 (lbf)	85	728	1419	2137	2851	3563	4297	5013	5727	6430	7150
Hoop-12 (lbf)	108	728	1427	2145	2857	3580	4290	4999	5719	6417	7143
Hoop-13 (lbf)	67	694	1438	2132	2859	3586	4288	4995	5714	6427	7139
Hoop-14 (lbf)	57	723	1423	2139	2867	3572	4286	5009	5729	6429	7138
Long-1 (lbf)	-3	690	1323	1983	2664	3357	4010	4657	5317	6028	6607
Long-2 (lbf)	2	658	1338	2005	2671	3336	4004	4674	5343	6017	6672
Long-3 (lbf)	-8	663	1325	2012	2673	3341	3995	4672	5335	6012	6664
Long-4 (lbf)	-3	668	1332	2014	2676	3334	4003	4676	5343	6004	6678
Long-5 (lbf)	0	670	1332	2005	2678	3330	4014	4674	5359	5998	6680
Long-6 (lbf)	6	673	1348	2016	2670	3342	4004	4678	5351	6006	6678
Long-7 (lbf)	11	698	1320	2010	2672	3357	4009	4690	5331	5997	6708
Long-8 (lbf)	2	643	1336	2009	2671	3336	3997	4669	5334	6021	6682
F01 ($\mu\epsilon$)	297	250	304	346	380	394	443	469	506	543	600
F02 ($\mu\epsilon$)	-353	-253	-211	-156	-96	-24	19	90	149	208	253
F03 ($\mu\epsilon$)	391	259	307	346	365	371	417	426	452	475	523
F04 ($\mu\epsilon$)	-466	-321	-269	-207	-131	-37	11	95	163	233	282

**Table F-19. Raw data, strain survey conducted after hot-wet conditioning, cold-dry environmental conditions (Run 1)
(continued)**

Load Step	0	1	2	3	4	5	6	7	8	9	10
Pressure (psi)	0.00	0.67	1.33	2.01	2.65	3.38	3.97	4.66	5.34	6.00	6.65
F05 ($\mu\epsilon$)	-	-	-	-	-	-	-	-	-	-	-
F06 ($\mu\epsilon$)	-480	-332	-292	-238	-171	-87	-43	36	102	164	214
F07 ($\mu\epsilon$)	254	152	207	248	281	288	337	351	381	409	457
F08 ($\mu\epsilon$)	-276	-139	-102	-55	6	83	123	194	253	314	356
IS16 ($\mu\epsilon$)	-175	-78	2	71	137	204	267	334	400	467	534
IS17 ($\mu\epsilon$)	-6	-43	-52	-46	-28	2	38	87	136	187	247
IS18 ($\mu\epsilon$)	78	11	-22	-36	-36	-25	-2	28	64	105	151
IS19 ($\mu\epsilon$)	-195	-150	-99	-52	-6	41	88	137	186	235	286
IS20 ($\mu\epsilon$)	-287	-223	-157	-98	-44	12	63	117	168	218	268
IS21 ($\mu\epsilon$)	-274	-217	-155	-100	-48	1	49	98	144	190	235
IS22 ($\mu\epsilon$)	139	46	0	-29	-42	-43	-27	-5	26	64	107
IS23 ($\mu\epsilon$)	286	197	142	105	77	58	52	51	56	67	85
IS24 ($\mu\epsilon$)	-333	-247	-163	-87	-16	52	115	179	240	297	353
IS25 ($\mu\epsilon$)	223	139	91	62	42	32	35	42	58	78	104
IS26 ($\mu\epsilon$)	-151	1	144	275	396	513	615	719	816	907	993
IS27 ($\mu\epsilon$)	284	200	159	138	127	124	135	151	176	205	240
IS28 ($\mu\epsilon$)	-128	13	146	271	385	494	589	688	781	867	950
IS29 ($\mu\epsilon$)	-203	-70	56	170	275	373	462	554	641	722	801
IS30 ($\mu\epsilon$)	-	-	-	-	-	-	-	-	-	-	-
IS31 ($\mu\epsilon$)	-13	69	151	226	299	370	436	504	570	634	693

**Table F-19. Raw data, strain survey conducted after hot-wet conditioning, cold-dry environmental conditions (Run 1)
(continued)**

Load Step	0	1	2	3	4	5	6	7	8	9	10
Pressure (psi)	0.00	0.67	1.33	2.01	2.65	3.38	3.97	4.66	5.34	6.00	6.65
IS32 ($\mu\epsilon$)	44	126	204	274	340	401	458	514	568	618	658
IS33 ($\mu\epsilon$)	55	141	223	298	366	430	491	551	608	659	701
IS34 ($\mu\epsilon$)	144	111	92	84	82	88	104	125	152	183	220
IS35 ($\mu\epsilon$)	481	394	325	273	229	192	171	153	142	137	139
IS36 ($\mu\epsilon$)	75	163	246	321	390	457	516	576	633	685	734
IS37 ($\mu\epsilon$)	388	291	219	166	121	87	69	54	48	49	57
IS38 ($\mu\epsilon$)	109	212	308	397	480	558	629	700	767	830	891
IS39 ($\mu\epsilon$)	383	275	203	152	112	83	73	67	70	81	99
IS40 ($\mu\epsilon$)	111	215	313	406	492	574	648	723	794	861	926
IS41 ($\mu\epsilon$)	-90	31	144	248	345	436	516	599	679	753	826
IS42 ($\mu\epsilon$)	-131	-20	83	167	247	327	398	475	546	613	684
IS43 ($\mu\epsilon$)	-101	-60	-7	43	100	162	223	291	357	424	492
IS44 ($\mu\epsilon$)	-174	-186	-175	-155	-126	-86	-45	6	57	111	168
IS45 ($\mu\epsilon$)	-65	7	75	138	201	263	319	378	434	489	541
IS46 ($\mu\epsilon$)	-57	23	99	167	233	299	356	416	473	526	578
IS47 ($\mu\epsilon$)	-79	-3	69	135	198	261	317	376	431	484	535
IS48 ($\mu\epsilon$)	-70	-69	-41	-8	34	83	136	195	257	320	385
IS49 ($\mu\epsilon$)	-82	-123	-148	-161	-165	-161	-149	-131	-110	-85	-57
IS50 ($\mu\epsilon$)	-71	19	101	175	246	316	376	440	500	557	610
IS51 ($\mu\epsilon$)	-107	-141	-160	-168	-166	-157	-141	-119	-95	-68	-37

**Table F-19. Raw data, strain survey conducted after hot-wet conditioning, cold-dry environmental conditions (Run 1)
(continued)**

Load Step	0	1	2	3	4	5	6	7	8	9	10
Pressure (psi)	0.00	0.67	1.33	2.01	2.65	3.38	3.97	4.66	5.34	6.00	6.65
IS52 ($\mu\epsilon$)	-70	49	157	257	353	448	530	616	697	773	846
IS53 ($\mu\epsilon$)	-154	-181	-190	-185	-171	-149	-121	-86	-47	-8	35
IS54 ($\mu\epsilon$)	-70	41	143	236	326	414	491	572	649	722	792
IS55 ($\mu\epsilon$)	-57	39	131	212	290	366	436	508	577	644	710
IS56 ($\mu\epsilon$)	-126	-33	42	108	170	232	291	353	414	476	539
IS57 ($\mu\epsilon$)	41	16	12	21	40	68	103	144	190	241	296
IS58 ($\mu\epsilon$)	181	103	61	40	34	38	56	80	112	150	194
IS59 ($\mu\epsilon$)	-195	-142	-86	-36	13	62	111	162	213	263	316
IS60 ($\mu\epsilon$)	-252	-181	-113	-53	3	57	108	161	212	259	309
IS61 ($\mu\epsilon$)	-262	-195	-129	-72	-20	32	82	131	180	226	272
IS62 ($\mu\epsilon$)	116	30	-11	-30	-37	-30	-10	16	52	90	136
IS63 ($\mu\epsilon$)	348	262	206	168	139	117	110	105	108	115	131
IS64 ($\mu\epsilon$)	-270	-175	-85	-6	68	137	201	266	327	383	440
IS65 ($\mu\epsilon$)	364	309	284	273	270	274	289	308	333	362	397
IS66 ($\mu\epsilon$)	-7	157	310	448	576	698	803	909	1009	1100	1188
IS67 ($\mu\epsilon$)	276	231	219	219	226	240	263	292	327	363	406
IS68 ($\mu\epsilon$)	-25	123	262	388	505	617	715	815	909	994	1078
IS69 ($\mu\epsilon$)	-93	39	163	275	377	474	561	650	735	813	890
IS70 ($\mu\epsilon$)	-258	-161	-81	-15	46	106	165	226	286	346	409
IS71 ($\mu\epsilon$)	-108	-111	-82	-46	-2	48	103	165	227	289	355

**Table F-19. Raw data, strain survey conducted after hot-wet conditioning, cold-dry environmental conditions (Run 1)
(continued)**

Load Step	0	1	2	3	4	5	6	7	8	9	10
Pressure (psi)	0.00	0.67	1.33	2.01	2.65	3.38	3.97	4.66	5.34	6.00	6.65
IS72 ($\mu\epsilon$)	-31	-61	-52	-28	6	48	96	150	208	266	327
IS73 ($\mu\epsilon$)	57	124	194	262	327	391	449	510	568	621	673
IS74 ($\mu\epsilon$)	-37	38	112	181	247	312	370	431	489	542	594
IS75 ($\mu\epsilon$)	2	79	154	226	293	360	420	482	541	596	648
IS76 ($\mu\epsilon$)	-7	-15	12	52	99	154	211	275	341	407	475
IS77 ($\mu\epsilon$)	31	-50	-83	-91	-88	-77	-57	-31	0	32	69
IS78 ($\mu\epsilon$)	-11	72	153	229	301	372	435	500	563	621	677
IS79 ($\mu\epsilon$)	-28	-110	-142	-151	-148	-137	-118	-94	-64	-32	3
IS80 ($\mu\epsilon$)	30	124	217	306	391	476	551	629	704	775	841
IS81 ($\mu\epsilon$)	16	-66	-95	-103	-100	-89	-68	-44	-12	20	55
IS82 ($\mu\epsilon$)	-33	51	135	216	293	371	441	513	584	651	715
IS83 ($\mu\epsilon$)	44	123	204	278	347	417	480	546	611	672	733
IS84 ($\mu\epsilon$)	-76	-5	69	136	201	268	331	397	462	527	593
IS85 ($\mu\epsilon$)	-76	-51	-4	50	108	173	238	308	379	449	522
IS86 ($\mu\epsilon$)	-94	-95	-70	-36	5	54	105	163	223	283	346
IS87 ($\mu\epsilon$)	-24	37	97	149	200	251	297	345	393	437	481
IS88 ($\mu\epsilon$)	-39	27	90	145	196	248	293	340	384	426	467
IS89 ($\mu\epsilon$)	-46	16	75	129	177	225	270	316	359	399	441
IS90 ($\mu\epsilon$)	-94	-90	-66	-32	8	57	110	169	231	292	357
IS91 ($\mu\epsilon$)	-72	-94	-102	-101	-94	-81	-61	-37	-9	21	55

**Table F-19. Raw data, strain survey conducted after hot-wet conditioning, cold-dry environmental conditions (Run 1)
(continued)**

Load Step	0	1	2	3	4	5	6	7	8	9	10
Pressure (psi)	0.00	0.67	1.33	2.01	2.65	3.38	3.97	4.66	5.34	6.00	6.65
IS92 ($\mu\epsilon$)	-42	37	110	173	231	289	340	391	441	486	532
IS93 ($\mu\epsilon$)	-98	-100	-88	-67	-42	-10	26	67	111	155	204
IS94 ($\mu\epsilon$)	-78	41	152	253	350	446	529	617	698	775	848
IS95 ($\mu\epsilon$)	-82	-72	-48	-18	14	51	92	137	183	228	278
IS96 ($\mu\epsilon$)	-93	14	113	205	291	376	453	532	606	676	745
IS97 ($\mu\epsilon$)	-26	76	168	252	330	408	479	551	620	686	753
L01 ($\mu\epsilon$)	-	-	-	-	-	-	-	-	-	-	-
L02 ($\mu\epsilon$)	162	185	190	201	215	229	243	258	273	288	301
L03 ($\mu\epsilon$)	34	45	39	46	55	67	79	96	111	127	141
L04 ($\mu\epsilon$)	84	107	116	131	148	166	182	202	219	237	252
L05 ($\mu\epsilon$)	69	88	96	105	114	124	134	144	152	160	168
L06 ($\mu\epsilon$)	42	71	89	106	122	136	156	171	184	197	212
L07 ($\mu\epsilon$)	-	-	-	-	-	-	-	-	-	-	-
L08 ($\mu\epsilon$)	181	233	263	297	326	355	381	409	433	459	480
L09 ($\mu\epsilon$)	75	131	165	201	230	263	293	321	345	369	392
L10 ($\mu\epsilon$)	-	-	-	-	-	-	-	-	-	-	-
RAC-A1 ($\mu\epsilon$)	-20	83	183	279	373	468	551	641	725	805	881
RAC-A2 ($\mu\epsilon$)	-43	50	142	228	312	396	471	549	624	694	762
RAC-A3 ($\mu\epsilon$)	26	107	185	259	326	395	456	519	580	638	693
RAC-F1 ($\mu\epsilon$)	-70	28	123	218	308	397	478	562	642	717	789

F-160

**Table F-19. Raw data, strain survey conducted after hot-wet conditioning, cold-dry environmental conditions (Run 1)
(continued)**

Load Step	0	1	2	3	4	5	6	7	8	9	10
Pressure (psi)	0.00	0.67	1.33	2.01	2.65	3.38	3.97	4.66	5.34	6.00	6.65
RAC-F2 ($\mu\epsilon$)	-51	39	126	213	294	374	447	523	595	663	728
RBC-A1 ($\mu\epsilon$)	212	351	476	589	692	790	874	959	1038	1110	1180
RBC-A2 ($\mu\epsilon$)	133	255	364	463	553	637	711	784	854	916	977
RBC-A3 ($\mu\epsilon$)	146	261	365	460	547	628	700	771	839	901	960
RBC-A4 ($\mu\epsilon$)	51	162	263	357	443	525	597	670	739	802	864
RBC-F1 ($\mu\epsilon$)	216	359	481	590	691	786	868	948	1023	1093	1160
RBC-F2 ($\mu\epsilon$)	178	308	419	517	607	693	766	838	906	968	1027
RBC-F3 ($\mu\epsilon$)	159	288	396	492	581	664	737	808	875	936	993
S16 ($\mu\epsilon$)	-314	-264	-199	-135	-70	-4	60	128	195	261	328
S17 ($\mu\epsilon$)	-	-	-	-	-	-	-	-	-	-	-
S18 ($\mu\epsilon$)	-558	-375	-219	-91	23	129	221	315	402	485	565
S20 ($\mu\epsilon$)	38	-332	-655	-944	-1209	-1457	-1660	-1858	-2030	-2186	-2318
S22 ($\mu\epsilon$)	-445	-281	-139	-21	85	184	272	360	442	519	594
S25 ($\mu\epsilon$)	-678	-472	-291	-133	17	165	294	429	555	674	789
S29 ($\mu\epsilon$)	44	87	136	188	243	303	358	418	478	537	596
S30 ($\mu\epsilon$)	-225	-82	56	178	290	398	492	588	676	762	844
S32 ($\mu\epsilon$)	507	344	215	95	-15	-119	-204	-290	-366	-433	-278
S34 ($\mu\epsilon$)	-270	-142	-10	106	215	322	416	511	602	688	771
S37 ($\mu\epsilon$)	-488	-286	-94	73	230	383	515	651	777	897	1014
S41 ($\mu\epsilon$)	59	125	192	261	330	403	469	539	607	672	735

**Table F-19. Raw data, strain survey conducted after hot-wet conditioning, cold-dry environmental conditions (Run 1)
(continued)**

Load Step	0	1	2	3	4	5	6	7	8	9	10
Pressure (psi)	0.00	0.67	1.33	2.01	2.65	3.38	3.97	4.66	5.34	6.00	6.65
S42 ($\mu\epsilon$)	-183	-141	-81	-23	42	112	177	249	319	388	457
S43 ($\mu\epsilon$)	-338	-241	-142	-56	30	116	192	274	352	426	498
S44 ($\mu\epsilon$)	-106	32	158	267	370	471	557	648	733	815	892
S46 ($\mu\epsilon$)	-293	-586	-838	-1070	-1290	-1505	-1683	-1864	-2030	-2181	-2321
S48 ($\mu\epsilon$)	-132	-4	111	212	307	400	480	565	644	720	795
S51 ($\mu\epsilon$)	-144	39	211	363	506	648	768	895	1015	1130	1241
S55 ($\mu\epsilon$)	-159	-95	-28	38	107	176	239	308	374	439	502
S56 ($\mu\epsilon$)	-266	-213	-147	-82	-17	50	114	184	252	321	390
S57 ($\mu\epsilon$)	-	-	-	-	-	-	-	-	-	-	-
S58 ($\mu\epsilon$)	-619	-415	-246	-107	15	129	229	328	420	508	592
S60 ($\mu\epsilon$)	-44	-472	-839	-1167	-1470	-1753	-1986	-2217	-2425	-2609	-2775
S62 ($\mu\epsilon$)	-485	-303	-156	-33	73	175	263	352	434	511	587
S65 ($\mu\epsilon$)	-635	-422	-239	-77	74	222	349	482	605	720	832
S69 ($\mu\epsilon$)	-145	-82	-19	45	110	177	239	307	373	437	500
S70 ($\mu\epsilon$)	5	54	119	186	254	327	394	467	541	612	683
S71 ($\mu\epsilon$)	-	-	-	-	-	-	-	-	-	-	-
S72 ($\mu\epsilon$)	-119	63	205	321	425	526	613	701	785	866	944
S74 ($\mu\epsilon$)	-169	-332	-478	-626	-768	-909	-1029	-1157	-1275	-1387	-1489
S76 ($\mu\epsilon$)	-162	8	143	256	357	455	539	627	709	788	864
S79 ($\mu\epsilon$)	-111	129	321	478	620	761	879	1002	1118	1227	1332

**Table F-19. Raw data, strain survey conducted after hot-wet conditioning, cold-dry environmental conditions (Run 1)
(continued)**

Load Step	0	1	2	3	4	5	6	7	8	9	10
Pressure (psi)	0.00	0.67	1.33	2.01	2.65	3.38	3.97	4.66	5.34	6.00	6.65
S83 ($\mu\epsilon$)	-85	14	95	168	237	307	368	434	497	558	618
S84 ($\mu\epsilon$)	-174	-109	-39	27	97	169	237	315	387	457	529
S85 ($\mu\epsilon$)	-	-	-	-	-	-	-	-	-	-	-
S86 ($\mu\epsilon$)	-152	-15	103	203	296	385	464	547	626	700	774
S88 ($\mu\epsilon$)	-233	-337	-420	-490	-552	-608	-647	-685	-713	-734	-748
S90 ($\mu\epsilon$)	-148	-16	99	199	290	377	453	533	609	683	755
S93 ($\mu\epsilon$)	-247	-83	70	204	331	457	566	680	789	893	993
S97 ($\mu\epsilon$)	-196	-119	-48	21	89	158	220	286	350	413	475
UAC-A1 ($\mu\epsilon$)	-108	33	163	283	398	511	607	707	800	888	971
UAC-A2 ($\mu\epsilon$)	-54	76	193	301	402	501	586	675	759	835	911
UAC-A3 ($\mu\epsilon$)	-91	17	116	204	288	369	440	514	583	649	712
UAC-F1 ($\mu\epsilon$)	-88	49	175	292	405	517	614	714	807	895	978
UAC-F2 ($\mu\epsilon$)	-96	25	136	237	334	430	513	598	678	753	825
UBC-A1 ($\mu\epsilon$)	26	236	431	607	767	920	1050	1181	1301	1411	1514
UBC-A2 ($\mu\epsilon$)	-56	119	281	429	563	689	798	907	1008	1100	1186
UBC-A3 ($\mu\epsilon$)	-89	73	223	359	482	598	698	798	892	977	1057
UBC-A4 ($\mu\epsilon$)	-115	35	174	299	414	521	614	709	798	880	958
UBC-F1 ($\mu\epsilon$)	-3	210	402	576	736	886	1016	1145	1264	1373	1475
UBC-F2 ($\mu\epsilon$)	-76	103	266	412	546	672	780	889	989	1081	1165
UBC-F3 ($\mu\epsilon$)	-71	97	247	383	508	625	726	827	921	1007	1086

**Table F-19. Raw data, strain survey conducted after hot-wet conditioning, cold-dry environmental conditions (Run 1)
(continued)**

Load Step	0	1	2	3	4	5	6	7	8	9	10
Pressure (psi)	0.00	0.67	1.33	2.01	2.65	3.38	3.97	4.66	5.34	6.00	6.65
UDAC-A1 ($\mu\epsilon$)	-58	75	198	313	421	528	620	716	804	886	965
UDAC-A2 ($\mu\epsilon$)	-52	68	177	278	371	464	545	628	705	777	846
UDAC-A3 ($\mu\epsilon$)	-45	59	152	238	316	394	463	533	599	661	722
UDAC-F1 ($\mu\epsilon$)	-50	83	207	323	434	544	638	736	826	910	991
UDAC-F2 ($\mu\epsilon$)	-48	65	171	270	364	457	537	621	697	769	839
UDBC-A1 ($\mu\epsilon$)	67	279	470	640	796	942	1065	1188	1302	1404	1500
UDBC-A2 ($\mu\epsilon$)	28	207	369	514	647	771	876	981	1080	1168	1250
UDBC-A3 ($\mu\epsilon$)	19	186	338	473	597	712	810	909	1002	1084	1161
UDBC-A4 ($\mu\epsilon$)	-55	98	238	363	477	584	677	770	857	934	1008
UDBC-F1 ($\mu\epsilon$)	45	281	492	680	851	1009	1144	1279	1403	1514	1619
UDBC-F2 ($\mu\epsilon$)	-11	183	357	512	653	784	895	1006	1108	1200	1287
UDBC-F3 ($\mu\epsilon$)	-44	137	300	445	577	697	801	904	999	1085	1167

Table F-20. Raw data, strain survey conducted after hot-wet conditioning, cold-dry environmental conditions (Run 2)

Load Step	0	1	2	3	4	5	6	7	8	9	10
Pressure (psi)	-0.10	0.65	1.35	1.96	2.65	3.35	3.98	4.68	5.33	6.03	6.68
Frame-1 (lbf)	6	137	256	325	480	575	656	819	912	998	1157
Frame-2 (lbf)	58	115	221	337	458	565	680	793	907	1020	1133
Frame-3 (lbf)	3	115	231	336	453	569	676	792	909	1014	1132
Frame-4 (lbf)	43	119	221	343	455	567	680	797	908	1020	1133
Frame-5 (lbf)	13	111	230	336	459	549	682	793	906	1022	1127
Frame-6 (lbf)	0	116	244	347	454	579	684	782	909	1007	1136
Frame-7 (lbf)	25	108	231	335	451	567	678	793	903	1017	1132
Frame-8 (lbf)	22	118	219	338	454	567	684	791	903	1018	1128
Frame-9 (lbf)	36	116	228	339	451	568	681	792	906	1020	1133
Frame-10 (lbf)	1	125	224	338	463	563	685	793	906	1020	1132
Frame-11 (lbf)	2	106	229	340	455	567	678	791	904	1022	1139
Frame-12 (lbf)	28	111	223	341	457	569	680	794	908	1017	1134
Hoop-1 (lbf)	61	709	1422	2142	2847	3565	4290	5001	5696	6421	7143
Hoop-2 (lbf)	207	746	1461	2170	2869	3558	4273	4972	5723	6438	7126
Hoop-3 (lbf)	107	708	1445	2153	2851	3575	4271	5003	5713	6422	7144
Hoop-4 (lbf)	51	704	1429	2148	2844	3562	4277	4994	5725	6418	7166
Hoop-5 (lbf)	39	708	1436	2137	2864	3587	4287	4992	5718	6427	7144
Hoop-6 (lbf)	49	713	1432	2132	2856	3567	4285	4989	5698	6428	7146
Hoop-7 (lbf)	-7	713	1443	2136	2844	3572	4271	4999	5723	6421	7154
Hoop-8 (lbf)	226	717	1441	2142	2852	3563	4270	4995	5714	6424	7144
Hoop-9 (lbf)	35	718	1447	2135	2855	3580	4289	5004	5716	6437	7151

**Table F-20. Raw data, strain survey conducted after hot-wet conditioning, cold-dry environmental conditions (Run 2)
(continued)**

Load Step	0	1	2	3	4	5	6	7	8	9	10
Pressure (psi)	-0.10	0.65	1.35	1.96	2.65	3.35	3.98	4.68	5.33	6.03	6.68
Hoop-10 (lb _f)	-24	705	1453	2128	2858	3580	4274	5004	5717	6429	7145
Hoop-11 (lb _f)	60	725	1471	2147	2841	3576	4281	5000	5729	6430	7144
Hoop-12 (lb _f)	113	696	1422	2134	2866	3574	4268	4997	5714	6425	7150
Hoop-13 (lb _f)	56	709	1427	2123	2846	3563	4275	4991	5706	6426	7140
Hoop-14 (lb _f)	24	710	1445	2138	2859	3571	4278	5003	5712	6417	7134
Long-1 (lb _f)	19	647	1358	2017	2617	3358	3983	4653	5325	5992	6707
Long-2 (lb _f)	0	677	1330	2001	2674	3338	4006	4671	5356	6015	6670
Long-3 (lb _f)	12	670	1330	2002	2673	3334	4008	4672	5349	6006	6666
Long-4 (lb _f)	-3	668	1319	2011	2671	3333	4008	4676	5341	6009	6678
Long-5 (lb _f)	2	664	1330	2009	2658	3337	4010	4669	5353	6003	6679
Long-6 (lb _f)	18	675	1335	2000	2669	3322	4004	4668	5361	6002	6676
Long-7 (lb _f)	-9	657	1323	1997	2663	3319	4033	4640	5336	5939	6678
Long-8 (lb _f)	-2	688	1338	2008	2670	3338	4025	4667	5334	5991	6675
F01 (μ ϵ)	333	255	279	332	363	385	430	454	498	531	568
F02 (μ ϵ)	-381	-255	-207	-153	-87	-27	29	101	156	221	276
F03 (μ ϵ)	444	277	293	335	351	370	399	407	440	455	481
F04 (μ ϵ)	-510	-328	-259	-201	-124	-39	22	111	176	253	320
F05 (μ ϵ)	-	-	-	-	-	-	-	-	-	-	-
F06 (μ ϵ)	-535	-355	-290	-239	-167	-96	-38	41	100	174	234
F07 (μ ϵ)	307	174	202	250	274	299	330	346	382	401	432

**Table F-20. Raw data, strain survey conducted after hot-wet conditioning, cold-dry environmental conditions (Run 2)
(continued)**

Load Step	0	1	2	3	4	5	6	7	8	9	10
Pressure (psi)	-0.10	0.65	1.35	1.96	2.65	3.35	3.98	4.68	5.33	6.03	6.68
F08 ($\mu\epsilon$)	-314	-153	-98	-53	9	77	128	201	256	322	378
IS16 ($\mu\epsilon$)	-183	-81	1	67	134	201	263	331	397	465	534
IS17 ($\mu\epsilon$)	-2	-45	-55	-48	-29	2	35	83	133	188	245
IS18 ($\mu\epsilon$)	84	7	-26	-39	-38	-25	-4	26	62	103	150
IS19 ($\mu\epsilon$)	-205	-162	-105	-59	-12	37	82	132	181	231	284
IS20 ($\mu\epsilon$)	-298	-236	-165	-107	-51	6	57	111	162	214	266
IS21 ($\mu\epsilon$)	-282	-228	-161	-108	-56	-4	42	93	139	186	233
IS22 ($\mu\epsilon$)	157	48	-3	-30	-43	-42	-30	-6	23	61	106
IS23 ($\mu\epsilon$)	292	193	137	101	74	58	49	48	54	65	81
IS24 ($\mu\epsilon$)	-345	-259	-167	-94	-21	48	110	175	234	294	352
IS25 ($\mu\epsilon$)	235	137	90	60	43	33	34	42	55	76	101
IS26 ($\mu\epsilon$)	-162	-1	153	278	400	515	615	721	813	905	994
IS27 ($\mu\epsilon$)	299	201	159	136	126	123	134	150	173	203	237
IS28 ($\mu\epsilon$)	-141	10	154	271	386	495	590	689	778	866	950
IS29 ($\mu\epsilon$)	-216	-75	61	168	272	372	460	553	635	719	802
IS30 ($\mu\epsilon$)	-	-	-	-	-	-	-	-	-	-	-
IS31 ($\mu\epsilon$)	-18	61	148	220	292	363	428	499	562	628	692
IS32 ($\mu\epsilon$)	34	115	196	263	328	390	446	504	555	607	656
IS33 ($\mu\epsilon$)	44	131	214	286	353	418	478	538	592	647	699
IS34 ($\mu\epsilon$)	148	108	87	80	77	84	99	121	147	180	217

**Table F-20. Raw data, strain survey conducted after hot-wet conditioning, cold-dry environmental conditions (Run 2)
(continued)**

Load Step	0	1	2	3	4	5	6	7	8	9	10
Pressure (psi)	-0.10	0.65	1.35	1.96	2.65	3.35	3.98	4.68	5.33	6.03	6.68
IS35 ($\mu\epsilon$)	487	391	319	267	223	189	166	148	137	133	135
IS36 ($\mu\epsilon$)	69	156	244	315	385	451	510	572	626	681	733
IS37 ($\mu\epsilon$)	401	291	217	163	120	86	66	51	45	46	54
IS38 ($\mu\epsilon$)	108	211	314	398	480	559	629	701	766	830	892
IS39 ($\mu\epsilon$)	401	275	199	147	108	81	69	64	67	78	99
IS40 ($\mu\epsilon$)	108	213	318	406	491	574	647	724	792	860	927
IS41 ($\mu\epsilon$)	-96	28	147	245	341	434	514	600	677	753	826
IS42 ($\mu\epsilon$)	-141	-21	84	161	239	320	388	466	534	610	681
IS43 ($\mu\epsilon$)	-104	-64	-7	39	95	159	217	287	349	421	490
IS44 ($\mu\epsilon$)	-172	-191	-177	-159	-130	-89	-49	2	50	108	165
IS45 ($\mu\epsilon$)	-72	0	77	137	199	261	316	377	429	486	539
IS46 ($\mu\epsilon$)	-64	17	100	166	232	297	354	415	469	524	577
IS47 ($\mu\epsilon$)	-84	-7	71	134	198	261	316	376	429	483	535
IS48 ($\mu\epsilon$)	-64	-73	-44	-11	32	82	132	193	252	317	385
IS49 ($\mu\epsilon$)	-79	-128	-149	-163	-167	-162	-152	-136	-116	-89	-60
IS50 ($\mu\epsilon$)	-78	14	104	174	245	314	375	440	497	554	609
IS51 ($\mu\epsilon$)	-101	-142	-158	-167	-165	-155	-143	-121	-101	-71	-39
IS52 ($\mu\epsilon$)	-79	47	164	259	355	447	529	616	693	771	847
IS53 ($\mu\epsilon$)	-150	-185	-191	-188	-174	-150	-125	-90	-56	-13	32
IS54 ($\mu\epsilon$)	-79	37	147	237	327	414	491	573	646	719	791

**Table F-20. Raw data, strain survey conducted after hot-wet conditioning, cold-dry environmental conditions (Run 2)
(continued)**

Load Step	0	1	2	3	4	5	6	7	8	9	10
Pressure (psi)	-0.10	0.65	1.35	1.96	2.65	3.35	3.98	4.68	5.33	6.03	6.68
IS55 ($\mu\epsilon$)	-62	34	133	211	290	366	434	506	573	640	707
IS56 ($\mu\epsilon$)	-131	-32	44	108	170	231	290	353	413	476	541
IS57 ($\mu\epsilon$)	45	13	9	19	38	66	101	145	190	240	295
IS58 ($\mu\epsilon$)	188	100	56	37	32	38	54	80	112	150	193
IS59 ($\mu\epsilon$)	-204	-150	-90	-39	10	60	108	160	211	263	317
IS60 ($\mu\epsilon$)	-263	-191	-118	-58	-2	54	104	157	207	258	309
IS61 ($\mu\epsilon$)	-272	-204	-133	-77	-22	30	78	128	176	223	272
IS62 ($\mu\epsilon$)	130	29	-15	-33	-38	-31	-13	16	50	89	137
IS63 ($\mu\epsilon$)	356	259	202	165	137	118	109	106	107	116	129
IS64 ($\mu\epsilon$)	-282	-183	-88	-10	64	134	197	263	323	382	440
IS65 ($\mu\epsilon$)	376	309	283	271	269	275	289	309	333	362	396
IS66 ($\mu\epsilon$)	-22	155	316	449	576	696	803	911	1007	1100	1190
IS67 ($\mu\epsilon$)	289	232	218	217	224	240	263	293	324	363	406
IS68 ($\mu\epsilon$)	-40	120	267	387	505	616	714	816	905	994	1079
IS69 ($\mu\epsilon$)	-109	34	165	272	374	472	559	649	729	811	891
IS70 ($\mu\epsilon$)	-257	-163	-85	-21	40	101	160	223	284	346	411
IS71 ($\mu\epsilon$)	-99	-113	-87	-50	-6	46	103	165	226	289	359
IS72 ($\mu\epsilon$)	-21	-66	-57	-32	3	46	94	149	205	264	328
IS73 ($\mu\epsilon$)	55	120	196	260	326	390	448	510	566	621	675
IS74 ($\mu\epsilon$)	-37	35	113	179	247	312	369	432	487	542	597

**Table F-20. Raw data, strain survey conducted after hot-wet conditioning, cold-dry environmental conditions (Run 2)
(continued)**

Load Step	0	1	2	3	4	5	6	7	8	9	10
Pressure (psi)	-0.10	0.65	1.35	1.96	2.65	3.35	3.98	4.68	5.33	6.03	6.68
IS75 ($\mu\epsilon$)	1	77	157	225	293	359	419	482	538	595	650
IS76 ($\mu\epsilon$)	0	-17	12	50	98	153	211	275	339	406	477
IS77 ($\mu\epsilon$)	49	-52	-85	-93	-89	-78	-58	-31	-3	31	69
IS78 ($\mu\epsilon$)	-15	67	153	226	299	370	433	501	560	620	678
IS79 ($\mu\epsilon$)	-7	-111	-144	-152	-149	-138	-118	-93	-65	-33	3
IS80 ($\mu\epsilon$)	26	121	220	304	391	474	549	630	702	773	843
IS81 ($\mu\epsilon$)	37	-68	-98	-107	-103	-91	-71	-44	-16	17	54
IS82 ($\mu\epsilon$)	-36	48	137	213	292	368	439	514	582	650	716
IS83 ($\mu\epsilon$)	38	118	203	272	342	413	477	545	605	667	730
IS84 ($\mu\epsilon$)	-65	-6	69	132	197	265	327	395	459	526	593
IS85 ($\mu\epsilon$)	-72	-57	-5	45	104	171	234	306	374	447	521
IS86 ($\mu\epsilon$)	-92	-99	-72	-40	1	52	102	162	218	282	345
IS87 ($\mu\epsilon$)	-34	29	94	144	195	247	293	343	388	435	481
IS88 ($\mu\epsilon$)	-47	19	86	138	190	242	287	336	380	424	467
IS89 ($\mu\epsilon$)	-54	8	71	121	170	220	264	312	353	398	440
IS90 ($\mu\epsilon$)	-96	-95	-68	-36	5	56	107	168	226	292	357
IS91 ($\mu\epsilon$)	-79	-101	-104	-104	-96	-81	-63	-38	-12	19	54
IS92 ($\mu\epsilon$)	-49	31	108	168	227	284	335	389	437	485	532
IS93 ($\mu\epsilon$)	-101	-101	-85	-66	-41	-7	26	68	109	154	204
IS94 ($\mu\epsilon$)	-80	44	161	258	354	449	531	619	696	775	851

**Table F-20. Raw data, strain survey conducted after hot-wet conditioning, cold-dry environmental conditions (Run 2)
(continued)**

Load Step	0	1	2	3	4	5	6	7	8	9	10
Pressure (psi)	-0.10	0.65	1.35	1.96	2.65	3.35	3.98	4.68	5.33	6.03	6.68
IS95 ($\mu\epsilon$)	-80	-70	-44	-16	15	54	92	137	180	228	277
IS96 ($\mu\epsilon$)	-96	16	121	208	294	378	454	533	604	677	746
IS97 ($\mu\epsilon$)	-31	75	174	253	332	409	478	551	617	686	752
L01 ($\mu\epsilon$)	-	-	-	-	-	-	-	-	-	-	-
L02 ($\mu\epsilon$)	150	185	194	205	218	232	245	261	275	290	306
L03 ($\mu\epsilon$)	13	41	38	46	55	67	80	96	111	129	147
L04 ($\mu\epsilon$)	65	105	117	131	148	165	182	201	220	240	259
L05 ($\mu\epsilon$)	60	91	98	109	117	126	135	145	153	164	172
L06 ($\mu\epsilon$)	37	76	92	111	126	141	159	173	187	201	213
L07 ($\mu\epsilon$)	-	-	-	-	-	-	-	-	-	-	-
L08 ($\mu\epsilon$)	161	231	264	297	329	357	380	408	434	461	486
L09 ($\mu\epsilon$)	58	132	164	203	230	260	292	317	343	373	393
L10 ($\mu\epsilon$)	-	-	-	-	-	-	-	-	-	-	-
RAC-A1 ($\mu\epsilon$)	-23	83	189	281	376	468	552	643	724	805	884
RAC-A2 ($\mu\epsilon$)	-48	48	145	226	312	394	468	550	620	693	764
RAC-A3 ($\mu\epsilon$)	22	104	187	256	325	393	454	519	577	635	693
RAC-F1 ($\mu\epsilon$)	-75	25	127	217	308	397	477	563	639	717	792
RAC-F2 ($\mu\epsilon$)	-55	35	129	211	293	374	446	524	592	663	731
RBC-A1 ($\mu\epsilon$)	213	358	490	596	700	797	880	967	1041	1113	1184
RBC-A2 ($\mu\epsilon$)	131	256	372	465	555	640	713	788	854	917	979

**Table F-20. Raw data, strain survey conducted after hot-wet conditioning, cold-dry environmental conditions (Run 2)
(continued)**

Load Step	0	1	2	3	4	5	6	7	8	9	10
Pressure (psi)	-0.10	0.65	1.35	1.96	2.65	3.35	3.98	4.68	5.33	6.03	6.68
RBC-A3 ($\mu\epsilon$)	141	259	370	459	546	629	700	774	838	901	962
RBC-A4 ($\mu\epsilon$)	47	160	268	356	442	525	597	671	737	802	865
RBC-F1 ($\mu\epsilon$)	214	363	493	596	696	790	871	954	1026	1096	1161
RBC-F2 ($\mu\epsilon$)	173	309	426	519	609	693	766	841	906	968	1028
RBC-F3 ($\mu\epsilon$)	152	286	401	492	581	663	735	808	873	935	994
S16 ($\mu\epsilon$)	-311	-263	-192	-129	-64	2	63	131	196	263	332
S17 ($\mu\epsilon$)	-	-	-	-	-	-	-	-	-	-	-
S18 ($\mu\epsilon$)	-567	-376	-212	-88	26	132	222	316	402	486	569
S20 ($\mu\epsilon$)	94	-319	-666	-940	-1204	-1446	-1650	-1851	-2021	-2178	-2319
S22 ($\mu\epsilon$)	-451	-283	-133	-19	89	188	272	362	440	520	598
S25 ($\mu\epsilon$)	-689	-475	-285	-130	21	166	294	430	553	676	795
S29 ($\mu\epsilon$)	43	87	138	189	245	303	359	420	478	538	599
S30 ($\mu\epsilon$)	-225	-82	66	183	296	401	492	589	676	763	847
S32 ($\mu\epsilon$)	656	496	366	261	159	66	-13	-93	-159	-222	-279
S34 ($\mu\epsilon$)	-266	-141	-5	108	217	321	415	512	599	687	774
S37 ($\mu\epsilon$)	-493	-288	-84	79	236	385	516	654	777	900	1018
S41 ($\mu\epsilon$)	49	123	194	262	333	404	470	541	606	672	737
S42 ($\mu\epsilon$)	-184	-142	-77	-20	45	115	176	250	314	386	457
S43 ($\mu\epsilon$)	-340	-238	-133	-50	34	119	191	275	346	425	500
S44 ($\mu\epsilon$)	-113	34	166	270	372	472	556	649	728	813	894

**Table F-20. Raw data, strain survey conducted after hot-wet conditioning, cold-dry environmental conditions (Run 2)
(continued)**

Load Step	0	1	2	3	4	5	6	7	8	9	10
Pressure (psi)	-0.10	0.65	1.35	1.96	2.65	3.35	3.98	4.68	5.33	6.03	6.68
S46 ($\mu\epsilon$)	-271	-594	-861	-1083	-1306	-1512	-1691	-1874	-2032	-2186	-2329
S48 ($\mu\epsilon$)	-132	-2	118	215	310	402	480	566	642	720	796
S51 ($\mu\epsilon$)	-155	37	217	363	505	644	767	896	1011	1129	1242
S55 ($\mu\epsilon$)	-163	-97	-25	39	106	176	238	307	370	437	502
S56 ($\mu\epsilon$)	-267	-216	-143	-78	-11	56	119	188	255	324	394
S57 ($\mu\epsilon$)	-	-	-	-	-	-	-	-	-	-	-
S58 ($\mu\epsilon$)	-631	-414	-237	-100	24	135	232	332	422	511	597
S60 ($\mu\epsilon$)	26	-445	-841	-1155	-1459	-1741	-1978	-2217	-2420	-2609	-2779
S62 ($\mu\epsilon$)	-497	-302	-147	-28	81	179	265	354	435	514	593
S65 ($\mu\epsilon$)	-656	-426	-232	-75	77	220	347	481	602	721	838
S69 ($\mu\epsilon$)	-146	-80	-13	48	113	180	242	310	374	439	504
S70 ($\mu\epsilon$)	3	50	122	188	258	329	397	471	541	613	686
S71 ($\mu\epsilon$)	-	-	-	-	-	-	-	-	-	-	-
S72 ($\mu\epsilon$)	-132	62	210	323	429	527	614	704	786	867	948
S74 ($\mu\epsilon$)	-159	-338	-497	-635	-777	-913	-1036	-1165	-1279	-1392	-1499
S76 ($\mu\epsilon$)	-172	7	148	257	359	454	539	627	708	789	868
S79 ($\mu\epsilon$)	-138	124	323	476	620	757	875	1002	1115	1227	1337
S83 ($\mu\epsilon$)	-96	14	98	168	238	307	368	435	495	557	618
S84 ($\mu\epsilon$)	-167	-105	-31	34	103	175	242	316	386	458	531
S85 ($\mu\epsilon$)	-	-	-	-	-	-	-	-	-	-	-

**Table F-20. Raw data, strain survey conducted after hot-wet conditioning, cold-dry environmental conditions (Run 2)
(continued)**

Load Step	0	1	2	3	4	5	6	7	8	9	10
Pressure (psi)	-0.10	0.65	1.35	1.96	2.65	3.35	3.98	4.68	5.33	6.03	6.68
S86 ($\mu\epsilon$)	-140	-8	112	208	300	388	466	550	626	702	777
S88 ($\mu\epsilon$)	-207	-339	-429	-496	-558	-610	-650	-687	-713	-734	-749
S90 ($\mu\epsilon$)	-133	-11	107	201	292	378	454	535	609	685	759
S93 ($\mu\epsilon$)	-231	-78	77	206	332	456	565	682	787	892	995
S97 ($\mu\epsilon$)	-196	-116	-41	25	93	160	222	290	352	415	479
UAC-A1 ($\mu\epsilon$)	-118	31	172	286	401	511	607	708	796	886	971
UAC-A2 ($\mu\epsilon$)	-65	71	199	302	403	501	586	676	754	834	910
UAC-A3 ($\mu\epsilon$)	-99	13	120	204	289	369	440	514	579	646	711
UAC-F1 ($\mu\epsilon$)	-92	51	187	298	412	521	617	717	806	895	981
UAC-F2 ($\mu\epsilon$)	-102	24	144	240	338	431	513	599	676	752	826
UBC-A1 ($\mu\epsilon$)	16	242	451	616	778	926	1054	1186	1301	1411	1517
UBC-A2 ($\mu\epsilon$)	-71	118	293	432	567	691	798	909	1005	1098	1187
UBC-A3 ($\mu\epsilon$)	-104	71	232	361	484	599	698	801	889	977	1059
UBC-A4 ($\mu\epsilon$)	-131	31	181	300	414	521	614	710	795	879	959
UBC-F1 ($\mu\epsilon$)	-11	216	421	586	744	891	1019	1150	1262	1372	1476
UBC-F2 ($\mu\epsilon$)	-91	101	275	413	548	671	780	889	985	1077	1165
UBC-F3 ($\mu\epsilon$)	-87	93	255	383	508	624	724	827	916	1003	1086
UDAC-A1 ($\mu\epsilon$)	-59	82	212	322	428	533	624	720	803	888	969
UDAC-A2 ($\mu\epsilon$)	-55	71	187	283	376	467	547	630	703	778	848
UDAC-A3 ($\mu\epsilon$)	-50	59	159	240	318	395	463	533	597	661	723

**Table F-20. Raw data, strain survey conducted after hot-wet conditioning, cold-dry environmental conditions (Run 2)
(continued)**

Load Step	0	1	2	3	4	5	6	7	8	9	10
Pressure (psi)	-0.10	0.65	1.35	1.96	2.65	3.35	3.98	4.68	5.33	6.03	6.68
UDAC-F1 ($\mu\epsilon$)	-53	88	222	332	442	549	642	740	826	913	995
UDAC-F2 ($\mu\epsilon$)	-52	68	182	276	368	460	539	623	696	771	841
UDBC-A1 ($\mu\epsilon$)	49	279	481	644	800	943	1067	1193	1301	1406	1503
UDBC-A2 ($\mu\epsilon$)	11	205	376	515	648	771	877	985	1078	1168	1253
UDBC-A3 ($\mu\epsilon$)	1	182	343	472	596	712	811	912	999	1084	1164
UDBC-A4 ($\mu\epsilon$)	-73	92	241	359	473	580	672	766	849	930	1007
UDBC-F1 ($\mu\epsilon$)	23	280	505	684	853	1012	1146	1283	1401	1514	1622
UDBC-F2 ($\mu\epsilon$)	-33	177	364	511	651	782	893	1007	1104	1199	1288
UDBC-F3 ($\mu\epsilon$)	-66	130	305	442	573	695	798	904	996	1085	1169

Table F-21. Raw data, strain survey conducted after hot-wet conditioning, cold-dry environmental conditions (Run 3)

Load Step	0	1	2	3	4	5	6	7	8	9	10
Pressure (psi)	-0.09	0.66	1.34	2.00	2.67	3.33	3.99	4.63	5.34	6.00	6.66
Frame-1 (lb _f)	9	71	243	315	421	588	673	771	919	995	1161
Frame-2 (lb _f)	72	111	225	342	461	567	684	790	908	1019	1133
Frame-3 (lb _f)	3	106	230	343	453	567	681	790	906	1019	1130
Frame-4 (lb _f)	36	116	227	340	457	574	677	794	908	1019	1133
Frame-5 (lb _f)	4	115	225	332	448	562	683	795	896	1017	1138
Frame-6 (lb _f)	-1	97	223	337	440	577	686	799	896	1016	1135
Frame-7 (lb _f)	22	112	227	338	451	565	681	794	906	1016	1136
Frame-8 (lb _f)	22	108	233	346	452	567	677	790	910	1019	1134
Frame-9 (lb _f)	41	113	220	340	454	571	680	793	904	1019	1134
Frame-10 (lb _f)	1	123	227	351	451	571	687	791	907	1021	1132
Frame-11 (lb _f)	10	116	224	335	457	562	680	786	908	1024	1132
Frame-12 (lb _f)	26	113	227	348	449	568	677	789	907	1013	1133
Hoop-1 (lb _f)	63	721	1416	2149	2854	3570	4294	5001	5707	6432	7141
Hoop-2 (lb _f)	203	706	1454	2125	2866	3569	4248	5000	5703	6438	7125
Hoop-3 (lb _f)	117	696	1431	2150	2857	3566	4294	4989	5702	6430	7150
Hoop-4 (lb _f)	53	716	1429	2151	2861	3581	4290	4995	5706	6442	7134
Hoop-5 (lb _f)	38	722	1433	2156	2860	3568	4295	5001	5700	6422	7137
Hoop-6 (lb _f)	49	707	1442	2147	2858	3581	4268	4993	5715	6419	7151

**Table F-21. Raw data, strain survey conducted after hot-wet conditioning, cold-dry environmental conditions (Run 3)
(continued)**

Load Step	0	1	2	3	4	5	6	7	8	9	10
Pressure (psi)	-0.09	0.66	1.34	2.00	2.67	3.33	3.99	4.63	5.34	6.00	6.66
Hoop-7 (lb _f)	8	729	1417	2139	2862	3573	4283	4991	5721	6437	7133
Hoop-8 (lb _f)	223	713	1453	2140	2857	3569	4280	5009	5713	6425	7138
Hoop-9 (lb _f)	11	721	1421	2142	2864	3579	4290	4996	5710	6430	7141
Hoop-10 (lb _f)	-17	708	1430	2138	2872	3573	4278	4981	5696	6421	7128
Hoop-11 (lb _f)	46	703	1441	2146	2848	3567	4282	5004	5720	6438	7140
Hoop-12 (lb _f)	93	711	1433	2148	2854	3572	4282	4988	5713	6420	7146
Hoop-13 (lb _f)	53	726	1410	2096	2862	3573	4284	4988	5714	6428	7138
Hoop-14 (lb _f)	19	695	1435	2144	2852	3583	4291	4974	5691	6420	7126
Long-1 (lb _f)	-13	675	1332	2019	2680	3330	4007	4663	5368	6040	6647
Long-2 (lb _f)	24	646	1337	2000	2674	3337	4007	4667	5342	6021	6680
Long-3 (lb _f)	3	651	1326	2001	2664	3338	4013	4671	5345	6024	6673
Long-4 (lb _f)	-18	667	1327	2002	2668	3337	4007	4667	5345	6005	6670
Long-5 (lb _f)	2	669	1316	2004	2673	3333	4015	4674	5362	6006	6681
Long-6 (lb _f)	9	673	1351	2003	2667	3334	4001	4676	5335	6011	6673
Long-7 (lb _f)	8	639	1332	2001	2678	3339	4001	4660	5319	5993	6666
Long-8 (lb _f)	-5	690	1328	2010	2662	3338	4003	4673	5340	6030	6679
F01 (μ ϵ)	335	243	276	316	344	383	420	467	498	526	573
F02 (μ ϵ)	-386	-252	-193	-142	-80	-19	39	90	162	219	277

**Table F-21. Raw data, strain survey conducted after hot-wet conditioning, cold-dry environmental conditions (Run 3)
(continued)**

Load Step	0	1	2	3	4	5	6	7	8	9	10
Pressure (psi)	-0.09	0.66	1.34	2.00	2.67	3.33	3.99	4.63	5.34	6.00	6.66
F03 ($\mu\epsilon$)	448	258	277	317	337	363	385	425	436	456	491
F04 ($\mu\epsilon$)	-514	-316	-247	-183	-109	-35	34	90	176	248	313
F05 ($\mu\epsilon$)	-	-	-	-	-	-	-	-	-	-	-
F06 ($\mu\epsilon$)	-548	-347	-276	-223	-155	-92	-31	20	104	166	230
F07 ($\mu\epsilon$)	322	160	191	233	261	292	323	363	380	402	439
F08 ($\mu\epsilon$)	-318	-146	-91	-42	19	76	135	183	256	317	370
IS16 ($\mu\epsilon$)	-182	-81	0	68	135	201	266	329	398	465	533
IS17 ($\mu\epsilon$)	0	-46	-57	-49	-29	1	40	80	132	187	243
IS18 ($\mu\epsilon$)	85	6	-28	-41	-39	-25	-2	26	63	103	149
IS19 ($\mu\epsilon$)	-208	-163	-108	-62	-13	36	83	130	181	231	282
IS20 ($\mu\epsilon$)	-301	-236	-167	-109	-51	5	58	109	163	214	265
IS21 ($\mu\epsilon$)	-285	-229	-164	-109	-58	-4	45	91	140	186	231
IS22 ($\mu\epsilon$)	157	45	-5	-33	-46	-42	-28	-6	25	62	106
IS23 ($\mu\epsilon$)	292	191	135	98	72	57	49	49	54	65	82
IS24 ($\mu\epsilon$)	-348	-258	-169	-94	-22	48	112	172	235	293	351
IS25 ($\mu\epsilon$)	235	136	88	58	40	34	35	43	57	76	102
IS26 ($\mu\epsilon$)	-165	0	152	278	402	516	620	716	815	906	994
IS27 ($\mu\epsilon$)	301	199	156	134	124	125	135	151	175	204	238
IS28 ($\mu\epsilon$)	-144	10	153	272	387	495	593	685	779	867	950
IS29 ($\mu\epsilon$)	-220	-74	59	168	273	372	463	548	637	720	800

**Table F-21. Raw data, strain survey conducted after hot-wet conditioning, cold-dry environmental conditions (Run 3)
(continued)**

Load Step	0	1	2	3	4	5	6	7	8	9	10
Pressure (psi)	-0.09	0.66	1.34	2.00	2.67	3.33	3.99	4.63	5.34	6.00	6.66
IS30 ($\mu\epsilon$)	-	-	-	-	-	-	-	-	-	-	-
IS31 ($\mu\epsilon$)	-22	60	145	217	291	362	430	495	562	628	691
IS32 ($\mu\epsilon$)	31	114	194	261	327	389	447	500	556	607	656
IS33 ($\mu\epsilon$)	40	130	214	285	353	419	478	535	593	646	699
IS34 ($\mu\epsilon$)	147	106	86	76	75	84	99	120	147	179	216
IS35 ($\mu\epsilon$)	488	388	316	263	220	188	163	148	137	133	136
IS36 ($\mu\epsilon$)	66	154	241	312	383	449	511	567	626	680	732
IS37 ($\mu\epsilon$)	401	288	213	159	116	86	64	52	45	46	54
IS38 ($\mu\epsilon$)	105	211	312	397	481	558	631	698	766	831	893
IS39 ($\mu\epsilon$)	404	274	198	145	107	83	69	67	70	81	100
IS40 ($\mu\epsilon$)	106	213	317	405	492	573	649	720	793	861	927
IS41 ($\mu\epsilon$)	-100	29	146	245	342	433	517	596	677	753	826
IS42 ($\mu\epsilon$)	-141	-20	82	159	242	319	394	461	537	610	683
IS43 ($\mu\epsilon$)	-105	-64	-11	38	97	159	224	283	354	421	492
IS44 ($\mu\epsilon$)	-174	-192	-180	-162	-130	-89	-44	1	56	109	166
IS45 ($\mu\epsilon$)	-76	2	75	136	201	262	320	375	432	487	540
IS46 ($\mu\epsilon$)	-68	18	98	166	233	296	356	412	470	525	577
IS47 ($\mu\epsilon$)	-88	-7	69	135	199	260	318	373	430	484	535
IS48 ($\mu\epsilon$)	-67	-73	-46	-13	32	81	134	190	254	319	384
IS49 ($\mu\epsilon$)	-83	-128	-152	-167	-167	-161	-149	-134	-112	-87	-60

**Table F-21. Raw data, strain survey conducted after hot-wet conditioning, cold-dry environmental conditions (Run 3)
(continued)**

Load Step	0	1	2	3	4	5	6	7	8	9	10
Pressure (psi)	-0.09	0.66	1.34	2.00	2.67	3.33	3.99	4.63	5.34	6.00	6.66
IS50 ($\mu\epsilon$)	-81	15	103	175	246	314	378	436	498	556	610
IS51 ($\mu\epsilon$)	-105	-142	-160	-170	-164	-155	-138	-120	-95	-69	-37
IS52 ($\mu\epsilon$)	-83	47	163	260	357	447	533	613	695	773	845
IS53 ($\mu\epsilon$)	-154	-185	-193	-191	-175	-150	-120	-89	-51	-11	32
IS54 ($\mu\epsilon$)	-83	39	147	238	328	413	494	569	647	721	790
IS55 ($\mu\epsilon$)	-65	36	132	211	290	365	438	504	575	643	707
IS56 ($\mu\epsilon$)	-132	-33	43	107	169	231	290	349	412	475	538
IS57 ($\mu\epsilon$)	45	11	7	16	36	66	100	141	188	239	293
IS58 ($\mu\epsilon$)	188	97	54	34	29	38	53	78	110	148	192
IS59 ($\mu\epsilon$)	-208	-150	-92	-42	9	60	108	157	209	260	314
IS60 ($\mu\epsilon$)	-268	-192	-120	-61	-3	53	104	154	206	256	306
IS61 ($\mu\epsilon$)	-277	-204	-136	-80	-25	29	78	124	173	222	269
IS62 ($\mu\epsilon$)	130	26	-17	-36	-41	-30	-13	14	49	89	135
IS63 ($\mu\epsilon$)	354	256	200	162	135	118	108	106	108	116	130
IS64 ($\mu\epsilon$)	-287	-184	-90	-13	62	133	197	259	322	380	438
IS65 ($\mu\epsilon$)	373	306	280	269	268	275	288	308	333	363	397
IS66 ($\mu\epsilon$)	-29	154	314	448	577	697	804	905	1006	1099	1189
IS67 ($\mu\epsilon$)	287	229	216	215	223	241	262	291	325	363	406
IS68 ($\mu\epsilon$)	-46	119	265	387	506	616	716	810	905	993	1078
IS69 ($\mu\epsilon$)	-118	34	165	273	376	472	560	644	730	811	890

**Table F-21. Raw data, strain survey conducted after hot-wet conditioning, cold-dry environmental conditions (Run 3)
(continued)**

Load Step	0	1	2	3	4	5	6	7	8	9	10
Pressure (psi)	-0.09	0.66	1.34	2.00	2.67	3.33	3.99	4.63	5.34	6.00	6.66
IS70 ($\mu\epsilon$)	-260	-166	-89	-25	38	101	159	219	280	343	406
IS71 ($\mu\epsilon$)	-103	-116	-90	-54	-8	47	101	160	222	288	355
IS72 ($\mu\epsilon$)	-24	-69	-59	-35	1	46	93	145	203	262	324
IS73 ($\mu\epsilon$)	51	119	194	260	326	390	449	506	565	620	673
IS74 ($\mu\epsilon$)	-42	35	112	179	247	312	371	428	487	541	594
IS75 ($\mu\epsilon$)	-3	76	155	224	293	359	420	478	538	594	649
IS76 ($\mu\epsilon$)	-3	-19	9	48	96	153	211	271	337	405	475
IS77 ($\mu\epsilon$)	44	-54	-87	-96	-92	-77	-58	-33	-3	30	67
IS78 ($\mu\epsilon$)	-20	66	152	225	299	369	434	496	560	619	677
IS79 ($\mu\epsilon$)	-12	-113	-145	-154	-151	-137	-119	-94	-66	-34	1
IS80 ($\mu\epsilon$)	21	121	219	304	391	474	551	625	702	774	842
IS81 ($\mu\epsilon$)	32	-71	-100	-109	-105	-90	-71	-46	-16	16	53
IS82 ($\mu\epsilon$)	-42	47	135	213	293	369	440	509	581	649	715
IS83 ($\mu\epsilon$)	32	117	202	273	344	412	477	541	606	669	729
IS84 ($\mu\epsilon$)	-69	-7	67	132	199	264	329	391	461	527	593
IS85 ($\mu\epsilon$)	-76	-57	-8	44	105	170	235	301	376	448	520
IS86 ($\mu\epsilon$)	-96	-100	-74	-42	2	52	104	157	221	282	345
IS87 ($\mu\epsilon$)	-37	29	91	143	195	246	293	339	388	435	480
IS88 ($\mu\epsilon$)	-51	19	84	137	190	240	288	332	380	424	465
IS89 ($\mu\epsilon$)	-59	7	70	120	170	219	263	307	355	397	439

**Table F-21. Raw data, strain survey conducted after hot-wet conditioning, cold-dry environmental conditions (Run 3)
(continued)**

Load Step	0	1	2	3	4	5	6	7	8	9	10
Pressure (psi)	-0.09	0.66	1.34	2.00	2.67	3.33	3.99	4.63	5.34	6.00	6.66
IS90 ($\mu\epsilon$)	-99	-95	-70	-38	6	56	109	164	229	291	355
IS91 ($\mu\epsilon$)	-80	-100	-106	-106	-97	-82	-63	-40	-11	20	54
IS92 ($\mu\epsilon$)	-52	30	106	167	227	283	336	385	437	485	531
IS93 ($\mu\epsilon$)	-102	-101	-86	-68	-40	-8	28	66	110	156	204
IS94 ($\mu\epsilon$)	-84	46	161	259	356	448	534	614	698	776	850
IS95 ($\mu\epsilon$)	-82	-70	-45	-19	16	54	93	134	181	228	277
IS96 ($\mu\epsilon$)	-100	16	120	208	295	378	455	528	605	677	745
IS97 ($\mu\epsilon$)	-35	75	172	252	332	408	479	547	618	686	751
L01 ($\mu\epsilon$)	-	-	-	-	-	-	-	-	-	-	-
L02 ($\mu\epsilon$)	151	185	194	205	218	231	244	258	273	288	303
L03 ($\mu\epsilon$)	13	42	41	47	56	67	80	92	109	126	143
L04 ($\mu\epsilon$)	64	106	117	132	149	166	184	200	219	237	255
L05 ($\mu\epsilon$)	59	91	99	108	117	127	135	144	153	161	170
L06 ($\mu\epsilon$)	38	77	94	110	126	144	161	176	189	200	213
L07 ($\mu\epsilon$)	-	-	-	-	-	-	-	-	-	-	-
L08 ($\mu\epsilon$)	160	231	266	296	325	354	380	404	430	455	477
L09 ($\mu\epsilon$)	55	132	167	201	233	262	291	318	346	369	394
L10 ($\mu\epsilon$)	-	-	-	-	-	-	-	-	-	-	-
RAC-A1 ($\mu\epsilon$)	-28	83	188	280	376	468	554	636	723	804	882
RAC-A2 ($\mu\epsilon$)	-53	47	143	226	312	393	470	542	620	693	761

**Table F-21. Raw data, strain survey conducted after hot-wet conditioning, cold-dry environmental conditions (Run 3)
(continued)**

Load Step	0	1	2	3	4	5	6	7	8	9	10
Pressure (psi)	-0.09	0.66	1.34	2.00	2.67	3.33	3.99	4.63	5.34	6.00	6.66
RAC-A3 ($\mu\epsilon$)	16	103	185	255	325	393	456	515	577	636	692
RAC-F1 ($\mu\epsilon$)	-80	26	127	216	309	397	479	557	639	716	790
RAC-F2 ($\mu\epsilon$)	-60	36	129	210	294	374	448	518	592	662	728
RBC-A1 ($\mu\epsilon$)	211	359	490	598	703	797	884	962	1042	1115	1184
RBC-A2 ($\mu\epsilon$)	129	256	371	466	557	640	715	784	853	919	978
RBC-A3 ($\mu\epsilon$)	139	260	369	460	548	628	701	770	839	903	962
RBC-A4 ($\mu\epsilon$)	44	161	267	356	444	524	598	668	738	804	865
RBC-F1 ($\mu\epsilon$)	211	365	493	598	700	791	873	950	1027	1097	1161
RBC-F2 ($\mu\epsilon$)	170	309	425	520	611	694	767	837	906	970	1028
RBC-F3 ($\mu\epsilon$)	149	286	400	493	582	663	735	804	873	936	993
S16 ($\mu\epsilon$)	-312	-264	-194	-131	-64	2	67	129	196	262	329
S17 ($\mu\epsilon$)	-	-	-	-	-	-	-	-	-	-	-
S18 ($\mu\epsilon$)	-568	-375	-214	-88	27	132	227	312	402	484	565
S20 ($\mu\epsilon$)	103	-318	-663	-942	-1207	-1443	-1652	-1835	-2018	-2177	-2316
S22 ($\mu\epsilon$)	-453	-283	-135	-18	89	188	278	358	442	519	595
S25 ($\mu\epsilon$)	-692	-473	-285	-129	23	167	300	422	552	673	790
S29 ($\mu\epsilon$)	42	87	138	190	245	303	361	417	478	538	597
S30 ($\mu\epsilon$)	-230	-81	65	184	297	402	499	587	678	764	847
S32 ($\mu\epsilon$)	663	494	365	258	155	65	-16	-89	-160	-222	-277
S34 ($\mu\epsilon$)	-268	-139	-5	109	218	322	418	507	599	688	772

**Table F-21. Raw data, strain survey conducted after hot-wet conditioning, cold-dry environmental conditions (Run 3)
(continued)**

Load Step	0	1	2	3	4	5	6	7	8	9	10
Pressure (psi)	-0.09	0.66	1.34	2.00	2.67	3.33	3.99	4.63	5.34	6.00	6.66
S37 ($\mu\epsilon$)	-498	-286	-84	81	238	387	524	648	778	899	1015
S41 ($\mu\epsilon$)	48	124	195	263	334	404	473	537	607	673	737
S42 ($\mu\epsilon$)	-186	-141	-78	-20	47	116	185	249	322	390	460
S43 ($\mu\epsilon$)	-341	-238	-135	-52	35	120	201	272	353	426	502
S44 ($\mu\epsilon$)	-114	35	166	271	375	472	564	645	734	815	896
S46 ($\mu\epsilon$)	-264	-601	-867	-1093	-1315	-1514	-1695	-1861	-2032	-2187	-2326
S48 ($\mu\epsilon$)	-134	-1	118	217	312	401	484	561	644	722	796
S51 ($\mu\epsilon$)	-154	38	216	365	508	644	772	890	1015	1131	1241
S55 ($\mu\epsilon$)	-163	-96	-25	40	107	176	243	306	374	439	503
S56 ($\mu\epsilon$)	-271	-215	-145	-80	-12	55	119	184	252	320	389
S57 ($\mu\epsilon$)	-	-	-	-	-	-	-	-	-	-	-
S58 ($\mu\epsilon$)	-635	-411	-237	-101	23	135	235	327	420	507	592
S60 ($\mu\epsilon$)	40	-443	-838	-1159	-1465	-1740	-1983	-2200	-2418	-2609	-2780
S62 ($\mu\epsilon$)	-500	-302	-149	-29	80	179	267	347	431	510	587
S65 ($\mu\epsilon$)	-660	-423	-233	-76	77	220	350	471	599	717	830
S69 ($\mu\epsilon$)	-147	-80	-15	48	114	179	243	306	373	437	502
S70 ($\mu\epsilon$)	1	52	121	189	259	330	398	466	540	612	683
S71 ($\mu\epsilon$)	-	-	-	-	-	-	-	-	-	-	-
S72 ($\mu\epsilon$)	-134	64	211	326	431	528	617	699	785	867	945
S74 ($\mu\epsilon$)	-156	-339	-498	-639	-781	-915	-1040	-1156	-1280	-1393	-1499

**Table F-21. Raw data, strain survey conducted after hot-wet conditioning, cold-dry environmental conditions (Run 3)
(continued)**

Load Step	0	1	2	3	4	5	6	7	8	9	10
Pressure (psi)	-0.09	0.66	1.34	2.00	2.67	3.33	3.99	4.63	5.34	6.00	6.66
S76 ($\mu\epsilon$)	-172	9	147	258	360	454	542	623	707	787	866
S79 ($\mu\epsilon$)	-140	124	322	476	622	755	878	993	1114	1225	1333
S83 ($\mu\epsilon$)	-100	15	99	170	240	307	370	431	495	558	617
S84 ($\mu\epsilon$)	-171	-106	-34	33	104	174	244	311	386	459	529
S85 ($\mu\epsilon$)	-	-	-	-	-	-	-	-	-	-	-
S86 ($\mu\epsilon$)	-144	-11	109	207	300	387	468	545	626	702	776
S88 ($\mu\epsilon$)	-210	-344	-434	-502	-563	-613	-653	-684	-714	-735	-750
S90 ($\mu\epsilon$)	-137	-13	105	201	292	377	456	531	611	684	756
S93 ($\mu\epsilon$)	-241	-84	70	202	329	450	564	671	783	889	989
S97 ($\mu\epsilon$)	-199	-118	-43	24	92	159	223	285	351	415	477
UAC-A1 ($\mu\epsilon$)	-122	32	171	289	404	511	612	703	799	888	970
UAC-A2 ($\mu\epsilon$)	-69	73	198	302	405	499	590	671	756	836	908
UAC-A3 ($\mu\epsilon$)	-103	14	119	206	289	368	443	512	582	649	710
UAC-F1 ($\mu\epsilon$)	-97	53	185	302	415	522	621	712	808	897	980
UAC-F2 ($\mu\epsilon$)	-108	25	142	242	340	431	516	595	677	754	825
UBC-A1 ($\mu\epsilon$)	13	244	450	619	779	927	1060	1180	1302	1414	1516
UBC-A2 ($\mu\epsilon$)	-74	119	292	433	568	691	803	903	1006	1100	1187
UBC-A3 ($\mu\epsilon$)	-107	72	231	362	485	599	702	795	891	978	1058
UBC-A4 ($\mu\epsilon$)	-135	32	179	300	415	522	617	706	796	880	958
UBC-F1 ($\mu\epsilon$)	-15	217	422	587	746	892	1025	1144	1265	1375	1477

**Table F-21. Raw data, strain survey conducted after hot-wet conditioning, cold-dry environmental conditions (Run 3)
(continued)**

Load Step	0	1	2	3	4	5	6	7	8	9	10
Pressure (psi)	-0.09	0.66	1.34	2.00	2.67	3.33	3.99	4.63	5.34	6.00	6.66
UBC-F2 ($\mu\epsilon$)	-96	102	275	415	549	672	783	884	987	1079	1166
UBC-F3 ($\mu\epsilon$)	-91	93	254	384	509	624	727	822	919	1005	1086
UDAC-A1 ($\mu\epsilon$)	-64	84	213	323	432	534	628	715	805	889	967
UDAC-A2 ($\mu\epsilon$)	-60	72	186	283	378	467	550	625	704	778	847
UDAC-A3 ($\mu\epsilon$)	-54	60	158	239	319	395	464	529	597	661	722
UDAC-F1 ($\mu\epsilon$)	-57	90	221	335	446	550	646	734	828	913	993
UDAC-F2 ($\mu\epsilon$)	-57	70	181	278	371	461	542	617	698	771	840
UDBC-A1 ($\mu\epsilon$)	43	279	480	645	802	944	1070	1185	1302	1406	1503
UDBC-A2 ($\mu\epsilon$)	4	204	375	516	650	771	879	979	1078	1169	1253
UDBC-A3 ($\mu\epsilon$)	-6	182	342	473	598	711	812	906	999	1084	1164
UDBC-A4 ($\mu\epsilon$)	-81	92	239	360	475	579	673	761	849	930	1007
UDBC-F1 ($\mu\epsilon$)	17	279	504	684	856	1011	1150	1275	1401	1515	1622
UDBC-F2 ($\mu\epsilon$)	-40	176	362	511	653	781	896	1000	1105	1200	1288
UDBC-F3 ($\mu\epsilon$)	-73	130	303	442	574	694	800	898	996	1085	1168

F.2.2.2 After 30,000 Cycles

Table F-22. Raw data, strain survey conducted after 30,000 cycles, cold-dry environmental conditions (Run 1)

Load Step	0	1	2	3	4	5	6	7	8	9	10
Pressure (psi)	-0.02	0.67	1.34	2.00	2.68	3.35	4.00	4.68	5.34	6.02	6.68
Frame-1 (lbf)	5	142	208	323	448	565	725	781	923	1001	1150
Frame-2 (lbf)	68	117	224	343	454	565	680	797	906	1019	1132
Frame-3 (lbf)	3	110	224	334	452	568	678	792	908	1018	1134
Frame-4 (lbf)	47	110	226	340	452	566	682	793	906	1020	1133
Frame-5 (lbf)	12	104	232	337	459	569	678	792	911	1014	1128
Frame-6 (lbf)	6	106	225	341	451	570	679	788	907	1018	1140
Frame-7 (lbf)	15	113	227	341	454	563	681	795	908	1023	1129
Frame-8 (lbf)	12	109	217	337	452	569	680	791	902	1021	1132
Frame-9 (lbf)	44	115	227	345	453	566	679	791	904	1020	1132
Frame-10 (lbf)	2	112	225	332	459	564	682	794	907	1018	1133
Frame-11 (lbf)	9	116	225	338	453	568	683	789	906	1023	1131
Frame-12 (lbf)	-2	114	225	343	452	566	681	790	907	1017	1136
Hoop-1 (lbf)	93	720	1439	2149	2860	3571	4279	4994	5711	6454	7146
Hoop-2 (lbf)	126	665	1409	2138	2864	3564	4292	4996	5701	6420	7159
Hoop-3 (lbf)	116	707	1433	2150	2857	3578	4282	5010	5710	6445	7130
Hoop-4 (lbf)	17	704	1425	2141	2848	3567	4277	5012	5723	6428	7137
Hoop-5 (lbf)	21	716	1435	2157	2858	3582	4281	4996	5701	6429	7150
Hoop-6 (lbf)	106	712	1433	2141	2866	3562	4270	4999	5720	6443	7146
Hoop-7 (lbf)	100	721	1423	2144	2863	3570	4290	5006	5716	6435	7142
Hoop-8 (lbf)	206	715	1423	2143	2855	3573	4286	5005	5707	6435	7145

Table F-22. Raw data, strain survey conducted after 30,000 cycles, cold-dry environmental conditions (Run 1) (continued)

Load Step	0	1	2	3	4	5	6	7	8	9	10
Pressure (psi)	-0.02	0.67	1.34	2.00	2.68	3.35	4.00	4.68	5.34	6.02	6.68
Hoop-9 (lbf)	3	701	1443	2139	2852	3569	4278	5007	5714	6434	7138
Hoop-10 (lbf)	-9	713	1430	2136	2866	3571	4281	5006	5711	6442	7146
Hoop-11 (lbf)	56	723	1434	2147	2868	3563	4283	4999	5727	6457	7165
Hoop-12 (lbf)	157	729	1439	2143	2855	3571	4273	5003	5710	6425	7143
Hoop-13 (lbf)	80	718	1384	2141	2863	3578	4285	5003	5710	6444	7147
Hoop-14 (lbf)	57	723	1427	2149	2839	3587	4285	5014	5705	6440	7144
Long-1 (lbf)	-6	620	1339	1999	2663	3376	3999	4667	5335	5970	6741
Long-2 (lbf)	-1	660	1335	2009	2674	3334	4005	4671	5312	6005	6676
Long-3 (lbf)	-10	655	1341	2002	2674	3345	4006	4671	5308	5993	6711
Long-4 (lbf)	4	671	1351	2001	2671	3331	4019	4702	5334	6010	6674
Long-5 (lbf)	-2	675	1342	2006	2667	3342	4006	4680	5323	6008	6672
Long-6 (lbf)	21	654	1354	2004	2667	3355	4005	4671	5340	6005	6679
Long-7 (lbf)	-28	659	1336	1993	2673	3326	3990	4662	5343	6007	6683
Long-8 (lbf)	6	680	1326	2009	2659	3306	4007	4674	5338	6007	6678
F01 ($\mu\epsilon$)	325	285	328	358	382	403	426	451	481	507	542
F02 ($\mu\epsilon$)	-363	-277	-228	-166	-104	-43	21	85	146	210	270
F03 ($\mu\epsilon$)	462	332	372	395	406	422	438	453	475	494	519
F04 ($\mu\epsilon$)	-479	-338	-285	-215	-141	-66	12	91	165	242	312
F05 ($\mu\epsilon$)	-	-	-	-	-	-	-	-	-	-	-
F06 ($\mu\epsilon$)	-471	-342	-297	-237	-167	-104	-31	37	108	182	248
F07 ($\mu\epsilon$)	232	146	183	211	227	249	273	294	316	340	369

Table F-22. Raw data, strain survey conducted after 30,000 cycles, cold-dry environmental conditions (Run 1) (continued)

Load Step	0	1	2	3	4	5	6	7	8	9	10
Pressure (psi)	-0.02	0.67	1.34	2.00	2.68	3.35	4.00	4.68	5.34	6.02	6.68
F08 ($\mu\epsilon$)	-213	-95	-46	15	80	143	208	275	335	401	458
IS16 ($\mu\epsilon$)	-182	-92	-13	52	113	172	233	296	356	424	490
IS17 ($\mu\epsilon$)	-39	-77	-88	-87	-71	-48	-12	27	74	127	182
IS18 ($\mu\epsilon$)	36	-37	-74	-94	-98	-90	-72	-46	-13	28	72
IS19 ($\mu\epsilon$)	-219	-185	-140	-103	-65	-27	13	56	99	147	195
IS20 ($\mu\epsilon$)	-339	-287	-228	-181	-136	-93	-48	-4	40	87	132
IS21 ($\mu\epsilon$)	-326	-276	-217	-171	-127	-84	-41	2	43	88	131
IS22 ($\mu\epsilon$)	86	-9	-62	-99	-119	-124	-118	-101	-75	-42	-2
IS23 ($\mu\epsilon$)	233	138	77	32	0	-22	-34	-39	-37	-27	-12
IS24 ($\mu\epsilon$)	-370	-302	-229	-169	-113	-60	-7	45	94	145	195
IS25 ($\mu\epsilon$)	182	99	53	20	-1	-11	-12	-6	7	26	51
IS26 ($\mu\epsilon$)	-141	5	149	275	390	496	597	692	781	869	952
IS27 ($\mu\epsilon$)	241	164	132	112	101	102	112	129	153	182	218
IS28 ($\mu\epsilon$)	-101	42	183	308	422	527	628	724	814	902	986
IS29 ($\mu\epsilon$)	-185	-50	79	192	294	388	479	567	651	733	812
IS30 ($\mu\epsilon$)	73	48	46	46	50	61	81	108	141	179	223
IS31 ($\mu\epsilon$)	-13	67	152	226	296	364	431	499	564	630	694
IS32 ($\mu\epsilon$)	34	111	191	258	320	378	434	487	538	589	637
IS33 ($\mu\epsilon$)	39	122	206	278	344	404	465	522	576	629	680
IS34 ($\mu\epsilon$)	109	72	51	35	28	29	39	55	76	104	136
IS35 ($\mu\epsilon$)	434	343	275	220	176	141	116	96	85	77	78

Table F-22. Raw data, strain survey conducted after 30,000 cycles, cold-dry environmental conditions (Run 1) (continued)

Load Step	0	1	2	3	4	5	6	7	8	9	10
Pressure (psi)	-0.02	0.67	1.34	2.00	2.68	3.35	4.00	4.68	5.34	6.02	6.68
IS36 ($\mu\epsilon$)	58	140	223	294	358	418	477	532	586	637	687
IS37 ($\mu\epsilon$)	350	248	178	122	77	42	19	2	-6	-8	-3
IS38 ($\mu\epsilon$)	111	209	307	393	471	545	616	684	747	810	869
IS39 ($\mu\epsilon$)	350	239	170	115	75	47	32	24	26	34	51
IS40 ($\mu\epsilon$)	123	222	324	414	497	574	650	722	790	857	922
IS41 ($\mu\epsilon$)	-57	62	180	284	380	468	553	637	714	791	864
IS42 ($\mu\epsilon$)	-179	-61	42	127	204	277	350	421	492	564	628
IS43 ($\mu\epsilon$)	-132	-87	-31	20	75	132	194	258	323	392	459
IS44 ($\mu\epsilon$)	-207	-225	-214	-197	-170	-135	-92	-46	6	62	118
IS45 ($\mu\epsilon$)	-59	9	79	139	198	252	308	363	415	469	520
IS46 ($\mu\epsilon$)	-72	0	74	136	194	247	301	352	401	450	497
IS47 ($\mu\epsilon$)	-90	-19	52	113	171	224	278	329	379	429	476
IS48 ($\mu\epsilon$)	-83	-91	-68	-40	-3	40	90	147	206	269	333
IS49 ($\mu\epsilon$)	-88	-138	-160	-174	-178	-175	-163	-147	-126	-101	-71
IS50 ($\mu\epsilon$)	-70	16	100	171	238	300	360	419	475	530	582
IS51 ($\mu\epsilon$)	-93	-134	-148	-154	-151	-142	-125	-104	-80	-50	-18
IS52 ($\mu\epsilon$)	-51	68	183	284	380	468	555	639	717	796	869
IS53 ($\mu\epsilon$)	-148	-182	-184	-179	-165	-143	-115	-81	-45	-3	41
IS54 ($\mu\epsilon$)	-55	54	161	255	344	426	507	585	658	732	802
IS55 ($\mu\epsilon$)	-54	41	138	220	297	369	439	510	575	643	707
IS56 ($\mu\epsilon$)	-129	-50	22	82	138	191	248	305	361	422	482

Table F-22. Raw data, strain survey conducted after 30,000 cycles, cold-dry environmental conditions (Run 1) (continued)

Load Step	0	1	2	3	4	5	6	7	8	9	10
Pressure (psi)	-0.02	0.67	1.34	2.00	2.68	3.35	4.00	4.68	5.34	6.02	6.68
IS57 ($\mu\epsilon$)	17	-14	-18	-15	-2	19	52	89	130	179	229
IS58 ($\mu\epsilon$)	145	67	25	1	-9	-6	9	32	62	100	144
IS59 ($\mu\epsilon$)	-190	-153	-105	-65	-26	15	58	103	148	198	248
IS60 ($\mu\epsilon$)	-265	-210	-148	-99	-54	-9	35	79	122	169	214
IS61 ($\mu\epsilon$)	-262	-203	-137	-85	-37	8	55	102	148	195	242
IS62 ($\mu\epsilon$)	92	15	-22	-44	-51	-45	-29	-4	30	70	114
IS63 ($\mu\epsilon$)	277	184	122	76	44	22	9	5	7	17	31
IS64 ($\mu\epsilon$)	-298	-234	-163	-107	-54	-4	46	94	140	188	235
IS65 ($\mu\epsilon$)	317	259	234	219	215	218	231	249	273	304	337
IS66 ($\mu\epsilon$)	11	155	297	419	530	633	731	822	908	991	1069
IS67 ($\mu\epsilon$)	258	220	216	217	227	245	271	300	336	376	419
IS68 ($\mu\epsilon$)	53	204	352	482	601	711	816	915	1007	1097	1182
IS69 ($\mu\epsilon$)	-12	124	255	366	469	565	656	742	824	905	984
IS70 ($\mu\epsilon$)	-256	-158	-75	-12	46	104	161	219	276	337	398
IS71 ($\mu\epsilon$)	-136	-132	-99	-63	-18	35	90	148	209	273	338
IS72 ($\mu\epsilon$)	-40	-67	-53	-30	5	49	96	150	204	265	327
IS73 ($\mu\epsilon$)	69	136	208	271	332	392	448	504	556	609	659
IS74 ($\mu\epsilon$)	-26	46	119	183	243	301	356	410	460	511	558
IS75 ($\mu\epsilon$)	-6	68	142	208	270	328	385	441	492	544	592
IS76 ($\mu\epsilon$)	4	-4	26	65	114	168	227	290	354	422	491
IS77 ($\mu\epsilon$)	49	-24	-51	-60	-56	-42	-23	2	31	64	100

Table F-22. Raw data, strain survey conducted after 30,000 cycles, cold-dry environmental conditions (Run 1) (continued)

Load Step	0	1	2	3	4	5	6	7	8	9	10
Pressure (psi)	-0.02	0.67	1.34	2.00	2.68	3.35	4.00	4.68	5.34	6.02	6.68
IS78 ($\mu\epsilon$)	8	86	166	237	303	366	428	487	542	597	648
IS79 ($\mu\epsilon$)	-8	-81	-107	-116	-111	-98	-79	-55	-28	4	39
IS80 ($\mu\epsilon$)	73	167	263	352	436	517	596	671	743	815	883
IS81 ($\mu\epsilon$)	21	-54	-78	-88	-83	-70	-50	-26	2	34	69
IS82 ($\mu\epsilon$)	1	83	171	250	328	403	476	547	615	683	747
IS83 ($\mu\epsilon$)	66	144	226	297	366	433	497	560	621	683	741
IS84 ($\mu\epsilon$)	-81	-13	62	125	186	245	305	367	427	492	555
IS85 ($\mu\epsilon$)	-109	-98	-57	-9	44	101	164	230	296	368	439
IS86 ($\mu\epsilon$)	-117	-131	-113	-86	-49	-7	43	97	152	213	275
IS87 ($\mu\epsilon$)	-27	22	73	116	157	196	236	275	313	353	391
IS88 ($\mu\epsilon$)	-60	-13	35	75	111	144	178	210	241	271	302
IS89 ($\mu\epsilon$)	-67	-22	24	62	97	128	162	192	223	254	285
IS90 ($\mu\epsilon$)	-124	-126	-104	-75	-36	9	62	116	173	236	299
IS91 ($\mu\epsilon$)	-90	-120	-132	-137	-133	-124	-107	-88	-64	-34	-2
IS92 ($\mu\epsilon$)	-52	15	80	133	181	226	269	311	350	389	426
IS93 ($\mu\epsilon$)	-104	-104	-87	-64	-37	-5	32	72	115	162	211
IS94 ($\mu\epsilon$)	-62	69	193	302	403	497	589	676	757	839	915
IS95 ($\mu\epsilon$)	-90	-77	-47	-15	20	55	99	141	186	235	286
IS96 ($\mu\epsilon$)	-85	28	136	231	319	401	482	559	631	704	773
IS97 ($\mu\epsilon$)	-27	77	176	260	339	412	484	554	620	687	753
L01 ($\mu\epsilon$)	-	-	-	-	-	-	-	-	-	-	-

Table F-22. Raw data, strain survey conducted after 30,000 cycles, cold-dry environmental conditions (Run 1) (continued)

Load Step	0	1	2	3	4	5	6	7	8	9	10
Pressure (psi)	-0.02	0.67	1.34	2.00	2.68	3.35	4.00	4.68	5.34	6.02	6.68
L02 ($\mu\epsilon$)	204	213	209	220	231	245	259	273	288	302	318
L03 ($\mu\epsilon$)	75	75	64	68	78	90	105	119	136	152	171
L04 ($\mu\epsilon$)	134	148	152	168	185	203	223	240	260	278	299
L05 ($\mu\epsilon$)	113	128	130	141	152	161	173	182	192	202	212
L06 ($\mu\epsilon$)	22	53	66	85	103	120	136	149	161	171	183
L07 ($\mu\epsilon$)	-	-	-	-	-	-	-	-	-	-	-
L08 ($\mu\epsilon$)	247	282	302	334	364	393	423	448	473	497	522
L09 ($\mu\epsilon$)	125	170	203	238	270	299	329	354	381	405	431
L10 ($\mu\epsilon$)	-	-	-	-	-	-	-	-	-	-	-
RAC-A1 ($\mu\epsilon$)	19	130	239	341	440	534	626	715	799	883	963
RAC-A2 ($\mu\epsilon$)	-9	87	182	271	355	436	515	591	664	738	807
RAC-A3 ($\mu\epsilon$)	51	131	212	284	352	418	480	542	600	658	714
RAC-F1 ($\mu\epsilon$)	-31	71	174	271	363	450	536	619	697	776	851
RAC-F2 ($\mu\epsilon$)	-19	72	165	250	331	408	485	558	627	697	763
RBC-A1 ($\mu\epsilon$)	260	403	538	655	762	859	951	1037	1117	1192	1262
RBC-A2 ($\mu\epsilon$)	152	271	384	482	570	650	726	797	863	926	985
RBC-A3 ($\mu\epsilon$)	156	267	373	466	549	626	699	768	832	894	952
RBC-A4 ($\mu\epsilon$)	62	170	274	365	449	527	600	671	737	801	862
RBC-F1 ($\mu\epsilon$)	268	410	541	654	756	850	936	1018	1091	1163	1228
RBC-F2 ($\mu\epsilon$)	206	331	445	542	630	711	786	856	920	983	1040
RBC-F3 ($\mu\epsilon$)	184	305	416	511	597	676	749	818	880	942	998

Table F-22. Raw data, strain survey conducted after 30,000 cycles, cold-dry environmental conditions (Run 1) (continued)

Load Step	0	1	2	3	4	5	6	7	8	9	10
Pressure (psi)	-0.02	0.67	1.34	2.00	2.68	3.35	4.00	4.68	5.34	6.02	6.68
S16 ($\mu\epsilon$)	21	94	177	246	312	375	410	455	506	563	618
S17 ($\mu\epsilon$)	-	-	-	-	-	-	-	-	-	-	-
S18 ($\mu\epsilon$)	-663	-464	-284	-142	-18	95	192	279	370	465	554
S20 ($\mu\epsilon$)	700	402	139	-87	-288	-465	-626	-773	-893	-997	-1082
S22 ($\mu\epsilon$)	-387	-228	-83	34	137	230	309	380	452	530	604
S25 ($\mu\epsilon$)	-617	-423	-245	-92	51	185	306	420	533	651	762
S29 ($\mu\epsilon$)	56	106	163	221	281	340	400	462	522	584	644
S30 ($\mu\epsilon$)	-215	-73	66	181	287	383	474	563	645	728	807
S32 ($\mu\epsilon$)	930	784	658	546	445	354	272	196	130	69	15
S34 ($\mu\epsilon$)	-	-	-	-	-	-	-	-	-	-	-
S37 ($\mu\epsilon$)	-452	-241	-42	125	277	418	554	684	805	926	1041
S41 ($\mu\epsilon$)	40	111	187	262	337	409	481	552	620	690	755
S42 ($\mu\epsilon$)	-	-	-	-	-	-	-	-	-	-	-
S43 ($\mu\epsilon$)	-284	-180	-77	10	91	169	240	305	375	448	519
S44 ($\mu\epsilon$)	-22	135	280	399	502	598	687	776	859	944	1024
S46 ($\mu\epsilon$)	-258	-541	-793	-1017	-1225	-1413	-1592	-1763	-1907	-2045	-2167
S48 ($\mu\epsilon$)	-120	24	150	255	350	436	521	602	680	759	831
S51 ($\mu\epsilon$)	-184	10	189	341	480	611	737	860	977	1094	1204
S55 ($\mu\epsilon$)	-176	-107	-35	34	100	166	232	299	364	431	495
S56 ($\mu\epsilon$)	-211	-172	-112	-55	6	67	129	187	249	315	380
S57 ($\mu\epsilon$)	-	-	-	-	-	-	-	-	-	-	-

Table F-22. Raw data, strain survey conducted after 30,000 cycles, cold-dry environmental conditions (Run 1) (continued)

Load Step	0	1	2	3	4	5	6	7	8	9	10
Pressure (psi)	-0.02	0.67	1.34	2.00	2.68	3.35	4.00	4.68	5.34	6.02	6.68
S58 ($\mu\epsilon$)	-523	-334	-163	-29	88	194	287	370	452	537	617
S60 ($\mu\epsilon$)	239	-37	-281	-484	-661	-813	-954	-1081	-1181	-1267	-1335
S62 ($\mu\epsilon$)	-416	-249	-101	15	118	211	293	368	443	519	592
S65 ($\mu\epsilon$)	-635	-388	-159	34	202	354	494	626	748	874	989
S69 ($\mu\epsilon$)	-62	-13	43	93	142	189	229	263	300	340	380
S70 ($\mu\epsilon$)	-1	50	121	188	256	327	396	468	536	608	678
S71 ($\mu\epsilon$)	-	-	-	-	-	-	-	-	-	-	-
S72 ($\mu\epsilon$)	-115	65	214	332	435	530	618	705	784	866	943
S74 ($\mu\epsilon$)	-113	-292	-455	-611	-761	-901	-1033	-1161	-1280	-1395	-1502
S76 ($\mu\epsilon$)	-122	53	196	310	410	502	589	675	753	834	911
S79 ($\mu\epsilon$)	-88	138	328	483	622	750	873	991	1101	1213	1316
S83 ($\mu\epsilon$)	-33	65	154	232	305	375	442	510	573	638	701
S84 ($\mu\epsilon$)	-123	-58	19	89	162	234	304	368	437	512	585
S85 ($\mu\epsilon$)	-	-	-	-	-	-	-	-	-	-	-
S86 ($\mu\epsilon$)	-207	-70	54	143	218	282	335	379	423	469	510
S88 ($\mu\epsilon$)	-243	-382	-491	-584	-663	-727	-788	-843	-880	-908	-926
S90 ($\mu\epsilon$)	-106	24	145	242	332	413	484	544	610	680	748
S93 ($\mu\epsilon$)	-106	62	222	357	482	600	708	809	909	1012	1110
S97 ($\mu\epsilon$)	-135	-63	11	80	148	213	271	323	380	441	500
UAC-A1 ($\mu\epsilon$)	-83	63	204	328	445	551	654	754	845	936	1021
UAC-A2 ($\mu\epsilon$)	-35	94	219	327	428	519	610	696	776	855	928

Table F-22. Raw data, strain survey conducted after 30,000 cycles, cold-dry environmental conditions (Run 1) (continued)

Load Step	0	1	2	3	4	5	6	7	8	9	10
Pressure (psi)	-0.02	0.67	1.34	2.00	2.68	3.35	4.00	4.68	5.34	6.02	6.68
UAC-A3 ($\mu\epsilon$)	-80	26	130	219	301	376	450	521	588	653	717
UAC-F1 ($\mu\epsilon$)	-56	86	225	349	466	575	680	781	874	969	1054
UAC-F2 ($\mu\epsilon$)	-74	48	166	271	368	460	548	632	711	789	860
UBC-A1 ($\mu\epsilon$)	-	-	-	-	-	-	-	-	-	-	-
UBC-A2 ($\mu\epsilon$)	-4	188	370	528	671	800	920	1033	1135	1234	1325
UBC-A3 ($\mu\epsilon$)	-57	111	269	408	532	645	750	850	942	1029	1112
UBC-A4 ($\mu\epsilon$)	-91	61	203	328	440	542	639	731	816	899	977
UBC-F1 ($\mu\epsilon$)	-	-	-	-	-	-	-	-	-	-	-
UBC-F2 ($\mu\epsilon$)	-19	177	360	519	662	790	910	1023	1125	1224	1314
UBC-F3 ($\mu\epsilon$)	-35	139	301	441	567	681	788	889	980	1070	1151
UDAC-A1 ($\mu\epsilon$)	-37	116	261	389	506	612	717	815	906	996	1080
UDAC-A2 ($\mu\epsilon$)	-38	92	215	323	421	511	599	682	758	835	906
UDAC-A3 ($\mu\epsilon$)	-42	65	166	252	333	405	477	545	609	673	734
UDAC-F1 ($\mu\epsilon$)	-27	120	263	389	506	614	718	817	908	999	1084
UDAC-F2 ($\mu\epsilon$)	-31	91	208	313	409	498	586	668	744	820	892
UDBC-A1 ($\mu\epsilon$)	-	-	-	-	-	-	-	-	-	-	-
UDBC-A2 ($\mu\epsilon$)	153	358	549	714	863	996	1120	1235	1339	1439	1529
UDBC-A3 ($\mu\epsilon$)	111	286	450	591	719	834	940	1040	1130	1217	1296
UDBC-A4 ($\mu\epsilon$)	35	189	335	461	574	678	775	867	950	1031	1107
UDBC-F1 ($\mu\epsilon$)	-	-	-	-	-	-	-	-	-	-	-
UDBC-F2 ($\mu\epsilon$)	126	349	556	735	894	1037	1170	1293	1405	1513	1610

Table F-22. Raw data, strain survey conducted after 30,000 cycles, cold-dry environmental conditions (Run 1) (continued)

Load Step	0	1	2	3	4	5	6	7	8	9	10
Pressure (psi)	-0.02	0.67	1.34	2.00	2.68	3.35	4.00	4.68	5.34	6.02	6.68
UDBC-F3 ($\mu\epsilon$)	50	236	409	559	692	811	922	1026	1120	1211	1293

Table F-23. Raw data, strain survey conducted after 30,000 cycles, cold-dry environmental conditions (Run 2)

Load Step	0	1	2	3	4	5	6	7	8	9	10
Pressure (psi)	-0.15	0.67	1.35	2.01	2.66	3.34	4.01	4.66	5.34	5.99	6.66
Frame-1 (lbf)	4	106	202	366	444	566	683	804	883	1009	1157
Frame-2 (lbf)	69	122	221	338	454	567	680	796	905	1018	1135
Frame-3 (lbf)	3	116	228	332	454	568	679	792	910	1019	1132
Frame-4 (lbf)	56	101	226	338	452	569	684	793	904	1021	1131
Frame-5 (lbf)	3	107	218	333	456	577	686	792	911	1018	1133
Frame-6 (lbf)	5	116	217	342	443	580	690	800	910	1025	1123
Frame-7 (lbf)	19	112	223	341	456	572	677	792	911	1020	1131
Frame-8 (lbf)	13	114	233	340	450	571	682	790	909	1016	1123
Frame-9 (lbf)	47	111	230	343	454	567	679	795	906	1019	1133
Frame-10 (lbf)	1	115	234	342	458	554	681	792	907	1019	1133
Frame-11 (lbf)	14	113	230	340	454	567	680	791	910	1020	1133
Frame-12 (lbf)	-3	115	236	344	452	570	680	795	905	1019	1134
Hoop-1 (lbf)	69	719	1437	2134	2877	3574	4289	4995	5716	6424	7125
Hoop-2 (lbf)	133	708	1427	2169	2872	3563	4263	4997	5724	6431	7132
Hoop-3 (lbf)	104	714	1435	2137	2867	3566	4278	4997	5709	6424	7159
Hoop-4 (lbf)	4	721	1431	2129	2864	3561	4272	4983	5703	6410	7127
Hoop-5 (lbf)	16	726	1425	2144	2861	3569	4299	5013	5710	6446	7151
Hoop-6 (lbf)	53	712	1424	2138	2870	3568	4292	5000	5717	6420	7135
Hoop-7 (lbf)	145	718	1420	2143	2859	3572	4285	4995	5703	6434	7136
Hoop-8 (lbf)	181	716	1425	2148	2866	3571	4285	4997	5715	6426	7141
Hoop-9 (lbf)	-18	719	1415	2089	2860	3574	4290	4998	5709	6431	7140

Table F-23. Raw data, strain survey conducted after 30,000 cycles, cold-dry environmental conditions (Run 2) (continued)

Load Step	0	1	2	3	4	5	6	7	8	9	10
Pressure (psi)	-0.15	0.67	1.35	2.01	2.66	3.34	4.01	4.66	5.34	5.99	6.66
Hoop-10 (lbf)	-26	724	1416	2142	2877	3569	4279	4994	5702	6428	7146
Hoop-11 (lbf)	41	739	1423	2163	2870	3585	4295	4998	5709	6415	7137
Hoop-12 (lbf)	111	708	1420	2135	2858	3570	4288	4995	5716	6432	7130
Hoop-13 (lbf)	57	707	1443	2149	2843	3572	4285	4997	5713	6436	7140
Hoop-14 (lbf)	18	701	1417	2143	2880	3576	4284	4986	5704	6415	7125
Long-1 (lbf)	-14	669	1325	2018	2672	3337	3946	4701	5368	5950	6686
Long-2 (lbf)	-5	679	1330	2008	2671	3347	4006	4675	5313	6010	6677
Long-3 (lbf)	-8	681	1341	1999	2671	3333	4005	4674	5338	5998	6683
Long-4 (lbf)	6	642	1341	2000	2667	3341	4001	4674	5365	6006	6678
Long-5 (lbf)	4	677	1335	2008	2669	3344	4004	4692	5337	6008	6676
Long-6 (lbf)	-32	688	1304	2011	2673	3353	4001	4649	5334	6006	6666
Long-7 (lbf)	14	616	1349	2010	2664	3341	4004	4676	5346	6004	6700
Long-8 (lbf)	-5	673	1332	2004	2653	3334	4009	4674	5340	6011	6644
F01 ($\mu\epsilon$)	409	281	322	348	372	406	434	459	482	513	542
F02 ($\mu\epsilon$)	-430	-265	-226	-165	-103	-39	17	80	149	211	269
F03 ($\mu\epsilon$)	583	326	370	388	402	422	446	465	476	498	523
F04 ($\mu\epsilon$)	-570	-341	-285	-215	-137	-65	3	83	165	239	309
F05 ($\mu\epsilon$)	-	-	-	-	-	-	-	-	-	-	-
F06 ($\mu\epsilon$)	-587	-357	-305	-241	-172	-108	-47	23	98	170	234
F07 ($\mu\epsilon$)	362	161	195	220	240	267	298	321	337	364	392
F08 ($\mu\epsilon$)	-312	-109	-62	1	70	132	189	254	322	384	442

Table F-23. Raw data, strain survey conducted after 30,000 cycles, cold-dry environmental conditions (Run 2) (continued)

Load Step	0	1	2	3	4	5	6	7	8	9	10
Pressure (psi)	-0.15	0.67	1.35	2.01	2.66	3.34	4.01	4.66	5.34	5.99	6.66
IS16 ($\mu\epsilon$)	-190	-91	-15	50	111	171	233	294	357	423	488
IS17 ($\mu\epsilon$)	-24	-79	-91	-89	-75	-46	-12	27	72	125	180
IS18 ($\mu\epsilon$)	54	-40	-77	-96	-100	-91	-71	-46	-13	27	71
IS19 ($\mu\epsilon$)	-225	-193	-148	-110	-72	-32	10	51	97	143	192
IS20 ($\mu\epsilon$)	-347	-295	-237	-189	-143	-97	-52	-8	38	83	129
IS21 ($\mu\epsilon$)	-330	-282	-224	-177	-131	-88	-44	-2	41	85	130
IS22 ($\mu\epsilon$)	118	-10	-64	-101	-120	-124	-117	-100	-75	-42	-2
IS23 ($\mu\epsilon$)	247	134	74	30	-2	-22	-33	-38	-37	-27	-12
IS24 ($\mu\epsilon$)	-379	-309	-237	-177	-119	-65	-11	40	91	141	192
IS25 ($\mu\epsilon$)	201	98	52	19	-1	-10	-10	-5	7	26	51
IS26 ($\mu\epsilon$)	-162	6	147	273	389	495	595	688	779	866	949
IS27 ($\mu\epsilon$)	265	166	132	110	101	103	114	130	152	183	218
IS28 ($\mu\epsilon$)	-125	42	181	306	420	527	626	719	811	899	982
IS29 ($\mu\epsilon$)	-207	-54	75	187	289	385	475	561	647	728	809
IS30 ($\mu\epsilon$)	100	48	43	40	45	59	82	108	140	179	221
IS31 ($\mu\epsilon$)	-21	66	148	223	295	363	431	496	562	627	691
IS32 ($\mu\epsilon$)	26	110	187	254	318	376	433	485	537	587	635
IS33 ($\mu\epsilon$)	31	123	204	275	343	405	465	521	575	628	680
IS34 ($\mu\epsilon$)	124	69	48	32	27	28	39	54	77	104	136
IS35 ($\mu\epsilon$)	449	342	273	219	174	143	118	98	86	79	79
IS36 ($\mu\epsilon$)	50	138	219	290	356	417	476	531	585	636	686

Table F-23. Raw data, strain survey conducted after 30,000 cycles, cold-dry environmental conditions (Run 2) (continued)

Load Step	0	1	2	3	4	5	6	7	8	9	10
Pressure (psi)	-0.15	0.67	1.35	2.01	2.66	3.34	4.01	4.66	5.34	5.99	6.66
IS37 ($\mu\epsilon$)	372	248	177	120	75	43	20	4	-5	-7	-2
IS38 ($\mu\epsilon$)	100	210	306	392	471	546	616	682	748	809	868
IS39 ($\mu\epsilon$)	383	240	169	114	73	48	33	26	27	35	51
IS40 ($\mu\epsilon$)	110	223	323	412	496	575	650	720	791	856	920
IS41 ($\mu\epsilon$)	-79	62	176	280	377	466	551	632	711	787	860
IS42 ($\mu\epsilon$)	-193	-58	40	121	198	272	345	413	485	554	625
IS43 ($\mu\epsilon$)	-135	-87	-34	17	72	130	193	254	321	387	456
IS44 ($\mu\epsilon$)	-199	-225	-217	-198	-170	-136	-93	-47	4	57	114
IS45 ($\mu\epsilon$)	-71	7	75	137	197	252	308	360	413	464	517
IS46 ($\mu\epsilon$)	-85	-1	70	132	192	246	299	349	399	447	494
IS47 ($\mu\epsilon$)	-100	-19	49	111	169	223	277	327	377	426	474
IS48 ($\mu\epsilon$)	-69	-93	-73	-45	-6	38	91	144	204	265	330
IS49 ($\mu\epsilon$)	-85	-139	-163	-176	-180	-175	-164	-149	-127	-104	-75
IS50 ($\mu\epsilon$)	-86	16	96	168	237	299	359	417	473	527	579
IS51 ($\mu\epsilon$)	-91	-133	-150	-156	-152	-142	-124	-106	-80	-53	-21
IS52 ($\mu\epsilon$)	-73	70	181	283	380	468	553	634	714	790	864
IS53 ($\mu\epsilon$)	-144	-180	-186	-181	-166	-144	-115	-83	-46	-6	38
IS54 ($\mu\epsilon$)	-77	55	158	253	343	425	505	581	656	728	798
IS55 ($\mu\epsilon$)	-66	43	136	218	296	368	439	506	575	640	705
IS56 ($\mu\epsilon$)	-130	-45	23	81	136	189	245	299	358	416	477
IS57 ($\mu\epsilon$)	25	-21	-26	-22	-8	15	46	82	125	172	225

Table F-23. Raw data, strain survey conducted after 30,000 cycles, cold-dry environmental conditions (Run 2) (continued)

Load Step	0	1	2	3	4	5	6	7	8	9	10
Pressure (psi)	-0.15	0.67	1.35	2.01	2.66	3.34	4.01	4.66	5.34	5.99	6.66
IS58 ($\mu\epsilon$)	161	62	21	-3	-12	-8	7	29	60	97	140
IS59 ($\mu\epsilon$)	-196	-160	-112	-72	-32	9	52	96	143	192	243
IS60 ($\mu\epsilon$)	-274	-217	-155	-106	-59	-15	29	73	118	163	209
IS61 ($\mu\epsilon$)	-270	-210	-146	-93	-45	2	49	95	141	188	235
IS62 ($\mu\epsilon$)	113	9	-28	-50	-56	-48	-31	-7	26	66	110
IS63 ($\mu\epsilon$)	292	178	119	73	41	20	9	3	6	15	30
IS64 ($\mu\epsilon$)	-311	-242	-172	-115	-61	-12	39	85	133	181	229
IS65 ($\mu\epsilon$)	334	257	231	215	211	216	228	246	270	300	334
IS66 ($\mu\epsilon$)	-15	151	290	412	524	628	724	813	901	984	1062
IS67 ($\mu\epsilon$)	277	217	212	212	223	241	265	295	331	371	414
IS68 ($\mu\epsilon$)	23	198	344	473	594	704	807	903	997	1088	1173
IS69 ($\mu\epsilon$)	-43	115	243	356	460	554	645	730	814	896	974
IS70 ($\mu\epsilon$)	-253	-159	-80	-18	40	97	155	212	271	332	393
IS71 ($\mu\epsilon$)	-122	-137	-105	-69	-26	28	82	140	202	267	332
IS72 ($\mu\epsilon$)	-23	-73	-60	-36	-1	42	90	142	198	258	321
IS73 ($\mu\epsilon$)	60	132	203	267	329	387	444	498	551	604	654
IS74 ($\mu\epsilon$)	-34	43	115	179	240	297	352	405	456	506	553
IS75 ($\mu\epsilon$)	-15	65	138	204	267	325	381	435	488	539	588
IS76 ($\mu\epsilon$)	10	-10	20	60	109	163	222	283	349	417	486
IS77 ($\mu\epsilon$)	68	-31	-56	-65	-61	-47	-28	-4	25	59	96
IS78 ($\mu\epsilon$)	-5	82	162	232	299	362	422	480	536	591	643

Table F-23. Raw data, strain survey conducted after 30,000 cycles, cold-dry environmental conditions (Run 2) (continued)

Load Step	0	1	2	3	4	5	6	7	8	9	10
Pressure (psi)	-0.15	0.67	1.35	2.01	2.66	3.34	4.01	4.66	5.34	5.99	6.66
IS79 ($\mu\epsilon$)	13	-88	-113	-121	-118	-104	-86	-62	-34	-2	33
IS80 ($\mu\epsilon$)	54	162	258	347	432	512	589	663	737	807	875
IS81 ($\mu\epsilon$)	46	-61	-85	-93	-90	-76	-57	-33	-5	28	63
IS82 ($\mu\epsilon$)	-17	78	165	246	323	397	469	538	607	675	740
IS83 ($\mu\epsilon$)	53	138	219	292	361	426	490	552	615	676	736
IS84 ($\mu\epsilon$)	-74	-12	59	120	182	242	304	364	426	489	552
IS85 ($\mu\epsilon$)	-97	-99	-60	-14	40	99	162	226	294	364	435
IS86 ($\mu\epsilon$)	-108	-134	-117	-90	-52	-9	41	93	150	210	270
IS87 ($\mu\epsilon$)	-34	21	70	114	156	195	234	272	311	350	388
IS88 ($\mu\epsilon$)	-64	-12	34	73	110	144	177	208	239	270	300
IS89 ($\mu\epsilon$)	-70	-22	22	59	95	128	161	191	221	252	282
IS90 ($\mu\epsilon$)	-117	-126	-106	-77	-36	9	60	114	172	233	296
IS91 ($\mu\epsilon$)	-87	-122	-135	-138	-134	-124	-108	-89	-66	-37	-5
IS92 ($\mu\epsilon$)	-60	16	78	131	180	225	268	309	348	387	423
IS93 ($\mu\epsilon$)	-106	-104	-90	-67	-38	-6	31	70	113	160	208
IS94 ($\mu\epsilon$)	-83	70	190	299	402	496	586	671	754	834	911
IS95 ($\mu\epsilon$)	-91	-76	-51	-19	17	56	97	140	183	233	281
IS96 ($\mu\epsilon$)	-104	29	132	227	317	399	479	554	628	700	769
IS97 ($\mu\epsilon$)	-42	78	173	257	337	410	482	550	617	685	749
L01 ($\mu\epsilon$)	-	-	-	-	-	-	-	-	-	-	-
L02 ($\mu\epsilon$)	174	207	203	215	226	239	251	265	279	293	308

Table F-23. Raw data, strain survey conducted after 30,000 cycles, cold-dry environmental conditions (Run 2) (continued)

Load Step	0	1	2	3	4	5	6	7	8	9	10
Pressure (psi)	-0.15	0.67	1.35	2.01	2.66	3.34	4.01	4.66	5.34	5.99	6.66
L03 ($\mu\epsilon$)	45	67	56	64	72	84	95	111	128	144	161
L04 ($\mu\epsilon$)	105	143	145	162	179	197	213	233	252	271	288
L05 ($\mu\epsilon$)	93	122	122	133	143	154	163	174	184	194	203
L06 ($\mu\epsilon$)	15	55	67	86	104	123	138	152	164	176	186
L07 ($\mu\epsilon$)	-	-	-	-	-	-	-	-	-	-	-
L08 ($\mu\epsilon$)	203	268	290	325	353	383	409	437	461	485	508
L09 ($\mu\epsilon$)	93	168	193	226	260	293	321	349	373	398	419
L10 ($\mu\epsilon$)	-	-	-	-	-	-	-	-	-	-	-
RAC-A1 ($\mu\epsilon$)	-1	125	234	336	436	529	619	706	792	875	956
RAC-A2 ($\mu\epsilon$)	-28	80	177	264	350	431	508	582	657	729	798
RAC-A3 ($\mu\epsilon$)	36	126	208	280	348	413	475	535	595	651	708
RAC-F1 ($\mu\epsilon$)	-49	66	168	265	358	446	530	611	691	769	844
RAC-F2 ($\mu\epsilon$)	-34	67	159	244	327	404	479	551	622	691	757
RBC-A1 ($\mu\epsilon$)	239	408	540	656	764	862	953	1036	1117	1192	1262
RBC-A2 ($\mu\epsilon$)	137	274	384	481	570	651	726	796	864	926	985
RBC-A3 ($\mu\epsilon$)	140	269	373	465	549	627	699	767	833	894	952
RBC-A4 ($\mu\epsilon$)	46	170	273	364	448	526	599	669	737	800	861
RBC-F1 ($\mu\epsilon$)	244	414	542	654	757	850	936	1015	1091	1160	1227
RBC-F2 ($\mu\epsilon$)	185	334	444	542	631	711	786	854	920	981	1039
RBC-F3 ($\mu\epsilon$)	162	308	416	510	597	675	748	815	879	939	997
S16 ($\mu\epsilon$)	-79	11	96	168	235	297	361	423	482	538	595

Table F-23. Raw data, strain survey conducted after 30,000 cycles, cold-dry environmental conditions (Run 2) (continued)

Load Step	0	1	2	3	4	5	6	7	8	9	10
Pressure (psi)	-0.15	0.67	1.35	2.01	2.66	3.34	4.01	4.66	5.34	5.99	6.66
S17 ($\mu\epsilon$)	-	-	-	-	-	-	-	-	-	-	-
S18 ($\mu\epsilon$)	-717	-492	-315	-176	-53	56	164	262	358	448	537
S20 ($\mu\epsilon$)	749	386	126	-102	-307	-477	-628	-762	-885	-990	-1079
S22 ($\mu\epsilon$)	-451	-265	-122	-6	96	189	278	361	440	514	589
S25 ($\mu\epsilon$)	-677	-456	-280	-127	15	148	277	401	520	633	745
S29 ($\mu\epsilon$)	49	108	164	222	282	341	401	460	522	583	644
S30 ($\mu\epsilon$)	-224	-72	64	180	287	381	474	559	644	725	803
S32 ($\mu\epsilon$)	985	797	673	559	456	365	283	209	139	77	23
S34 ($\mu\epsilon$)	-	-	-	-	-	-	-	-	-	-	-
S37 ($\mu\epsilon$)	-465	-240	-45	122	278	417	552	678	803	921	1036
S41 ($\mu\epsilon$)	22	112	186	262	337	409	479	549	620	687	753
S42 ($\mu\epsilon$)	-	-	-	-	-	-	-	-	-	-	-
S43 ($\mu\epsilon$)	-336	-215	-116	-28	54	132	210	285	359	427	499
S44 ($\mu\epsilon$)	-34	142	282	397	502	599	688	775	862	943	1025
S46 ($\mu\epsilon$)	-220	-567	-814	-1042	-1251	-1436	-1601	-1757	-1906	-2044	-2170
S48 ($\mu\epsilon$)	-135	30	151	254	351	436	522	600	679	755	828
S51 ($\mu\epsilon$)	-203	13	187	339	483	611	736	857	975	1089	1200
S55 ($\mu\epsilon$)	-185	-106	-37	31	100	165	231	297	364	428	493
S56 ($\mu\epsilon$)	-252	-206	-143	-83	-20	40	104	167	233	295	361
S57 ($\mu\epsilon$)	-	-	-	-	-	-	-	-	-	-	-
S58 ($\mu\epsilon$)	-578	-361	-194	-62	55	157	255	346	434	515	596

Table F-23. Raw data, strain survey conducted after 30,000 cycles, cold-dry environmental conditions (Run 2) (continued)

Load Step	0	1	2	3	4	5	6	7	8	9	10
Pressure (psi)	-0.15	0.67	1.35	2.01	2.66	3.34	4.01	4.66	5.34	5.99	6.66
S60 ($\mu\epsilon$)	309	-36	-280	-486	-671	-822	-954	-1070	-1174	-1261	-1332
S62 ($\mu\epsilon$)	-470	-279	-133	-17	86	176	263	344	423	499	572
S65 ($\mu\epsilon$)	-726	-434	-204	-15	156	306	450	587	719	842	961
S69 ($\mu\epsilon$)	-132	-69	-13	37	85	131	178	224	269	312	355
S70 ($\mu\epsilon$)	-7	48	118	186	256	323	392	461	532	603	674
S71 ($\mu\epsilon$)	-	-	-	-	-	-	-	-	-	-	-
S72 ($\mu\epsilon$)	-141	70	215	332	436	528	616	699	781	861	940
S74 ($\mu\epsilon$)	-64	-287	-448	-605	-755	-895	-1025	-1151	-1272	-1386	-1494
S76 ($\mu\epsilon$)	-141	57	197	310	412	502	589	670	752	831	909
S79 ($\mu\epsilon$)	-127	139	326	479	619	745	866	981	1095	1204	1309
S83 ($\mu\epsilon$)	-61	63	150	228	302	370	438	503	569	633	696
S84 ($\mu\epsilon$)	-171	-94	-19	53	125	197	273	346	421	493	567
S85 ($\mu\epsilon$)	-	-	-	-	-	-	-	-	-	-	-
S86 ($\mu\epsilon$)	-309	-146	-23	68	147	213	276	332	386	434	481
S88 ($\mu\epsilon$)	-242	-417	-525	-621	-702	-765	-815	-857	-893	-920	-939
S90 ($\mu\epsilon$)	-168	-22	96	192	281	360	440	514	588	657	726
S93 ($\mu\epsilon$)	-158	25	182	314	441	557	672	782	888	990	1089
S97 ($\mu\epsilon$)	-194	-100	-28	40	107	171	236	299	361	421	481
UAC-A1 ($\mu\epsilon$)	-110	64	201	327	444	550	652	748	842	930	1015
UAC-A2 ($\mu\epsilon$)	-59	95	215	325	428	518	608	692	773	849	922
UAC-A3 ($\mu\epsilon$)	-98	28	128	217	300	374	449	518	586	650	712

Table F-23. Raw data, strain survey conducted after 30,000 cycles, cold-dry environmental conditions (Run 2) (continued)

Load Step	0	1	2	3	4	5	6	7	8	9	10
Pressure (psi)	-0.15	0.67	1.35	2.01	2.66	3.34	4.01	4.66	5.34	5.99	6.66
UAC-F1 ($\mu\epsilon$)	-81	89	223	348	467	575	678	776	872	961	1049
UAC-F2 ($\mu\epsilon$)	-96	50	164	268	369	459	545	628	708	783	856
UBC-A1 ($\mu\epsilon$)	-	-	-	-	-	-	-	-	-	-	-
UBC-A2 ($\mu\epsilon$)	-34	191	370	528	672	801	920	1030	1134	1232	1324
UBC-A3 ($\mu\epsilon$)	-85	112	268	406	532	646	750	847	939	1027	1110
UBC-A4 ($\mu\epsilon$)	-118	59	200	325	438	542	638	727	814	896	976
UBC-F1 ($\mu\epsilon$)	-	-	-	-	-	-	-	-	-	-	-
UBC-F2 ($\mu\epsilon$)	-56	179	357	516	660	789	909	1018	1123	1220	1310
UBC-F3 ($\mu\epsilon$)	-69	139	297	438	566	680	787	885	979	1066	1148
UDAC-A1 ($\mu\epsilon$)	-64	118	257	386	505	612	714	810	903	992	1076
UDAC-A2 ($\mu\epsilon$)	-61	94	213	319	420	510	597	678	755	830	901
UDAC-A3 ($\mu\epsilon$)	-60	67	164	250	331	405	476	542	606	670	730
UDAC-F1 ($\mu\epsilon$)	-54	121	259	387	506	613	715	812	905	995	1079
UDAC-F2 ($\mu\epsilon$)	-54	91	205	310	409	498	583	664	741	817	887
UDBC-A1 ($\mu\epsilon$)	-	-	-	-	-	-	-	-	-	-	-
UDBC-A2 ($\mu\epsilon$)	112	355	543	708	858	992	1114	1226	1332	1431	1521
UDBC-A3 ($\mu\epsilon$)	73	280	442	584	713	828	933	1030	1123	1209	1289
UDBC-A4 ($\mu\epsilon$)	-1	181	325	451	566	670	766	855	941	1022	1099
UDBC-F1 ($\mu\epsilon$)	-	-	-	-	-	-	-	-	-	-	-
UDBC-F2 ($\mu\epsilon$)	83	346	551	729	890	1034	1165	1286	1400	1505	1602
UDBC-F3 ($\mu\epsilon$)	8	229	401	550	684	806	916	1018	1114	1203	1287

Table F-24. Raw data, strain survey conducted after 30,000 cycles, cold-dry environmental conditions (Run 3)

Load Step	0	1	2	3	4	5	6	7	8	9	10
Pressure (psi)	-0.01	0.66	1.34	2.01	2.65	3.33	4.02	4.67	5.35	5.98	6.67
Frame-1 (lbf)	4	108	243	351	450	576	663	789	929	1010	1128
Frame-2 (lbf)	76	112	224	339	453	567	678	795	906	1019	1135
Frame-3 (lbf)	2	115	224	341	455	565	678	793	903	1019	1135
Frame-4 (lbf)	36	119	234	337	457	568	679	794	907	1019	1132
Frame-5 (lbf)	9	104	223	335	453	561	678	798	907	1017	1135
Frame-6 (lbf)	-8	118	214	337	456	559	682	784	905	1025	1135
Frame-7 (lbf)	16	112	225	340	453	562	676	795	904	1016	1133
Frame-8 (lbf)	10	113	220	341	457	566	685	792	910	1023	1132
Frame-9 (lbf)	45	110	228	343	444	566	680	791	906	1020	1133
Frame-10 (lbf)	0	113	222	342	443	565	681	793	905	1020	1134
Frame-11 (lbf)	3	112	227	336	455	562	682	799	898	1016	1133
Frame-12 (lbf)	17	111	222	342	462	568	681	795	906	1019	1137
Hoop-1 (lbf)	89	717	1415	2146	2846	3574	4292	5005	5696	6440	7142
Hoop-2 (lbf)	140	709	1413	2110	2867	3586	4292	5005	5697	6422	7141
Hoop-3 (lbf)	99	719	1410	2133	2864	3567	4300	5014	5718	6424	7154
Hoop-4 (lbf)	-5	711	1429	2144	2853	3580	4302	4998	5725	6428	7143
Hoop-5 (lbf)	45	711	1425	2152	2838	3550	4291	4998	5697	6430	7128
Hoop-6 (lbf)	45	705	1434	2138	2865	3582	4274	5010	5719	6412	7145
Hoop-7 (lbf)	98	721	1411	2147	2845	3568	4287	5004	5718	6420	7142
Hoop-8 (lbf)	231	717	1430	2140	2854	3577	4290	5006	5717	6420	7142
Hoop-9 (lbf)	3	702	1415	2149	2852	3569	4283	5006	5721	6427	7147

Table F-24. Raw data, strain survey conducted after 30,000 cycles, cold-dry environmental conditions (Run 3) (continued)

Load Step	0	1	2	3	4	5	6	7	8	9	10
Pressure (psi)	-0.01	0.66	1.34	2.01	2.65	3.33	4.02	4.67	5.35	5.98	6.67
Hoop-10 (lbf)	6	701	1429	2144	2848	3577	4305	5017	5716	6421	7142
Hoop-11 (lbf)	89	721	1425	2146	2865	3559	4283	4989	5694	6423	7137
Hoop-12 (lbf)	104	722	1421	2152	2862	3573	4277	5002	5723	6425	7129
Hoop-13 (lbf)	64	707	1456	2136	2855	3580	4291	5010	5710	6425	7147
Hoop-14 (lbf)	32	710	1435	2133	2846	3562	4283	5013	5714	6426	7151
Long-1 (lbf)	67	668	1337	2006	2697	3320	4016	4679	5297	6022	6684
Long-2 (lbf)	-13	662	1326	2004	2666	3349	4004	4676	5333	6011	6696
Long-3 (lbf)	2	683	1337	2000	2667	3345	4000	4675	5348	6009	6674
Long-4 (lbf)	-9	664	1317	2005	2669	3339	3999	4673	5337	6011	6672
Long-5 (lbf)	2	645	1338	2002	2669	3340	4004	4694	5323	6004	6677
Long-6 (lbf)	-7	692	1337	2004	2673	3333	3998	4654	5326	6016	6651
Long-7 (lbf)	-19	697	1328	1995	2678	3329	3993	4671	5341	6015	6672
Long-8 (lbf)	6	649	1334	2003	2667	3333	4005	4660	5340	5991	6677
F01 ($\mu\epsilon$)	308	286	332	359	385	412	433	455	485	519	546
F02 ($\mu\epsilon$)	-357	-279	-229	-170	-110	-50	20	86	146	201	265
F03 ($\mu\epsilon$)	448	341	384	405	419	437	448	462	483	510	528
F04 ($\mu\epsilon$)	-479	-351	-297	-228	-155	-81	4	84	158	224	303
F05 ($\mu\epsilon$)	-	-	-	-	-	-	-	-	-	-	-
F06 ($\mu\epsilon$)	-477	-362	-319	-254	-192	-124	-48	26	92	150	226
F07 ($\mu\epsilon$)	257	178	217	238	264	288	301	323	348	380	403
F08 ($\mu\epsilon$)	-238	-127	-81	-19	47	111	183	249	309	364	431

Table F-24. Raw data, strain survey conducted after 30,000 cycles, cold-dry environmental conditions (Run 3) (continued)

Load Step	0	1	2	3	4	5	6	7	8	9	10
Pressure (psi)	-0.01	0.66	1.34	2.01	2.65	3.33	4.02	4.67	5.35	5.98	6.67
IS16 ($\mu\epsilon$)	-172	-89	-12	52	113	174	236	298	360	424	492
IS17 ($\mu\epsilon$)	-33	-75	-87	-85	-71	-44	-10	31	76	128	184
IS18 ($\mu\epsilon$)	37	-36	-74	-93	-96	-87	-70	-43	-11	28	73
IS19 ($\mu\epsilon$)	-226	-192	-146	-108	-70	-30	11	54	97	144	194
IS20 ($\mu\epsilon$)	-347	-295	-236	-187	-142	-96	-51	-6	38	83	131
IS21 ($\mu\epsilon$)	-331	-281	-223	-175	-131	-87	-43	0	41	85	132
IS22 ($\mu\epsilon$)	89	-5	-59	-96	-116	-122	-115	-98	-74	-41	0
IS23 ($\mu\epsilon$)	227	137	76	33	2	-19	-33	-37	-35	-25	-10
IS24 ($\mu\epsilon$)	-378	-310	-237	-177	-119	-65	-11	41	91	141	193
IS25 ($\mu\epsilon$)	181	102	54	22	2	-8	-10	-4	8	28	52
IS26 ($\mu\epsilon$)	-145	2	146	271	386	493	596	692	779	865	949
IS27 ($\mu\epsilon$)	245	171	135	114	105	104	115	133	155	184	219
IS28 ($\mu\epsilon$)	-108	37	178	302	416	524	626	722	810	896	983
IS29 ($\mu\epsilon$)	-193	-58	74	185	287	384	477	565	646	728	810
IS30 ($\mu\epsilon$)	83	55	48	45	48	63	83	110	142	180	224
IS31 ($\mu\epsilon$)	-17	64	147	221	292	362	431	498	562	626	692
IS32 ($\mu\epsilon$)	31	109	187	254	316	376	433	487	538	587	637
IS33 ($\mu\epsilon$)	38	122	203	275	341	405	465	523	576	628	680
IS34 ($\mu\epsilon$)	113	75	53	37	31	33	42	58	79	106	139
IS35 ($\mu\epsilon$)	433	345	275	221	178	145	118	99	87	82	81
IS36 ($\mu\epsilon$)	54	137	219	288	355	416	476	532	585	636	687

Table F-24. Raw data, strain survey conducted after 30,000 cycles, cold-dry environmental conditions (Run 3) (continued)

Load Step	0	1	2	3	4	5	6	7	8	9	10
Pressure (psi)	-0.01	0.66	1.34	2.01	2.65	3.33	4.02	4.67	5.35	5.98	6.67
IS37 ($\mu\epsilon$)	351	252	180	123	78	45	20	3	-5	-5	-1
IS38 ($\mu\epsilon$)	110	208	305	390	469	544	616	684	747	809	869
IS39 ($\mu\epsilon$)	358	247	173	118	77	51	33	26	28	37	53
IS40 ($\mu\epsilon$)	119	220	320	410	493	572	650	722	790	855	920
IS41 ($\mu\epsilon$)	-66	55	172	274	372	462	550	633	710	784	859
IS42 ($\mu\epsilon$)	-169	-57	41	123	198	274	348	419	487	557	630
IS43 ($\mu\epsilon$)	-128	-86	-33	20	74	133	196	260	323	390	460
IS44 ($\mu\epsilon$)	-207	-224	-215	-197	-169	-134	-91	-44	5	58	117
IS45 ($\mu\epsilon$)	-61	7	75	137	195	253	308	363	413	466	518
IS46 ($\mu\epsilon$)	-74	-1	70	132	190	246	300	352	400	447	495
IS47 ($\mu\epsilon$)	-91	-20	49	110	168	223	276	329	378	425	474
IS48 ($\mu\epsilon$)	-85	-92	-71	-43	-5	40	92	147	205	266	332
IS49 ($\mu\epsilon$)	-95	-139	-163	-176	-179	-175	-163	-147	-128	-103	-74
IS50 ($\mu\epsilon$)	-73	14	96	168	235	299	360	419	473	526	580
IS51 ($\mu\epsilon$)	-99	-133	-150	-156	-151	-141	-125	-104	-81	-53	-20
IS52 ($\mu\epsilon$)	-54	66	178	280	375	466	554	637	713	788	865
IS53 ($\mu\epsilon$)	-151	-180	-186	-180	-164	-142	-114	-81	-45	-5	40
IS54 ($\mu\epsilon$)	-59	52	156	251	340	424	506	584	656	726	799
IS55 ($\mu\epsilon$)	-54	43	137	220	296	370	442	511	576	642	708
IS56 ($\mu\epsilon$)	-121	-44	24	80	134	188	244	300	355	414	475
IS57 ($\mu\epsilon$)	12	-18	-25	-21	-7	14	46	83	124	171	221

Table F-24. Raw data, strain survey conducted after 30,000 cycles, cold-dry environmental conditions (Run 3) (continued)

Load Step	0	1	2	3	4	5	6	7	8	9	10
Pressure (psi)	-0.01	0.66	1.34	2.01	2.65	3.33	4.02	4.67	5.35	5.98	6.67
IS58 ($\mu\epsilon$)	140	65	23	-2	-11	-8	6	29	58	96	139
IS59 ($\mu\epsilon$)	-202	-163	-115	-75	-34	7	51	96	141	189	241
IS60 ($\mu\epsilon$)	-277	-219	-158	-109	-63	-17	28	73	116	160	207
IS61 ($\mu\epsilon$)	-274	-214	-149	-97	-49	-1	46	92	138	184	232
IS62 ($\mu\epsilon$)	90	11	-27	-48	-55	-48	-32	-7	25	64	109
IS63 ($\mu\epsilon$)	266	180	119	74	42	21	7	3	5	14	28
IS64 ($\mu\epsilon$)	-314	-247	-177	-120	-66	-15	36	83	130	177	225
IS65 ($\mu\epsilon$)	311	259	231	217	211	216	226	245	269	299	332
IS66 ($\mu\epsilon$)	-5	142	284	405	516	621	721	812	898	979	1059
IS67 ($\mu\epsilon$)	254	219	212	213	222	240	263	294	329	368	411
IS68 ($\mu\epsilon$)	34	187	335	466	584	696	802	902	993	1082	1168
IS69 ($\mu\epsilon$)	-35	104	235	348	449	547	640	728	810	888	968
IS70 ($\mu\epsilon$)	-251	-160	-82	-21	36	95	153	211	268	328	391
IS71 ($\mu\epsilon$)	-142	-140	-109	-73	-28	24	79	139	199	262	330
IS72 ($\mu\epsilon$)	-47	-75	-62	-38	-4	40	88	141	196	255	318
IS73 ($\mu\epsilon$)	61	128	199	263	324	383	442	497	549	601	652
IS74 ($\mu\epsilon$)	-31	40	112	175	235	294	350	404	454	503	552
IS75 ($\mu\epsilon$)	-12	61	135	200	261	321	379	434	485	535	585
IS76 ($\mu\epsilon$)	-7	-14	16	56	104	160	220	282	345	412	482
IS77 ($\mu\epsilon$)	35	-34	-61	-69	-65	-51	-32	-7	22	55	92
IS78 ($\mu\epsilon$)	-1	78	157	227	293	357	420	478	533	587	641

Table F-24. Raw data, strain survey conducted after 30,000 cycles, cold-dry environmental conditions (Run 3) (continued)

Load Step	0	1	2	3	4	5	6	7	8	9	10
Pressure (psi)	-0.01	0.66	1.34	2.01	2.65	3.33	4.02	4.67	5.35	5.98	6.67
IS79 ($\mu\epsilon$)	-23	-92	-119	-127	-123	-109	-90	-66	-38	-6	29
IS80 ($\mu\epsilon$)	60	155	252	339	423	505	585	661	732	801	871
IS81 ($\mu\epsilon$)	10	-64	-89	-98	-94	-80	-61	-36	-8	24	60
IS82 ($\mu\epsilon$)	-14	71	158	238	314	390	465	535	602	668	736
IS83 ($\mu\epsilon$)	55	134	216	287	355	421	488	551	611	672	734
IS84 ($\mu\epsilon$)	-74	-11	60	121	180	242	305	366	427	488	552
IS85 ($\mu\epsilon$)	-108	-98	-60	-13	38	98	162	228	294	363	434
IS86 ($\mu\epsilon$)	-120	-133	-118	-89	-54	-9	41	95	149	208	269
IS87 ($\mu\epsilon$)	-29	20	69	113	153	194	234	274	311	349	388
IS88 ($\mu\epsilon$)	-61	-14	32	71	107	142	176	208	239	269	298
IS89 ($\mu\epsilon$)	-68	-23	20	59	92	127	160	191	221	251	281
IS90 ($\mu\epsilon$)	-124	-124	-106	-75	-38	8	61	116	173	232	297
IS91 ($\mu\epsilon$)	-95	-122	-137	-139	-135	-124	-109	-89	-66	-38	-6
IS92 ($\mu\epsilon$)	-53	14	76	129	177	223	267	309	347	385	422
IS93 ($\mu\epsilon$)	-108	-103	-91	-67	-40	-6	30	71	113	158	207
IS94 ($\mu\epsilon$)	-64	67	186	296	396	493	585	672	753	831	908
IS95 ($\mu\epsilon$)	-92	-75	-51	-18	16	55	96	140	184	231	280
IS96 ($\mu\epsilon$)	-89	25	128	224	311	396	477	555	627	697	767
IS97 ($\mu\epsilon$)	-28	76	171	256	334	410	483	552	619	685	750
L01 ($\mu\epsilon$)	-	-	-	-	-	-	-	-	-	-	-
L02 ($\mu\epsilon$)	177	194	192	204	214	226	239	253	267	280	296

Table F-24. Raw data, strain survey conducted after 30,000 cycles, cold-dry environmental conditions (Run 3) (continued)

Load Step	0	1	2	3	4	5	6	7	8	9	10
Pressure (psi)	-0.01	0.66	1.34	2.01	2.65	3.33	4.02	4.67	5.35	5.98	6.67
L03 ($\mu\epsilon$)	46	54	43	51	59	72	84	100	115	130	149
L04 ($\mu\epsilon$)	108	130	134	151	166	184	203	222	240	257	277
L05 ($\mu\epsilon$)	90	111	113	125	135	145	154	165	175	184	194
L06 ($\mu\epsilon$)	16	53	67	87	106	124	139	153	166	178	188
L07 ($\mu\epsilon$)	-	-	-	-	-	-	-	-	-	-	-
L08 ($\mu\epsilon$)	212	255	280	313	343	370	397	423	447	472	496
L09 ($\mu\epsilon$)	90	153	176	216	246	278	306	332	357	381	404
L10 ($\mu\epsilon$)	-	-	-	-	-	-	-	-	-	-	-
RAC-A1 ($\mu\epsilon$)	7	117	227	329	426	521	615	703	787	869	951
RAC-A2 ($\mu\epsilon$)	-23	73	169	257	340	423	505	579	652	722	793
RAC-A3 ($\mu\epsilon$)	40	121	203	275	342	408	472	534	591	648	705
RAC-F1 ($\mu\epsilon$)	-43	59	162	258	350	439	527	609	687	763	839
RAC-F2 ($\mu\epsilon$)	-30	61	154	239	320	399	477	549	618	686	754
RBC-A1 ($\mu\epsilon$)	258	402	537	653	760	859	952	1038	1117	1191	1263
RBC-A2 ($\mu\epsilon$)	150	270	382	478	566	649	727	798	864	924	985
RBC-A3 ($\mu\epsilon$)	153	265	370	462	546	625	699	769	832	893	952
RBC-A4 ($\mu\epsilon$)	58	167	270	361	444	524	600	671	736	799	860
RBC-F1 ($\mu\epsilon$)	266	410	539	650	753	848	936	1018	1091	1161	1229
RBC-F2 ($\mu\epsilon$)	203	329	442	538	627	709	786	857	921	981	1041
RBC-F3 ($\mu\epsilon$)	180	304	412	506	593	673	748	817	880	940	998
S16 ($\mu\epsilon$)	-78	-1	86	159	227	290	353	416	473	533	594

Table F-24. Raw data, strain survey conducted after 30,000 cycles, cold-dry environmental conditions (Run 3) (continued)

Load Step	0	1	2	3	4	5	6	7	8	9	10
Pressure (psi)	-0.01	0.66	1.34	2.01	2.65	3.33	4.02	4.67	5.35	5.98	6.67
S17 ($\mu\epsilon$)	-	-	-	-	-	-	-	-	-	-	-
S18 ($\mu\epsilon$)	-694	-502	-322	-180	-58	55	161	262	353	446	529
S20 ($\mu\epsilon$)	701	393	130	-96	-292	-469	-627	-765	-882	-981	-1071
S22 ($\mu\epsilon$)	-428	-275	-129	-11	92	184	274	357	432	511	590
S25 ($\mu\epsilon$)	-652	-468	-290	-136	6	141	272	398	512	627	744
S29 ($\mu\epsilon$)	58	107	164	221	280	341	402	463	523	583	645
S30 ($\mu\epsilon$)	-212	-73	66	181	285	382	476	563	645	725	806
S32 ($\mu\epsilon$)	962	810	683	570	467	375	290	213	146	86	29
S34 ($\mu\epsilon$)	-	-	-	-	-	-	-	-	-	-	-
S37 ($\mu\epsilon$)	-445	-241	-43	123	274	417	555	683	803	920	1038
S41 ($\mu\epsilon$)	37	109	184	259	333	407	481	552	619	685	753
S42 ($\mu\epsilon$)	-	-	-	-	-	-	-	-	-	-	-
S43 ($\mu\epsilon$)	-329	-227	-125	-35	46	124	203	280	349	422	498
S44 ($\mu\epsilon$)	-13	144	285	400	503	606	696	783	864	945	1030
S46 ($\mu\epsilon$)	-275	-561	-807	-1032	-1235	-1426	-1602	-1762	-1906	-2039	-2163
S48 ($\mu\epsilon$)	-110	29	153	256	350	438	523	604	681	754	830
S51 ($\mu\epsilon$)	-174	13	189	341	480	612	742	864	978	1089	1203
S55 ($\mu\epsilon$)	-176	-108	-37	31	98	165	234	300	364	428	495
S56 ($\mu\epsilon$)	-261	-221	-155	-93	-31	30	94	159	220	286	355
S57 ($\mu\epsilon$)	-	-	-	-	-	-	-	-	-	-	-
S58 ($\mu\epsilon$)	-559	-376	-208	-74	42	147	246	339	421	505	591

Table F-24. Raw data, strain survey conducted after 30,000 cycles, cold-dry environmental conditions (Run 3) (continued)

Load Step	0	1	2	3	4	5	6	7	8	9	10
Pressure (psi)	-0.01	0.66	1.34	2.01	2.65	3.33	4.02	4.67	5.35	5.98	6.67
S60 ($\mu\epsilon$)	270	-24	-270	-475	-653	-811	-952	-1071	-1171	-1253	-1325
S62 ($\mu\epsilon$)	-455	-291	-144	-27	74	167	255	338	413	490	568
S65 ($\mu\epsilon$)	-696	-452	-220	-33	136	294	443	581	706	829	954
S69 ($\mu\epsilon$)	-132	-85	-29	23	71	118	165	212	255	300	347
S70 ($\mu\epsilon$)	-6	43	115	184	252	321	392	462	529	600	672
S71 ($\mu\epsilon$)	-	-	-	-	-	-	-	-	-	-	-
S72 ($\mu\epsilon$)	-108	67	213	330	432	526	616	701	780	858	938
S74 ($\mu\epsilon$)	-93	-273	-437	-595	-741	-882	-1020	-1147	-1265	-1376	-1485
S76 ($\mu\epsilon$)	-112	57	197	310	409	501	590	672	751	828	907
S79 ($\mu\epsilon$)	-84	136	323	475	613	742	867	983	1092	1200	1307
S83 ($\mu\epsilon$)	-42	59	146	224	296	366	436	503	566	629	693
S84 ($\mu\epsilon$)	-169	-105	-29	44	116	189	265	340	412	487	564
S85 ($\mu\epsilon$)	-	-	-	-	-	-	-	-	-	-	-
S86 ($\mu\epsilon$)	-284	-150	-26	68	145	214	279	339	389	439	491
S88 ($\mu\epsilon$)	-279	-423	-531	-625	-703	-769	-824	-867	-900	-924	-940
S90 ($\mu\epsilon$)	-156	-35	83	181	269	350	430	508	576	648	723
S93 ($\mu\epsilon$)	-144	12	171	306	430	549	666	778	880	982	1086
S97 ($\mu\epsilon$)	-184	-114	-41	29	96	162	228	292	352	414	478
UAC-A1 ($\mu\epsilon$)	-87	60	198	324	439	548	653	751	840	928	1015
UAC-A2 ($\mu\epsilon$)	-39	91	213	322	423	518	608	694	772	848	924
UAC-A3 ($\mu\epsilon$)	-82	26	127	217	299	376	451	521	587	651	715

Table F-24. Raw data, strain survey conducted after 30,000 cycles, cold-dry environmental conditions (Run 3) (continued)

Load Step	0	1	2	3	4	5	6	7	8	9	10
Pressure (psi)	-0.01	0.66	1.34	2.01	2.65	3.33	4.02	4.67	5.35	5.98	6.67
UAC-F1 ($\mu\epsilon$)	-59	84	220	345	461	573	679	779	871	960	1048
UAC-F2 ($\mu\epsilon$)	-77	46	161	266	363	457	546	630	707	781	856
UBC-A1 ($\mu\epsilon$)	-	-	-	-	-	-	-	-	-	-	-
UBC-A2 ($\mu\epsilon$)	-8	185	367	526	668	798	921	1034	1134	1230	1324
UBC-A3 ($\mu\epsilon$)	-63	106	266	404	528	643	751	850	940	1026	1111
UBC-A4 ($\mu\epsilon$)	-99	54	198	322	435	539	639	730	814	895	977
UBC-F1 ($\mu\epsilon$)	-	-	-	-	-	-	-	-	-	-	-
UBC-F2 ($\mu\epsilon$)	-26	173	354	513	656	787	909	1022	1123	1218	1311
UBC-F3 ($\mu\epsilon$)	-42	134	295	435	562	679	787	887	979	1065	1149
UDAC-A1 ($\mu\epsilon$)	-40	114	254	382	498	609	714	812	901	988	1073
UDAC-A2 ($\mu\epsilon$)	-41	91	209	317	415	508	596	679	754	827	899
UDAC-A3 ($\mu\epsilon$)	-44	65	161	249	327	404	476	544	607	669	730
UDAC-F1 ($\mu\epsilon$)	-30	116	256	383	499	610	715	814	904	991	1077
UDAC-F2 ($\mu\epsilon$)	-34	87	202	307	403	495	583	665	740	813	885
UDBC-A1 ($\mu\epsilon$)	-	-	-	-	-	-	-	-	-	-	-
UDBC-A2 ($\mu\epsilon$)	134	342	534	700	848	984	1110	1225	1329	1426	1518
UDBC-A3 ($\mu\epsilon$)	90	268	433	575	703	819	929	1029	1119	1204	1286
UDBC-A4 ($\mu\epsilon$)	12	170	316	443	556	662	761	853	937	1016	1094
UDBC-F1 ($\mu\epsilon$)	-	-	-	-	-	-	-	-	-	-	-
UDBC-F2 ($\mu\epsilon$)	108	332	541	720	880	1027	1163	1286	1397	1501	1599
UDBC-F3 ($\mu\epsilon$)	28	217	393	543	677	800	914	1017	1112	1201	1285

F.2.2.3 After 60,000 Cycles

Table F-25. Raw data, strain survey conducted after 60,000 cycles, cold-dry environmental conditions (Run 1)

Load Step	0	1	2	3	4	5	6	7	8	9	10
Pressure (psi)	-0.03	0.68	1.31	1.99	2.67	3.32	3.98	4.66	5.32	6.02	6.65
Frame-1 (lb _f)	0	140	232	302	504	514	652	832	951	958	1094
Frame-2 (lb _f)	51	118	241	342	439	571	703	769	919	997	1132
Frame-3 (lb _f)	1	109	222	336	443	581	653	793	905	1020	1131
Frame-4 (lb _f)	25	126	224	337	447	555	675	804	933	999	1132
Frame-5 (lb _f)	4	106	230	334	455	562	669	800	913	1030	1132
Frame-6 (lb _f)	-8	132	213	325	452	553	664	803	897	1004	1148
Frame-7 (lb _f)	-8	112	235	345	455	559	677	794	904	1023	1133
Frame-8 (lb _f)	2	107	238	334	465	551	683	807	907	1020	1134
Frame-9 (lb _f)	17	110	222	352	451	570	682	796	907	1020	1132
Frame-10 (lb _f)	1	120	233	332	450	566	692	797	905	1032	1136
Frame-11 (lb _f)	8	116	227	322	456	577	681	794	904	1024	1133
Frame-12 (lb _f)	0	108	233	340	448	581	674	793	910	1029	1133
Hoop-1 (lb _f)	31	732	1439	2172	2851	3595	4278	4979	5707	6446	7161
Hoop-2 (lb _f)	77	671	1416	2102	2819	3530	4318	5023	5707	6428	7127
Hoop-3 (lb _f)	54	721	1436	2147	2850	3570	4278	4996	5698	6427	7147
Hoop-4 (lb _f)	12	714	1434	2154	2855	3582	4279	5003	5713	6431	7143
Hoop-5 (lb _f)	46	706	1416	2148	2850	3586	4293	4992	5706	6445	7123
Hoop-6 (lb _f)	14	729	1426	2141	2861	3579	4293	5008	5699	6412	7135
Hoop-7 (lb _f)	42	682	1435	2152	2870	3575	4301	4996	5713	6425	7126
Hoop-8 (lb _f)	12	716	1418	2143	2860	3574	4283	5011	5710	6422	7141

Table F-25. Raw data, strain survey conducted after 60,000 cycles, cold-dry environmental conditions (Run 1) (continued)

Load Step	0	1	2	3	4	5	6	7	8	9	10
Pressure (psi)	-0.03	0.68	1.31	1.99	2.67	3.32	3.98	4.66	5.32	6.02	6.65
Hoop-9 (lbf)	-22	760	1405	2138	2867	3551	4283	5003	5702	6431	7132
Hoop-10 (lbf)	11	716	1392	2159	2847	3567	4289	4984	5717	6421	7126
Hoop-11 (lbf)	1	704	1469	2145	2805	3574	4295	4991	5709	6432	7139
Hoop-12 (lbf)	74	695	1410	2123	2869	3558	4285	4998	5708	6424	7138
Hoop-13 (lbf)	9	723	1440	2165	2873	3583	4268	5027	5701	6427	7154
Hoop-14 (lbf)	41	748	1452	2154	2861	3569	4284	5011	5727	6435	7136
Long-1 (lbf)	-4	673	1341	1959	2690	3325	3997	4718	5349	6001	6702
Long-2 (lbf)	13	677	1340	2006	2677	3343	4009	4671	5342	6006	6671
Long-3 (lbf)	16	661	1337	1999	2667	3339	4006	4674	5341	6004	6676
Long-4 (lbf)	-13	677	1332	2008	2687	3320	4002	4673	5344	6006	6676
Long-5 (lbf)	-19	671	1332	2001	2672	3336	4010	4675	5337	6011	6673
Long-6 (lbf)	-18	655	1340	2026	2685	3339	4004	4651	5323	6020	6677
Long-7 (lbf)	-65	718	1303	2002	2680	3329	4008	4657	5341	6013	6671
Long-8 (lbf)	0	637	1326	1999	2673	3333	4004	4680	5318	5994	6676
F01 ($\mu\epsilon$)	-	-	-	-	-	-	-	-	-	-	-
F02 ($\mu\epsilon$)	-	-	-	-	-	-	-	-	-	-	-
F03 ($\mu\epsilon$)	-	-	-	-	-	-	-	-	-	-	-
F04 ($\mu\epsilon$)	-	-	-	-	-	-	-	-	-	-	-
F05 ($\mu\epsilon$)	-	-	-	-	-	-	-	-	-	-	-
F06 ($\mu\epsilon$)	-	-	-	-	-	-	-	-	-	-	-
F07 ($\mu\epsilon$)	-	-	-	-	-	-	-	-	-	-	-

Table F-25. Raw data, strain survey conducted after 60,000 cycles, cold-dry environmental conditions (Run 1) (continued)

Load Step	0	1	2	3	4	5	6	7	8	9	10
Pressure (psi)	-0.03	0.68	1.31	1.99	2.67	3.32	3.98	4.66	5.32	6.02	6.65
F08 ($\mu\epsilon$)	-	-	-	-	-	-	-	-	-	-	-
IS18 ($\mu\epsilon$)	75	-33	-93	-127	-144	-143	-132	-111	-81	-47	-2
IS20 ($\mu\epsilon$)	-324	-283	-240	-204	-167	-127	-89	-50	-8	31	75
IS22 ($\mu\epsilon$)	157	48	-16	-55	-80	-84	-77	-61	-35	-3	40
IS25 ($\mu\epsilon$)	220	90	19	-28	-61	-78	-85	-83	-73	-57	-32
IS26 ($\mu\epsilon$)	-186	-76	33	130	227	314	396	476	552	624	695
IS27 ($\mu\epsilon$)	309	189	131	97	78	74	82	95	120	148	185
IS28 ($\mu\epsilon$)	-85	52	188	312	433	541	644	744	840	929	1016
IS29 ($\mu\epsilon$)	-152	-26	95	200	304	397	489	576	663	743	824
IS30 ($\mu\epsilon$)	151	126	111	104	102	114	134	158	190	227	273
IS32 ($\mu\epsilon$)	19	107	186	254	321	383	441	496	550	601	652
IS34 ($\mu\epsilon$)	157	110	77	57	43	47	55	70	94	122	159
IS37 ($\mu\epsilon$)	383	266	184	120	66	31	4	-14	-23	-26	-19
IS38 ($\mu\epsilon$)	89	202	302	391	478	556	630	701	770	835	899
IS39 ($\mu\epsilon$)	376	254	174	116	70	44	29	22	26	36	55
IS40 ($\mu\epsilon$)	99	214	318	411	503	586	664	741	814	885	953
IS41 ($\mu\epsilon$)	-88	40	154	256	354	444	529	610	691	767	843
IS44 ($\mu\epsilon$)	-143	-189	-199	-194	-176	-149	-115	-74	-29	20	74
IS46 ($\mu\epsilon$)	-34	27	86	142	198	250	300	349	397	444	489
IS48 ($\mu\epsilon$)	-39	-52	-44	-23	8	49	94	144	199	255	317
IS51 ($\mu\epsilon$)	-118	-167	-179	-181	-172	-159	-141	-119	-94	-65	-31

Table F-25. Raw data, strain survey conducted after 60,000 cycles, cold-dry environmental conditions (Run 1) (continued)

Load Step	0	1	2	3	4	5	6	7	8	9	10
Pressure (psi)	-0.03	0.68	1.31	1.99	2.67	3.32	3.98	4.66	5.32	6.02	6.65
IS52 ($\mu\epsilon$)	-56	55	161	259	359	448	536	622	704	782	859
IS55 ($\mu\epsilon$)	-19	75	168	249	330	405	478	549	618	686	753
IS58 ($\mu\epsilon$)	163	55	-4	-34	-48	-44	-28	-2	32	70	118
IS60 ($\mu\epsilon$)	-301	-243	-193	-148	-106	-65	-25	16	55	95	138
IS62 ($\mu\epsilon$)	122	30	-17	-40	-51	-43	-26	2	36	75	124
IS65 ($\mu\epsilon$)	360	258	206	178	160	156	161	177	199	224	258
IS66 ($\mu\epsilon$)	-87	30	136	233	322	403	480	556	626	692	758
IS67 ($\mu\epsilon$)	327	262	240	237	241	257	282	314	352	393	439
IS68 ($\mu\epsilon$)	53	222	376	517	645	760	868	975	1073	1166	1253
IS69 ($\mu\epsilon$)	-11	139	270	386	493	588	681	774	859	940	1019
IS72 ($\mu\epsilon$)	29	-24	-29	-9	20	60	105	160	218	276	342
IS74 ($\mu\epsilon$)	-38	33	100	163	226	284	338	394	446	496	546
IS76 ($\mu\epsilon$)	31	5	24	60	104	155	212	275	340	406	478
IS79 ($\mu\epsilon$)	79	-19	-50	-55	-50	-38	-20	7	36	66	104
IS80 ($\mu\epsilon$)	60	155	249	341	431	513	593	674	750	823	894
IS83 ($\mu\epsilon$)	102	187	271	350	425	495	563	634	699	762	825
IS86 ($\mu\epsilon$)	-55	-91	-90	-72	-39	4	48	98	153	212	274
IS88 ($\mu\epsilon$)	-62	-14	29	67	105	140	171	201	231	261	291
IS90 ($\mu\epsilon$)	-99	-109	-103	-81	-49	-4	41	93	149	208	270
IS93 ($\mu\epsilon$)	-56	-70	-58	-40	-10	25	61	101	145	192	244
IS94 ($\mu\epsilon$)	-78	54	174	280	387	485	575	664	748	830	908

Table F-25. Raw data, strain survey conducted after 60,000 cycles, cold-dry environmental conditions (Run 1) (continued)

Load Step	0	1	2	3	4	5	6	7	8	9	10
Pressure (psi)	-0.03	0.68	1.31	1.99	2.67	3.32	3.98	4.66	5.32	6.02	6.65
IS95 ($\mu\epsilon$)	-59	-56	-31	-4	32	75	114	158	204	253	305
IS96 ($\mu\epsilon$)	-96	18	121	212	306	391	470	548	623	697	767
IS97 ($\mu\epsilon$)	-34	72	167	247	329	407	478	548	615	685	751
IS104 ($\mu\epsilon$)	62	-54	-134	-185	-219	-236	-241	-237	-221	-201	-172
IS105 ($\mu\epsilon$)	-549	-488	-433	-384	-341	-299	-258	-215	-174	-135	-93
IS106 ($\mu\epsilon$)	137	-32	-151	-234	-296	-336	-363	-377	-382	-380	-367
IS107 ($\mu\epsilon$)	207	166	129	106	88	80	80	86	100	119	146
IS108 ($\mu\epsilon$)	-197	24	208	371	520	654	779	898	1009	1114	1213
IS109 ($\mu\epsilon$)	-	-	-	-	-	-	-	-	-	-	-
IS110 ($\mu\epsilon$)	49	-44	-109	-149	-173	-176	-169	-153	-125	-92	-49
IS111 ($\mu\epsilon$)	-471	-402	-334	-274	-215	-155	-98	-41	17	73	132
IS112 ($\mu\epsilon$)	163	29	-56	-114	-153	-170	-176	-171	-155	-132	-100
IS113 ($\mu\epsilon$)	234	191	162	141	123	119	121	128	141	160	186
IS114 ($\mu\epsilon$)	-192	3	182	338	482	614	738	855	966	1070	1172
IS115 ($\mu\epsilon$)	-	-	-	-	-	-	-	-	-	-	-
L01 ($\mu\epsilon$)	-	-	-	-	-	-	-	-	-	-	-
L02 ($\mu\epsilon$)	-	-	-	-	-	-	-	-	-	-	-
L03 ($\mu\epsilon$)	-	-	-	-	-	-	-	-	-	-	-
L04 ($\mu\epsilon$)	-	-	-	-	-	-	-	-	-	-	-
L05 ($\mu\epsilon$)	-	-	-	-	-	-	-	-	-	-	-
L06 ($\mu\epsilon$)	-	-	-	-	-	-	-	-	-	-	-

Table F-25. Raw data, strain survey conducted after 60,000 cycles, cold-dry environmental conditions (Run 1) (continued)

Load Step	0	1	2	3	4	5	6	7	8	9	10
Pressure (psi)	-0.03	0.68	1.31	1.99	2.67	3.32	3.98	4.66	5.32	6.02	6.65
L07 ($\mu\epsilon$)	-	-	-	-	-	-	-	-	-	-	-
L08 ($\mu\epsilon$)	-	-	-	-	-	-	-	-	-	-	-
L09 ($\mu\epsilon$)	-	-	-	-	-	-	-	-	-	-	-
L10 ($\mu\epsilon$)	-	-	-	-	-	-	-	-	-	-	-
RAC-A1 ($\mu\epsilon$)	36	146	255	360	464	558	651	746	834	920	1004
RAC-F1 ($\mu\epsilon$)	-44	59	158	254	351	441	526	611	693	772	852
RBC-A1 ($\mu\epsilon$)	269	450	606	741	873	986	1092	1192	1287	1374	1457
RBC-A2 ($\mu\epsilon$)	135	276	397	502	603	691	772	849	923	989	1055
RBC-A3 ($\mu\epsilon$)	139	270	382	478	573	657	734	806	876	941	1004
RBC-F1 ($\mu\epsilon$)	257	430	579	707	832	939	1037	1129	1216	1297	1372
RBC-F2 ($\mu\epsilon$)	162	305	429	535	638	725	806	881	953	1019	1080
RBC-F3 ($\mu\epsilon$)	128	268	388	489	588	673	751	824	893	958	1018
S18 ($\mu\epsilon$)	-514	-323	-175	-61	44	134	218	302	379	454	529
S20 ($\mu\epsilon$)	532	326	150	0	-133	-243	-337	-419	-486	-538	-580
S22 ($\mu\epsilon$)	-591	-311	-106	57	188	325	440	549	647	743	837
S25 ($\mu\epsilon$)	-587	-377	-206	-57	88	220	346	472	590	704	816
S29 ($\mu\epsilon$)	13	70	126	182	244	301	360	421	482	542	603
S30 ($\mu\epsilon$)	-265	-98	48	177	296	402	501	595	684	769	855
S32 ($\mu\epsilon$)	1006	830	679	554	430	329	236	149	72	3	-59
S34 ($\mu\epsilon$)	-331	-210	-87	21	127	223	313	397	480	562	641
S37 ($\mu\epsilon$)	-435	-201	-4	167	331	479	617	752	877	999	1118

Table F-25. Raw data, strain survey conducted after 60,000 cycles, cold-dry environmental conditions (Run 1) (continued)

Load Step	0	1	2	3	4	5	6	7	8	9	10
Pressure (psi)	-0.03	0.68	1.31	1.99	2.67	3.32	3.98	4.66	5.32	6.02	6.65
S41 ($\mu\epsilon$)	-33	32	103	175	252	323	393	464	533	601	669
S42 ($\mu\epsilon$)	-	-	-	-	-	-	-	-	-	-	-
S43 ($\mu\epsilon$)	-	-	-	-	-	-	-	-	-	-	-
S44 ($\mu\epsilon$)	-30	120	238	341	437	524	608	689	768	844	920
S46 ($\mu\epsilon$)	-295	-360	-414	-465	-509	-544	-575	-601	-621	-636	-646
S48 ($\mu\epsilon$)	-1225	-1090	-978	-885	-793	-711	-632	-557	-483	-411	-342
S51 ($\mu\epsilon$)	-21	172	327	467	602	728	849	970	1086	1199	1310
S55 ($\mu\epsilon$)	-141	-61	12	83	156	225	293	363	431	499	566
S58 ($\mu\epsilon$)	-1008	-761	-557	-388	-254	-121	-2	113	217	313	412
S60 ($\mu\epsilon$)	290	39	-163	-330	-476	-592	-692	-774	-839	-890	-926
S62 ($\mu\epsilon$)	-520	-285	-106	38	165	274	376	476	564	649	734
S65 ($\mu\epsilon$)	-609	-362	-171	-2	161	306	443	578	703	825	942
S69 ($\mu\epsilon$)	-403	-312	-215	-123	-34	59	150	242	330	415	497
S72 ($\mu\epsilon$)	-171	36	183	303	412	505	593	679	761	840	919
S74 ($\mu\epsilon$)	-155	-271	-381	-489	-592	-683	-772	-860	-941	-1017	-1088
S76 ($\mu\epsilon$)	-227	-40	93	204	307	398	485	570	652	731	810
S79 ($\mu\epsilon$)	-153	110	297	453	599	732	857	980	1096	1209	1318
S83 ($\mu\epsilon$)	-105	22	120	207	292	366	439	512	582	648	715
S86 ($\mu\epsilon$)	-176	-6	124	229	328	413	493	572	646	720	792
S88 ($\mu\epsilon$)	-283	-421	-521	-603	-670	-726	-768	-804	-827	-842	-847
S90 ($\mu\epsilon$)	-190	-46	75	178	275	359	439	518	595	670	744

Table F-25. Raw data, strain survey conducted after 60,000 cycles, cold-dry environmental conditions (Run 1) (continued)

Load Step	0	1	2	3	4	5	6	7	8	9	10
Pressure (psi)	-0.03	0.68	1.31	1.99	2.67	3.32	3.98	4.66	5.32	6.02	6.65
S93 ($\mu\epsilon$)	-201	-15	142	277	409	525	638	750	855	960	1060
S97 ($\mu\epsilon$)	-265	-185	-109	-38	37	104	170	236	300	365	429
S104 ($\mu\epsilon$)	-559	-360	-194	-51	73	185	288	386	478	564	648
S105 ($\mu\epsilon$)	612	267	-12	-249	-460	-644	-809	-957	-1089	-1206	-1305
S106 ($\mu\epsilon$)	-510	-251	-44	124	276	407	530	649	755	856	954
S107 ($\mu\epsilon$)	-591	-391	-203	-29	138	297	449	599	742	880	1012
S109 ($\mu\epsilon$)	-64	-43	5	65	133	201	273	347	420	494	567
S110 ($\mu\epsilon$)	-470	-276	-105	40	173	293	403	508	606	700	793
S111 ($\mu\epsilon$)	551	250	-3	-205	-384	-533	-661	-770	-860	-933	-993
S112 ($\mu\epsilon$)	-488	-269	-95	50	182	296	402	503	597	688	777
S113 ($\mu\epsilon$)	-587	-390	-207	-41	125	276	422	565	700	833	962
S115 ($\mu\epsilon$)	13	51	103	164	233	301	373	449	525	607	706
UAC-A1 ($\mu\epsilon$)	-79	56	187	307	426	534	638	739	834	925	1012
UAC-F1 ($\mu\epsilon$)	-56	77	202	322	443	553	658	760	858	952	1041
UB-A1 ($\mu\epsilon$)	-	-	-	-	-	-	-	-	-	-	-
UB-A2 ($\mu\epsilon$)	-36	216	447	644	827	989	1140	1282	1414	1536	1651
UB-A3 ($\mu\epsilon$)	-75	150	355	529	690	834	970	1096	1215	1324	1430
UB-F1 ($\mu\epsilon$)	-	-	-	-	-	-	-	-	-	-	-
UB-F2 ($\mu\epsilon$)	-264	-31	174	347	501	648	784	907	1025	1132	1233
UB-F3 ($\mu\epsilon$)	-562	-312	-117	27	99	234	339	423	484	516	554
UBC-A1 ($\mu\epsilon$)	-	-	-	-	-	-	-	-	-	-	-

Table F-25. Raw data, strain survey conducted after 60,000 cycles, cold-dry environmental conditions (Run 1) (continued)

Load Step	0	1	2	3	4	5	6	7	8	9	10
Pressure (psi)	-0.03	0.68	1.31	1.99	2.67	3.32	3.98	4.66	5.32	6.02	6.65
UBC-A2 ($\mu\epsilon$)	103	337	555	750	936	1097	1247	1389	1519	1640	1753
UBC-A3 ($\mu\epsilon$)	-21	152	315	458	597	717	830	937	1036	1128	1216
UBC-F1 ($\mu\epsilon$)	-	-	-	-	-	-	-	-	-	-	-
UBC-F2 ($\mu\epsilon$)	82	319	540	735	924	1085	1235	1376	1507	1628	1740
UBC-F3 ($\mu\epsilon$)	3	180	347	493	635	757	870	977	1076	1170	1256
UDAC-A1 ($\mu\epsilon$)	-53	104	244	368	492	605	707	807	902	994	1080
UDAC-F1 ($\mu\epsilon$)	-44	108	245	369	492	605	709	809	905	997	1083
UDB-A1 ($\mu\epsilon$)	-	-	-	-	-	-	-	-	-	-	-
UDB-A2 ($\mu\epsilon$)	-527	-343	-213	-105	-20	75	156	230	295	349	400
UDB-A3 ($\mu\epsilon$)	-157	94	303	486	655	800	935	1061	1177	1287	1389
UDB-F1 ($\mu\epsilon$)	-	-	-	-	-	-	-	-	-	-	-
UDB-F2 ($\mu\epsilon$)	-23	312	583	829	1052	1248	1428	1596	1749	1895	2026
UDB-F3 ($\mu\epsilon$)	-5	258	468	660	836	990	1132	1267	1390	1508	1615
UDBC-A1 ($\mu\epsilon$)	-	-	-	-	-	-	-	-	-	-	-
UDBC-A2 ($\mu\epsilon$)	-	-	-	-	-	-	-	-	-	-	-
UDBC-A3 ($\mu\epsilon$)	146	362	548	713	860	988	1106	1220	1321	1413	1499
UDBC-F1 ($\mu\epsilon$)	-	-	-	-	-	-	-	-	-	-	-
UDBC-F2 ($\mu\epsilon$)	-	-	-	-	-	-	-	-	-	-	-
UDBC-F3 ($\mu\epsilon$)	92	326	524	702	859	996	1123	1241	1350	1445	1537

Table F-26. Raw data, strain survey conducted after 60,000 cycles, cold-dry environmental conditions (Run 2)

Load Step	0	1	2	3	4	5	6	7	8	9	10
Pressure (psi)	-0.02	0.67	1.33	1.98	2.66	3.32	4.01	4.68	5.35	5.99	6.71
Frame-1 (lbf)	-2	131	241	283	512	550	733	826	947	1063	1128
Frame-2 (lbf)	52	132	236	329	467	561	676	806	923	1017	1138
Frame-3 (lbf)	2	122	210	325	468	553	671	764	867	1018	1135
Frame-4 (lbf)	32	108	218	337	474	554	682	803	910	1019	1144
Frame-5 (lbf)	-3	132	212	345	474	580	696	787	898	1001	1120
Frame-6 (lbf)	10	138	237	329	464	569	668	792	926	1022	1134
Frame-7 (lbf)	1	128	223	333	451	564	678	787	906	1018	1134
Frame-8 (lbf)	9	131	220	339	450	571	694	791	897	1017	1140
Frame-9 (lbf)	23	105	231	342	454	570	678	788	907	1022	1127
Frame-10 (lbf)	1	106	219	353	465	572	672	803	901	1018	1125
Frame-11 (lbf)	13	112	225	333	448	570	683	795	907	1016	1139
Frame-12 (lbf)	0	104	209	336	449	551	673	794	901	1018	1125
Hoop-1 (lbf)	50	691	1427	2158	2824	3585	4269	4985	5686	6414	7149
Hoop-2 (lbf)	108	677	1453	2182	2893	3612	4325	4997	5717	6435	7165
Hoop-3 (lbf)	31	726	1433	2140	2861	3559	4295	4994	5721	6433	7162
Hoop-4 (lbf)	24	704	1416	2132	2849	3564	4281	5000	5722	6409	7157
Hoop-5 (lbf)	-12	720	1465	2137	2843	3571	4273	4989	5707	6422	7163
Hoop-6 (lbf)	14	720	1404	2136	2847	3565	4300	4997	5726	6431	7160
Hoop-7 (lbf)	28	713	1439	2158	2844	3568	4294	5002	5720	6431	7146
Hoop-8 (lbf)	30	721	1434	2146	2860	3558	4294	4995	5721	6423	7162
Hoop-9 (lbf)	-4	720	1431	2142	2831	3574	4302	5008	5723	6429	7169

Table F-26. Raw data, strain survey conducted after 60,000 cycles, cold-dry environmental conditions (Run 2) (continued)

Load Step	0	1	2	3	4	5	6	7	8	9	10
Pressure (psi)	-0.02	0.67	1.33	1.98	2.66	3.32	4.01	4.68	5.35	5.99	6.71
Hoop-10 (lbf)	4	691	1414	2133	2832	3597	4295	5025	5730	6430	7164
Hoop-11 (lbf)	-16	709	1428	2132	2863	3566	4294	5016	5718	6433	7151
Hoop-12 (lbf)	44	765	1430	2122	2889	3561	4291	5008	5705	6423	7166
Hoop-13 (lbf)	-1	734	1447	2130	2869	3585	4292	4951	5725	6429	7159
Hoop-14 (lbf)	10	694	1442	2129	2853	3558	4300	5002	5716	6437	7146
Long-1 (lbf)	-8	702	1307	1995	2650	3328	3918	4679	5327	6010	6625
Long-2 (lbf)	-5	645	1336	2006	2669	3331	3998	4671	5339	6009	6663
Long-3 (lbf)	2	670	1340	2015	2670	3342	3999	4680	5338	6007	6673
Long-4 (lbf)	-19	657	1331	2006	2669	3348	3990	4660	5344	6009	6674
Long-5 (lbf)	-1	668	1338	2003	2665	3337	4001	4676	5339	6021	6660
Long-6 (lbf)	43	671	1337	1984	2664	3358	3952	4673	5340	6013	6658
Long-7 (lbf)	-65	663	1281	1977	2680	3301	4005	4680	5338	5989	6728
Long-8 (lbf)	20	677	1335	2008	2662	3341	3999	4678	5357	6012	6690
F01 ($\mu\epsilon$)	-	-	-	-	-	-	-	-	-	-	-
F02 ($\mu\epsilon$)	-	-	-	-	-	-	-	-	-	-	-
F03 ($\mu\epsilon$)	-	-	-	-	-	-	-	-	-	-	-
F04 ($\mu\epsilon$)	-	-	-	-	-	-	-	-	-	-	-
F05 ($\mu\epsilon$)	-	-	-	-	-	-	-	-	-	-	-
F06 ($\mu\epsilon$)	-	-	-	-	-	-	-	-	-	-	-
F07 ($\mu\epsilon$)	-	-	-	-	-	-	-	-	-	-	-
F08 ($\mu\epsilon$)	-	-	-	-	-	-	-	-	-	-	-

Table F-26. Raw data, strain survey conducted after 60,000 cycles, cold-dry environmental conditions (Run 2) (continued)

Load Step	0	1	2	3	4	5	6	7	8	9	10
Pressure (psi)	-0.02	0.67	1.33	1.98	2.66	3.32	4.01	4.68	5.35	5.99	6.71
IS18 ($\mu\epsilon$)	68	-36	-96	-129	-143	-144	-129	-109	-78	-42	2
IS20 ($\mu\epsilon$)	-330	-286	-246	-209	-169	-134	-90	-51	-8	34	78
IS22 ($\mu\epsilon$)	155	49	-16	-57	-78	-86	-76	-60	-32	3	43
IS25 ($\mu\epsilon$)	217	92	20	-28	-59	-78	-82	-81	-69	-52	-29
IS26 ($\mu\epsilon$)	-185	-71	34	129	225	311	400	478	556	627	701
IS27 ($\mu\epsilon$)	316	196	135	98	81	74	86	99	125	155	189
IS28 ($\mu\epsilon$)	-82	61	192	312	433	541	651	749	845	933	1024
IS29 ($\mu\epsilon$)	-154	-19	97	198	303	395	494	580	667	748	831
IS30 ($\mu\epsilon$)	149	121	105	97	100	109	131	156	191	230	273
IS32 ($\mu\epsilon$)	18	111	187	254	320	380	443	497	552	603	654
IS34 ($\mu\epsilon$)	156	111	76	54	45	42	54	70	95	125	159
IS37 ($\mu\epsilon$)	378	266	185	119	68	28	5	-15	-22	-23	-20
IS38 ($\mu\epsilon$)	90	207	306	391	477	554	635	704	774	837	902
IS39 ($\mu\epsilon$)	375	255	176	116	73	43	30	23	29	40	54
IS40 ($\mu\epsilon$)	100	219	321	410	502	584	669	744	819	887	956
IS41 ($\mu\epsilon$)	-88	44	156	253	353	441	534	614	696	769	846
IS44 ($\mu\epsilon$)	-142	-186	-197	-194	-176	-148	-112	-72	-26	23	79
IS46 ($\mu\epsilon$)	-32	28	89	142	197	249	302	350	398	445	493
IS48 ($\mu\epsilon$)	-39	-50	-41	-22	9	48	95	145	202	258	322
IS51 ($\mu\epsilon$)	-117	-161	-173	-177	-171	-156	-137	-116	-89	-60	-28
IS52 ($\mu\epsilon$)	-53	59	165	261	358	449	540	624	705	783	865

Table F-26. Raw data, strain survey conducted after 60,000 cycles, cold-dry environmental conditions (Run 2) (continued)

Load Step	0	1	2	3	4	5	6	7	8	9	10
Pressure (psi)	-0.02	0.67	1.33	1.98	2.66	3.32	4.01	4.68	5.35	5.99	6.71
IS55 ($\mu\epsilon$)	-18	81	171	250	330	406	483	551	621	688	758
IS58 ($\mu\epsilon$)	150	49	-7	-38	-47	-46	-27	-3	34	75	123
IS60 ($\mu\epsilon$)	-303	-242	-193	-154	-107	-70	-25	14	57	99	141
IS62 ($\mu\epsilon$)	118	31	-18	-45	-49	-46	-24	1	38	81	129
IS65 ($\mu\epsilon$)	356	263	209	178	164	159	167	179	203	232	264
IS66 ($\mu\epsilon$)	-91	34	138	229	322	402	485	557	629	697	763
IS67 ($\mu\epsilon$)	322	267	243	236	244	259	286	315	355	399	444
IS68 ($\mu\epsilon$)	47	226	378	512	645	761	876	978	1077	1171	1261
IS69 ($\mu\epsilon$)	-23	140	268	380	491	587	683	772	859	942	1022
IS72 ($\mu\epsilon$)	24	-25	-27	-12	21	58	111	160	221	281	347
IS74 ($\mu\epsilon$)	-36	35	102	163	227	283	343	397	450	500	550
IS76 ($\mu\epsilon$)	32	9	28	58	107	155	218	277	343	410	482
IS79 ($\mu\epsilon$)	76	-18	-47	-58	-50	-39	-15	8	39	73	107
IS80 ($\mu\epsilon$)	58	156	252	340	432	514	600	677	754	826	899
IS83 ($\mu\epsilon$)	93	185	269	346	424	493	564	632	699	765	826
IS86 ($\mu\epsilon$)	-58	-91	-87	-71	-39	1	51	101	158	215	279
IS88 ($\mu\epsilon$)	-60	-10	33	68	105	138	173	203	235	264	294
IS90 ($\mu\epsilon$)	-102	-108	-100	-80	-47	-6	45	96	153	211	276
IS93 ($\mu\epsilon$)	-59	-65	-53	-36	-9	25	65	104	150	196	248
IS94 ($\mu\epsilon$)	-76	60	179	283	386	483	580	666	752	831	915
IS95 ($\mu\epsilon$)	-61	-50	-27	-2	33	72	118	160	209	256	309

Table F-26. Raw data, strain survey conducted after 60,000 cycles, cold-dry environmental conditions (Run 2) (continued)

Load Step	0	1	2	3	4	5	6	7	8	9	10
Pressure (psi)	-0.02	0.67	1.33	1.98	2.66	3.32	4.01	4.68	5.35	5.99	6.71
IS96 ($\mu\epsilon$)	-95	23	125	214	304	389	474	551	627	698	774
IS97 ($\mu\epsilon$)	-36	78	169	249	329	404	481	549	621	686	756
IS104 ($\mu\epsilon$)	70	-52	-132	-184	-219	-235	-237	-232	-217	-196	-167
IS105 ($\mu\epsilon$)	-558	-492	-438	-390	-345	-304	-256	-216	-174	-134	-87
IS106 ($\mu\epsilon$)	140	-31	-149	-231	-292	-335	-360	-376	-378	-374	-363
IS107 ($\mu\epsilon$)	212	168	134	108	88	81	83	89	104	123	151
IS108 ($\mu\epsilon$)	-194	27	212	369	517	652	785	901	1014	1116	1223
IS109 ($\mu\epsilon$)	-	-	-	-	-	-	-	-	-	-	-
IS110 ($\mu\epsilon$)	58	-38	-105	-146	-167	-175	-165	-148	-120	-86	-44
IS111 ($\mu\epsilon$)	-478	-399	-335	-276	-213	-159	-96	-40	19	76	137
IS112 ($\mu\epsilon$)	156	28	-59	-115	-152	-173	-174	-169	-152	-129	-97
IS113 ($\mu\epsilon$)	235	197	164	142	127	120	124	130	145	163	188
IS114 ($\mu\epsilon$)	-194	18	188	340	486	615	746	861	974	1075	1181
IS115 ($\mu\epsilon$)	-	-	-	-	-	-	-	-	-	-	-
L01 ($\mu\epsilon$)	-	-	-	-	-	-	-	-	-	-	-
L02 ($\mu\epsilon$)	-	-	-	-	-	-	-	-	-	-	-
L03 ($\mu\epsilon$)	-	-	-	-	-	-	-	-	-	-	-
L04 ($\mu\epsilon$)	-	-	-	-	-	-	-	-	-	-	-
L05 ($\mu\epsilon$)	-	-	-	-	-	-	-	-	-	-	-
L06 ($\mu\epsilon$)	-	-	-	-	-	-	-	-	-	-	-
L07 ($\mu\epsilon$)	-	-	-	-	-	-	-	-	-	-	-

Table F-26. Raw data, strain survey conducted after 60,000 cycles, cold-dry environmental conditions (Run 2) (continued)

Load Step	0	1	2	3	4	5	6	7	8	9	10
Pressure (psi)	-0.02	0.67	1.33	1.98	2.66	3.32	4.01	4.68	5.35	5.99	6.71
L08 ($\mu\epsilon$)	-	-	-	-	-	-	-	-	-	-	-
L09 ($\mu\epsilon$)	-	-	-	-	-	-	-	-	-	-	-
L10 ($\mu\epsilon$)	-	-	-	-	-	-	-	-	-	-	-
RAC-A1 ($\mu\epsilon$)	37	148	257	359	464	560	657	748	837	922	1009
RAC-F1 ($\mu\epsilon$)	-44	59	160	253	351	438	532	615	699	776	857
RBC-A1 ($\mu\epsilon$)	272	462	614	745	872	986	1100	1197	1293	1376	1462
RBC-A2 ($\mu\epsilon$)	136	283	402	502	602	689	778	853	927	992	1057
RBC-A3 ($\mu\epsilon$)	139	275	385	478	572	653	738	809	881	943	1006
RBC-F1 ($\mu\epsilon$)	258	442	586	712	830	937	1043	1133	1220	1297	1376
RBC-F2 ($\mu\epsilon$)	161	315	434	538	635	722	810	884	956	1020	1084
RBC-F3 ($\mu\epsilon$)	126	275	390	491	585	669	755	826	895	958	1022
S18 ($\mu\epsilon$)	-508	-316	-176	-61	44	133	222	301	381	455	536
S20 ($\mu\epsilon$)	569	344	167	21	-115	-229	-331	-413	-481	-532	-581
S22 ($\mu\epsilon$)	-645	-359	-152	14	165	287	414	519	628	729	833
S25 ($\mu\epsilon$)	-583	-373	-208	-60	85	216	349	471	592	705	827
S29 ($\mu\epsilon$)	18	72	128	183	243	301	364	424	486	546	611
S30 ($\mu\epsilon$)	-258	-89	55	178	298	402	506	598	688	772	861
S32 ($\mu\epsilon$)	1018	832	688	562	445	339	237	154	76	9	-62
S34 ($\mu\epsilon$)	-347	-216	-95	11	114	207	306	390	477	557	642
S37 ($\mu\epsilon$)	-426	-194	-2	166	331	476	621	751	880	999	1126
S41 ($\mu\epsilon$)	-31	33	104	175	251	322	397	466	537	603	674

Table F-26. Raw data, strain survey conducted after 60,000 cycles, cold-dry environmental conditions (Run 2) (continued)

Load Step	0	1	2	3	4	5	6	7	8	9	10
Pressure (psi)	-0.02	0.67	1.33	1.98	2.66	3.32	4.01	4.68	5.35	5.99	6.71
S42 ($\mu\epsilon$)	-	-	-	-	-	-	-	-	-	-	-
S43 ($\mu\epsilon$)	-	-	-	-	-	-	-	-	-	-	-
S44 ($\mu\epsilon$)	-21	123	240	341	437	526	612	692	770	846	927
S46 ($\mu\epsilon$)	-299	-367	-425	-472	-516	-555	-584	-609	-625	-637	-647
S48 ($\mu\epsilon$)	-1249	-1113	-999	-906	-812	-729	-646	-571	-493	-426	-351
S51 ($\mu\epsilon$)	-12	173	328	465	601	728	853	971	1087	1198	1318
S55 ($\mu\epsilon$)	-135	-60	13	83	155	225	297	365	433	500	571
S58 ($\mu\epsilon$)	-1065	-803	-608	-453	-302	-183	-51	54	164	267	375
S60 ($\mu\epsilon$)	316	46	-155	-318	-464	-584	-688	-770	-835	-884	-924
S62 ($\mu\epsilon$)	-541	-298	-117	23	155	261	371	462	556	644	735
S65 ($\mu\epsilon$)	-606	-365	-173	-9	154	298	444	574	703	823	950
S69 ($\mu\epsilon$)	-437	-345	-247	-152	-55	33	128	216	309	399	487
S72 ($\mu\epsilon$)	-161	42	187	302	411	504	598	682	765	843	927
S74 ($\mu\epsilon$)	-161	-277	-389	-493	-594	-691	-783	-866	-946	-1018	-1094
S76 ($\mu\epsilon$)	-225	-42	92	199	304	394	485	569	652	731	815
S79 ($\mu\epsilon$)	-148	111	296	450	598	728	859	979	1097	1208	1326
S83 ($\mu\epsilon$)	-103	23	121	207	290	366	441	513	583	650	718
S86 ($\mu\epsilon$)	-166	0	126	230	325	411	495	571	648	720	798
S88 ($\mu\epsilon$)	-270	-414	-520	-600	-671	-727	-769	-803	-825	-838	-846
S90 ($\mu\epsilon$)	-178	-40	78	179	273	359	443	521	598	673	753
S93 ($\mu\epsilon$)	-190	-9	143	275	403	522	640	749	857	958	1067

Table F-26. Raw data, strain survey conducted after 60,000 cycles, cold-dry environmental conditions (Run 2) (continued)

Load Step	0	1	2	3	4	5	6	7	8	9	10
Pressure (psi)	-0.02	0.67	1.33	1.98	2.66	3.32	4.01	4.68	5.35	5.99	6.71
S97 ($\mu\epsilon$)	-261	-185	-110	-40	31	100	169	234	301	365	433
S104 ($\mu\epsilon$)	-572	-365	-198	-58	70	180	292	386	478	563	657
S105 ($\mu\epsilon$)	651	291	6	-223	-440	-625	-798	-946	-1080	-1196	-1307
S106 ($\mu\epsilon$)	-515	-253	-52	120	274	406	535	647	755	855	963
S107 ($\mu\epsilon$)	-599	-394	-210	-38	133	291	452	598	743	877	1024
S109 ($\mu\epsilon$)	-64	-43	4	64	131	201	277	348	422	493	574
S110 ($\mu\epsilon$)	-480	-273	-105	39	174	290	406	508	607	699	800
S111 ($\mu\epsilon$)	584	258	15	-188	-369	-519	-654	-762	-856	-930	-995
S112 ($\mu\epsilon$)	-481	-263	-92	52	183	296	408	506	601	691	787
S113 ($\mu\epsilon$)	-590	-386	-206	-42	123	273	426	566	703	832	973
S115 ($\mu\epsilon$)	17	53	107	167	236	304	380	454	531	618	1199
UAC-A1 ($\mu\epsilon$)	-76	62	192	307	426	535	642	740	835	924	1019
UAC-F1 ($\mu\epsilon$)	-48	82	210	325	443	555	663	765	862	954	1050
UB-A1 ($\mu\epsilon$)	-	-	-	-	-	-	-	-	-	-	-
UB-A2 ($\mu\epsilon$)	-41	235	453	646	831	991	1150	1289	1422	1541	1661
UB-A3 ($\mu\epsilon$)	-84	164	357	527	691	832	975	1100	1220	1328	1437
UB-F1 ($\mu\epsilon$)	-	-	-	-	-	-	-	-	-	-	-
UB-F2 ($\mu\epsilon$)	-304	-46	148	321	483	626	769	891	1009	1115	1224
UB-F3 ($\mu\epsilon$)	-768	-452	-273	-134	-20	60	173	238	323	399	475
UBC-A1 ($\mu\epsilon$)	-	-	-	-	-	-	-	-	-	-	-
UBC-A2 ($\mu\epsilon$)	113	353	566	755	938	1100	1259	1396	1527	1643	1761

Table F-26. Raw data, strain survey conducted after 60,000 cycles, cold-dry environmental conditions (Run 2) (continued)

Load Step	0	1	2	3	4	5	6	7	8	9	10
Pressure (psi)	-0.02	0.67	1.33	1.98	2.66	3.32	4.01	4.68	5.35	5.99	6.71
UBC-A3 ($\mu\epsilon$)	-17	162	320	459	597	717	838	941	1042	1131	1222
UBC-F1 ($\mu\epsilon$)	-	-	-	-	-	-	-	-	-	-	-
UBC-F2 ($\mu\epsilon$)	91	336	550	742	925	1087	1247	1384	1514	1630	1748
UBC-F3 ($\mu\epsilon$)	4	190	351	495	633	755	877	980	1081	1171	1262
UDAC-A1 ($\mu\epsilon$)	-52	109	248	371	492	603	713	810	908	995	1088
UDAC-F1 ($\mu\epsilon$)	-42	109	250	370	492	604	713	813	909	998	1092
UDB-A1 ($\mu\epsilon$)	-	-	-	-	-	-	-	-	-	-	-
UDB-A2 ($\mu\epsilon$)	-600	-419	-278	-166	-63	23	115	185	256	317	378
UDB-A3 ($\mu\epsilon$)	-148	106	315	492	657	804	945	1069	1187	1292	1400
UDB-F1 ($\mu\epsilon$)	-	-	-	-	-	-	-	-	-	-	-
UDB-F2 ($\mu\epsilon$)	-12	319	596	832	1052	1250	1437	1603	1758	1896	2037
UDB-F3 ($\mu\epsilon$)	2	261	477	661	833	991	1140	1272	1397	1509	1626
UDBC-A1 ($\mu\epsilon$)	-	-	-	-	-	-	-	-	-	-	-
UDBC-A2 ($\mu\epsilon$)	-	-	-	-	-	-	-	-	-	-	-
UDBC-A3 ($\mu\epsilon$)	138	366	550	709	860	990	1115	1223	1324	1418	1506
UDBC-F1 ($\mu\epsilon$)	-	-	-	-	-	-	-	-	-	-	-
UDBC-F2 ($\mu\epsilon$)	-	-	-	-	-	-	-	-	-	-	-
UDBC-F3 ($\mu\epsilon$)	82	329	528	694	857	995	1130	1244	1352	1449	1543

Table F-27. Raw data, strain survey conducted after 60,000 cycles, cold-dry environmental conditions (Run 3)

Load Step	0	1	2	3	4	5	6	7	8	9	10
Pressure (psi)	-0.01	0.67	1.33	1.98	2.74	3.32	4.01	4.61	5.39	6.02	6.62
Frame-1 (lbf)	0	146	166	385	425	549	704	832	924	995	1139
Frame-2 (lbf)	50	126	235	374	431	580	681	792	904	1017	1146
Frame-3 (lbf)	1	124	218	355	453	554	674	798	906	1025	1129
Frame-4 (lbf)	49	124	227	344	455	562	674	794	908	1026	1134
Frame-5 (lbf)	0	122	234	356	452	555	679	802	911	1005	1113
Frame-6 (lbf)	-6	105	218	340	437	568	697	780	904	1026	1144
Frame-7 (lbf)	-7	116	225	333	440	566	679	790	908	1016	1131
Frame-8 (lbf)	9	118	226	335	438	565	677	781	904	1019	1132
Frame-9 (lbf)	24	117	227	343	438	569	677	787	904	1019	1134
Frame-10 (lbf)	1	126	234	326	450	573	682	800	907	1022	1141
Frame-11 (lbf)	14	104	234	337	456	567	686	801	907	1022	1129
Frame-12 (lbf)	0	123	226	342	453	560	683	798	901	1020	1122
Hoop-1 (lbf)	58	697	1449	2149	2873	3576	4295	4972	5714	6450	7106
Hoop-2 (lbf)	101	688	1385	2136	2906	3580	4319	4984	5723	6430	7134
Hoop-3 (lbf)	31	708	1441	2152	2867	3564	4279	4976	5729	6437	7119
Hoop-4 (lbf)	28	704	1440	2099	2903	3569	4278	4977	5733	6443	7111
Hoop-5 (lbf)	-15	716	1448	2124	2862	3582	4291	4968	5725	6442	7141
Hoop-6 (lbf)	19	701	1435	2139	2858	3566	4287	4982	5732	6443	7124
Hoop-7 (lbf)	22	712	1432	2134	2863	3563	4278	4973	5728	6433	7112
Hoop-8 (lbf)	40	709	1429	2148	2892	3569	4295	4974	5734	6436	7112
Hoop-9 (lbf)	-2	713	1444	2121	2875	3592	4279	4970	5729	6448	7123

Table F-27. Raw data, strain survey conducted after 60,000 cycles, cold-dry environmental conditions (Run 3) (continued)

Load Step	0	1	2	3	4	5	6	7	8	9	10
Pressure (psi)	-0.01	0.67	1.33	1.98	2.74	3.32	4.01	4.61	5.39	6.02	6.62
Hoop-10 (lbf)	-3	688	1422	2157	2910	3563	4302	4926	5748	6445	7101
Hoop-11 (lbf)	-1	718	1439	2136	2856	3582	4279	4985	5740	6425	7127
Hoop-12 (lbf)	39	718	1431	2151	2896	3550	4285	4994	5721	6441	7123
Hoop-13 (lbf)	5	741	1370	2175	2852	3572	4289	4969	5744	6443	7131
Hoop-14 (lbf)	12	702	1448	2119	2880	3569	4284	4970	5720	6446	7113
Long-1 (lbf)	15	626	1308	2045	2670	3412	4027	4652	5346	6023	6641
Long-2 (lbf)	6	692	1335	2011	2644	3334	4007	4678	5333	5985	6679
Long-3 (lbf)	27	663	1337	1997	2653	3336	3998	4683	5327	6000	6683
Long-4 (lbf)	-14	673	1312	2047	2648	3333	4004	4679	5320	6007	6679
Long-5 (lbf)	3	666	1332	2010	2684	3347	3997	4661	5365	6009	6671
Long-6 (lbf)	56	655	1321	2008	2659	3333	3999	4692	5349	6006	6688
Long-7 (lbf)	-42	672	1335	2056	2688	3347	3995	4664	5326	6005	6654
Long-8 (lbf)	-4	629	1348	2008	2660	3345	4007	4674	5341	6013	6648
F01 ($\mu\epsilon$)	-	-	-	-	-	-	-	-	-	-	-
F02 ($\mu\epsilon$)	-	-	-	-	-	-	-	-	-	-	-
F03 ($\mu\epsilon$)	-	-	-	-	-	-	-	-	-	-	-
F04 ($\mu\epsilon$)	-	-	-	-	-	-	-	-	-	-	-
F05 ($\mu\epsilon$)	-	-	-	-	-	-	-	-	-	-	-
F06 ($\mu\epsilon$)	-	-	-	-	-	-	-	-	-	-	-
F07 ($\mu\epsilon$)	-	-	-	-	-	-	-	-	-	-	-
F08 ($\mu\epsilon$)	-	-	-	-	-	-	-	-	-	-	-

Table F-27. Raw data, strain survey conducted after 60,000 cycles, cold-dry environmental conditions (Run 3) (continued)

Load Step	0	1	2	3	4	5	6	7	8	9	10
Pressure (psi)	-0.01	0.67	1.33	1.98	2.74	3.32	4.01	4.61	5.39	6.02	6.62
IS18 ($\mu\epsilon$)	65	-39	-98	-130	-148	-146	-132	-112	-79	-43	-4
IS20 ($\mu\epsilon$)	-331	-288	-249	-210	-170	-134	-91	-55	-9	33	73
IS22 ($\mu\epsilon$)	154	49	-17	-56	-84	-87	-79	-63	-35	-1	37
IS25 ($\mu\epsilon$)	213	91	19	-27	-66	-77	-84	-81	-71	-52	-30
IS26 ($\mu\epsilon$)	-184	-74	33	131	231	310	399	471	558	627	692
IS27 ($\mu\epsilon$)	312	197	135	102	74	75	84	98	123	153	186
IS28 ($\mu\epsilon$)	-81	58	191	315	441	539	650	741	848	933	1012
IS29 ($\mu\epsilon$)	-154	-23	94	201	308	394	491	572	668	747	820
IS30 ($\mu\epsilon$)	146	119	101	93	91	106	127	152	188	226	267
IS32 ($\mu\epsilon$)	17	106	185	253	323	379	442	492	553	601	648
IS34 ($\mu\epsilon$)	155	110	74	54	39	43	53	70	94	122	156
IS37 ($\mu\epsilon$)	374	261	181	120	60	29	2	-13	-27	-27	-20
IS38 ($\mu\epsilon$)	90	203	303	393	483	555	634	698	775	838	895
IS39 ($\mu\epsilon$)	372	253	173	117	65	43	28	24	24	37	54
IS40 ($\mu\epsilon$)	100	215	319	413	509	584	669	737	819	887	949
IS41 ($\mu\epsilon$)	-87	39	153	255	359	441	533	607	695	768	836
IS44 ($\mu\epsilon$)	-145	-186	-197	-195	-174	-150	-113	-78	-26	24	71
IS46 ($\mu\epsilon$)	-33	29	89	140	202	247	301	344	400	445	487
IS48 ($\mu\epsilon$)	-40	-49	-40	-24	12	46	94	139	202	259	315
IS51 ($\mu\epsilon$)	-122	-160	-172	-178	-167	-156	-137	-118	-90	-59	-29
IS52 ($\mu\epsilon$)	-54	59	166	260	369	448	540	615	710	785	855

Table F-27. Raw data, strain survey conducted after 60,000 cycles, cold-dry environmental conditions (Run 3) (continued)

Load Step	0	1	2	3	4	5	6	7	8	9	10
Pressure (psi)	-0.01	0.67	1.33	1.98	2.74	3.32	4.01	4.61	5.39	6.02	6.62
IS55 ($\mu\epsilon$)	-20	81	172	249	338	404	481	545	624	690	751
IS58 ($\mu\epsilon$)	144	46	-12	-39	-53	-47	-29	-4	33	74	117
IS60 ($\mu\epsilon$)	-304	-246	-198	-152	-111	-74	-30	7	55	94	133
IS62 ($\mu\epsilon$)	115	29	-21	-44	-56	-47	-26	-1	37	78	122
IS65 ($\mu\epsilon$)	356	268	212	179	158	160	167	182	204	233	264
IS66 ($\mu\epsilon$)	-90	34	136	230	325	400	483	551	630	695	755
IS67 ($\mu\epsilon$)	321	271	244	235	239	259	286	316	356	398	441
IS68 ($\mu\epsilon$)	49	230	379	513	653	760	876	971	1082	1171	1253
IS69 ($\mu\epsilon$)	-22	141	267	379	494	585	683	767	864	942	1016
IS72 ($\mu\epsilon$)	21	-26	-33	-13	18	57	108	158	220	279	338
IS74 ($\mu\epsilon$)	-34	36	101	164	229	284	342	392	451	499	545
IS76 ($\mu\epsilon$)	31	9	25	61	107	155	216	274	345	410	475
IS79 ($\mu\epsilon$)	75	-14	-51	-56	-54	-37	-17	8	38	71	106
IS80 ($\mu\epsilon$)	60	160	252	340	437	514	599	671	756	826	891
IS83 ($\mu\epsilon$)	93	188	268	342	425	492	565	628	701	763	822
IS86 ($\mu\epsilon$)	-63	-93	-90	-75	-37	0	47	96	158	214	270
IS88 ($\mu\epsilon$)	-60	-11	32	66	106	137	170	200	234	263	290
IS90 ($\mu\epsilon$)	-104	-111	-103	-84	-45	-8	40	89	152	208	264
IS93 ($\mu\epsilon$)	-64	-69	-54	-39	-4	24	63	101	149	195	242
IS94 ($\mu\epsilon$)	-76	58	178	279	398	481	578	658	754	831	902
IS95 ($\mu\epsilon$)	-66	-54	-29	-5	38	71	114	157	209	255	302

Table F-27. Raw data, strain survey conducted after 60,000 cycles, cold-dry environmental conditions (Run 3) (continued)

Load Step	0	1	2	3	4	5	6	7	8	9	10
Pressure (psi)	-0.01	0.67	1.33	1.98	2.74	3.32	4.01	4.61	5.39	6.02	6.62
IS96 ($\mu\epsilon$)	-96	20	124	211	314	387	472	544	629	698	763
IS97 ($\mu\epsilon$)	-39	73	166	244	335	401	479	543	621	686	747
IS104 ($\mu\epsilon$)	71	-52	-132	-183	-218	-233	-237	-234	-216	-195	-169
IS105 ($\mu\epsilon$)	-559	-497	-441	-392	-338	-307	-258	-226	-174	-135	-98
IS106 ($\mu\epsilon$)	139	-29	-150	-232	-300	-336	-362	-376	-379	-375	-365
IS107 ($\mu\epsilon$)	210	166	133	108	91	82	83	87	104	124	148
IS108 ($\mu\epsilon$)	-194	25	213	370	536	652	785	889	1019	1118	1208
IS109 ($\mu\epsilon$)	-	-	-	-	-	-	-	-	-	-	-
IS110 ($\mu\epsilon$)	60	-38	-105	-142	-170	-173	-166	-149	-120	-87	-48
IS111 ($\mu\epsilon$)	-479	-406	-338	-273	-210	-159	-97	-46	20	74	127
IS112 ($\mu\epsilon$)	153	26	-62	-117	-159	-173	-177	-172	-155	-131	-103
IS113 ($\mu\epsilon$)	234	194	161	142	122	120	119	128	142	161	185
IS114 ($\mu\epsilon$)	-192	11	186	343	496	614	744	851	976	1074	1167
IS115 ($\mu\epsilon$)	-	-	-	-	-	-	-	-	-	-	-
L01 ($\mu\epsilon$)	-	-	-	-	-	-	-	-	-	-	-
L02 ($\mu\epsilon$)	-	-	-	-	-	-	-	-	-	-	-
L03 ($\mu\epsilon$)	-	-	-	-	-	-	-	-	-	-	-
L04 ($\mu\epsilon$)	-	-	-	-	-	-	-	-	-	-	-
L05 ($\mu\epsilon$)	-	-	-	-	-	-	-	-	-	-	-
L06 ($\mu\epsilon$)	-	-	-	-	-	-	-	-	-	-	-
L07 ($\mu\epsilon$)	-	-	-	-	-	-	-	-	-	-	-

Table F-27. Raw data, strain survey conducted after 60,000 cycles, cold-dry environmental conditions (Run 3) (continued)

Load Step	0	1	2	3	4	5	6	7	8	9	10
Pressure (psi)	-0.01	0.67	1.33	1.98	2.74	3.32	4.01	4.61	5.39	6.02	6.62
L08 ($\mu\epsilon$)	-	-	-	-	-	-	-	-	-	-	-
L09 ($\mu\epsilon$)	-	-	-	-	-	-	-	-	-	-	-
L10 ($\mu\epsilon$)	-	-	-	-	-	-	-	-	-	-	-
RAC-A1 ($\mu\epsilon$)	39	151	257	359	471	559	658	741	840	923	999
RAC-F1 ($\mu\epsilon$)	-42	58	157	254	357	439	529	607	701	775	846
RBC-A1 ($\mu\epsilon$)	272	455	613	748	886	988	1101	1190	1295	1378	1453
RBC-A2 ($\mu\epsilon$)	136	278	400	505	611	691	779	847	928	992	1050
RBC-A3 ($\mu\epsilon$)	139	270	382	480	580	655	737	803	881	942	999
RBC-F1 ($\mu\epsilon$)	257	433	584	711	842	937	1043	1127	1225	1299	1367
RBC-F2 ($\mu\epsilon$)	161	307	431	536	644	722	810	879	959	1021	1077
RBC-F3 ($\mu\epsilon$)	125	267	387	489	593	668	754	820	898	958	1014
S18 ($\mu\epsilon$)	-504	-316	-174	-59	51	132	223	295	385	459	525
S20 ($\mu\epsilon$)	571	353	173	21	-129	-222	-324	-400	-479	-530	-567
S22 ($\mu\epsilon$)	-657	-377	-168	-1	164	272	400	498	617	716	800
S25 ($\mu\epsilon$)	-578	-376	-208	-58	99	215	350	461	598	710	811
S29 ($\mu\epsilon$)	20	73	128	184	248	301	364	420	490	548	604
S30 ($\mu\epsilon$)	-255	-88	57	179	303	400	503	588	690	772	849
S32 ($\mu\epsilon$)	1019	843	692	563	428	342	239	163	74	10	-45
S34 ($\mu\epsilon$)	-356	-228	-102	5	117	203	303	380	475	552	626
S37 ($\mu\epsilon$)	-423	-192	0	165	338	472	619	740	883	1000	1108
S41 ($\mu\epsilon$)	-29	33	104	175	256	321	397	460	539	604	664

Table F-27. Raw data, strain survey conducted after 60,000 cycles, cold-dry environmental conditions (Run 3) (continued)

Load Step	0	1	2	3	4	5	6	7	8	9	10
Pressure (psi)	-0.01	0.67	1.33	1.98	2.74	3.32	4.01	4.61	5.39	6.02	6.62
S42 ($\mu\epsilon$)	-	-	-	-	-	-	-	-	-	-	-
S43 ($\mu\epsilon$)	-	-	-	-	-	-	-	-	-	-	-
S44 ($\mu\epsilon$)	-16	125	243	340	444	523	611	683	774	847	914
S46 ($\mu\epsilon$)	-298	-367	-426	-475	-527	-557	-586	-608	-630	-640	-647
S48 ($\mu\epsilon$)	-1251	-1124	-1009	-915	-813	-745	-660	-590	-505	-440	-375
S51 ($\mu\epsilon$)	-7	174	328	464	610	723	852	957	1092	1199	1298
S55 ($\mu\epsilon$)	-131	-58	15	83	161	223	296	358	437	501	562
S58 ($\mu\epsilon$)	-1095	-842	-649	-478	-326	-219	-90	7	128	226	314
S60 ($\mu\epsilon$)	316	51	-151	-317	-475	-580	-683	-759	-834	-881	-916
S62 ($\mu\epsilon$)	-546	-309	-128	19	157	253	364	449	551	637	714
S65 ($\mu\epsilon$)	-604	-370	-179	-8	168	292	441	559	705	822	928
S69 ($\mu\epsilon$)	-447	-354	-257	-164	-59	23	121	202	304	389	466
S72 ($\mu\epsilon$)	-156	43	188	307	418	504	599	676	769	845	917
S74 ($\mu\epsilon$)	-164	-281	-392	-493	-607	-691	-783	-861	-953	-1023	-1085
S76 ($\mu\epsilon$)	-224	-44	90	201	310	393	486	562	655	731	804
S79 ($\mu\epsilon$)	-146	109	297	451	608	726	859	968	1101	1209	1309
S83 ($\mu\epsilon$)	-100	23	122	208	297	366	443	509	586	651	712
S86 ($\mu\epsilon$)	-161	3	128	229	331	410	495	564	650	722	787
S88 ($\mu\epsilon$)	-266	-412	-522	-598	-684	-726	-768	-799	-827	-839	-843
S90 ($\mu\epsilon$)	-172	-36	81	182	283	358	444	515	602	675	741
S93 ($\mu\epsilon$)	-184	-6	143	274	413	520	640	738	861	961	1052

Table F-27. Raw data, strain survey conducted after 60,000 cycles, cold-dry environmental conditions (Run 3) (continued)

Load Step	0	1	2	3	4	5	6	7	8	9	10
Pressure (psi)	-0.01	0.67	1.33	1.98	2.74	3.32	4.01	4.61	5.39	6.02	6.62
S97 ($\mu\epsilon$)	-256	-183	-110	-40	39	98	170	229	303	367	424
S104 ($\mu\epsilon$)	-572	-371	-200	-57	83	176	289	372	481	564	641
S105 ($\mu\epsilon$)	654	293	5	-222	-464	-619	-796	-924	-1084	-1194	-1285
S106 ($\mu\epsilon$)	-515	-259	-49	118	288	400	533	632	760	857	944
S107 ($\mu\epsilon$)	-599	-399	-210	-36	150	287	451	582	749	880	1002
S109 ($\mu\epsilon$)	-64	-45	5	64	140	199	277	339	426	495	561
S110 ($\mu\epsilon$)	-482	-282	-108	41	185	288	405	497	611	699	784
S111 ($\mu\epsilon$)	583	268	20	-187	-380	-513	-649	-749	-855	-925	-981
S112 ($\mu\epsilon$)	-479	-269	-91	54	196	295	410	497	607	693	773
S113 ($\mu\epsilon$)	-589	-391	-208	-37	139	271	427	554	710	834	952
S115 ($\mu\epsilon$)	18	52	107	168	243	304	382	449	535	614	916
UAC-A1 ($\mu\epsilon$)	-77	62	193	307	440	532	642	730	840	927	1007
UAC-F1 ($\mu\epsilon$)	-47	85	212	325	459	554	664	755	868	958	1039
UB-A1 ($\mu\epsilon$)	-	-	-	-	-	-	-	-	-	-	-
UB-A2 ($\mu\epsilon$)	-39	227	451	649	842	990	1148	1277	1425	1540	1645
UB-A3 ($\mu\epsilon$)	-84	155	354	530	701	831	973	1089	1222	1326	1422
UB-F1 ($\mu\epsilon$)	-	-	-	-	-	-	-	-	-	-	-
UB-F2 ($\mu\epsilon$)	-316	-68	135	310	483	609	752	862	995	1096	1188
UB-F3 ($\mu\epsilon$)	-844	-540	-342	-187	-50	11	112	167	252	314	371
UBC-A1 ($\mu\epsilon$)	0	0	0	0	1203	1202	1203	1203	1202	1203	1203
UBC-A2 ($\mu\epsilon$)	115	350	566	756	952	1098	1257	1384	1531	1643	1745

Table F-27. Raw data, strain survey conducted after 60,000 cycles, cold-dry environmental conditions (Run 3) (continued)

Load Step	0	1	2	3	4	5	6	7	8	9	10
Pressure (psi)	-0.01	0.67	1.33	1.98	2.74	3.32	4.01	4.61	5.39	6.02	6.62
UBC-A3 ($\mu\epsilon$)	-16	159	319	461	606	715	836	932	1044	1131	1210
UBC-F1 ($\mu\epsilon$)	-	-	-	-	-	-	-	-	-	-	-
UBC-F2 ($\mu\epsilon$)	93	329	549	740	939	1083	1244	1370	1519	1630	1731
UBC-F3 ($\mu\epsilon$)	5	184	350	493	644	751	873	970	1084	1170	1249
UDAC-A1 ($\mu\epsilon$)	-53	105	247	367	506	600	710	802	910	995	1074
UDAC-F1 ($\mu\epsilon$)	-42	108	249	367	507	602	712	803	912	998	1077
UDB-A1 ($\mu\epsilon$)	-	-	-	-	-	-	-	-	-	-	-
UDB-A2 ($\mu\epsilon$)	-614	-435	-292	-178	-60	8	99	161	246	305	353
UDB-A3 ($\mu\epsilon$)	-144	110	321	496	677	806	949	1060	1196	1298	1391
UDB-F1 ($\mu\epsilon$)	-	-	-	-	-	-	-	-	-	-	-
UDB-F2 ($\mu\epsilon$)	-13	321	601	833	1080	1253	1440	1590	1769	1903	2022
UDB-F3 ($\mu\epsilon$)	2	263	481	661	858	992	1142	1261	1407	1515	1611
UDBC-A1 ($\mu\epsilon$)	-	-	-	-	-	-	-	-	-	-	-
UDBC-A2 ($\mu\epsilon$)	-	-	-	-	-	-	-	-	-	-	-
UDBC-A3 ($\mu\epsilon$)	142	370	552	709	871	991	1116	1217	1331	1419	1498
UDBC-F1 ($\mu\epsilon$)	-	-	-	-	-	-	-	-	-	-	-
UDBC-F2 ($\mu\epsilon$)	-	-	-	-	-	-	-	-	-	-	-
UDBC-F3 ($\mu\epsilon$)	83	326	525	697	869	995	1128	1236	1357	1450	1532

F.2.2.4 After 90,000 Cycles

Table F-28. Raw data, strain survey conducted after 90,000 cycles, cold-dry environmental conditions (Run 1)

Load Step	0	1	2	3	4	5	6	7	8	9	10
Pressure (psi)	-0.01	0.67	1.32	1.96	2.70	3.37	3.99	4.66	5.34	5.99	6.66
Frame-1 (lbf)	7	11	252	395	458	573	684	750	909	1006	1074
Frame-2 (lbf)	66	46	236	339	443	570	684	790	907	1023	1131
Frame-3 (lbf)	1	110	250	329	472	551	681	798	903	1018	1132
Frame-4 (lbf)	34	68	226	335	441	568	684	799	913	1014	1132
Frame-5 (lbf)	6	6	250	321	418	574	678	802	926	1029	1136
Frame-6 (lbf)	-1	112	199	355	458	583	678	801	908	1022	1137
Frame-7 (lbf)	6	5	224	344	450	570	679	792	908	1020	1132
Frame-8 (lbf)	8	3	226	346	458	552	679	797	912	1021	1137
Frame-9 (lbf)	38	111	225	335	449	569	683	792	906	1020	1132
Frame-10 (lbf)	0	124	237	342	447	563	667	811	894	1024	1150
Frame-11 (lbf)	4	4	227	341	454	568	676	792	901	1016	1133
Frame-12 (lbf)	3	107	233	336	475	563	670	798	903	1020	1149
Hoop-1 (lbf)	93	712	1417	2149	2841	3581	4278	5001	5713	6417	7139
Hoop-2 (lbf)	19	690	1439	2046	2879	3576	4250	4999	5716	6428	7151
Hoop-3 (lbf)	47	718	1431	2129	2852	3571	4277	4989	5721	6422	7130
Hoop-4 (lbf)	8	717	1396	2156	2873	3574	4283	4993	5707	6420	7145
Hoop-5 (lbf)	7	718	1441	2113	2860	3563	4270	4981	5692	6405	7138
Hoop-6 (lbf)	12	731	1432	2130	2854	3568	4278	5004	5724	6406	7155
Hoop-7 (lbf)	74	721	1426	2132	2862	3583	4269	4975	5712	6417	7131
Hoop-8 (lbf)	15	714	1430	2119	2858	3574	4276	4990	5718	6424	7142

Table F-28. Raw data, strain survey conducted after 90,000 cycles, cold-dry environmental conditions (Run 1) (continued)

Load Step	0	1	2	3	4	5	6	7	8	9	10
Pressure (psi)	-0.01	0.67	1.32	1.96	2.70	3.37	3.99	4.66	5.34	5.99	6.66
Hoop-9 (lbf)	12	729	1448	2160	2864	3552	4275	4991	5723	6397	7131
Hoop-10 (lbf)	113	724	1442	2122	2844	3584	4260	4982	5714	6414	7138
Hoop-11 (lbf)	47	700	1421	2127	2857	3583	4284	4986	5731	6416	7123
Hoop-12 (lbf)	56	729	1441	2168	2836	3586	4281	4998	5714	6427	7141
Hoop-13 (lbf)	28	726	1420	2129	2893	3571	4293	4994	5716	6411	7158
Hoop-14 (lbf)	-9	718	1404	2127	2855	3573	4281	4990	5712	6408	7129
Long-1 (lbf)	40	686	1368	2026	2674	3304	4031	4618	5328	5976	6616
Long-2 (lbf)	6	657	1351	1998	2680	3337	4021	4676	5349	6021	6678
Long-3 (lbf)	-24	640	1346	2006	2678	3331	4017	4676	5341	6004	6674
Long-4 (lbf)	-18	675	1323	2005	2660	3346	4014	4675	5346	6015	6676
Long-5 (lbf)	9	652	1346	2009	2677	3315	4026	4672	5337	6023	6669
Long-6 (lbf)	-3	663	1350	2007	2685	3354	4011	4676	5341	6027	6690
Long-7 (lbf)	-18	636	1350	1991	2643	3341	3992	4677	5344	5998	6654
Long-8 (lbf)	-1	639	1337	2015	2671	3354	4023	4670	5361	6006	6676
F01 ($\mu\epsilon$)	-	-	-	-	-	-	-	-	-	-	-
F02 ($\mu\epsilon$)	-	-	-	-	-	-	-	-	-	-	-
F03 ($\mu\epsilon$)	-	-	-	-	-	-	-	-	-	-	-
F04 ($\mu\epsilon$)	-	-	-	-	-	-	-	-	-	-	-
F05 ($\mu\epsilon$)	-	-	-	-	-	-	-	-	-	-	-
F06 ($\mu\epsilon$)	-	-	-	-	-	-	-	-	-	-	-
F07 ($\mu\epsilon$)	-	-	-	-	-	-	-	-	-	-	-

Table F-28. Raw data, strain survey conducted after 90,000 cycles, cold-dry environmental conditions (Run 1) (continued)

Load Step	0	1	2	3	4	5	6	7	8	9	10
Pressure (psi)	-0.01	0.67	1.32	1.96	2.70	3.37	3.99	4.66	5.34	5.99	6.66
F08 ($\mu\epsilon$)	-	-	-	-	-	-	-	-	-	-	-
IS18 ($\mu\epsilon$)	64	-42	-98	-129	-147	-143	-129	-105	-71	-35	13
IS20 ($\mu\epsilon$)	-303	-274	-226	-189	-155	-117	-80	-41	0	39	82
IS22 ($\mu\epsilon$)	142	23	-26	-63	-87	-87	-76	-57	-26	7	51
IS25 ($\mu\epsilon$)	178	36	-33	-80	-121	-136	-141	-139	-126	-111	-85
IS26 ($\mu\epsilon$)	-243	-173	-91	-21	47	113	171	230	289	341	396
IS27 ($\mu\epsilon$)	292	158	110	80	57	60	69	86	111	139	177
IS28 ($\mu\epsilon$)	-50	87	228	354	477	588	688	784	882	965	1051
IS29 ($\mu\epsilon$)	-118	0	125	232	336	432	519	603	690	766	846
IS30 ($\mu\epsilon$)	135	98	93	84	83	94	113	140	173	208	253
IS32 ($\mu\epsilon$)	18	101	181	249	317	378	433	488	543	589	640
IS34 ($\mu\epsilon$)	150	96	76	58	44	47	59	77	103	129	166
IS37 ($\mu\epsilon$)	-	-	-	-	-	-	-	-	-	-	-
IS38 ($\mu\epsilon$)	-	-	-	-	-	-	-	-	-	-	-
IS39 ($\mu\epsilon$)	336	211	145	93	48	26	17	14	20	29	49
IS40 ($\mu\epsilon$)	97	207	313	405	499	583	661	736	811	875	943
IS41 ($\mu\epsilon$)	-72	51	167	268	370	462	546	627	709	778	852
IS44 ($\mu\epsilon$)	-145	-183	-207	-200	-183	-156	-122	-82	-36	12	66
IS46 ($\mu\epsilon$)	-26	35	89	144	200	249	296	343	390	433	478
IS48 ($\mu\epsilon$)	-28	-46	-34	-12	20	59	103	154	210	263	325
IS51 ($\mu\epsilon$)	-123	-151	-183	-180	-173	-159	-140	-119	-91	-63	-31

Table F-28. Raw data, strain survey conducted after 90,000 cycles, cold-dry environmental conditions (Run 1) (continued)

Load Step	0	1	2	3	4	5	6	7	8	9	10
Pressure (psi)	-0.01	0.67	1.32	1.96	2.70	3.37	3.99	4.66	5.34	5.99	6.66
IS52 ($\mu\epsilon$)	-25	95	192	290	393	482	566	651	736	812	889
IS55 ($\mu\epsilon$)	-15	84	169	251	334	407	478	550	620	685	752
IS58 ($\mu\epsilon$)	-703	-802	-851	-874	-888	-871	-851	-819	-775	-729	-674
IS60 ($\mu\epsilon$)	-292	-243	-191	-151	-115	-74	-37	1	41	77	117
IS62 ($\mu\epsilon$)	103	10	-34	-56	-67	-57	-37	-10	29	68	119
IS65 ($\mu\epsilon$)	297	195	137	107	84	83	90	104	126	152	187
IS66 ($\mu\epsilon$)	-176	-85	-9	62	132	198	258	318	378	430	486
IS67 ($\mu\epsilon$)	285	221	195	190	189	209	233	264	302	341	388
IS68 ($\mu\epsilon$)	12	195	326	458	587	702	804	904	1002	1086	1172
IS69 ($\mu\epsilon$)	-36	137	242	356	468	565	656	745	832	909	990
IS72 ($\mu\epsilon$)	-1	-53	-59	-39	-10	34	81	134	194	249	315
IS74 ($\mu\epsilon$)	-21	49	113	176	240	299	353	406	459	507	557
IS76 ($\mu\epsilon$)	7	-10	5	41	86	141	198	259	328	390	462
IS79 ($\mu\epsilon$)	29	-50	-93	-97	-96	-79	-58	-34	-4	24	61
IS80 ($\mu\epsilon$)	43	150	233	322	417	500	579	657	735	804	876
IS83 ($\mu\epsilon$)	69	169	236	311	388	457	524	591	656	714	779
IS86 ($\mu\epsilon$)	-43	-65	-76	-51	-15	24	68	122	178	234	297
IS88 ($\mu\epsilon$)	-48	2	41	80	120	153	184	215	245	273	303
IS90 ($\mu\epsilon$)	-87	-91	-89	-63	-26	15	60	115	171	226	289
IS93 ($\mu\epsilon$)	-45	-30	-42	-17	14	44	79	121	165	210	261
IS94 ($\mu\epsilon$)	-64	86	190	300	414	507	595	684	771	849	928

Table F-28. Raw data, strain survey conducted after 90,000 cycles, cold-dry environmental conditions (Run 1) (continued)

Load Step	0	1	2	3	4	5	6	7	8	9	10
Pressure (psi)	-0.01	0.67	1.32	1.96	2.70	3.37	3.99	4.66	5.34	5.99	6.66
IS95 ($\mu\epsilon$)	-48	-24	-19	14	52	89	128	174	220	266	318
IS96 ($\mu\epsilon$)	-82	47	136	231	330	411	488	567	644	713	785
IS97 ($\mu\epsilon$)	-20	97	180	263	348	420	490	561	631	693	761
IS104 ($\mu\epsilon$)	46	-45	-129	-173	-206	-216	-219	-209	-191	-168	-137
IS105 ($\mu\epsilon$)	-504	-445	-396	-352	-313	-270	-233	-195	-155	-118	-77
IS106 ($\mu\epsilon$)	141	-48	-152	-231	-294	-330	-351	-362	-362	-355	-340
IS107 ($\mu\epsilon$)	155	121	74	47	28	21	22	31	48	69	97
IS108 ($\mu\epsilon$)	-286	-126	-8	102	211	306	393	479	564	640	715
IS109 ($\mu\epsilon$)	-	-	-	-	-	-	-	-	-	-	-
IS110 ($\mu\epsilon$)	38	-49	-114	-149	-173	-171	-162	-141	-109	-75	-30
IS111 ($\mu\epsilon$)	-435	-373	-309	-254	-201	-145	-94	-40	15	67	122
IS112 ($\mu\epsilon$)	117	-35	-110	-163	-203	-171	-156	-167	-149	-123	-84
IS113 ($\mu\epsilon$)	228	171	136	110	85	78	77	83	96	112	136
IS114 ($\mu\epsilon$)	-263	-119	14	128	236	335	422	510	597	672	750
IS115 ($\mu\epsilon$)	-	-	-	-	-	-	-	-	-	-	-
L01 ($\mu\epsilon$)	-	-	-	-	-	-	-	-	-	-	-
L02 ($\mu\epsilon$)	-	-	-	-	-	-	-	-	-	-	-
L03 ($\mu\epsilon$)	-	-	-	-	-	-	-	-	-	-	-
L04 ($\mu\epsilon$)	-	-	-	-	-	-	-	-	-	-	-
L05 ($\mu\epsilon$)	-	-	-	-	-	-	-	-	-	-	-
L06 ($\mu\epsilon$)	-	-	-	-	-	-	-	-	-	-	-

Table F-28. Raw data, strain survey conducted after 90,000 cycles, cold-dry environmental conditions (Run 1) (continued)

Load Step	0	1	2	3	4	5	6	7	8	9	10
Pressure (psi)	-0.01	0.67	1.32	1.96	2.70	3.37	3.99	4.66	5.34	5.99	6.66
L07 ($\mu\epsilon$)	-	-	-	-	-	-	-	-	-	-	-
L08 ($\mu\epsilon$)	-	-	-	-	-	-	-	-	-	-	-
L09 ($\mu\epsilon$)	-	-	-	-	-	-	-	-	-	-	-
L10 ($\mu\epsilon$)	-	-	-	-	-	-	-	-	-	-	-
RAC-A1 ($\mu\epsilon$)	0	122	220	322	431	527	618	709	801	884	968
RAC-F1 ($\mu\epsilon$)	-48	57	151	247	348	438	522	607	691	767	846
RBC-A1 ($\mu\epsilon$)	-	-	-	-	-	-	-	-	-	-	-
RBC-A2 ($\mu\epsilon$)	151	291	415	522	628	719	802	879	955	1018	1083
RBC-A3 ($\mu\epsilon$)	144	270	382	480	577	661	737	810	881	940	1001
RBC-F1 ($\mu\epsilon$)	-	-	-	-	-	-	-	-	-	-	-
RBC-F2 ($\mu\epsilon$)	163	315	438	545	653	744	824	901	975	1037	1100
RBC-F3 ($\mu\epsilon$)	125	271	387	489	591	678	754	827	897	957	1018
S18 ($\mu\epsilon$)	-457	-284	-134	-26	74	161	238	314	389	459	533
S20 ($\mu\epsilon$)	-	-	-	-	-	-	-	-	-	-	-
S22 ($\mu\epsilon$)	-655	-411	-228	-100	27	126	229	320	408	483	567
S25 ($\mu\epsilon$)	-543	-334	-164	-20	126	255	372	489	606	713	822
S29 ($\mu\epsilon$)	-4	61	120	181	245	307	365	426	491	550	612
S30 ($\mu\epsilon$)	-	-	-	-	-	-	-	-	-	-	-
S32 ($\mu\epsilon$)	-	-	-	-	-	-	-	-	-	-	-
S34 ($\mu\epsilon$)	-372	-269	-162	-59	37	123	205	284	364	431	503
S37 ($\mu\epsilon$)	-388	-177	27	190	355	499	630	759	887	1001	1119

Table F-28. Raw data, strain survey conducted after 90,000 cycles, cold-dry environmental conditions (Run 1) (continued)

Load Step	0	1	2	3	4	5	6	7	8	9	10
Pressure (psi)	-0.01	0.67	1.32	1.96	2.70	3.37	3.99	4.66	5.34	5.99	6.66
S41 ($\mu\epsilon$)	-25	48	119	193	275	349	418	489	561	626	695
S42 ($\mu\epsilon$)	-	-	-	-	-	-	-	-	-	-	-
S43 ($\mu\epsilon$)	-	-	-	-	-	-	-	-	-	-	-
S44 ($\mu\epsilon$)	-12	115	249	347	449	536	614	694	774	847	923
S46 ($\mu\epsilon$)	-	-	-	-	-	-	-	-	-	-	-
S48 ($\mu\epsilon$)	-196	-65	50	141	233	307	379	452	522	587	655
S51 ($\mu\epsilon$)	-11	155	329	463	605	729	846	964	1083	1193	1304
S55 ($\mu\epsilon$)	-127	-49	25	94	171	240	306	374	443	509	577
S58 ($\mu\epsilon$)	-1040	-963	-922	-892	-860	-832	-804	-776	-746	-725	-700
S60 ($\mu\epsilon$)	-	-	-	-	-	-	-	-	-	-	-
S62 ($\mu\epsilon$)	-510	-302	-123	7	127	225	315	402	489	566	648
S65 ($\mu\epsilon$)	-571	-339	-152	3	163	300	426	551	676	788	901
S69 ($\mu\epsilon$)	-480	-397	-300	-221	-130	-56	24	108	189	262	344
S72 ($\mu\epsilon$)	-139	54	205	319	427	521	604	686	770	844	923
S74 ($\mu\epsilon$)	-853	-855	-852	-839	-852	-843	-858	-852	-852	-837	-839
S76 ($\mu\epsilon$)	-222	-55	85	190	293	384	466	548	632	707	785
S79 ($\mu\epsilon$)	-131	116	307	456	608	737	856	975	1095	1204	1314
S83 ($\mu\epsilon$)	-105	23	113	195	280	353	422	492	561	624	691
S86 ($\mu\epsilon$)	-149	0	145	245	348	432	509	584	659	729	801
S88 ($\mu\epsilon$)	-	-	-	-	-	-	-	-	-	-	-
S90 ($\mu\epsilon$)	-194	-57	73	173	275	362	439	517	593	665	739

Table F-28. Raw data, strain survey conducted after 90,000 cycles, cold-dry environmental conditions (Run 1) (continued)

Load Step	0	1	2	3	4	5	6	7	8	9	10
Pressure (psi)	-0.01	0.67	1.32	1.96	2.70	3.37	3.99	4.66	5.34	5.99	6.66
S93 ($\mu\epsilon$)	-173	-10	163	293	433	551	659	769	877	977	1079
S97 ($\mu\epsilon$)	-250	-167	-88	-18	61	129	193	259	325	386	452
S104 ($\mu\epsilon$)	-518	-350	-180	-51	72	180	272	365	457	540	623
S105 ($\mu\epsilon$)	-	-	-	-	-	-	-	-	-	-	-
S106 ($\mu\epsilon$)	-485	-218	-20	141	296	421	533	638	746	842	937
S107 ($\mu\epsilon$)	-532	-352	-170	-7	159	310	448	588	731	860	989
S109 ($\mu\epsilon$)	-53	-21	33	95	170	242	313	386	465	536	611
S110 ($\mu\epsilon$)	-435	-254	-84	50	182	295	395	494	594	682	771
S111 ($\mu\epsilon$)	-289	-282	-288	-283	-295	-284	-288	-290	-288	-282	-286
S112 ($\mu\epsilon$)	-503	-280	-115	21	151	260	356	450	546	630	717
S113 ($\mu\epsilon$)	-551	-354	-176	-19	146	293	426	562	699	821	946
S115 ($\mu\epsilon$)	-	-	-	-	-	-	-	-	-	-	-
UAC-A1 ($\mu\epsilon$)	-67	82	200	322	446	554	653	752	851	939	1026
UAC-F1 ($\mu\epsilon$)	-53	95	204	327	456	565	666	769	870	962	1053
UB-A1 ($\mu\epsilon$)	-	-	-	-	-	-	-	-	-	-	-
UB-A2 ($\mu\epsilon$)	-	-	-	-	-	-	-	-	-	-	-
UB-A3 ($\mu\epsilon$)	-	-	-	-	-	-	-	-	-	-	-
UB-F1 ($\mu\epsilon$)	-	-	-	-	-	-	-	-	-	-	-
UB-F2 ($\mu\epsilon$)	-	-	-	-	-	-	-	-	-	-	-
UB-F3 ($\mu\epsilon$)	-567	-504	-461	-437	-417	-404	-377	-351	-330	-309	-293
UBC-A1 ($\mu\epsilon$)	-	-	-	-	-	-	-	-	-	-	-

Table F-28. Raw data, strain survey conducted after 90,000 cycles, cold-dry environmental conditions (Run 1) (continued)

Load Step	0	1	2	3	4	5	6	7	8	9	10
Pressure (psi)	-0.01	0.67	1.32	1.96	2.70	3.37	3.99	4.66	5.34	5.99	6.66
UBC-A2 ($\mu\epsilon$)	-	-	-	-	-	-	-	-	-	-	-
UBC-A3 ($\mu\epsilon$)	67	268	457	623	786	923	1044	1159	1272	1366	1459
UBC-F1 ($\mu\epsilon$)	-	-	-	-	-	-	-	-	-	-	-
UBC-F2 ($\mu\epsilon$)	-	-	-	-	-	-	-	-	-	-	-
UBC-F3 ($\mu\epsilon$)	74	290	483	652	820	959	1082	1199	1312	1407	1500
UDAC-A1 ($\mu\epsilon$)	-46	133	253	383	515	622	721	823	918	1006	1093
UDAC-F1 ($\mu\epsilon$)	-39	138	252	381	515	622	722	823	920	1008	1097
UDB-A1 ($\mu\epsilon$)	-	-	-	-	-	-	-	-	-	-	-
UDB-A2 ($\mu\epsilon$)	-	-	-	-	-	-	-	-	-	-	-
UDB-A3 ($\mu\epsilon$)	-110	196	423	631	828	992	1136	1272	1402	1514	1622
UDB-F1 ($\mu\epsilon$)	-	-	-	-	-	-	-	-	-	-	-
UDB-F2 ($\mu\epsilon$)	-	-	-	-	-	-	-	-	-	-	-
UDB-F3 ($\mu\epsilon$)	66	407	643	867	1087	1267	1423	1579	1725	1848	1970
UDBC-A1 ($\mu\epsilon$)	-	-	-	-	-	-	-	-	-	-	-
UDBC-A2 ($\mu\epsilon$)	-	-	-	-	-	-	-	-	-	-	-
UDBC-A3 ($\mu\epsilon$)	-175	-19	80	181	276	357	428	493	555	607	657
UDBC-F1 ($\mu\epsilon$)	-	-	-	-	-	-	-	-	-	-	-
UDBC-F2 ($\mu\epsilon$)	-	-	-	-	-	-	-	-	-	-	-
UDBC-F3 ($\mu\epsilon$)	-	-	-	-	-	-	-	-	-	-	-

Table F-29. Raw data, strain survey conducted after 90,000 cycles, cold-dry environmental conditions (Run 2)

Load Step	0	1	2	3	4	5	6	7	8	9	10
Pressure (psi)	-0.02	0.67	1.33	1.98	2.70	3.30	3.97	4.73	5.37	6.04	6.69
Frame-1 (lbf)	12	120	227	396	415	580	755	830	878	1071	1185
Frame-2 (lbf)	49	52	227	336	446	566	681	790	906	1022	1129
Frame-3 (lbf)	1	121	219	338	442	566	678	796	906	1022	1129
Frame-4 (lbf)	38	69	224	345	446	575	670	792	906	1019	1132
Frame-5 (lbf)	3	154	204	359	465	591	657	802	899	1021	1114
Frame-6 (lbf)	-3	104	235	337	451	564	689	800	916	1005	1133
Frame-7 (lbf)	6	120	224	346	454	570	678	792	903	1029	1130
Frame-8 (lbf)	10	112	231	346	460	564	683	797	911	1022	1131
Frame-9 (lbf)	39	115	225	341	451	568	684	792	910	1021	1131
Frame-10 (lbf)	0	129	231	347	465	572	678	822	917	1036	1114
Frame-11 (lbf)	0	112	223	341	454	569	680	798	903	1022	1132
Frame-12 (lbf)	-1	115	261	353	473	570	675	794	907	1020	1128
Hoop-1 (lbf)	31	681	1427	2115	2886	3553	4264	4998	5714	6426	7137
Hoop-2 (lbf)	127	760	1413	2126	2788	3576	4275	4979	5703	6429	7139
Hoop-3 (lbf)	39	737	1420	2147	2865	3568	4281	4994	5711	6451	7143
Hoop-4 (lbf)	0	717	1436	2140	2878	3553	4289	5012	5708	6450	7126
Hoop-5 (lbf)	25	714	1425	2146	2872	3537	4288	4994	5708	6446	7149
Hoop-6 (lbf)	3	717	1431	2145	2881	3561	4283	5014	5716	6461	7132
Hoop-7 (lbf)	46	704	1429	2145	2878	3554	4285	5023	5721	6454	7133
Hoop-8 (lbf)	32	717	1420	2141	2861	3562	4293	5009	5716	6449	7141
Hoop-9 (lbf)	9	710	1443	2153	2860	3555	4274	5006	5716	6455	7138

Table F-29. Raw data, strain survey conducted after 90,000 cycles, cold-dry environmental conditions (Run 2) (continued)

Load Step	0	1	2	3	4	5	6	7	8	9	10
Pressure (psi)	-0.02	0.67	1.33	1.98	2.70	3.30	3.97	4.73	5.37	6.04	6.69
Hoop-10 (lbf)	-9	707	1477	2134	2866	3533	4295	5015	5709	6468	7150
Hoop-11 (lbf)	22	711	1397	2146	2862	3578	4293	5010	5700	6444	7133
Hoop-12 (lbf)	105	722	1439	2145	2885	3566	4288	5000	5708	6440	7129
Hoop-13 (lbf)	-19	737	1415	2140	2857	3556	4299	5013	5727	6432	7133
Hoop-14 (lbf)	-10	702	1399	2129	2854	3568	4284	4980	5717	6446	7138
Long-1 (lbf)	-18	694	1339	2058	2614	3278	4006	4671	5339	6038	6693
Long-2 (lbf)	8	668	1338	1997	2661	3347	3999	4665	5350	6006	6684
Long-3 (lbf)	2	642	1333	1998	2666	3344	4009	4665	5328	6010	6675
Long-4 (lbf)	4	682	1338	2016	2668	3348	3988	4672	5342	6005	6675
Long-5 (lbf)	-8	661	1324	1998	2669	3320	3978	4659	5340	6037	6675
Long-6 (lbf)	-10	655	1281	1986	2663	3346	3975	4696	5345	6021	6683
Long-7 (lbf)	-2	641	1372	2015	2677	3324	3970	4673	5342	6000	6686
Long-8 (lbf)	3	678	1315	2008	2665	3339	3989	4666	5337	6005	6675
F01 ($\mu\epsilon$)	-	-	-	-	-	-	-	-	-	-	-
F02 ($\mu\epsilon$)	-	-	-	-	-	-	-	-	-	-	-
F03 ($\mu\epsilon$)	-	-	-	-	-	-	-	-	-	-	-
F04 ($\mu\epsilon$)	-	-	-	-	-	-	-	-	-	-	-
F05 ($\mu\epsilon$)	-	-	-	-	-	-	-	-	-	-	-
F06 ($\mu\epsilon$)	-	-	-	-	-	-	-	-	-	-	-
F07 ($\mu\epsilon$)	-	-	-	-	-	-	-	-	-	-	-
F08 ($\mu\epsilon$)	-	-	-	-	-	-	-	-	-	-	-

Table F-29. Raw data, strain survey conducted after 90,000 cycles, cold-dry environmental conditions (Run 2) (continued)

Load Step	0	1	2	3	4	5	6	7	8	9	10
Pressure (psi)	-0.02	0.67	1.33	1.98	2.70	3.30	3.97	4.73	5.37	6.04	6.69
IS18 ($\mu\epsilon$)	57	-42	-101	-132	-146	-141	-127	-104	-73	-31	14
IS20 ($\mu\epsilon$)	-309	-272	-232	-196	-158	-122	-81	-42	-4	39	80
IS22 ($\mu\epsilon$)	136	31	-28	-65	-88	-88	-78	-61	-32	8	50
IS25 ($\mu\epsilon$)	170	43	-33	-83	-122	-134	-141	-143	-131	-110	-85
IS26 ($\mu\epsilon$)	-249	-170	-95	-24	45	106	170	230	285	342	395
IS27 ($\mu\epsilon$)	292	173	113	79	58	59	68	81	105	142	178
IS28 ($\mu\epsilon$)	-49	96	228	355	478	580	688	788	877	968	1051
IS29 ($\mu\epsilon$)	-120	10	124	232	335	424	518	605	686	768	846
IS30 ($\mu\epsilon$)	136	105	86	79	80	92	112	135	168	210	252
IS32 ($\mu\epsilon$)	17	108	179	249	315	372	432	487	538	591	640
IS34 ($\mu\epsilon$)	150	102	74	54	43	48	58	73	96	131	167
IS37 ($\mu\epsilon$)	-	-	-	-	-	-	-	-	-	-	-
IS38 ($\mu\epsilon$)	-	-	-	-	-	-	-	-	-	-	-
IS39 ($\mu\epsilon$)	340	225	146	92	46	29	16	9	14	31	50
IS40 ($\mu\epsilon$)	97	215	312	407	499	577	659	737	807	879	944
IS41 ($\mu\epsilon$)	-73	57	164	268	369	453	542	626	702	781	854
IS44 ($\mu\epsilon$)	-151	-194	-205	-204	-185	-160	-123	-83	-39	13	64
IS46 ($\mu\epsilon$)	-31	30	89	141	198	243	294	342	388	433	476
IS48 ($\mu\epsilon$)	-34	-46	-34	-16	20	55	103	153	207	265	324
IS51 ($\mu\epsilon$)	-129	-163	-177	-180	-173	-161	-140	-119	-95	-64	-32
IS52 ($\mu\epsilon$)	-29	86	191	288	393	473	566	654	733	812	887

Table F-29. Raw data, strain survey conducted after 90,000 cycles, cold-dry environmental conditions (Run 2) (continued)

Load Step	0	1	2	3	4	5	6	7	8	9	10
Pressure (psi)	-0.02	0.67	1.33	1.98	2.70	3.30	3.97	4.73	5.37	6.04	6.69
IS55 ($\mu\epsilon$)	-20	82	169	249	332	401	476	550	615	684	750
IS58 ($\mu\epsilon$)	-715	-811	-864	-885	-889	-876	-851	-821	-782	-733	-673
IS60 ($\mu\epsilon$)	-297	-243	-199	-157	-116	-78	-38	-1	35	77	117
IS62 ($\mu\epsilon$)	96	8	-37	-59	-69	-58	-37	-12	24	69	118
IS65 ($\mu\epsilon$)	291	198	141	108	84	84	90	100	122	154	187
IS66 ($\mu\epsilon$)	-182	-91	-15	59	131	193	257	318	373	430	485
IS67 ($\mu\epsilon$)	280	225	196	188	189	208	232	260	296	342	387
IS68 ($\mu\epsilon$)	7	181	322	457	586	694	804	906	996	1087	1171
IS69 ($\mu\epsilon$)	-43	115	235	352	463	557	655	745	828	911	988
IS72 ($\mu\epsilon$)	-2	-51	-62	-42	-12	29	81	131	188	252	317
IS74 ($\mu\epsilon$)	-20	49	111	176	238	293	352	406	456	509	557
IS76 ($\mu\epsilon$)	4	-13	3	40	84	136	197	258	321	392	462
IS79 ($\mu\epsilon$)	29	-54	-94	-97	-99	-82	-59	-40	-12	25	61
IS80 ($\mu\epsilon$)	44	144	230	323	414	492	578	658	731	806	876
IS83 ($\mu\epsilon$)	67	160	229	308	383	450	521	587	650	717	777
IS86 ($\mu\epsilon$)	-48	-76	-74	-55	-18	17	70	122	177	238	298
IS88 ($\mu\epsilon$)	-48	1	43	80	119	148	184	214	244	275	303
IS90 ($\mu\epsilon$)	-90	-95	-86	-65	-26	9	63	114	168	231	291
IS93 ($\mu\epsilon$)	-48	-44	-38	-20	12	40	82	121	164	214	261
IS94 ($\mu\epsilon$)	-62	78	192	299	413	498	597	689	770	853	929
IS95 ($\mu\epsilon$)	-50	-32	-16	12	51	83	130	173	218	271	319

Table F-29. Raw data, strain survey conducted after 90,000 cycles, cold-dry environmental conditions (Run 2) (continued)

Load Step	0	1	2	3	4	5	6	7	8	9	10
Pressure (psi)	-0.02	0.67	1.33	1.98	2.70	3.30	3.97	4.73	5.37	6.04	6.69
IS96 ($\mu\epsilon$)	-82	40	137	230	328	402	489	570	642	716	786
IS97 ($\mu\epsilon$)	-22	95	180	261	347	414	491	562	628	698	761
IS104 ($\mu\epsilon$)	52	-53	-124	-173	-205	-216	-215	-209	-193	-168	-136
IS105 ($\mu\epsilon$)	-510	-454	-400	-357	-311	-275	-232	-192	-157	-117	-78
IS106 ($\mu\epsilon$)	133	-43	-154	-235	-298	-330	-351	-365	-365	-355	-340
IS107 ($\mu\epsilon$)	151	113	77	47	27	21	23	29	45	68	97
IS108 ($\mu\epsilon$)	-296	-142	-13	97	209	296	393	483	561	639	713
IS109 ($\mu\epsilon$)	-	-	-	-	-	-	-	-	-	-	-
IS110 ($\mu\epsilon$)	39	-46	-110	-147	-168	-168	-157	-137	-110	-70	-27
IS111 ($\mu\epsilon$)	-443	-374	-314	-258	-200	-149	-93	-38	14	69	124
IS112 ($\mu\epsilon$)	134	-4	-85	-140	-172	-185	-186	-175	-149	-106	-60
IS113 ($\mu\epsilon$)	223	178	140	111	87	82	81	82	94	115	139
IS114 ($\mu\epsilon$)	-270	-114	14	128	238	330	426	514	595	676	752
IS115 ($\mu\epsilon$)	-	-	-	-	-	-	-	-	-	-	-
L01 ($\mu\epsilon$)	-	-	-	-	-	-	-	-	-	-	-
L02 ($\mu\epsilon$)	-	-	-	-	-	-	-	-	-	-	-
L03 ($\mu\epsilon$)	-	-	-	-	-	-	-	-	-	-	-
L04 ($\mu\epsilon$)	-	-	-	-	-	-	-	-	-	-	-
L05 ($\mu\epsilon$)	-	-	-	-	-	-	-	-	-	-	-
L06 ($\mu\epsilon$)	-	-	-	-	-	-	-	-	-	-	-
L07 ($\mu\epsilon$)	-	-	-	-	-	-	-	-	-	-	-

Table F-29. Raw data, strain survey conducted after 90,000 cycles, cold-dry environmental conditions (Run 2) (continued)

Load Step	0	1	2	3	4	5	6	7	8	9	10
Pressure (psi)	-0.02	0.67	1.33	1.98	2.70	3.30	3.97	4.73	5.37	6.04	6.69
L08 ($\mu\epsilon$)	-	-	-	-	-	-	-	-	-	-	-
L09 ($\mu\epsilon$)	-	-	-	-	-	-	-	-	-	-	-
L10 ($\mu\epsilon$)	-	-	-	-	-	-	-	-	-	-	-
RAC-A1 ($\mu\epsilon$)	2	116	217	323	428	519	617	712	797	884	967
RAC-F1 ($\mu\epsilon$)	-47	54	148	247	345	428	521	607	687	769	847
RBC-A1 ($\mu\epsilon$)	-	-	-	-	-	-	-	-	-	-	-
RBC-A2 ($\mu\epsilon$)	153	302	416	527	629	713	801	880	951	1022	1084
RBC-A3 ($\mu\epsilon$)	145	279	382	483	577	654	736	810	876	944	1004
RBC-F1 ($\mu\epsilon$)	-	-	-	-	-	-	-	-	-	-	-
RBC-F2 ($\mu\epsilon$)	169	327	442	552	655	737	823	902	971	1039	1100
RBC-F3 ($\mu\epsilon$)	129	281	389	494	592	670	752	828	893	959	1018
S18 ($\mu\epsilon$)	-445	-276	-137	-27	74	155	239	317	389	463	535
S20 ($\mu\epsilon$)	-	-	-	-	-	-	-	-	-	-	-
S22 ($\mu\epsilon$)	-699	-458	-284	-141	2	105	212	308	394	485	563
S25 ($\mu\epsilon$)	-532	-335	-169	-23	124	243	371	495	604	716	824
S29 ($\mu\epsilon$)	-4	59	120	182	247	303	367	431	491	552	613
S30 ($\mu\epsilon$)	-	-	-	-	-	-	-	-	-	-	-
S32 ($\mu\epsilon$)	-	-	-	-	-	-	-	-	-	-	-
S34 ($\mu\epsilon$)	-392	-272	-170	-70	29	112	199	281	354	433	505
S37 ($\mu\epsilon$)	-390	-172	21	189	356	487	628	764	883	1004	1120
S41 ($\mu\epsilon$)	-25	46	118	194	275	342	417	492	559	630	697

Table F-29. Raw data, strain survey conducted after 90,000 cycles, cold-dry environmental conditions (Run 2) (continued)

Load Step	0	1	2	3	4	5	6	7	8	9	10
Pressure (psi)	-0.02	0.67	1.33	1.98	2.70	3.30	3.97	4.73	5.37	6.04	6.69
S42 ($\mu\epsilon$)	-	-	-	-	-	-	-	-	-	-	-
S43 ($\mu\epsilon$)	-	-	-	-	-	-	-	-	-	-	-
S44 ($\mu\epsilon$)	-10	128	248	350	450	529	614	698	773	849	922
S46 ($\mu\epsilon$)	-	-	-	-	-	-	-	-	-	-	-
S48 ($\mu\epsilon$)	-215	-82	28	124	222	294	373	450	517	586	650
S51 ($\mu\epsilon$)	-9	166	323	462	606	719	845	971	1082	1196	1303
S55 ($\mu\epsilon$)	-123	-49	23	94	170	233	304	376	441	508	575
S58 ($\mu\epsilon$)	-1053	-995	-951	-913	-868	-841	-806	-778	-754	-727	-699
S60 ($\mu\epsilon$)	-	-	-	-	-	-	-	-	-	-	-
S62 ($\mu\epsilon$)	-522	-304	-142	-8	116	211	312	401	482	565	645
S65 ($\mu\epsilon$)	-566	-346	-166	-6	158	284	422	554	671	787	900
S69 ($\mu\epsilon$)	-523	-435	-347	-261	-162	-82	8	94	174	259	336
S72 ($\mu\epsilon$)	-135	59	205	322	431	516	605	691	768	847	923
S74 ($\mu\epsilon$)	-856	-850	-848	-847	-843	-838	-834	-839	-848	-849	-834
S76 ($\mu\epsilon$)	-218	-49	79	187	292	375	464	550	627	707	784
S79 ($\mu\epsilon$)	-130	115	299	454	608	727	855	982	1093	1205	1313
S83 ($\mu\epsilon$)	-105	18	111	195	279	347	421	493	558	625	688
S86 ($\mu\epsilon$)	-142	14	138	246	345	422	505	586	658	732	801
S88 ($\mu\epsilon$)	-	-	-	-	-	-	-	-	-	-	-
S90 ($\mu\epsilon$)	-182	-49	70	175	274	352	437	518	591	668	742
S93 ($\mu\epsilon$)	-166	3	155	294	430	537	656	773	877	982	1081

Table F-29. Raw data, strain survey conducted after 90,000 cycles, cold-dry environmental conditions (Run 2) (continued)

Load Step	0	1	2	3	4	5	6	7	8	9	10
Pressure (psi)	-0.02	0.67	1.33	1.98	2.70	3.30	3.97	4.73	5.37	6.04	6.69
S97 ($\mu\epsilon$)	-245	-171	-95	-20	56	118	189	258	321	389	452
S104 ($\mu\epsilon$)	-523	-344	-183	-51	78	174	278	374	459	541	623
S105 ($\mu\epsilon$)	-	-	-	-	-	-	-	-	-	-	-
S106 ($\mu\epsilon$)	-475	-223	-22	141	298	412	534	649	748	844	936
S107 ($\mu\epsilon$)	-531	-355	-177	-12	161	298	452	601	733	861	987
S109 ($\mu\epsilon$)	-50	-25	29	93	168	234	311	390	462	536	610
S110 ($\mu\epsilon$)	-438	-255	-89	49	186	290	399	504	594	685	773
S111 ($\mu\epsilon$)	-295	-301	-285	-285	-292	-287	-286	-285	-293	-295	-289
S112 ($\mu\epsilon$)	-498	-282	-116	23	156	256	361	461	547	634	719
S113 ($\mu\epsilon$)	-548	-359	-182	-19	150	283	429	573	699	825	949
S115 ($\mu\epsilon$)	-	-	-	-	-	-	-	-	-	-	-
UAC-A1 ($\mu\epsilon$)	-70	72	202	321	447	545	654	759	850	940	1027
UAC-F1 ($\mu\epsilon$)	-53	81	209	327	456	556	670	777	873	965	1055
UB-A1 ($\mu\epsilon$)	-	-	-	-	-	-	-	-	-	-	-
UB-A2 ($\mu\epsilon$)	-	-	-	-	-	-	-	-	-	-	-
UB-A3 ($\mu\epsilon$)	-	-	-	-	-	-	-	-	-	-	-
UB-F1 ($\mu\epsilon$)	-	-	-	-	-	-	-	-	-	-	-
UB-F2 ($\mu\epsilon$)	-	-	-	-	-	-	-	-	-	-	-
UB-F3 ($\mu\epsilon$)	-	-	-	-	-	-	-	-	-	-	-
UBC-A1 ($\mu\epsilon$)	-	-	-	-	-	-	-	-	-	-	-
UBC-A2 ($\mu\epsilon$)	-	-	-	-	-	-	-	-	-	-	-

Table F-29. Raw data, strain survey conducted after 90,000 cycles, cold-dry environmental conditions (Run 2) (continued)

Load Step	0	1	2	3	4	5	6	7	8	9	10
Pressure (psi)	-0.02	0.67	1.33	1.98	2.70	3.30	3.97	4.73	5.37	6.04	6.69
UBC-A3 ($\mu\epsilon$)	73	283	462	630	789	915	1047	1167	1269	1370	1461
UBC-F1 ($\mu\epsilon$)	-	-	-	-	-	-	-	-	-	-	-
UBC-F2 ($\mu\epsilon$)	-	-	-	-	-	-	-	-	-	-	-
UBC-F3 ($\mu\epsilon$)	80	302	486	658	821	949	1080	1204	1308	1410	1501
UDAC-A1 ($\mu\epsilon$)	-46	120	256	381	514	610	724	827	919	1012	1097
UDAC-F1 ($\mu\epsilon$)	-39	117	256	380	514	610	725	829	921	1012	1100
UDB-A1 ($\mu\epsilon$)	-	-	-	-	-	-	-	-	-	-	-
UDB-A2 ($\mu\epsilon$)	-	-	-	-	-	-	-	-	-	-	-
UDB-A3 ($\mu\epsilon$)	-115	187	431	635	829	977	1133	1275	1397	1512	1618
UDB-F1 ($\mu\epsilon$)	-	-	-	-	-	-	-	-	-	-	-
UDB-F2 ($\mu\epsilon$)	-	-	-	-	-	-	-	-	-	-	-
UDB-F3 ($\mu\epsilon$)	63	387	650	870	1090	1257	1433	1594	1731	1856	1974
UDBC-A1 ($\mu\epsilon$)	-	-	-	-	-	-	-	-	-	-	-
UDBC-A2 ($\mu\epsilon$)	-	-	-	-	-	-	-	-	-	-	-
UDBC-A3 ($\mu\epsilon$)	-169	-25	86	190	286	360	435	503	561	615	665
UDBC-F1 ($\mu\epsilon$)	-	-	-	-	-	-	-	-	-	-	-
UDBC-F2 ($\mu\epsilon$)	-	-	-	-	-	-	-	-	-	-	-
UDBC-F3 ($\mu\epsilon$)	-	-	-	-	-	-	-	-	-	-	-

Table F-30. Raw data, strain survey conducted after 90,000 cycles, cold-dry environmental conditions (Run 3)

Load Step	0	1	2	3	4	5	6	7	8	9	10
Pressure (psi)	-0.01	0.66	1.34	1.99	2.68	3.34	3.96	4.67	5.36	6.02	6.67
Frame-1 (lbf)	13	138	174	403	524	610	622	802	950	1043	1083
Frame-2 (lbf)	48	99	214	334	443	561	678	793	905	1018	1133
Frame-3 (lbf)	2	108	242	338	469	570	669	793	907	1020	1131
Frame-4 (lbf)	35	104	221	342	443	568	677	792	911	1025	1130
Frame-5 (lbf)	2	123	235	311	461	544	652	804	907	1027	1130
Frame-6 (lbf)	-2	119	213	337	471	577	694	793	904	1033	1140
Frame-7 (lbf)	2	112	229	342	452	568	680	787	905	1016	1130
Frame-8 (lbf)	9	115	227	340	460	565	668	789	902	1023	1135
Frame-9 (lbf)	39	114	224	343	455	561	673	793	906	1019	1132
Frame-10 (lbf)	0	112	216	344	457	556	692	803	908	1021	1135
Frame-11 (lbf)	3	110	232	337	440	569	679	796	910	1019	1130
Frame-12 (lbf)	-1	108	226	328	453	570	679	806	905	1023	1136
Hoop-1 (lbf)	40	724	1443	2133	2836	3544	4282	5022	5706	6420	7135
Hoop-2 (lbf)	114	710	1465	2158	2891	3554	4309	4944	5718	6445	7139
Hoop-3 (lbf)	39	701	1426	2155	2818	3559	4280	5026	5695	6427	7130
Hoop-4 (lbf)	5	711	1436	2136	2844	3566	4288	5008	5701	6431	7132
Hoop-5 (lbf)	28	723	1438	2158	2834	3561	4264	5008	5724	6430	7145
Hoop-6 (lbf)	7	694	1434	2159	2869	3569	4277	5006	5700	6428	7133
Hoop-7 (lbf)	47	708	1432	2168	2844	3571	4283	5002	5712	6431	7147
Hoop-8 (lbf)	203	717	1433	2151	2852	3567	4290	5006	5703	6431	7140
Hoop-9 (lbf)	5	723	1457	2187	2837	3573	4284	5000	5715	6442	7138

Table F-30. Raw data, strain survey conducted after 90,000 cycles, cold-dry environmental conditions (Run 3) (continued)

Load Step	0	1	2	3	4	5	6	7	8	9	10
Pressure (psi)	-0.01	0.66	1.34	1.99	2.68	3.34	3.96	4.67	5.36	6.02	6.67
Hoop-10 (lbf)	4	697	1450	2143	2857	3560	4282	5008	5712	6441	7137
Hoop-11 (lbf)	18	694	1406	2155	2854	3570	4284	5007	5705	6427	7128
Hoop-12 (lbf)	46	703	1414	2149	2854	3571	4279	5000	5707	6436	7122
Hoop-13 (lbf)	26	694	1420	2165	2867	3557	4257	5000	5714	6416	7142
Hoop-14 (lbf)	-27	727	1454	2166	2839	3563	4282	5007	5699	6436	7142
Long-1 (lbf)	-53	586	1343	2008	2682	3327	4056	4689	5337	6019	6634
Long-2 (lbf)	-1	637	1331	2002	2680	3336	4011	4666	5330	6020	6675
Long-3 (lbf)	8	685	1331	2005	2677	3342	4010	4665	5339	6020	6674
Long-4 (lbf)	-8	625	1324	1955	2669	3343	3979	4674	5337	6027	6669
Long-5 (lbf)	-7	666	1315	2005	2662	3330	4016	4658	5339	6016	6674
Long-6 (lbf)	-3	623	1343	1981	2680	3348	3999	4671	5339	5983	6722
Long-7 (lbf)	-50	694	1342	2025	2731	3348	3985	4692	5335	6002	6667
Long-8 (lbf)	-6	654	1321	2000	2684	3332	4006	4659	5341	6018	6671
F01 ($\mu\epsilon$)	-	-	-	-	-	-	-	-	-	-	-
F02 ($\mu\epsilon$)	-	-	-	-	-	-	-	-	-	-	-
F03 ($\mu\epsilon$)	-	-	-	-	-	-	-	-	-	-	-
F04 ($\mu\epsilon$)	-	-	-	-	-	-	-	-	-	-	-
F05 ($\mu\epsilon$)	-	-	-	-	-	-	-	-	-	-	-
F06 ($\mu\epsilon$)	-	-	-	-	-	-	-	-	-	-	-
F07 ($\mu\epsilon$)	-	-	-	-	-	-	-	-	-	-	-
F08 ($\mu\epsilon$)	-	-	-	-	-	-	-	-	-	-	-

Table F-30. Raw data, strain survey conducted after 90,000 cycles, cold-dry environmental conditions (Run 3) (continued)

Load Step	0	1	2	3	4	5	6	7	8	9	10
Pressure (psi)	-0.01	0.66	1.34	1.99	2.68	3.34	3.96	4.67	5.36	6.02	6.67
IS18 ($\mu\epsilon$)	56	-46	-101	-132	-145	-142	-127	-103	-72	-31	14
IS20 ($\mu\epsilon$)	-311	-271	-232	-196	-161	-123	-84	-43	-5	37	80
IS22 ($\mu\epsilon$)	136	31	-29	-68	-88	-92	-80	-60	-34	5	49
IS25 ($\mu\epsilon$)	170	40	-34	-86	-119	-137	-142	-141	-131	-111	-86
IS26 ($\mu\epsilon$)	-250	-169	-95	-25	42	107	167	229	284	341	394
IS27 ($\mu\epsilon$)	294	173	114	78	60	57	65	82	106	139	175
IS28 ($\mu\epsilon$)	-50	99	232	357	473	584	683	786	878	967	1049
IS29 ($\mu\epsilon$)	-121	12	127	232	331	426	513	604	685	767	844
IS30 ($\mu\epsilon$)	133	100	86	80	80	88	109	136	166	207	251
IS32 ($\mu\epsilon$)	17	107	182	250	313	373	429	486	538	590	638
IS34 ($\mu\epsilon$)	150	104	74	53	44	46	57	75	98	130	166
IS37 ($\mu\epsilon$)	-	-	-	-	-	-	-	-	-	-	-
IS38 ($\mu\epsilon$)	-	-	-	-	-	-	-	-	-	-	-
IS39 ($\mu\epsilon$)	343	225	146	90	51	25	15	10	15	29	48
IS40 ($\mu\epsilon$)	99	216	316	408	496	580	656	735	806	878	942
IS41 ($\mu\epsilon$)	-73	57	166	268	364	455	538	625	703	781	851
IS44 ($\mu\epsilon$)	-152	-197	-209	-203	-189	-160	-125	-84	-40	11	63
IS46 ($\mu\epsilon$)	-31	30	88	143	194	245	293	341	386	433	476
IS48 ($\mu\epsilon$)	-33	-46	-38	-15	14	56	100	151	205	264	324
IS51 ($\mu\epsilon$)	-127	-165	-181	-181	-175	-160	-143	-120	-97	-65	-32
IS52 ($\mu\epsilon$)	-30	85	188	290	384	478	562	649	730	810	885

Table F-30. Raw data, strain survey conducted after 90,000 cycles, cold-dry environmental conditions (Run 3) (continued)

Load Step	0	1	2	3	4	5	6	7	8	9	10
Pressure (psi)	-0.01	0.66	1.34	1.99	2.68	3.34	3.96	4.67	5.36	6.02	6.67
IS55 ($\mu\epsilon$)	-20	79	167	251	326	402	474	546	614	683	749
IS58 ($\mu\epsilon$)	-718	-811	-861	-886	-888	-876	-855	-818	-775	-730	-673
IS60 ($\mu\epsilon$)	-296	-241	-197	-156	-117	-78	-42	-1	37	76	116
IS62 ($\mu\epsilon$)	95	8	-38	-62	-68	-61	-41	-11	24	69	117
IS65 ($\mu\epsilon$)	289	194	137	103	85	79	85	101	122	151	185
IS66 ($\mu\epsilon$)	-182	-90	-14	59	129	194	253	317	374	429	483
IS67 ($\mu\epsilon$)	279	221	194	185	190	204	227	261	297	339	385
IS68 ($\mu\epsilon$)	6	179	323	458	584	697	797	903	997	1086	1169
IS69 ($\mu\epsilon$)	-46	112	237	353	461	559	647	742	827	910	988
IS72 ($\mu\epsilon$)	-4	-55	-60	-43	-11	30	75	131	188	251	313
IS74 ($\mu\epsilon$)	-20	49	113	175	237	295	348	405	457	507	555
IS76 ($\mu\epsilon$)	3	-14	4	39	85	137	193	257	321	391	459
IS79 ($\mu\epsilon$)	27	-61	-94	-103	-96	-85	-65	-40	-12	23	58
IS80 ($\mu\epsilon$)	43	141	232	322	412	495	572	655	731	805	873
IS83 ($\mu\epsilon$)	65	153	231	308	381	449	514	585	649	713	775
IS86 ($\mu\epsilon$)	-50	-79	-78	-55	-24	22	66	119	176	235	295
IS88 ($\mu\epsilon$)	-48	1	43	81	115	150	181	213	243	273	302
IS90 ($\mu\epsilon$)	-89	-97	-87	-62	-30	15	60	113	170	229	290
IS93 ($\mu\epsilon$)	-48	-49	-42	-17	8	44	80	119	163	210	259
IS94 ($\mu\epsilon$)	-63	76	191	304	405	506	594	684	769	850	926
IS95 ($\mu\epsilon$)	-50	-37	-19	13	46	87	128	171	218	267	316

Table F-30. Raw data, strain survey conducted after 90,000 cycles, cold-dry environmental conditions (Run 3) (continued)

Load Step	0	1	2	3	4	5	6	7	8	9	10
Pressure (psi)	-0.01	0.66	1.34	1.99	2.68	3.34	3.96	4.67	5.36	6.02	6.67
IS96 ($\mu\epsilon$)	-83	37	136	233	321	408	486	565	641	714	783
IS97 ($\mu\epsilon$)	-22	89	178	264	341	418	488	559	627	695	759
IS104 ($\mu\epsilon$)	53	-52	-126	-174	-203	-214	-213	-207	-191	-166	-134
IS105 ($\mu\epsilon$)	-509	-448	-398	-353	-314	-270	-230	-193	-156	-117	-74
IS106 ($\mu\epsilon$)	132	-44	-156	-239	-295	-331	-350	-364	-365	-357	-339
IS107 ($\mu\epsilon$)	157	115	76	47	28	22	24	31	45	69	98
IS108 ($\mu\epsilon$)	-293	-137	-12	102	202	303	391	479	560	638	713
IS109 ($\mu\epsilon$)	-	-	-	-	-	-	-	-	-	-	-
IS110 ($\mu\epsilon$)	38	-47	-111	-148	-166	-169	-157	-136	-107	-69	-25
IS111 ($\mu\epsilon$)	-443	-370	-314	-258	-203	-146	-94	-38	14	69	125
IS112 ($\mu\epsilon$)	137	1	-83	-138	-167	-175	-167	-152	-118	-77	-34
IS113 ($\mu\epsilon$)	222	177	140	108	89	80	80	84	96	115	140
IS114 ($\mu\epsilon$)	-271	-111	15	127	233	334	422	513	595	676	752
IS115 ($\mu\epsilon$)	-	-	-	-	-	-	-	-	-	-	-
L01 ($\mu\epsilon$)	-	-	-	-	-	-	-	-	-	-	-
L02 ($\mu\epsilon$)	-	-	-	-	-	-	-	-	-	-	-
L03 ($\mu\epsilon$)	-	-	-	-	-	-	-	-	-	-	-
L04 ($\mu\epsilon$)	-	-	-	-	-	-	-	-	-	-	-
L05 ($\mu\epsilon$)	-	-	-	-	-	-	-	-	-	-	-
L06 ($\mu\epsilon$)	-	-	-	-	-	-	-	-	-	-	-
L07 ($\mu\epsilon$)	-	-	-	-	-	-	-	-	-	-	-

Table F-30. Raw data, strain survey conducted after 90,000 cycles, cold-dry environmental conditions (Run 3) (continued)

Load Step	0	1	2	3	4	5	6	7	8	9	10
Pressure (psi)	-0.01	0.66	1.34	1.99	2.68	3.34	3.96	4.67	5.36	6.02	6.67
L08 ($\mu\epsilon$)	-	-	-	-	-	-	-	-	-	-	-
L09 ($\mu\epsilon$)	-	-	-	-	-	-	-	-	-	-	-
L10 ($\mu\epsilon$)	-	-	-	-	-	-	-	-	-	-	-
RAC-A1 ($\mu\epsilon$)	2	113	218	323	425	522	612	709	797	885	966
RAC-F1 ($\mu\epsilon$)	-49	54	151	246	343	433	515	605	688	769	843
RBC-A1 ($\mu\epsilon$)	-	-	-	-	-	-	-	-	-	-	-
RBC-A2 ($\mu\epsilon$)	154	303	421	528	627	718	797	880	952	1022	1083
RBC-A3 ($\mu\epsilon$)	145	279	387	483	575	658	732	809	877	943	1002
RBC-F1 ($\mu\epsilon$)	-	-	-	-	-	-	-	-	-	-	-
RBC-F2 ($\mu\epsilon$)	171	326	448	556	654	743	822	902	973	1040	1101
RBC-F3 ($\mu\epsilon$)	132	280	395	498	591	675	752	828	895	960	1018
S18 ($\mu\epsilon$)	-437	-263	-131	-21	72	161	238	319	390	465	538
S20 ($\mu\epsilon$)	-	-	-	-	-	-	-	-	-	-	-
S22 ($\mu\epsilon$)	-700	-462	-279	-129	-8	106	203	304	390	480	563
S25 ($\mu\epsilon$)	-526	-326	-164	-16	119	251	369	494	606	718	824
S29 ($\mu\epsilon$)	-3	61	120	182	243	306	365	430	491	554	615
S30 ($\mu\epsilon$)	-	-	-	-	-	-	-	-	-	-	-
S32 ($\mu\epsilon$)	-	-	-	-	-	-	-	-	-	-	-
S34 ($\mu\epsilon$)	-394	-276	-168	-68	26	112	195	280	354	432	503
S37 ($\mu\epsilon$)	-392	-169	22	192	344	490	623	758	881	1004	1117
S41 ($\mu\epsilon$)	-24	48	120	195	271	346	415	490	560	630	695

Table F-30. Raw data, strain survey conducted after 90,000 cycles, cold-dry environmental conditions (Run 3) (continued)

Load Step	0	1	2	3	4	5	6	7	8	9	10
Pressure (psi)	-0.01	0.66	1.34	1.99	2.68	3.34	3.96	4.67	5.36	6.02	6.67
S42 ($\mu\epsilon$)	-	-	-	-	-	-	-	-	-	-	-
S43 ($\mu\epsilon$)	-	-	-	-	-	-	-	-	-	-	-
S44 ($\mu\epsilon$)	-8	133	252	353	445	533	612	696	772	848	920
S46 ($\mu\epsilon$)	-	-	-	-	-	-	-	-	-	-	-
S48 ($\mu\epsilon$)	-222	-88	27	125	209	291	368	443	512	583	649
S51 ($\mu\epsilon$)	-10	170	329	468	599	726	841	967	1081	1195	1302
S55 ($\mu\epsilon$)	-123	-48	24	96	165	235	301	373	440	508	574
S58 ($\mu\epsilon$)	-1047	-988	-945	-905	-870	-836	-810	-776	-749	-724	-698
S60 ($\mu\epsilon$)	-	-	-	-	-	-	-	-	-	-	-
S62 ($\mu\epsilon$)	-518	-300	-139	-1	111	217	307	400	482	566	644
S65 ($\mu\epsilon$)	-559	-338	-160	3	152	294	417	552	673	788	898
S69 ($\mu\epsilon$)	-527	-439	-349	-256	-170	-84	-4	87	171	255	334
S72 ($\mu\epsilon$)	-133	66	207	324	425	518	602	689	768	847	921
S74 ($\mu\epsilon$)	-842	-835	-840	-837	-837	-829	-830	-832	-835	-833	-825
S76 ($\mu\epsilon$)	-218	-46	80	190	288	379	462	548	628	707	783
S79 ($\mu\epsilon$)	-130	120	303	459	599	733	851	977	1092	1205	1310
S83 ($\mu\epsilon$)	-105	20	112	197	276	349	417	489	557	624	688
S86 ($\mu\epsilon$)	-132	24	145	249	339	427	504	585	658	732	802
S88 ($\mu\epsilon$)	-	-	-	-	-	-	-	-	-	-	-
S90 ($\mu\epsilon$)	-172	-37	78	180	270	358	435	518	593	670	742
S93 ($\mu\epsilon$)	-158	16	163	299	422	545	653	771	876	982	1080

Table F-30. Raw data, strain survey conducted after 90,000 cycles, cold-dry environmental conditions (Run 3) (continued)

Load Step	0	1	2	3	4	5	6	7	8	9	10
Pressure (psi)	-0.01	0.66	1.34	1.99	2.68	3.34	3.96	4.67	5.36	6.02	6.67
S97 ($\mu\epsilon$)	-238	-162	-89	-16	52	123	187	256	322	388	451
S104 ($\mu\epsilon$)	-522	-336	-177	-44	74	184	278	375	460	545	629
S105 ($\mu\epsilon$)	-	-	-	-	-	-	-	-	-	-	-
S106 ($\mu\epsilon$)	-477	-215	-15	151	293	423	534	647	748	845	940
S107 ($\mu\epsilon$)	-534	-349	-174	-5	153	309	451	598	732	864	990
S109 ($\mu\epsilon$)	-50	-21	32	96	165	239	310	388	462	538	611
S110 ($\mu\epsilon$)	-437	-245	-87	55	180	297	397	502	595	688	776
S111 ($\mu\epsilon$)	-287	-283	-292	-292	-289	-281	-287	-291	-285	-287	-281
S112 ($\mu\epsilon$)	-495	-275	-113	30	153	264	361	460	549	638	722
S113 ($\mu\epsilon$)	-546	-350	-180	-13	142	292	426	570	700	828	951
S115 ($\mu\epsilon$)	-	-	-	-	-	-	-	-	-	-	-
UAC-A1 ($\mu\epsilon$)	-70	71	199	325	438	552	651	753	848	940	1025
UAC-F1 ($\mu\epsilon$)	-51	82	207	334	448	565	667	772	871	965	1054
UB-A1 ($\mu\epsilon$)	-	-	-	-	-	-	-	-	-	-	-
UB-A2 ($\mu\epsilon$)	-	-	-	-	-	-	-	-	-	-	-
UB-A3 ($\mu\epsilon$)	-	-	-	-	-	-	-	-	-	-	-
UB-F1 ($\mu\epsilon$)	-	-	-	-	-	-	-	-	-	-	-
UB-F2 ($\mu\epsilon$)	-	-	-	-	-	-	-	-	-	-	-
UB-F3 ($\mu\epsilon$)	-583	-511	-458	-425	-388	-361	-338	-311	-298	-275	-260
UBC-A1 ($\mu\epsilon$)	-	-	-	-	-	-	-	-	-	-	-
UBC-A2 ($\mu\epsilon$)	-	-	-	-	-	-	-	-	-	-	-

Table F-30. Raw data, strain survey conducted after 90,000 cycles, cold-dry environmental conditions (Run 3) (continued)

Load Step	0	1	2	3	4	5	6	7	8	9	10
Pressure (psi)	-0.01	0.66	1.34	1.99	2.68	3.34	3.96	4.67	5.36	6.02	6.67
UBC-A3 ($\mu\epsilon$)	73	285	468	633	784	922	1041	1163	1270	1370	1459
UBC-F1 ($\mu\epsilon$)	-	-	-	-	-	-	-	-	-	-	-
UBC-F2 ($\mu\epsilon$)	-	-	-	-	-	-	-	-	-	-	-
UBC-F3 ($\mu\epsilon$)	81	301	492	662	817	957	1079	1202	1310	1411	1499
UDAC-A1 ($\mu\epsilon$)	-47	118	255	386	506	621	720	822	919	1009	1093
UDAC-F1 ($\mu\epsilon$)	-38	119	255	389	506	623	722	824	921	1012	1097
UDB-A1 ($\mu\epsilon$)	-	-	-	-	-	-	-	-	-	-	-
UDB-A2 ($\mu\epsilon$)	-	-	-	-	-	-	-	-	-	-	-
UDB-A3 ($\mu\epsilon$)	-112	191	430	640	819	987	1132	1271	1396	1512	1617
UDB-F1 ($\mu\epsilon$)	-	-	-	-	-	-	-	-	-	-	-
UDB-F2 ($\mu\epsilon$)	-	-	-	-	-	-	-	-	-	-	-
UDB-F3 ($\mu\epsilon$)	71	391	648	881	1081	1270	1431	1587	1726	1856	1972
UDBC-A1 ($\mu\epsilon$)	-	-	-	-	-	-	-	-	-	-	-
UDBC-A2 ($\mu\epsilon$)	-	-	-	-	-	-	-	-	-	-	-
UDBC-A3 ($\mu\epsilon$)	-162	-17	98	199	291	372	440	510	568	624	673
UDBC-F1 ($\mu\epsilon$)	-	-	-	-	-	-	-	-	-	-	-
UDBC-F2 ($\mu\epsilon$)	-	-	-	-	-	-	-	-	-	-	-
UDBC-F3 ($\mu\epsilon$)	-	-	-	-	-	-	-	-	-	-	-

F.2.3 Hot-Wet Environmental Conditions

F.2.3.1 After Hot-Wet Conditioning

Table F-31. Raw data, strain survey conducted after hot-wet conditioning, hot-wet environmental conditions (Run 1)

Load Step	0	1	2	3	4	5	6	7	8	9	10
Pressure (psi)	-0.02	0.67	1.33	1.99	2.66	3.35	4.02	4.65	5.35	6.02	6.66
Frame-1 (lb _f)	3	157	220	354	453	601	726	766	901	1038	1118
Frame-2 (lb _f)	69	109	216	333	444	569	680	793	903	1019	1132
Frame-3 (lb _f)	0	116	232	343	452	565	678	793	907	1016	1133
Frame-4 (lb _f)	38	113	224	339	460	567	679	793	905	1019	1132
Frame-5 (lb _f)	-1	115	224	341	459	563	678	802	902	1025	1134
Frame-6 (lb _f)	-1	107	227	340	459	567	679	798	913	1016	1137
Frame-7 (lb _f)	11	113	223	338	453	568	681	795	902	1021	1133
Frame-8 (lb _f)	1	117	228	344	454	564	674	790	907	1026	1137
Frame-9 (lb _f)	33	111	231	340	454	567	679	791	905	1022	1129
Frame-10 (lb _f)	0	106	225	342	432	562	677	793	904	1021	1134
Frame-11 (lb _f)	0	115	223	346	457	565	689	794	911	1021	1124
Frame-12 (lb _f)	29	116	225	339	459	570	680	792	908	1019	1131
Hoop-1 (lb _f)	9	723	1438	2128	2856	3558	4270	5004	5720	6433	7123
Hoop-2 (lb _f)	178	744	1438	2173	2829	3575	4281	5005	5706	6427	7125
Hoop-3 (lb _f)	0	712	1438	2136	2865	3570	4275	4987	5717	6415	7155
Hoop-4 (lb _f)	65	667	1423	2134	2854	3574	4289	4993	5718	6412	7147
Hoop-5 (lb _f)	55	722	1437	2140	2851	3575	4297	5013	5720	6459	7152
Hoop-6 (lb _f)	18	726	1425	2135	2848	3589	4281	4988	5702	6433	7115

**Table F-31. Raw data, strain survey conducted after hot-wet conditioning, hot-wet environmental conditions (Run 1)
(continued)**

Load Step	0	1	2	3	4	5	6	7	8	9	10
Pressure (psi)	-0.02	0.67	1.33	1.99	2.66	3.35	4.02	4.65	5.35	6.02	6.66
Hoop-7 (lb _f)	1	718	1430	2141	2858	3590	4289	5004	5727	6416	7141
Hoop-8 (lb _f)	112	698	1426	2133	2857	3580	4283	5001	5711	6429	7135
Hoop-9 (lb _f)	57	716	1469	2125	2857	3584	4294	4990	5709	6427	7141
Hoop-10 (lb _f)	11	733	1409	2158	2857	3600	4289	5002	5718	6429	7132
Hoop-11 (lb _f)	68	716	1430	2116	2862	3584	4288	4984	5716	6429	7148
Hoop-12 (lb _f)	184	724	1442	2139	2852	3583	4288	5003	5729	6429	7135
Hoop-13 (lb _f)	65	725	1446	2115	2838	3548	4278	4999	5706	6429	7131
Hoop-14 (lb _f)	-11	718	1422	2140	2853	3568	4286	4997	5709	6420	7146
Long-1 (lb _f)	-9	691	1348	2010	2688	3340	4014	4687	5297	6046	6613
Long-2 (lb _f)	1	671	1336	2006	2671	3332	4008	4669	5331	6003	6675
Long-3 (lb _f)	2	665	1336	2003	2675	3340	4008	4671	5345	6005	6674
Long-4 (lb _f)	33	645	1343	2002	2674	3337	4003	4675	5338	6005	6644
Long-5 (lb _f)	6	673	1295	1993	2668	3342	4003	4676	5339	6002	6665
Long-6 (lb _f)	1	672	1334	2000	2661	3341	4008	4671	5341	6033	6677
Long-7 (lb _f)	0	667	1322	2014	2652	3341	4001	4673	5345	6000	6679
Long-8 (lb _f)	4	686	1341	2007	2674	3341	4007	4664	5339	5997	6665
F01 (μ ϵ)	-289	-284	-239	-181	-133	-81	-35	20	67	116	172
F02 (μ ϵ)	270	367	400	448	504	552	605	653	705	753	797
F03 (μ ϵ)	-367	-412	-361	-309	-267	-222	-191	-147	-107	-65	-17
F04 (μ ϵ)	400	496	544	591	649	702	762	814	873	927	974

**Table F-31. Raw data, strain survey conducted after hot-wet conditioning, hot-wet environmental conditions (Run 1)
(continued)**

Load Step	0	1	2	3	4	5	6	7	8	9	10
Pressure (psi)	-0.02	0.67	1.33	1.99	2.66	3.35	4.02	4.65	5.35	6.02	6.66
F05 ($\mu\epsilon$)	-	-	-	-	-	-	-	-	-	-	-
F06 ($\mu\epsilon$)	419	519	559	601	647	694	747	790	842	890	928
F07 ($\mu\epsilon$)	-213	-246	-199	-154	-123	-74	-37	5	44	85	132
F08 ($\mu\epsilon$)	220	311	351	396	448	500	550	597	647	695	738
IS16 ($\mu\epsilon$)	56	99	175	247	321	397	473	547	625	700	777
IS17 ($\mu\epsilon$)	-62	-58	-25	17	69	127	188	251	318	384	453
IS18 ($\mu\epsilon$)	-211	-215	-199	-168	-127	-77	-23	35	98	161	229
IS19 ($\mu\epsilon$)	-25	2	36	72	111	153	196	241	289	338	389
IS20 ($\mu\epsilon$)	165	199	247	288	329	368	405	442	478	512	547
IS21 ($\mu\epsilon$)	137	173	218	255	291	325	356	386	416	443	470
IS22 ($\mu\epsilon$)	-238	-255	-241	-219	-184	-141	-94	-41	18	78	141
IS23 ($\mu\epsilon$)	-368	-357	-361	-351	-331	-305	-275	-241	-202	-160	-114
IS24 ($\mu\epsilon$)	201	256	320	377	432	485	533	579	626	670	713
IS25 ($\mu\epsilon$)	-360	-331	-315	-288	-249	-205	-158	-106	-50	8	71
IS26 ($\mu\epsilon$)	81	196	313	417	522	620	714	801	889	973	1055
IS27 ($\mu\epsilon$)	-355	-313	-279	-236	-183	-125	-66	-4	63	131	201
IS28 ($\mu\epsilon$)	55	164	272	370	469	561	649	731	813	891	968
IS29 ($\mu\epsilon$)	97	181	278	368	459	545	628	706	787	863	940
IS30 ($\mu\epsilon$)	-	-	-	-	-	-	-	-	-	-	-
IS31 ($\mu\epsilon$)	-40	-7	54	112	177	241	304	367	431	493	556

**Table F-31. Raw data, strain survey conducted after hot-wet conditioning, hot-wet environmental conditions (Run 1)
(continued)**

Load Step	0	1	2	3	4	5	6	7	8	9	10
Pressure (psi)	-0.02	0.67	1.33	1.99	2.66	3.35	4.02	4.65	5.35	6.02	6.66
IS32 ($\mu\epsilon$)	-88	-59	-12	30	73	114	153	190	227	262	298
IS33 ($\mu\epsilon$)	-84	-49	1	46	93	136	176	215	253	290	327
IS34 ($\mu\epsilon$)	-311	-282	-242	-204	-158	-109	-56	0	59	119	184
IS35 ($\mu\epsilon$)	-527	-584	-602	-606	-593	-574	-547	-516	-479	-438	-393
IS36 ($\mu\epsilon$)	-89	-57	-7	38	84	128	169	208	248	286	324
IS37 ($\mu\epsilon$)	-462	-520	-533	-531	-512	-486	-452	-414	-369	-321	-268
IS38 ($\mu\epsilon$)	-138	-91	-27	30	91	148	204	257	310	361	412
IS39 ($\mu\epsilon$)	-465	-519	-522	-509	-479	-441	-396	-346	-289	-229	-166
IS40 ($\mu\epsilon$)	-145	-89	-21	41	108	170	231	288	345	401	455
IS41 ($\mu\epsilon$)	7	83	166	243	324	399	472	541	611	679	745
IS42 ($\mu\epsilon$)	136	151	205	262	323	388	451	516	583	649	717
IS43 ($\mu\epsilon$)	37	4	38	80	133	193	255	320	389	457	529
IS44 ($\mu\epsilon$)	103	20	21	37	67	108	154	205	261	319	381
IS45 ($\mu\epsilon$)	-5	29	105	173	242	308	370	430	491	548	606
IS46 ($\mu\epsilon$)	-21	25	105	174	243	308	371	430	489	545	601
IS47 ($\mu\epsilon$)	-13	35	113	181	248	313	374	433	492	548	604
IS48 ($\mu\epsilon$)	-23	-37	1	35	80	131	186	244	306	369	436
IS49 ($\mu\epsilon$)	-22	-86	-81	-72	-52	-27	2	35	73	113	157
IS50 ($\mu\epsilon$)	-16	41	128	204	280	352	421	485	550	612	672
IS51 ($\mu\epsilon$)	8	-45	-30	-11	18	52	90	130	175	221	271

**Table F-31. Raw data, strain survey conducted after hot-wet conditioning, hot-wet environmental conditions (Run 1)
(continued)**

Load Step	0	1	2	3	4	5	6	7	8	9	10
Pressure (psi)	-0.02	0.67	1.33	1.99	2.66	3.35	4.02	4.65	5.35	6.02	6.66
IS52 ($\mu\epsilon$)	-13	72	189	292	398	497	592	682	771	856	938
IS53 ($\mu\epsilon$)	30	-25	-6	21	60	104	152	203	258	315	376
IS54 ($\mu\epsilon$)	-24	57	168	266	365	459	549	633	717	797	875
IS55 ($\mu\epsilon$)	-56	29	136	229	320	407	489	567	645	719	794
IS56 ($\mu\epsilon$)	91	119	161	210	259	316	375	434	497	562	627
IS57 ($\mu\epsilon$)	-108	-130	-119	-92	-57	-13	36	88	145	204	265
IS58 ($\mu\epsilon$)	-227	-266	-267	-249	-224	-189	-148	-103	-51	2	59
IS59 ($\mu\epsilon$)	26	21	50	82	116	152	189	227	269	311	355
IS60 ($\mu\epsilon$)	185	200	243	279	314	349	381	411	443	472	500
IS61 ($\mu\epsilon$)	173	193	237	274	308	341	370	397	425	450	476
IS62 ($\mu\epsilon$)	-204	-232	-215	-193	-165	-128	-87	-43	9	62	118
IS63 ($\mu\epsilon$)	-391	-431	-432	-423	-408	-389	-365	-339	-306	-272	-235
IS64 ($\mu\epsilon$)	194	229	290	342	395	445	492	536	581	623	664
IS65 ($\mu\epsilon$)	-407	-427	-398	-361	-318	-271	-220	-168	-109	-48	16
IS66 ($\mu\epsilon$)	20	117	234	340	448	547	642	731	822	908	992
IS67 ($\mu\epsilon$)	-359	-371	-329	-281	-227	-171	-112	-51	17	86	156
IS68 ($\mu\epsilon$)	16	109	216	313	410	500	587	668	751	830	907
IS69 ($\mu\epsilon$)	57	143	237	321	406	484	562	636	715	788	860
IS70 ($\mu\epsilon$)	210	199	230	270	313	366	420	475	535	594	656
IS71 ($\mu\epsilon$)	3	-31	-15	19	60	112	167	224	287	351	416

**Table F-31. Raw data, strain survey conducted after hot-wet conditioning, hot-wet environmental conditions (Run 1)
(continued)**

Load Step	0	1	2	3	4	5	6	7	8	9	10
Pressure (psi)	-0.02	0.67	1.33	1.99	2.66	3.35	4.02	4.65	5.35	6.02	6.66
IS72 ($\mu\epsilon$)	-101	-126	-109	-76	-36	13	66	122	184	248	313
IS73 ($\mu\epsilon$)	-203	-118	-26	56	137	212	283	350	417	481	543
IS74 ($\mu\epsilon$)	-134	-57	30	107	185	256	325	390	455	517	576
IS75 ($\mu\epsilon$)	-113	-34	54	131	209	281	350	416	481	544	604
IS76 ($\mu\epsilon$)	-119	-68	-14	41	98	158	221	284	352	422	492
IS77 ($\mu\epsilon$)	-206	-194	-169	-138	-103	-66	-26	16	63	112	162
IS78 ($\mu\epsilon$)	-115	-29	65	149	233	310	384	453	523	590	654
IS79 ($\mu\epsilon$)	-183	-164	-134	-97	-58	-18	25	70	120	171	224
IS80 ($\mu\epsilon$)	-144	-35	76	177	279	373	464	550	636	719	798
IS81 ($\mu\epsilon$)	-232	-225	-202	-172	-137	-101	-60	-17	31	82	134
IS82 ($\mu\epsilon$)	-116	-15	88	182	276	363	448	528	609	688	762
IS83 ($\mu\epsilon$)	-175	-82	20	104	189	264	339	411	483	553	621
IS84 ($\mu\epsilon$)	10	39	103	162	227	293	359	425	493	561	631
IS85 ($\mu\epsilon$)	-10	-31	4	43	98	158	223	288	358	427	500
IS86 ($\mu\epsilon$)	-19	-57	-43	-19	22	71	127	184	246	310	377
IS87 ($\mu\epsilon$)	-69	-17	38	85	133	179	224	266	309	350	392
IS88 ($\mu\epsilon$)	-41	19	84	137	190	241	289	335	381	425	468
IS89 ($\mu\epsilon$)	-33	25	89	140	193	243	291	337	383	427	472
IS90 ($\mu\epsilon$)	-36	-45	-20	8	50	100	156	214	275	338	405
IS91 ($\mu\epsilon$)	-80	-101	-99	-93	-75	-48	-15	20	61	105	154

**Table F-31. Raw data, strain survey conducted after hot-wet conditioning, hot-wet environmental conditions (Run 1)
(continued)**

Load Step	0	1	2	3	4	5	6	7	8	9	10
Pressure (psi)	-0.02	0.67	1.33	1.99	2.66	3.35	4.02	4.65	5.35	6.02	6.66
IS92 ($\mu\epsilon$)	-54	18	92	154	216	274	330	382	434	484	533
IS93 ($\mu\epsilon$)	-70	-76	-57	-35	1	43	90	140	193	248	309
IS94 ($\mu\epsilon$)	-40	78	196	299	405	506	602	692	781	867	950
IS95 ($\mu\epsilon$)	-74	-74	-47	-17	26	75	129	184	242	302	367
IS96 ($\mu\epsilon$)	-39	65	171	263	359	449	538	620	701	780	859
IS97 ($\mu\epsilon$)	-82	12	107	191	276	359	438	512	587	660	733
L01 ($\mu\epsilon$)	-	-	-	-	-	-	-	-	-	-	-
L02 ($\mu\epsilon$)	-324	-236	-223	-206	-190	-176	-160	-147	-133	-117	-104
L03 ($\mu\epsilon$)	-216	-155	-147	-134	-116	-100	-80	-61	-41	-20	-2
L04 ($\mu\epsilon$)	-237	-152	-126	-100	-70	-46	-19	5	29	53	73
L05 ($\mu\epsilon$)	-225	-196	-195	-191	-184	-179	-172	-166	-159	-151	-142
L06 ($\mu\epsilon$)	-252	-201	-180	-163	-147	-135	-126	-116	-110	-104	-95
L07 ($\mu\epsilon$)	-	-	-	-	-	-	-	-	-	-	-
L08 ($\mu\epsilon$)	-278	-211	-201	-183	-163	-146	-126	-108	-89	-68	-51
L09 ($\mu\epsilon$)	-203	-137	-126	-107	-88	-68	-48	-25	-4	19	37
L10 ($\mu\epsilon$)	-	-	-	-	-	-	-	-	-	-	-
RAC-A1 ($\mu\epsilon$)	-100	8	121	224	331	432	529	621	714	804	890
RAC-A2 ($\mu\epsilon$)	-71	29	133	226	321	409	495	576	657	735	810
RAC-A3 ($\mu\epsilon$)	-158	-68	28	110	193	269	342	411	480	547	612
RAC-F1 ($\mu\epsilon$)	-47	61	170	271	374	471	564	652	740	825	906

**Table F-31. Raw data, strain survey conducted after hot-wet conditioning, hot-wet environmental conditions (Run 1)
(continued)**

Load Step	0	1	2	3	4	5	6	7	8	9	10
Pressure (psi)	-0.02	0.67	1.33	1.99	2.66	3.35	4.02	4.65	5.35	6.02	6.66
RAC-F2 ($\mu\epsilon$)	-65	38	141	234	329	417	501	580	661	737	810
RBC-A1 ($\mu\epsilon$)	-222	-161	-88	-23	45	107	167	223	278	330	381
RBC-A2 ($\mu\epsilon$)	-153	-103	-40	15	74	127	179	227	275	320	364
RBC-A3 ($\mu\epsilon$)	-169	-117	-52	5	66	121	175	226	276	325	372
RBC-A4 ($\mu\epsilon$)	-105	-46	22	84	148	208	266	321	376	428	480
RBC-F1 ($\mu\epsilon$)	-227	-163	-91	-28	38	98	155	209	261	310	358
RBC-F2 ($\mu\epsilon$)	-190	-134	-69	-14	45	98	149	197	244	288	332
RBC-F3 ($\mu\epsilon$)	-168	-111	-47	9	67	120	172	220	267	313	357
S16 ($\mu\epsilon$)	321	304	375	442	511	581	649	717	787	857	927
S17 ($\mu\epsilon$)	-	-	-	-	-	-	-	-	-	-	-
S18 ($\mu\epsilon$)	334	362	467	558	643	725	801	874	948	1019	1090
S20 ($\mu\epsilon$)	-480	-767	-999	-1204	-1403	-1571	-1721	-1848	-1962	-2056	-2132
S22 ($\mu\epsilon$)	-243	-169	-79	-4	66	138	199	254	310	367	418
S25 ($\mu\epsilon$)	91	165	345	478	658	804	949	1056	1165	1272	1376
S29 ($\mu\epsilon$)	-238	-134	-50	29	109	186	261	333	406	477	547
S30 ($\mu\epsilon$)	49	159	275	371	463	550	632	710	789	865	940
S32 ($\mu\epsilon$)	-	-	-	-	-	-	-	-	-	-	-
S34 ($\mu\epsilon$)	85	131	223	308	393	477	558	637	717	794	871
S37 ($\mu\epsilon$)	310	463	616	744	864	976	1082	1182	1281	1375	1466
S41 ($\mu\epsilon$)	-	-	-	-	-	-	-	-	-	-	-

**Table F-31. Raw data, strain survey conducted after hot-wet conditioning, hot-wet environmental conditions (Run 1)
(continued)**

Load Step	0	1	2	3	4	5	6	7	8	9	10
Pressure (psi)	-0.02	0.67	1.33	1.99	2.66	3.35	4.02	4.65	5.35	6.02	6.66
S42 ($\mu\epsilon$)	73	149	237	314	390	464	537	609	681	752	823
S43 ($\mu\epsilon$)	183	297	401	487	566	641	711	777	844	907	970
S44 ($\mu\epsilon$)	-8	134	256	362	460	551	635	715	794	870	945
S46 ($\mu\epsilon$)	137	-42	-360	-531	-766	-975	-1229	-1373	-1561	-1694	-1836
S48 ($\mu\epsilon$)	-41	33	135	228	318	402	483	559	636	709	780
S51 ($\mu\epsilon$)	3	145	274	392	507	607	710	808	907	1001	1093
S55 ($\mu\epsilon$)	39	108	168	233	301	370	438	504	572	639	705
S56 ($\mu\epsilon$)	233	285	354	419	483	546	604	664	728	787	848
S57 ($\mu\epsilon$)	-	-	-	-	-	-	-	-	-	-	-
S58 ($\mu\epsilon$)	653	750	813	913	986	1071	1138	1172	1192	1279	1374
S60 ($\mu\epsilon$)	-675	-903	-1164	-1402	-1628	-1823	-1994	-2143	-2278	-2393	-2493
S62 ($\mu\epsilon$)	368	437	524	603	675	748	815	878	943	1006	1067
S65 ($\mu\epsilon$)	523	663	782	892	1003	1112	1217	1316	1417	1515	1610
S69 ($\mu\epsilon$)	-138	-43	55	117	190	262	332	404	476	546	616
S70 ($\mu\epsilon$)	-159	-74	23	106	187	264	338	409	484	556	628
S71 ($\mu\epsilon$)	-	-	-	-	-	-	-	-	-	-	-
S72 ($\mu\epsilon$)	-2	119	245	347	441	529	611	688	766	839	912
S74 ($\mu\epsilon$)	-9	-192	-357	-513	-674	-823	-965	-1098	-1229	-1355	-1473
S76 ($\mu\epsilon$)	58	107	202	289	375	459	539	616	694	770	844
S79 ($\mu\epsilon$)	-	-	-	-	-	-	-	-	-	-	-

**Table F-31. Raw data, strain survey conducted after hot-wet conditioning, hot-wet environmental conditions (Run 1)
(continued)**

Load Step	0	1	2	3	4	5	6	7	8	9	10
Pressure (psi)	-0.02	0.67	1.33	1.99	2.66	3.35	4.02	4.65	5.35	6.02	6.66
S83 ($\mu\epsilon$)	-143	-118	-62	-5	49	95	151	215	271	332	400
S84 ($\mu\epsilon$)	58	118	200	270	343	414	485	554	625	695	765
S85 ($\mu\epsilon$)	-	-	-	-	-	-	-	-	-	-	-
S86 ($\mu\epsilon$)	99	229	356	458	553	639	719	794	870	942	1013
S88 ($\mu\epsilon$)	79	-49	-142	-215	-285	-342	-392	-431	-465	-491	-510
S90 ($\mu\epsilon$)	118	232	348	447	541	628	707	784	860	934	1007
S93 ($\mu\epsilon$)	127	265	412	540	663	779	888	992	1094	1193	1288
S97 ($\mu\epsilon$)	127	194	262	327	394	462	528	593	660	727	792
UAC-A1 ($\mu\epsilon$)	25	129	268	392	516	632	742	845	947	1042	1134
UAC-A2 ($\mu\epsilon$)	-15	74	193	298	403	500	592	677	762	841	917
UAC-A3 ($\mu\epsilon$)	-23	67	177	273	368	456	540	617	695	768	840
UAC-F1 ($\mu\epsilon$)	-13	89	230	356	483	603	718	824	930	1029	1124
UAC-F2 ($\mu\epsilon$)	0	88	211	319	427	529	626	716	805	889	970
UBC-A1 ($\mu\epsilon$)	-63	91	240	368	497	612	720	818	913	1003	1090
UBC-A2 ($\mu\epsilon$)	14	136	253	356	457	549	635	713	790	861	931
UBC-A3 ($\mu\epsilon$)	39	146	252	345	436	519	597	669	739	805	869
UBC-A4 ($\mu\epsilon$)	53	149	249	337	426	506	582	653	723	790	855
UBC-F1 ($\mu\epsilon$)	-66	116	263	391	517	630	735	832	926	1013	1097
UBC-F2 ($\mu\epsilon$)	5	160	280	382	484	575	660	738	814	885	954
UBC-F3 ($\mu\epsilon$)	6	149	259	354	447	532	610	683	755	822	887

**Table F-31. Raw data, strain survey conducted after hot-wet conditioning, hot-wet environmental conditions (Run 1)
(continued)**

Load Step	0	1	2	3	4	5	6	7	8	9	10
Pressure (psi)	-0.02	0.67	1.33	1.99	2.66	3.35	4.02	4.65	5.35	6.02	6.66
UDAC-A1 ($\mu\epsilon$)	-59	77	214	332	452	565	672	771	867	959	1048
UDAC-A2 ($\mu\epsilon$)	-58	61	179	281	385	482	574	660	743	823	900
UDAC-A3 ($\mu\epsilon$)	-82	20	120	206	293	376	456	529	602	672	741
UDAC-F1 ($\mu\epsilon$)	-72	69	213	334	458	574	684	786	885	979	1070
UDAC-F2 ($\mu\epsilon$)	-67	52	175	277	383	481	574	661	745	826	903
UDBC-A1 ($\mu\epsilon$)	-45	84	229	355	481	594	701	801	900	993	1083
UDBC-A2 ($\mu\epsilon$)	-14	97	217	320	423	514	600	681	761	836	908
UDBC-A3 ($\mu\epsilon$)	-12	93	204	299	394	477	558	632	708	779	847
UDBC-A4 ($\mu\epsilon$)	29	126	227	314	402	479	554	625	698	765	832
UDBC-F1 ($\mu\epsilon$)	-18	103	256	391	525	647	763	870	976	1075	1171
UDBC-F2 ($\mu\epsilon$)	29	128	251	359	465	562	652	735	818	894	968
UDBC-F3 ($\mu\epsilon$)	42	135	248	348	446	535	618	695	772	843	913

Table F-32. Raw data, strain survey conducted after hot-wet conditioning, hot-wet environmental conditions (Run 2)

Load Step	0	1	2	3	4	5	6	7	8	9	10
Pressure (psi)	-0.01	0.68	1.34	1.98	2.66	3.34	4.01	4.69	5.35	6.02	6.67
Frame-1 (lbf)	1	117	240	348	470	547	725	800	932	989	1166
Frame-2 (lbf)	70	49	230	336	448	568	680	792	906	1022	1133
Frame-3 (lbf)	0	115	224	332	455	564	681	795	906	1019	1133
Frame-4 (lbf)	45	112	227	343	450	567	682	792	908	1022	1132
Frame-5 (lbf)	-14	104	243	343	456	570	699	784	904	1028	1128
Frame-6 (lbf)	2	112	235	337	452	561	674	779	901	1018	1135
Frame-7 (lbf)	11	116	226	335	455	569	682	791	901	1018	1132
Frame-8 (lbf)	-1	106	223	345	458	566	679	795	898	1019	1133
Frame-9 (lbf)	33	112	228	339	454	556	678	792	907	1018	1133
Frame-10 (lbf)	0	121	238	340	454	564	678	786	896	1018	1133
Frame-11 (lbf)	0	110	226	344	451	571	677	794	909	1024	1135
Frame-12 (lbf)	24	108	228	341	459	566	683	794	907	1018	1135
Hoop-1 (lbf)	-6	703	1415	2144	2853	3571	4265	5014	5704	6430	7133
Hoop-2 (lbf)	144	722	1455	2149	2841	3583	4281	5000	5721	6447	7138
Hoop-3 (lbf)	49	713	1414	2140	2853	3579	4283	4998	5711	6418	7141
Hoop-4 (lbf)	33	719	1428	2136	2848	3580	4279	5003	5726	6453	7137
Hoop-5 (lbf)	33	682	1414	2142	2859	3587	4271	5004	5698	6418	7128
Hoop-6 (lbf)	-12	717	1435	2130	2858	3580	4275	5021	5726	6426	7159
Hoop-7 (lbf)	-6	716	1433	2147	2853	3566	4291	4998	5712	6420	7148
Hoop-8 (lbf)	131	711	1421	2132	2854	3583	4285	5007	5719	6438	7137
Hoop-9 (lbf)	28	709	1441	2164	2866	3581	4294	4983	5717	6428	7132

**Table F-32. Raw data, strain survey conducted after hot-wet conditioning, hot-wet environmental conditions (Run 2)
(continued)**

Load Step	0	1	2	3	4	5	6	7	8	9	10
Pressure (psi)	-0.01	0.68	1.34	1.98	2.66	3.34	4.01	4.69	5.35	6.02	6.67
Hoop-10 (lbf)	10	713	1428	2131	2827	3573	4279	5010	5723	6435	7146
Hoop-11 (lbf)	38	700	1411	2155	2858	3575	4288	5005	5727	6437	7155
Hoop-12 (lbf)	149	716	1432	2134	2847	3570	4289	5011	5714	6423	7141
Hoop-13 (lbf)	56	771	1452	2130	2837	3585	4273	5005	5713	6431	7142
Hoop-14 (lbf)	4	701	1428	2142	2864	3574	4283	5027	5719	6431	7143
Long-1 (lbf)	21	650	1356	1994	2698	3370	3980	4682	5322	5946	6646
Long-2 (lbf)	0	648	1340	2001	2668	3338	4010	4678	5342	6002	6684
Long-3 (lbf)	-3	668	1336	2005	2675	3333	4008	4683	5342	6006	6674
Long-4 (lbf)	-3	681	1369	2005	2668	3336	4004	4670	5343	6006	6674
Long-5 (lbf)	2	664	1338	2006	2676	3340	4017	4669	5337	5999	6676
Long-6 (lbf)	-3	639	1329	2013	2674	3338	4006	4669	5340	5997	6673
Long-7 (lbf)	3	663	1349	2002	2671	3333	4009	4659	5331	6004	6677
Long-8 (lbf)	-4	650	1334	2010	2646	3341	4019	4664	5343	6000	6669
F01 ($\mu\epsilon$)	-287	-270	-221	-165	-126	-74	-19	23	72	119	177
F02 ($\mu\epsilon$)	269	347	394	441	495	545	599	647	697	751	795
F03 ($\mu\epsilon$)	-356	-385	-345	-296	-266	-224	-183	-145	-103	-68	-18
F04 ($\mu\epsilon$)	405	469	526	577	645	699	756	818	871	934	982
F05 ($\mu\epsilon$)	-	-	-	-	-	-	-	-	-	-	-
F06 ($\mu\epsilon$)	443	507	554	593	653	689	744	789	834	887	929
F07 ($\mu\epsilon$)	-236	-249	-191	-146	-118	-73	-33	5	46	84	129

**Table F-32. Raw data, strain survey conducted after hot-wet conditioning, hot-wet environmental conditions (Run 2)
(continued)**

Load Step	0	1	2	3	4	5	6	7	8	9	10
Pressure (psi)	-0.01	0.68	1.34	1.98	2.66	3.34	4.01	4.69	5.35	6.02	6.67
F08 ($\mu\epsilon$)	252	280	343	390	445	495	544	595	641	695	737
IS16 ($\mu\epsilon$)	34	95	168	240	313	389	463	542	617	694	768
IS17 ($\mu\epsilon$)	-77	-57	-28	15	64	123	181	248	311	378	445
IS18 ($\mu\epsilon$)	-221	-212	-198	-168	-129	-79	-28	33	93	157	222
IS19 ($\mu\epsilon$)	-32	7	39	74	108	150	190	236	283	331	380
IS20 ($\mu\epsilon$)	144	193	239	280	318	358	394	432	468	503	537
IS21 ($\mu\epsilon$)	113	163	206	243	276	312	342	375	404	432	460
IS22 ($\mu\epsilon$)	-246	-252	-242	-219	-188	-144	-99	-42	14	74	135
IS23 ($\mu\epsilon$)	-374	-362	-364	-352	-336	-309	-280	-243	-204	-162	-117
IS24 ($\mu\epsilon$)	184	252	315	372	424	478	525	574	619	664	706
IS25 ($\mu\epsilon$)	-350	-322	-307	-277	-243	-199	-153	-99	-45	13	72
IS26 ($\mu\epsilon$)	78	204	319	425	526	626	717	809	894	978	1058
IS27 ($\mu\epsilon$)	-345	-307	-273	-228	-179	-121	-63	2	67	134	202
IS28 ($\mu\epsilon$)	48	165	272	373	467	562	647	734	813	891	966
IS29 ($\mu\epsilon$)	79	178	276	367	453	542	623	706	784	860	935
IS30 ($\mu\epsilon$)	-	-	-	-	-	-	-	-	-	-	-
IS31 ($\mu\epsilon$)	-69	-14	46	107	168	235	297	363	426	488	549
IS32 ($\mu\epsilon$)	-110	-63	-17	27	67	110	148	187	224	259	294
IS33 ($\mu\epsilon$)	-109	-55	-4	42	85	132	170	211	250	287	323
IS34 ($\mu\epsilon$)	-314	-275	-239	-200	-158	-107	-58	1	59	119	180

**Table F-32. Raw data, strain survey conducted after hot-wet conditioning, hot-wet environmental conditions (Run 2)
(continued)**

Load Step	0	1	2	3	4	5	6	7	8	9	10
Pressure (psi)	-0.01	0.68	1.34	1.98	2.66	3.34	4.01	4.69	5.35	6.02	6.67
IS35 ($\mu\epsilon$)	-530	-580	-600	-601	-593	-569	-544	-510	-473	-432	-389
IS36 ($\mu\epsilon$)	-109	-60	-10	36	79	125	165	208	247	284	321
IS37 ($\mu\epsilon$)	-458	-510	-526	-521	-507	-477	-446	-404	-361	-314	-264
IS38 ($\mu\epsilon$)	-149	-88	-25	35	92	152	205	262	314	365	415
IS39 ($\mu\epsilon$)	-468	-514	-519	-502	-476	-434	-390	-337	-281	-222	-160
IS40 ($\mu\epsilon$)	-158	-89	-21	45	107	172	231	292	348	403	456
IS41 ($\mu\epsilon$)	-9	79	164	244	320	398	469	543	611	678	743
IS42 ($\mu\epsilon$)	118	149	200	259	320	383	445	513	579	646	711
IS43 ($\mu\epsilon$)	24	9	37	80	132	192	251	319	386	455	523
IS44 ($\mu\epsilon$)	91	25	20	37	67	107	150	204	258	316	375
IS45 ($\mu\epsilon$)	-36	23	98	167	235	302	361	425	484	542	598
IS46 ($\mu\epsilon$)	-40	26	102	172	241	307	367	429	487	544	597
IS47 ($\mu\epsilon$)	-31	35	111	179	246	311	371	432	490	547	601
IS48 ($\mu\epsilon$)	-42	-34	-2	35	78	131	180	242	303	368	431
IS49 ($\mu\epsilon$)	-32	-80	-81	-70	-51	-24	3	38	75	115	157
IS50 ($\mu\epsilon$)	-31	43	128	204	280	352	419	486	549	611	669
IS51 ($\mu\epsilon$)	-1	-40	-30	-8	21	56	91	133	177	223	270
IS52 ($\mu\epsilon$)	-25	77	191	296	400	500	592	685	772	857	937
IS53 ($\mu\epsilon$)	23	-18	-3	27	65	111	156	208	262	319	377
IS54 ($\mu\epsilon$)	-35	62	170	269	367	461	548	635	717	797	873

**Table F-32. Raw data, strain survey conducted after hot-wet conditioning, hot-wet environmental conditions (Run 2)
(continued)**

Load Step	0	1	2	3	4	5	6	7	8	9	10
Pressure (psi)	-0.01	0.68	1.34	1.98	2.66	3.34	4.01	4.69	5.35	6.02	6.67
IS55 ($\mu\epsilon$)	-72	33	137	230	319	406	486	566	642	716	788
IS56 ($\mu\epsilon$)	72	118	159	204	254	309	369	430	494	557	622
IS57 ($\mu\epsilon$)	-115	-126	-118	-94	-61	-18	32	85	142	199	259
IS58 ($\mu\epsilon$)	-228	-259	-263	-249	-226	-192	-150	-104	-53	-1	55
IS59 ($\mu\epsilon$)	6	20	47	76	106	142	177	218	259	300	344
IS60 ($\mu\epsilon$)	157	192	231	267	301	336	367	401	432	462	491
IS61 ($\mu\epsilon$)	138	180	222	258	291	325	354	385	413	439	465
IS62 ($\mu\epsilon$)	-209	-225	-213	-193	-167	-132	-89	-43	7	58	114
IS63 ($\mu\epsilon$)	-389	-422	-430	-421	-410	-389	-364	-334	-303	-270	-232
IS64 ($\mu\epsilon$)	172	226	283	336	386	438	484	532	576	618	658
IS65 ($\mu\epsilon$)	-396	-406	-387	-350	-312	-264	-210	-156	-99	-41	22
IS66 ($\mu\epsilon$)	15	128	240	348	451	552	647	742	829	914	997
IS67 ($\mu\epsilon$)	-347	-347	-316	-268	-220	-163	-100	-37	27	91	160
IS68 ($\mu\epsilon$)	9	115	216	315	408	501	588	674	754	832	908
IS69 ($\mu\epsilon$)	37	143	233	317	399	481	560	640	714	787	859
IS70 ($\mu\epsilon$)	189	203	229	266	309	360	414	469	531	589	651
IS71 ($\mu\epsilon$)	-6	-25	-16	15	55	105	161	220	284	345	411
IS72 ($\mu\epsilon$)	-101	-116	-108	-77	-39	9	63	121	183	244	310
IS73 ($\mu\epsilon$)	-210	-114	-27	55	133	210	280	351	417	480	541
IS74 ($\mu\epsilon$)	-143	-54	29	106	181	254	322	391	454	515	574

**Table F-32. Raw data, strain survey conducted after hot-wet conditioning, hot-wet environmental conditions (Run 2)
(continued)**

Load Step	0	1	2	3	4	5	6	7	8	9	10
Pressure (psi)	-0.01	0.68	1.34	1.98	2.66	3.34	4.01	4.69	5.35	6.02	6.67
IS75 ($\mu\epsilon$)	-123	-31	52	130	205	279	348	417	481	542	602
IS76 ($\mu\epsilon$)	-117	-64	-13	40	95	154	218	284	352	418	488
IS77 ($\mu\epsilon$)	-196	-182	-167	-137	-105	-66	-26	19	65	112	163
IS78 ($\mu\epsilon$)	-123	-25	64	148	229	308	381	455	523	589	653
IS79 ($\mu\epsilon$)	-171	-151	-131	-96	-60	-19	27	72	122	170	223
IS80 ($\mu\epsilon$)	-146	-28	77	179	278	374	465	554	638	719	798
IS81 ($\mu\epsilon$)	-217	-210	-199	-170	-138	-100	-57	-12	36	82	134
IS82 ($\mu\epsilon$)	-115	-7	89	183	274	363	448	533	611	687	761
IS83 ($\mu\epsilon$)	-182	-73	17	102	181	264	337	414	484	551	618
IS84 ($\mu\epsilon$)	-9	40	99	161	224	293	353	423	489	559	626
IS85 ($\mu\epsilon$)	-24	-26	-1	42	95	159	216	286	354	426	495
IS86 ($\mu\epsilon$)	-28	-51	-46	-19	20	73	121	182	244	310	374
IS87 ($\mu\epsilon$)	-100	-30	26	74	122	169	210	255	298	340	380
IS88 ($\mu\epsilon$)	-53	17	79	132	185	236	283	331	377	422	464
IS89 ($\mu\epsilon$)	-44	26	85	137	188	240	286	333	381	426	470
IS90 ($\mu\epsilon$)	-44	-39	-23	7	48	101	151	212	273	338	401
IS91 ($\mu\epsilon$)	-82	-95	-100	-92	-73	-46	-17	21	62	107	154
IS92 ($\mu\epsilon$)	-65	17	90	152	213	272	326	380	432	483	531
IS93 ($\mu\epsilon$)	-72	-68	-56	-31	4	49	90	142	195	253	310
IS94 ($\mu\epsilon$)	-45	83	199	303	409	510	602	695	784	870	951

**Table F-32. Raw data, strain survey conducted after hot-wet conditioning, hot-wet environmental conditions (Run 2)
(continued)**

Load Step	0	1	2	3	4	5	6	7	8	9	10
Pressure (psi)	-0.01	0.68	1.34	1.98	2.66	3.34	4.01	4.69	5.35	6.02	6.67
IS95 ($\mu\epsilon$)	-75	-65	-45	-12	31	82	131	187	247	308	369
IS96 ($\mu\epsilon$)	-46	71	173	266	361	453	537	621	704	783	859
IS97 ($\mu\epsilon$)	-98	12	105	190	275	357	433	510	585	657	727
L01 ($\mu\epsilon$)	-	-	-	-	-	-	-	-	-	-	-
L02 ($\mu\epsilon$)	-292	-229	-216	-201	-184	-172	-157	-142	-127	-112	-96
L03 ($\mu\epsilon$)	-179	-145	-140	-127	-109	-92	-74	-54	-33	-11	9
L04 ($\mu\epsilon$)	-200	-144	-118	-94	-65	-40	-14	11	35	60	82
L05 ($\mu\epsilon$)	-198	-190	-190	-187	-180	-175	-170	-163	-153	-144	-135
L06 ($\mu\epsilon$)	-228	-203	-177	-161	-147	-134	-125	-117	-107	-99	-92
L07 ($\mu\epsilon$)	-	-	-	-	-	-	-	-	-	-	-
L08 ($\mu\epsilon$)	-245	-212	-198	-180	-160	-141	-123	-103	-83	-62	-44
L09 ($\mu\epsilon$)	-166	-133	-117	-100	-76	-59	-37	-12	5	30	49
L10 ($\mu\epsilon$)	-	-	-	-	-	-	-	-	-	-	-
RAC-A1 ($\mu\epsilon$)	-102	16	123	228	331	434	530	627	717	805	890
RAC-A2 ($\mu\epsilon$)	-75	36	133	227	320	410	495	580	658	735	809
RAC-A3 ($\mu\epsilon$)	-160	-60	27	110	190	269	341	415	481	547	609
RAC-F1 ($\mu\epsilon$)	-49	67	173	275	375	473	564	658	742	827	907
RAC-F2 ($\mu\epsilon$)	-68	43	143	237	328	417	500	585	662	738	810
RBC-A1 ($\mu\epsilon$)	-232	-156	-83	-16	48	113	171	230	283	335	384
RBC-A2 ($\mu\epsilon$)	-164	-99	-37	21	75	132	181	233	279	324	367

**Table F-32. Raw data, strain survey conducted after hot-wet conditioning, hot-wet environmental conditions (Run 2)
(continued)**

Load Step	0	1	2	3	4	5	6	7	8	9	10
Pressure (psi)	-0.01	0.68	1.34	1.98	2.66	3.34	4.01	4.69	5.35	6.02	6.67
RBC-A3 ($\mu\epsilon$)	-177	-112	-48	11	67	126	178	232	281	329	375
RBC-A4 ($\mu\epsilon$)	-114	-44	24	88	148	211	267	325	379	431	481
RBC-F1 ($\mu\epsilon$)	-236	-158	-87	-22	40	104	159	215	266	315	361
RBC-F2 ($\mu\epsilon$)	-198	-129	-66	-8	47	104	153	203	249	292	334
RBC-F3 ($\mu\epsilon$)	-175	-106	-44	14	69	125	175	226	272	317	359
S16 ($\mu\epsilon$)	301	309	377	444	511	580	645	716	784	853	921
S17 ($\mu\epsilon$)	-	-	-	-	-	-	-	-	-	-	-
S18 ($\mu\epsilon$)	296	348	456	547	632	712	785	861	931	999	1064
S20 ($\mu\epsilon$)	-399	-711	-947	-1155	-1348	-1522	-1669	-1808	-1926	-2032	-2120
S22 ($\mu\epsilon$)	-297	-185	-94	-19	50	118	185	253	297	352	405
S25 ($\mu\epsilon$)	258	327	465	582	698	815	919	1033	1138	1239	1335
S29 ($\mu\epsilon$)	-230	-135	-49	29	107	184	257	332	403	475	543
S30 ($\mu\epsilon$)	30	157	271	368	457	546	626	708	786	861	936
S32 ($\mu\epsilon$)	-946	-1006	-1054	-1094	-1133	-1168	-1198	-1226	-1250	-1271	-1289
S34 ($\mu\epsilon$)	55	128	216	302	385	470	548	631	708	785	861
S37 ($\mu\epsilon$)	277	456	606	733	851	964	1067	1171	1268	1363	1453
S41 ($\mu\epsilon$)	-	-	-	-	-	-	-	-	-	-	-
S42 ($\mu\epsilon$)	68	157	242	318	393	467	537	612	683	754	823
S43 ($\mu\epsilon$)	161	290	394	479	557	633	701	772	838	904	966
S44 ($\mu\epsilon$)	-31	127	254	359	456	547	629	713	790	867	939

**Table F-32. Raw data, strain survey conducted after hot-wet conditioning, hot-wet environmental conditions (Run 2)
(continued)**

Load Step	0	1	2	3	4	5	6	7	8	9	10
Pressure (psi)	-0.01	0.68	1.34	1.98	2.66	3.34	4.01	4.69	5.35	6.02	6.67
S46 ($\mu\epsilon$)	171	-111	-378	-546	-805	-1021	-1210	-1393	-1558	-1715	-1861
S48 ($\mu\epsilon$)	-62	28	130	225	312	401	475	555	630	706	774
S51 ($\mu\epsilon$)	-20	131	260	376	487	595	697	800	897	993	1083
S55 ($\mu\epsilon$)	41	101	165	229	297	365	432	501	568	634	698
S56 ($\mu\epsilon$)	212	280	352	415	475	538	595	660	717	779	842
S57 ($\mu\epsilon$)	-	-	-	-	-	-	-	-	-	-	-
S58 ($\mu\epsilon$)	550	705	812	898	979	1057	1084	1131	1204	1284	1362
S60 ($\mu\epsilon$)	-574	-853	-1114	-1351	-1569	-1766	-1940	-2103	-2243	-2371	-2484
S62 ($\mu\epsilon$)	339	430	518	595	668	738	805	871	935	996	1058
S65 ($\mu\epsilon$)	508	655	779	887	999	1105	1207	1312	1410	1509	1603
S69 ($\mu\epsilon$)	-74	0	75	142	212	283	352	425	491	558	626
S70 ($\mu\epsilon$)	-168	-75	21	104	183	259	334	407	481	552	623
S71 ($\mu\epsilon$)	-	-	-	-	-	-	-	-	-	-	-
S72 ($\mu\epsilon$)	-35	107	236	337	431	519	601	681	759	832	904
S74 ($\mu\epsilon$)	-21	-205	-368	-526	-684	-832	-973	-1113	-1240	-1364	-1480
S76 ($\mu\epsilon$)	23	100	195	281	366	450	530	610	687	762	835
S79 ($\mu\epsilon$)	-	-	-	-	-	-	-	-	-	-	-
S83 ($\mu\epsilon$)	-131	-94	-49	-4	45	96	159	224	278	331	380
S84 ($\mu\epsilon$)	45	121	200	271	342	416	482	555	623	694	761
S85 ($\mu\epsilon$)	-	-	-	-	-	-	-	-	-	-	-

**Table F-32. Raw data, strain survey conducted after hot-wet conditioning, hot-wet environmental conditions (Run 2)
(continued)**

Load Step	0	1	2	3	4	5	6	7	8	9	10
Pressure (psi)	-0.01	0.68	1.34	1.98	2.66	3.34	4.01	4.69	5.35	6.02	6.67
S86 ($\mu\epsilon$)	76	223	350	453	546	634	711	791	863	937	1005
S88 ($\mu\epsilon$)	67	-54	-146	-220	-290	-347	-394	-435	-468	-494	-515
S90 ($\mu\epsilon$)	98	227	345	445	536	623	702	781	854	927	999
S93 ($\mu\epsilon$)	106	260	408	537	658	774	881	988	1088	1187	1278
S97 ($\mu\epsilon$)	132	196	263	329	396	463	528	595	660	725	787
UAC-A1 ($\mu\epsilon$)	12	138	273	397	520	636	743	849	948	1043	1133
UAC-A2 ($\mu\epsilon$)	-36	76	194	299	403	501	589	678	761	840	914
UAC-A3 ($\mu\epsilon$)	-33	72	179	275	368	457	538	618	694	767	836
UAC-F1 ($\mu\epsilon$)	-26	98	235	362	488	609	719	830	932	1031	1123
UAC-F2 ($\mu\epsilon$)	-14	94	213	322	430	532	626	719	806	890	968
UBC-A1 ($\mu\epsilon$)	-76	97	242	374	497	617	721	825	919	1009	1093
UBC-A2 ($\mu\epsilon$)	0	136	253	358	456	550	634	717	791	863	931
UBC-A3 ($\mu\epsilon$)	25	146	251	346	434	520	596	672	740	806	869
UBC-A4 ($\mu\epsilon$)	37	148	247	337	421	505	579	654	723	789	853
UBC-F1 ($\mu\epsilon$)	-82	120	266	397	518	635	738	839	931	1018	1100
UBC-F2 ($\mu\epsilon$)	-12	160	279	385	483	577	660	742	816	887	955
UBC-F3 ($\mu\epsilon$)	-12	149	258	356	445	533	610	687	757	824	887
UDAC-A1 ($\mu\epsilon$)	-64	85	217	337	457	570	672	774	870	963	1049
UDAC-A2 ($\mu\epsilon$)	-65	67	181	285	387	485	573	661	745	825	900
UDAC-A3 ($\mu\epsilon$)	-89	23	121	207	294	377	453	529	602	672	739

**Table F-32. Raw data, strain survey conducted after hot-wet conditioning, hot-wet environmental conditions (Run 2)
(continued)**

Load Step	0	1	2	3	4	5	6	7	8	9	10
Pressure (psi)	-0.01	0.68	1.34	1.98	2.66	3.34	4.01	4.69	5.35	6.02	6.67
UDAC-F1 ($\mu\epsilon$)	-74	77	215	339	463	579	684	790	888	983	1071
UDAC-F2 ($\mu\epsilon$)	-71	59	176	280	385	485	573	663	747	828	904
UDBC-A1 ($\mu\epsilon$)	-53	94	232	361	483	601	708	814	910	1002	1091
UDBC-A2 ($\mu\epsilon$)	-24	103	216	323	421	517	604	690	767	841	913
UDBC-A3 ($\mu\epsilon$)	-21	99	203	301	392	481	562	642	714	784	852
UDBC-A4 ($\mu\epsilon$)	18	130	225	314	398	481	556	633	702	769	836
UDBC-F1 ($\mu\epsilon$)	-26	117	264	402	532	657	773	886	988	1087	1181
UDBC-F2 ($\mu\epsilon$)	16	134	254	365	467	567	657	745	825	901	974
UDBC-F3 ($\mu\epsilon$)	27	138	249	351	446	538	621	704	778	849	918

Table F-33. Raw data, strain survey conducted after hot-wet conditioning, hot-wet environmental conditions (Run 3)

Load Step	0	1	2	3	4	5	6	7	8	9	10
Pressure (psi)	0.00	0.67	1.34	1.99	2.69	3.34	4.01	4.70	5.35	6.00	6.65
Frame-1 (lbf)	0	78	248	338	442	623	712	801	904	1007	1114
Frame-2 (lbf)	67	100	215	329	457	565	679	793	902	1019	1133
Frame-3 (lbf)	0	114	232	346	451	566	680	793	908	1017	1135
Frame-4 (lbf)	35	109	229	345	451	559	682	798	904	1022	1135
Frame-5 (lbf)	-8	121	216	347	463	564	690	789	900	1020	1140
Frame-6 (lbf)	4	108	239	334	457	560	684	794	897	1016	1136
Frame-7 (lbf)	11	114	227	339	451	564	681	790	904	1020	1130
Frame-8 (lbf)	0	105	224	341	449	570	682	795	905	1020	1135
Frame-9 (lbf)	39	116	227	334	442	566	681	791	909	1021	1129
Frame-10 (lbf)	1	110	232	343	451	571	684	788	906	1019	1132
Frame-11 (lbf)	10	118	222	342	456	567	680	790	908	1020	1127
Frame-12 (lbf)	31	116	227	337	454	570	676	795	908	1016	1131
Hoop-1 (lbf)	57	709	1418	2141	2863	3562	4278	4997	5715	6438	7149
Hoop-2 (lbf)	215	695	1467	2145	2883	3557	4290	4996	5705	6415	7151
Hoop-3 (lbf)	41	728	1428	2143	2860	3567	4282	5002	5714	6422	7138
Hoop-4 (lbf)	31	716	1450	2143	2869	3568	4296	5005	5708	6412	7127
Hoop-5 (lbf)	32	704	1437	2130	2857	3564	4292	5007	5735	6429	7156
Hoop-6 (lbf)	0	719	1437	2145	2870	3567	4289	5005	5699	6427	7143
Hoop-7 (lbf)	-4	717	1420	2140	2857	3570	4290	5004	5710	6422	7137
Hoop-8 (lbf)	129	720	1431	2139	2864	3578	4288	5007	5715	6426	7146
Hoop-9 (lbf)	66	706	1409	2128	2857	3562	4290	5004	5717	6434	7140

**Table F-33. Raw data, strain survey conducted after hot-wet conditioning, hot-wet environmental conditions (Run 3)
(continued)**

Load Step	0	1	2	3	4	5	6	7	8	9	10
Pressure (psi)	0.00	0.67	1.34	1.99	2.69	3.34	4.01	4.70	5.35	6.00	6.65
Hoop-10 (lbf)	10	713	1446	2138	2853	3573	4296	5003	5722	6415	7138
Hoop-11 (lbf)	45	716	1468	2137	2873	3559	4285	5017	5733	6418	7141
Hoop-12 (lbf)	158	707	1425	2141	2862	3571	4283	5011	5698	6427	7139
Hoop-13 (lbf)	66	740	1403	2148	2844	3565	4289	5000	5712	6426	7139
Hoop-14 (lbf)	15	697	1439	2148	2876	3562	4282	4994	5704	6435	7139
Long-1 (lbf)	-18	673	1320	2001	2658	3348	3988	4627	5343	5976	6690
Long-2 (lbf)	13	672	1333	2005	2679	3338	3996	4668	5343	6009	6677
Long-3 (lbf)	0	666	1337	2002	2672	3338	4005	4666	5346	6005	6684
Long-4 (lbf)	4	682	1321	2011	2670	3338	4014	4664	5339	6014	6669
Long-5 (lbf)	-3	666	1343	2002	2667	3335	4007	4669	5329	6012	6677
Long-6 (lbf)	0	631	1327	2012	2664	3356	3995	4660	5360	5999	6648
Long-7 (lbf)	6	659	1349	1973	2670	3347	4004	4681	5350	6000	6673
Long-8 (lbf)	0	660	1328	2015	2666	3339	4016	4671	5326	6007	6672
F01 ($\mu\epsilon$)	-291	-266	-233	-166	-121	-67	-23	29	72	125	177
F02 ($\mu\epsilon$)	276	341	392	439	498	537	593	646	699	743	789
F03 ($\mu\epsilon$)	-358	-381	-343	-295	-268	-214	-180	-138	-102	-57	-14
F04 ($\mu\epsilon$)	405	464	526	574	644	687	755	812	872	923	975
F05 ($\mu\epsilon$)	-	-	-	-	-	-	-	-	-	-	-
F06 ($\mu\epsilon$)	448	502	548	591	650	686	744	786	839	883	929
F07 ($\mu\epsilon$)	-242	-231	-190	-145	-115	-62	-28	13	48	95	136

**Table F-33. Raw data, strain survey conducted after hot-wet conditioning, hot-wet environmental conditions (Run 3)
(continued)**

Load Step	0	1	2	3	4	5	6	7	8	9	10
Pressure (psi)	0.00	0.67	1.34	1.99	2.69	3.34	4.01	4.70	5.35	6.00	6.65
F08 ($\mu\epsilon$)	259	288	335	380	444	485	540	588	641	686	733
IS16 ($\mu\epsilon$)	41	94	169	239	315	387	464	539	616	692	768
IS17 ($\mu\epsilon$)	-68	-57	-26	15	67	122	183	245	311	377	445
IS18 ($\mu\epsilon$)	-212	-210	-196	-167	-126	-79	-25	32	94	157	223
IS19 ($\mu\epsilon$)	-21	7	41	73	109	147	189	232	278	326	376
IS20 ($\mu\epsilon$)	142	188	234	274	314	352	390	426	463	499	534
IS21 ($\mu\epsilon$)	107	155	199	235	271	304	337	368	398	427	456
IS22 ($\mu\epsilon$)	-242	-247	-237	-216	-184	-143	-95	-42	15	74	137
IS23 ($\mu\epsilon$)	-364	-358	-361	-350	-332	-306	-276	-241	-201	-159	-113
IS24 ($\mu\epsilon$)	185	249	313	368	424	474	524	571	617	662	705
IS25 ($\mu\epsilon$)	-329	-313	-298	-271	-234	-192	-145	-94	-38	19	80
IS26 ($\mu\epsilon$)	91	211	326	430	536	630	725	814	901	983	1065
IS27 ($\mu\epsilon$)	-324	-298	-265	-222	-170	-115	-56	7	73	140	209
IS28 ($\mu\epsilon$)	55	168	276	374	473	562	651	735	817	894	970
IS29 ($\mu\epsilon$)	79	178	277	366	457	540	625	705	785	861	937
IS30 ($\mu\epsilon$)	-	-	-	-	-	-	-	-	-	-	-
IS31 ($\mu\epsilon$)	-73	-18	43	102	168	230	295	360	423	485	548
IS32 ($\mu\epsilon$)	-113	-64	-17	25	69	108	148	187	223	259	294
IS33 ($\mu\epsilon$)	-113	-57	-5	40	87	128	169	211	248	284	321
IS34 ($\mu\epsilon$)	-305	-270	-233	-196	-152	-106	-53	3	61	120	182

**Table F-33. Raw data, strain survey conducted after hot-wet conditioning, hot-wet environmental conditions (Run 3)
(continued)**

Load Step	0	1	2	3	4	5	6	7	8	9	10
Pressure (psi)	0.00	0.67	1.34	1.99	2.69	3.34	4.01	4.70	5.35	6.00	6.65
IS35 ($\mu\epsilon$)	-516	-569	-590	-593	-580	-561	-535	-502	-466	-425	-381
IS36 ($\mu\epsilon$)	-111	-60	-10	35	82	124	167	209	248	285	323
IS37 ($\mu\epsilon$)	-443	-498	-515	-512	-494	-469	-436	-397	-353	-307	-256
IS38 ($\mu\epsilon$)	-144	-82	-20	38	100	155	212	266	319	370	420
IS39 ($\mu\epsilon$)	-453	-502	-508	-494	-463	-426	-381	-329	-273	-214	-153
IS40 ($\mu\epsilon$)	-154	-84	-16	47	115	174	236	296	352	407	461
IS41 ($\mu\epsilon$)	-7	81	167	243	324	397	471	543	612	678	744
IS42 ($\mu\epsilon$)	117	148	201	257	319	382	447	513	580	645	712
IS43 ($\mu\epsilon$)	24	9	40	80	133	191	255	320	387	455	526
IS44 ($\mu\epsilon$)	91	25	23	37	67	106	153	204	259	315	377
IS45 ($\mu\epsilon$)	-43	17	96	162	233	296	360	421	481	538	596
IS46 ($\mu\epsilon$)	-39	26	105	172	243	305	369	429	488	543	599
IS47 ($\mu\epsilon$)	-30	36	113	179	248	310	373	432	490	546	602
IS48 ($\mu\epsilon$)	-41	-34	1	34	80	129	185	241	304	367	433
IS49 ($\mu\epsilon$)	-28	-77	-76	-67	-47	-22	8	40	78	117	161
IS50 ($\mu\epsilon$)	-28	44	131	206	283	352	421	487	550	611	671
IS51 ($\mu\epsilon$)	5	-36	-24	-5	25	58	96	136	180	225	274
IS52 ($\mu\epsilon$)	-19	80	197	299	406	500	597	687	775	857	940
IS53 ($\mu\epsilon$)	32	-12	5	32	72	114	162	212	267	322	382
IS54 ($\mu\epsilon$)	-29	65	175	272	373	461	552	637	720	798	876

**Table F-33. Raw data, strain survey conducted after hot-wet conditioning, hot-wet environmental conditions (Run 3)
(continued)**

Load Step	0	1	2	3	4	5	6	7	8	9	10
Pressure (psi)	0.00	0.67	1.34	1.99	2.69	3.34	4.01	4.70	5.35	6.00	6.65
IS55 ($\mu\epsilon$)	-69	34	140	230	323	405	487	566	643	716	789
IS56 ($\mu\epsilon$)	72	114	158	206	259	311	370	430	495	558	623
IS57 ($\mu\epsilon$)	-115	-128	-116	-90	-55	-15	33	86	144	200	260
IS58 ($\mu\epsilon$)	-228	-259	-260	-244	-220	-188	-147	-102	-50	1	57
IS59 ($\mu\epsilon$)	1	12	43	73	104	137	173	211	253	294	338
IS60 ($\mu\epsilon$)	149	183	226	261	296	330	364	395	427	458	488
IS61 ($\mu\epsilon$)	126	169	214	251	286	317	349	378	407	435	461
IS62 ($\mu\epsilon$)	-205	-220	-208	-187	-162	-127	-88	-41	9	62	116
IS63 ($\mu\epsilon$)	-383	-417	-419	-412	-401	-382	-357	-328	-297	-263	-226
IS64 ($\mu\epsilon$)	170	221	281	334	386	435	484	529	573	616	657
IS65 ($\mu\epsilon$)	-382	-397	-371	-335	-298	-252	-202	-146	-90	-32	30
IS66 ($\mu\epsilon$)	24	131	249	356	461	558	656	748	836	920	1003
IS67 ($\mu\epsilon$)	-332	-336	-300	-254	-206	-151	-92	-27	35	101	169
IS68 ($\mu\epsilon$)	12	114	222	319	415	503	592	678	757	835	912
IS69 ($\mu\epsilon$)	33	140	236	320	403	481	563	643	715	790	861
IS70 ($\mu\epsilon$)	186	196	226	267	312	361	413	470	531	590	651
IS71 ($\mu\epsilon$)	-9	-31	-16	17	58	106	160	220	283	345	410
IS72 ($\mu\epsilon$)	-101	-120	-105	-74	-35	12	64	122	184	246	311
IS73 ($\mu\epsilon$)	-207	-114	-23	57	137	209	282	351	417	480	542
IS74 ($\mu\epsilon$)	-139	-53	33	108	184	254	325	391	454	516	575

**Table F-33. Raw data, strain survey conducted after hot-wet conditioning, hot-wet environmental conditions (Run 3)
(continued)**

Load Step	0	1	2	3	4	5	6	7	8	9	10
Pressure (psi)	0.00	0.67	1.34	1.99	2.69	3.34	4.01	4.70	5.35	6.00	6.65
IS75 ($\mu\epsilon$)	-119	-31	57	132	209	279	350	416	481	542	602
IS76 ($\mu\epsilon$)	-111	-64	-11	43	98	157	218	284	352	419	488
IS77 ($\mu\epsilon$)	-190	-183	-160	-132	-100	-63	-22	21	66	115	165
IS78 ($\mu\epsilon$)	-118	-25	69	151	233	308	384	455	524	589	653
IS79 ($\mu\epsilon$)	-165	-153	-125	-91	-55	-14	28	75	123	173	226
IS80 ($\mu\epsilon$)	-138	-26	85	184	283	375	468	555	640	720	799
IS81 ($\mu\epsilon$)	-207	-209	-190	-163	-132	-94	-53	-9	37	87	138
IS82 ($\mu\epsilon$)	-107	-5	97	188	279	365	452	534	612	688	763
IS83 ($\mu\epsilon$)	-174	-70	27	107	188	263	342	417	483	552	618
IS84 ($\mu\epsilon$)	-8	40	102	161	226	289	357	422	489	557	626
IS85 ($\mu\epsilon$)	-23	-26	3	42	98	155	221	286	354	424	495
IS86 ($\mu\epsilon$)	-26	-52	-41	-19	24	70	125	183	244	308	374
IS87 ($\mu\epsilon$)	-114	-39	20	65	116	160	205	248	291	332	375
IS88 ($\mu\epsilon$)	-51	16	80	132	187	234	283	330	376	420	464
IS89 ($\mu\epsilon$)	-40	26	89	138	192	238	286	335	380	424	469
IS90 ($\mu\epsilon$)	-39	-39	-18	7	51	99	155	213	273	336	402
IS91 ($\mu\epsilon$)	-76	-93	-96	-89	-68	-44	-13	24	65	109	157
IS92 ($\mu\epsilon$)	-62	18	92	153	217	271	327	381	433	482	532
IS93 ($\mu\epsilon$)	-62	-63	-48	-27	11	50	97	146	199	255	314
IS94 ($\mu\epsilon$)	-36	88	205	307	416	511	607	698	787	870	954

**Table F-33. Raw data, strain survey conducted after hot-wet conditioning, hot-wet environmental conditions (Run 3)
(continued)**

Load Step	0	1	2	3	4	5	6	7	8	9	10
Pressure (psi)	0.00	0.67	1.34	1.99	2.69	3.34	4.01	4.70	5.35	6.00	6.65
IS95 ($\mu\epsilon$)	-62	-59	-36	-6	40	85	137	193	251	311	373
IS96 ($\mu\epsilon$)	-38	75	179	270	369	453	540	625	707	784	861
IS97 ($\mu\epsilon$)	-96	13	107	192	280	356	434	511	586	657	729
L01 ($\mu\epsilon$)	-	-	-	-	-	-	-	-	-	-	-
L02 ($\mu\epsilon$)	-280	-228	-212	-197	-182	-169	-155	-141	-124	-111	-96
L03 ($\mu\epsilon$)	-169	-147	-136	-125	-106	-90	-72	-53	-31	-12	8
L04 ($\mu\epsilon$)	-190	-144	-115	-92	-62	-39	-14	11	37	58	81
L05 ($\mu\epsilon$)	-196	-191	-187	-185	-179	-175	-170	-162	-153	-146	-137
L06 ($\mu\epsilon$)	-223	-197	-176	-160	-146	-134	-126	-116	-110	-101	-93
L07 ($\mu\epsilon$)	-	-	-	-	-	-	-	-	-	-	-
L08 ($\mu\epsilon$)	-234	-209	-194	-177	-158	-139	-120	-100	-80	-62	-42
L09 ($\mu\epsilon$)	-161	-124	-116	-94	-74	-56	-33	-13	12	35	55
L10 ($\mu\epsilon$)	-	-	-	-	-	-	-	-	-	-	-
RAC-A1 ($\mu\epsilon$)	-93	19	132	232	337	434	535	628	719	806	892
RAC-A2 ($\mu\epsilon$)	-68	37	140	231	324	410	498	580	659	735	810
RAC-A3 ($\mu\epsilon$)	-151	-56	36	115	195	269	345	416	482	547	610
RAC-F1 ($\mu\epsilon$)	-42	70	179	278	380	473	569	658	745	828	909
RAC-F2 ($\mu\epsilon$)	-61	45	148	239	333	417	504	585	663	738	812
RBC-A1 ($\mu\epsilon$)	-223	-148	-76	-11	58	117	178	235	289	340	390
RBC-A2 ($\mu\epsilon$)	-156	-93	-31	25	84	135	187	237	284	328	372

F-300

**Table F-33. Raw data, strain survey conducted after hot-wet conditioning, hot-wet environmental conditions (Run 3)
(continued)**

Load Step	0	1	2	3	4	5	6	7	8	9	10
Pressure (psi)	0.00	0.67	1.34	1.99	2.69	3.34	4.01	4.70	5.35	6.00	6.65
RBC-A3 ($\mu\epsilon$)	-168	-105	-42	16	76	130	184	236	286	334	381
RBC-A4 ($\mu\epsilon$)	-107	-38	29	91	156	213	272	328	382	434	486
RBC-F1 ($\mu\epsilon$)	-227	-151	-80	-17	50	108	166	220	271	320	367
RBC-F2 ($\mu\epsilon$)	-190	-122	-59	-3	56	107	159	208	253	297	339
RBC-F3 ($\mu\epsilon$)	-167	-99	-37	19	78	129	181	230	277	321	365
S16 ($\mu\epsilon$)	294	307	378	442	511	576	645	714	784	852	920
S17 ($\mu\epsilon$)	-	-	-	-	-	-	-	-	-	-	-
S18 ($\mu\epsilon$)	267	322	430	520	605	680	750	835	907	975	1041
S20 ($\mu\epsilon$)	-377	-689	-928	-1131	-1333	-1496	-1654	-1791	-1914	-2020	-2115
S22 ($\mu\epsilon$)	-289	-194	-102	-29	44	108	175	237	297	354	414
S25 ($\mu\epsilon$)	168	250	386	496	617	724	839	947	1050	1147	1239
S29 ($\mu\epsilon$)	-226	-133	-47	30	111	183	259	332	404	474	544
S30 ($\mu\epsilon$)	26	155	269	367	460	543	626	707	785	861	936
S32 ($\mu\epsilon$)	-940	-999	-1045	-1085	-1128	-1160	-1193	-1221	-1246	-1267	-1288
S34 ($\mu\epsilon$)	49	123	212	295	382	461	544	623	703	780	857
S37 ($\mu\epsilon$)	263	446	600	726	847	953	1062	1164	1262	1356	1448
S41 ($\mu\epsilon$)	-	-	-	-	-	-	-	-	-	-	-
S42 ($\mu\epsilon$)	72	160	247	321	398	469	544	616	688	757	829
S43 ($\mu\epsilon$)	159	286	391	475	556	627	701	770	838	902	967
S44 ($\mu\epsilon$)	-36	124	252	356	456	542	630	711	790	864	940

F-301

**Table F-33. Raw data, strain survey conducted after hot-wet conditioning, hot-wet environmental conditions (Run 3)
(continued)**

Load Step	0	1	2	3	4	5	6	7	8	9	10
Pressure (psi)	0.00	0.67	1.34	1.99	2.69	3.34	4.01	4.70	5.35	6.00	6.65
S46 ($\mu\epsilon$)	150	-115	-380	-607	-843	-1040	-1188	-1368	-1540	-1704	-1845
S48 ($\mu\epsilon$)	-67	25	131	220	313	394	477	551	627	700	771
S51 ($\mu\epsilon$)	-25	126	257	372	486	589	696	796	895	988	1082
S55 ($\mu\epsilon$)	39	99	164	228	297	362	432	499	567	632	698
S56 ($\mu\epsilon$)	204	275	351	412	481	535	596	656	720	779	841
S57 ($\mu\epsilon$)	-	-	-	-	-	-	-	-	-	-	-
S58 ($\mu\epsilon$)	559	685	777	870	947	1028	1079	1144	1218	1288	1358
S60 ($\mu\epsilon$)	-524	-814	-1090	-1323	-1551	-1741	-1924	-2086	-2235	-2365	-2485
S62 ($\mu\epsilon$)	328	420	510	589	665	732	800	866	932	994	1055
S65 ($\mu\epsilon$)	504	649	772	882	997	1099	1205	1305	1408	1504	1600
S69 ($\mu\epsilon$)	-66	7	81	149	220	285	357	428	493	561	627
S70 ($\mu\epsilon$)	-167	-72	23	106	186	258	333	407	481	552	623
S71 ($\mu\epsilon$)	-	-	-	-	-	-	-	-	-	-	-
S72 ($\mu\epsilon$)	-36	108	235	336	432	515	600	680	757	830	903
S74 ($\mu\epsilon$)	-34	-210	-377	-532	-692	-834	-980	-1114	-1244	-1364	-1483
S76 ($\mu\epsilon$)	14	97	192	279	367	446	527	607	684	758	832
S79 ($\mu\epsilon$)	-	-	-	-	-	-	-	-	-	-	-
S83 ($\mu\epsilon$)	-140	-103	-51	0	54	109	174	235	277	333	391
S84 ($\mu\epsilon$)	45	121	202	269	344	411	485	554	623	692	761
S85 ($\mu\epsilon$)	-	-	-	-	-	-	-	-	-	-	-

**Table F-33. Raw data, strain survey conducted after hot-wet conditioning, hot-wet environmental conditions (Run 3)
(continued)**

Load Step	0	1	2	3	4	5	6	7	8	9	10
Pressure (psi)	0.00	0.67	1.34	1.99	2.69	3.34	4.01	4.70	5.35	6.00	6.65
S86 ($\mu\epsilon$)	69	218	347	448	544	625	710	785	858	930	1001
S88 ($\mu\epsilon$)	55	-61	-152	-224	-295	-349	-397	-437	-471	-496	-516
S90 ($\mu\epsilon$)	88	220	340	437	532	613	698	775	850	921	994
S93 ($\mu\epsilon$)	97	254	404	531	655	765	877	982	1083	1179	1274
S97 ($\mu\epsilon$)	132	194	262	326	395	459	527	593	659	723	789
UAC-A1 ($\mu\epsilon$)	20	142	281	401	527	637	748	852	951	1045	1136
UAC-A2 ($\mu\epsilon$)	-37	75	196	299	406	499	592	678	762	839	916
UAC-A3 ($\mu\epsilon$)	-28	74	184	277	373	456	540	619	695	767	838
UAC-F1 ($\mu\epsilon$)	-18	103	243	366	496	609	725	832	936	1032	1127
UAC-F2 ($\mu\epsilon$)	-8	98	221	325	436	533	630	721	809	891	972
UBC-A1 ($\mu\epsilon$)	-68	101	251	379	509	620	729	831	927	1015	1100
UBC-A2 ($\mu\epsilon$)	4	139	257	360	462	552	639	719	796	868	937
UBC-A3 ($\mu\epsilon$)	28	148	254	347	439	520	600	673	744	810	874
UBC-A4 ($\mu\epsilon$)	37	148	249	337	426	505	582	655	725	791	856
UBC-F1 ($\mu\epsilon$)	-77	126	273	401	529	638	746	845	938	1024	1108
UBC-F2 ($\mu\epsilon$)	-9	164	283	387	490	579	666	746	821	892	960
UBC-F3 ($\mu\epsilon$)	-9	152	262	357	452	534	615	690	761	828	893
UDAC-A1 ($\mu\epsilon$)	-54	90	225	342	466	570	677	778	874	963	1051
UDAC-A2 ($\mu\epsilon$)	-56	71	187	288	395	485	577	664	748	825	902
UDAC-A3 ($\mu\epsilon$)	-83	26	125	211	301	378	456	531	604	672	741

**Table F-33. Raw data, strain survey conducted after hot-wet conditioning, hot-wet environmental conditions (Run 3)
(continued)**

Load Step	0	1	2	3	4	5	6	7	8	9	10
Pressure (psi)	0.00	0.67	1.34	1.99	2.69	3.34	4.01	4.70	5.35	6.00	6.65
UDAC-F1 ($\mu\epsilon$)	-63	82	223	343	471	579	690	792	891	983	1073
UDAC-F2 ($\mu\epsilon$)	-62	63	184	284	393	484	577	666	749	828	905
UDBC-A1 ($\mu\epsilon$)	-46	99	243	370	494	606	718	821	917	1009	1098
UDBC-A2 ($\mu\epsilon$)	-22	104	224	328	429	520	611	695	772	846	919
UDBC-A3 ($\mu\epsilon$)	-18	100	211	306	400	483	568	647	718	789	857
UDBC-A4 ($\mu\epsilon$)	18	129	231	319	405	482	562	638	706	774	840
UDBC-F1 ($\mu\epsilon$)	-14	127	280	414	547	667	786	897	999	1097	1192
UDBC-F2 ($\mu\epsilon$)	19	138	263	371	477	571	666	753	832	908	982
UDBC-F3 ($\mu\epsilon$)	28	140	256	356	454	542	629	711	785	856	926

F.2.3.2 After 30,000 Cycles

Table F-34. Raw data, strain survey conducted after 30,000 cycles, hot-wet environmental conditions (Run 1)

Load Step	0	1	2	3	4	5	6	7	8	9	10
Pressure (psi)	-0.01	0.66	1.33	2.01	2.68	3.34	4.02	4.65	5.33	5.99	6.66
Frame-1 (lbf)	1	99	215	338	471	548	666	812	907	1002	1162
Frame-2 (lbf)	75	113	224	340	441	564	681	793	906	1021	1130
Frame-3 (lbf)	2	111	228	337	452	568	678	793	908	1019	1131
Frame-4 (lbf)	55	114	226	344	452	569	684	791	906	1020	1133
Frame-5 (lbf)	6	109	229	342	451	562	682	790	903	1029	1135
Frame-6 (lbf)	-9	118	234	343	454	562	687	786	901	1020	1134
Frame-7 (lbf)	15	121	226	338	455	568	679	795	908	1025	1132
Frame-8 (lbf)	10	109	223	334	459	568	676	797	909	1019	1129
Frame-9 (lbf)	51	112	224	336	453	566	680	792	907	1019	1134
Frame-10 (lbf)	1	113	223	342	444	571	681	797	909	1018	1132
Frame-11 (lbf)	2	111	229	344	458	569	677	790	903	1018	1134
Frame-12 (lbf)	25	111	226	345	455	566	682	793	908	1017	1137
Hoop-1 (lbf)	70	730	1436	2146	2844	3571	4287	4994	5719	6431	7144
Hoop-2 (lbf)	179	680	1457	2152	2846	3586	4289	5005	5702	6415	7147
Hoop-3 (lbf)	79	727	1444	2147	2863	3579	4293	4990	5699	6432	7122
Hoop-4 (lbf)	53	740	1421	2137	2853	3569	4299	5013	5720	6426	7131
Hoop-5 (lbf)	109	697	1413	2150	2860	3576	4281	4989	5713	6429	7135
Hoop-6 (lbf)	54	714	1435	2155	2850	3562	4283	4983	5707	6415	7148
Hoop-7 (lbf)	0	705	1419	2143	2856	3567	4290	4997	5720	6437	7140
Hoop-8 (lbf)	171	716	1436	2144	2856	3572	4292	4995	5712	6430	7138

Table F-34. Raw data, strain survey conducted after 30,000 cycles, hot-wet environmental conditions (Run 1) (continued)

Load Step	0	1	2	3	4	5	6	7	8	9	10
Pressure (psi)	-0.01	0.66	1.33	2.01	2.68	3.34	4.02	4.65	5.33	5.99	6.66
Hoop-9 (lbf)	56	736	1412	2149	2858	3569	4280	4993	5711	6424	7142
Hoop-10 (lbf)	22	710	1428	2136	2844	3584	4290	4998	5714	6417	7137
Hoop-11 (lbf)	93	725	1432	2135	2866	3580	4308	5013	5725	6448	7150
Hoop-12 (lbf)	173	702	1429	2133	2861	3562	4281	4994	5718	6417	7120
Hoop-13 (lbf)	70	710	1448	2151	2861	3566	4279	4987	5706	6424	7144
Hoop-14 (lbf)	-4	709	1418	2143	2857	3569	4293	4990	5703	6434	7135
Long-1 (lbf)	-32	627	1341	2001	2668	3352	3981	4674	5345	6009	6648
Long-2 (lbf)	14	669	1336	1983	2664	3334	4000	4677	5350	6008	6675
Long-3 (lbf)	3	673	1340	1986	2662	3339	4017	4666	5346	6009	6670
Long-4 (lbf)	23	694	1331	2008	2663	3340	4002	4672	5341	6005	6677
Long-5 (lbf)	1	677	1343	1999	2662	3333	4000	4673	5336	6012	6686
Long-6 (lbf)	26	636	1337	2004	2654	3343	4006	4668	5327	6012	6673
Long-7 (lbf)	-3	665	1324	1995	2678	3342	4000	4673	5336	5994	6635
Long-8 (lbf)	2	691	1324	2010	2677	3355	4000	4673	5334	6040	6707
F01 ($\mu\epsilon$)	-405	-422	-368	-330	-281	-227	-183	-134	-93	-43	5
F02 ($\mu\epsilon$)	352	443	484	532	577	619	671	715	761	812	861
F03 ($\mu\epsilon$)	-459	-521	-467	-421	-381	-341	-304	-261	-221	-180	-135
F04 ($\mu\epsilon$)	498	590	629	680	734	787	848	898	956	1015	1069
F05 ($\mu\epsilon$)	-	-	-	-	-	-	-	-	-	-	-
F06 ($\mu\epsilon$)	487	598	631	672	717	763	814	853	902	953	1005
F07 ($\mu\epsilon$)	-246	-319	-266	-218	-183	-138	-96	-53	-16	26	68

Table F-34. Raw data, strain survey conducted after 30,000 cycles, hot-wet environmental conditions (Run 1) (continued)

Load Step	0	1	2	3	4	5	6	7	8	9	10
Pressure (psi)	-0.01	0.66	1.33	2.01	2.68	3.34	4.02	4.65	5.33	5.99	6.66
F08 ($\mu\epsilon$)	248	369	401	448	494	542	592	636	685	738	786
IS16 ($\mu\epsilon$)	73	76	156	226	296	367	437	509	582	655	731
IS17 ($\mu\epsilon$)	-70	-94	-57	-17	32	86	143	204	268	333	402
IS18 ($\mu\epsilon$)	-213	-238	-219	-191	-153	-107	-55	1	62	125	193
IS19 ($\mu\epsilon$)	50	64	85	96	109	124	140	159	180	203	230
IS20 ($\mu\epsilon$)	206	220	267	303	337	370	404	438	471	505	541
IS21 ($\mu\epsilon$)	177	196	243	278	312	345	379	412	446	480	515
IS22 ($\mu\epsilon$)	-282	-309	-295	-276	-246	-207	-161	-110	-54	6	69
IS23 ($\mu\epsilon$)	-381	-385	-389	-383	-365	-341	-310	-272	-228	-181	-128
IS24 ($\mu\epsilon$)	219	256	319	366	411	453	494	534	573	611	650
IS25 ($\mu\epsilon$)	-387	-371	-352	-325	-286	-244	-195	-140	-81	-20	46
IS26 ($\mu\epsilon$)	89	197	320	427	530	624	714	801	885	965	1044
IS27 ($\mu\epsilon$)	-379	-349	-310	-263	-208	-150	-87	-20	51	121	197
IS28 ($\mu\epsilon$)	70	174	289	393	492	584	674	759	843	922	1002
IS29 ($\mu\epsilon$)	109	181	281	370	457	538	620	699	777	853	931
IS30 ($\mu\epsilon$)	-266	-294	-256	-218	-173	-121	-65	-5	57	122	191
IS31 ($\mu\epsilon$)	0	33	96	153	212	269	327	383	439	495	552
IS32 ($\mu\epsilon$)	-102	-75	-22	22	66	108	148	187	224	262	298
IS33 ($\mu\epsilon$)	-95	-62	-5	42	88	132	175	216	254	293	332
IS34 ($\mu\epsilon$)	-359	-348	-310	-274	-234	-188	-137	-85	-30	29	90
IS35 ($\mu\epsilon$)	-569	-621	-638	-638	-623	-600	-569	-533	-492	-447	-397

Table F-34. Raw data, strain survey conducted after 30,000 cycles, hot-wet environmental conditions (Run 1) (continued)

Load Step	0	1	2	3	4	5	6	7	8	9	10
Pressure (psi)	-0.01	0.66	1.33	2.01	2.68	3.34	4.02	4.65	5.33	5.99	6.66
IS36 ($\mu\epsilon$)	-96	-66	-10	37	83	127	170	211	250	289	327
IS37 ($\mu\epsilon$)	-520	-572	-585	-580	-559	-529	-492	-447	-400	-346	-288
IS38 ($\mu\epsilon$)	-165	-117	-48	13	74	132	189	244	297	349	400
IS39 ($\mu\epsilon$)	-506	-547	-546	-527	-492	-450	-399	-343	-282	-218	-150
IS40 ($\mu\epsilon$)	-161	-103	-29	39	106	170	233	294	353	411	469
IS41 ($\mu\epsilon$)	22	97	185	265	343	418	491	562	631	699	766
IS42 ($\mu\epsilon$)	114	119	175	233	294	356	419	481	546	612	679
IS43 ($\mu\epsilon$)	5	-26	10	55	108	166	229	293	360	429	501
IS44 ($\mu\epsilon$)	57	-14	-12	7	37	77	124	174	230	288	349
IS45 ($\mu\epsilon$)	-13	26	101	168	230	291	349	405	461	515	570
IS46 ($\mu\epsilon$)	-25	19	93	158	219	276	332	384	436	486	536
IS47 ($\mu\epsilon$)	-13	33	107	172	233	291	348	401	454	506	557
IS48 ($\mu\epsilon$)	-65	-77	-40	-3	40	89	142	198	259	323	388
IS49 ($\mu\epsilon$)	-52	-97	-97	-86	-68	-43	-15	18	55	94	138
IS50 ($\mu\epsilon$)	-20	36	122	199	270	338	404	465	525	583	641
IS51 ($\mu\epsilon$)	-36	-71	-60	-38	-9	25	63	102	146	192	241
IS52 ($\mu\epsilon$)	-23	65	184	294	398	496	591	680	768	852	935
IS53 ($\mu\epsilon$)	-9	-46	-29	2	41	86	133	184	239	295	355
IS54 ($\mu\epsilon$)	-25	57	169	271	367	459	548	631	714	793	871
IS55 ($\mu\epsilon$)	-50	29	136	230	318	402	482	558	634	708	781
IS56 ($\mu\epsilon$)	78	83	122	162	207	257	311	367	426	486	550

Table F-34. Raw data, strain survey conducted after 30,000 cycles, hot-wet environmental conditions (Run 1) (continued)

Load Step	0	1	2	3	4	5	6	7	8	9	10
Pressure (psi)	-0.01	0.66	1.33	2.01	2.68	3.34	4.02	4.65	5.33	5.99	6.66
IS57 ($\mu\epsilon$)	-139	-169	-158	-137	-106	-67	-21	30	83	139	200
IS58 ($\mu\epsilon$)	-260	-296	-294	-281	-257	-224	-183	-137	-87	-33	27
IS59 ($\mu\epsilon$)	71	62	85	97	108	119	132	146	160	177	196
IS60 ($\mu\epsilon$)	198	200	243	274	303	333	363	394	424	456	489
IS61 ($\mu\epsilon$)	220	227	274	309	341	372	404	436	468	500	535
IS62 ($\mu\epsilon$)	-268	-295	-273	-253	-225	-190	-147	-99	-48	6	68
IS63 ($\mu\epsilon$)	-426	-450	-449	-443	-430	-411	-386	-355	-320	-280	-234
IS64 ($\mu\epsilon$)	217	240	294	334	371	406	441	475	508	541	574
IS65 ($\mu\epsilon$)	-479	-476	-440	-402	-357	-310	-257	-200	-140	-78	-11
IS66 ($\mu\epsilon$)	0	99	219	325	425	517	605	689	769	846	922
IS67 ($\mu\epsilon$)	-457	-441	-386	-331	-271	-209	-142	-73	-3	69	145
IS68 ($\mu\epsilon$)	-19	86	204	312	415	511	605	694	781	864	947
IS69 ($\mu\epsilon$)	53	139	240	326	411	491	573	649	723	799	873
IS70 ($\mu\epsilon$)	161	130	162	198	240	287	340	396	453	510	573
IS71 ($\mu\epsilon$)	-42	-78	-53	-20	23	73	129	188	249	311	378
IS72 ($\mu\epsilon$)	-147	-165	-138	-104	-61	-12	43	102	162	224	292
IS73 ($\mu\epsilon$)	-177	-99	-8	70	145	214	281	344	405	463	521
IS74 ($\mu\epsilon$)	-129	-63	21	93	163	228	292	352	410	466	521
IS75 ($\mu\epsilon$)	-96	-28	56	130	200	265	329	390	449	505	561
IS76 ($\mu\epsilon$)	-154	-105	-43	14	73	134	199	265	333	400	473
IS77 ($\mu\epsilon$)	-257	-233	-199	-166	-129	-92	-51	-7	38	85	136

Table F-34. Raw data, strain survey conducted after 30,000 cycles, hot-wet environmental conditions (Run 1) (continued)

Load Step	0	1	2	3	4	5	6	7	8	9	10
Pressure (psi)	-0.01	0.66	1.33	2.01	2.68	3.34	4.02	4.65	5.33	5.99	6.66
IS78 ($\mu\epsilon$)	-114	-37	54	134	211	282	352	418	482	543	604
IS79 ($\mu\epsilon$)	-260	-227	-187	-149	-108	-67	-22	24	72	120	174
IS80 ($\mu\epsilon$)	-153	-47	67	171	271	364	456	542	626	708	788
IS81 ($\mu\epsilon$)	-313	-291	-258	-225	-188	-150	-108	-63	-17	30	82
IS82 ($\mu\epsilon$)	-136	-39	67	162	254	340	425	506	584	661	737
IS83 ($\mu\epsilon$)	-184	-102	-1	85	166	243	319	392	460	529	598
IS84 ($\mu\epsilon$)	-23	-6	61	122	184	249	314	377	443	510	578
IS85 ($\mu\epsilon$)	-48	-77	-46	-5	45	104	166	230	296	365	435
IS86 ($\mu\epsilon$)	-53	-97	-90	-67	-31	15	67	122	181	243	309
IS87 ($\mu\epsilon$)	-68	-24	25	68	109	150	190	228	267	305	344
IS88 ($\mu\epsilon$)	-47	-6	45	87	127	167	204	239	274	308	343
IS89 ($\mu\epsilon$)	-45	-4	47	89	129	168	206	242	278	313	350
IS90 ($\mu\epsilon$)	-58	-70	-49	-20	20	69	124	180	239	301	366
IS91 ($\mu\epsilon$)	-89	-112	-122	-119	-105	-82	-54	-21	16	57	103
IS92 ($\mu\epsilon$)	-53	8	73	129	181	232	280	324	368	410	452
IS93 ($\mu\epsilon$)	-86	-87	-75	-51	-18	24	69	118	169	225	284
IS94 ($\mu\epsilon$)	-27	96	219	330	436	537	634	724	814	900	984
IS95 ($\mu\epsilon$)	-96	-94	-72	-40	0	49	100	154	210	270	333
IS96 ($\mu\epsilon$)	-36	70	177	274	367	456	543	625	705	783	861
IS97 ($\mu\epsilon$)	-78	10	106	192	274	355	432	506	580	651	723
L01 ($\mu\epsilon$)	-	-	-	-	-	-	-	-	-	-	-

Table F-34. Raw data, strain survey conducted after 30,000 cycles, hot-wet environmental conditions (Run 1) (continued)

Load Step	0	1	2	3	4	5	6	7	8	9	10
Pressure (psi)	-0.01	0.66	1.33	2.01	2.68	3.34	4.02	4.65	5.33	5.99	6.66
L02 ($\mu\epsilon$)	-321	-225	-217	-203	-186	-173	-158	-143	-127	-113	-96
L03 ($\mu\epsilon$)	-208	-130	-129	-115	-98	-81	-63	-43	-23	-2	19
L04 ($\mu\epsilon$)	-224	-130	-112	-87	-60	-36	-11	13	36	59	81
L05 ($\mu\epsilon$)	-215	-177	-182	-177	-170	-163	-155	-146	-137	-127	-118
L06 ($\mu\epsilon$)	-256	-190	-172	-154	-137	-123	-113	-103	-96	-91	-84
L07 ($\mu\epsilon$)	-	-	-	-	-	-	-	-	-	-	-
L08 ($\mu\epsilon$)	-264	-192	-191	-175	-156	-138	-119	-99	-80	-60	-41
L09 ($\mu\epsilon$)	-184	-112	-112	-100	-82	-61	-41	-22	-3	18	39
L10 ($\mu\epsilon$)	-	-	-	-	-	-	-	-	-	-	-
RAC-A1 ($\mu\epsilon$)	-125	-19	102	213	322	424	526	622	717	808	898
RAC-A2 ($\mu\epsilon$)	-94	2	110	207	302	390	477	559	640	718	795
RAC-A3 ($\mu\epsilon$)	-167	-83	13	96	177	252	326	396	463	529	594
RAC-F1 ($\mu\epsilon$)	-62	43	160	266	370	467	562	653	742	828	913
RAC-F2 ($\mu\epsilon$)	-77	22	130	226	319	406	491	571	650	726	801
RBC-A1 ($\mu\epsilon$)	-269	-205	-125	-55	14	78	140	197	253	307	360
RBC-A2 ($\mu\epsilon$)	-188	-137	-69	-9	49	103	155	204	252	297	341
RBC-A3 ($\mu\epsilon$)	-194	-141	-73	-12	47	102	156	206	255	302	349
RBC-A4 ($\mu\epsilon$)	-121	-61	11	76	139	198	256	310	364	415	466
RBC-F1 ($\mu\epsilon$)	-261	-194	-117	-49	17	78	137	191	243	294	342
RBC-F2 ($\mu\epsilon$)	-215	-158	-90	-31	27	81	132	180	225	269	311
RBC-F3 ($\mu\epsilon$)	-188	-130	-64	-5	52	105	156	203	249	293	335

Table F-34. Raw data, strain survey conducted after 30,000 cycles, hot-wet environmental conditions (Run 1) (continued)

Load Step	0	1	2	3	4	5	6	7	8	9	10
Pressure (psi)	-0.01	0.66	1.33	2.01	2.68	3.34	4.02	4.65	5.33	5.99	6.66
S16 ($\mu\epsilon$)	-144	-130	-99	-76	-54	-35	-16	2	30	47	65
S17 ($\mu\epsilon$)	-	-	-	-	-	-	-	-	-	-	-
S18 ($\mu\epsilon$)	239	-162	-13	100	188	282	361	432	498	576	647
S20 ($\mu\epsilon$)	-	-	-	-	-	-	-	-	-	-	-
S22 ($\mu\epsilon$)	131	203	312	396	473	558	634	705	780	842	914
S25 ($\mu\epsilon$)	552	622	765	882	999	1105	1207	1304	1398	1491	1576
S29 ($\mu\epsilon$)	-190	-82	4	85	163	237	311	381	452	522	592
S30 ($\mu\epsilon$)	-271	-193	-99	-26	42	104	163	219	273	327	379
S32 ($\mu\epsilon$)	-1456	-1504	-1557	-1595	-1652	-1697	-1746	-1776	-1811	-1826	-1837
S34 ($\mu\epsilon$)	-	-	-	-	-	-	-	-	-	-	-
S37 ($\mu\epsilon$)	347	477	635	761	873	978	1077	1169	1259	1347	1433
S41 ($\mu\epsilon$)	-207	-85	10	98	183	263	340	413	486	557	628
S42 ($\mu\epsilon$)	-	-	-	-	-	-	-	-	-	-	-
S43 ($\mu\epsilon$)	128	212	300	371	434	493	551	604	658	705	756
S44 ($\mu\epsilon$)	-	-	-	-	-	-	-	-	-	-	-
S46 ($\mu\epsilon$)	273	35	-211	-424	-617	-787	-945	-1082	-1211	-1334	-1452
S48 ($\mu\epsilon$)	-163	-101	3	93	178	259	334	403	473	543	611
S51 ($\mu\epsilon$)	12	119	253	370	478	581	681	773	865	954	1042
S55 ($\mu\epsilon$)	-9	50	112	176	241	306	372	435	499	563	627
S56 ($\mu\epsilon$)	142	183	258	320	380	437	495	553	612	667	725
S57 ($\mu\epsilon$)	-	-	-	-	-	-	-	-	-	-	-

Table F-34. Raw data, strain survey conducted after 30,000 cycles, hot-wet environmental conditions (Run 1) (continued)

Load Step	0	1	2	3	4	5	6	7	8	9	10
Pressure (psi)	-0.01	0.66	1.33	2.01	2.68	3.34	4.02	4.65	5.33	5.99	6.66
S58 ($\mu\epsilon$)	522	591	700	784	858	927	995	1059	1123	1183	1245
S60 ($\mu\epsilon$)	-1001	-1121	-1211	-1361	-1480	-1585	-1677	-1770	-1838	-1910	-1947
S62 ($\mu\epsilon$)	434	480	567	640	706	770	834	895	956	1014	1076
S65 ($\mu\epsilon$)	526	629	742	840	933	1018	1101	1177	1249	1318	1385
S69 ($\mu\epsilon$)	79	118	161	200	237	274	309	342	374	404	428
S70 ($\mu\epsilon$)	-80	5	98	178	254	324	394	465	531	600	672
S71 ($\mu\epsilon$)	-	-	-	-	-	-	-	-	-	-	-
S72 ($\mu\epsilon$)	35	128	245	341	426	508	586	658	730	800	871
S74 ($\mu\epsilon$)	-859	-991	-1163	-1301	-1430	-1550	-1660	-1781	-1893	-1987	-2091
S76 ($\mu\epsilon$)	-119	-89	1	82	159	235	310	380	452	522	595
S79 ($\mu\epsilon$)	-110	-48	62	159	252	344	437	521	607	692	775
S83 ($\mu\epsilon$)	55	74	131	185	243	306	363	422	476	539	592
S84 ($\mu\epsilon$)	107	168	255	333	408	483	559	633	707	780	853
S85 ($\mu\epsilon$)	-	-	-	-	-	-	-	-	-	-	-
S86 ($\mu\epsilon$)	78	86	128	175	206	214	211	213	238	251	251
S88 ($\mu\epsilon$)	18	-134	-239	-328	-405	-467	-518	-559	-592	-619	-639
S90 ($\mu\epsilon$)	-130	-31	91	193	282	365	445	520	596	665	736
S93 ($\mu\epsilon$)	566	690	850	983	1105	1220	1330	1433	1534	1631	1724
S97 ($\mu\epsilon$)	107	166	233	298	363	427	491	554	619	680	741
UAC-A1 ($\mu\epsilon$)	12	123	269	401	525	642	753	856	958	1055	1148
UAC-A2 ($\mu\epsilon$)	-9	80	201	308	406	498	586	666	745	820	893

Table F-34. Raw data, strain survey conducted after 30,000 cycles, hot-wet environmental conditions (Run 1) (continued)

Load Step	0	1	2	3	4	5	6	7	8	9	10
Pressure (psi)	-0.01	0.66	1.33	2.01	2.68	3.34	4.02	4.65	5.33	5.99	6.66
UAC-A3 ($\mu\epsilon$)	-23	64	174	272	363	449	531	607	682	754	825
UAC-F1 ($\mu\epsilon$)	-20	97	245	383	512	635	752	860	967	1068	1166
UAC-F2 ($\mu\epsilon$)	-5	93	220	335	443	544	641	731	820	904	985
UBC-A1 ($\mu\epsilon$)	-	-	-	-	-	-	-	-	-	-	-
UBC-A2 ($\mu\epsilon$)	-24	95	227	346	459	560	657	747	834	915	994
UBC-A3 ($\mu\epsilon$)	15	118	233	335	431	518	601	680	756	827	898
UBC-A4 ($\mu\epsilon$)	45	138	243	337	426	507	587	662	737	808	879
UBC-F1 ($\mu\epsilon$)	-	-	-	-	-	-	-	-	-	-	-
UBC-F2 ($\mu\epsilon$)	-31	130	265	384	497	600	697	786	871	953	1030
UBC-F3 ($\mu\epsilon$)	-25	128	246	351	449	539	625	704	780	853	923
UDAC-A1 ($\mu\epsilon$)	-48	100	245	375	497	613	722	823	922	1016	1108
UDAC-A2 ($\mu\epsilon$)	-51	74	197	306	408	506	599	684	767	847	926
UDAC-A3 ($\mu\epsilon$)	-69	31	132	220	305	386	464	536	608	676	745
UDAC-F1 ($\mu\epsilon$)	-50	98	245	377	501	618	729	830	931	1026	1118
UDAC-F2 ($\mu\epsilon$)	-51	72	194	304	407	505	598	683	767	847	926
UDBC-A1 ($\mu\epsilon$)	-	-	-	-	-	-	-	-	-	-	-
UDBC-A2 ($\mu\epsilon$)	-97	23	161	286	405	515	620	718	811	899	983
UDBC-A3 ($\mu\epsilon$)	-69	44	166	274	376	469	558	641	721	797	870
UDBC-A4 ($\mu\epsilon$)	-1	103	213	308	399	484	566	643	717	791	862
UDBC-F1 ($\mu\epsilon$)	-	-	-	-	-	-	-	-	-	-	-
UDBC-F2 ($\mu\epsilon$)	-59	47	194	329	456	572	684	787	885	977	1066

Table F-34. Raw data, strain survey conducted after 30,000 cycles, hot-wet environmental conditions (Run 1) (continued)

Load Step	0	1	2	3	4	5	6	7	8	9	10
Pressure (psi)	-0.01	0.66	1.33	2.01	2.68	3.34	4.02	4.65	5.33	5.99	6.66
UDBC-F3 ($\mu\epsilon$)	-9	90	216	329	436	532	625	711	793	870	945

Table F-35. Raw data, strain survey conducted after 30,000 cycles, hot-wet environmental conditions (Run 2)

Load Step	0	1	2	3	4	5	6	7	8	9	10
Pressure (psi)	-0.11	0.67	1.33	2.00	2.66	3.34	4.02	4.66	5.36	6.01	6.67
Frame-1 (lbf)	4	71	213	362	449	545	635	782	927	1035	1124
Frame-2 (lbf)	72	62	227	339	453	568	680	792	906	1021	1132
Frame-3 (lbf)	3	111	235	334	455	565	679	794	905	1020	1135
Frame-4 (lbf)	55	82	231	340	452	568	683	793	907	1021	1131
Frame-5 (lbf)	1	121	225	350	452	568	679	796	912	1019	1133
Frame-6 (lbf)	-11	112	226	334	451	559	675	791	910	1019	1129
Frame-7 (lbf)	16	114	227	334	449	570	678	795	907	1019	1134
Frame-8 (lbf)	18	121	230	337	456	567	689	797	906	1020	1135
Frame-9 (lbf)	50	112	230	335	453	567	678	792	907	1017	1134
Frame-10 (lbf)	1	108	224	344	453	567	681	794	892	1019	1133
Frame-11 (lbf)	-5	116	225	338	453	569	678	797	905	1022	1137
Frame-12 (lbf)	28	31	221	343	457	567	677	793	906	1019	1134
Hoop-1 (lbf)	64	711	1427	2131	2868	3578	4300	4996	5710	6416	7149
Hoop-2 (lbf)	166	698	1437	2170	2884	3550	4289	4994	5701	6406	7131
Hoop-3 (lbf)	76	703	1434	2131	2854	3571	4296	4998	5730	6429	7132
Hoop-4 (lbf)	30	736	1429	2131	2842	3577	4285	4986	5741	6417	7134
Hoop-5 (lbf)	105	713	1415	2129	2854	3576	4294	5001	5725	6422	7151
Hoop-6 (lbf)	56	712	1419	2157	2844	3572	4281	4984	5729	6423	7143
Hoop-7 (lbf)	39	706	1426	2140	2853	3571	4288	5001	5715	6427	7140
Hoop-8 (lbf)	157	711	1423	2145	2860	3577	4285	4992	5722	6426	7142
Hoop-9 (lbf)	27	672	1420	2132	2849	3577	4287	4995	5730	6425	7144

Table F-35. Raw data, strain survey conducted after 30,000 cycles, hot-wet environmental conditions (Run 2) (continued)

Load Step	0	1	2	3	4	5	6	7	8	9	10
Pressure (psi)	-0.11	0.67	1.33	2.00	2.66	3.34	4.02	4.66	5.36	6.01	6.67
Hoop-10 (lbf)	-2	707	1421	2129	2853	3567	4286	4992	5731	6428	7146
Hoop-11 (lbf)	58	724	1450	2147	2845	3561	4301	5010	5721	6419	7126
Hoop-12 (lbf)	157	727	1437	2142	2848	3564	4282	4999	5720	6428	7129
Hoop-13 (lbf)	94	710	1432	2125	2857	3559	4279	4992	5719	6417	7143
Hoop-14 (lbf)	2	711	1413	2147	2855	3568	4296	4993	5735	6424	7138
Long-1 (lbf)	-21	667	1303	1993	2655	3345	3988	4671	5349	6010	6605
Long-2 (lbf)	12	673	1345	2012	2669	3341	4007	4674	5333	6001	6702
Long-3 (lbf)	-2	674	1333	2018	2673	3335	4007	4677	5333	6010	6684
Long-4 (lbf)	-10	664	1340	2009	2670	3336	4002	4675	5343	6009	6677
Long-5 (lbf)	18	664	1343	2009	2671	3339	4008	4671	5339	6010	6680
Long-6 (lbf)	-28	639	1342	2025	2672	3338	4005	4676	5323	6038	6674
Long-7 (lbf)	5	654	1345	2006	2663	3337	4012	4667	5333	6010	6670
Long-8 (lbf)	8	686	1341	1996	2672	3315	3983	4665	5342	5960	6649
F01 ($\mu\epsilon$)	-351	-408	-358	-312	-264	-209	-166	-117	-75	-37	12
F02 ($\mu\epsilon$)	309	444	475	527	564	608	659	702	761	805	854
F03 ($\mu\epsilon$)	-368	-525	-447	-410	-367	-325	-287	-242	-206	-166	-124
F04 ($\mu\epsilon$)	435	577	614	670	717	773	830	880	949	1001	1056
F05 ($\mu\epsilon$)	-	-	-	-	-	-	-	-	-	-	-
F06 ($\mu\epsilon$)	435	598	613	667	704	749	795	837	893	940	993
F07 ($\mu\epsilon$)	-211	-339	-260	-221	-177	-135	-94	-51	-17	22	62
F08 ($\mu\epsilon$)	234	364	399	448	492	540	589	633	689	737	787

Table F-35. Raw data, strain survey conducted after 30,000 cycles, hot-wet environmental conditions (Run 2) (continued)

Load Step	0	1	2	3	4	5	6	7	8	9	10
Pressure (psi)	-0.11	0.67	1.33	2.00	2.66	3.34	4.02	4.66	5.36	6.01	6.67
IS16 ($\mu\epsilon$)	36	71	148	219	288	360	433	504	581	652	728
IS17 ($\mu\epsilon$)	-96	-96	-63	-22	27	81	140	200	267	331	399
IS18 ($\mu\epsilon$)	-229	-235	-220	-193	-154	-109	-56	0	64	125	192
IS19 ($\mu\epsilon$)	15	56	73	85	99	114	131	151	174	196	224
IS20 ($\mu\epsilon$)	177	211	257	292	327	361	396	430	466	500	536
IS21 ($\mu\epsilon$)	150	187	232	267	303	337	371	405	441	474	510
IS22 ($\mu\epsilon$)	-279	-306	-294	-277	-246	-208	-161	-110	-51	6	70
IS23 ($\mu\epsilon$)	-395	-381	-389	-383	-365	-341	-308	-270	-225	-179	-126
IS24 ($\mu\epsilon$)	186	249	308	355	401	444	487	526	568	605	644
IS25 ($\mu\epsilon$)	-403	-363	-349	-322	-284	-241	-190	-136	-76	-17	48
IS26 ($\mu\epsilon$)	50	201	317	425	528	623	716	802	889	967	1046
IS27 ($\mu\epsilon$)	-396	-341	-306	-260	-205	-146	-81	-16	57	126	200
IS28 ($\mu\epsilon$)	32	176	285	390	490	583	674	759	847	924	1004
IS29 ($\mu\epsilon$)	70	179	275	363	451	535	618	697	780	854	931
IS30 ($\mu\epsilon$)	-266	-295	-258	-220	-175	-123	-67	-8	59	122	190
IS31 ($\mu\epsilon$)	-34	25	85	142	202	260	319	375	436	490	546
IS32 ($\mu\epsilon$)	-120	-75	-25	19	64	106	147	186	227	262	299
IS33 ($\mu\epsilon$)	-115	-62	-8	39	87	130	173	214	257	293	332
IS34 ($\mu\epsilon$)	-368	-349	-311	-277	-235	-189	-139	-86	-27	28	89
IS35 ($\mu\epsilon$)	-565	-619	-638	-638	-622	-599	-568	-531	-486	-442	-393
IS36 ($\mu\epsilon$)	-114	-65	-12	34	82	126	170	211	253	290	328

Table F-35. Raw data, strain survey conducted after 30,000 cycles, hot-wet environmental conditions (Run 2) (continued)

Load Step	0	1	2	3	4	5	6	7	8	9	10
Pressure (psi)	-0.11	0.67	1.33	2.00	2.66	3.34	4.02	4.66	5.36	6.01	6.67
IS37 ($\mu\epsilon$)	-509	-567	-582	-577	-555	-526	-488	-444	-393	-342	-284
IS38 ($\mu\epsilon$)	-182	-112	-47	14	76	134	192	247	304	353	404
IS39 ($\mu\epsilon$)	-496	-544	-544	-524	-489	-446	-395	-338	-274	-212	-145
IS40 ($\mu\epsilon$)	-179	-98	-28	40	108	172	236	297	360	416	473
IS41 ($\mu\epsilon$)	-3	99	183	262	342	417	491	561	635	700	768
IS42 ($\mu\epsilon$)	89	109	167	225	286	350	415	479	548	612	679
IS43 ($\mu\epsilon$)	-4	-28	7	52	106	165	229	293	364	433	504
IS44 ($\mu\epsilon$)	58	-15	-15	3	35	75	123	173	231	288	350
IS45 ($\mu\epsilon$)	-45	21	92	159	223	284	344	400	459	513	568
IS46 ($\mu\epsilon$)	-49	19	90	155	216	275	332	384	439	488	538
IS47 ($\mu\epsilon$)	-37	33	105	169	231	290	347	401	457	508	559
IS48 ($\mu\epsilon$)	-76	-77	-43	-6	37	87	142	199	262	324	389
IS49 ($\mu\epsilon$)	-55	-92	-96	-85	-66	-42	-12	21	59	99	142
IS50 ($\mu\epsilon$)	-45	38	121	197	270	338	405	466	530	587	644
IS51 ($\mu\epsilon$)	-46	-67	-60	-38	-8	25	64	104	150	196	245
IS52 ($\mu\epsilon$)	-53	71	186	295	399	498	594	683	774	857	940
IS53 ($\mu\epsilon$)	-21	-43	-29	2	42	85	135	186	242	298	358
IS54 ($\mu\epsilon$)	-56	62	168	270	367	459	549	632	718	796	874
IS55 ($\mu\epsilon$)	-85	32	133	227	316	400	482	559	638	710	784
IS56 ($\mu\epsilon$)	42	77	115	157	202	253	308	363	425	485	550
IS57 ($\mu\epsilon$)	-152	-171	-162	-141	-109	-70	-24	26	82	138	199

Table F-35. Raw data, strain survey conducted after 30,000 cycles, hot-wet environmental conditions (Run 2) (continued)

Load Step	0	1	2	3	4	5	6	7	8	9	10
Pressure (psi)	-0.11	0.67	1.33	2.00	2.66	3.34	4.02	4.66	5.36	6.01	6.67
IS58 ($\mu\epsilon$)	-260	-294	-294	-282	-257	-224	-183	-138	-84	-31	28
IS59 ($\mu\epsilon$)	51	56	76	87	98	109	122	135	152	168	187
IS60 ($\mu\epsilon$)	175	195	237	267	298	328	358	389	422	453	486
IS61 ($\mu\epsilon$)	197	221	267	301	334	366	399	430	465	496	531
IS62 ($\mu\epsilon$)	-264	-294	-273	-254	-225	-190	-148	-101	-45	8	69
IS63 ($\mu\epsilon$)	-412	-444	-445	-442	-428	-409	-383	-352	-315	-275	-229
IS64 ($\mu\epsilon$)	192	234	286	325	363	399	434	468	503	535	568
IS65 ($\mu\epsilon$)	-460	-463	-430	-395	-351	-303	-250	-194	-131	-69	-4
IS66 ($\mu\epsilon$)	-21	103	219	324	423	517	606	689	773	849	924
IS67 ($\mu\epsilon$)	-436	-424	-374	-321	-262	-199	-133	-65	8	80	154
IS68 ($\mu\epsilon$)	-32	92	206	313	415	513	607	696	787	869	951
IS69 ($\mu\epsilon$)	29	143	237	325	410	491	572	649	730	803	876
IS70 ($\mu\epsilon$)	138	121	154	191	234	283	337	391	451	509	571
IS71 ($\mu\epsilon$)	-44	-80	-57	-24	20	70	127	184	249	311	377
IS72 ($\mu\epsilon$)	-139	-161	-137	-104	-60	-11	44	101	166	227	294
IS73 ($\mu\epsilon$)	-189	-93	-7	71	145	215	282	345	410	467	524
IS74 ($\mu\epsilon$)	-143	-60	21	94	163	229	293	352	414	468	523
IS75 ($\mu\epsilon$)	-110	-25	57	130	200	266	331	390	453	508	564
IS76 ($\mu\epsilon$)	-159	-101	-42	13	73	134	200	265	336	404	475
IS77 ($\mu\epsilon$)	-241	-221	-194	-163	-127	-89	-48	-5	43	89	140
IS78 ($\mu\epsilon$)	-128	-33	55	135	211	283	354	419	486	546	606

Table F-35. Raw data, strain survey conducted after 30,000 cycles, hot-wet environmental conditions (Run 2) (continued)

Load Step	0	1	2	3	4	5	6	7	8	9	10
Pressure (psi)	-0.11	0.67	1.33	2.00	2.66	3.34	4.02	4.66	5.36	6.01	6.67
IS79 ($\mu\epsilon$)	-241	-213	-180	-144	-104	-63	-19	27	77	126	178
IS80 ($\mu\epsilon$)	-165	-38	72	175	273	368	459	545	634	714	793
IS81 ($\mu\epsilon$)	-293	-278	-252	-221	-185	-147	-105	-60	-11	36	87
IS82 ($\mu\epsilon$)	-146	-30	71	165	256	343	428	508	591	666	741
IS83 ($\mu\epsilon$)	-199	-93	4	89	169	247	322	394	469	536	603
IS84 ($\mu\epsilon$)	-36	-8	58	118	182	246	312	377	447	510	579
IS85 ($\mu\epsilon$)	-54	-78	-49	-9	44	101	164	229	299	365	436
IS86 ($\mu\epsilon$)	-54	-95	-92	-69	-31	14	66	122	185	245	311
IS87 ($\mu\epsilon$)	-99	-29	18	61	104	144	184	223	264	301	341
IS88 ($\mu\epsilon$)	-67	-5	43	86	127	166	204	239	276	309	344
IS89 ($\mu\epsilon$)	-64	-3	45	88	129	168	206	243	282	315	352
IS90 ($\mu\epsilon$)	-70	-70	-52	-22	20	68	121	178	241	301	367
IS91 ($\mu\epsilon$)	-95	-107	-121	-118	-101	-80	-52	-18	21	61	107
IS92 ($\mu\epsilon$)	-75	10	72	128	182	232	280	325	371	412	454
IS93 ($\mu\epsilon$)	-97	-81	-74	-50	-14	25	71	120	175	228	288
IS94 ($\mu\epsilon$)	-59	102	219	331	437	538	635	726	820	903	987
IS95 ($\mu\epsilon$)	-107	-87	-71	-38	6	51	103	158	218	274	339
IS96 ($\mu\epsilon$)	-66	76	176	274	368	457	544	626	711	786	865
IS97 ($\mu\epsilon$)	-113	13	103	189	273	353	432	505	583	652	724
L01 ($\mu\epsilon$)	-	-	-	-	-	-	-	-	-	-	-
L02 ($\mu\epsilon$)	-296	-209	-207	-192	-179	-167	-153	-137	-124	-108	-92

Table F-35. Raw data, strain survey conducted after 30,000 cycles, hot-wet environmental conditions (Run 2) (continued)

Load Step	0	1	2	3	4	5	6	7	8	9	10
Pressure (psi)	-0.11	0.67	1.33	2.00	2.66	3.34	4.02	4.66	5.36	6.01	6.67
L03 ($\mu\epsilon$)	-181	-115	-122	-105	-91	-76	-58	-38	-19	2	23
L04 ($\mu\epsilon$)	-206	-119	-107	-79	-54	-32	-9	16	40	62	85
L05 ($\mu\epsilon$)	-190	-171	-178	-171	-165	-159	-152	-143	-134	-124	-114
L06 ($\mu\epsilon$)	-237	-195	-177	-156	-138	-126	-116	-106	-101	-96	-88
L07 ($\mu\epsilon$)	-	-	-	-	-	-	-	-	-	-	-
L08 ($\mu\epsilon$)	-239	-185	-185	-168	-152	-136	-117	-98	-79	-58	-39
L09 ($\mu\epsilon$)	-165	-92	-105	-86	-67	-50	-32	-11	10	28	53
L10 ($\mu\epsilon$)	-	-	-	-	-	-	-	-	-	-	-
RAC-A1 ($\mu\epsilon$)	-139	-10	106	218	325	429	530	626	725	813	903
RAC-A2 ($\mu\epsilon$)	-107	10	114	211	303	393	480	561	647	722	798
RAC-A3 ($\mu\epsilon$)	-177	-74	18	101	180	256	330	399	471	534	598
RAC-F1 ($\mu\epsilon$)	-78	51	162	269	372	470	565	655	750	831	916
RAC-F2 ($\mu\epsilon$)	-92	29	132	228	320	407	493	573	656	729	803
RBC-A1 ($\mu\epsilon$)	-292	-199	-124	-54	16	80	142	199	259	311	364
RBC-A2 ($\mu\epsilon$)	-208	-132	-68	-9	50	105	158	206	257	300	344
RBC-A3 ($\mu\epsilon$)	-213	-136	-71	-11	49	104	158	209	261	306	352
RBC-A4 ($\mu\epsilon$)	-139	-56	12	76	140	200	258	313	369	419	470
RBC-F1 ($\mu\epsilon$)	-283	-186	-116	-47	19	81	140	194	249	298	347
RBC-F2 ($\mu\epsilon$)	-235	-150	-89	-29	29	83	135	182	231	273	315
RBC-F3 ($\mu\epsilon$)	-209	-123	-63	-4	53	106	158	205	254	296	339
S16 ($\mu\epsilon$)	-152	-136	-104	-79	-55	-31	-9	11	32	49	67

Table F-35. Raw data, strain survey conducted after 30,000 cycles, hot-wet environmental conditions (Run 2) (continued)

Load Step	0	1	2	3	4	5	6	7	8	9	10
Pressure (psi)	-0.11	0.67	1.33	2.00	2.66	3.34	4.02	4.66	5.36	6.01	6.67
S17 ($\mu\epsilon$)	-	-	-	-	-	-	-	-	-	-	-
S18 ($\mu\epsilon$)	-34	-6	106	196	278	354	430	500	572	636	701
S20 ($\mu\epsilon$)	-	-	-	-	-	-	-	-	-	-	-
S22 ($\mu\epsilon$)	97	195	306	393	470	548	626	696	768	838	906
S25 ($\mu\epsilon$)	527	620	755	873	989	1098	1200	1291	1397	1483	1573
S29 ($\mu\epsilon$)	-192	-76	7	88	164	240	314	384	459	526	595
S30 ($\mu\epsilon$)	-268	-167	-75	-7	63	123	182	237	295	345	396
S32 ($\mu\epsilon$)	-1307	-1388	-1430	-1475	-1514	-1549	-1585	-1613	-1642	-1661	-1680
S34 ($\mu\epsilon$)	-	-	-	-	-	-	-	-	-	-	-
S37 ($\mu\epsilon$)	281	451	607	732	845	951	1051	1142	1238	1323	1409
S41 ($\mu\epsilon$)	-213	-76	16	104	187	268	345	418	495	563	632
S42 ($\mu\epsilon$)	-	-	-	-	-	-	-	-	-	-	-
S43 ($\mu\epsilon$)	103	210	295	367	430	490	548	601	656	706	758
S44 ($\mu\epsilon$)	-	-	-	-	-	-	-	-	-	-	-
S46 ($\mu\epsilon$)	404	90	-172	-399	-589	-753	-901	-1101	-1254	-1370	-1528
S48 ($\mu\epsilon$)	-201	-116	-12	82	166	246	323	393	468	548	616
S51 ($\mu\epsilon$)	-27	110	245	361	469	574	675	768	866	954	1043
S55 ($\mu\epsilon$)	-19	43	105	169	234	300	366	429	497	559	624
S56 ($\mu\epsilon$)	125	180	253	314	374	432	489	545	605	661	718
S57 ($\mu\epsilon$)	-	-	-	-	-	-	-	-	-	-	-
S58 ($\mu\epsilon$)	477	584	693	777	851	921	989	1051	1118	1178	1240

Table F-35. Raw data, strain survey conducted after 30,000 cycles, hot-wet environmental conditions (Run 2) (continued)

Load Step	0	1	2	3	4	5	6	7	8	9	10
Pressure (psi)	-0.11	0.67	1.33	2.00	2.66	3.34	4.02	4.66	5.36	6.01	6.67
S60 ($\mu\epsilon$)	-888	-1211	-1188	-1527	-2098	-2186	-2405	-2170	-1923	-2364	-2412
S62 ($\mu\epsilon$)	398	475	561	635	702	767	831	890	954	1013	1074
S65 ($\mu\epsilon$)	437	582	690	786	876	962	1044	1112	1185	1249	1313
S69 ($\mu\epsilon$)	79	117	156	195	232	266	302	334	369	400	430
S70 ($\mu\epsilon$)	-96	-1	92	171	245	316	388	455	526	591	660
S71 ($\mu\epsilon$)	-	-	-	-	-	-	-	-	-	-	-
S72 ($\mu\epsilon$)	-17	116	236	333	419	501	580	652	728	798	869
S74 ($\mu\epsilon$)	-684	-881	-1038	-1178	-1309	-1436	-1581	-1688	-1794	-1890	-2001
S76 ($\mu\epsilon$)	-158	-97	-4	78	156	234	312	382	460	530	602
S79 ($\mu\epsilon$)	-164	-63	51	149	244	338	430	515	606	689	773
S83 ($\mu\epsilon$)	59	95	147	201	259	318	378	442	504	567	626
S84 ($\mu\epsilon$)	87	171	255	333	409	486	561	635	713	784	857
S85 ($\mu\epsilon$)	-	-	-	-	-	-	-	-	-	-	-
S86 ($\mu\epsilon$)	16	49	103	111	152	163	207	208	239	251	250
S88 ($\mu\epsilon$)	62	-129	-227	-319	-394	-456	-509	-550	-585	-610	-631
S90 ($\mu\epsilon$)	-158	-38	84	184	274	359	439	513	575	645	714
S93 ($\mu\epsilon$)	525	650	809	942	1064	1181	1291	1394	1506	1586	1678
S97 ($\mu\epsilon$)	102	164	230	295	360	424	489	551	617	677	738
UAC-A1 ($\mu\epsilon$)	-23	131	270	403	527	644	756	859	965	1060	1153
UAC-A2 ($\mu\epsilon$)	-51	79	194	302	402	495	585	666	750	824	897
UAC-A3 ($\mu\epsilon$)	-56	68	172	270	362	448	531	607	685	756	826

Table F-35. Raw data, strain survey conducted after 30,000 cycles, hot-wet environmental conditions (Run 2) (continued)

Load Step	0	1	2	3	4	5	6	7	8	9	10
Pressure (psi)	-0.11	0.67	1.33	2.00	2.66	3.34	4.02	4.66	5.36	6.01	6.67
UAC-F1 ($\mu\epsilon$)	-53	105	247	385	514	637	755	863	974	1073	1171
UAC-F2 ($\mu\epsilon$)	-35	99	221	335	443	545	643	733	825	908	989
UBC-A1 ($\mu\epsilon$)	-	-	-	-	-	-	-	-	-	-	-
UBC-A2 ($\mu\epsilon$)	-61	101	228	348	460	564	662	752	842	921	1000
UBC-A3 ($\mu\epsilon$)	-18	125	234	336	432	521	606	684	763	832	902
UBC-A4 ($\mu\epsilon$)	14	143	243	336	426	509	590	665	743	812	883
UBC-F1 ($\mu\epsilon$)	-	-	-	-	-	-	-	-	-	-	-
UBC-F2 ($\mu\epsilon$)	-68	138	266	387	500	604	702	791	881	959	1036
UBC-F3 ($\mu\epsilon$)	-56	136	248	353	452	543	630	709	789	860	930
UDAC-A1 ($\mu\epsilon$)	-86	106	243	375	498	612	722	824	928	1018	1111
UDAC-A2 ($\mu\epsilon$)	-85	80	194	305	409	505	598	684	772	849	928
UDAC-A3 ($\mu\epsilon$)	-99	36	130	220	306	386	464	537	612	678	747
UDAC-F1 ($\mu\epsilon$)	-87	104	244	377	502	618	729	831	936	1029	1122
UDAC-F2 ($\mu\epsilon$)	-83	77	194	304	408	505	598	684	773	850	929
UDBC-A1 ($\mu\epsilon$)	-	-	-	-	-	-	-	-	-	-	-
UDBC-A2 ($\mu\epsilon$)	-110	33	167	292	410	521	627	724	822	907	991
UDBC-A3 ($\mu\epsilon$)	-77	55	172	279	380	475	565	647	732	805	878
UDBC-A4 ($\mu\epsilon$)	-12	112	216	312	402	488	571	648	727	798	868
UDBC-F1 ($\mu\epsilon$)	-	-	-	-	-	-	-	-	-	-	-
UDBC-F2 ($\mu\epsilon$)	-81	53	198	332	459	578	690	792	895	985	1072
UDBC-F3 ($\mu\epsilon$)	-25	97	221	333	439	538	631	717	803	878	952

Table F-36. Raw data, strain survey conducted after 30,000 cycles, hot-wet environmental conditions (Run 3)

Load Step	0	1	2	3	4	5	6	7	8	9	10
Pressure (psi)	-0.11	0.67	1.33	1.98	2.66	3.35	4.01	4.66	5.32	5.99	6.67
Frame-1 (lbf)	5	146	249	352	474	581	654	766	916	997	1115
Frame-2 (lbf)	79	121	223	333	455	565	680	794	906	1021	1134
Frame-3 (lbf)	2	117	230	343	451	568	675	792	908	1015	1132
Frame-4 (lbf)	55	113	221	340	457	563	679	795	905	1020	1132
Frame-5 (lbf)	1	126	229	345	436	560	680	793	895	1020	1127
Frame-6 (lbf)	-8	112	228	333	449	559	678	780	907	1020	1135
Frame-7 (lbf)	16	110	227	345	452	565	677	793	912	1021	1133
Frame-8 (lbf)	10	108	226	343	454	568	687	795	908	1013	1133
Frame-9 (lbf)	46	115	228	334	448	565	680	795	904	1020	1132
Frame-10 (lbf)	1	118	224	348	453	568	671	793	907	1019	1134
Frame-11 (lbf)	6	117	234	340	453	564	683	796	906	1020	1131
Frame-12 (lbf)	21	112	224	337	460	569	677	792	907	1018	1132
Hoop-1 (lbf)	68	703	1419	2129	2856	3565	4305	5010	5711	6433	7135
Hoop-2 (lbf)	173	729	1418	2114	2841	3576	4297	4990	5712	6410	7123
Hoop-3 (lbf)	78	720	1424	2154	2853	3581	4284	4995	5701	6428	7151
Hoop-4 (lbf)	36	710	1435	2137	2862	3564	4292	4994	5698	6411	7139
Hoop-5 (lbf)	105	694	1426	2137	2851	3559	4286	5002	5736	6438	7145
Hoop-6 (lbf)	48	709	1438	2149	2849	3576	4296	5000	5717	6421	7140
Hoop-7 (lbf)	26	716	1431	2135	2860	3576	4289	5000	5714	6425	7135
Hoop-8 (lbf)	140	722	1425	2137	2857	3571	4291	5000	5714	6422	7141
Hoop-9 (lbf)	37	731	1426	2145	2854	3571	4286	5010	5711	6429	7140

Table F-36. Raw data, strain survey conducted after 30,000 cycles, hot-wet environmental conditions (Run 3) (continued)

Load Step	0	1	2	3	4	5	6	7	8	9	10
Pressure (psi)	-0.11	0.67	1.33	1.98	2.66	3.35	4.01	4.66	5.32	5.99	6.67
Hoop-10 (lbf)	3	724	1433	2123	2854	3569	4292	4997	5707	6411	7139
Hoop-11 (lbf)	53	685	1407	2132	2860	3553	4291	4987	5729	6419	7144
Hoop-12 (lbf)	148	723	1438	2142	2863	3564	4279	5015	5710	6428	7148
Hoop-13 (lbf)	62	688	1451	2126	2860	3585	4295	4993	5709	6441	7141
Hoop-14 (lbf)	10	729	1424	2143	2852	3563	4299	4999	5697	6414	7121
Long-1 (lbf)	99	618	1323	1996	2677	3352	3974	4610	5345	6030	6637
Long-2 (lbf)	30	678	1342	2000	2682	3347	4011	4677	5334	6016	6677
Long-3 (lbf)	3	674	1339	2008	2678	3340	4008	4675	5366	6011	6673
Long-4 (lbf)	38	690	1340	2001	2675	3337	4010	4673	5343	6007	6676
Long-5 (lbf)	-8	650	1329	2003	2683	3334	4017	4671	5327	5999	6672
Long-6 (lbf)	1	656	1326	2003	2674	3336	4002	4655	5341	6005	6675
Long-7 (lbf)	16	690	1335	2005	2678	3341	4013	4663	5344	6006	6681
Long-8 (lbf)	-14	675	1341	2005	2669	3337	4009	4683	5363	6032	6675
F01 ($\mu\epsilon$)	-343	-393	-359	-304	-256	-202	-159	-113	-71	-25	18
F02 ($\mu\epsilon$)	303	428	469	519	560	602	654	701	748	797	846
F03 ($\mu\epsilon$)	-366	-493	-446	-401	-356	-315	-281	-237	-198	-156	-117
F04 ($\mu\epsilon$)	424	561	608	655	710	762	825	881	934	990	1045
F05 ($\mu\epsilon$)	-	-	-	-	-	-	-	-	-	-	-
F06 ($\mu\epsilon$)	428	571	606	646	692	737	783	833	879	925	975
F07 ($\mu\epsilon$)	-213	-309	-261	-213	-169	-123	-84	-42	-5	34	72
F08 ($\mu\epsilon$)	235	360	393	434	482	526	579	626	674	723	773

Table F-36. Raw data, strain survey conducted after 30,000 cycles, hot-wet environmental conditions (Run 3) (continued)

Load Step	0	1	2	3	4	5	6	7	8	9	10
Pressure (psi)	-0.11	0.67	1.33	1.98	2.66	3.35	4.01	4.66	5.32	5.99	6.67
IS16 ($\mu\epsilon$)	31	67	145	213	285	357	430	502	575	650	726
IS17 ($\mu\epsilon$)	-99	-99	-65	-26	23	79	137	198	262	328	397
IS18 ($\mu\epsilon$)	-228	-236	-220	-194	-155	-108	-56	1	61	125	193
IS19 ($\mu\epsilon$)	15	55	74	85	98	113	130	149	170	194	222
IS20 ($\mu\epsilon$)	170	207	252	288	324	359	393	428	462	497	534
IS21 ($\mu\epsilon$)	144	184	229	265	300	335	369	403	438	472	509
IS22 ($\mu\epsilon$)	-278	-304	-294	-276	-246	-207	-160	-109	-54	6	70
IS23 ($\mu\epsilon$)	-392	-384	-389	-384	-367	-341	-308	-270	-227	-178	-125
IS24 ($\mu\epsilon$)	182	245	305	352	398	442	484	524	563	603	642
IS25 ($\mu\epsilon$)	-399	-366	-349	-323	-285	-241	-190	-137	-78	-17	49
IS26 ($\mu\epsilon$)	49	197	318	424	527	624	717	803	887	967	1047
IS27 ($\mu\epsilon$)	-391	-342	-305	-260	-205	-145	-80	-15	55	127	202
IS28 ($\mu\epsilon$)	30	171	285	387	488	583	675	760	843	924	1005
IS29 ($\mu\epsilon$)	67	174	274	361	449	534	618	697	775	853	931
IS30 ($\mu\epsilon$)	-267	-292	-258	-220	-175	-123	-67	-7	56	121	190
IS31 ($\mu\epsilon$)	-37	20	83	140	200	259	318	375	431	487	545
IS32 ($\mu\epsilon$)	-121	-76	-25	20	64	107	149	188	226	263	300
IS33 ($\mu\epsilon$)	-115	-63	-8	40	86	131	175	216	255	293	332
IS34 ($\mu\epsilon$)	-370	-348	-311	-276	-235	-189	-139	-86	-31	27	88
IS35 ($\mu\epsilon$)	-562	-619	-636	-636	-621	-597	-565	-528	-487	-441	-390
IS36 ($\mu\epsilon$)	-115	-66	-12	35	82	127	171	212	252	291	329

Table F-36. Raw data, strain survey conducted after 30,000 cycles, hot-wet environmental conditions (Run 3) (continued)

Load Step	0	1	2	3	4	5	6	7	8	9	10
Pressure (psi)	-0.11	0.67	1.33	1.98	2.66	3.35	4.01	4.66	5.32	5.99	6.67
IS37 ($\mu\epsilon$)	-506	-566	-580	-575	-554	-524	-485	-442	-393	-340	-282
IS38 ($\mu\epsilon$)	-182	-113	-45	16	77	137	195	249	303	355	407
IS39 ($\mu\epsilon$)	-493	-541	-541	-522	-487	-443	-391	-335	-274	-210	-143
IS40 ($\mu\epsilon$)	-179	-98	-25	41	109	175	240	300	360	418	476
IS41 ($\mu\epsilon$)	-3	98	185	263	342	418	494	564	633	701	769
IS42 ($\mu\epsilon$)	83	104	164	222	285	348	413	478	544	610	679
IS43 ($\mu\epsilon$)	-5	-29	8	52	106	166	229	295	363	432	505
IS44 ($\mu\epsilon$)	56	-19	-17	1	33	73	120	172	228	286	348
IS45 ($\mu\epsilon$)	-49	15	90	155	220	281	341	398	455	510	566
IS46 ($\mu\epsilon$)	-49	17	91	155	217	275	332	386	438	488	539
IS47 ($\mu\epsilon$)	-37	32	106	169	231	290	347	402	455	507	560
IS48 ($\mu\epsilon$)	-77	-76	-41	-6	38	88	142	200	260	324	391
IS49 ($\mu\epsilon$)	-54	-95	-94	-85	-66	-41	-12	21	59	99	144
IS50 ($\mu\epsilon$)	-47	36	122	197	269	338	405	467	528	586	645
IS51 ($\mu\epsilon$)	-45	-71	-59	-38	-9	25	63	104	149	195	246
IS52 ($\mu\epsilon$)	-53	68	188	295	400	499	595	686	773	857	941
IS53 ($\mu\epsilon$)	-21	-48	-29	1	40	85	134	185	241	298	359
IS54 ($\mu\epsilon$)	-57	58	170	269	367	459	549	634	716	796	875
IS55 ($\mu\epsilon$)	-85	29	135	226	316	400	482	560	636	710	785
IS56 ($\mu\epsilon$)	36	70	112	155	202	254	309	366	425	487	552
IS57 ($\mu\epsilon$)	-155	-174	-163	-141	-109	-68	-22	29	83	139	200

Table F-36. Raw data, strain survey conducted after 30,000 cycles, hot-wet environmental conditions (Run 3) (continued)

Load Step	0	1	2	3	4	5	6	7	8	9	10
Pressure (psi)	-0.11	0.67	1.33	1.98	2.66	3.35	4.01	4.66	5.32	5.99	6.67
IS58 ($\mu\epsilon$)	-259	-293	-291	-278	-253	-219	-179	-132	-82	-28	32
IS59 ($\mu\epsilon$)	53	57	78	89	99	111	122	135	150	166	186
IS60 ($\mu\epsilon$)	170	194	235	266	297	328	359	390	421	453	487
IS61 ($\mu\epsilon$)	193	222	267	301	335	368	400	432	464	497	532
IS62 ($\mu\epsilon$)	-263	-289	-271	-252	-223	-186	-144	-97	-45	10	70
IS63 ($\mu\epsilon$)	-407	-440	-442	-437	-424	-404	-379	-348	-311	-271	-224
IS64 ($\mu\epsilon$)	187	231	284	323	361	398	433	467	500	533	568
IS65 ($\mu\epsilon$)	-454	-457	-424	-387	-343	-295	-242	-186	-126	-64	3
IS66 ($\mu\epsilon$)	-23	102	222	326	427	521	610	694	774	851	927
IS67 ($\mu\epsilon$)	-428	-416	-364	-310	-251	-188	-123	-54	16	88	162
IS68 ($\mu\epsilon$)	-32	93	211	317	421	519	613	703	790	873	956
IS69 ($\mu\epsilon$)	28	143	243	330	416	498	579	657	733	807	882
IS70 ($\mu\epsilon$)	130	116	151	189	233	284	336	391	449	508	570
IS71 ($\mu\epsilon$)	-48	-82	-57	-24	20	72	127	185	247	310	376
IS72 ($\mu\epsilon$)	-137	-159	-133	-100	-56	-6	48	105	166	229	296
IS73 ($\mu\epsilon$)	-188	-92	-3	74	149	218	285	348	409	468	526
IS74 ($\mu\epsilon$)	-142	-59	24	96	166	232	295	355	413	469	524
IS75 ($\mu\epsilon$)	-109	-23	61	133	203	269	334	394	453	509	566
IS76 ($\mu\epsilon$)	-155	-98	-38	16	76	138	202	267	336	404	476
IS77 ($\mu\epsilon$)	-236	-219	-189	-158	-122	-84	-44	-2	44	92	142
IS78 ($\mu\epsilon$)	-128	-32	59	138	214	286	356	422	486	547	607

Table F-36. Raw data, strain survey conducted after 30,000 cycles, hot-wet environmental conditions (Run 3) (continued)

Load Step	0	1	2	3	4	5	6	7	8	9	10
Pressure (psi)	-0.11	0.67	1.33	1.98	2.66	3.35	4.01	4.66	5.32	5.99	6.67
IS79 ($\mu\epsilon$)	-235	-211	-174	-138	-99	-57	-14	31	79	129	182
IS80 ($\mu\epsilon$)	-163	-37	77	179	278	372	463	550	635	715	796
IS81 ($\mu\epsilon$)	-287	-276	-246	-215	-180	-141	-101	-57	-10	38	90
IS82 ($\mu\epsilon$)	-144	-29	76	169	260	347	432	513	592	667	743
IS83 ($\mu\epsilon$)	-196	-90	11	95	177	254	328	401	472	539	607
IS84 ($\mu\epsilon$)	-39	-9	58	119	181	247	312	378	444	510	580
IS85 ($\mu\epsilon$)	-55	-80	-49	-9	42	102	164	229	296	364	436
IS86 ($\mu\epsilon$)	-53	-97	-90	-68	-32	15	67	124	183	245	311
IS87 ($\mu\epsilon$)	-100	-33	17	59	101	143	183	222	261	299	339
IS88 ($\mu\epsilon$)	-67	-6	44	86	127	167	204	240	275	309	344
IS89 ($\mu\epsilon$)	-64	-4	46	88	128	169	207	244	280	315	352
IS90 ($\mu\epsilon$)	-69	-71	-50	-21	19	69	122	179	239	300	366
IS91 ($\mu\epsilon$)	-91	-109	-118	-115	-102	-78	-50	-16	21	62	109
IS92 ($\mu\epsilon$)	-74	8	74	129	182	233	281	327	371	412	455
IS93 ($\mu\epsilon$)	-93	-85	-71	-48	-15	27	72	122	174	229	289
IS94 ($\mu\epsilon$)	-57	98	222	331	437	539	637	729	818	903	989
IS95 ($\mu\epsilon$)	-102	-89	-67	-35	5	55	106	161	218	276	339
IS96 ($\mu\epsilon$)	-64	72	179	274	367	459	546	629	709	787	865
IS97 ($\mu\epsilon$)	-112	9	105	189	271	353	431	507	580	652	724
L01 ($\mu\epsilon$)	-	-	-	-	-	-	-	-	-	-	-
L02 ($\mu\epsilon$)	-290	-209	-202	-189	-176	-163	-149	-136	-120	-105	-91

Table F-36. Raw data, strain survey conducted after 30,000 cycles, hot-wet environmental conditions (Run 3) (continued)

Load Step	0	1	2	3	4	5	6	7	8	9	10
Pressure (psi)	-0.11	0.67	1.33	1.98	2.66	3.35	4.01	4.66	5.32	5.99	6.67
L03 ($\mu\epsilon$)	-176	-119	-118	-105	-90	-75	-57	-38	-17	3	23
L04 ($\mu\epsilon$)	-203	-120	-104	-79	-55	-31	-6	16	40	62	84
L05 ($\mu\epsilon$)	-189	-170	-176	-170	-164	-158	-150	-143	-133	-124	-115
L06 ($\mu\epsilon$)	-235	-194	-179	-160	-143	-128	-119	-112	-105	-100	-93
L07 ($\mu\epsilon$)	-	-	-	-	-	-	-	-	-	-	-
L08 ($\mu\epsilon$)	-236	-186	-181	-167	-150	-134	-114	-96	-76	-56	-37
L09 ($\mu\epsilon$)	-157	-97	-98	-81	-65	-45	-22	-4	16	36	55
L10 ($\mu\epsilon$)	-	-	-	-	-	-	-	-	-	-	-
RAC-A1 ($\mu\epsilon$)	-138	-9	111	221	329	433	534	630	725	815	905
RAC-A2 ($\mu\epsilon$)	-106	10	118	213	307	396	482	565	645	723	800
RAC-A3 ($\mu\epsilon$)	-174	-71	24	106	186	262	335	405	472	537	602
RAC-F1 ($\mu\epsilon$)	-77	51	166	271	374	472	569	659	747	832	917
RAC-F2 ($\mu\epsilon$)	-91	30	135	229	322	410	496	576	654	729	805
RBC-A1 ($\mu\epsilon$)	-292	-201	-122	-53	16	81	145	202	258	312	366
RBC-A2 ($\mu\epsilon$)	-208	-134	-66	-8	51	106	160	208	256	301	346
RBC-A3 ($\mu\epsilon$)	-212	-136	-69	-10	50	107	162	212	261	308	355
RBC-A4 ($\mu\epsilon$)	-138	-56	15	78	142	202	262	315	369	421	472
RBC-F1 ($\mu\epsilon$)	-281	-189	-113	-45	20	83	143	197	249	300	350
RBC-F2 ($\mu\epsilon$)	-233	-153	-86	-27	31	85	138	185	231	275	318
RBC-F3 ($\mu\epsilon$)	-207	-126	-60	-2	54	108	160	208	254	297	341
S16 ($\mu\epsilon$)	-152	-141	-110	-85	-61	-37	-17	2	29	51	72

Table F-36. Raw data, strain survey conducted after 30,000 cycles, hot-wet environmental conditions (Run 3) (continued)

Load Step	0	1	2	3	4	5	6	7	8	9	10
Pressure (psi)	-0.11	0.67	1.33	1.98	2.66	3.35	4.01	4.66	5.32	5.99	6.67
S17 ($\mu\epsilon$)	-	-	-	-	-	-	-	-	-	-	-
S18 ($\mu\epsilon$)	-24	11	115	192	261	329	394	465	528	584	635
S20 ($\mu\epsilon$)	-	-	-	-	-	-	-	-	-	-	-
S22 ($\mu\epsilon$)	104	207	316	407	487	567	621	710	779	848	919
S25 ($\mu\epsilon$)	518	617	756	877	994	1100	1202	1302	1389	1482	1573
S29 ($\mu\epsilon$)	-187	-73	12	90	168	243	318	389	459	529	599
S30 ($\mu\epsilon$)	-241	-139	-49	21	87	148	204	260	314	366	416
S32 ($\mu\epsilon$)	-1228	-1252	-1303	-1350	-1398	-1435	-1478	-1511	-1543	-1579	-1612
S34 ($\mu\epsilon$)	-	-	-	-	-	-	-	-	-	-	-
S37 ($\mu\epsilon$)	252	424	580	703	817	922	1022	1116	1206	1294	1381
S41 ($\mu\epsilon$)	-210	-75	19	105	190	270	348	422	494	564	635
S42 ($\mu\epsilon$)	-	-	-	-	-	-	-	-	-	-	-
S43 ($\mu\epsilon$)	96	208	294	364	430	489	545	598	650	702	757
S44 ($\mu\epsilon$)	-	-	-	-	-	-	-	-	-	-	-
S46 ($\mu\epsilon$)	277	7	-224	-418	-606	-772	-1301	-1426	-1551	-1638	-1728
S48 ($\mu\epsilon$)	-216	-127	-23	67	152	238	325	397	466	533	602
S51 ($\mu\epsilon$)	-32	110	244	358	469	573	674	770	863	953	1043
S55 ($\mu\epsilon$)	-23	38	100	163	229	295	362	426	491	555	620
S56 ($\mu\epsilon$)	114	175	248	308	368	427	484	540	596	653	713
S57 ($\mu\epsilon$)	-	-	-	-	-	-	-	-	-	-	-
S58 ($\mu\epsilon$)	464	578	686	769	846	917	984	1048	1110	1172	1236

Table F-36. Raw data, strain survey conducted after 30,000 cycles, hot-wet environmental conditions (Run 3) (continued)

Load Step	0	1	2	3	4	5	6	7	8	9	10
Pressure (psi)	-0.11	0.67	1.33	1.98	2.66	3.35	4.01	4.66	5.32	5.99	6.67
S60 ($\mu\epsilon$)	-2065	-2130	-2253	-2434	-2610	-2553	-2787	-2975	-2356	-3378	-2708
S62 ($\mu\epsilon$)	389	472	559	632	701	768	831	891	951	1011	1073
S65 ($\mu\epsilon$)	411	542	651	741	831	916	999	1073	1144	1214	1283
S69 ($\mu\epsilon$)	60	106	146	184	222	258	294	327	360	393	427
S70 ($\mu\epsilon$)	-113	-14	81	158	235	307	378	445	514	584	654
S71 ($\mu\epsilon$)	-	-	-	-	-	-	-	-	-	-	-
S72 ($\mu\epsilon$)	-23	114	234	329	418	501	579	654	725	796	868
S74 ($\mu\epsilon$)	-593	-776	-932	-1076	-1222	-1351	-1480	-1597	-1706	-1815	-1918
S76 ($\mu\epsilon$)	-147	-79	14	95	177	257	332	405	478	552	623
S79 ($\mu\epsilon$)	-173	-67	46	144	241	335	426	513	600	683	767
S83 ($\mu\epsilon$)	59	87	141	200	258	319	379	440	494	560	624
S84 ($\mu\epsilon$)	84	174	258	335	412	489	564	636	710	782	859
S85 ($\mu\epsilon$)	-	-	-	-	-	-	-	-	-	-	-
S86 ($\mu\epsilon$)	9	32	93	107	143	140	168	175	195	209	225
S88 ($\mu\epsilon$)	67	-111	-219	-305	-381	-444	-498	-542	-576	-602	-622
S90 ($\mu\epsilon$)	-186	-63	60	159	251	335	415	490	561	632	705
S93 ($\mu\epsilon$)	475	628	789	922	1046	1162	1273	1376	1476	1573	1670
S97 ($\mu\epsilon$)	94	159	226	289	355	420	484	546	608	670	733
UAC-A1 ($\mu\epsilon$)	-24	127	273	401	527	644	756	862	963	1059	1154
UAC-A2 ($\mu\epsilon$)	-56	71	193	299	401	495	585	669	750	826	902
UAC-A3 ($\mu\epsilon$)	-57	63	172	268	360	446	529	607	682	753	825

Table F-36. Raw data, strain survey conducted after 30,000 cycles, hot-wet environmental conditions (Run 3) (continued)

Load Step	0	1	2	3	4	5	6	7	8	9	10
Pressure (psi)	-0.11	0.67	1.33	1.98	2.66	3.35	4.01	4.66	5.32	5.99	6.67
UAC-F1 ($\mu\epsilon$)	-53	101	250	384	515	637	755	866	972	1073	1172
UAC-F2 ($\mu\epsilon$)	-35	97	223	334	443	546	644	736	824	908	990
UBC-A1 ($\mu\epsilon$)	-	-	-	-	-	-	-	-	-	-	-
UBC-A2 ($\mu\epsilon$)	-63	96	229	346	460	565	665	754	841	923	1003
UBC-A3 ($\mu\epsilon$)	-19	121	235	335	432	523	609	686	762	834	905
UBC-A4 ($\mu\epsilon$)	13	139	245	335	426	511	592	667	742	813	885
UBC-F1 ($\mu\epsilon$)	-	-	-	-	-	-	-	-	-	-	-
UBC-F2 ($\mu\epsilon$)	-70	133	267	386	500	604	704	794	879	960	1039
UBC-F3 ($\mu\epsilon$)	-56	131	250	353	453	545	632	712	788	861	932
UDAC-A1 ($\mu\epsilon$)	-86	100	246	373	496	613	723	826	924	1017	1110
UDAC-A2 ($\mu\epsilon$)	-84	74	197	304	407	506	599	686	770	849	928
UDAC-A3 ($\mu\epsilon$)	-97	32	132	220	304	387	465	539	610	679	747
UDAC-F1 ($\mu\epsilon$)	-86	99	248	376	501	618	730	835	934	1028	1122
UDAC-F2 ($\mu\epsilon$)	-82	73	197	304	407	506	599	687	770	850	929
UDBC-A1 ($\mu\epsilon$)	-	-	-	-	-	-	-	-	-	-	-
UDBC-A2 ($\mu\epsilon$)	-110	35	173	297	417	528	634	733	825	912	997
UDBC-A3 ($\mu\epsilon$)	-76	58	179	285	387	482	572	656	735	811	884
UDBC-A4 ($\mu\epsilon$)	-12	114	222	316	409	494	577	655	730	802	874
UDBC-F1 ($\mu\epsilon$)	-	-	-	-	-	-	-	-	-	-	-
UDBC-F2 ($\mu\epsilon$)	-84	53	202	334	463	582	695	798	896	988	1076
UDBC-F3 ($\mu\epsilon$)	-26	99	226	337	444	543	637	723	805	882	958

F.3 REDUCTION PROCEDURE

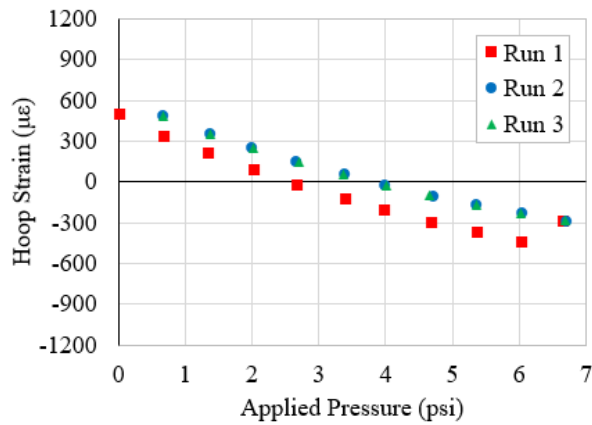
During post-processing of strain survey results, the initial measurement by each strain gauge (i.e., that which was acquired while the applied was equal to zero), was shifted to zero. Subsequently, all other values (i.e., those measured while the applied load was greater than zero) were also shifted by the same amount. A brief example of this reduction procedure is shown in figure F-1.

Figure F-1 shows results for strain gauge S32 obtained during a strain survey conducted in cold-dry environmental conditions following the completion of hot-wet conditioning. Figure F-1a shows the applied pressures, figure F-1b shows the raw strain data recorded by the strain gauge as a function of the applied pressure, and figure F-1c shows the strain data following the completion of post-processing. As shown in figure F-1b, the initial data points differed from zero by 507.335 $\mu\epsilon$, 656.094 $\mu\epsilon$, and 663.1 $\mu\epsilon$ for strain survey runs 1, 2, and 3, respectively. Adhering to the aforementioned reduction procedure, each strain value recorded during run 1 was reduced by 507.335 $\mu\epsilon$, each strain value recorded during run 2 was reduced by 656.094 $\mu\epsilon$, and each strain value recorded during run 3 was reduced by 663.1 (i.e., values in each run were offset by the corresponding zero-shift value). As shown in figure F-1c, application of the reduction procedure results in each array of values beginning with 0 $\mu\epsilon$ for the lowest applied pressure point. A graphical representation of this procedure is shown in figure F-2. Figure F-2a shows the raw strain results recorded by strain gauge S32 (i.e., those listed in figure F-1b), whereas figure F-2b depicts the same strain results after post-processing (i.e., those listed in figure F-1c).

	(a) Applied Pressure	(b) Raw Strain Data	(c) Offset Strain Data
Run 1	Pressure (psi)	S32 ($\mu\epsilon$)	S32 ($\mu\epsilon$)
	0.003	507.335	0
	0.668	344.314	-163.021
	1.333	214.583	-292.752
	2.007	95.419	-411.916
	2.653	-15.3409	-522.6759
	3.377	-119.058	-626.393
	3.975	-203.568	-710.903
	4.663	-289.675	-797.01
	5.339	-365.845	-873.18
	6.003	-433.277	-940.612
6.646	-278.318	-785.653	
Run 2	Pressure (psi)	S32 ($\mu\epsilon$)	S32 ($\mu\epsilon$)
	-0.098	656.094	0
	0.653	496.498	-159.596
	1.348	365.706	-290.388
	1.961	260.809	-395.285
	2.646	158.565	-497.529
	3.349	65.6275	-590.4665
	3.976	-12.9961	-669.0901
	4.679	-93.0257	-749.1197
	5.331	-159.124	-815.218
	6.026	-221.925	-878.019
6.679	-278.704	-934.798	
Run 3	Pressure (psi)	S32 ($\mu\epsilon$)	S32 ($\mu\epsilon$)
	-0.088	663.1	0
	0.656	493.956	-169.144
	1.343	364.501	-298.599
	1.996	258.051	-405.049
	2.675	155.486	-507.614
	3.335	65.3235	-597.7765
	3.991	-16.3137	-679.4137
	4.630	-88.5724	-751.6724
	5.344	-159.821	-822.921
	5.998	-222.292	-885.392
6.655	-277.259	-940.359	

Figure F-1. Tabulated example of the post-processing procedure applied to strain survey results: (a) applied pressure, (b) raw strain response, and (c) reduced strain response

(a) Strain Results Before Zero-Shift Post-Processing



(b) Strain Results After Zero-Shift Post-Processing

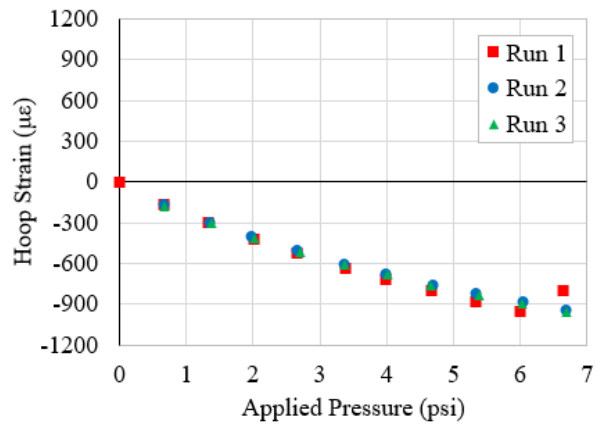


Figure F-2. Graphical example of the post-processing procedure applied to strain survey results: (a) strain results before zero-shift post-processing and (b) strain results after zero-shift post-processing

F.4 REDUCED STRAIN GAUGE RESPONSE DURING STRAIN SURVEYS, GRAPHED

F.4.1 Repair Patch RAC

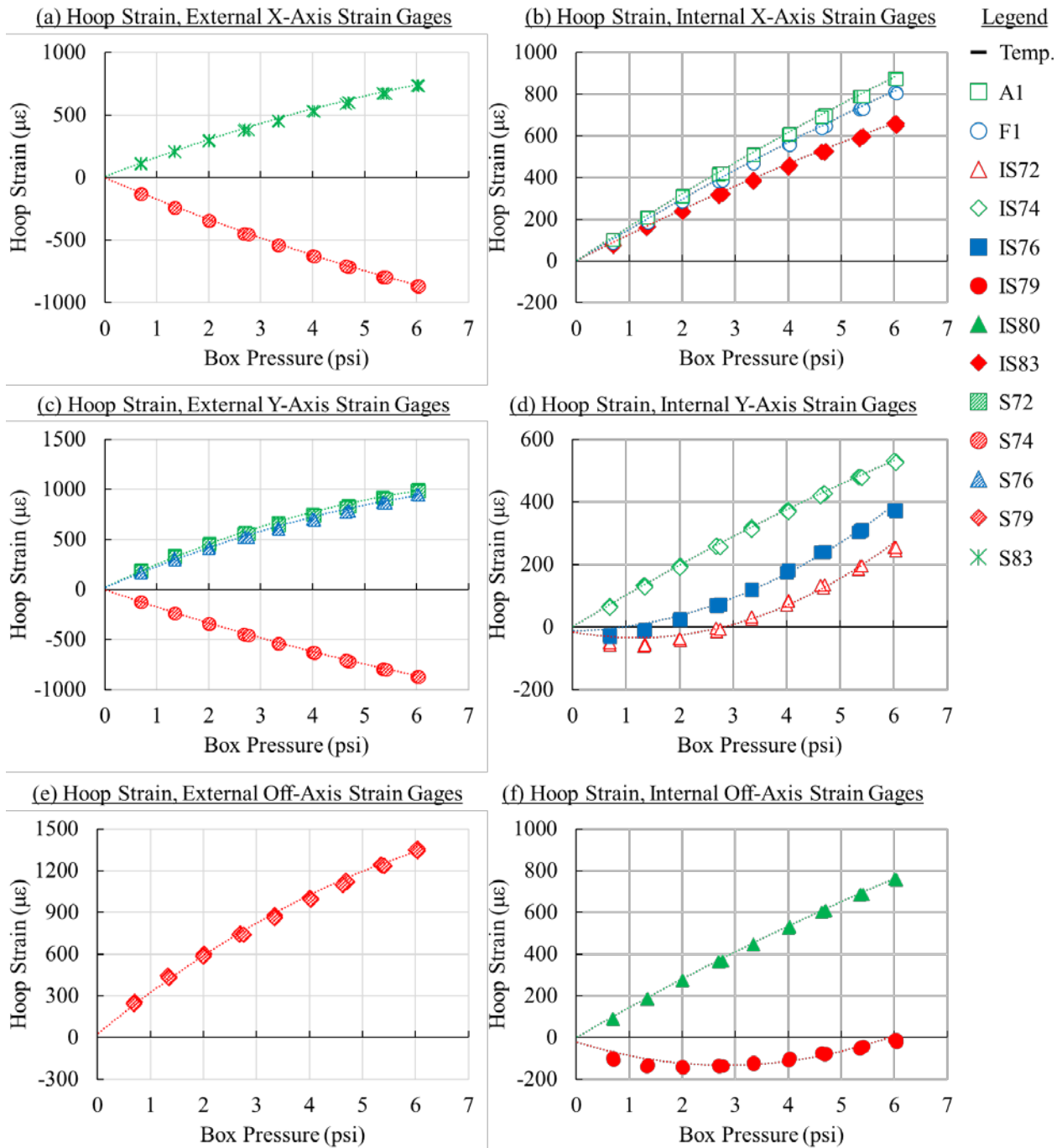


Figure F-3. Reduced strain response measured by strain gauges installed in the vicinity of repair patch RAC during a strain survey conducted following the completion of 60,000 cycles: (a) hoop strain, external X-axis strain gauges, (b) hoop strain, internal X-axis strain gauges, (c) hoop strain, external Y-axis strain gauges, (d) hoop strain, external Y-axis strain gauges, (e) hoop strain, external off-axis strain gauges, and (f) hoop strain, internal off-axis strain gauges

F.4.2 Repair Patch RBC

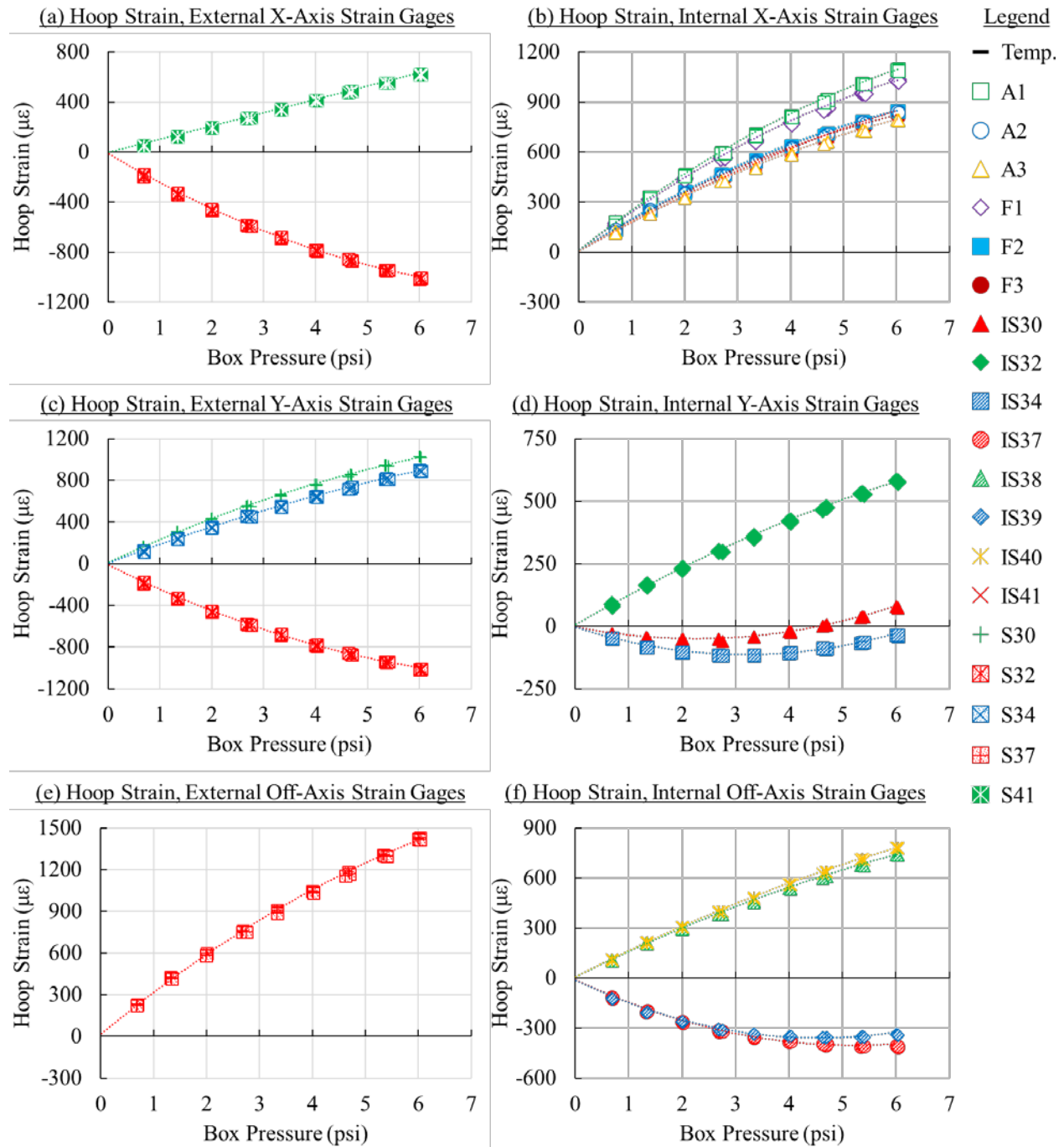


Figure F-4. Reduced strain response measured by strain gauges installed in the vicinity of repair patch RBC during a strain survey conducted following the completion of 60,000 cycles: (a) hoop strain, external X-axis strain gauges, (b) hoop strain, internal X-axis strain gauges, (c) hoop strain, external Y-axis strain gauges, (d) hoop strain, external Y-axis strain gauges, (e) hoop strain, external off-axis strain gauges, and (f) hoop strain, internal off-axis strain gauges

F.4.3 Repair Patch UAC

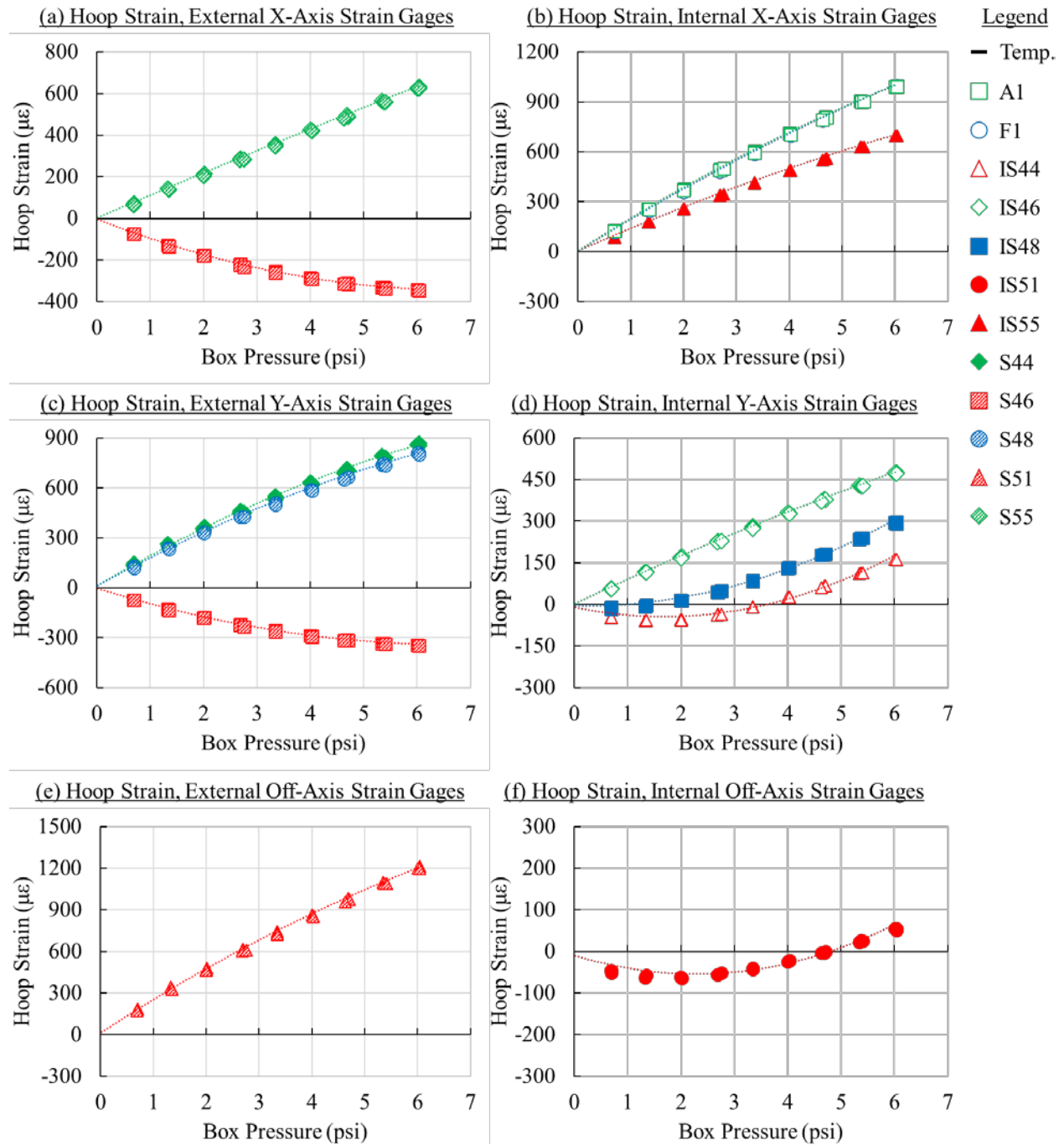


Figure F-5. Reduced strain response measured by strain gauges installed in the vicinity of repair patch UAC during a strain survey conducted following the completion of 60,000 cycles: (a) hoop strain, external X-axis strain gauges, (b) hoop strain, internal X-axis strain gauges, (c) hoop strain, external Y-axis strain gauges, (d) hoop strain, external Y-axis strain gauges, (e) hoop strain, external off-axis strain gauges, and (f) hoop strain, internal off-axis strain gauges

F.4.4 Repair Patch UB

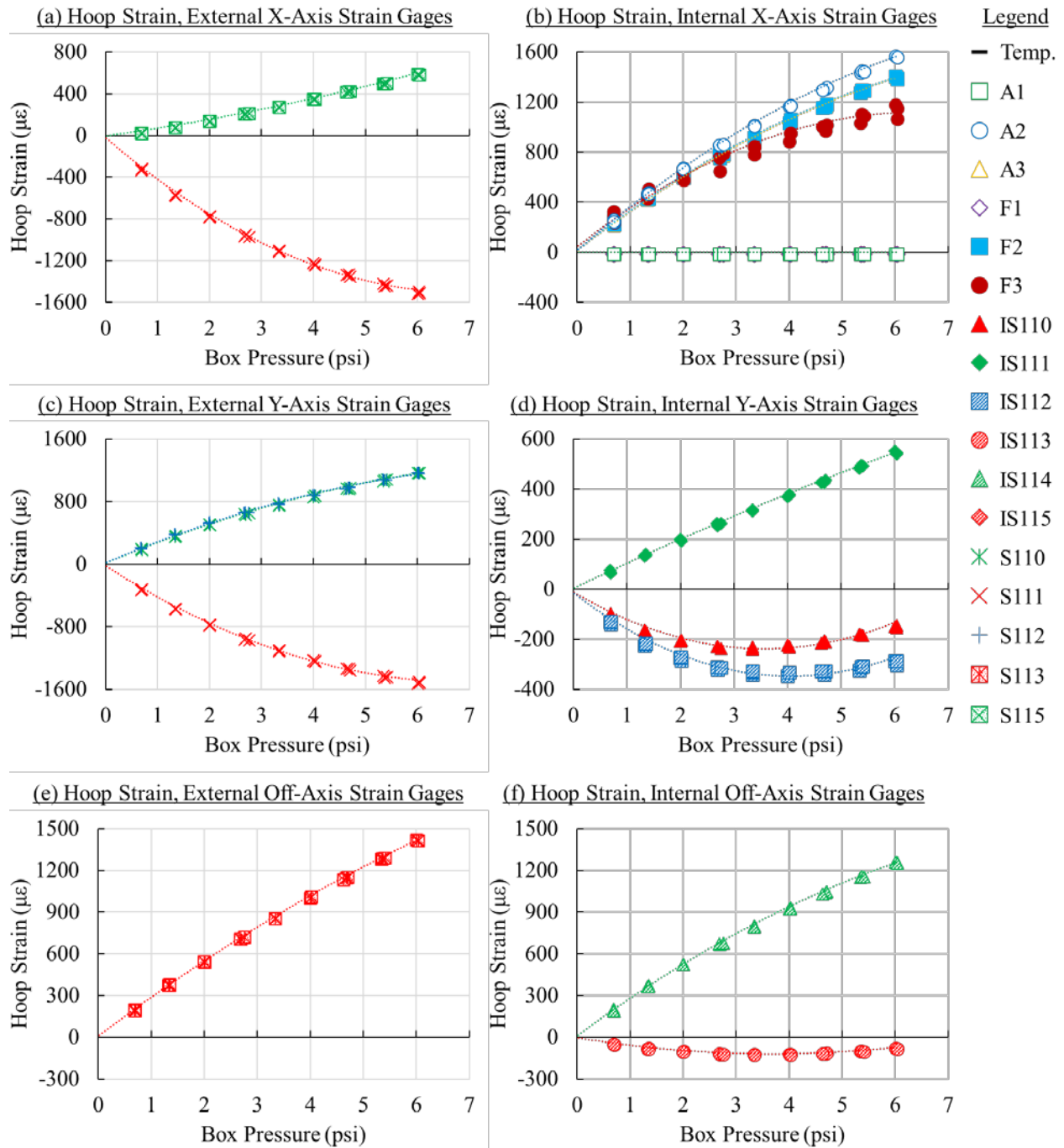


Figure F-6. Reduced strain response measured by strain gauges installed in the vicinity of repair patch UB during a strain survey conducted following the completion of 60,000 cycles: (a) hoop strain, external X-axis strain gauges, (b) hoop strain, internal X-axis strain gauges, (c) hoop strain, external Y-axis strain gauges, (d) hoop strain, external Y-axis strain gauges, (e) hoop strain, external off-axis strain gauges, and (f) hoop strain, internal off-axis strain gauges

F.4.5 Repair Patch UBC

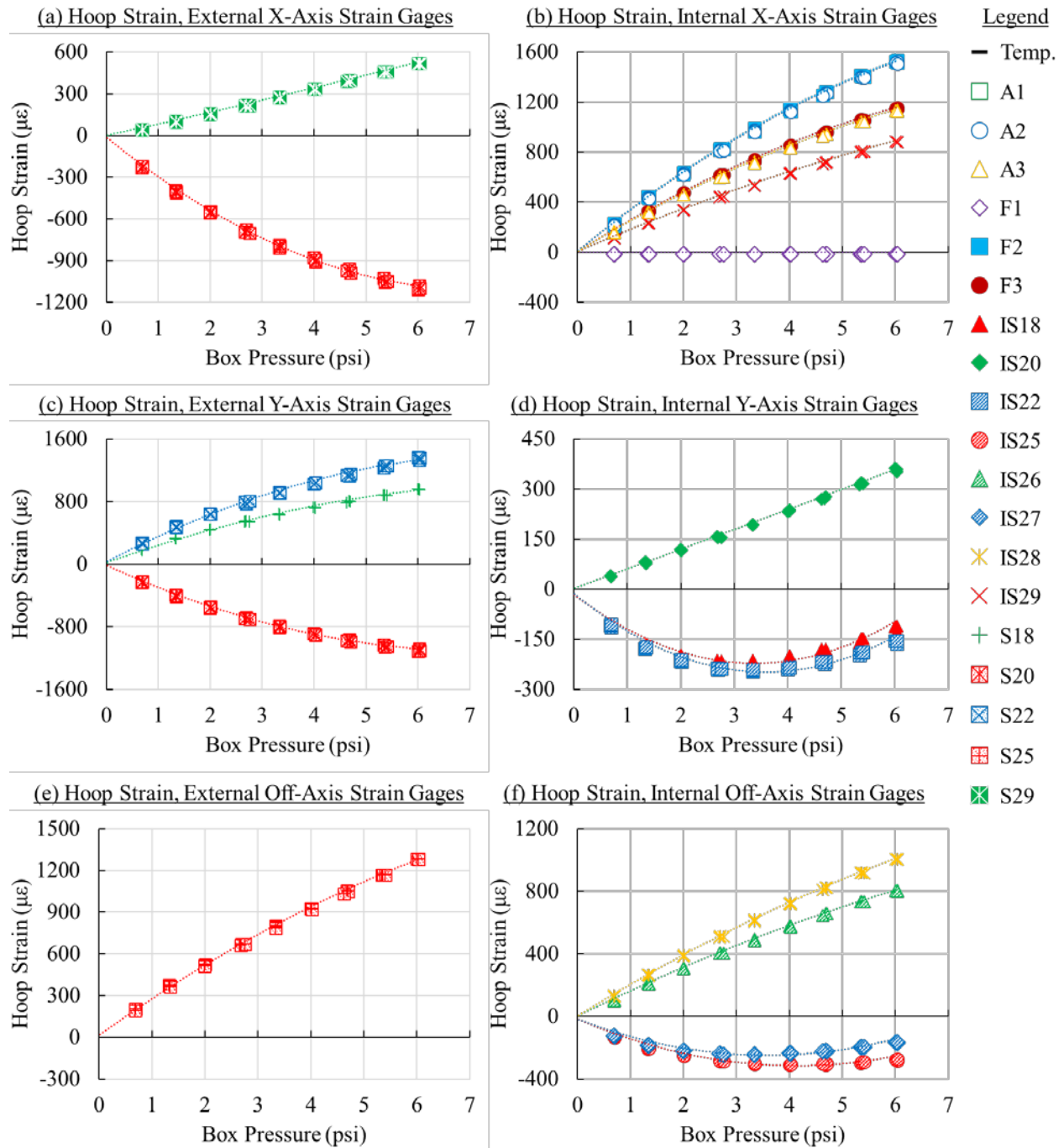


Figure F-7. Reduced strain response measured by strain gauges installed in the vicinity of repair patch UBC during a strain survey conducted following the completion of 60,000 cycles: (a) hoop strain, external X-axis strain gauges, (b) hoop strain, internal X-axis strain gauges, (c) hoop strain, external Y-axis strain gauges, (d) hoop strain, external Y-axis strain gauges, (e) hoop strain, external off-axis strain gauges, and (f) hoop strain, internal off-axis strain gauges

F.4.6 Repair Patch UDAC

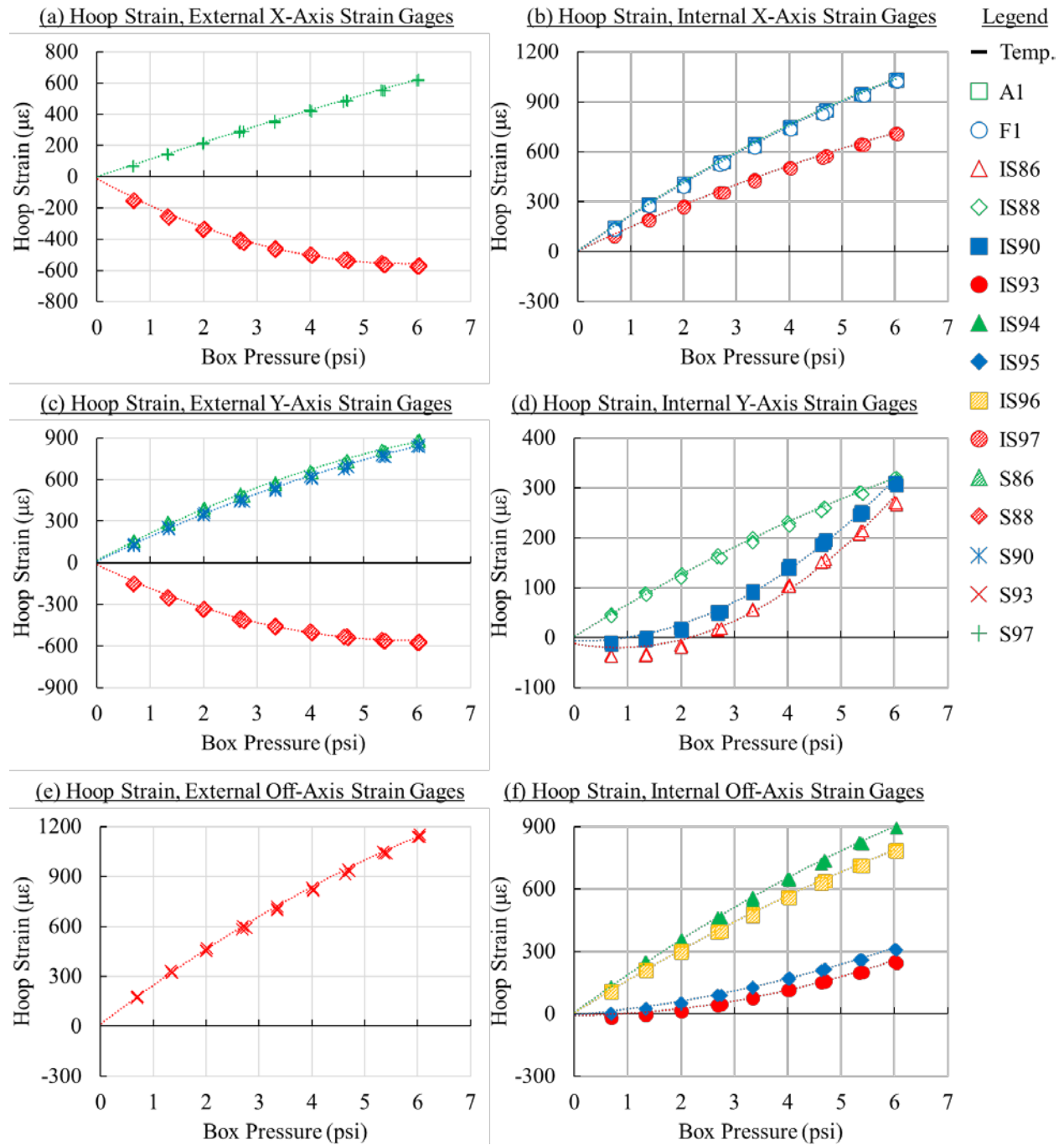


Figure F-8. Reduced strain response measured by strain gauges installed in the vicinity of repair patch UDAC during a strain survey conducted following the completion of 60,000 cycles: (a) hoop strain, external X-axis strain gauges, (b) hoop strain, internal X-axis strain gauges, (c) hoop strain, external Y-axis strain gauges, (d) hoop strain, external Y-axis strain gauges, (e) hoop strain, external off-axis strain gauges, and (f) hoop strain, internal off-axis strain gauges

F.4.7 Repair Patch UDB

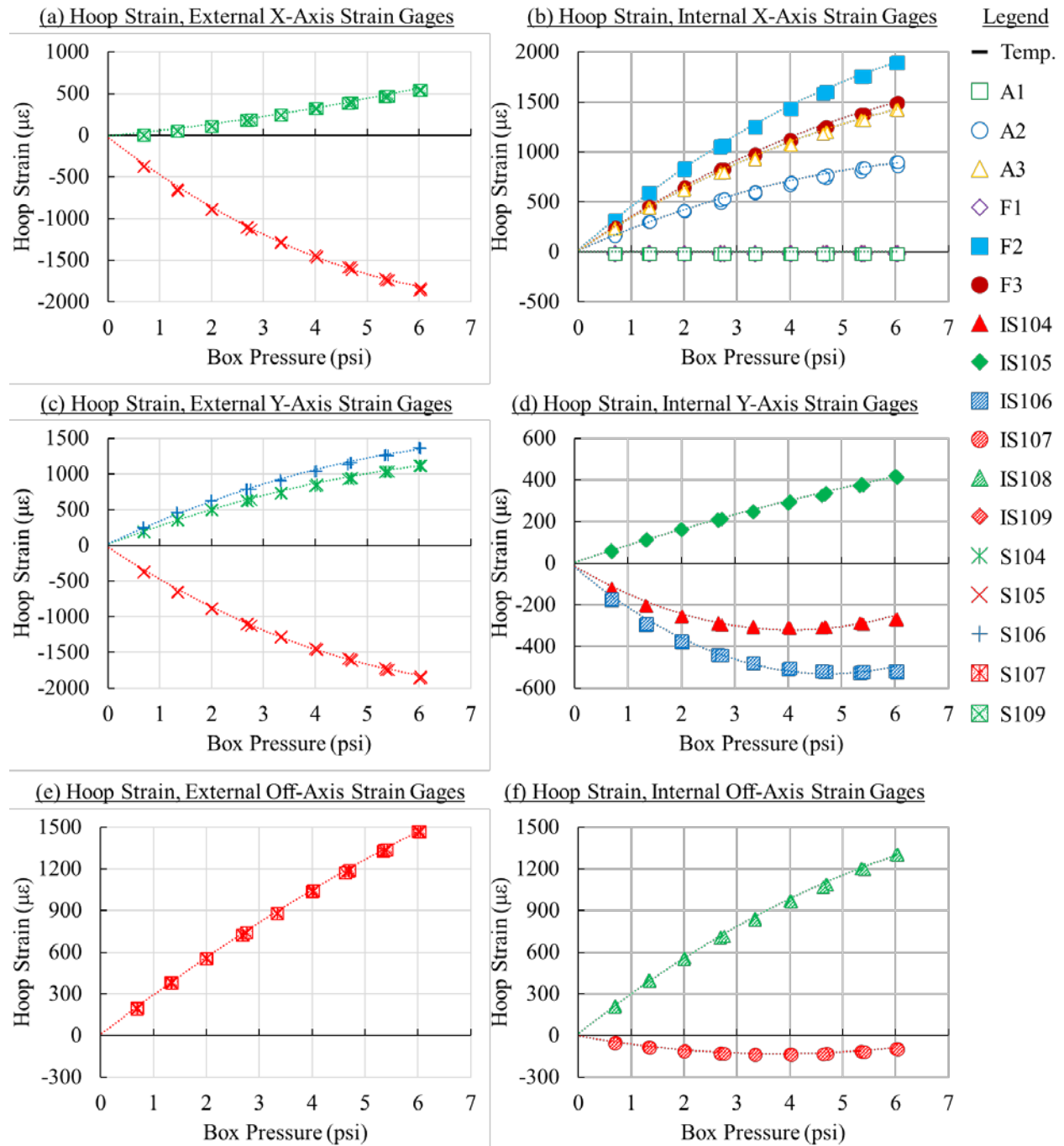


Figure F-9. Reduced strain response measured by strain gauges installed in the vicinity of repair patch UDB during a strain survey conducted following the completion of 60,000 cycles: (a) hoop strain, external X-axis strain gauges, (b) hoop strain, internal X-axis strain gauges, (c) hoop strain, external Y-axis strain gauges, (d) hoop strain, external Y-axis strain gauges, (e) hoop strain, external off-axis strain gauges, and (f) hoop strain, internal off-axis strain gauges

F.4.8 Repair Patch UDBC

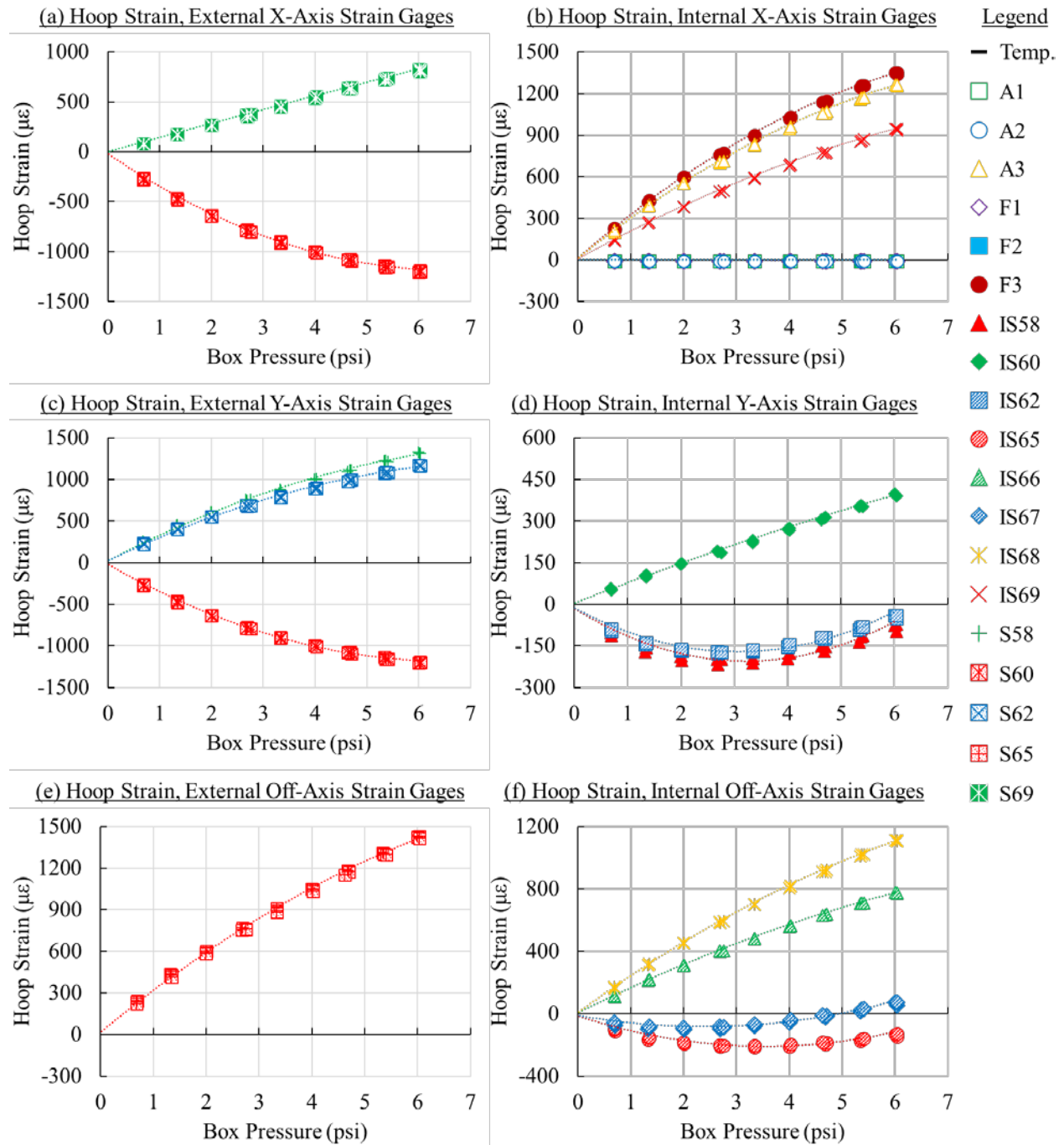


Figure F-10. Reduced strain response measured by strain gauges installed in the vicinity of repair patch UDBC during a strain survey conducted following the completion of 60,000 cycles: (a) hoop strain, external X-axis strain gauges, (b) hoop strain, internal X-axis strain gauges, (c) hoop strain, external Y-axis strain gauges, (d) hoop strain, external Y-axis strain gauges, (e) hoop strain, external off-axis strain gauges, and (f) hoop strain, internal off-axis strain gauges

APPENDIX G—3D DIGITAL IMAGE CORRELATION RESULTS

G.1 INTRODUCTION

Three-dimensional (3D) digital image correlation (DIC) is a non-contact, material-independent NDI method that utilizes sequential digital images of a specimen subjected to mechanical loading to measure in-plane deformation, displacement, and strain. Throughout the duration of the test, a 5M ARAMIS 3D DIC system was used to monitor strains exhibited in the vicinity of each repair patch during quasistatic strain surveys. The 5M ARAMIS 3D DIC system consisted of a sensor unit, a sensor controller, a high-performance PC system, and ARAMIS 3D DIC analysis software. The sensor unit, which featured two 5-megapixel cameras with 12-mm focal length lenses, a laser pointer, and two adjustable LED spotlights mounted on a circular support bar, was connected to the sensor controller and the high-performance PC system, both of which were located in the laboratory control room. Before each inspection, the sensor support bar was mounted on the motion control assembly of the RCCM system, as shown in figure G-1a. Similar to the high-magnification cameras that were also attached to the RCCM system, this connection facilitated the ability to precisely and efficiently relocate the ARAMIS sensor unit throughout the test section of the fuselage panel.

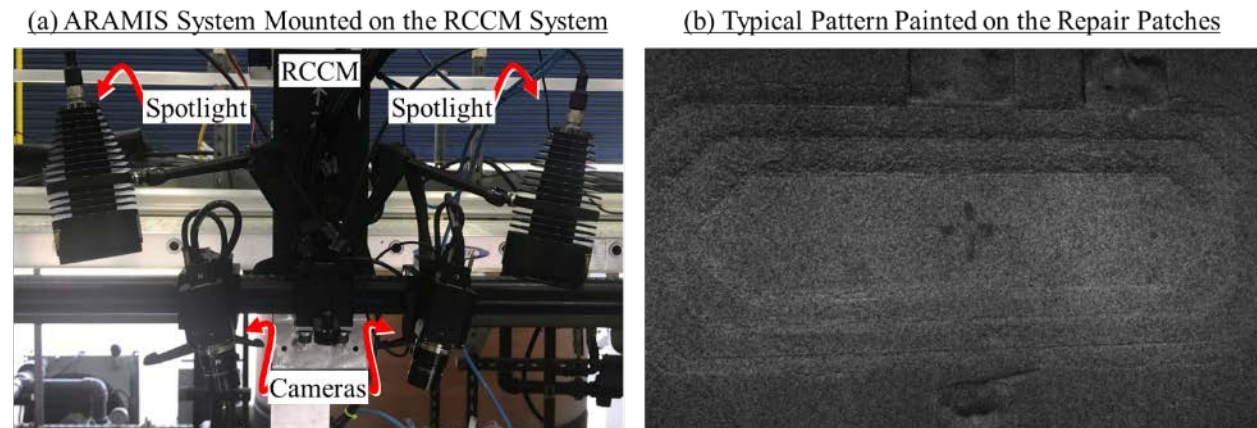


Figure G-1. (a) ARAMIS 3D DIC system mounted on the motion control assembly of the RCCM system, and (b) typical stochastic pattern painted on, and in the vicinity of, each repair patch

Specimen preparations, sensor unit configurations, pre-processing parameters, data-capture procedures, post-processing parameters, and post-processing procedures were generally consistent throughout the test. Prior to each inspection, the top surface of each repair patch and the external fuselage panel surface in the immediate vicinity of each repair patch were coated with a dull, highly contrasted, monochromatic, stochastic pattern by sporadically spraying flat black paint over a consistent layer of flat white paint, as shown in figure G-1b. To ensure appropriate resolution of results, digital images of each repair patch were captured independently using two fields of view: 1) narrow field-of-view (NFOV), which was 7.87 inches by 6.69 inches, and 2) wide field-of-view (WFOV), which was 11.81 inches by 9.84 inches. For each field-of-view, a rotational inspection approach was applied in which the RCCM system was used to position the sensor unit directly above each repair patch. When in position, the fuselage panel was subjected to the strain survey load spectrum while the high-resolution cameras captured digital images of the repair patch at each

load stage. Irrespective of the inspection, the facet sizes and step sizes were consistent for each field-of-view. For NFOV, the facet size was 20 square pixels, and the facet step size was 10 pixels. Irrespective of the field-of-view, the computation size was governed by a three-by-three grid of computation points and the validity quote (i.e., the percentage of computation points within a computation area that must exist for a computation to successfully execute) was 55%. A brief overview of the post-processing steps executed for each measurement is provided in section G.2.

G.2 POST-PROCESSING PROCEDURE

During post-processing, a median filter was applied three times for each computation point over a 5 by 5 grid of computation points using a filter quote (analogous to the validity quote) of 50%. A 3-2-1 coordinate transformation was applied to reorient each result such that the inspection region was parallel with the x - y plane. A brief example of this post-processing procedure is provided in figure G-2 using actual results obtained during the test. A raw measurement obtained for repair patch UB during a strain survey conducted in ambient environmental conditions following the completion of 40,000 cycles (i.e., immediately after repair patch UB was installed on the fuselage panel) was used for the example. Shown in figure G-2 is a comparison of the 3D ARAMIS DIC results before and after a 3-2-1 coordinate transformation. Shown in figure G-3 is a comparison of the 3D ARAMIS DIC results before and after the application of a median filter.

(a) Result Before a 3-2-1 Coordinate Transformation

(b) Result After a 3-2-1 Coordinate Transformation

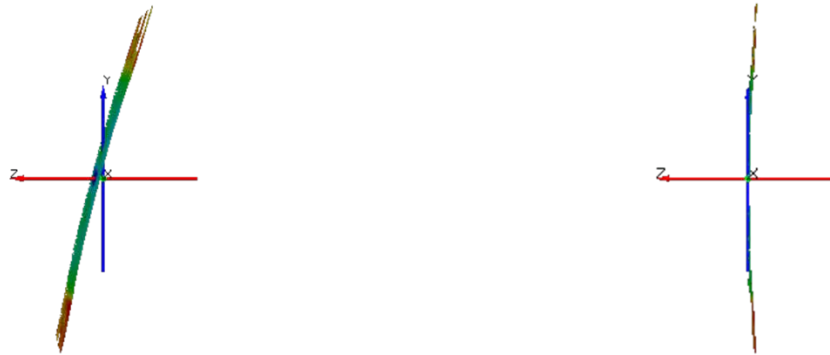
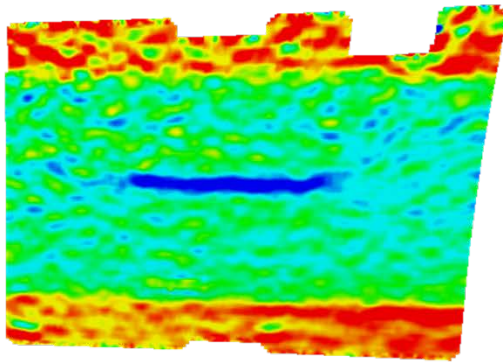


Figure G-2. Comparison of 3D ARAMIS DIC result captured in NFOV for repair patch RBC: (a) before a 3-2-1 coordinate transformation, and (b) after a 3-2-1 coordinate transformation

(a) Result Before Application of a Median Filter



(b) Result After Application of a Median Filter

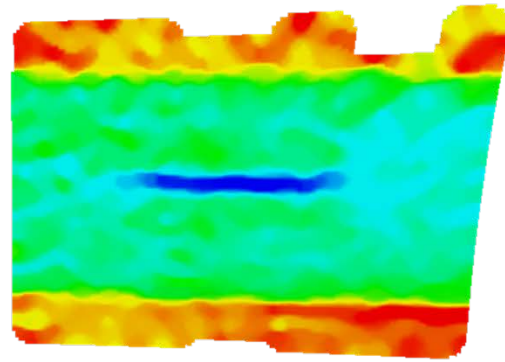


Figure G-3. Comparison of 3D ARAMIS DIC result captured in NFOV for repair patch RBC: (a) before application of a median filter and (b) after application of a median filter.

G.3 NARROW FIELD OF VIEW MEASUREMENTS

The inspection periods during which strain surveys were conducted with the 3D DIC system in the NFOV setting were strategically chosen to ensure the ability to evaluate the effect that some event (e.g., the accumulation of fatigue cycles) had on the distribution of strain. A summary of the inspection periods during which NFOV strain surveys were conducted and the applied loads during said surveys is provided in table G-1.

Table G-1. Summary of strain surveys conducted with 3D DIC system in the NFOV setting

Inspection Period	Maximum Mechanical Load	Environmental Load
Before Phase I Notch Cutting	75% of SSL Conditions	Ambient
After Phase I Notch Cutting	75% of SSL Conditions	Ambient
After Phase I Pre-Cracking	75% of SSL Conditions	Ambient
After Phase I Patch Installation	75% of SSL Conditions	Ambient
After Hot-Wet Conditioning	75% of SSL Conditions	Ambient
After 10,000 Cycles	75% of SSL Conditions	Ambient
After 20,000 Cycles	75% of SSL Conditions	Ambient
After 30,000 Cycles	75% of SSL Conditions	Ambient
After 40,000 Cycles	75% of SSL Conditions	Ambient
After 50,000 Cycles	75% of SSL Conditions	Ambient
After 60,000 Cycles	75% of SSL Conditions	Ambient
After 70,000 Cycles	75% of SSL Conditions	Ambient
After 80,000 Cycles	75% of SSL Conditions	Ambient
After 90,000 Cycles	75% of SSL Conditions	Ambient

Provided in the subsequent sections are representative results captured in the NFOV for each repair patch throughout the duration of the test. For repair patches RAC, RBC, UAC, UBC, UDAC, and

UDBC, results are provided for strain surveys conducted after patch installation, after hot-wet conditioning, after 20,000 cycles, after 40,000 cycles, and after 60,000 cycles. For repair patches UB and UDB, results are provided for strain surveys conducted after patch installation, after 10,000 cycles, and after 20,000 cycles. Results for repair patches RAC, RBC, UAC, UB, UBC, UDAC, UDB, and UDBC are provided in figures G-4 through G-11, respectively.

G.2.1 REPAIR PATCH RAC

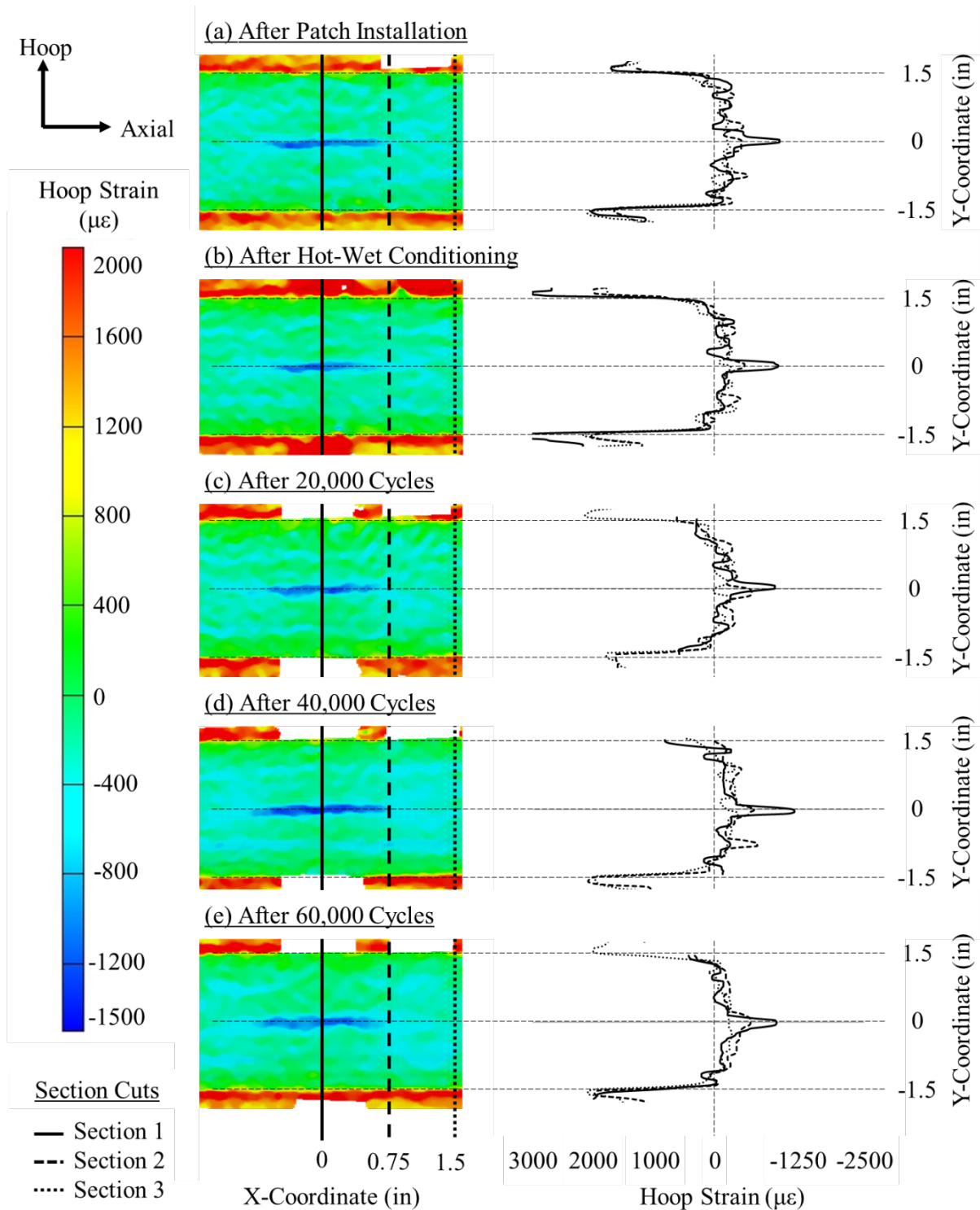


Figure G-4. Digital image correlation results captured in the NFOV for repair patch RAC: (a) after patch installation, (b) after hot-wet conditioning, (c) after 20,000 cycles, (d) after 40,000 cycles, and (e) after 60,000 cycles

G.2.2 REPAIR PATCH RBC

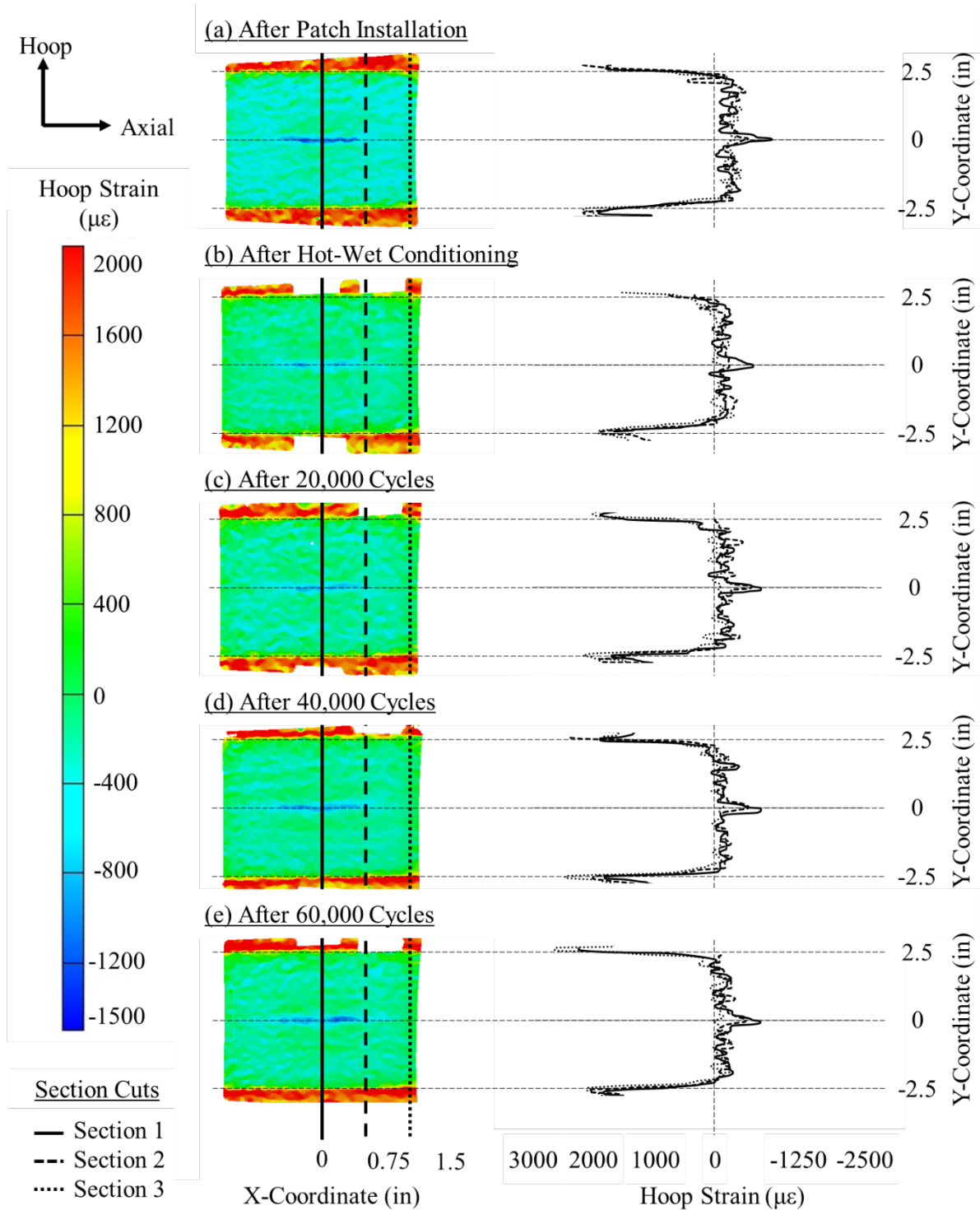


Figure G-5. Digital image correlation results captured in the NFOV for repair patch RBC; (a) after patch installation, (b) after hot-wet conditioning, (c) after 20,000 cycles, (d) after 40,000 cycles, and (e) after 60,000 cycles

G.2.3 REPAIR PATCH UAC

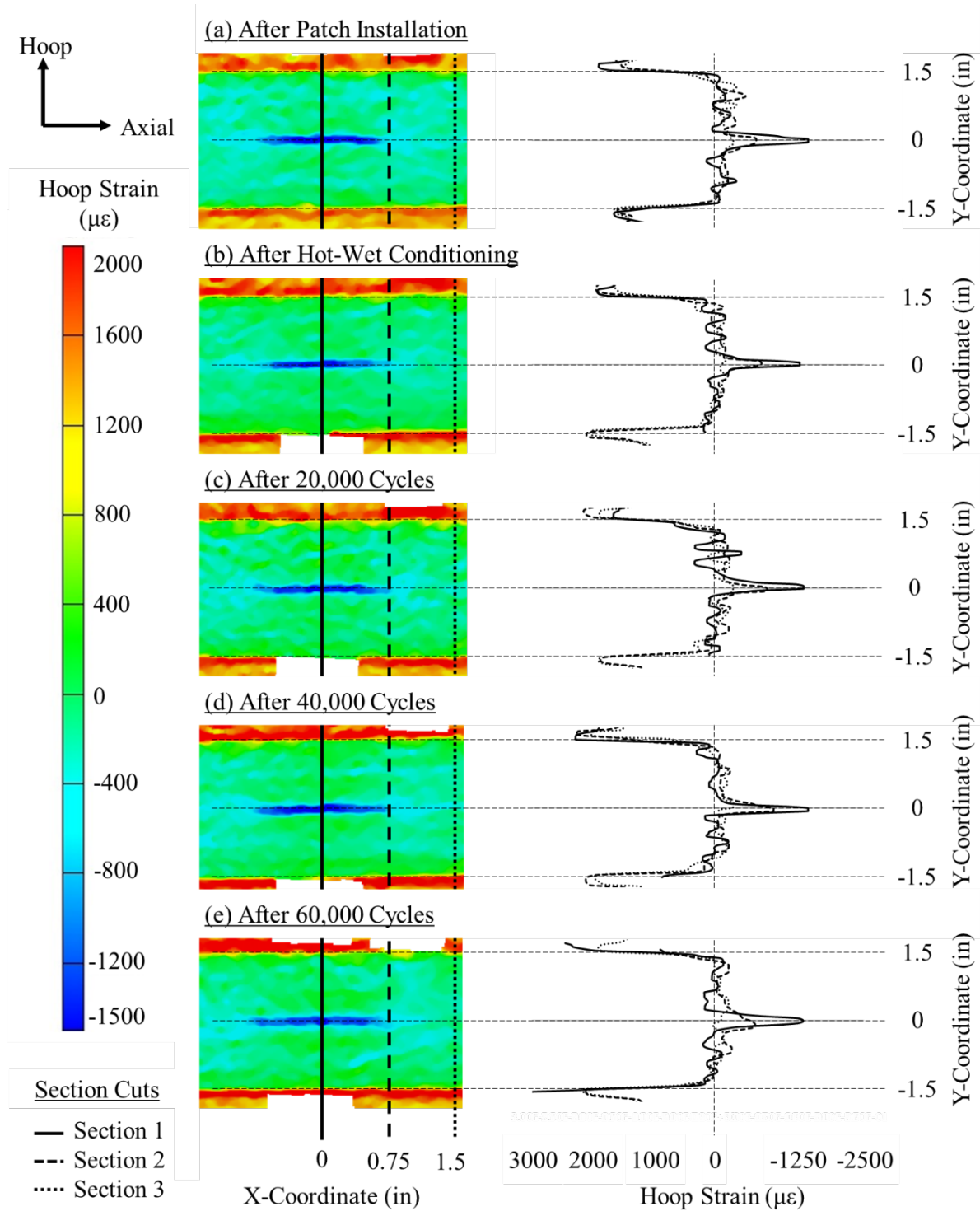


Figure G-6. Digital image correlation results captured in the NFOV for repair patch UAC: (a) after patch installation, (b) after hot-wet conditioning, (c) after 20,000 cycles, (d) after 40,000 cycles, and (e) after 60,000 cycles

G.2.4 REPAIR PATCH UB

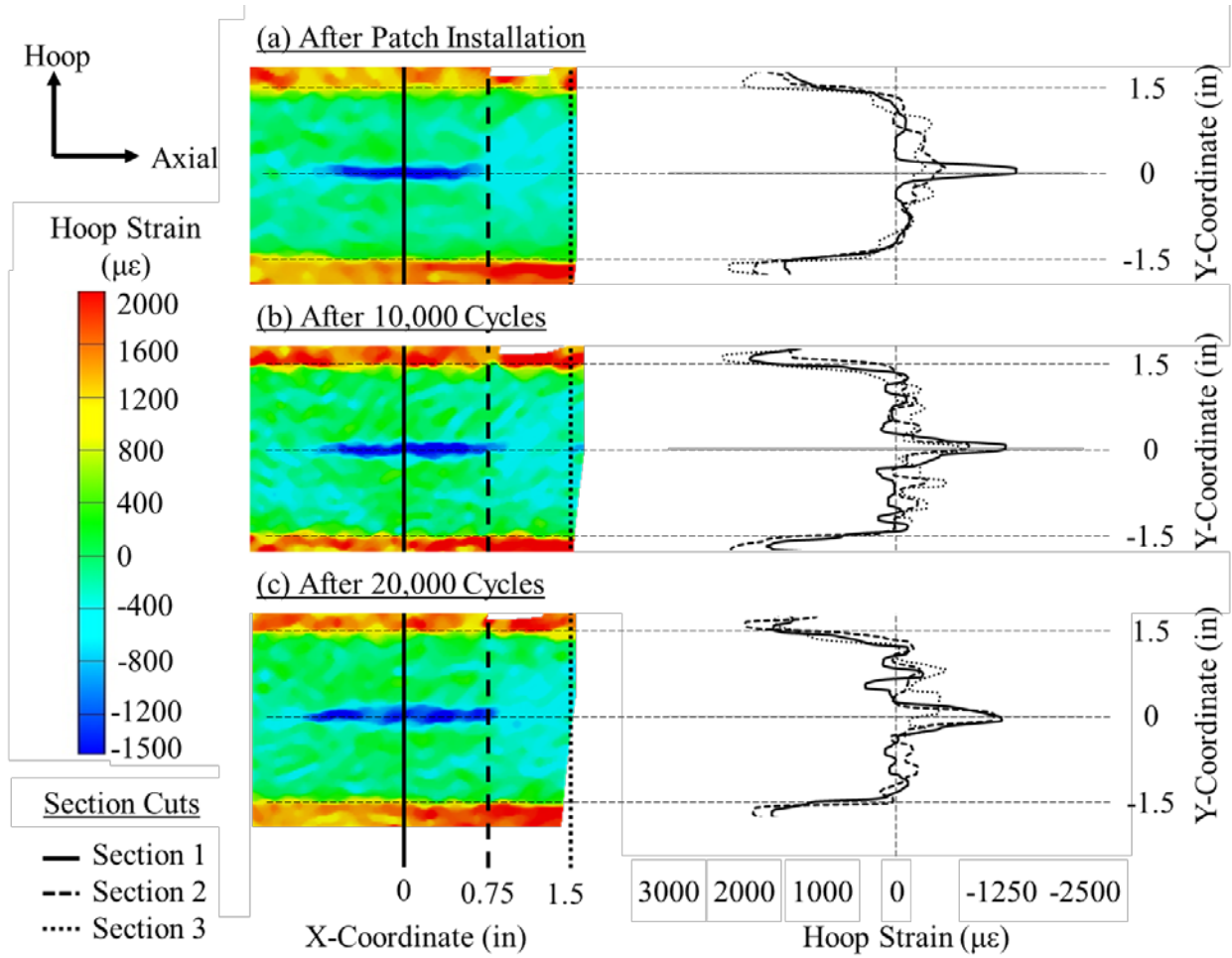


Figure G-7. Digital image correlation results captured in the NFOV for repair patch UB: (a) after patch installation, (b) after 10,000 cycles, and (c) after 20,000 cycles

G.2.5 REPAIR PATCH UBC

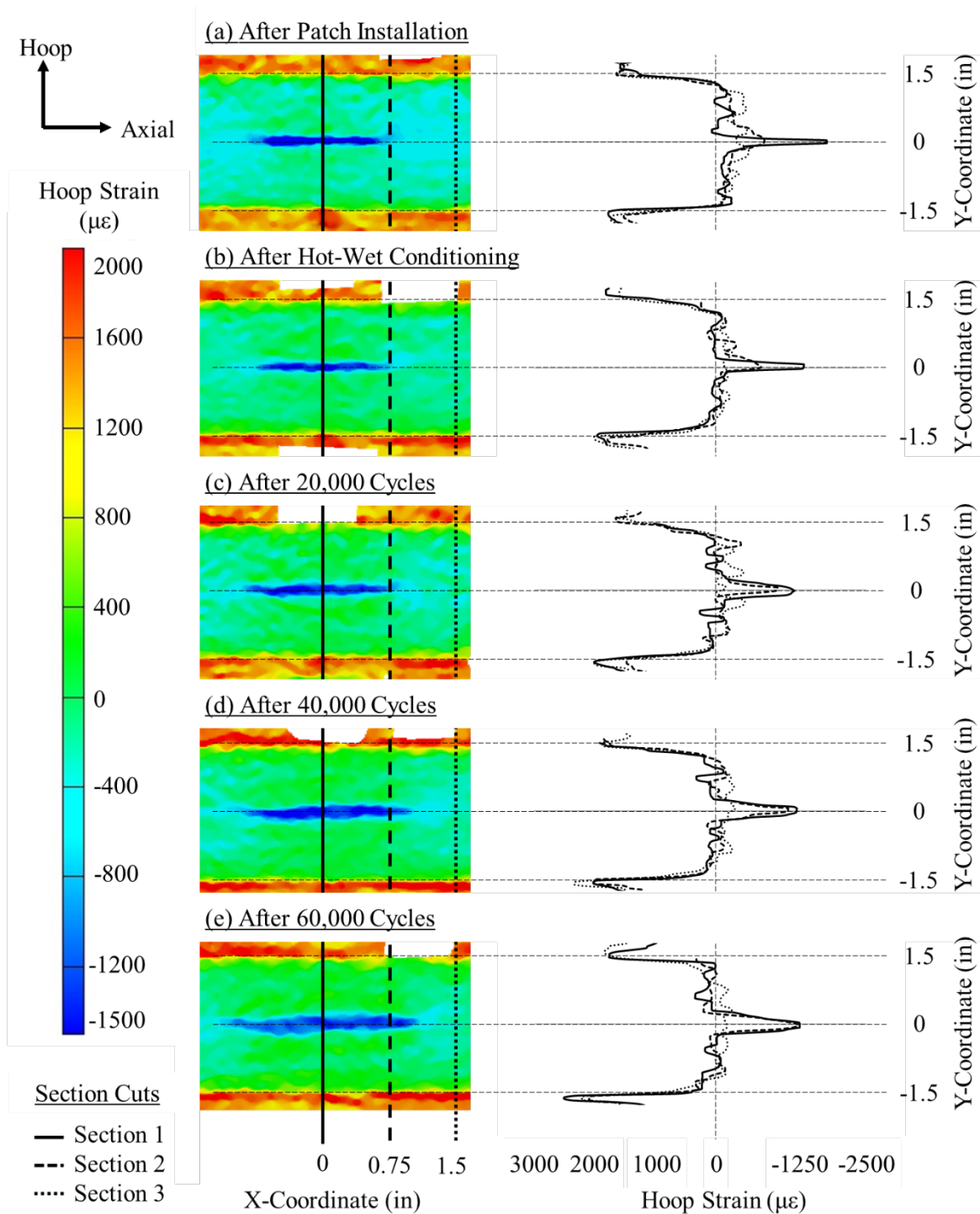


Figure G-8. Digital image correlation results captured in the NFOV for repair patch UBC: (a) after patch installation, (b) after hot-wet conditioning, (c) after 20,000 cycles, (d) after 40,000 cycles, and (e) after 60,000 cycles

G.2.6 REPAIR PATCH UDAC

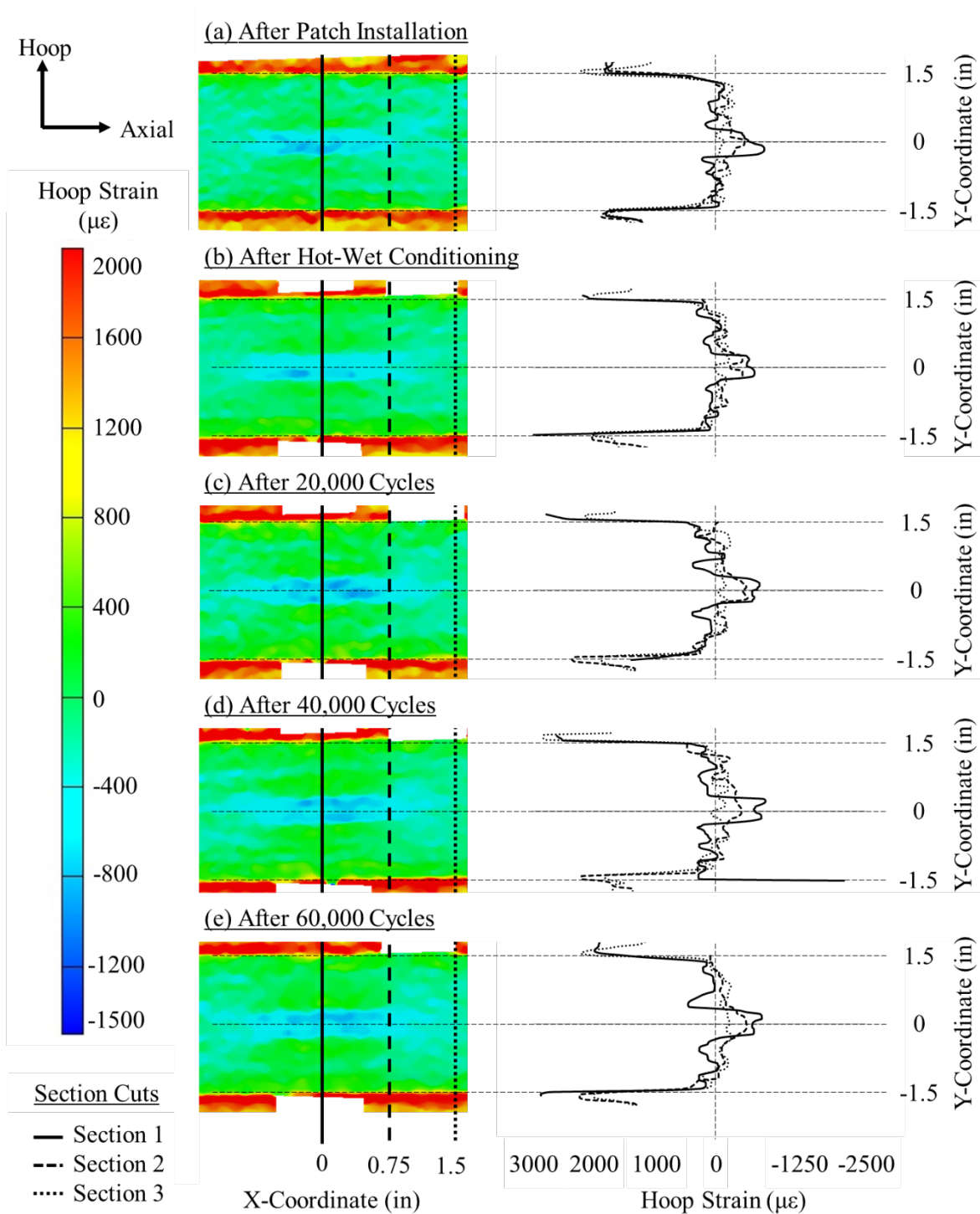


Figure G-9. Digital image correlation results captured in the NFOV for repair patch UDAC: (a) after patch installation, (b) after hot-wet conditioning, (c) after 20,000 cycles, (d) after 40,000 cycles, and (e) after 60,000 cycles

G.2.7 REPAIR PATCH UDB

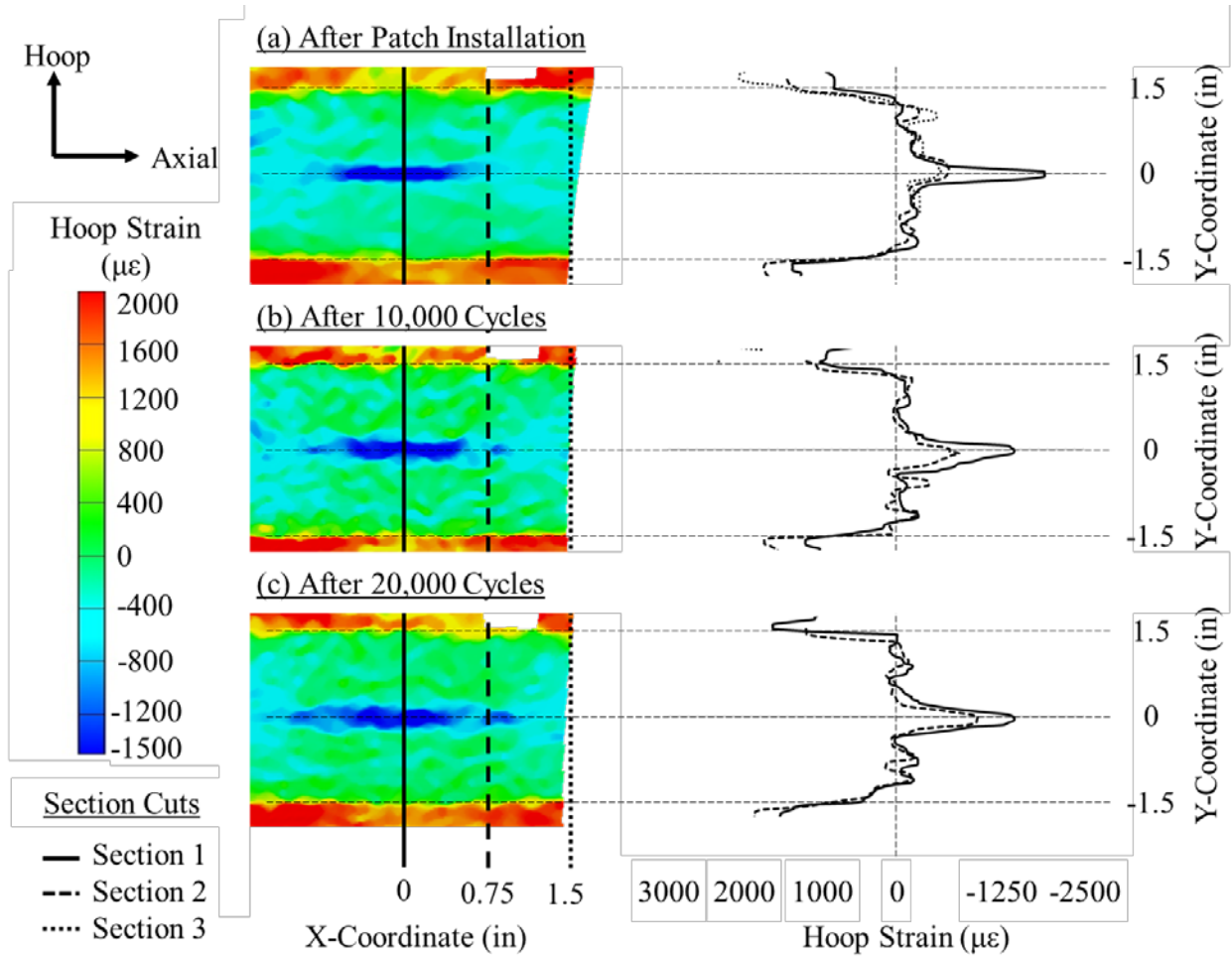


Figure G-10. Digital image correlation results captured in the NFOV for repair patch UDB: (a) after patch installation, (b) after 10,000 cycles, and (c) after 20,000 cycles

G.2.8 REPAIR PATCH UDBC

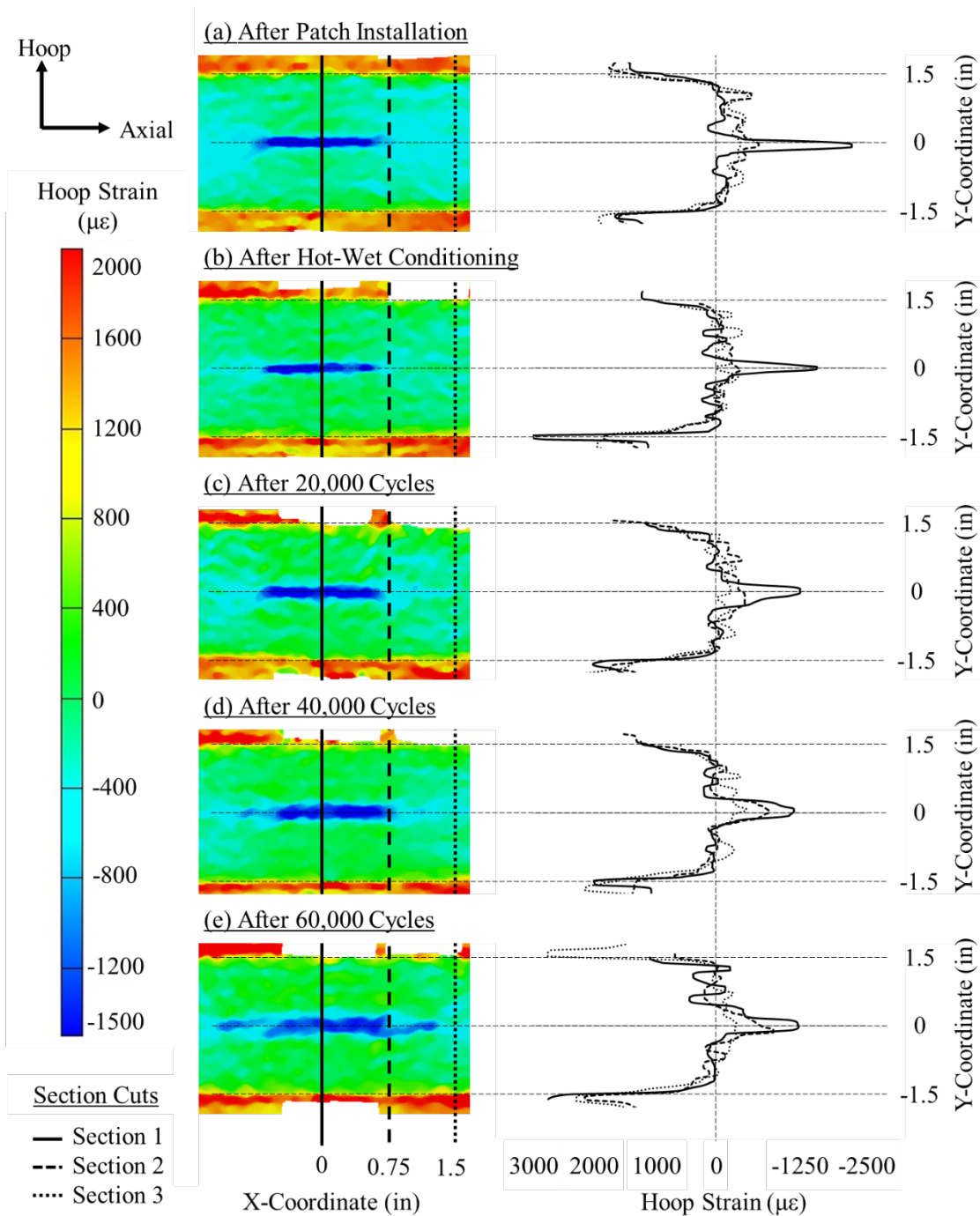


Figure G-11. Digital image correlation results captured in the NFOV for repair patch UDBC: (a) after patch installation, (b) after hot-wet conditioning, (c) after 20,000 cycles, (d) after 40,000 cycles, and (e) after 60,000 cycles

APPENDIX H—FATIGUE CRACK GROWTH RESULTS

H.1 INTRODUCTION

Throughout the duration of the test, visual and eddy current inspections were conducted to monitor the growth of each through-thickness, center-bay crack in the fuselage panel. Visual inspections were conducted quasi-continuously (during fatigue cycling), whereas eddy current inspections were conducted intermittently (during inspection periods when fatigue cycling was paused). For the visual inspections, two high-magnification camera systems were used. A remote-controlled camera system situated above the FASTER fixture was used to monitor the external surface of the fuselage panel, whereas a remote-controlled camera system situated inside the pressure box was used to monitor the internal surface of the fuselage panel.

H.1.1 High-Magnification Camera Inspections

The remote-controlled camera situated above the FASTER fixture was attached to the RCCM system, which consists of a mechanical frame assembly, a motion control assembly, and a video data-acquisition system. The mechanical frame assembly, shown in figure H-1a, includes a rectangular frame mounted on top of the four columns at the corners of the test fixture, and two nesting frames that provide the capability to adjust the axial and transverse position of the attached assembly. The motion control assembly, attached to the mechanical frame assembly as shown in figure H-1b, is comprised of three bidirectional and two unidirectional translation stages that provide additional translational ability and the attachment point for four high-magnification cameras. Controlled by a laboratory computer, the motion control system is capable of precisely and efficiently positioning the high-magnification cameras, two of which are shown in figure H-1c, above any specified location within the test section. When in position, the video data-acquisition system is capable of providing real-time crack-length measurements, recording images, and recording videos with frame rates of up to 30 frames per second.

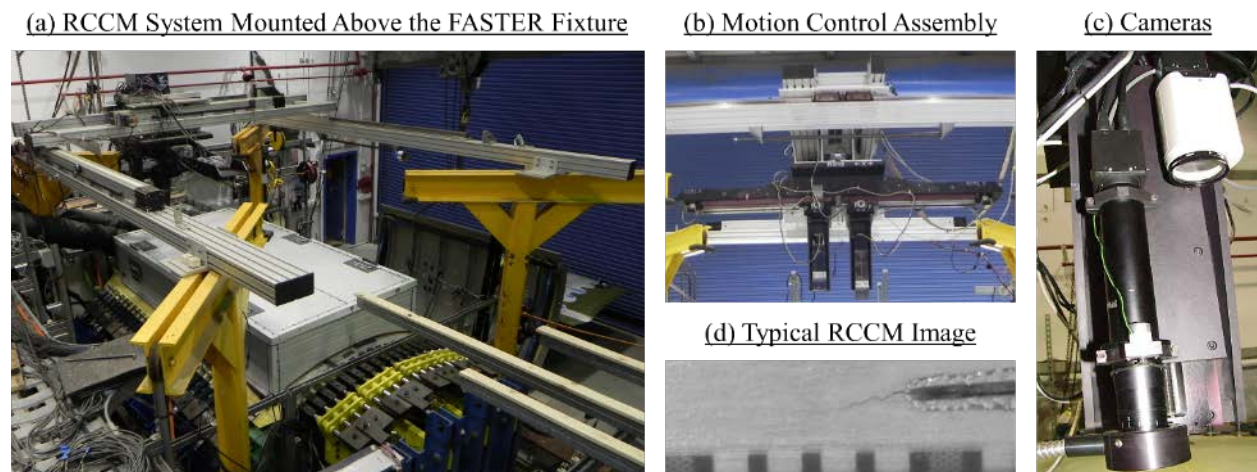


Figure H-1. (a) RCCM system mounted above the FASTER fixture, (b) motion control assembly, (c) cameras, and (d) typical image captured by RCCM system during pre-cracking

Because of the nature of the test, which used an environmental chamber to simulate environmental conditions, the external surface of the panel was not visible during fatigue cracking; therefore, the RCCM system was only used during fatigue pre-cracking, which was conducted with the environmental chamber removed. A typical image captured by this system during fatigue pre-cracking is shown in figure H-1d. Because of the limitations of the camera system, which only allowed for monitoring of a single instance of damage at a given time, a rotational inspection approach was applied. Every 100 to 500 cycles during fatigue pre-cracking, a test administrator moved the camera over each instance of damage to conduct visual measurements of each half-crack. If an appreciable difference in crack length was observed when compared to the previous inspection, a digital image of the half-crack was recorded and archived. For each instance of damage, translucent grids featuring 0.05-inch spacing, taped next to each crack tip, as shown in figure H-1d, were used to aid in the visual assessments of crack length.

The remote-controlled camera situated inside the pressure box consists of a Spectrum 120™ high-definition camera, a MicroTrac Flat Platform, a tether, and a Versatrax Rack Mount Controller. Mounted to the chassis of the MicroTrac Flat Platform, the Spectrum 120 high-definition camera features four high-intensity LEDs and is capable of zooming up to 432x, tilting up to 280°, and panning up to 360°. The complete system is tether-connected to a break-out box that connects to a laboratory computer monitor and the Versatrax Rack Mount Controller, both of which were located in the laboratory control room. The Spectrum 120 high-definition camera, the MicroTrac Flat Platform, and the tether, shown in figure H-2a, are each rated to operate under a hydrostatic pressure of approximately 42 psi.

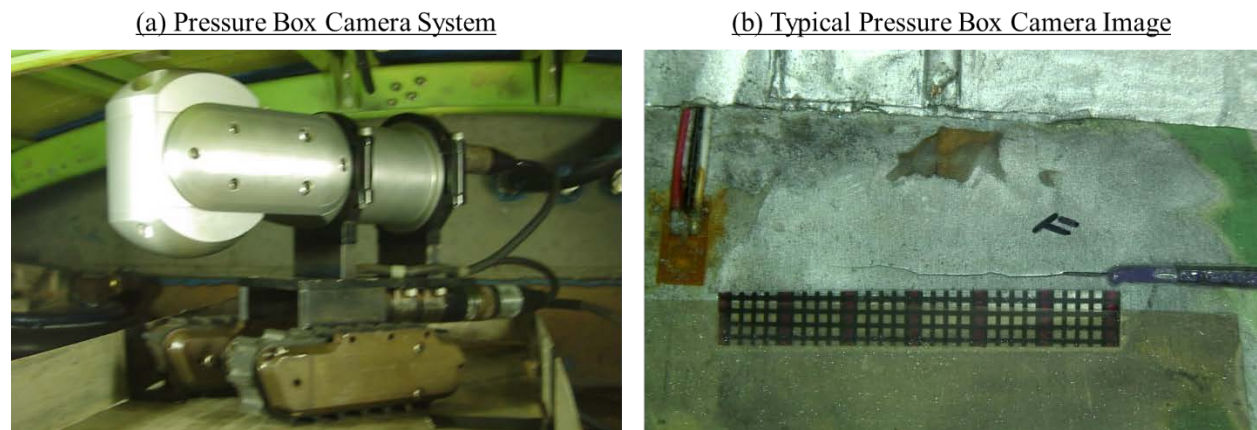


Figure H-2. (a) The pressure box camera system underneath a fuselage panel and (b) a typical image captured by the pressure box camera system during fatigue cracking

Because of the nature of the test, which used an environmental chamber to simulate environmental conditions, only the internal surface of the panel was viewable during fatigue cracking; therefore, the pressure box camera system was the only system capable of monitoring the formation and growth of damage in the fuselage panel during fatigue cracking. A typical image captured by this system during fatigue cracking is shown in figure H-2b. Because of the limitations of the camera system, which only allowed for monitoring of a single instance of damage at a given time, a rotational inspection approach was applied. Every 100 to 500 cycles during fatigue cracking, a test administrator moved the camera below each instance of damage to conduct visual measurements

of each half-crack. If an appreciable difference in crack length was observed when compared to the previous inspection, a digital image of the half-crack was recorded and archived. For each instance of damage, translucent grids featuring 0.05-inch spacing, taped next to each crack tip as shown in figure H-2b, were used to aid in the visual assessments of crack length.

H.1.2 Eddy Current Inspections

Eddy current is a non-destructive inspection method that utilizes measured changes in electrical impedance to detect surface and subsurface flaws (e.g., cracks or voids) in electrically conductive specimens. Throughout the duration of the test, an Olympus Nortec® 500D Eddy Current Flow Detector (P/N 7720140.00), a system capable of inducing AC signals with frequencies ranging from 50 Hz to 12 MHz, shown in figure H-3a, was used in conjunction with two detachable probes to monitor the growth of the through-thickness, center-bay cracks underneath each adhesively bonded repair patch. A PowerLink™ Standard Bridge Detachable Surface Probe (P/N 9222161) featuring a tip diameter of 0.31 inch and an operating frequency range of 1 to 50 kHz, shown in figure H-3c, was used to conduct LFEC inspections on the top of each repair patch; a PowerLink™ Absolute Shielded Metal Detachable Pencil Probe (P/N 9403410) featuring a tip diameter of 0.13 inch and an operating frequency range of 50 to 500 kHz, shown in figure H-3b, was used to conduct HFEC inspections on the internal fuselage panel surface under each repair patch. Specimen preparations, pre-processing parameters, data-capture procedures, and post-processing procedures were generally consistent throughout the duration of the test. Because of the requirements of the digital image correlation system, each inspection region was coated with a dull, highly contrasted, monochromatic, stochastic pattern. Prior to each inspection, this coating was removed. When the coating was removed, the system was configured and inspections were conducted.

(a) Olympus Nortec® 500D Eddy Current Flow Detector



(b) PowerLink™ Detachable Pencil Probe



(c) PowerLink™ Detachable Surface Probe



Figure H-3. (a) Portable Eddy Current Flow Detector, (b) PowerLink™ Absolute Shielded Metal Detachable Pencil Probe, and (c) PowerLink™ Standard Bridge Detachable Surface Probe

Adjustable parameters prior to and during acquisition included the: 1) phase angle, 2) horizontal signal gain, 3) vertical signal gain, and 4) frequency. Prior to HFEC inspections, the phase angle was set to 100 degrees, the horizontal signal gain was set to 57.1 dB, the vertical signal gain was set to 72.1 dB, and the frequency was set to 210 kHz. Prior to LFEC inspections, the phase angle was set to 4 degrees, the horizontal signal gain was set to 53.5 dB, the vertical signal gain was set

to 68.9 dB, and the frequency was set to 3 kHz. Subsequently, for each inspection type, using each damage and repair patch scenario, these values were adjusted to ensure that specific indications for each repair type (e.g., those caused by detection of a crack while passing the LFEC probe over the top surface of the repair patch) were appropriately distributed in the instrument's plot of inductive reactance versus the impedance of the metal wire coil in the probe. Specific indications included those which were observed during: 1) inspection of an area with no known imperfections; 2) suspension of the probe in air (i.e., during liftoff); 3) inspection of the crack from the internal surface of the fuselage panel; and 4) inspection of the crack from the top surface of the repair patch. In each case, the system was calibrated to ensure that the indications for each case were visible within the instrument plot, as shown in figure H-3a.

During each inspection period, the LFEC and HFEC probes were methodically relocated over the top surface of each repair patch and the internal fuselage panel surface underneath the footprint of each repair patch, respectively. Irrespective of the probe that was used, an imperfection that resulted in a vertical response on the plot of inductive reactance versus impedance, as shown in figure H-3a, was deemed a significant indication that a crack was present. When the crack was found with a probe, the indications were followed horizontally outward from the geometric center of the repair patch footprint to the point at which indications were no longer present. At this point, the half-crack was measured and recorded. For each instance of damage (i.e., each half-crack), translucent grids featuring 0.05-inch spacing, taped next to each crack tip, as shown in figure H-2a, were used to aid in the HFEC and LFEC assessments of crack length.

H.2 FATIGUE PRE-CRACKING RESULTS

As mentioned previously, inspections during fatigue pre-cracking were conducted exclusively from the external fuselage panel surface. Visual inspections were conducted with the remote-controlled camera system situated directly above the FASTER fixture, whereas HFEC inspections were conducted with the Olympus Nortec® 500D eddy current flaw detector and the PowerLink™ Absolute Shielded Metal Detachable Pencil Probe. Because of the limitations of the camera system, which only allowed for monitoring of a single instance of damage at a given time, a rotational inspection approach was applied. Every 100 to 500 cycles during fatigue pre-cracking, a test administrator moved the high-magnification camera over each instance of damage to conduct visual measurements of each half-crack. If an appreciable difference in crack length was observed when compared to the previous inspection, a digital image of the half-crack was recorded and archived. When visual inspections indicated a crack had grown to approximately 3 inches in length, fatigue pre-cracking was halted and HFEC inspections were conducted to verify the measurements. Results recorded during fatigue pre-cracking are provided in the subsequent sections.

H.2.1 HALF-CRACK MEASUREMENTS, TABULATED

Provided in the subsequent sections are tables containing half-crack measurements obtained via visual and HFEC inspections during fatigue pre-cracking for repair patches RAC, RBC, UAC, UB, UBC, UDAC, UDB, and UDBC, respectively.

H.2.1.1 REPAIR PATCH RAC

Table H-1. Raw data, half-crack length measurements obtained during fatigue pre-cracking for repair patch RAC

Cycles	Visual			High Frequency Eddy Current			Low Frequency Eddy Current		
	a _{fwd} (inches)	a _{aft} (inches)	a _{avg} (inches)	a _{fwd} (inches)	a _{aft} (inches)	a _{avg} (inches)	a _{fwd} (inches)	a _{aft} (inches)	a _{avg} (inches)
0	1.40	1.40	1.40	-	-	-	-	-	-
531	1.41	1.43	1.42	-	-	-	-	-	-
747	1.44	1.43	1.44	-	-	-	-	-	-
1073	1.47	1.45	1.46	-	-	-	-	-	-
1243	1.49	1.48	1.49	-	-	-	-	-	-
1355	1.50	1.49	1.50	-	-	-	-	-	-
1359	-	-	-	1.50	1.49	1.49	-	-	-

H.2.1.2 REPAIR PATCH RBC

Table H-2. Raw data, half-crack length measurements obtained during fatigue pre-cracking for repair patch RBC

Cycles	Visual			High Frequency Eddy Current			Low Frequency Eddy Current		
	a _{fwd} (inches)	a _{aft} (inches)	a _{avg} (inches)	a _{fwd} (inches)	a _{aft} (inches)	a _{avg} (inches)	a _{fwd} (inches)	a _{aft} (inches)	a _{avg} (inches)
0	1.40	1.40	1.40	-	-	-	-	-	-
540	1.42	1.41	1.42	-	-	-	-	-	-
770	1.43	1.45	1.44	-	-	-	-	-	-
1033	1.44	1.44	1.44	-	-	-	-	-	-
1233	1.47	1.47	1.47	-	-	-	-	-	-
1346	1.47	1.48	1.48	-	-	-	-	-	-
1359	-	-	-	1.46	1.49	1.48	-	-	-

H.2.1.3 REPAIR PATCH UAC

Table H-3. Raw data, half-crack length measurements obtained during fatigue pre-cracking for repair patch UAC

Cycles	Visual			High Frequency Eddy Current			Low Frequency Eddy Current		
	a _{fwd} (inches)	a _{aft} (inches)	a _{avg} (inches)	a _{fwd} (inches)	a _{aft} (inches)	a _{avg} (inches)	a _{fwd} (inches)	a _{aft} (inches)	a _{avg} (inches)
0	1.40	1.40	1.40	-	-	-	-	-	-
495	1.41	1.42	1.41	-	-	-	-	-	-
810	1.44	1.45	1.45	-	-	-	-	-	-
996	1.45	1.45	1.45	-	-	-	-	-	-
1204	1.47	1.47	1.47	-	-	-	-	-	-
1337	1.48	1.49	1.49	-	-	-	-	-	-
1359	-	-	-	1.50	1.50	1.50	-	-	-

H.2.1.4 REPAIR PATCH UB

Table H-4. Raw data, half-crack length measurements obtained during fatigue pre-cracking for repair patch UB

Cycles	Visual			High Frequency Eddy Current			Low Frequency Eddy Current		
	a _{fwd} (inches)	a _{aft} (inches)	a _{avg} (inches)	a _{fwd} (inches)	a _{aft} (inches)	a _{avg} (inches)	a _{fwd} (inches)	a _{aft} (inches)	a _{avg} (inches)
0	1.40	1.40	1.40	-	-	-	-	-	-
923	1.47	1.47	1.47	-	-	-	-	-	-
1200	1.51	1.50	1.50	-	-	-	-	-	-
1284	1.50	1.49	1.49	-	-	-	-	-	-
1302	1.49	1.49	1.49	-	-	-	-	-	-
1337	1.51	1.50	1.95	-	-	-	-	-	-
1377	1.50	1.50	1.50	-	-	-	-	-	-
1433	1.50	1.51	1.50	-	-	-	-	-	-
1500	-	-	-	1.54	1.53	1.54	-	-	-

H.2.1.5 REPAIR PATCH UBC

Table H-5. Raw data, half-crack length measurements obtained during fatigue pre-cracking for repair patch UBC

Cycles	Visual			High Frequency Eddy Current			Low Frequency Eddy Current		
	a _{fwd} (inches)	a _{aft} (inches)	a _{avg} (inches)	a _{fwd} (inches)	a _{aft} (inches)	a _{avg} (inches)	a _{fwd} (inches)	a _{aft} (inches)	a _{avg} (inches)
0	1.40	1.40	1.40	-	-	-	-	-	-
484	1.41	1.42	1.42	-	-	-	-	-	-
760	1.43	1.45	1.44	-	-	-	-	-	-
1047	1.45	1.45	1.45	-	-	-	-	-	-
1237	1.48	1.46	1.47	-	-	-	-	-	-
1341	1.49	1.46	1.48	-	-	-	-	-	-
1359	-	-	-	1.48	1.49	1.48	-	-	-

H.2.1.6 REPAIR PATCH UDAC

Table H-6. Raw data, half-crack length measurements obtained during fatigue pre-cracking for repair patch UDAC

Cycles	Visual			High Frequency Eddy Current			Low Frequency Eddy Current		
	a _{fwd} (inches)	a _{aft} (inches)	a _{avg} (inches)	a _{fwd} (inches)	a _{aft} (inches)	a _{avg} (inches)	a _{fwd} (inches)	a _{aft} (inches)	a _{avg} (inches)
0	1.40	1.40	1.40	-	-	-	-	-	-
451	1.42	1.41	1.42	-	-	-	-	-	-
793	1.44	1.44	1.44	-	-	-	-	-	-
988	1.45	1.45	1.45	-	-	-	-	-	-
1207	1.46	1.46	1.46	-	-	-	-	-	-
1329	1.47	1.48	1.47	-	-	-	-	-	-
1359	-	-	-	1.50	1.49	1.50	-	-	-

H.2.1.7 REPAIR PATCH UDB

Table H-7. Raw data, half-crack length measurements obtained during fatigue pre-cracking for repair patch UDB

Cycles	Visual			High Frequency Eddy Current			Low Frequency Eddy Current		
	a _{fwd} (inches)	a _{aft} (inches)	a _{avg} (inches)	a _{fwd} (inches)	a _{aft} (inches)	a _{avg} (inches)	a _{fwd} (inches)	a _{aft} (inches)	a _{avg} (inches)
0	1.40	1.40	1.40	-	-	-	-	-	-
350	1.42	1.42	1.42	-	-	-	-	-	-
573	1.43	1.43	1.43	-	-	-	-	-	-
749	1.44	1.43	1.44	-	-	-	-	-	-
935	1.46	1.45	1.46	-	-	-	-	-	-
1200	1.47	1.49	1.48	-	-	-	-	-	-
1272	1.49	1.50	1.50	-	-	-	-	-	-
1298	1.49	1.49	1.49	-	-	-	-	-	-
1331	1.50	1.50	1.50	-	-	-	-	-	-
1377	1.50	1.50	1.50	-	-	-	-	-	-
1428	1.50	1.50	1.50	-	-	-	-	-	-
1500	-	-	-	1.51	1.52	1.52	-	-	-

H.2.1.8 REPAIR PATCH UDBC

Table H-8. Raw data, half-crack length measurements obtained during fatigue pre-cracking for repair patch UDBC

Cycles	Visual			High Frequency Eddy Current			Low Frequency Eddy Current		
	a _{fwd} (inches)	a _{aft} (inches)	a _{avg} (inches)	a _{fwd} (inches)	a _{aft} (inches)	a _{avg} (inches)	a _{fwd} (inches)	a _{aft} (inches)	a _{avg} (inches)
0	1.40	1.40	1.40	-	-	-	-	-	-
470	1.43	1.42	1.43	-	-	-	-	-	-
739	1.45	1.42	1.44	-	-	-	-	-	-
1066	1.46	1.45	1.45	-	-	-	-	-	-
1240	1.48	1.46	1.47	-	-	-	-	-	-
1359	1.50	1.48	1.49	1.50	1.50	1.50	-	-	-

H.2.2 HALF-CRACK MEASUREMENTS, GRAPHED

Provided in the subsequent sections are plots displaying half-crack measurements obtained via visual and HFEC inspections during fatigue pre-cracking for repair patches RAC, RBC, UAC, UB, UBC, UDAC, UDB, and UDBC, respectively.

H.2.2.1 REPAIR PATCH RAC

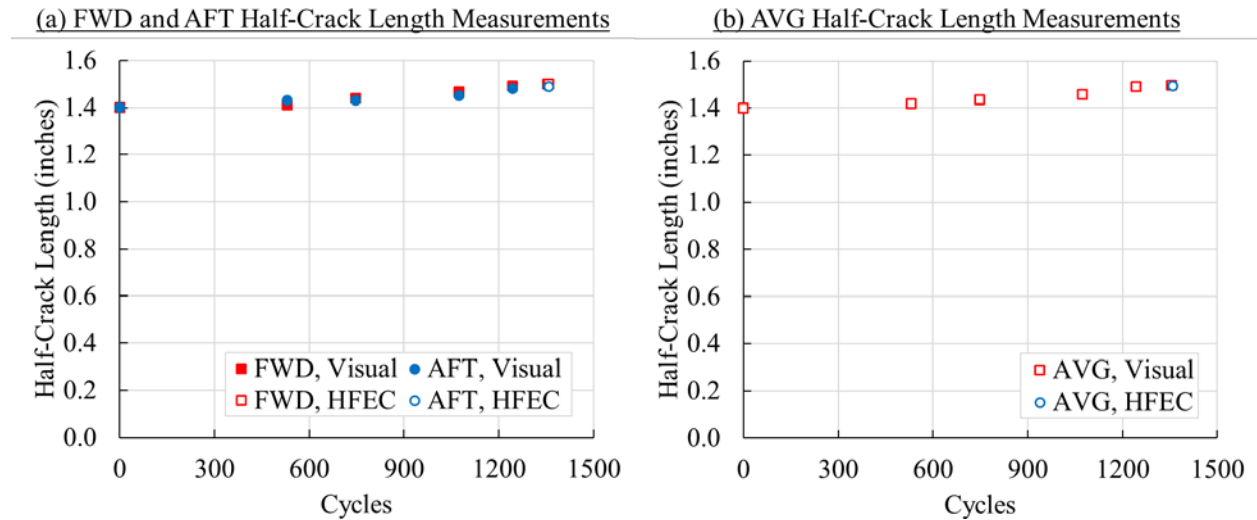


Figure H-4. Half-crack length measurements conducted during fatigue pre-cracking for repair patch RAC: (a) FWD and AFT half-crack results and (b) AVG half-crack results

H.2.2.2 REPAIR PATCH RBC

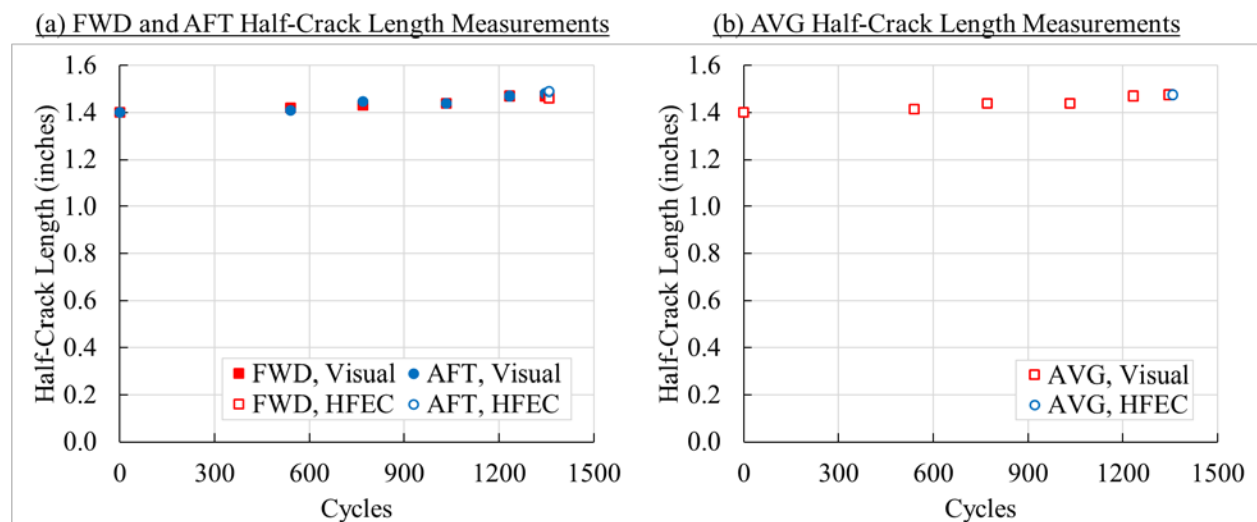


Figure H-5. Half-crack length measurements conducted during fatigue pre-cracking for repair patch RBC: (a) FWD and AFT half-crack results and (b) AVG half-crack results

H.2.2.3 REPAIR PATCH UAC

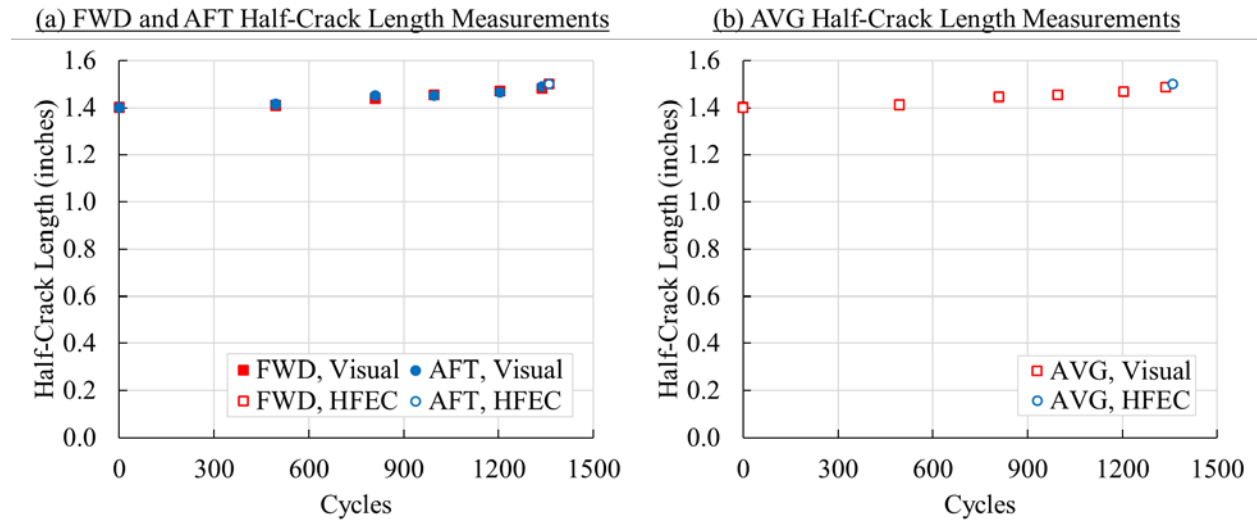


Figure H-6. Half-crack length measurements conducted during fatigue pre-cracking for repair patch UAC: (a) FWD and AFT half-crack results and (b) AVG half-crack results

H.2.2.4 REPAIR PATCH UB

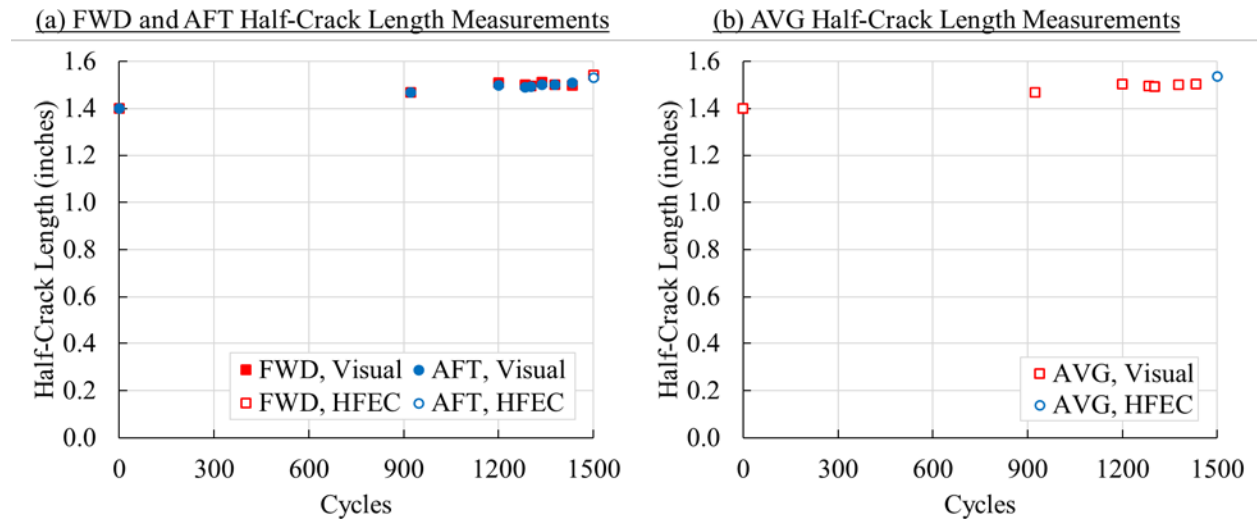


Figure H-7. Half-crack length measurements conducted during fatigue pre-cracking for repair patch UB: (a) FWD and AFT half-crack results and (b) AVG half-crack results

H.2.2.5 REPAIR PATCH UBC

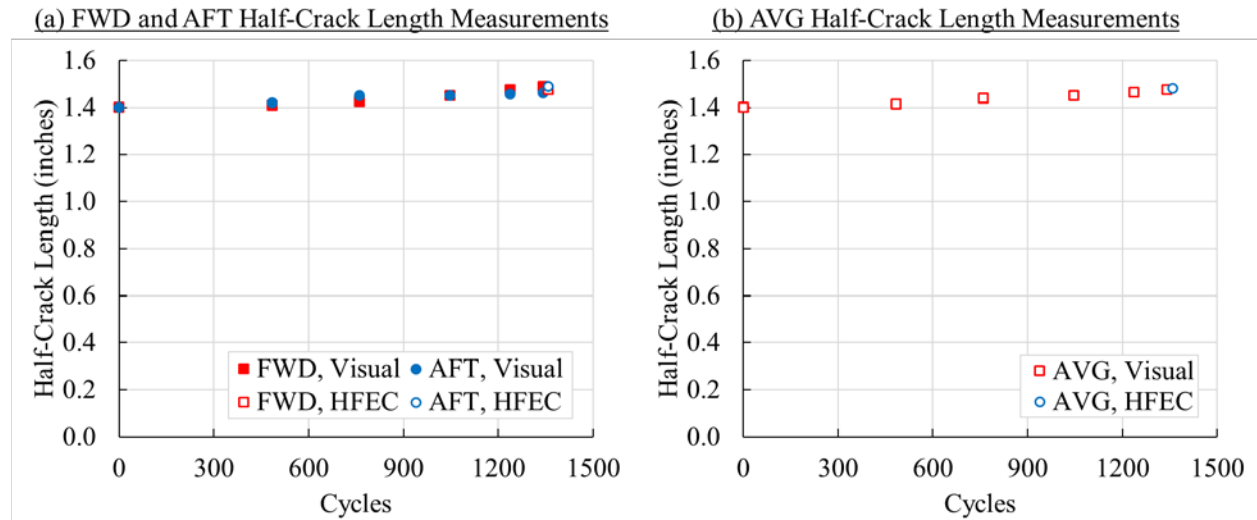


Figure H-8. Half-crack length measurements conducted during fatigue pre-cracking for repair patch UBC: (a) FWD and AFT half-crack results and (b) AVG half-crack results

H.2.2.6 REPAIR PATCH UDAC

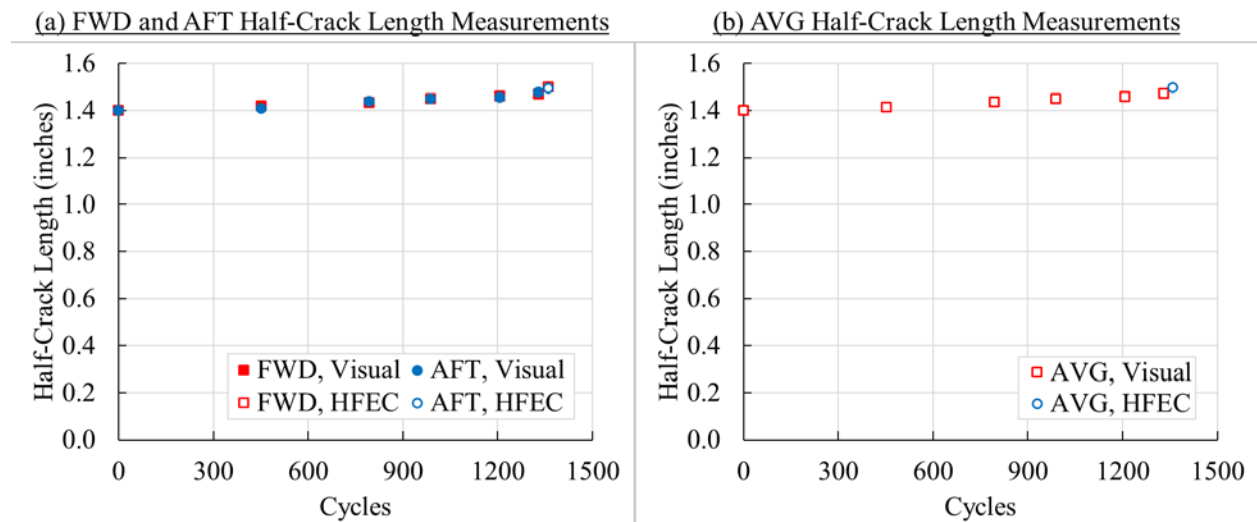


Figure H-9. Half-crack length measurements conducted during fatigue pre-cracking for repair patch UDAC: (a) FWD and AFT half-crack results and (b) AVG half-crack results

H.2.2.7 REPAIR PATCH UDB

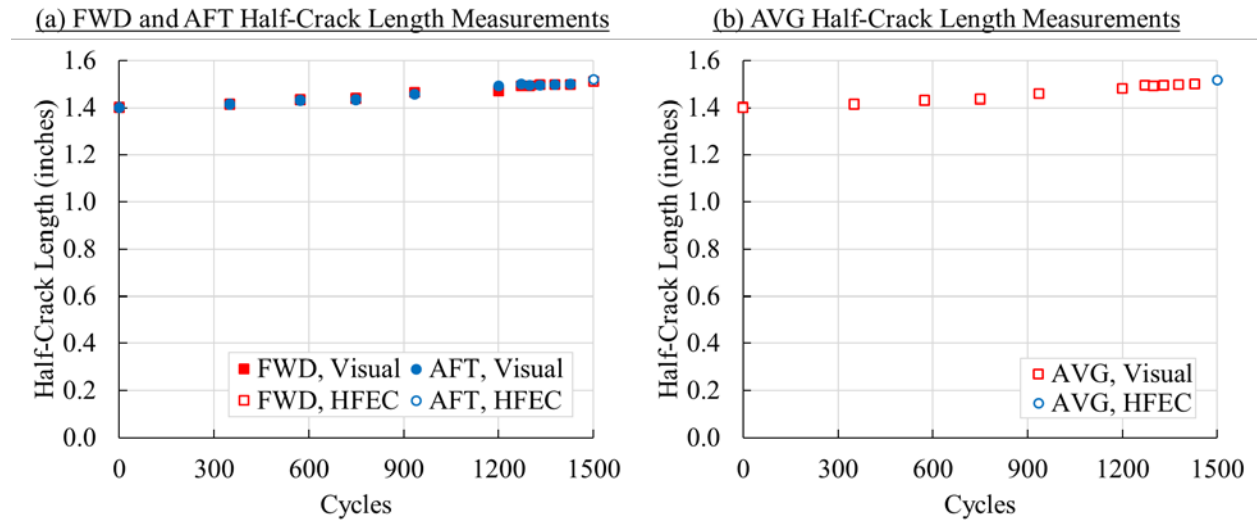


Figure H-10. Half-crack length measurements conducted during fatigue pre-cracking for repair patch UDB: (a) FWD and AFT half-crack results and (b) AVG half-crack results

H.2.2.8 REPAIR PATCH UDBC

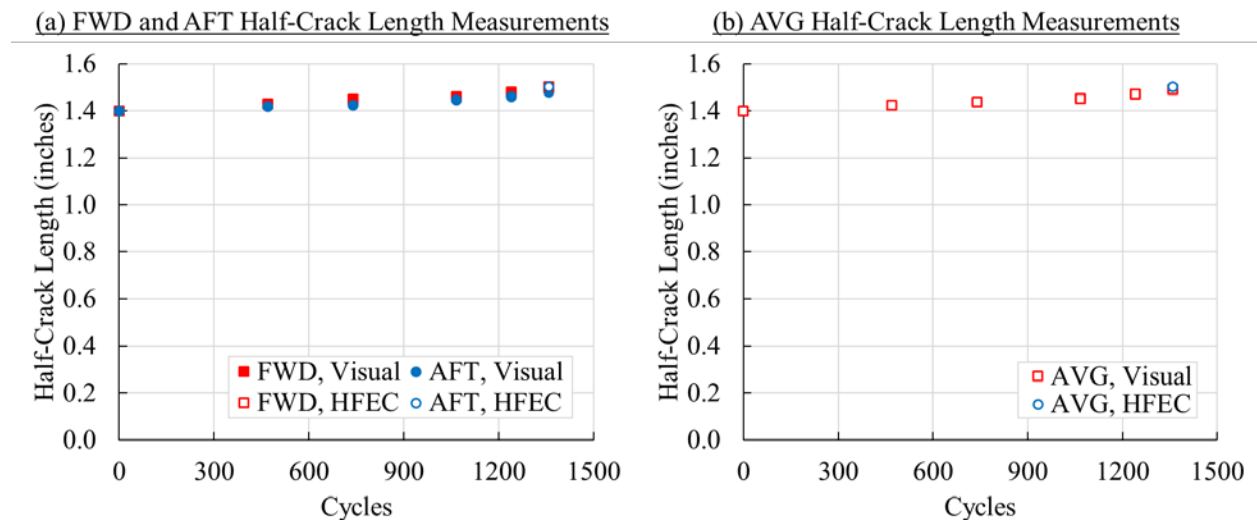


Figure H-11. Half-crack length measurements conducted during fatigue pre-cracking for repair patch UDBC: (a) FWD and AFT half-crack results and (b) AVG half-crack results

H.3 FATIGUE CRACKING RESULTS

Inspections during fatigue cracking were conducted from both the internal and the external fuselage panel surfaces. Visual inspections were conducted with the remote-controlled camera system situated inside the pressure box, HFEC inspections were conducted with the Olympus Nortec[®] 500D eddy current flaw detector and the PowerLink[™] Absolute Shielded Metal Detachable Pencil Probe, and LFEC inspections were conducted with the Olympus Nortec[®] 500D

eddy current flaw detector and the PowerLink™ Standard Bridge Detachable Surface Probe. Because of the limitations of the camera system, which only allowed for monitoring of a single instance of damage at a given time, a rotational inspection approach was applied. Every 100 to 500 cycles during fatigue cracking, a test administrator moved the high-magnification camera underneath each instance of damage to conduct visual measurements of each half-crack. If an appreciable difference in crack length was observed when compared to the previous inspection, a digital image of the half-crack was recorded and archived. Subsequently, during inspection periods, eddy current inspections were conducted. A summary of the inspection periods during which eddy current inspections were conducted is provided in table H-9. Results recorded during fatigue cracking are provided in the subsequent sections.

Table H-9. Summary of flash thermography inspections

Inspection Period	Repair Patches Inspected
After Phase I Patch Installation	RAC, RBC, UAC, UBC, UDAC, UDBC
After 10,000 Cycles	RAC, RBC, UAC, UBC, UDAC, UDBC
After 20,000 Cycles	RAC, RBC, UAC, UBC, UDAC, UDBC
After 40,000 Cycles	RAC, RBC, UAC, UBC, UDAC, UDBC
After 50,000 Cycles	RAC, RBC, UAC, UB, UBC, UDAC, UDB, UDBC
After 60,000 Cycles	RAC, RBC, UAC, UB, UBC, UDAC, UDB, UDBC
After 80,000 Cycles	RAC, RBC, UAC, UB, UBC, UDAC, UDB, UDBC
After 92,834 Cycles	RAC, RBC, UAC, UB, UBC, UDAC, UDB, UDBC

H.3.1 HALF-CRACK MEASUREMENTS, TABULATED

Provided in the subsequent sections are tables containing half-crack measurements obtained via visual, HFEC, and LFEC inspections during fatigue cracking for repair patches RAC, RBC, UAC, UB, UBC, UDAC, UDB, and UDBC, respectively.

H.3.1.1 REPAIR PATCH RAC

Table H-10. Raw data, half-crack length measurements obtained during fatigue cracking for repair patch RAC

Cycles	Visual			High Frequency Eddy Current			Low Frequency Eddy Current		
	a _{fwd} (inches)	a _{aft} (inches)	a _{avg} (inches)	a _{fwd} (inches)	a _{aft} (inches)	a _{avg} (inches)	a _{fwd} (inches)	a _{aft} (inches)	a _{avg} (inches)
0	1.50	1.49	1.50	1.50	1.49	1.49	1.46	1.40	1.43
200	1.50	1.49	1.50	-	-	-	-	-	-
400	1.50	1.49	1.50	-	-	-	-	-	-
600	1.50	1.49	1.50	-	-	-	-	-	-
800	1.50	1.49	1.50	-	-	-	-	-	-
1,000	1.50	1.49	1.50	-	-	-	-	-	-
1,200	1.50	1.49	1.50	-	-	-	-	-	-
1,400	1.50	1.49	1.50	-	-	-	-	-	-
1,600	1.50	1.50	1.50	-	-	-	-	-	-
1,800	1.50	1.50	1.50	-	-	-	-	-	-
2,000	1.50	1.50	1.50	-	-	-	-	-	-
2,200	1.50	1.50	1.50	-	-	-	-	-	-
2,400	1.50	1.50	1.50	-	-	-	-	-	-
2,600	1.50	1.50	1.50	-	-	-	-	-	-
2,800	1.50	1.50	1.50	-	-	-	-	-	-
3,000	1.50	1.50	1.50	-	-	-	-	-	-
3,200	1.50	1.50	1.50	-	-	-	-	-	-
3,400	1.50	1.50	1.50	-	-	-	-	-	-
3,600	1.50	1.50	1.50	-	-	-	-	-	-

Table H-10. Raw data, half-crack length measurements obtained during fatigue cracking for repair patch RAC (continued)

Cycles	Visual			High Frequency Eddy Current			Low Frequency Eddy Current		
	a _{fwd} (inches)	a _{aft} (inches)	a _{avg} (inches)	a _{fwd} (inches)	a _{aft} (inches)	a _{avg} (inches)	a _{fwd} (inches)	a _{aft} (inches)	a _{avg} (inches)
3,800	1.50	1.50	1.50	-	-	-	-	-	-
4,000	1.50	1.50	1.50	-	-	-	-	-	-
4,200	1.50	1.50	1.50	-	-	-	-	-	-
4,400	1.50	1.50	1.50	-	-	-	-	-	-
4,600	1.50	1.50	1.50	-	-	-	-	-	-
5,000	1.50	1.50	1.50	-	-	-	-	-	-
5,500	1.50	1.50	1.50	-	-	-	-	-	-
6,000	1.50	1.50	1.50	-	-	-	-	-	-
6,500	1.50	1.50	1.50	-	-	-	-	-	-
7,000	1.50	1.50	1.50	-	-	-	-	-	-
7,500	1.50	1.50	1.50	-	-	-	-	-	-
8,000	1.50	1.50	1.50	-	-	-	-	-	-
8,500	1.50	1.50	1.50	-	-	-	-	-	-
9,000	1.50	1.50	1.50	-	-	-	-	-	-
9,500	1.50	1.50	1.50	-	-	-	-	-	-
10,000	1.50	1.50	1.50	1.51	1.48	1.49	1.50	1.50	1.50
10,500	1.50	1.50	1.50	-	-	-	-	-	-
11,000	1.50	1.50	1.50	-	-	-	-	-	-
11,500	1.50	1.50	1.50	-	-	-	-	-	-
12,000	1.50	1.50	1.50	-	-	-	-	-	-

Table H-10. Raw data, half-crack length measurements obtained during fatigue cracking for repair patch RAC (continued)

Cycles	Visual			High Frequency Eddy Current			Low Frequency Eddy Current		
	a _{fwd} (inches)	a _{aft} (inches)	a _{avg} (inches)	a _{fwd} (inches)	a _{aft} (inches)	a _{avg} (inches)	a _{fwd} (inches)	a _{aft} (inches)	a _{avg} (inches)
12,500	1.50	1.50	1.50	-	-	-	-	-	-
13,000	1.50	1.50	1.50	-	-	-	-	-	-
13,500	1.50	1.50	1.50	-	-	-	-	-	-
14,000	1.50	1.50	1.50	-	-	-	-	-	-
14,500	1.50	1.50	1.50	-	-	-	-	-	-
15,000	1.50	1.50	1.50	-	-	-	-	-	-
15,500	1.50	1.50	1.50	-	-	-	-	-	-
16,000	1.50	1.50	1.50	-	-	-	-	-	-
16,500	1.50	1.50	1.50	-	-	-	-	-	-
17,000	1.50	1.50	1.50	-	-	-	-	-	-
17,500	1.50	1.50	1.50	-	-	-	-	-	-
18,000	1.50	1.50	1.50	-	-	-	-	-	-
18,500	1.50	1.50	1.50	-	-	-	-	-	-
19,000	1.50	1.50	1.50	-	-	-	-	-	-
19,500	1.50	1.50	1.50	-	-	-	-	-	-
20,000	1.50	1.50	1.50	1.53	1.48	1.50	1.50	1.48	1.49
20,500	1.50	1.50	1.50	-	-	-	-	-	-
21,000	1.50	1.50	1.50	-	-	-	-	-	-
21,500	1.50	1.50	1.50	-	-	-	-	-	-
22,000	1.50	1.50	1.50	-	-	-	-	-	-

H-20

Table H-10. Raw data, half-crack length measurements obtained during fatigue cracking for repair patch RAC (continued)

Cycles	Visual			High Frequency Eddy Current			Low Frequency Eddy Current		
	a _{fwd} (inches)	a _{aft} (inches)	a _{avg} (inches)	a _{fwd} (inches)	a _{aft} (inches)	a _{avg} (inches)	a _{fwd} (inches)	a _{aft} (inches)	a _{avg} (inches)
22,500	1.50	1.50	1.50	-	-	-	-	-	-
23,000	1.50	1.50	1.50	-	-	-	-	-	-
23,500	1.50	1.50	1.50	-	-	-	-	-	-
24,000	1.50	1.50	1.50	-	-	-	-	-	-
24,500	1.50	1.50	1.50	-	-	-	-	-	-
25,000	1.50	1.50	1.50	-	-	-	-	-	-
25,500	1.50	1.50	1.50	-	-	-	-	-	-
26,000	1.50	1.50	1.50	-	-	-	-	-	-
26,500	1.50	1.50	1.50	-	-	-	-	-	-
27,000	1.50	1.50	1.50	-	-	-	-	-	-
27,500	1.50	1.50	1.50	-	-	-	-	-	-
28,000	1.50	1.50	1.50	-	-	-	-	-	-
28,500	1.50	1.50	1.50	-	-	-	-	-	-
29,000	1.50	1.50	1.50	-	-	-	-	-	-
29,500	1.50	1.50	1.50	-	-	-	-	-	-
30,000	1.50	1.50	1.50	-	-	-	-	-	-
30,500	1.50	1.50	1.50	-	-	-	-	-	-
31,000	1.50	1.50	1.50	-	-	-	-	-	-
31,500	1.50	1.50	1.50	-	-	-	-	-	-
32,000	1.50	1.50	1.50	-	-	-	-	-	-

Table H-10. Raw data, half-crack length measurements obtained during fatigue cracking for repair patch RAC (continued)

Cycles	Visual			High Frequency Eddy Current			Low Frequency Eddy Current		
	a _{fwd} (inches)	a _{aft} (inches)	a _{avg} (inches)	a _{fwd} (inches)	a _{aft} (inches)	a _{avg} (inches)	a _{fwd} (inches)	a _{aft} (inches)	a _{avg} (inches)
32,500	1.50	1.50	1.50	-	-	-	-	-	-
33,000	1.50	1.50	1.50	-	-	-	-	-	-
33,500	1.50	1.50	1.50	-	-	-	-	-	-
34,000	1.50	1.50	1.50	-	-	-	-	-	-
34,500	1.50	1.50	1.50	-	-	-	-	-	-
35,000	1.50	1.50	1.50	-	-	-	-	-	-
35,500	1.50	1.50	1.50	-	-	-	-	-	-
36,000	1.50	1.50	1.50	-	-	-	-	-	-
36,500	1.50	1.50	1.50	-	-	-	-	-	-
37,000	1.50	1.50	1.50	-	-	-	-	-	-
37,500	1.50	1.50	1.50	-	-	-	-	-	-
38,000	1.50	1.50	1.50	-	-	-	-	-	-
38,500	1.50	1.50	1.50	-	-	-	-	-	-
39,000	1.50	1.50	1.50	-	-	-	-	-	-
39,500	1.50	1.50	1.50	-	-	-	-	-	-
40,000	1.50	1.50	1.50	1.55	1.48	1.51	1.54	1.46	1.50
40,500	1.50	1.50	1.50	-	-	-	-	-	-
41,000	1.50	1.50	1.50	-	-	-	-	-	-
41,500	1.50	1.50	1.50	-	-	-	-	-	-
42,000	1.50	1.50	1.50	-	-	-	-	-	-

Table H-10. Raw data, half-crack length measurements obtained during fatigue cracking for repair patch RAC (continued)

Cycles	Visual			High Frequency Eddy Current			Low Frequency Eddy Current		
	a _{fwd} (inches)	a _{aft} (inches)	a _{avg} (inches)	a _{fwd} (inches)	a _{aft} (inches)	a _{avg} (inches)	a _{fwd} (inches)	a _{aft} (inches)	a _{avg} (inches)
42,500	1.53	1.50	1.51	-	-	-	-	-	-
43,000	1.53	1.50	1.51	-	-	-	-	-	-
43,500	1.53	1.50	1.51	-	-	-	-	-	-
44,000	1.53	1.50	1.51	-	-	-	-	-	-
45,000	1.53	1.50	1.51	-	-	-	-	-	-
46,000	1.53	1.50	1.51	-	-	-	-	-	-
47,000	1.53	1.50	1.51	-	-	-	-	-	-
48,000	1.53	1.50	1.51	-	-	-	-	-	-
49,000	1.53	1.50	1.51	-	-	-	-	-	-
50,000	1.53	1.50	1.51	1.55	1.49	1.52	1.55	1.47	1.51
51,000	1.53	1.50	1.51	-	-	-	-	-	-
52,000	1.53	1.50	1.51	-	-	-	-	-	-
53,000	1.53	1.50	1.51	-	-	-	-	-	-
54,000	1.53	1.50	1.51	-	-	-	-	-	-
55,000	1.53	1.50	1.51	-	-	-	-	-	-
56,000	1.53	1.50	1.51	-	-	-	-	-	-
57,000	1.53	1.50	1.51	-	-	-	-	-	-
58,000	1.53	1.50	1.51	-	-	-	-	-	-
59,000	1.53	1.50	1.51	-	-	-	-	-	-
60,000	1.53	1.50	1.51	1.55	1.49	1.52	1.50	1.45	1.48

H-23

Table H-10. Raw data, half-crack length measurements obtained during fatigue cracking for repair patch RAC (continued)

Cycles	Visual			High Frequency Eddy Current			Low Frequency Eddy Current		
	a _{fwd} (inches)	a _{aft} (inches)	a _{avg} (inches)	a _{fwd} (inches)	a _{aft} (inches)	a _{avg} (inches)	a _{fwd} (inches)	a _{aft} (inches)	a _{avg} (inches)
61,000	1.53	1.50	1.51	-	-	-	-	-	-
62,000	1.53	1.50	1.51	-	-	-	-	-	-
63,000	1.53	1.50	1.51	-	-	-	-	-	-
64,000	1.53	1.50	1.51	-	-	-	-	-	-
65,000	1.53	1.50	1.51	-	-	-	-	-	-
70,000	1.53	1.50	1.51	-	-	-	-	-	-
72,000	1.53	1.50	1.51	-	-	-	-	-	-
74,000	1.53	1.50	1.51	-	-	-	-	-	-
77,000	1.53	1.50	1.51	-	-	-	-	-	-
79,000	1.53	1.50	1.51	-	-	-	-	-	-
80,000	1.53	1.50	1.51	1.55	1.49	1.52	-	-	-
84,000	1.53	1.50	1.51	-	-	-	-	-	-
86,000	1.53	1.50	1.51	-	-	-	-	-	-
88,000	1.53	1.50	1.51	-	-	-	-	-	-
90,000	1.53	1.50	1.51	-	-	-	-	-	-
92,000	1.53	1.50	1.51	-	-	-	-	-	-
92,834	1.53	1.50	1.51	1.55	1.49	1.52	1.48	1.50	1.49

H.3.1.2 REPAIR PATCH RBC

Table H-11. Raw data, half-crack length measurements obtained during fatigue cracking for repair patch RBC

Cycles	Visual			High Frequency Eddy Current			Low Frequency Eddy Current		
	a _{fwd} (inches)	a _{aft} (inches)	a _{avg} (inches)	a _{fwd} (inches)	a _{aft} (inches)	a _{avg} (inches)	a _{fwd} (inches)	a _{aft} (inches)	a _{avg} (inches)
0	1.47	1.48	1.48	1.46	1.49	1.48	1.55	1.45	1.50
200	1.47	1.48	1.48	-	-	-	-	-	-
400	1.47	1.48	1.48	-	-	-	-	-	-
600	1.47	1.48	1.48	-	-	-	-	-	-
800	1.50	1.48	1.49	-	-	-	-	-	-
1,000	1.50	1.48	1.49	-	-	-	-	-	-
1,200	1.50	1.48	1.49	-	-	-	-	-	-
1,400	1.50	1.48	1.49	-	-	-	-	-	-
1,600	1.50	1.48	1.49	-	-	-	-	-	-
1,800	1.50	1.48	1.49	-	-	-	-	-	-
2,000	1.50	1.48	1.49	-	-	-	-	-	-
2,200	1.50	1.48	1.49	-	-	-	-	-	-
2,400	1.50	1.48	1.49	-	-	-	-	-	-
2,600	1.50	1.48	1.49	-	-	-	-	-	-
2,800	1.50	1.48	1.49	-	-	-	-	-	-
3,000	1.50	1.48	1.49	-	-	-	-	-	-
3,200	1.50	1.48	1.49	-	-	-	-	-	-
3,400	1.50	1.48	1.49	-	-	-	-	-	-
3,600	1.50	1.48	1.49	-	-	-	-	-	-

Table H-11. Raw data, half-crack length measurements obtained during fatigue cracking for repair patch RBC (continued)

Cycles	Visual			High Frequency Eddy Current			Low Frequency Eddy Current		
	a _{fwd} (inches)	a _{aft} (inches)	a _{avg} (inches)	a _{fwd} (inches)	a _{aft} (inches)	a _{avg} (inches)	a _{fwd} (inches)	a _{aft} (inches)	a _{avg} (inches)
3,800	1.50	1.48	1.49	-	-	-	-	-	-
4,000	1.50	1.48	1.49	-	-	-	-	-	-
4,200	1.50	1.48	1.49	-	-	-	-	-	-
4,400	1.50	1.48	1.49	-	-	-	-	-	-
4,600	1.50	1.48	1.49	-	-	-	-	-	-
5,000	1.50	1.48	1.49	-	-	-	-	-	-
5,500	1.50	1.48	1.49	-	-	-	-	-	-
6,000	1.50	1.48	1.49	-	-	-	-	-	-
6,500	1.50	1.48	1.49	-	-	-	-	-	-
7,000	1.50	1.48	1.49	-	-	-	-	-	-
7,500	1.50	1.48	1.49	-	-	-	-	-	-
8,000	1.50	1.48	1.49	-	-	-	-	-	-
8,500	1.50	1.48	1.49	-	-	-	-	-	-
9,000	1.50	1.48	1.49	-	-	-	-	-	-
9,500	1.50	1.48	1.49	-	-	-	-	-	-
10,000	1.50	1.48	1.49	1.49	1.50	1.49	1.67	1.43	1.55
10,500	1.50	1.48	1.49	-	-	-	-	-	-
11,000	1.50	1.48	1.49	-	-	-	-	-	-
11,500	1.50	1.48	1.49	-	-	-	-	-	-
12,000	1.50	1.48	1.49	-	-	-	-	-	-

Table H-11. Raw data, half-crack length measurements obtained during fatigue cracking for repair patch RBC (continued)

Cycles	Visual			High Frequency Eddy Current			Low Frequency Eddy Current		
	a _{fwd} (inches)	a _{aft} (inches)	a _{avg} (inches)	a _{fwd} (inches)	a _{aft} (inches)	a _{avg} (inches)	a _{fwd} (inches)	a _{aft} (inches)	a _{avg} (inches)
12,500	1.50	1.48	1.49	-	-	-	-	-	-
13,000	1.50	1.48	1.49	-	-	-	-	-	-
13,500	1.50	1.48	1.49	-	-	-	-	-	-
14,000	1.50	1.48	1.49	-	-	-	-	-	-
14,500	1.50	1.48	1.49	-	-	-	-	-	-
15,000	1.50	1.48	1.49	-	-	-	-	-	-
15,500	1.50	1.48	1.49	-	-	-	-	-	-
16,000	1.50	1.48	1.49	-	-	-	-	-	-
16,500	1.50	1.48	1.49	-	-	-	-	-	-
17,000	1.50	1.48	1.49	-	-	-	-	-	-
17,500	1.50	1.48	1.49	-	-	-	-	-	-
18,000	1.50	1.48	1.49	-	-	-	-	-	-
18,500	1.50	1.48	1.49	-	-	-	-	-	-
19,000	1.50	1.48	1.49	-	-	-	-	-	-
19,500	1.50	1.48	1.49	-	-	-	-	-	-
20,000	1.50	1.48	1.49	1.51	1.54	1.53	1.60	1.50	1.55
20,500	1.50	1.48	1.49	-	-	-	-	-	-
21,000	1.50	1.48	1.49	-	-	-	-	-	-
21,500	1.50	1.48	1.49	-	-	-	-	-	-
22,000	1.50	1.48	1.49	-	-	-	-	-	-

Table H-11. Raw data, half-crack length measurements obtained during fatigue cracking for repair patch RBC (continued)

Cycles	Visual			High Frequency Eddy Current			Low Frequency Eddy Current		
	a _{fwd} (inches)	a _{aft} (inches)	a _{avg} (inches)	a _{fwd} (inches)	a _{aft} (inches)	a _{avg} (inches)	a _{fwd} (inches)	a _{aft} (inches)	a _{avg} (inches)
22,500	1.50	1.48	1.49	-	-	-	-	-	-
23,000	1.50	1.48	1.49	-	-	-	-	-	-
23,500	1.50	1.48	1.49	-	-	-	-	-	-
24,000	1.50	1.48	1.49	-	-	-	-	-	-
24,500	1.50	1.48	1.49	-	-	-	-	-	-
25,000	1.50	1.48	1.49	-	-	-	-	-	-
25,500	1.50	1.48	1.49	-	-	-	-	-	-
26,000	1.50	1.48	1.49	-	-	-	-	-	-
26,500	1.50	1.48	1.49	-	-	-	-	-	-
27,000	1.50	1.48	1.49	-	-	-	-	-	-
27,500	1.50	1.53	1.51	-	-	-	-	-	-
28,000	1.50	1.53	1.51	-	-	-	-	-	-
28,500	1.50	1.53	1.51	-	-	-	-	-	-
29,000	1.50	1.53	1.51	-	-	-	-	-	-
29,500	1.50	1.53	1.51	-	-	-	-	-	-
30,000	1.50	1.56	1.53	-	-	-	-	-	-
30,500	1.50	1.56	1.53	-	-	-	-	-	-
31,000	1.50	1.56	1.53	-	-	-	-	-	-
31,500	1.50	1.56	1.53	-	-	-	-	-	-
32,000	1.50	1.56	1.53	-	-	-	-	-	-

Table H-11. Raw data, half-crack length measurements obtained during fatigue cracking for repair patch RBC (continued)

Cycles	Visual			High Frequency Eddy Current			Low Frequency Eddy Current		
	a _{fwd} (inches)	a _{aft} (inches)	a _{avg} (inches)	a _{fwd} (inches)	a _{aft} (inches)	a _{avg} (inches)	a _{fwd} (inches)	a _{aft} (inches)	a _{avg} (inches)
32,500	1.52	1.56	1.54	-	-	-	-	-	-
33,000	1.52	1.56	1.54	-	-	-	-	-	-
33,500	1.52	1.56	1.54	-	-	-	-	-	-
34,000	1.52	1.56	1.54	-	-	-	-	-	-
34,500	1.52	1.56	1.54	-	-	-	-	-	-
35,000	1.52	1.58	1.55	-	-	-	-	-	-
35,500	1.52	1.58	1.55	-	-	-	-	-	-
36,000	1.52	1.58	1.55	-	-	-	-	-	-
36,500	1.52	1.58	1.55	-	-	-	-	-	-
37,000	1.52	1.58	1.55	-	-	-	-	-	-
37,500	1.55	1.58	1.56	-	-	-	-	-	-
38,000	1.55	1.58	1.56	-	-	-	-	-	-
38,500	1.55	1.58	1.56	-	-	-	-	-	-
39,000	1.55	1.58	1.56	-	-	-	-	-	-
39,500	1.55	1.58	1.56	-	-	-	-	-	-
40,000	1.55	1.58	1.56	1.59	1.61	1.60	1.77	1.57	1.67
40,500	1.57	1.58	1.58	-	-	-	-	-	-
41,000	1.57	1.58	1.58	-	-	-	-	-	-
41,500	1.57	1.58	1.58	-	-	-	-	-	-
42,000	1.57	1.58	1.58	-	-	-	-	-	-

Table H-11. Raw data, half-crack length measurements obtained during fatigue cracking for repair patch RBC (continued)

Cycles	Visual			High Frequency Eddy Current			Low Frequency Eddy Current		
	a _{fwd} (inches)	a _{aft} (inches)	a _{avg} (inches)	a _{fwd} (inches)	a _{aft} (inches)	a _{avg} (inches)	a _{fwd} (inches)	a _{aft} (inches)	a _{avg} (inches)
42,500	1.57	1.58	1.58	-	-	-	-	-	-
43,000	1.57	1.58	1.58	-	-	-	-	-	-
43,500	1.57	1.58	1.58	-	-	-	-	-	-
44,000	1.57	1.58	1.58	-	-	-	-	-	-
45,000	1.57	1.63	1.60	-	-	-	-	-	-
46,000	1.57	1.63	1.60	-	-	-	-	-	-
47,000	1.57	1.63	1.60	-	-	-	-	-	-
48,000	1.57	1.63	1.60	-	-	-	-	-	-
49,000	1.57	1.63	1.60	-	-	-	-	-	-
50,000	1.57	1.63	1.60	1.59	1.64	1.61	1.75	1.54	1.65
51,000	1.57	1.63	1.60	-	-	-	-	-	-
52,000	1.60	1.63	1.61	-	-	-	-	-	-
53,000	1.62	1.63	1.63	-	-	-	-	-	-
54,000	1.62	1.63	1.63	-	-	-	-	-	-
55,000	1.62	1.63	1.63	-	-	-	-	-	-
56,000	1.62	1.63	1.63	-	-	-	-	-	-
57,000	1.62	1.63	1.63	-	-	-	-	-	-
58,000	1.62	1.63	1.63	-	-	-	-	-	-
59,000	1.62	1.63	1.63	-	-	-	-	-	-
60,000	1.62	1.63	1.63	1.61	1.66	1.64	1.81	1.75	1.78

H-30

Table H-11. Raw data, half-crack length measurements obtained during fatigue cracking for repair patch RBC (continued)

Cycles	Visual			High Frequency Eddy Current			Low Frequency Eddy Current		
	a _{fwd} (inches)	a _{aft} (inches)	a _{avg} (inches)	a _{fwd} (inches)	a _{aft} (inches)	a _{avg} (inches)	a _{fwd} (inches)	a _{aft} (inches)	a _{avg} (inches)
61,000	1.65	1.68	1.66	-	-	-	-	-	-
62,000	1.65	1.68	1.66	-	-	-	-	-	-
63,000	1.65	1.68	1.66	-	-	-	-	-	-
64,000	1.65	1.68	1.66	-	-	-	-	-	-
65,000	1.67	1.68	1.68	-	-	-	-	-	-
66,000	1.67	1.68	1.68	-	-	-	-	-	-
67,000	1.67	1.68	1.68	-	-	-	-	-	-
68,000	1.67	1.68	1.68	-	-	-	-	-	-
69,000	1.67	1.71	1.69	-	-	-	-	-	-
70,000	1.70	1.71	1.70	-	-	-	-	-	-
71,000	1.70	1.71	1.70	-	-	-	-	-	-
72,000	1.70	1.73	1.71	-	-	-	-	-	-
73,000	1.70	1.73	1.71	-	-	-	-	-	-
74,000	1.70	1.73	1.71	-	-	-	-	-	-
75,000	1.70	1.73	1.71	-	-	-	-	-	-
76,000	1.70	1.73	1.71	-	-	-	-	-	-
77,000	1.70	1.73	1.71	-	-	-	-	-	-
78,000	1.70	1.73	1.71	-	-	-	-	-	-
79,000	1.72	1.76	1.74	-	-	-	-	-	-
80,000	1.72	1.76	1.74	1.76	1.81	1.79	-	-	-

Table H-11. Raw data, half-crack length measurements obtained during fatigue cracking for repair patch RBC (continued)

Cycles	Visual			High Frequency Eddy Current			Low Frequency Eddy Current		
	a _{fwd} (inches)	a _{aft} (inches)	a _{avg} (inches)	a _{fwd} (inches)	a _{aft} (inches)	a _{avg} (inches)	a _{fwd} (inches)	a _{aft} (inches)	a _{avg} (inches)
81,000	1.75	1.78	1.76	-	-	-	-	-	-
82,000	1.75	1.78	1.76	-	-	-	-	-	-
83,000	1.77	1.78	1.78	-	-	-	-	-	-
84,000	1.77	1.78	1.78	-	-	-	-	-	-
85,000	1.77	1.78	1.78	-	-	-	-	-	-
86,000	1.77	1.78	1.78	-	-	-	-	-	-
87,000	1.77	1.78	1.78	-	-	-	-	-	-
88,000	1.77	1.78	1.78	-	-	-	-	-	-
89,000	1.77	1.78	1.78	-	-	-	-	-	-
90,000	1.77	1.78	1.78	-	-	-	-	-	-
91,000	1.77	1.78	1.78	-	-	-	-	-	-
92,000	1.77	1.78	1.78	-	-	-	-	-	-
92,834	1.77	1.78	1.78	1.81	1.86	1.84	1.86	1.88	1.87

H.3.1.3 REPAIR PATCH UAC

Table H-12. Raw data, half-crack length measurements obtained during fatigue cracking for repair patch UAC

Cycles	Visual			High Frequency Eddy Current			Low Frequency Eddy Current		
	a _{fwd} (inches)	a _{aft} (inches)	a _{avg} (inches)	a _{fwd} (inches)	a _{aft} (inches)	a _{avg} (inches)	a _{fwd} (inches)	a _{aft} (inches)	a _{avg} (inches)
0	1.48	1.49	1.49	1.50	1.50	1.50	1.52	1.45	1.49
200	1.48	1.49	1.49	-	-	-	-	-	-
400	1.48	1.49	1.49	-	-	-	-	-	-
600	1.48	1.49	1.49	-	-	-	-	-	-
800	1.48	1.49	1.49	-	-	-	-	-	-
1,000	1.48	1.49	1.49	-	-	-	-	-	-
1,200	1.48	1.49	1.49	-	-	-	-	-	-
1,400	1.48	1.49	1.49	-	-	-	-	-	-
1,600	1.48	1.49	1.49	-	-	-	-	-	-
1,800	1.48	1.49	1.49	-	-	-	-	-	-
2,000	1.48	1.49	1.49	-	-	-	-	-	-
2,200	1.48	1.49	1.49	-	-	-	-	-	-
2,400	1.48	1.49	1.49	-	-	-	-	-	-
2,600	1.48	1.50	1.49	-	-	-	-	-	-
2,800	1.48	1.50	1.49	-	-	-	-	-	-
3,000	1.48	1.50	1.49	-	-	-	-	-	-
3,200	1.48	1.50	1.49	-	-	-	-	-	-
3,400	1.48	1.50	1.49	-	-	-	-	-	-
3,600	1.48	1.50	1.49	-	-	-	-	-	-

Table H-12. Raw data, half-crack length measurements obtained during fatigue cracking for repair patch UAC (continued)

Cycles	Visual			High Frequency Eddy Current			Low Frequency Eddy Current		
	a _{fwd} (inches)	a _{aft} (inches)	a _{avg} (inches)	a _{fwd} (inches)	a _{aft} (inches)	a _{avg} (inches)	a _{fwd} (inches)	a _{aft} (inches)	a _{avg} (inches)
3,800	1.48	1.50	1.49	-	-	-	-	-	-
4,000	1.48	1.50	1.49	-	-	-	-	-	-
4,200	1.48	1.50	1.49	-	-	-	-	-	-
4,400	1.48	1.50	1.49	-	-	-	-	-	-
4,600	1.48	1.50	1.49	-	-	-	-	-	-
5,000	1.48	1.50	1.49	-	-	-	-	-	-
5,500	1.48	1.50	1.49	-	-	-	-	-	-
6,000	1.48	1.50	1.49	-	-	-	-	-	-
6,500	1.48	1.50	1.49	-	-	-	-	-	-
7,000	1.48	1.50	1.49	-	-	-	-	-	-
7,500	1.48	1.50	1.49	-	-	-	-	-	-
8,000	1.48	1.50	1.49	-	-	-	-	-	-
8,500	1.48	1.50	1.49	-	-	-	-	-	-
9,000	1.48	1.50	1.49	-	-	-	-	-	-
9,500	1.48	1.50	1.49	-	-	-	-	-	-
10,000	1.48	1.50	1.49	1.50	1.50	1.50	1.55	1.45	1.50
10,500	1.48	1.50	1.49	-	-	-	-	-	-
11,000	1.48	1.50	1.49	-	-	-	-	-	-
11,500	1.48	1.50	1.49	-	-	-	-	-	-
12,000	1.48	1.50	1.49	-	-	-	-	-	-

Table H-12. Raw data, half-crack length measurements obtained during fatigue cracking for repair patch UAC (continued)

Cycles	Visual			High Frequency Eddy Current			Low Frequency Eddy Current		
	a _{fwd} (inches)	a _{aft} (inches)	a _{avg} (inches)	a _{fwd} (inches)	a _{aft} (inches)	a _{avg} (inches)	a _{fwd} (inches)	a _{aft} (inches)	a _{avg} (inches)
12,500	1.48	1.50	1.49	-	-	-	-	-	-
13,000	1.48	1.50	1.49	-	-	-	-	-	-
13,500	1.48	1.50	1.49	-	-	-	-	-	-
14,000	1.48	1.50	1.49	-	-	-	-	-	-
14,500	1.48	1.50	1.49	-	-	-	-	-	-
15,000	1.48	1.50	1.49	-	-	-	-	-	-
15,500	1.48	1.50	1.49	-	-	-	-	-	-
16,000	1.48	1.50	1.49	-	-	-	-	-	-
16,500	1.48	1.50	1.49	-	-	-	-	-	-
17,000	1.48	1.50	1.49	-	-	-	-	-	-
17,500	1.48	1.50	1.49	-	-	-	-	-	-
18,000	1.48	1.50	1.49	-	-	-	-	-	-
18,500	1.48	1.50	1.49	-	-	-	-	-	-
19,000	1.48	1.50	1.49	-	-	-	-	-	-
19,500	1.48	1.50	1.49	-	-	-	-	-	-
20,000	1.48	1.50	1.49	1.50	1.51	1.51	1.55	1.42	1.49
20,500	1.48	1.50	1.49	-	-	-	-	-	-
21,000	1.48	1.50	1.49	-	-	-	-	-	-
21,500	1.48	1.50	1.49	-	-	-	-	-	-
22,000	1.48	1.50	1.49	-	-	-	-	-	-

Table H-12. Raw data, half-crack length measurements obtained during fatigue cracking for repair patch UAC (continued)

Cycles	Visual			High Frequency Eddy Current			Low Frequency Eddy Current		
	a _{fwd} (inches)	a _{aft} (inches)	a _{avg} (inches)	a _{fwd} (inches)	a _{aft} (inches)	a _{avg} (inches)	a _{fwd} (inches)	a _{aft} (inches)	a _{avg} (inches)
22,500	1.48	1.50	1.49	-	-	-	-	-	-
23,000	1.48	1.50	1.49	-	-	-	-	-	-
23,500	1.48	1.50	1.49	-	-	-	-	-	-
24,000	1.48	1.50	1.49	-	-	-	-	-	-
24,500	1.48	1.50	1.49	-	-	-	-	-	-
25,000	1.48	1.50	1.49	-	-	-	-	-	-
25,500	1.48	1.50	1.49	-	-	-	-	-	-
26,000	1.48	1.50	1.49	-	-	-	-	-	-
26,500	1.48	1.50	1.49	-	-	-	-	-	-
27,000	1.48	1.50	1.49	-	-	-	-	-	-
27,500	1.48	1.50	1.49	-	-	-	-	-	-
28,000	1.48	1.50	1.49	-	-	-	-	-	-
28,500	1.48	1.50	1.49	-	-	-	-	-	-
29,000	1.48	1.50	1.49	-	-	-	-	-	-
29,500	1.48	1.50	1.49	-	-	-	-	-	-
30,000	1.48	1.50	1.49	-	-	-	-	-	-
30,500	1.48	1.50	1.49	-	-	-	-	-	-
31,000	1.48	1.50	1.49	-	-	-	-	-	-
31,500	1.48	1.50	1.49	-	-	-	-	-	-
32,000	1.48	1.50	1.49	-	-	-	-	-	-

Table H-12. Raw data, half-crack length measurements obtained during fatigue cracking for repair patch UAC (continued)

Cycles	Visual			High Frequency Eddy Current			Low Frequency Eddy Current		
	a _{fwd} (inches)	a _{aft} (inches)	a _{avg} (inches)	a _{fwd} (inches)	a _{aft} (inches)	a _{avg} (inches)	a _{fwd} (inches)	a _{aft} (inches)	a _{avg} (inches)
32,500	1.48	1.50	1.49	-	-	-	-	-	-
33,000	1.48	1.50	1.49	-	-	-	-	-	-
33,500	1.48	1.50	1.49	-	-	-	-	-	-
34,000	1.48	1.50	1.49	-	-	-	-	-	-
34,500	1.48	1.50	1.49	-	-	-	-	-	-
35,000	1.48	1.50	1.49	-	-	-	-	-	-
35,500	1.48	1.50	1.49	-	-	-	-	-	-
36,000	1.48	1.50	1.49	-	-	-	-	-	-
36,500	1.48	1.50	1.49	-	-	-	-	-	-
37,000	1.48	1.50	1.49	-	-	-	-	-	-
37,500	1.48	1.50	1.49	-	-	-	-	-	-
38,000	1.48	1.50	1.49	-	-	-	-	-	-
38,500	1.48	1.50	1.49	-	-	-	-	-	-
39,000	1.48	1.50	1.49	-	-	-	-	-	-
39,500	1.48	1.50	1.49	-	-	-	-	-	-
40,000	1.48	1.50	1.49	1.50	1.51	1.51	1.58	1.37	1.48
40,500	1.48	1.50	1.49	-	-	-	-	-	-
41,000	1.48	1.50	1.49	-	-	-	-	-	-
41,500	1.48	1.50	1.49	-	-	-	-	-	-
42,000	1.48	1.50	1.49	-	-	-	-	-	-

Table H-12. Raw data, half-crack length measurements obtained during fatigue cracking for repair patch UAC (continued)

Cycles	Visual			High Frequency Eddy Current			Low Frequency Eddy Current		
	a _{fwd} (inches)	a _{aft} (inches)	a _{avg} (inches)	a _{fwd} (inches)	a _{aft} (inches)	a _{avg} (inches)	a _{fwd} (inches)	a _{aft} (inches)	a _{avg} (inches)
42,500	1.49	1.50	1.50	-	-	-	-	-	-
43,000	1.49	1.50	1.50	-	-	-	-	-	-
43,500	1.49	1.50	1.50	-	-	-	-	-	-
44,000	1.49	1.50	1.50	-	-	-	-	-	-
45,000	1.49	1.50	1.50	-	-	-	-	-	-
46,000	1.49	1.50	1.50	-	-	-	-	-	-
47,000	1.49	1.50	1.50	-	-	-	-	-	-
48,000	1.49	1.50	1.50	-	-	-	-	-	-
49,000	1.49	1.50	1.50	-	-	-	-	-	-
50,000	1.49	1.50	1.50	1.53	1.53	1.53	1.55	1.50	1.53
51,000	1.49	1.50	1.50	-	-	-	-	-	-
52,000	1.49	1.50	1.50	-	-	-	-	-	-
53,000	1.49	1.50	1.50	-	-	-	-	-	-
54,000	1.49	1.50	1.50	-	-	-	-	-	-
55,000	1.49	1.50	1.50	-	-	-	-	-	-
56,000	1.49	1.50	1.50	-	-	-	-	-	-
57,000	1.49	1.50	1.50	-	-	-	-	-	-
58,000	1.49	1.50	1.50	-	-	-	-	-	-
59,000	1.49	1.50	1.50	-	-	-	-	-	-
60,000	1.49	1.50	1.50	1.53	1.53	1.53	1.60	1.40	1.50

Table H-12. Raw data, half-crack length measurements obtained during fatigue cracking for repair patch UAC (continued)

Cycles	Visual			High Frequency Eddy Current			Low Frequency Eddy Current		
	a _{fwd} (inches)	a _{aft} (inches)	a _{avg} (inches)	a _{fwd} (inches)	a _{aft} (inches)	a _{avg} (inches)	a _{fwd} (inches)	a _{aft} (inches)	a _{avg} (inches)
61,000	1.49	1.50	1.50	-	-	-	-	-	-
62,000	1.49	1.50	1.50	-	-	-	-	-	-
63,000	1.49	1.50	1.50	-	-	-	-	-	-
64,000	1.49	1.50	1.50	-	-	-	-	-	-
65,000	1.49	1.50	1.50	-	-	-	-	-	-
70,000	1.49	1.50	1.50	-	-	-	-	-	-
72,000	1.49	1.50	1.50	-	-	-	-	-	-
74,000	1.49	1.50	1.50	-	-	-	-	-	-
77,000	1.49	1.50	1.50	-	-	-	-	-	-
79,000	1.49	1.50	1.50	-	-	-	-	-	-
80,000	1.49	1.50	1.50	1.53	1.53	1.53	-	-	-
84,000	1.49	1.50	1.50	-	-	-	-	-	-
86,000	1.49	1.50	1.50	-	-	-	-	-	-
88,000	1.49	1.50	1.50	-	-	-	-	-	-
90,000	1.49	1.50	1.50	-	-	-	-	-	-
92,000	1.49	1.50	1.50	-	-	-	-	-	-
92,834	1.49	1.50	1.50	1.53	1.53	1.53	1.38	1.70	1.54

H.3.1.4 REPAIR PATCH UB

Table H-13. Raw data, half-crack length measurements obtained during fatigue cracking for repair patch UB

Cycles	Visual			High Frequency Eddy Current			Low Frequency Eddy Current		
	a _{fwd} (inches)	a _{aft} (inches)	a _{avg} (inches)	a _{fwd} (inches)	a _{aft} (inches)	a _{avg} (inches)	a _{fwd} (inches)	a _{aft} (inches)	a _{avg} (inches)
0	1.50	1.51	1.50	1.54	1.53	1.54	1.56	1.58	1.57
500	1.52	1.53	1.53	-	-	-	-	-	-
1,000	1.52	1.53	1.53	-	-	-	-	-	-
2,000	1.55	1.58	1.57	-	-	-	-	-	-
2,500	1.57	1.61	1.59	-	-	-	-	-	-
3,000	1.57	1.61	1.59	-	-	-	-	-	-
3,500	1.57	1.61	1.59	-	-	-	-	-	-
4,000	1.57	1.61	1.59	-	-	-	-	-	-
4,500	1.57	1.61	1.59	-	-	-	-	-	-
5,000	1.57	1.63	1.60	-	-	-	-	-	-
5,500	1.57	1.63	1.60	-	-	-	-	-	-
6,000	1.57	1.63	1.60	-	-	-	-	-	-
6,500	1.60	1.63	1.62	-	-	-	-	-	-
7,000	1.60	1.63	1.62	-	-	-	-	-	-
7,500	1.60	1.66	1.63	-	-	-	-	-	-
8,000	1.60	1.66	1.63	-	-	-	-	-	-
8,500	1.60	1.66	1.63	-	-	-	-	-	-
9,000	1.60	1.68	1.64	-	-	-	-	-	-
9,500	1.62	1.68	1.65	-	-	-	-	-	-

H-40

Table H-13. Raw data, half-crack length measurements obtained during fatigue cracking for repair patch UB (continued)

Cycles	Visual			High Frequency Eddy Current			Low Frequency Eddy Current		
	a _{fwd} (inches)	a _{aft} (inches)	a _{avg} (inches)	a _{fwd} (inches)	a _{aft} (inches)	a _{avg} (inches)	a _{fwd} (inches)	a _{aft} (inches)	a _{avg} (inches)
10,000	1.65	1.71	1.68	1.68	1.70	1.69	1.70	1.68	1.69
10,500	1.67	1.73	1.70	-	-	-	-	-	-
11,000	1.67	1.73	1.70	-	-	-	-	-	-
11,500	1.67	1.73	1.70	-	-	-	-	-	-
12,000	1.67	1.73	1.70	-	-	-	-	-	-
12,500	1.67	1.73	1.70	-	-	-	-	-	-
13,000	1.67	1.73	1.70	-	-	-	-	-	-
13,500	1.70	1.73	1.72	-	-	-	-	-	-
14,000	1.70	1.76	1.73	-	-	-	-	-	-
14,500	1.72	1.78	1.75	-	-	-	-	-	-
15,000	1.72	1.78	1.75	-	-	-	-	-	-
15,500	1.72	1.78	1.75	-	-	-	-	-	-
16,000	1.72	1.78	1.75	-	-	-	-	-	-
16,500	1.72	1.81	1.77	-	-	-	-	-	-
17,000	1.75	1.83	1.79	-	-	-	-	-	-
17,500	1.77	1.83	1.80	-	-	-	-	-	-
18,000	1.77	1.83	1.80	-	-	-	-	-	-
18,500	1.80	1.86	1.83	-	-	-	-	-	-
19,000	1.80	1.86	1.83	-	-	-	-	-	-
19,500	1.80	1.86	1.83	-	-	-	-	-	-

Table H-13. Raw data, half-crack length measurements obtained during fatigue cracking for repair patch UB (continued)

Cycles	Visual			High Frequency Eddy Current			Low Frequency Eddy Current		
	a _{fwd} (inches)	a _{aft} (inches)	a _{avg} (inches)	a _{fwd} (inches)	a _{aft} (inches)	a _{avg} (inches)	a _{fwd} (inches)	a _{aft} (inches)	a _{avg} (inches)
20,000	1.80	1.86	1.83	1.81	1.83	1.82	2.01	1.92	1.97
20,500	1.80	1.88	1.84	-	-	-	-	-	-
21,000	1.80	1.88	1.84	-	-	-	-	-	-
22,000	1.82	1.88	1.85	-	-	-	-	-	-
23,000	1.82	1.88	1.85	-	-	-	-	-	-
24,000	1.82	1.88	1.85	-	-	-	-	-	-
25,000	1.87	1.96	1.92	-	-	-	-	-	-
26,000	1.87	1.96	1.92	-	-	-	-	-	-
27,000	1.90	1.98	1.94	-	-	-	-	-	-
28,000	1.92	2.01	1.97	-	-	-	-	-	-
29,000	1.92	2.03	1.98	-	-	-	-	-	-
30,000	1.92	2.03	1.98	-	-	-	-	-	-
31,000	1.95	2.03	1.99	-	-	-	-	-	-
32,000	1.97	2.06	2.02	-	-	-	-	-	-
33,000	1.97	2.06	2.02	-	-	-	-	-	-
34,000	1.97	2.06	2.02	-	-	-	-	-	-
35,000	1.97	2.08	2.03	-	-	-	-	-	-
36,000	2.00	2.11	2.05	-	-	-	-	-	-
37,000	2.02	2.16	2.09	-	-	-	-	-	-
38,000	2.02	2.16	2.09	-	-	-	-	-	-

Table H-13. Raw data, half-crack length measurements obtained during fatigue cracking for repair patch UB (continued)

Cycles	Visual			High Frequency Eddy Current			Low Frequency Eddy Current		
	a _{fwd} (inches)	a _{aft} (inches)	a _{avg} (inches)	a _{fwd} (inches)	a _{aft} (inches)	a _{avg} (inches)	a _{fwd} (inches)	a _{aft} (inches)	a _{avg} (inches)
39,000	2.02	2.16	2.09	-	-	-	-	-	-
40,000	2.02	2.16	2.09	2.08	2.15	2.12	-	-	-
41,000	2.07	2.18	2.13	-	-	-	-	-	-
42,000	2.07	2.21	2.14	-	-	-	-	-	-
43,000	2.10	2.23	2.17	-	-	-	-	-	-
44,000	2.10	2.23	2.17	-	-	-	-	-	-
45,000	2.10	2.23	2.17	-	-	-	-	-	-
46,000	2.12	2.23	2.18	-	-	-	-	-	-
47,000	2.12	2.23	2.18	-	-	-	-	-	-
48,000	2.17	2.26	2.22	-	-	-	-	-	-
49,000	2.17	2.28	2.23	-	-	-	-	-	-
50,000	2.20	2.28	2.24	-	-	-	-	-	-
51,000	2.20	2.28	2.24	-	-	-	-	-	-
52,000	2.20	2.33	2.27	-	-	-	-	-	-
52,834	2.20	2.33	2.27	2.26	2.35	2.30	2.26	2.32	2.29

H.3.1.5 REPAIR PATCH UBC

Table H-14. Raw data, half-crack length measurements obtained during fatigue cracking for repair patch UBC

Cycles	Visual			High Frequency Eddy Current			Low Frequency Eddy Current		
	a _{fwd} (inches)	a _{aft} (inches)	a _{avg} (inches)	a _{fwd} (inches)	a _{aft} (inches)	a _{avg} (inches)	a _{fwd} (inches)	a _{aft} (inches)	a _{avg} (inches)
0	1.49	1.46	1.48	1.48	1.49	1.48	1.50	1.50	1.50
200	1.49	1.46	1.48	-	-	-	-	-	-
400	1.49	1.46	1.48	-	-	-	-	-	-
600	1.49	1.46	1.48	-	-	-	-	-	-
800	1.49	1.46	1.48	-	-	-	-	-	-
1,000	1.49	1.46	1.48	-	-	-	-	-	-
1,200	1.49	1.46	1.48	-	-	-	-	-	-
1,400	1.49	1.46	1.48	-	-	-	-	-	-
1,600	1.49	1.46	1.48	-	-	-	-	-	-
1,800	1.49	1.46	1.48	-	-	-	-	-	-
2,000	1.49	1.46	1.48	-	-	-	-	-	-
2,200	1.49	1.46	1.48	-	-	-	-	-	-
2,400	1.49	1.46	1.48	-	-	-	-	-	-
2,600	1.49	1.46	1.48	-	-	-	-	-	-
2,800	1.49	1.46	1.48	-	-	-	-	-	-
3,000	1.49	1.46	1.48	-	-	-	-	-	-
3,200	1.49	1.46	1.48	-	-	-	-	-	-
3,400	1.49	1.46	1.48	-	-	-	-	-	-
3,600	1.49	1.46	1.48	-	-	-	-	-	-

H-44

Table H-14. Raw data, half-crack length measurements obtained during fatigue cracking for repair patch UBC (continued)

Cycles	Visual			High Frequency Eddy Current			Low Frequency Eddy Current		
	a _{fwd} (inches)	a _{aft} (inches)	a _{avg} (inches)	a _{fwd} (inches)	a _{aft} (inches)	a _{avg} (inches)	a _{fwd} (inches)	a _{aft} (inches)	a _{avg} (inches)
3,800	1.49	1.46	1.48	-	-	-	-	-	-
4,000	1.49	1.46	1.48	-	-	-	-	-	-
4,200	1.49	1.46	1.48	-	-	-	-	-	-
4,400	1.49	1.46	1.48	-	-	-	-	-	-
4,600	1.49	1.46	1.48	-	-	-	-	-	-
5,000	1.49	1.47	1.48	-	-	-	-	-	-
5,500	1.49	1.47	1.48	-	-	-	-	-	-
6,000	1.49	1.47	1.48	-	-	-	-	-	-
6,500	1.49	1.47	1.48	-	-	-	-	-	-
7,000	1.49	1.47	1.48	-	-	-	-	-	-
7,500	1.50	1.50	1.50	-	-	-	-	-	-
8,000	1.50	1.50	1.50	-	-	-	-	-	-
8,500	1.53	1.50	1.51	-	-	-	-	-	-
9,000	1.53	1.50	1.51	-	-	-	-	-	-
9,500	1.54	1.52	1.53	-	-	-	-	-	-
10,000	1.54	1.52	1.53	1.55	1.54	1.54	1.65	1.60	1.63
10,500	1.54	1.52	1.53	-	-	-	-	-	-
11,000	1.54	1.52	1.53	-	-	-	-	-	-
11,500	1.58	1.52	1.55	-	-	-	-	-	-
12,000	1.58	1.52	1.55	-	-	-	-	-	-

H-45

Table H-14. Raw data, half-crack length measurements obtained during fatigue cracking for repair patch UBC (continued)

Cycles	Visual			High Frequency Eddy Current			Low Frequency Eddy Current		
	a _{fwd} (inches)	a _{aft} (inches)	a _{avg} (inches)	a _{fwd} (inches)	a _{aft} (inches)	a _{avg} (inches)	a _{fwd} (inches)	a _{aft} (inches)	a _{avg} (inches)
12,500	1.58	1.52	1.55	-	-	-	-	-	-
13,000	1.58	1.52	1.55	-	-	-	-	-	-
13,500	1.58	1.55	1.56	-	-	-	-	-	-
14,000	1.58	1.55	1.56	-	-	-	-	-	-
14,500	1.59	1.55	1.57	-	-	-	-	-	-
15,000	1.62	1.55	1.58	-	-	-	-	-	-
15,500	1.62	1.57	1.59	-	-	-	-	-	-
16,000	1.62	1.60	1.61	-	-	-	-	-	-
16,500	1.62	1.60	1.61	-	-	-	-	-	-
17,000	1.62	1.60	1.61	-	-	-	-	-	-
17,500	1.62	1.60	1.61	-	-	-	-	-	-
18,000	1.62	1.60	1.61	-	-	-	-	-	-
18,500	1.62	1.62	1.62	-	-	-	-	-	-
19,000	1.64	1.62	1.63	-	-	-	-	-	-
19,500	1.64	1.62	1.63	-	-	-	-	-	-
20,000	1.64	1.62	1.63	1.68	1.66	1.67	1.75	1.63	1.69
20,500	1.64	1.62	1.63	-	-	-	-	-	-
21,000	1.67	1.67	1.67	-	-	-	-	-	-
21,500	1.67	1.67	1.67	-	-	-	-	-	-
22,000	1.67	1.67	1.67	-	-	-	-	-	-

Table H-14. Raw data, half-crack length measurements obtained during fatigue cracking for repair patch UBC (continued)

Cycles	Visual			High Frequency Eddy Current			Low Frequency Eddy Current		
	a _{fwd} (inches)	a _{aft} (inches)	a _{avg} (inches)	a _{fwd} (inches)	a _{aft} (inches)	a _{avg} (inches)	a _{fwd} (inches)	a _{aft} (inches)	a _{avg} (inches)
22,500	1.68	1.67	1.68	-	-	-	-	-	-
23,000	1.69	1.67	1.68	-	-	-	-	-	-
23,500	1.69	1.67	1.68	-	-	-	-	-	-
24,000	1.69	1.67	1.68	-	-	-	-	-	-
24,500	1.74	1.67	1.71	-	-	-	-	-	-
25,000	1.74	1.70	1.72	-	-	-	-	-	-
25,500	1.74	1.70	1.72	-	-	-	-	-	-
26,000	1.74	1.70	1.72	-	-	-	-	-	-
26,500	1.74	1.70	1.72	-	-	-	-	-	-
27,000	1.74	1.72	1.73	-	-	-	-	-	-
27,500	1.74	1.72	1.73	-	-	-	-	-	-
28,000	1.74	1.72	1.73	-	-	-	-	-	-
28,500	1.74	1.72	1.73	-	-	-	-	-	-
29,000	1.74	1.72	1.73	-	-	-	-	-	-
29,500	1.74	1.72	1.73	-	-	-	-	-	-
30,000	1.74	1.72	1.73	-	-	-	-	-	-
30,500	1.79	1.75	1.77	-	-	-	-	-	-
31,000	1.79	1.75	1.77	-	-	-	-	-	-
31,500	1.79	1.77	1.78	-	-	-	-	-	-
32,000	1.79	1.77	1.78	-	-	-	-	-	-

Table H-14. Raw data, half-crack length measurements obtained during fatigue cracking for repair patch UBC (continued)

Cycles	Visual			High Frequency Eddy Current			Low Frequency Eddy Current		
	a _{fwd} (inches)	a _{aft} (inches)	a _{avg} (inches)	a _{fwd} (inches)	a _{aft} (inches)	a _{avg} (inches)	a _{fwd} (inches)	a _{aft} (inches)	a _{avg} (inches)
32,500	1.79	1.77	1.78	-	-	-	-	-	-
33,000	1.79	1.82	1.81	-	-	-	-	-	-
33,500	1.79	1.82	1.81	-	-	-	-	-	-
34,000	1.80	1.82	1.81	-	-	-	-	-	-
34,500	1.80	1.82	1.81	-	-	-	-	-	-
35,000	1.80	1.82	1.81	-	-	-	-	-	-
35,500	1.84	1.82	1.83	-	-	-	-	-	-
36,000	1.84	1.82	1.83	-	-	-	-	-	-
36,500	1.84	1.82	1.83	-	-	-	-	-	-
37,000	1.84	1.82	1.83	-	-	-	-	-	-
37,500	1.84	1.82	1.83	-	-	-	-	-	-
38,000	1.84	1.82	1.83	-	-	-	-	-	-
38,500	1.84	1.82	1.83	-	-	-	-	-	-
39,000	1.84	1.82	1.83	-	-	-	-	-	-
39,500	1.84	1.82	1.83	-	-	-	-	-	-
40,000	1.84	1.82	1.83	1.88	1.89	1.88	2.00	1.96	1.98
40,500	1.89	1.87	1.88	-	-	-	-	-	-
41,000	1.89	1.87	1.88	-	-	-	-	-	-
41,500	1.89	1.87	1.88	-	-	-	-	-	-
42,000	1.89	1.87	1.88	-	-	-	-	-	-

Table H-14. Raw data, half-crack length measurements obtained during fatigue cracking for repair patch UBC (continued)

Cycles	Visual			High Frequency Eddy Current			Low Frequency Eddy Current		
	a _{fwd} (inches)	a _{aft} (inches)	a _{avg} (inches)	a _{fwd} (inches)	a _{aft} (inches)	a _{avg} (inches)	a _{fwd} (inches)	a _{aft} (inches)	a _{avg} (inches)
42,500	1.89	1.90	1.89	-	-	-	-	-	-
43,000	1.92	1.90	1.91	-	-	-	-	-	-
43,500	1.94	1.92	1.93	-	-	-	-	-	-
44,000	1.94	1.92	1.93	-	-	-	-	-	-
45,000	1.94	1.92	1.93	-	-	-	-	-	-
46,000	1.94	1.92	1.93	-	-	-	-	-	-
47,000	1.97	1.95	1.96	-	-	-	-	-	-
48,000	1.97	1.97	1.97	-	-	-	-	-	-
49,000	1.97	1.97	1.97	-	-	-	-	-	-
50,000	1.99	1.97	1.98	2.03	2.04	2.03	2.15	2.05	2.10
51,000	1.99	2.02	2.01	-	-	-	-	-	-
52,000	2.02	2.02	2.02	-	-	-	-	-	-
53,000	2.02	2.02	2.02	-	-	-	-	-	-
54,000	2.04	2.02	2.03	-	-	-	-	-	-
55,000	2.07	2.02	2.04	-	-	-	-	-	-
56,000	2.07	2.02	2.04	-	-	-	-	-	-
57,000	2.09	2.02	2.06	-	-	-	-	-	-
58,000	2.09	2.05	2.07	-	-	-	-	-	-
59,000	2.09	2.07	2.08	-	-	-	-	-	-
60,000	2.09	2.07	2.08	2.10	2.06	2.08	2.22	2.20	2.21

Table H-14. Raw data, half-crack length measurements obtained during fatigue cracking for repair patch UBC (continued)

Cycles	Visual			High Frequency Eddy Current			Low Frequency Eddy Current		
	a _{fwd} (inches)	a _{aft} (inches)	a _{avg} (inches)	a _{fwd} (inches)	a _{aft} (inches)	a _{avg} (inches)	a _{fwd} (inches)	a _{aft} (inches)	a _{avg} (inches)
61,000	2.12	2.10	2.11	-	-	-	-	-	-
62,000	2.12	2.10	2.11	-	-	-	-	-	-
63,000	2.14	2.12	2.13	-	-	-	-	-	-
64,000	2.14	2.12	2.13	-	-	-	-	-	-
65,000	2.17	2.12	2.14	-	-	-	-	-	-
66,000	2.17	2.12	2.14	-	-	-	-	-	-
67,000	2.19	2.12	2.16	-	-	-	-	-	-
68,000	2.19	2.15	2.17	-	-	-	-	-	-
69,000	2.19	2.17	2.18	-	-	-	-	-	-
70,000	2.19	2.17	2.18	-	-	-	-	-	-
71,000	2.24	2.20	2.22	-	-	-	-	-	-
72,000	2.24	2.20	2.22	-	-	-	-	-	-
73,000	2.24	2.22	2.23	-	-	-	-	-	-
74,000	2.27	2.22	2.24	-	-	-	-	-	-
75,000	2.29	2.22	2.26	-	-	-	-	-	-
76,000	2.32	2.25	2.28	-	-	-	-	-	-
77,000	2.32	2.25	2.28	-	-	-	-	-	-
78,000	2.32	2.27	2.29	-	-	-	-	-	-
79,000	2.34	2.30	2.32	-	-	-	-	-	-
80,000	2.34	2.30	2.32	2.35	2.34	2.34	-	-	-

H-50

Table H-14. Raw data, half-crack length measurements obtained during fatigue cracking for repair patch UBC (continued)

Cycles	Visual			High Frequency Eddy Current			Low Frequency Eddy Current		
	a _{fwd} (inches)	a _{aft} (inches)	a _{avg} (inches)	a _{fwd} (inches)	a _{aft} (inches)	a _{avg} (inches)	a _{fwd} (inches)	a _{aft} (inches)	a _{avg} (inches)
81,000	2.34	2.30	2.32	-	-	-	-	-	-
82,000	2.34	2.32	2.33	-	-	-	-	-	-
83,000	2.39	2.32	2.36	-	-	-	-	-	-
84,000	2.39	2.32	2.36	-	-	-	-	-	-
85,000	2.39	2.32	2.36	-	-	-	-	-	-
86,000	2.39	2.37	2.38	-	-	-	-	-	-
87,000	2.42	2.37	2.39	-	-	-	-	-	-
88,000	2.42	2.37	2.39	-	-	-	-	-	-
89,000	2.44	2.42	2.43	-	-	-	-	-	-
90,000	2.44	2.45	2.44	-	-	-	-	-	-
91,000	2.49	2.45	2.47	-	-	-	-	-	-
92,000	2.49	2.45	2.47	-	-	-	-	-	-
92,834	2.49	2.45	2.47	2.50	2.49	2.49	2.58	2.52	2.55

H.3.1.6 REPAIR PATCH UDAC

Table H-15. Raw data, half-crack length measurements obtained during fatigue cracking for repair patch UDAC

Cycles	Visual			High Frequency Eddy Current			Low Frequency Eddy Current		
	a _{fwd} (inches)	a _{aft} (inches)	a _{avg} (inches)	a _{fwd} (inches)	a _{aft} (inches)	a _{avg} (inches)	a _{fwd} (inches)	a _{aft} (inches)	a _{avg} (inches)
0	1.47	1.48	1.47	1.50	1.49	1.50	1.52	1.48	1.50
200	1.47	1.48	1.47	-	-	-	-	-	-
400	1.47	1.48	1.47	-	-	-	-	-	-
600	1.47	1.48	1.47	-	-	-	-	-	-
800	1.47	1.48	1.47	-	-	-	-	-	-
1,000	1.47	1.48	1.47	-	-	-	-	-	-
1,200	1.47	1.48	1.47	-	-	-	-	-	-
1,400	1.47	1.48	1.47	-	-	-	-	-	-
1,600	1.47	1.48	1.47	-	-	-	-	-	-
1,800	1.47	1.48	1.47	-	-	-	-	-	-
2,000	1.47	1.48	1.47	-	-	-	-	-	-
2,200	1.47	1.48	1.47	-	-	-	-	-	-
2,400	1.47	1.48	1.47	-	-	-	-	-	-
2,600	1.47	1.48	1.47	-	-	-	-	-	-
2,800	1.47	1.48	1.47	-	-	-	-	-	-
3,000	1.47	1.48	1.47	-	-	-	-	-	-
3,200	1.47	1.48	1.47	-	-	-	-	-	-
3,400	1.48	1.48	1.48	-	-	-	-	-	-
3,600	1.48	1.48	1.48	-	-	-	-	-	-

Table H-15. Raw data, half-crack length measurements obtained during fatigue cracking for repair patch UDAC (continued)

Cycles	Visual			High Frequency Eddy Current			Low Frequency Eddy Current		
	a _{fwd} (inches)	a _{aft} (inches)	a _{avg} (inches)	a _{fwd} (inches)	a _{aft} (inches)	a _{avg} (inches)	a _{fwd} (inches)	a _{aft} (inches)	a _{avg} (inches)
3,800	1.48	1.48	1.48	-	-	-	-	-	-
4,000	1.48	1.48	1.48	-	-	-	-	-	-
4,200	1.48	1.48	1.48	-	-	-	-	-	-
4,400	1.48	1.48	1.48	-	-	-	-	-	-
4,600	1.48	1.48	1.48	-	-	-	-	-	-
5,000	1.48	1.48	1.48	-	-	-	-	-	-
5,500	1.48	1.48	1.48	-	-	-	-	-	-
6,000	1.48	1.48	1.48	-	-	-	-	-	-
6,500	1.48	1.48	1.48	-	-	-	-	-	-
7,000	1.48	1.48	1.48	-	-	-	-	-	-
7,500	1.48	1.48	1.48	-	-	-	-	-	-
8,000	1.48	1.48	1.48	-	-	-	-	-	-
8,500	1.48	1.48	1.48	-	-	-	-	-	-
9,000	1.48	1.48	1.48	-	-	-	-	-	-
9,500	1.48	1.48	1.48	-	-	-	-	-	-
10,000	1.48	1.48	1.48	1.55	1.52	1.53	1.55	1.46	1.51
10,500	1.48	1.48	1.48	-	-	-	-	-	-
11,000	1.48	1.48	1.48	-	-	-	-	-	-
11,500	1.48	1.49	1.49	-	-	-	-	-	-
12,000	1.48	1.49	1.49	-	-	-	-	-	-

Table H-15. Raw data, half-crack length measurements obtained during fatigue cracking for repair patch UDAC (continued)

Cycles	Visual			High Frequency Eddy Current			Low Frequency Eddy Current		
	a _{fwd} (inches)	a _{aft} (inches)	a _{avg} (inches)	a _{fwd} (inches)	a _{aft} (inches)	a _{avg} (inches)	a _{fwd} (inches)	a _{aft} (inches)	a _{avg} (inches)
12,500	1.48	1.49	1.49	-	-	-	-	-	-
13,000	1.48	1.49	1.49	-	-	-	-	-	-
13,500	1.48	1.49	1.49	-	-	-	-	-	-
14,000	1.48	1.49	1.49	-	-	-	-	-	-
14,500	1.48	1.49	1.49	-	-	-	-	-	-
15,000	1.48	1.49	1.49	-	-	-	-	-	-
15,500	1.48	1.49	1.49	-	-	-	-	-	-
16,000	1.48	1.49	1.49	-	-	-	-	-	-
16,500	1.48	1.49	1.49	-	-	-	-	-	-
17,000	1.48	1.49	1.49	-	-	-	-	-	-
17,500	1.48	1.49	1.49	-	-	-	-	-	-
18,000	1.48	1.49	1.49	-	-	-	-	-	-
18,500	1.48	1.49	1.49	-	-	-	-	-	-
19,000	1.48	1.49	1.49	-	-	-	-	-	-
19,500	1.48	1.49	1.49	-	-	-	-	-	-
20,000	1.48	1.49	1.49	1.55	1.51	1.53	1.56	1.43	1.50
20,500	1.48	1.49	1.49	-	-	-	-	-	-
21,000	1.48	1.49	1.49	-	-	-	-	-	-
21,500	1.48	1.49	1.49	-	-	-	-	-	-
22,000	1.48	1.49	1.49	-	-	-	-	-	-

H-54

Table H-15. Raw data, half-crack length measurements obtained during fatigue cracking for repair patch UDAC (continued)

Cycles	Visual			High Frequency Eddy Current			Low Frequency Eddy Current		
	a _{fwd} (inches)	a _{aft} (inches)	a _{avg} (inches)	a _{fwd} (inches)	a _{aft} (inches)	a _{avg} (inches)	a _{fwd} (inches)	a _{aft} (inches)	a _{avg} (inches)
22,500	1.48	1.49	1.49	-	-	-	-	-	-
23,000	1.48	1.49	1.49	-	-	-	-	-	-
23,500	1.48	1.49	1.49	-	-	-	-	-	-
24,000	1.48	1.49	1.49	-	-	-	-	-	-
24,500	1.48	1.49	1.49	-	-	-	-	-	-
25,000	1.48	1.49	1.49	-	-	-	-	-	-
25,500	1.48	1.49	1.49	-	-	-	-	-	-
26,000	1.48	1.49	1.49	-	-	-	-	-	-
26,500	1.48	1.49	1.49	-	-	-	-	-	-
27,000	1.48	1.49	1.49	-	-	-	-	-	-
27,500	1.48	1.49	1.49	-	-	-	-	-	-
28,000	1.48	1.49	1.49	-	-	-	-	-	-
28,500	1.48	1.49	1.49	-	-	-	-	-	-
29,000	1.48	1.49	1.49	-	-	-	-	-	-
29,500	1.48	1.49	1.49	-	-	-	-	-	-
30,000	1.48	1.49	1.49	-	-	-	-	-	-
30,500	1.48	1.49	1.49	-	-	-	-	-	-
31,000	1.48	1.49	1.49	-	-	-	-	-	-
31,500	1.48	1.49	1.49	-	-	-	-	-	-
32,000	1.48	1.49	1.49	-	-	-	-	-	-

Table H-15. Raw data, half-crack length measurements obtained during fatigue cracking for repair patch UDAC (continued)

Cycles	Visual			High Frequency Eddy Current			Low Frequency Eddy Current		
	a _{fwd} (inches)	a _{aft} (inches)	a _{avg} (inches)	a _{fwd} (inches)	a _{aft} (inches)	a _{avg} (inches)	a _{fwd} (inches)	a _{aft} (inches)	a _{avg} (inches)
32,500	1.48	1.49	1.49	-	-	-	-	-	-
33,000	1.48	1.49	1.49	-	-	-	-	-	-
33,500	1.48	1.49	1.49	-	-	-	-	-	-
34,000	1.48	1.49	1.49	-	-	-	-	-	-
34,500	1.48	1.49	1.49	-	-	-	-	-	-
35,000	1.48	1.49	1.49	-	-	-	-	-	-
35,500	1.48	1.49	1.49	-	-	-	-	-	-
36,000	1.48	1.49	1.49	-	-	-	-	-	-
36,500	1.48	1.49	1.49	-	-	-	-	-	-
37,000	1.48	1.49	1.49	-	-	-	-	-	-
37,500	1.48	1.49	1.49	-	-	-	-	-	-
38,000	1.48	1.49	1.49	-	-	-	-	-	-
38,500	1.48	1.49	1.49	-	-	-	-	-	-
39,000	1.48	1.49	1.49	-	-	-	-	-	-
39,500	1.48	1.49	1.49	-	-	-	-	-	-
40,000	1.48	1.49	1.49	1.55	1.51	1.53	1.52	1.45	1.49
40,500	1.48	1.49	1.49	-	-	-	-	-	-
41,000	1.48	1.49	1.49	-	-	-	-	-	-
41,500	1.48	1.49	1.49	-	-	-	-	-	-
42,000	1.48	1.49	1.49	-	-	-	-	-	-

H-56

Table H-15. Raw data, half-crack length measurements obtained during fatigue cracking for repair patch UDAC (continued)

Cycles	Visual			High Frequency Eddy Current			Low Frequency Eddy Current		
	a _{fwd} (inches)	a _{aft} (inches)	a _{avg} (inches)	a _{fwd} (inches)	a _{aft} (inches)	a _{avg} (inches)	a _{fwd} (inches)	a _{aft} (inches)	a _{avg} (inches)
42,500	1.48	1.49	1.49	-	-	-	-	-	-
43,000	1.48	1.49	1.49	-	-	-	-	-	-
43,500	1.48	1.49	1.49	-	-	-	-	-	-
44,000	1.48	1.49	1.49	-	-	-	-	-	-
45,000	1.48	1.49	1.49	-	-	-	-	-	-
46,000	1.48	1.49	1.49	-	-	-	-	-	-
47,000	1.48	1.49	1.49	-	-	-	-	-	-
48,000	1.48	1.49	1.49	-	-	-	-	-	-
49,000	1.48	1.49	1.49	-	-	-	-	-	-
50,000	1.48	1.49	1.49	1.50	1.51	1.50	1.50	1.50	1.50
51,000	1.48	1.49	1.49	-	-	-	-	-	-
52,000	1.48	1.49	1.49	-	-	-	-	-	-
53,000	1.48	1.49	1.49	-	-	-	-	-	-
54,000	1.48	1.49	1.49	-	-	-	-	-	-
55,000	1.48	1.51	1.50	-	-	-	-	-	-
56,000	1.48	1.51	1.50	-	-	-	-	-	-
57,000	1.48	1.51	1.50	-	-	-	-	-	-
58,000	1.48	1.51	1.50	-	-	-	-	-	-
59,000	1.48	1.51	1.50	-	-	-	-	-	-
60,000	1.48	1.51	1.50	1.53	1.51	1.52	1.60	1.40	1.50

Table H-15. Raw data, half-crack length measurements obtained during fatigue cracking for repair patch UDAC (continued)

Cycles	Visual			High Frequency Eddy Current			Low Frequency Eddy Current		
	a _{fwd} (inches)	a _{aft} (inches)	a _{avg} (inches)	a _{fwd} (inches)	a _{aft} (inches)	a _{avg} (inches)	a _{fwd} (inches)	a _{aft} (inches)	a _{avg} (inches)
61,000	1.48	1.51	1.50	-	-	-	-	-	-
62,000	1.48	1.51	1.50	-	-	-	-	-	-
63,000	1.48	1.51	1.50	-	-	-	-	-	-
64,000	1.48	1.51	1.50	-	-	-	-	-	-
65,000	1.48	1.51	1.50	-	-	-	-	-	-
70,000	1.48	1.51	1.50	-	-	-	-	-	-
72,000	1.48	1.51	1.50	-	-	-	-	-	-
74,000	1.48	1.51	1.50	-	-	-	-	-	-
77,000	1.48	1.51	1.50	-	-	-	-	-	-
79,000	1.48	1.51	1.50	-	-	-	-	-	-
80,000	1.48	1.51	1.50	1.53	1.51	1.52	-	-	-
84,000	1.48	1.50	1.49	-	-	-	-	-	-
86,000	1.48	1.50	1.49	-	-	-	-	-	-
88,000	1.48	1.50	1.49	-	-	-	-	-	-
90,000	1.48	1.50	1.49	-	-	-	-	-	-
92,000	1.48	1.50	1.49	-	-	-	-	-	-
92,834	1.48	1.50	1.49	1.53	1.51	1.52	1.54	1.45	1.50

H.3.1.7 REPAIR PATCH UDB

Table H-16. Raw data, half-crack length measurements obtained during fatigue cracking for repair patch UDB

Cycles	Visual			High Frequency Eddy Current			Low Frequency Eddy Current		
	a _{fwd} (inches)	a _{aft} (inches)	a _{avg} (inches)	a _{fwd} (inches)	a _{aft} (inches)	a _{avg} (inches)	a _{fwd} (inches)	a _{aft} (inches)	a _{avg} (inches)
0	1.50	1.50	1.50	1.51	1.52	1.52	1.52	1.56	1.54
500	1.52	1.51	1.52	-	-	-	-	-	-
1,000	1.55	1.54	1.54	-	-	-	-	-	-
2,000	1.57	1.56	1.57	-	-	-	-	-	-
2,500	1.57	1.56	1.57	-	-	-	-	-	-
3,000	1.60	1.59	1.59	-	-	-	-	-	-
3,500	1.60	1.59	1.59	-	-	-	-	-	-
4,000	1.62	1.61	1.62	-	-	-	-	-	-
4,500	1.62	1.61	1.62	-	-	-	-	-	-
5,000	1.62	1.64	1.63	-	-	-	-	-	-
5,500	1.62	1.66	1.64	-	-	-	-	-	-
6,000	1.62	1.66	1.64	-	-	-	-	-	-
6,500	1.67	1.66	1.67	-	-	-	-	-	-
7,000	1.70	1.66	1.68	-	-	-	-	-	-
7,500	1.70	1.66	1.68	-	-	-	-	-	-
8,000	1.70	1.66	1.68	-	-	-	-	-	-
8,500	1.70	1.71	1.71	-	-	-	-	-	-
9,000	1.72	1.74	1.73	-	-	-	-	-	-
9,500	1.72	1.74	1.73	-	-	-	-	-	-

Table H-16. Raw data, half-crack length measurements obtained during fatigue cracking for repair patch UDB (continued)

Cycles	Visual			High Frequency Eddy Current			Low Frequency Eddy Current		
	a _{fwd} (inches)	a _{aft} (inches)	a _{avg} (inches)	a _{fwd} (inches)	a _{aft} (inches)	a _{avg} (inches)	a _{fwd} (inches)	a _{aft} (inches)	a _{avg} (inches)
10,000	1.75	1.74	1.74	1.73	1.81	1.77	1.80	1.85	1.83
10,500	1.75	1.74	1.74	-	-	-	-	-	-
11,000	1.77	1.76	1.77	-	-	-	-	-	-
11,500	1.77	1.76	1.77	-	-	-	-	-	-
12,000	1.77	1.76	1.77	-	-	-	-	-	-
12,500	1.78	1.81	1.80	-	-	-	-	-	-
13,000	1.78	1.81	1.80	-	-	-	-	-	-
13,500	1.82	1.81	1.82	-	-	-	-	-	-
14,000	1.82	1.81	1.82	-	-	-	-	-	-
14,500	1.85	1.84	1.84	-	-	-	-	-	-
15,000	1.85	1.84	1.84	-	-	-	-	-	-
15,500	1.87	1.86	1.87	-	-	-	-	-	-
16,000	1.87	1.86	1.87	-	-	-	-	-	-
16,500	1.87	1.89	1.88	-	-	-	-	-	-
17,000	1.90	1.89	1.89	-	-	-	-	-	-
17,500	1.90	1.89	1.89	-	-	-	-	-	-
18,000	1.90	1.91	1.91	-	-	-	-	-	-
18,500	1.92	1.94	1.93	-	-	-	-	-	-
19,000	1.92	1.94	1.93	-	-	-	-	-	-
19,500	1.92	1.94	1.93	-	-	-	-	-	-

Table H-16. Raw data, half-crack length measurements obtained during fatigue cracking for repair patch UDB (continued)

Cycles	Visual			High Frequency Eddy Current			Low Frequency Eddy Current		
	a _{fwd} (inches)	a _{aft} (inches)	a _{avg} (inches)	a _{fwd} (inches)	a _{aft} (inches)	a _{avg} (inches)	a _{fwd} (inches)	a _{aft} (inches)	a _{avg} (inches)
20,000	1.92	1.94	1.93	1.96	2.04	2.00	2.02	2.03	2.03
20,500	1.92	1.94	1.93	-	-	-	-	-	-
21,000	1.92	1.94	1.93	-	-	-	-	-	-
22,000	1.92	1.94	1.93	-	-	-	-	-	-
23,000	1.97	2.04	2.01	-	-	-	-	-	-
24,000	1.97	2.04	2.01	-	-	-	-	-	-
25,000	2.02	2.04	2.03	-	-	-	-	-	-
26,000	2.02	2.06	2.04	-	-	-	-	-	-
27,000	2.02	2.06	2.04	-	-	-	-	-	-
28,000	2.07	2.09	2.08	-	-	-	-	-	-
29,000	2.12	2.11	2.12	-	-	-	-	-	-
30,000	2.12	2.11	2.12	-	-	-	-	-	-
31,000	2.12	2.14	2.13	-	-	-	-	-	-
32,000	2.15	2.16	2.16	-	-	-	-	-	-
33,000	2.20	2.16	2.18	-	-	-	-	-	-
34,000	2.22	2.16	2.19	-	-	-	-	-	-
35,000	2.22	2.19	2.21	-	-	-	-	-	-
36,000	2.25	2.24	2.24	-	-	-	-	-	-
37,000	2.27	2.24	2.26	-	-	-	-	-	-
38,000	2.30	2.26	2.28	-	-	-	-	-	-

Table H-16. Raw data, half-crack length measurements obtained during fatigue cracking for repair patch UDB (continued)

Cycles	Visual			High Frequency Eddy Current			Low Frequency Eddy Current		
	a _{fwd} (inches)	a _{aft} (inches)	a _{avg} (inches)	a _{fwd} (inches)	a _{aft} (inches)	a _{avg} (inches)	a _{fwd} (inches)	a _{aft} (inches)	a _{avg} (inches)
39,000	2.30	2.26	2.28	-	-	-	-	-	-
40,000	2.32	2.29	2.31	2.38	2.39	2.38	-	-	-
41,000	2.35	2.34	2.34	-	-	-	-	-	-
42,000	2.37	2.34	2.36	-	-	-	-	-	-
43,000	2.40	2.36	2.38	-	-	-	-	-	-
44,000	2.40	2.36	2.38	-	-	-	-	-	-
45,000	2.42	2.39	2.41	-	-	-	-	-	-
46,000	2.42	2.39	2.41	-	-	-	-	-	-
47,000	2.45	2.39	2.42	-	-	-	-	-	-
48,000	2.47	2.41	2.44	-	-	-	-	-	-
49,000	2.50	2.44	2.47	-	-	-	-	-	-
50,000	2.50	2.44	2.47	-	-	-	-	-	-
51,000	2.50	2.44	2.47	-	-	-	-	-	-
52,000	2.55	2.44	2.49	-	-	-	-	-	-
52,834	2.55	2.44	2.49	2.58	2.61	2.60	2.60	2.56	2.58

H.3.1.8 REPAIR PATCH UDBC

Table H-16. Raw data, half-crack length measurements obtained during fatigue cracking for repair patch UDBC

Cycles	Visual			High Frequency Eddy Current			Low Frequency Eddy Current		
	a _{fwd} (inches)	a _{aft} (inches)	a _{avg} (inches)	a _{fwd} (inches)	a _{aft} (inches)	a _{avg} (inches)	a _{fwd} (inches)	a _{aft} (inches)	a _{avg} (inches)
0	1.50	1.48	1.49	1.50	1.50	1.50	1.45	1.55	1.50
200	1.50	1.48	1.49	-	-	-	-	-	-
400	1.50	1.48	1.49	-	-	-	-	-	-
600	1.50	1.48	1.49	-	-	-	-	-	-
800	1.51	1.48	1.50	-	-	-	-	-	-
1,000	1.51	1.48	1.50	-	-	-	-	-	-
1,200	1.51	1.47	1.49	-	-	-	-	-	-
1,400	1.51	1.47	1.49	-	-	-	-	-	-
1,600	1.51	1.47	1.49	-	-	-	-	-	-
1,800	1.51	1.48	1.50	-	-	-	-	-	-
2,000	1.51	1.48	1.50	-	-	-	-	-	-
2,200	1.51	1.48	1.50	-	-	-	-	-	-
2,400	1.51	1.48	1.50	-	-	-	-	-	-
2,600	1.51	1.48	1.50	-	-	-	-	-	-
2,800	1.51	1.48	1.50	-	-	-	-	-	-
3,000	1.51	1.48	1.50	-	-	-	-	-	-
3,200	1.51	1.48	1.50	-	-	-	-	-	-
3,400	1.51	1.48	1.50	-	-	-	-	-	-
3,600	1.51	1.48	1.50	-	-	-	-	-	-

Table H-16. Raw data, half-crack length measurements obtained during fatigue cracking for repair patch UDBC (continued)

Cycles	Visual			High Frequency Eddy Current			Low Frequency Eddy Current		
	a _{fwd} (inches)	a _{aft} (inches)	a _{avg} (inches)	a _{fwd} (inches)	a _{aft} (inches)	a _{avg} (inches)	a _{fwd} (inches)	a _{aft} (inches)	a _{avg} (inches)
3,800	1.51	1.48	1.50	-	-	-	-	-	-
4,000	1.51	1.48	1.50	-	-	-	-	-	-
4,200	1.51	1.48	1.50	-	-	-	-	-	-
4,400	1.51	1.48	1.50	-	-	-	-	-	-
4,600	1.51	1.48	1.50	-	-	-	-	-	-
5,000	1.51	1.48	1.50	-	-	-	-	-	-
5,500	1.51	1.48	1.50	-	-	-	-	-	-
6,000	1.59	1.53	1.56	-	-	-	-	-	-
6,500	1.58	1.54	1.56	-	-	-	-	-	-
7,000	1.58	1.54	1.56	-	-	-	-	-	-
7,500	1.59	1.54	1.56	-	-	-	-	-	-
8,000	1.61	1.57	1.59	-	-	-	-	-	-
8,500	1.61	1.57	1.59	-	-	-	-	-	-
9,000	1.61	1.57	1.59	-	-	-	-	-	-
9,500	1.63	1.57	1.60	-	-	-	-	-	-
10,000	1.63	1.59	1.61	1.63	1.61	1.62	1.66	1.70	1.68
10,500	1.66	1.59	1.63	-	-	-	-	-	-
11,000	1.66	1.59	1.63	-	-	-	-	-	-
11,500	1.69	1.59	1.64	-	-	-	-	-	-
12,000	1.69	1.59	1.64	-	-	-	-	-	-

Table H-16. Raw data, half-crack length measurements obtained during fatigue cracking for repair patch UDBC (continued)

Cycles	Visual			High Frequency Eddy Current			Low Frequency Eddy Current		
	a _{fwd} (inches)	a _{aft} (inches)	a _{avg} (inches)	a _{fwd} (inches)	a _{aft} (inches)	a _{avg} (inches)	a _{fwd} (inches)	a _{aft} (inches)	a _{avg} (inches)
12,500	1.69	1.62	1.65	-	-	-	-	-	-
13,000	1.69	1.62	1.65	-	-	-	-	-	-
13,500	1.71	1.64	1.68	-	-	-	-	-	-
14,000	1.71	1.64	1.68	-	-	-	-	-	-
14,500	1.74	1.65	1.70	-	-	-	-	-	-
15,000	1.74	1.65	1.70	-	-	-	-	-	-
15,500	1.74	1.65	1.70	-	-	-	-	-	-
16,000	1.74	1.67	1.70	-	-	-	-	-	-
16,500	1.74	1.67	1.70	-	-	-	-	-	-
17,000	1.74	1.67	1.70	-	-	-	-	-	-
17,500	1.76	1.69	1.73	-	-	-	-	-	-
18,000	1.76	1.69	1.73	-	-	-	-	-	-
18,500	1.76	1.69	1.73	-	-	-	-	-	-
19,000	1.76	1.69	1.73	-	-	-	-	-	-
19,500	1.76	1.72	1.74	-	-	-	-	-	-
20,000	1.84	1.72	1.78	1.83	1.75	1.79	1.65	1.85	1.75
20,500	1.84	1.72	1.78	-	-	-	-	-	-
21,000	1.84	1.74	1.79	-	-	-	-	-	-
21,500	1.84	1.74	1.79	-	-	-	-	-	-
22,000	1.84	1.74	1.79	-	-	-	-	-	-

H-65

Table H-16. Raw data, half-crack length measurements obtained during fatigue cracking for repair patch UDBC (continued)

Cycles	Visual			High Frequency Eddy Current			Low Frequency Eddy Current		
	a _{fwd} (inches)	a _{aft} (inches)	a _{avg} (inches)	a _{fwd} (inches)	a _{aft} (inches)	a _{avg} (inches)	a _{fwd} (inches)	a _{aft} (inches)	a _{avg} (inches)
22,500	1.86	1.74	1.80	-	-	-	-	-	-
23,000	1.86	1.77	1.81	-	-	-	-	-	-
23,500	1.86	1.77	1.81	-	-	-	-	-	-
24,000	1.86	1.79	1.83	-	-	-	-	-	-
24,500	1.86	1.82	1.84	-	-	-	-	-	-
25,000	1.89	1.82	1.85	-	-	-	-	-	-
25,500	1.91	1.83	1.87	-	-	-	-	-	-
26,000	1.91	1.84	1.88	-	-	-	-	-	-
26,500	1.91	1.84	1.88	-	-	-	-	-	-
27,000	1.94	1.84	1.89	-	-	-	-	-	-
27,500	1.94	1.84	1.89	-	-	-	-	-	-
28,000	1.94	1.87	1.90	-	-	-	-	-	-
28,500	1.94	1.87	1.90	-	-	-	-	-	-
29,000	1.94	1.87	1.90	-	-	-	-	-	-
29,500	1.94	1.87	1.90	-	-	-	-	-	-
30,000	1.94	1.89	1.91	-	-	-	-	-	-
30,500	1.96	1.89	1.93	-	-	-	-	-	-
31,000	1.96	1.89	1.93	-	-	-	-	-	-
31,500	1.96	1.92	1.94	-	-	-	-	-	-
32,000	1.96	1.92	1.94	-	-	-	-	-	-

Table H-16. Raw data, half-crack length measurements obtained during fatigue cracking for repair patch UDBC (continued)

Cycles	Visual			High Frequency Eddy Current			Low Frequency Eddy Current		
	a _{fwd} (inches)	a _{aft} (inches)	a _{avg} (inches)	a _{fwd} (inches)	a _{aft} (inches)	a _{avg} (inches)	a _{fwd} (inches)	a _{aft} (inches)	a _{avg} (inches)
32,500	1.96	1.92	1.94	-	-	-	-	-	-
33,000	1.96	1.92	1.94	-	-	-	-	-	-
33,500	1.99	1.94	1.96	-	-	-	-	-	-
34,000	1.99	1.94	1.96	-	-	-	-	-	-
34,500	2.01	1.94	1.98	-	-	-	-	-	-
35,000	2.01	1.97	1.99	-	-	-	-	-	-
35,500	2.01	1.97	1.99	-	-	-	-	-	-
36,000	2.01	1.97	1.99	-	-	-	-	-	-
36,500	2.01	1.97	1.99	-	-	-	-	-	-
37,000	2.04	1.97	2.00	-	-	-	-	-	-
37,500	2.04	1.99	2.01	-	-	-	-	-	-
38,000	2.04	1.99	2.01	-	-	-	-	-	-
38,500	2.04	1.99	2.01	-	-	-	-	-	-
39,000	2.04	1.99	2.01	-	-	-	-	-	-
39,500	2.06	2.02	2.04	-	-	-	-	-	-
40,000	2.06	2.02	2.04	2.10	2.04	2.07	2.08	2.15	2.12
40,500	2.06	2.02	2.04	-	-	-	-	-	-
41,000	2.09	2.02	2.05	-	-	-	-	-	-
41,500	2.09	2.02	2.05	-	-	-	-	-	-
42,000	2.09	2.02	2.05	-	-	-	-	-	-

Table H-16. Raw data, half-crack length measurements obtained during fatigue cracking for repair patch UDBC (continued)

Cycles	Visual			High Frequency Eddy Current			Low Frequency Eddy Current		
	a _{fwd} (inches)	a _{aft} (inches)	a _{avg} (inches)	a _{fwd} (inches)	a _{aft} (inches)	a _{avg} (inches)	a _{fwd} (inches)	a _{aft} (inches)	a _{avg} (inches)
42,500	2.09	2.04	2.06	-	-	-	-	-	-
43,000	2.11	2.04	2.08	-	-	-	-	-	-
43,500	2.11	2.04	2.08	-	-	-	-	-	-
44,000	2.14	2.09	2.11	-	-	-	-	-	-
44,500	2.14	2.09	2.11	-	-	-	-	-	-
45,000	2.14	2.09	2.11	-	-	-	-	-	-
45,500	2.14	2.09	2.11	-	-	-	-	-	-
46,000	2.14	2.09	2.11	-	-	-	-	-	-
46,500	2.16	2.09	2.13	-	-	-	-	-	-
47,000	2.16	2.09	2.13	-	-	-	-	-	-
47,500	2.16	2.12	2.14	-	-	-	-	-	-
48,000	2.16	2.12	2.14	-	-	-	-	-	-
49,000	2.16	2.14	2.15	-	-	-	-	-	-
49,500	2.19	2.14	2.16	-	-	-	-	-	-
50,000	2.19	2.14	2.16	2.20	2.15	2.18	2.18	2.25	2.22
50,500	2.24	2.17	2.20	-	-	-	-	-	-
51,000	2.24	2.17	2.20	-	-	-	-	-	-
51,500	2.24	2.17	2.20	-	-	-	-	-	-
52,000	2.24	2.17	2.20	-	-	-	-	-	-
52,500	2.24	2.17	2.20	-	-	-	-	-	-

Table H-16. Raw data, half-crack length measurements obtained during fatigue cracking for repair patch UDBC (continued)

Cycles	Visual			High Frequency Eddy Current			Low Frequency Eddy Current		
	a _{fwd} (inches)	a _{aft} (inches)	a _{avg} (inches)	a _{fwd} (inches)	a _{aft} (inches)	a _{avg} (inches)	a _{fwd} (inches)	a _{aft} (inches)	a _{avg} (inches)
53,000	2.26	2.19	2.23	-	-	-	-	-	-
53,500	2.31	2.19	2.25	-	-	-	-	-	-
54,000	2.31	2.19	2.25	-	-	-	-	-	-
54,500	2.31	2.19	2.25	-	-	-	-	-	-
55,000	2.31	2.19	2.25	-	-	-	-	-	-
55,500	2.31	2.19	2.25	-	-	-	-	-	-
56,000	2.31	2.22	2.26	-	-	-	-	-	-
56,500	2.31	2.22	2.26	-	-	-	-	-	-
57,000	2.31	2.27	2.29	-	-	-	-	-	-
57,500	2.31	2.27	2.29	-	-	-	-	-	-
58,000	2.34	2.27	2.30	-	-	-	-	-	-
58,500	2.34	2.27	2.30	-	-	-	-	-	-
59,000	2.34	2.27	2.30	-	-	-	-	-	-
59,500	2.36	2.29	2.33	-	-	-	-	-	-
60,000	2.36	2.29	2.33	2.38	2.33	2.35	2.35	2.53	2.44
60,500	2.36	2.29	2.33	-	-	-	-	-	-
61,000	2.36	2.29	2.33	-	-	-	-	-	-
62,000	2.39	2.29	2.34	-	-	-	-	-	-
63,000	2.39	2.32	2.35	-	-	-	-	-	-
64,000	2.44	2.32	2.38	-	-	-	-	-	-

Table H-16. Raw data, half-crack length measurements obtained during fatigue cracking for repair patch UDBC (continued)

Cycles	Visual			High Frequency Eddy Current			Low Frequency Eddy Current		
	a _{fwd} (inches)	a _{aft} (inches)	a _{avg} (inches)	a _{fwd} (inches)	a _{aft} (inches)	a _{avg} (inches)	a _{fwd} (inches)	a _{aft} (inches)	a _{avg} (inches)
65,000	2.44	2.34	2.39	-	-	-	-	-	-
66,000	2.44	2.37	2.40	-	-	-	-	-	-
67,000	2.46	2.39	2.43	-	-	-	-	-	-
68,000	2.46	2.39	2.43	-	-	-	-	-	-
69,000	2.46	2.39	2.43	-	-	-	-	-	-
70,000	2.46	2.42	2.44	-	-	-	-	-	-
71,000	2.49	2.44	2.46	-	-	-	-	-	-
72,000	2.51	2.44	2.48	-	-	-	-	-	-
73,000	2.51	2.44	2.48	-	-	-	-	-	-
74,000	2.54	2.47	2.50	-	-	-	-	-	-
75,000	2.54	2.49	2.51	-	-	-	-	-	-
76,000	2.56	2.49	2.53	-	-	-	-	-	-
77,000	2.56	2.49	2.53	-	-	-	-	-	-
78,000	2.61	2.49	2.55	-	-	-	-	-	-
79,000	2.61	2.49	2.55	-	-	-	-	-	-
80,000	2.61	2.49	2.55	2.65	2.55	2.60	-	-	-
81,000	2.61	2.52	2.56	-	-	-	-	-	-
82,000	2.61	2.54	2.58	-	-	-	-	-	-
83,000	2.61	2.59	2.60	-	-	-	-	-	-
84,000	2.66	2.59	2.63	-	-	-	-	-	-

H-70

Table H-16. Raw data, half-crack length measurements obtained during fatigue cracking for repair patch UDBC (continued)

Cycles	Visual			High Frequency Eddy Current			Low Frequency Eddy Current		
	a _{fwd} (inches)	a _{aft} (inches)	a _{avg} (inches)	a _{fwd} (inches)	a _{aft} (inches)	a _{avg} (inches)	a _{fwd} (inches)	a _{aft} (inches)	a _{avg} (inches)
85,000	2.66	2.59	2.63	-	-	-	-	-	-
86,000	2.66	2.59	2.63	-	-	-	-	-	-
87,000	2.66	2.59	2.63	-	-	-	-	-	-
88,000	2.69	2.64	2.66	-	-	-	-	-	-
89,000	2.71	2.64	2.68	-	-	-	-	-	-
90,000	2.71	2.64	2.68	-	-	-	-	-	-
91,000	2.71	2.67	2.69	-	-	-	-	-	-
92,000	2.71	2.69	2.70	-	-	-	-	-	-
92,834	2.71	2.69	2.70	2.80	2.75	2.78	2.98	2.68	2.83

H.3.2 HALF-CRACK MEASUREMENTS, GRAPHED

Provided in the subsequent sections are plots displaying half-crack measurements obtained via visual, HFEC, and LFEC inspections during fatigue cracking for repair patches RAC, RBC, UAC, UB, UBC, UDAC, UDB, and UDBC, respectively.

H.3.2.1 REPAIR PATCH RAC

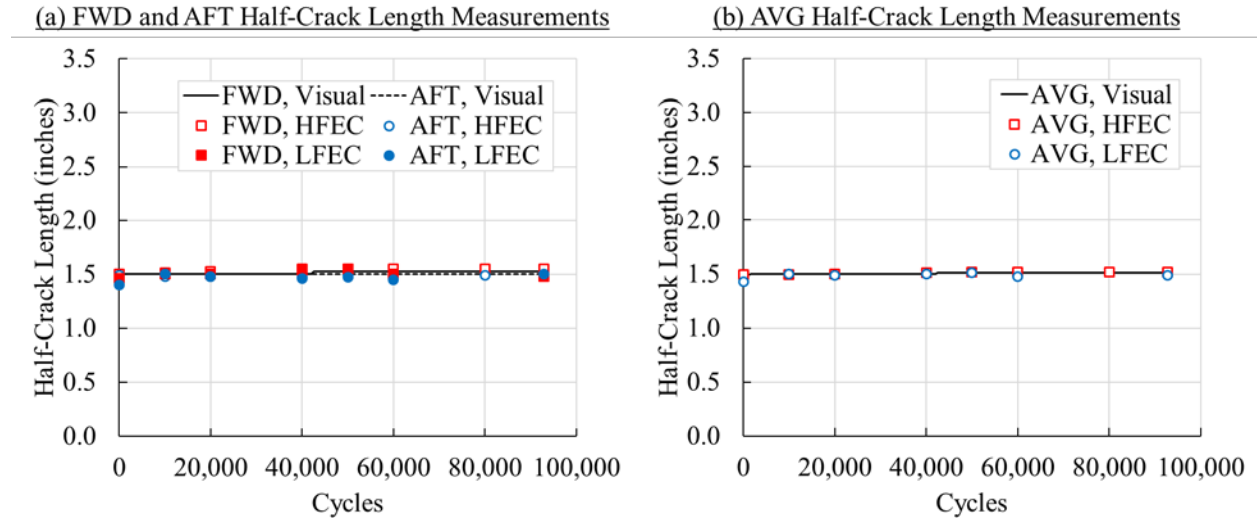


Figure H-12. Half-crack length measurements conducted during fatigue cracking for repair patch RAC: (a) FWD and AFT half-crack results and (b) AVG half-crack results

H.3.2.2 REPAIR PATCH RBC

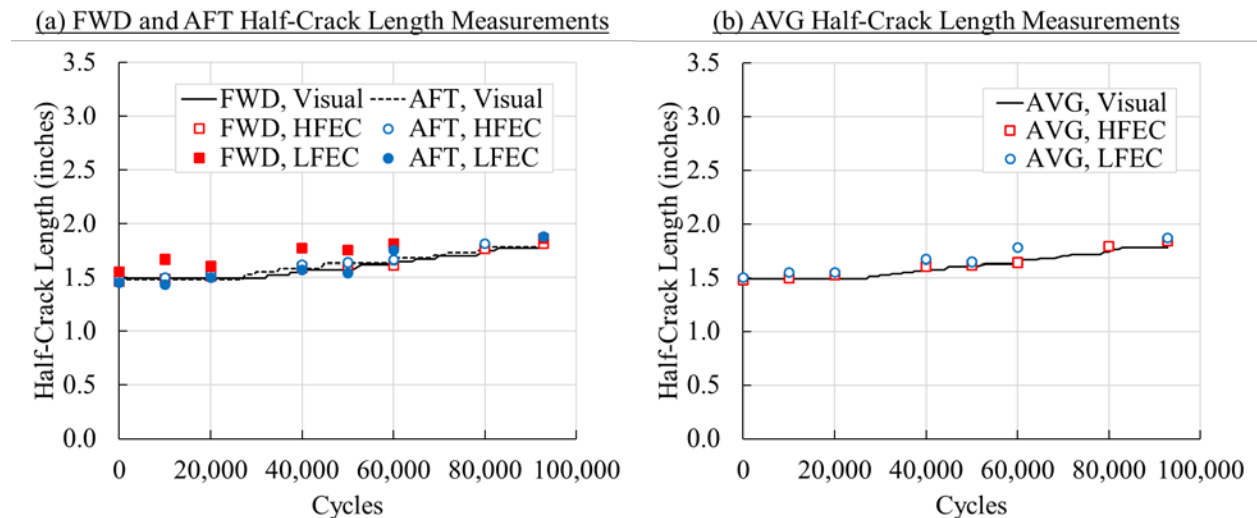


Figure H-13. Half-crack length measurements conducted during fatigue cracking for repair patch RBC: (a) FWD and AFT half-crack results and (b) AVG half-crack results

H.3.2.3 REPAIR PATCH UAC

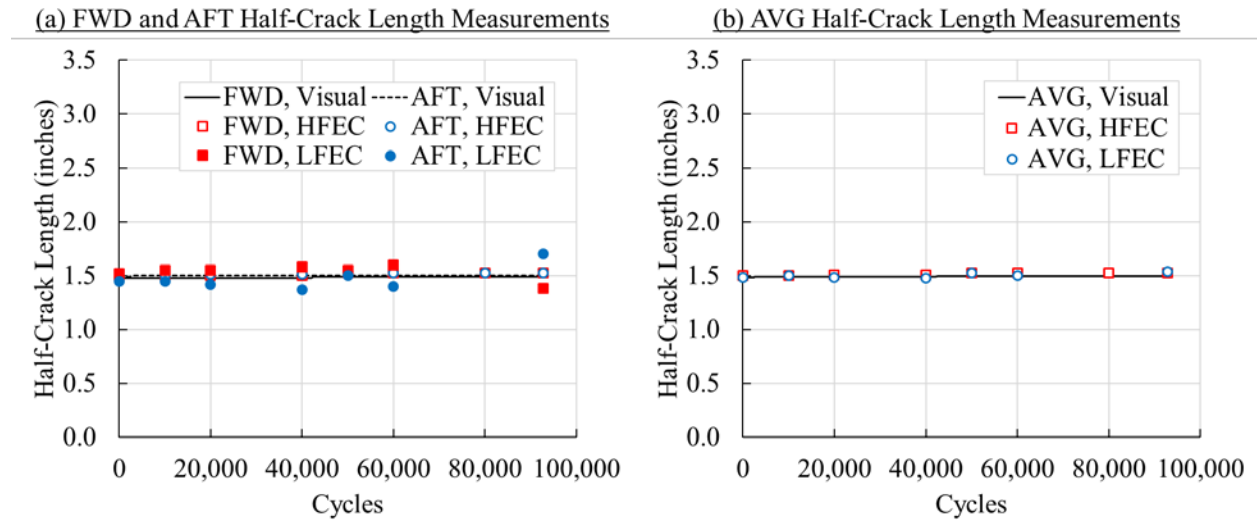


Figure H-14. Half-crack length measurements conducted during fatigue cracking for repair patch UAC: (a) FWD and AFT half-crack results and (b) AVG half-crack results

H.3.2.4 REPAIR PATCH UB

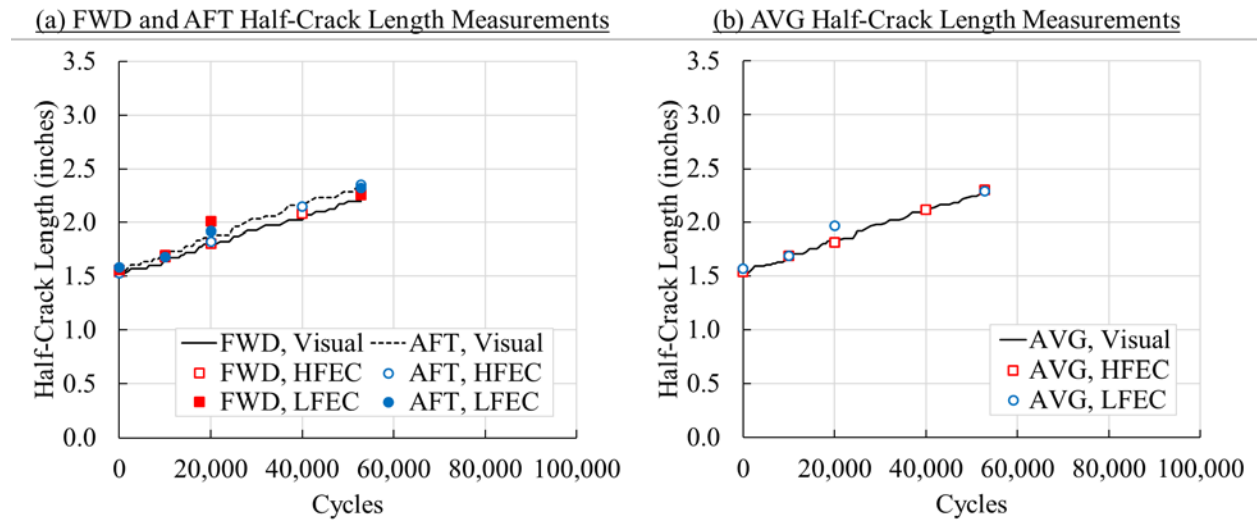


Figure H-15. Half-crack length measurements conducted during fatigue cracking for repair patch UB: (a) FWD and AFT half-crack results and (b) AVG half-crack results

H.3.2.5 REPAIR PATCH UBC

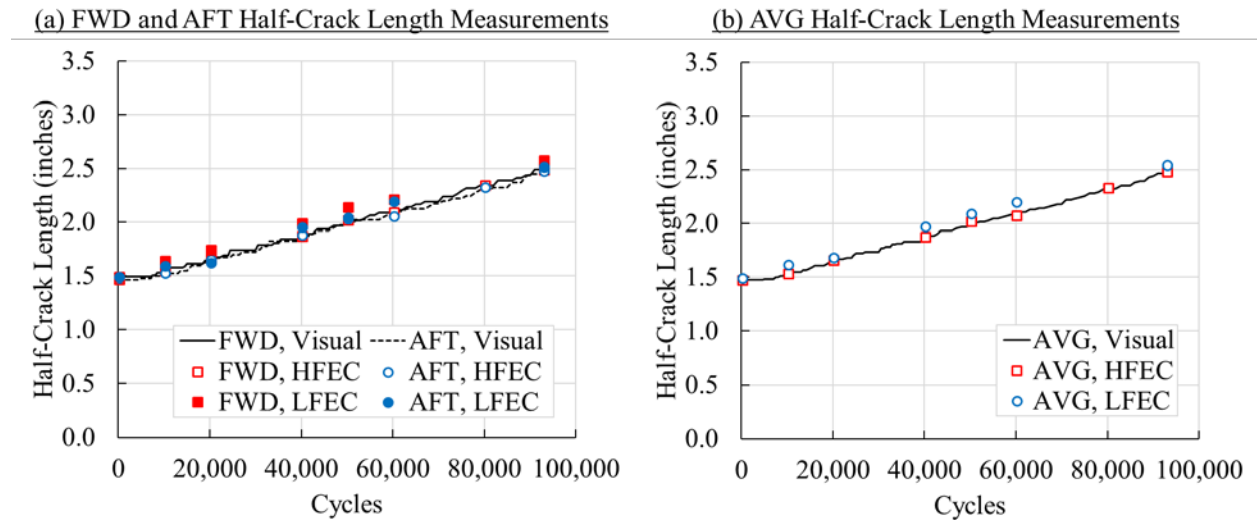


Figure H-16. Half-crack length measurements conducted during fatigue cracking for repair patch UBC: (a) FWD and AFT half-crack results and (b) AVG half-crack results

H.3.2.6 REPAIR PATCH UDAC

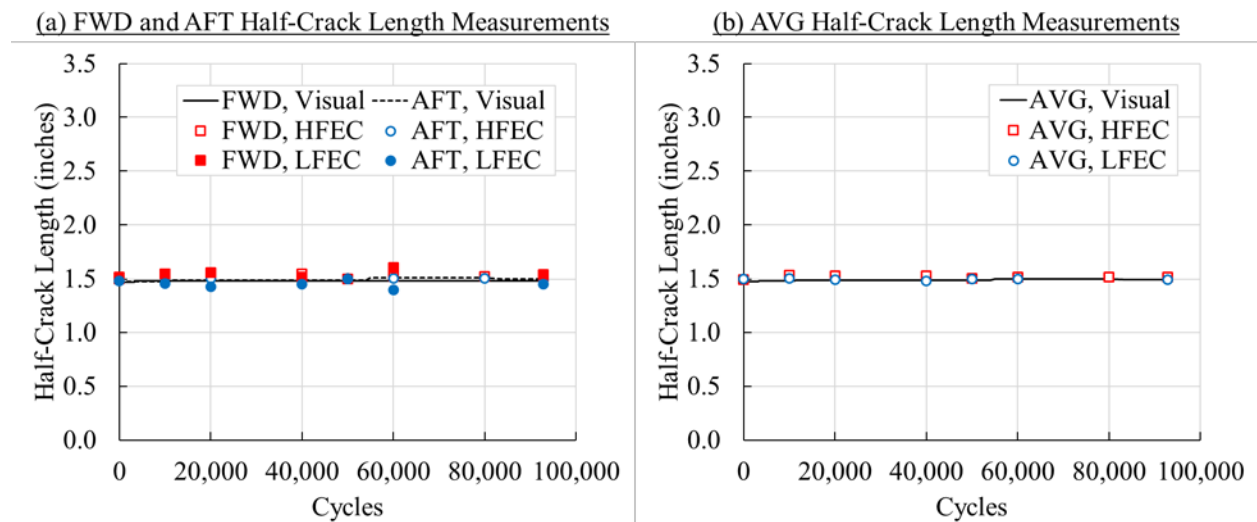


Figure H-17. Half-crack length measurements conducted during fatigue cracking for repair patch UDAC: (a) FWD and AFT half-crack results and (b) AVG half-crack results

H.3.2.7 REPAIR PATCH UDB

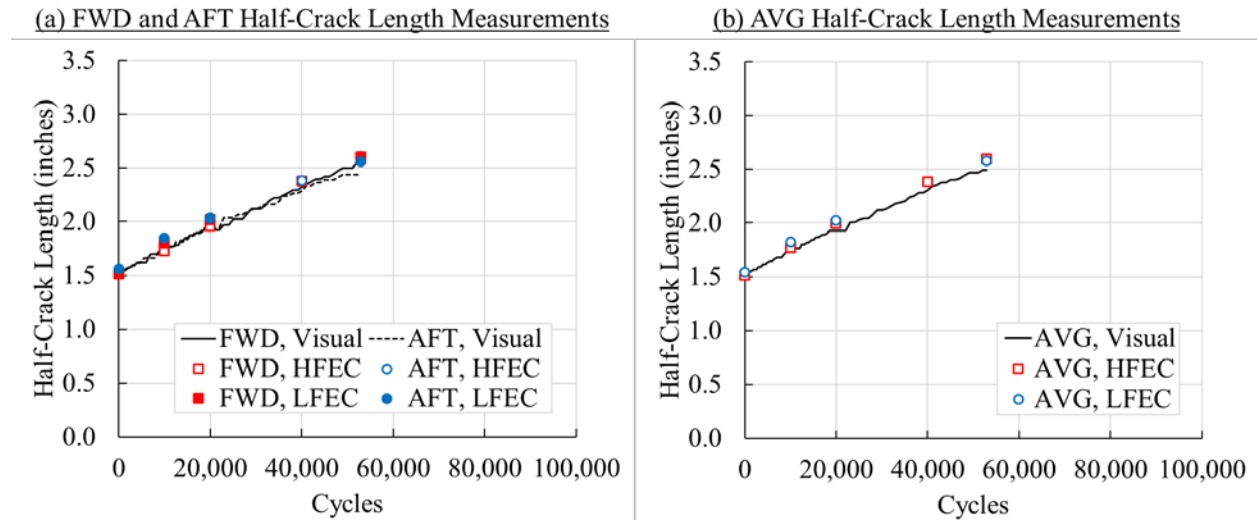


Figure H-18. Half-crack length measurements conducted during fatigue cracking for repair patch UDB: (a) FWD and AFT half-crack results and (b) AVG half-crack results

H.3.2.8 REPAIR PATCH UDBC

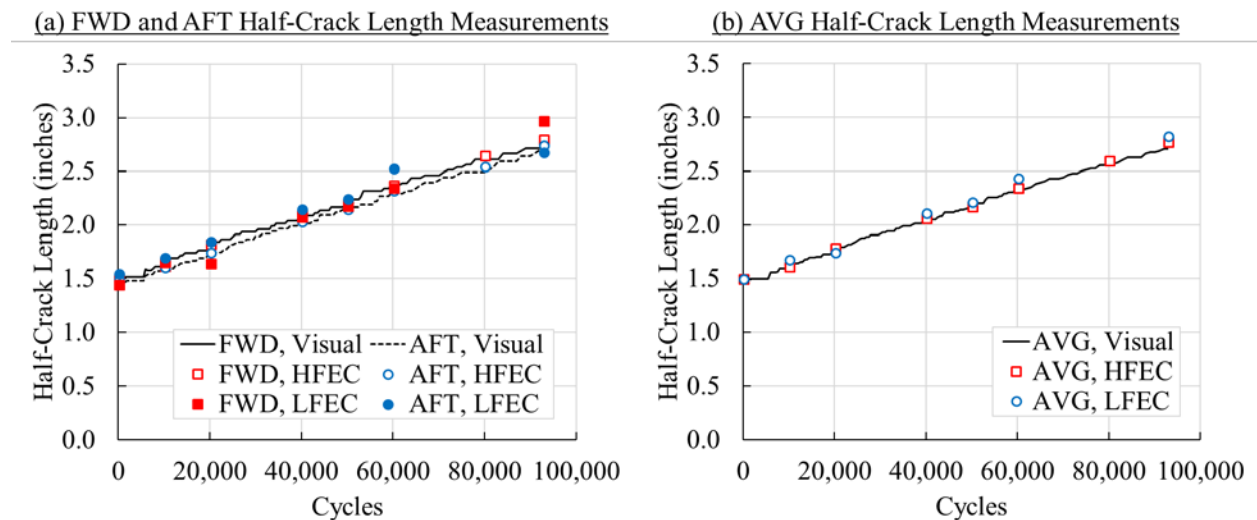


Figure H-19. Half-crack length measurements conducted during fatigue cracking for repair patch UDBC: (a) FWD and AFT half-crack results and (b) AVG half-crack results

APPENDIX I—FLASH THERMOGRAPHY RESULTS

I.1 INTRODUCTION

Flash thermography is a non-destructive inspection method that utilizes measured changes in the surface temperature of a specimen subjected to a spatially uniform flash of light, captured via sequential, digital, infrared images, to detect subsurface irregularities (e.g., voids or inclusions). Throughout the duration of the test, a Thermal Wave Imaging (TWI) ThermoScope® II system was used to monitor the formation and growth of areas of disbond, cracks, and general damage in the vicinity of each B/Ep repair patch. The ThermoScope® II system consisted of a portable high-performance PC system pre-equipped with MOSAIQ® analysis software, shown in figure I-1a, and an integrated illumination head comprised of two xenon flash lamps, an infrared camera, and an LCD monitor, shown in figure I-1b. The MOSAIQ® software, which utilizes the thermographic signal reconstruction (TSR) method to process the digital, infrared images captured during each inspection, allowed for full-field and pointwise observation of the surface temperature response, logarithm of the surface temperature response, first logarithmic derivative of the surface temperature response, and the second logarithmic derivative of the surface temperature response.

(a) TWI Portable High-Performance PC System



(b) TWI Integrated Illumination Head



Figure I-1. (a) TWI ThermoScope® II high-performance PC system complete with MOSAIQ® analysis software, and (b) TWI ThermoScope® II integrated illumination head

Specimen preparations, pre-processing parameters, data capture procedures, post-processing parameters, and post-processing procedures were generally consistent throughout the duration of the test. Because of the requirements of the digital image correlation system, each inspection region (i.e., the top surface of each B/Ep repair patch and the external fuselage panel skin in the immediate vicinity of each B/Ep repair patch) was coated with a dull, highly contrasted, monochromatic, stochastic pattern. Prior to each inspection, this coating was removed. Subsequently, the system was configured, and inspections were conducted. Adjustable parameters prior to acquisition included: 1) acquisition length, 2) capture rate, 3) TSR skip frames, 4) trigger mode, 5) flash frame, 6) precision flash duration, and 7) flash trigger offset (FTO). For each inspection, the acquisition length was 19.89 seconds, the capture rate was 29.97 frames/second, the number of TSR skip frames was 2, the trigger mode was internal, the flash frame was 10, the precision flash duration was 4.1 milliseconds, and the FTO was 0.2 milliseconds. Because of the field-of-view limitations of the integrated illumination head, multiple images of each B/Ep repair

patch were captured and stitched together during post-processing to create a single image for each repair patch.

During each inspection period, the integrated illumination head was used to inspect the left side of each repair patch, followed by the right half of each repair patch. When the inspection of both halves of a repair patch was complete, imperfections of the repair patch, clearly visible in the flash thermography results, were used to stitch the two images together. When this post-processing was complete, full-field, monochromatic indications of the surface temperature response, logarithm of the surface temperature response, first logarithmic derivative of the surface temperature response, and the second logarithmic derivative of the surface temperature response were evaluated at several time marks into acquisition. When the inspection process was complete for each repair patch, digital images depicting these results were captured and archived.

I.2 FLASH THERMOGRAPHY RESULTS

The periods during which flash thermography inspections were conducted were strategically chosen to ensure the ability to evaluate whether the accumulation of fatigue cycles caused the formation or growth of areas of disbond, cracks, and general damage in the vicinity of each B/Ep repair patch. A summary of the inspection periods during which flash thermography inspections were conducted is provided in table I-1.

Table I-1. Summary of flash thermography inspections

Inspection Period	Repair Patches Inspected
After Phase I Patch Installation	RBC, UBC, UDBC
After 10,000 Cycles	RBC, UBC, UDBC
After 20,000 Cycles	RBC, UBC, UDBC
After 40,000 Cycles	RBC, UB, UBC, UDB, UDBC
After 50,000 Cycles	RBC, UB, UBC, UDB, UDBC
After 60,000 Cycles	RBC, UB, UBC, UDB, UDBC
After 92,834 Cycles	RBC, UB, UBC, UDB, UDBC

I.2.1 Second Logarithmic Derivative of Surface Temperature Measurements

Provided in the subsequent sections are full-field, monochromatic results displaying the second logarithmic derivative of surface temperature for repair patches RBC, UB, UBC, UDB, and UDBC, respectively. In each case, results shown were captured 2.502 seconds into acquisition. Results for repair patches RBC, UB, UBC, UDB, and UDBC are provided in figures I-2 through I-6, respectively.

I.2.1.1 REPAIR PATCH RBC

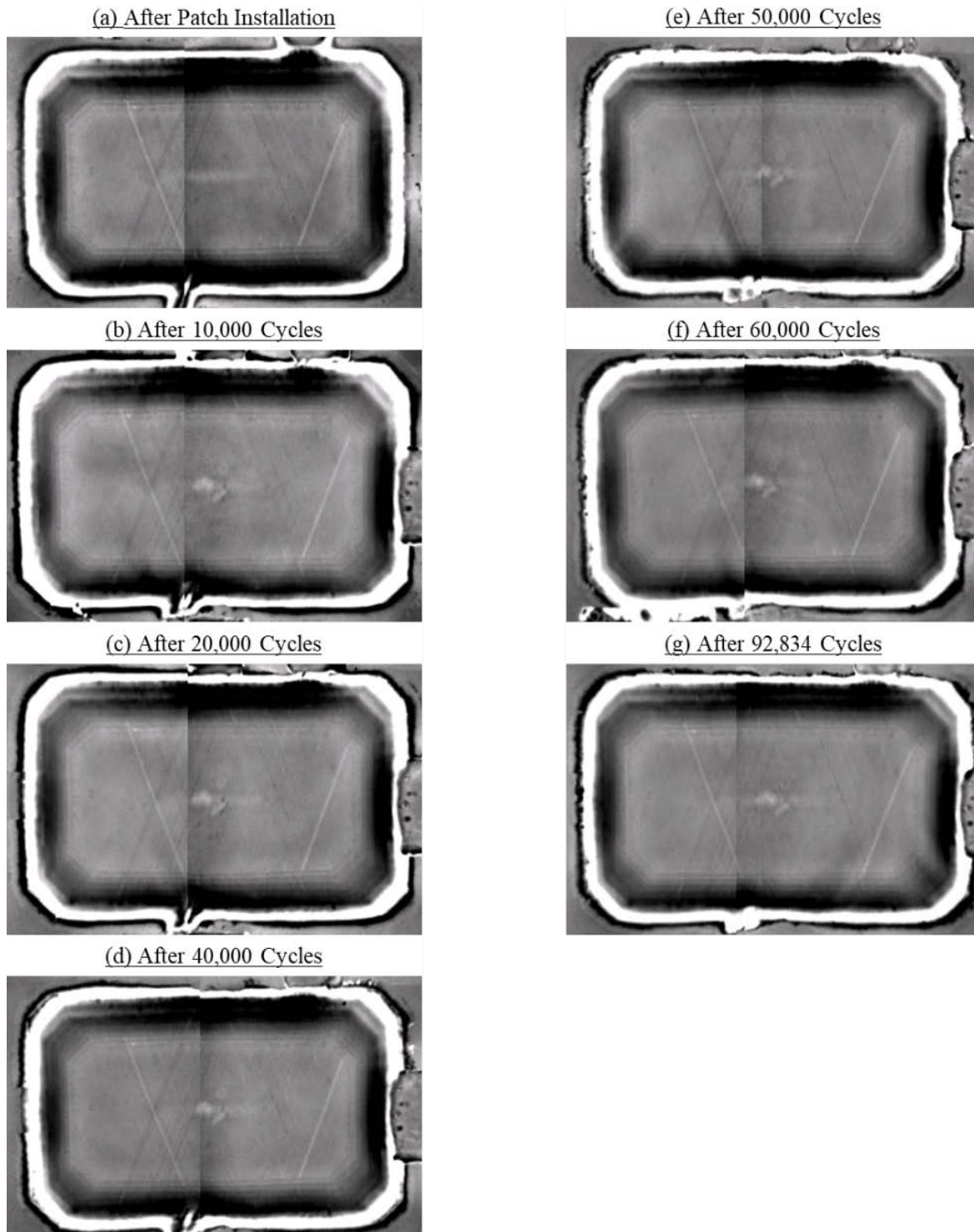


Figure I-2. Flash thermography results captured for repair patch RBC: (a) after patch installation, (b) after 10,000 cycles, (c) after 20,000 cycles, (d) after 40,000 cycles, (e) after 50,000 cycles, (f) after 60,000 cycles, and (g) after 92,834 cycles

I.2.1.2 REPAIR PATCH UB

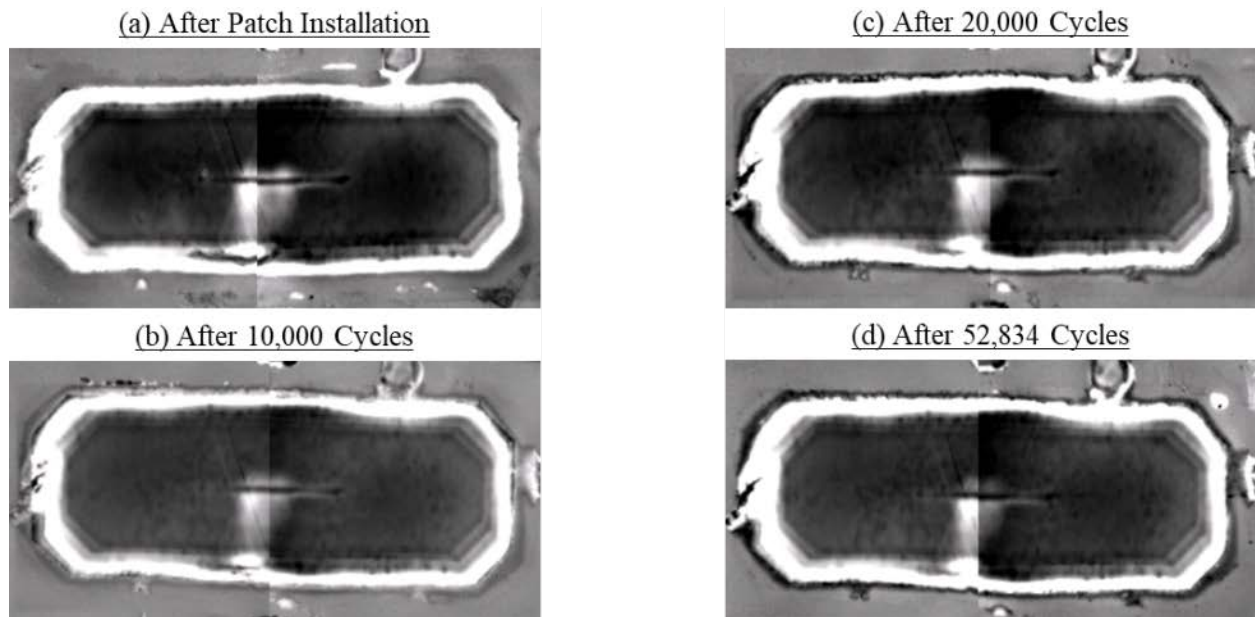


Figure I-3. Flash thermography results captured for repair patch UB: (a) after patch installation, (b) after 10,000 cycles, (c) after 20,000 cycles, and (d) after 52,834 cycles

I.2.1.3 REPAIR PATCH UBC

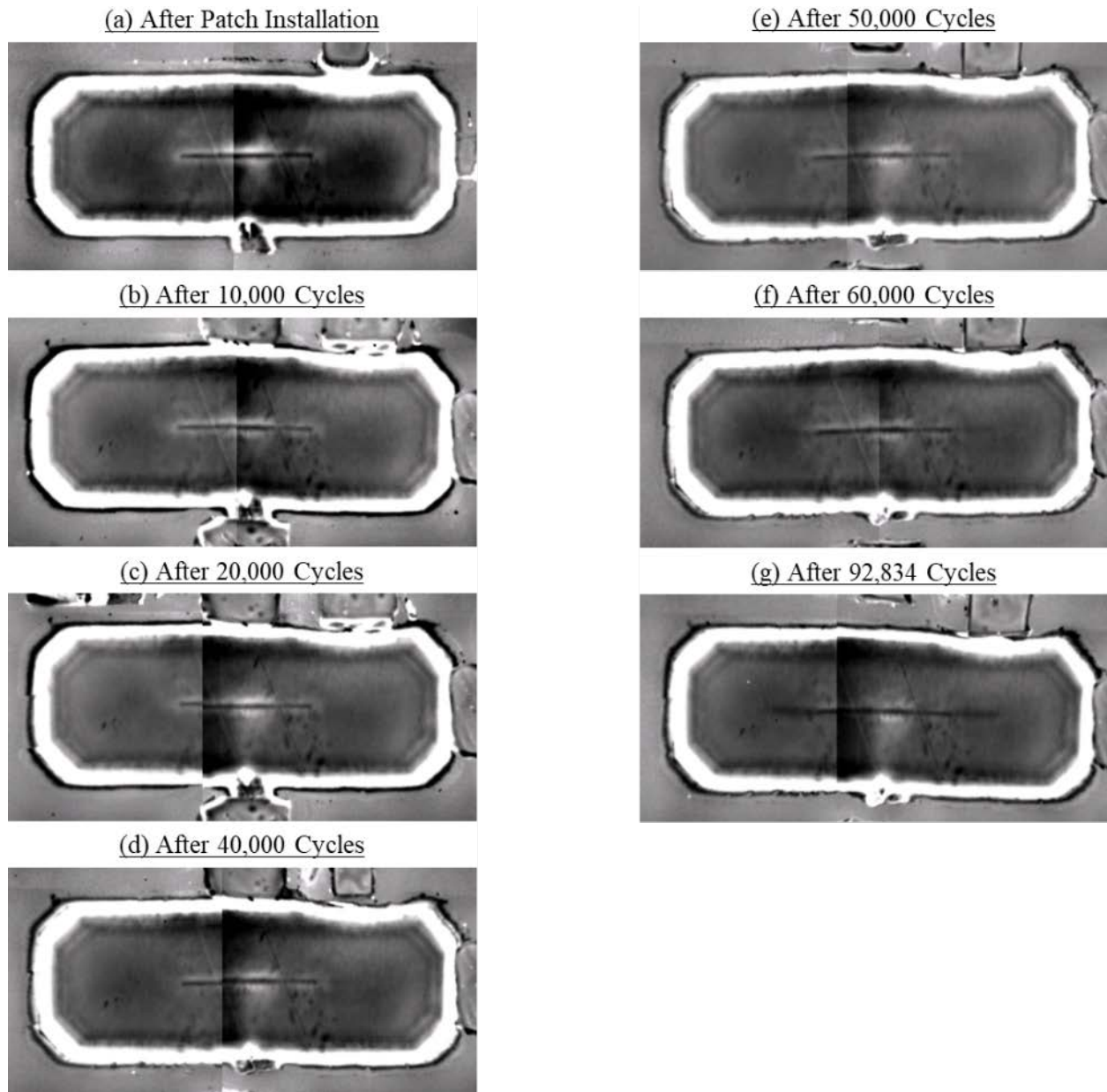


Figure I-4. Flash thermography results captured for repair patch UBC: a) after patch installation, (b) after 10,000 cycles, (c) after 20,000 cycles, (d) after 40,000 cycles, (e) after 50,000 cycles, (f) after 60,000 cycles, and (g) after 92,834 cycles

I.2.1.4 REPAIR PATCH UDB

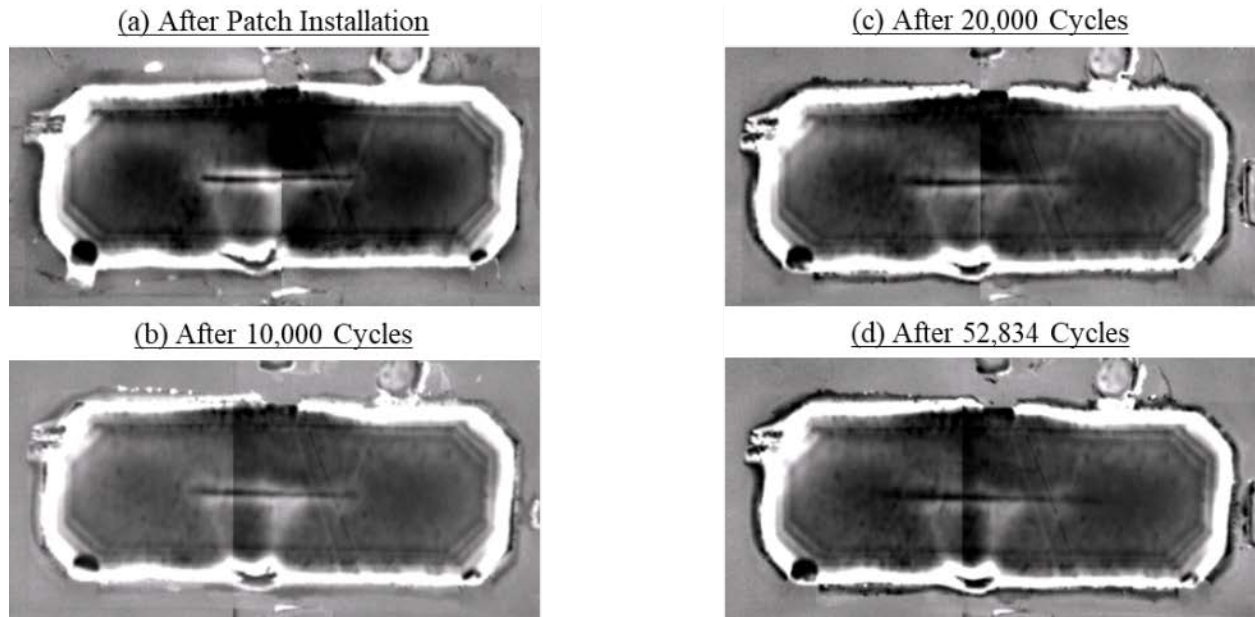


Figure I-5. Flash thermography results captured for repair patch UDB: (a) after patch installation, (b) after 10,000 cycles, (c) after 20,000 cycles, and (d) after 52834 cycles

I.2.1.5 REPAIR PATCH UDBC

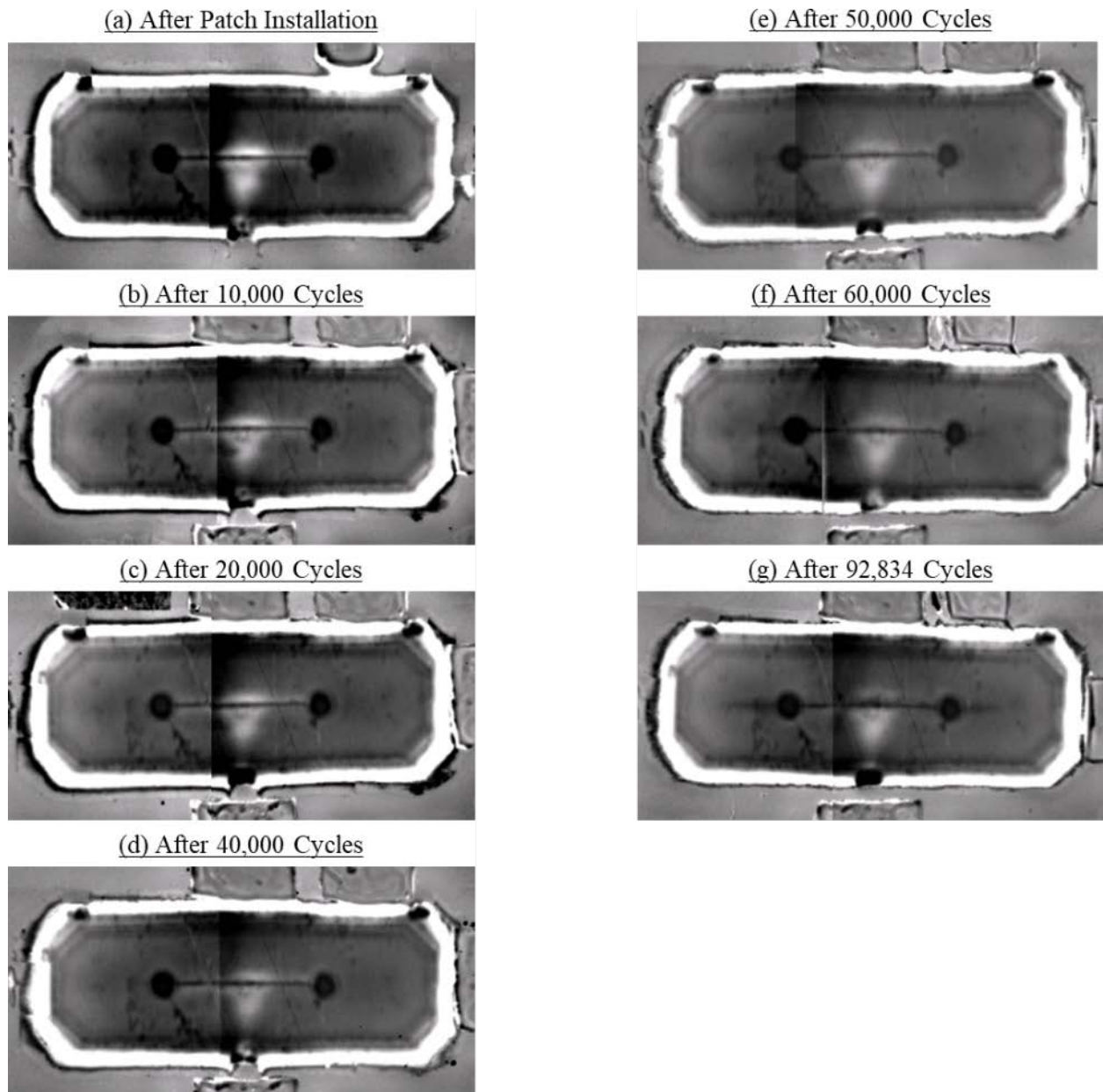


Figure I-6. Flash thermography results captured for repair patch UDBC: (a) after patch installation, (b) after 10,000 cycles, (c) after 20,000 cycles, (d) after 40,000 cycles, (e) after 50,000 cycles, (f) after 60,000 cycles, and (g) after 92,834 cycles

APPENDIX J—RESONANCE ULTRASONIC RESULTS

J.1 INTRODUCTION

Resonance ultrasonic is a non-destructive inspection method that utilizes measured changes in the phase and amplitude of ultrasonic waveforms induced in a specimen to detect subsurface irregularities (e.g., voids or inclusions). Throughout the duration of the test, an Olympus BondMaster 1000e+ instrument (P/N 7720140.00), a system capable of generating waveforms with frequencies ranging from 250 Hz to 1.5 MHz, shown in figure J-1a, was used in conjunction with ultrasonic couplant and a detachable resonance probe to monitor the formation and growth of areas of disbond, cracks, and general damage in the vicinity of each repair patch. Sonotech ULTRAGEL II® (P/N 25-901), shown in figure J-1a, and an S-PR-5 - 250 kHz Resonance Probe (P/N 9317795) featuring a tip diameter of 0.37 inch and an operating frequency range of 240 to 260 kHz, shown in figure J-1b, were used to conduct inspections on the top of each repair patch. Specimen preparations, pre-processing parameters, data capture procedures, post-processing parameters, and post-processing procedures were generally consistent throughout the duration of the test. Because of the requirements of the digital image correlation system, each inspection region was coated with a dull, highly contrasted, monochromatic, stochastic pattern. Prior to each inspection, this coating was removed. When the coating was removed, the system was configured and inspections were conducted.

(a) Olympus BondMaster 1000e+ Instrument



(b) S-PR-5 - 250 kHz Resonance Probe



Figure J-1. (a) Olympus BondMaster 1000e+, and (b) S-PR-5 - 250 kHz resonance probe

Adjustable parameters prior to and during acquisition included the: 1) phase angle, 2) horizontal signal gain, 3) vertical signal gain, and 4) frequency. Prior to each inspection, the phase angle was set at 169 degrees, the horizontal signal gain was set to -5.0 dB, the vertical signal gain was set to -5.0 dB, and the frequency was set to 248 kHz. Subsequently, using reference standards provided by The Boeing Company, these values were adjusted to ensure that specific indications for each repair type (e.g., those caused by detection of an FEP insert) were appropriately distributed in the instrument's polar-coordinate plot of phase (angular rotation) and amplitude (radius). Specific indications included those observed during: 1) inspection of an area with no known imperfections; 2) suspension of the probe in air (i.e., during lift-off); 3) inspection of an area with an FEP tab insert; and 4) inspection of an area with an Al shim insert. In each case, the system was calibrated to ensure that indication recorded during inspection of an area with no known imperfection was located at the origin of the polar-coordinate plot. Indications recorded during inspection of an area

with an Al shim insert, during inspection of an area with an FEP tab insert, and during suspension of the probe in air were likewise located in the top right, middle right, and right of the first quadrant of the polar-coordinate plot.

During each inspection period, the resonance probe was methodically relocated throughout the top surface of each repair patch. In each case, an indication whose radius exceeded a certain value (dictated by the parameters specified during the calibration process), represented by a square as shown for example in figure J-1a, was considered significant. At any point, if the indication radius exceeded this critical value, a pencil was used to lightly mark the top surface of the repair patch at the geometric center of the probe. When such an indication was found, further investigations of the immediate area were conducted to map out the boundary of the imperfection. This process was completed for the entire top surface of each repair patch. When the inspection process was complete, pictures of the top surface of each repair patch were captured and archived.

J.2 RESONANCE ULTRASONIC RESULTS

The periods during which resonance ultrasonic inspections were conducted were strategically chosen to ensure the ability to evaluate whether the accumulation of fatigue cycles caused the formation or growth of areas of disbond and general damage in the vicinity of each repair patch. A summary of the inspection periods during which resonance ultrasonic inspections were conducted is shown in table J-1.

Table J-1. Summary of resonance ultrasonic inspections

Inspection Period	Repair Patches Inspected
After Phase-I Patch Installation	RAC, RBC, UAC, UBC, UDAC, UDBC
After 10,000 Cycles	RAC, RBC, UAC, UBC, UDAC, UDBC
After 20,000 Cycles	RAC, RBC, UAC, UBC, UDAC, UDBC
After 40,000 Cycles	RAC, RBC, UAC, UB, UBC, UDAC, UDB, UDBC
After 60,000 Cycles	RAC, RBC, UAC, UB, UBC, UDAC, UDB, UDBC
After 92,834 Cycles	RAC, RBC, UAC, UB, UBC, UDAC, UDB, UDBC

J.2.1 Photographs of Pencil-Marked Repair Patches

Provided in the subsequent sections are representative resonance ultrasonic results for repair patches UDAC and UDBC. In each case, results are provided in the form of pictures that were captured following the completion of each inspection. Visible pencil and marker markings represent the boundary of imperfections detected by the resonance ultrasonic system. Results for repair patches UDAC and UDBC are provided in figures J-2 and J-3, respectively.

J.2.1.1 REPAIR PATCH UDAC

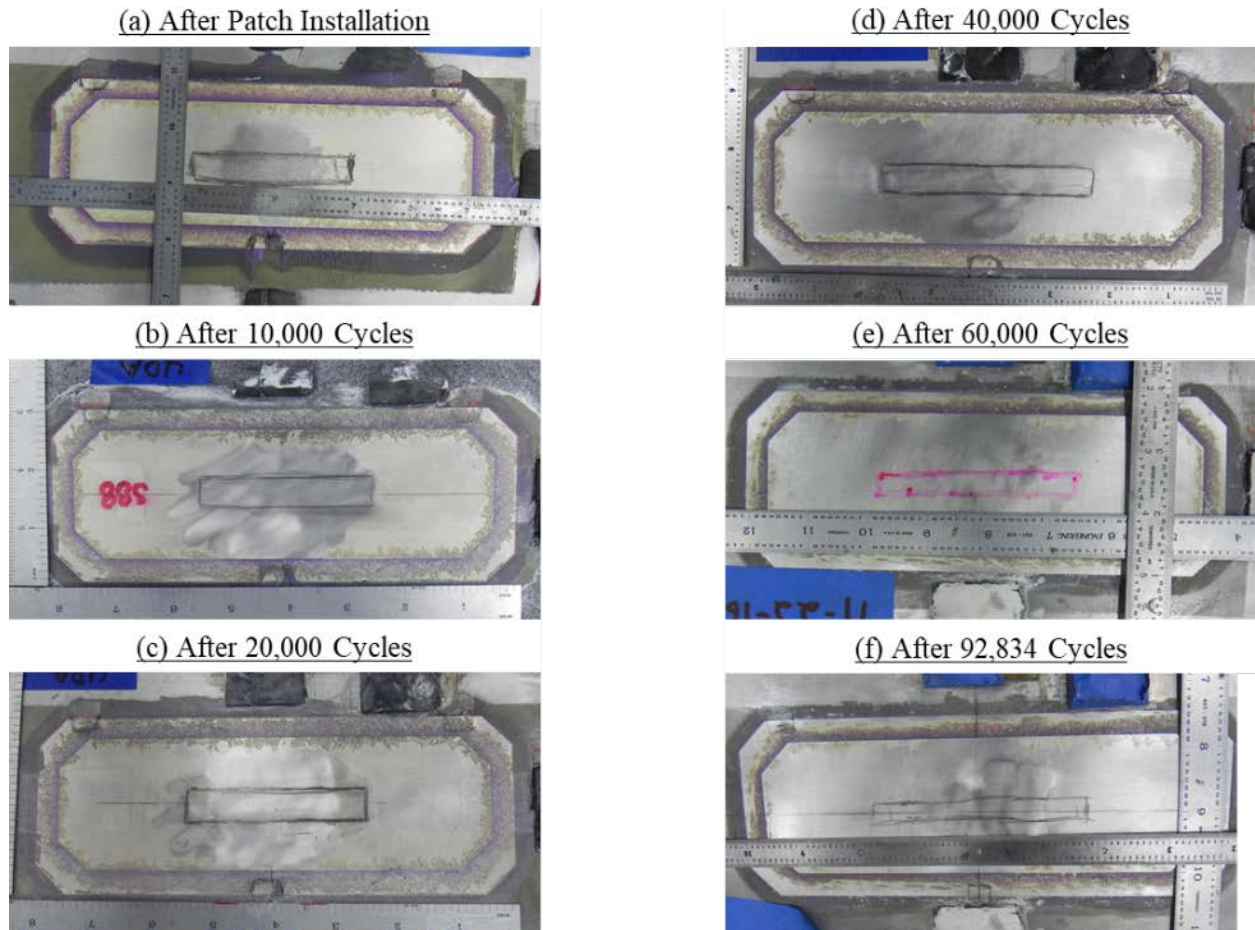


Figure J-2. Flash thermography results captured for repair patch UDAC: a) after patch installation, (b) after 10,000 cycles, (c) after 20,000 cycles, (d) after 40,000 cycles, (e) after 60,000 cycles, and (f) after 92,834 cycles

J.2.1.2 REPAIR PATCH UDBC

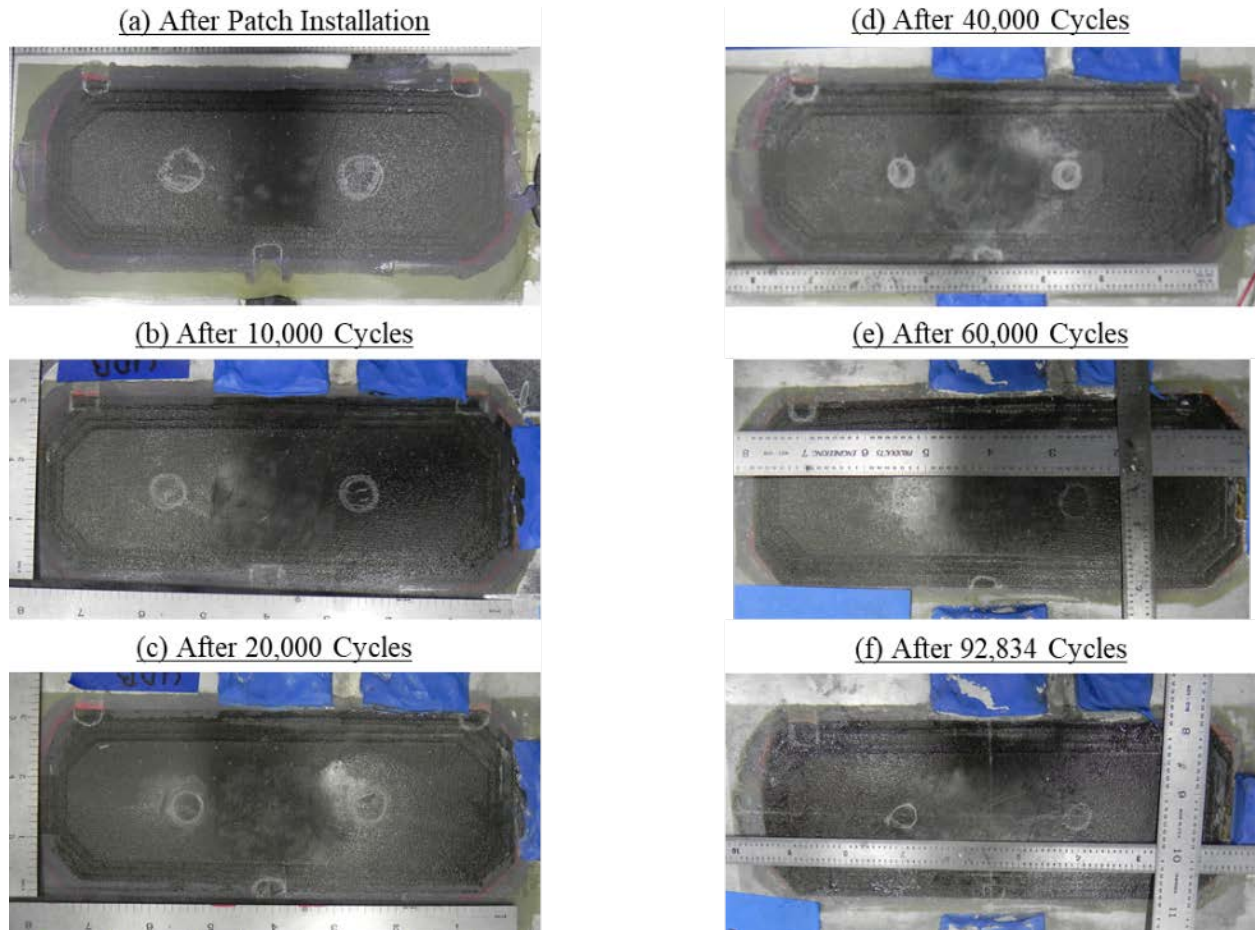


Figure J-3. Flash thermography results captured for repair patch UDBC: a) after patch installation, (b) after 10,000 cycles, (c) after 20,000 cycles, (d) after 40,000 cycles, (e) after 60,000 cycles, and (f) after 92,834 cycles

APPENDIX K–PRELIMINARY THERMAL RESIDUAL STRESS ANALYSIS BY
VISCOELASTIC MODELING

All previous thermal residual stress analyses used a thermo-elastic model in which the modulus of the adhesive across the glass transition temperature was assumed to change according to a step function, as shown in figure K-1. However, most adhesives actually behave viscoelastically, as shown in figure K-2, for a generic adhesive at various curing levels. As shown, time-dependent modulus curves (and temperature-dependent modulus curves, not shown) for curing levels $c = 0.74$, $c = 0.87$, $c = 0.95$, and $c = 0.99$ (i.e., a 74% cure, an 87% cure, a 95% cure, and a 99% cure, respectively) are smooth; therefore, the change of the modulus of the adhesive across the glass transition is a smooth curve, not a step function as idealized in the thermo-elastic model. In an effort to improve the predictive capability of thermal residual stresses in adhesively bonded repair patches, especially B/Ep repair patches, a study was conducted using a viscoelastic material model newly developed by the Inhar University (see figure K-3).

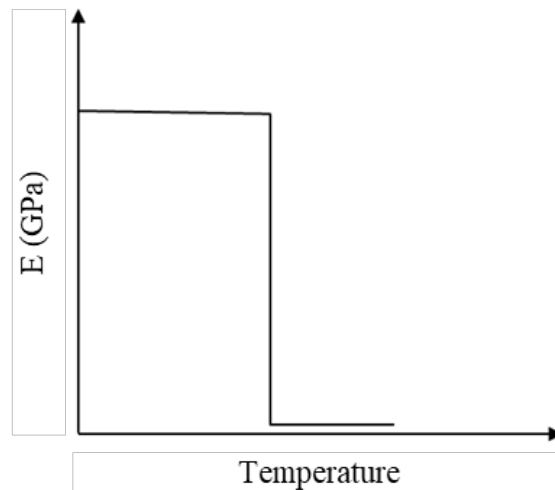


Figure K-1. Temperature-dependent mechanical behavior of a generic adhesive across glass transition temperatures based on a thermo-elastic model

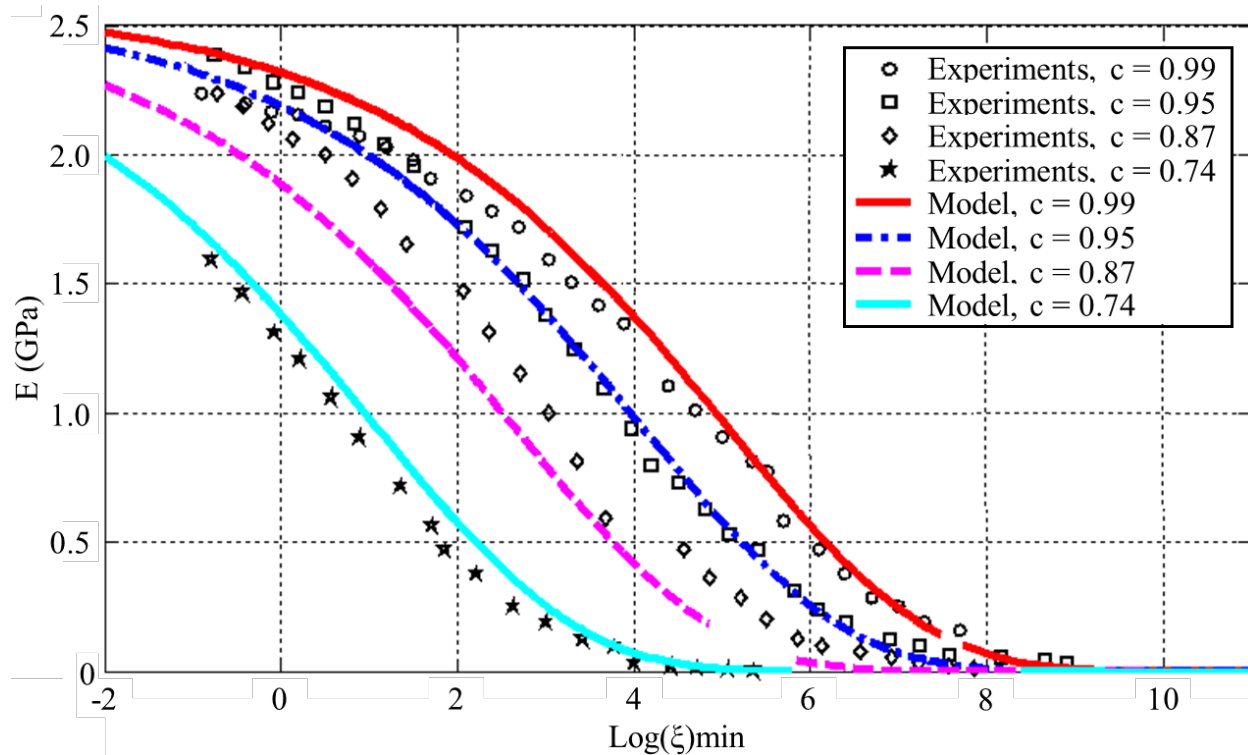


Figure K-2. Time-dependent mechanical behavior of a generic adhesive across glass transition temperatures based on a thermo-viscoelastic model

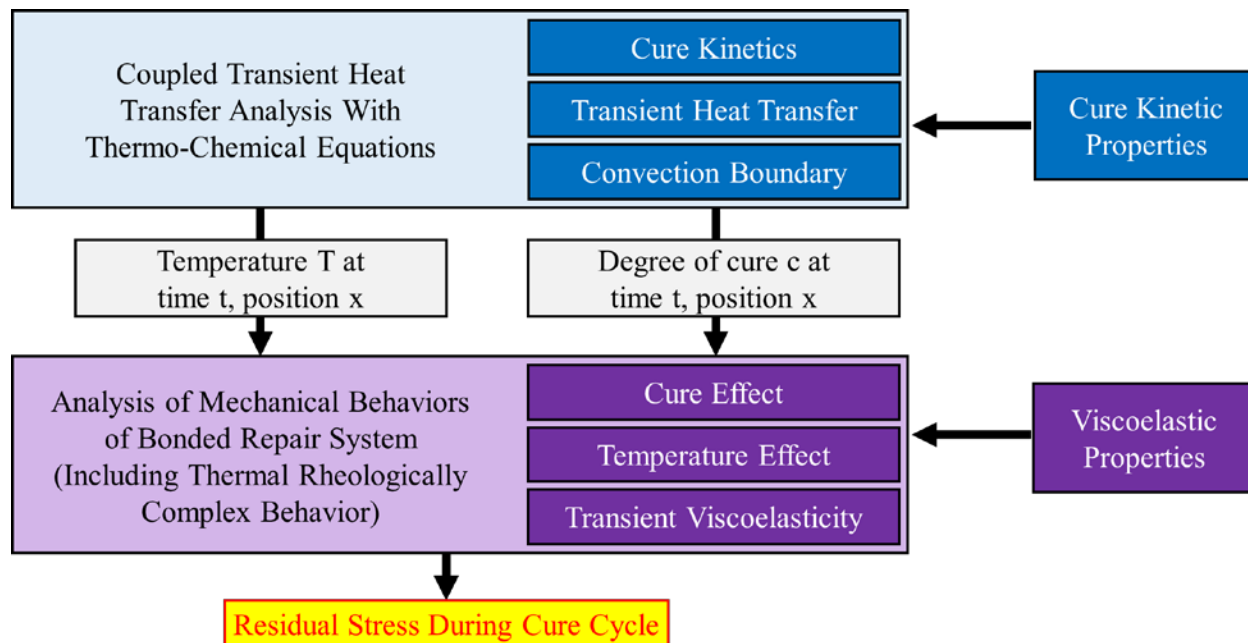


Figure K-3. Inhar University's thermo-chemical-mechanical model for adhesive curing

Recently sponsored by The Boeing Company, Inhar University of South Korea has developed a new thermo-chemical-mechanical model for adhesive curing. This new adhesive curing model,

shown in figure K-3, consists of two coupled analyses: 1) a thermo-chemical analysis, and 2) a thermo-mechanical analysis. In the thermo-chemical analysis, a coupled transient heat transfer analysis with thermo-chemical equations is performed using the cure kinetic properties as shown in the upper part of figure K-3. Both temperature and the degree of cure at time t and position x of a curing bonded structure are calculated from this thermo-chemical analysis. The calculated temperature and the degree of cure are then fed into a second thermo-mechanical analysis. The thermo-mechanical analysis calculates thermal residual stresses in the bonded structure using adhesive viscoelastic properties, as shown in the lower part of figure K-3. However, the adhesive viscoelastic properties are functions of time, temperature, and the degrees of cure.

To assess the improvement of the new viscoelastic model for the adhesive on predicting thermal residual stresses in bonded repair, ABAQUS finite element analyses of a curved panel repaired with both Al and B/Ep patches were performed to simulate the curing process of the adhesive bond. For simplicity, the thermo-chemical analysis was assumed to be decoupled from the thermo-mechanical analysis, and the degree of cure of the adhesive bond as a function of time is already obtained from this analysis. Therefore, only thermo-mechanical analysis of the curved panel using a viscoelastic model will be performed. In the thermo-viscoelastic analysis, the temperature distributions for different regions of the curved panel and for repaired patch are assumed to be uniform and steady at the initial time and during heat-up and cool-down phases, as shown in figure K-4. Figures K-5 and K-6 show comparisons of the analytical predictions with strain gauge data for Al and B/Ep patches from a Panel-3 test. Because no good correlation was found for Panel 3, a post-test analysis based on the present viscoelastic model was not performed for Panel 4. Until a further improvement of the thermo-viscoelastic stress model is made, test results of Panels 3 and 4 will be used to determine empirical knock-down factors for the previous CRAS simple thermo-stress model.

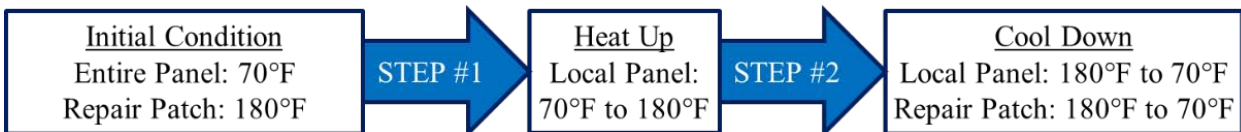
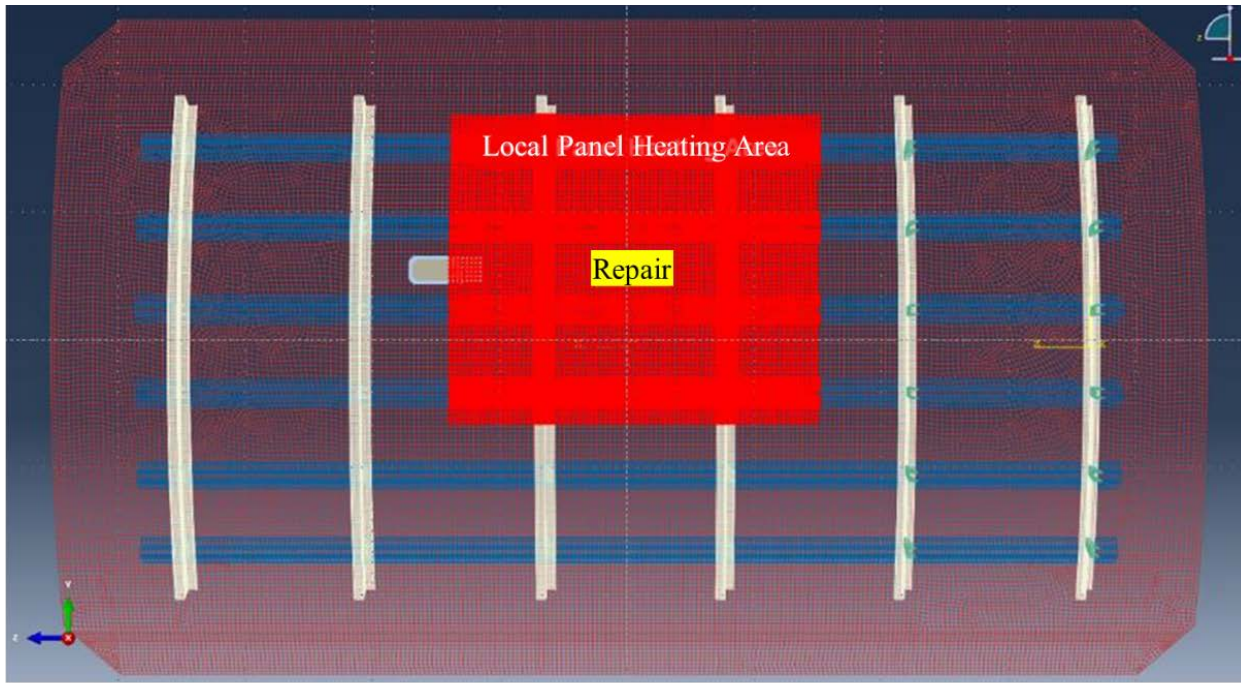


Figure K-4. Assumed temperature distribution in the panel and the repair patch at the initial time, during heat up, and during the cool-down curing process in the ABAQUS analysis

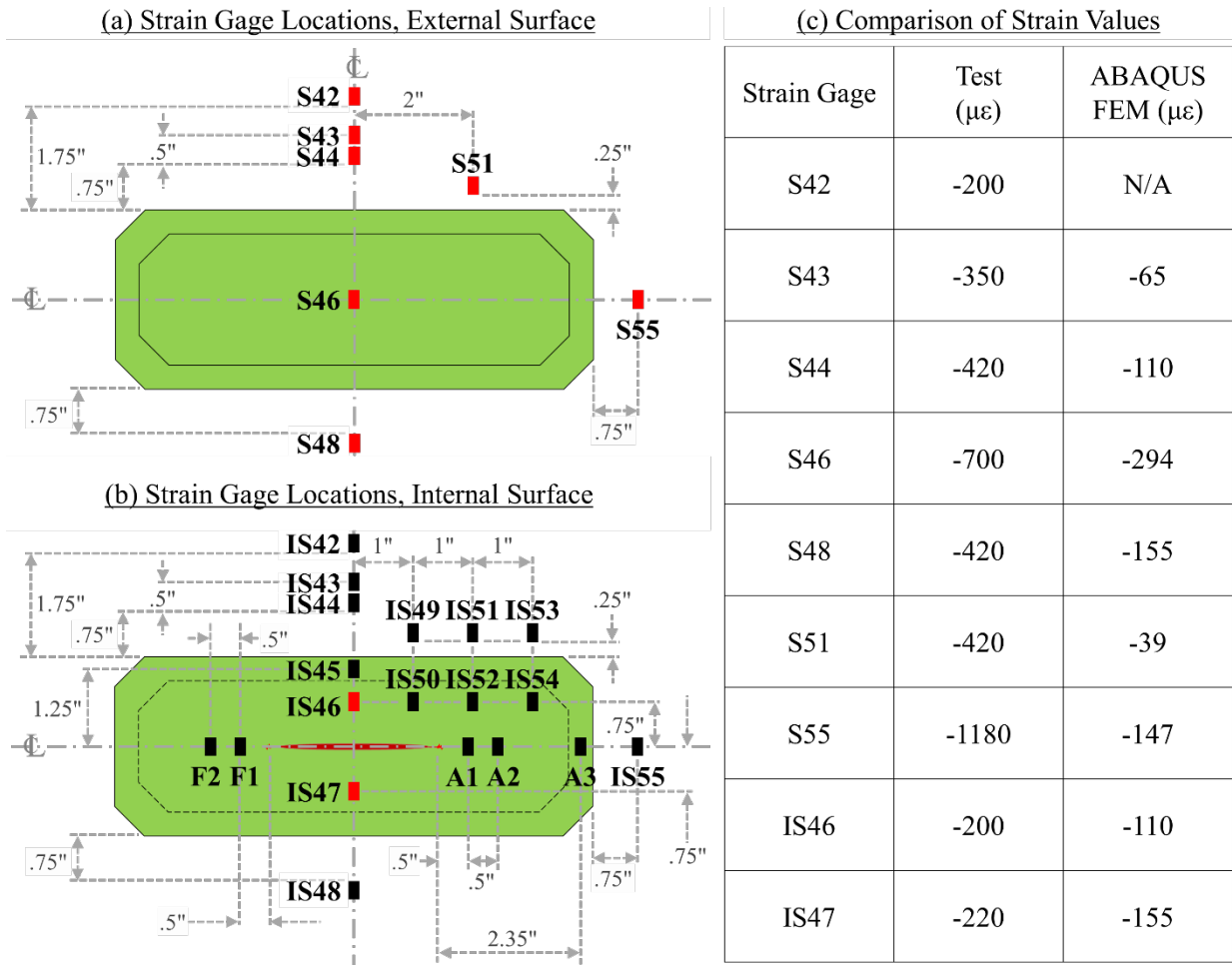


Figure K-5. A comparison between strain values obtained via analytical predictions and those obtained via strain gauges for the Type-2 (under-designed) Al repair patch, UAC: (a) strain gage locations, external surface, (b) strain gage locations, internal surface, (c) comparison of strain values

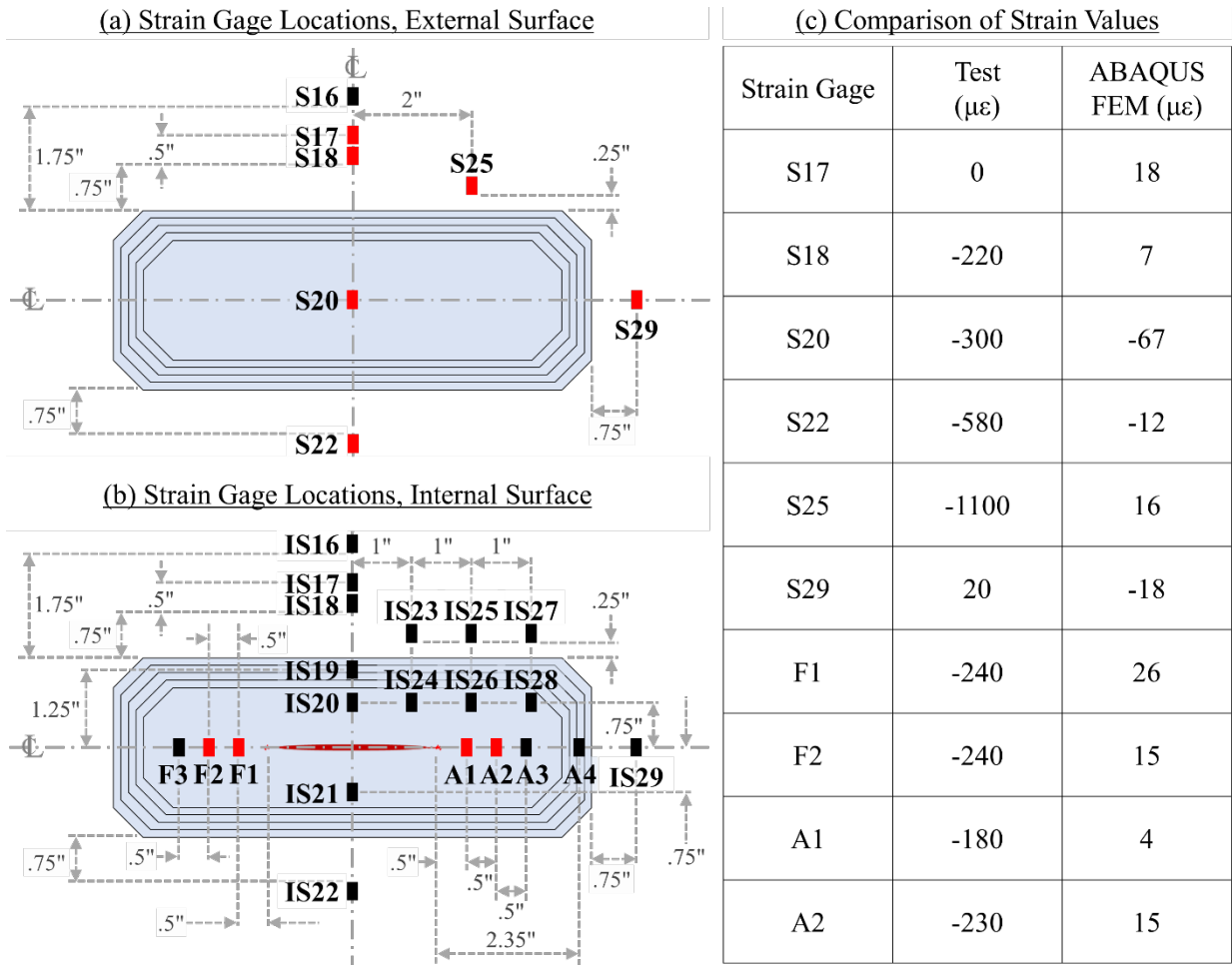


Figure K-6. A comparison between strain values obtained via analytical predictions and those obtained via strain gauges for the Type-2 (under-designed) B/Ep repair patch, UBC: (a) strain gage locations, external surface, (b) strain gage locations, internal surface, (c) comparison of strain values